URBAN AIR QUALITY: MONITORING AND MODELLING

URBAN AIR QUALITY:
MONITORING AND MODELLING

Proceedings of the First International Conference on
Urban Air Quality: Monitoring and Modelling
University of Hertfordshire, Hatfield, U.K.
11–12 July 1996

Guest edited by

Ranjeet S. Sokhi
Atmospheric Science Research Group
Department of Environmental Sciences
University of Hertfordshire
College Lane, Hatfield, Hertfordshire
AL10 9AB, U.K.

Organised by

The Environmental Physics Group of the Institute of Physics, U.K.

in collaboration with

The Royal Meteorological Society, U.K.
The National Society for Clean Air and Environmental Protection, U.K.
The Royal Society of Chemistry, U.K.

Printed on acid-free paper

TABLE OF CONTENTS

URBAN AIR QUALITY:
MONITORING AND MODELLING

Proceedings of the First International Conference on
Urban Air Quality: Monitoring and Modelling
University of Hertfordshire, Hatfield, U.K.
11–12 July 1996

Preface

The increasing concern over environmental and health impact of urban air pollution has lead to a growing need for an international conference focussing specifically on urbanised regions. Although, air quality has gained importance through out the world, it is especially in areas of high urban development that the problems are particularly acute. Scientific interest in this field is particularly evident from the growing number of journal publications and conference presentations. The numerous conferences held every year on air pollution, however, have tended to encompass a broad theme and have not specifically focussed on the urban environment.

In order to address this need an international conference on urban air quality was organised by the Environmental Physics Group of the Institute of Physics in collaboration with the Royal Society of Chemistry (RSC), The Royal Meteorological Society (RMS) and the National Society for Clean Air and Environmental Protection (NSCA). Over 100 participants from various countries attended this first international conference on urban air quality.

The aim of the conference was to provide a forum for open scientific discussion on the latest advances in the field of urban air quality monitoring and modelling. The range of topics included: chemical and biogenic pollutants, monitoring techniques, instrumentation, analysis of pollutants, spatial and temporal interpretation of air quality data, emission sources and modelling of air quality.

All papers submitted for publication were peer reviewed and consequently, some articles were not successful in the refereeing process and have not been included in this special issue. The quality of the presentations was especially high and thus no differentiation was made during the refereeing process between oral and poster contributions.

The success of this conference can be attributed to the excellent organisation by the main sponsoring and collaborating bodies. The dedication of the Scientific and Editorial Panel is acknowledged especially during the reviewing stages of this special issue. Most of all, it is the hard work of the researchers in this field that requires special mention. It is their continued effort that is leading to advances in the field and is providing improved understanding of urban atmospheric pollution in relation to its generation, its dispersion, and its impact on the environment as a whole.

Ranjeet S Sokhi
University of Hertfordshire, UK

PM$_{10}$ CONCENTRATION MEASUREMENTS IN DUBLIN CITY

J. KEARY[1], S. G. JENNINGS[1], T. C. O'CONNOR[1], B. MCMANUS[2] AND M. LEE[2]

[1] Departmental of Experimental Physics, University College Galway, Galway, Ireland.
[2] Atmospheric Pollution and Noise Unit, Dublin Corporation, Dublin, Ireland.

Abstract. Mass Concentration of ambient particulate matter with an aerodynamic diameter less than 10μm (PM$_{10}$) are reported for the first time for a range of sites in Dublin City over a 6 month period from January 1st 1996 to June 30th 1996. PM$_{10}$ gravimetric mass concentration measurements are made with low flow Partisol 2000 air samplers using an impaction type PM$_{10}$ inlet and 47mm diameter glass fibre filters. In addition, much finer time resolution measurements (minimum sampling frequency of 30 minutes) are made using a tapered element oscillating microbalance (TEOM) PM$_{10}$ mass monitor. These PM$_{10}$ mass concentrations methods are also compared with mass concentration inferred using the standard black smoke method. Analysis of the ambient mass concentration data with reference to traffic density and meteorological influences are presented. Results for the first six months of 1996 show that the average PM$_{10}$ values range from a high of 49 μg m^{-3} at the Dublin city centre site to 14 μg m^{-3} at one of the suburban sites. Intercomparison between PM$_{10}$ and black smoke mass concentrations show that the relationship is site specific. Statistical analysis between PM$_{10}$ levels and car traffic number show a positive correlation while a weak negative correlation is found between PM$_{10}$ levels and rainfall amount, wind speed and air temperature.

1. Introduction

The quality of the air we breathe has become a significant factor in the environment, with increasing interest in both indoor and outdoor air properties. Interest in measurements of the concentration of particulate matter with a diameter less than 10μm (PM$_{10}$) has increased dramatically in recent years due to concerns about its likely role in human health in urban areas in particular. The well known severe episodes of air pollution in Europe and North America before 1960 provided indisputable evidence that high levels of air pollution have important short-term effects on human health, including possible related increases in mortality. Since then, air quality guidelines and standards set by national and international organizations have contributed to a decrease in air pollution to moderate or low levels in several large conurbation areas. However, recent work (Katsouyanni et al.,1995) indicates that moderate and even low levels of air pollution have short-term effects on mortality and morbidity, and that these effects are measurable at levels of air pollution which do not exceed the set safety limits. Historically, measurements of sulphur dioxide and total suspended particulates were used as indicators of air pollution but more recent studies have tended to focus on the inhalable fraction of particulate matter, PM$_{10}$ and its role in air pollution. Several recent studies have shown that there is a relationship between PM$_{10}$ particulate concentration and various health indicators such as hospital admissions, frequencies of respiratory illness, reduced lung capacity and death. Studies from the USA indicate statistically significant increases in mortality and morbidity as a result of short-term exposure to PM$_{10}$. These studies use data from different cities and include Utah Valley (Pope et al.,1992), Philadelphia (Schwartz and Dockery,1992a) and Steubenville, Ohio (Schwartz and Dockery,1992b). Studies from other areas, such as Australia (Glikson et al.,1995),

Canada (Delfino et al.,1994) and Europe (Spix et al.,1993) and have also indicated similar associations between PM_{10} and health effects.

Analysis of epidemiological data from the USA (Schwartz,1994) has suggested that a rise of 10 μg m^{-3} in PM_{10} levels are accompanied by an increase in relative risk of mortality of about 1% in the exposed population. This evidence has led to the new World Health Organisation report (Air Quality Guidelines for Europe,1995), which recommends new European safety standards for air pollution, and declines a proposed safe limit for PM_{10} "because there is no evident threshold for effects on morbidity and mortality, there does not seem to be a safe level - the more there is, the worse it is".

Emission of PM_{10} particulate matter into the atmosphere can arise from a number of different sources. Emissions are generally categorised into two sources, primary and secondary. Primary sources of PM_{10} include road transport vehicles. Motor vehicles are an important source of primary PM_{10}, especially in urban areas. For example, in London more than 80 per cent of primary PM_{10} emissions comes from vehicles, with medium-sized lorries accounting for nearly a quarter of the total (Quality of Air Review Group, QUARG,1996). Other primary sources of PM_{10} include stationary combustion sources, such as domestic fires, industrial processes such as construction works, pharmaceutical companies, oil storage depots and garages. These stationary sources are significant contributors to PM_{10} emissions and they account for about one half of PM_{10} emissions in the UK. However in cities these contribution may become quite small: in London they account for about 5% of all the emissions (QUARG,1996). Secondary sources of PM_{10} are particles formed within the atmosphere from the condensation of vapors or as a result of chemical reaction processes. Main sources of secondary particles include the atmospheric oxidation of sulphur dioxide to sulphuric acid and the oxidation of nitrogen dioxide to nitric acid.

To date there have been no comprehensive measurements of the concentrations of PM_{10} particulate species in urban air in Ireland. In the absence of historical PM_{10} data in Dublin City, black smoke data is the only available measurement of fine suspended particulate concentrations. There is a comprehensive data base of black smoke measurements in Dublin City dating back to the early 1970's. Clearly it would be of interest to establish if any relationship exists between the PM_{10} and black smoke measurements. A number of recent studies have investigated this relationship with a view to using it for epidemiological studies (Muir and Laxen,1995; Ostro,1993).

The principal objectives of this PM_{10} measuring programme are to establish ambient mass concentrations of particulate matter with diameter less than 10μm (PM_{10}) at a number of sites in Dublin city and to determine relationships between PM_{10} mass concentration with that inferred using the standard black smoke method at these sites. Diurnal variation of PM_{10} at some of the sites is also examined.

2. Measurement Methods

2.1.   AREA OF STUDY

The city of Dublin is located on the east coast of Ireland. Physically the region is divided into two by the river Liffey which flows from west to east through the city and enters the sea in Dublin Bay. The city is surrounded on the southern side by the Wicklow mountain range, the hills start about 10 km from the city centre and extend a further 50 km to the

south. The highest peak rises to a height of 930 meters. The population within the city boundary in 1991 was 477,675 according to the 1991 census. The PM_{10} measurements were carried out at a series of sites in Dublin City, as shown in Figure 1. The sites can be grouped into three categories: urban, suburban and suburban background. Specific site details are outlined in Table I.

TABLE I
PM_{10} Measurement sites in Dublin City

Site Name	Site Type	PM_{10} Equipment Position
College Green	Urban (city centre)	Kerbside-heavy traffic junction
Rathmines	Urban	2nd floor level-adjacent to major road
Ashtown Grove	Suburban	1st floor level 200m from major road
Clontarf	Suburban	1st floor level-adjacent to major road
Phoenix Park	Suburban (background)	1st floor level-remote from traffic routes

2.2. PM_{10} EQUIPMENT

PM_{10} mass concentrations were measured using two different instruments: the Rupprecht and Patashnick Partisol Model 2000 Air Sampler and the Rupprecht and Patashnick Tapered Element Oscillating Microbalance, TEOM, (Patashnick and Rupprecht,1991).

The Partisol sampler is a US Environmental Protection Agency (EPA) reference method for the measurement for PM_{10} mass concentrations. The sampler is a low flow gravimetric PM_{10} sampler which can be operated as a stand-alone unit or with three additional satellites PM_{10} sampling heads and filter units. Use of the satellite heads enables four consecutive daily samples to be taken without manual attention. Air is drawn through the PM_{10} inlet at a flow rate of 16.7 1 min^{-1}. The particles are collected on a 47mm diameter glass fibre filter. The filter conditioning and sampling procedures followed were in accordance with the U.S. EPA guidelines for PM_{10} sampling (Federal Register, 1987). Before use, each filter was inspected for any defects and the filters were preconditioned in a controlled environment chamber at a constant temperature (21°C ± 3°) and relative humidity (RH), 31% ± 5% RH. The filters were preweighed using a Mettler-Toledo AG245 semi-micro balance with a resolution of 0.01mg. After exposure,

6

Fig. 1.   PM$_{10}$ measurement sites in Dublin City.

1. COLLEGE STREET
2. MERCHANTS QUAY
3. RATHMINES ROAD LWR.
4. CLONTARF ROAD
5. ASHTOWN GROVE/
   NAVAN RD.
6. ORDNANCE SURVEY/
   PHOENIX PARK

E.P.A. PROJECT
PM$_{10}$ SITES

the filters were stored in an environmental chamber for at least 24 hours before weighing. Five Partisol units were used during the study.

A Tapered Element Oscillating Microbalance (TEOM) was also used during the work. The TEOM air sampler has been given US EPA reference equivalent status for the measurement of PM_{10} mass concentrations. The TEOM air sampler is capable of yielding continuous hourly average PM_{10} mass concentrations, unattended. The TEOM consists of a filter cartridge located on top of a hollow tapered crystal element which vibrates at its natural frequency. Air is drawn through the standard PM_{10} inlet at a rate of 16.7 l min^{-1}. The air flow is then split into two streams: a reference bypass flow of 13.7 l min^{-1} and a sample flow 3 l min^{-1} which passes through a 16mm diameter filter connected to the top of a hollow tapered element. As the particles collect on the filter, the tube's natural frequency of vibration decreases. The change in frequency is indirectly proportional to the particulate mass collected on the filter head. Average PM_{10} mass concentration (hourly or half-hourly) based on the change in vibrational frequency of the hollow element is calculated. The inlet temperature including the sensing element is maintained at 30°C to minimize any losses from the more volatile organic compounds. One TEOM unit was available during the study and this was rotated between the various sites.

Black smoke measurements were also performed at the various sites. The measurements were made using the automatic 8-port sampler to collect daily filters for smoke stain analysis according to the British Standard method (BS1747 Part 2,1969). Studies have shown that this method samples particles of less than about 4μm in diameter (Mark and Hall, 1993). The results are presented as concentrations of black smoke in micrograms per cubic meter (μg m^{-3}) using the OECD standard calibration curve for an EEL reflectometer and Whatman #1 filter paper.

Meteorological parameters of air temperature, wind speed, wind direction and rainfall were recorded by the National Meteorological Service (Met Eireann) at Dublin Airport. This site is 8.5 km north of the city centre and is surrounded by flat open agricultural land. The traffic data used in this study were obtained from the Road, Traffic and Planning Division of Dublin Corporation.

3. Results

3.1.   *PM_{10} MEASUREMENTS*

A range of PM_{10} mass concentrations were measured at the various sites for the first six months of 1996. The highest average PM_{10} mass concentration (49 μg m^{-3}) for this period was recorded at the College Green city centre site. The other urban site at Rathmines, had an average PM_{10} mass concentration of 28 μg m^{-3} during this period. The two suburban sites, Ashtown Grove and Clontarf had average concentrations of 31 and 14 μg m^{-3} respectively. The background Phoenix Park site had a mean value of 17 μg m^{-3}.

Figure 2 shows the daily PM_{10} mass concentrations for the College Green and Rathmines sites. The PM_{10} mass concentrations at the College Green site are generally higher than at the Rathmines site and it is noticeable that the values for the first three months of 1996 are higher than the following three months. The PM_{10} levels at the two sites track each other quite well. Figure 3 shows the measurements for the College Green site and the Phoenix Park background site. Again, it can be observed that the mass concentrations levels at each site track each other but the values at the College Green site
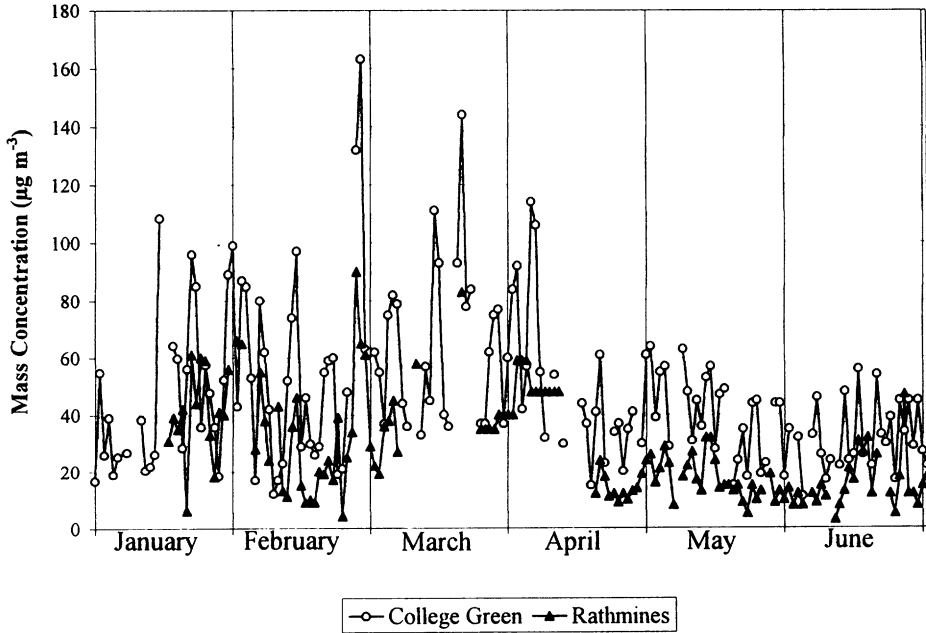
Fig. 2.   Partisol PM$_{10}$ mass concentration (μg m^{-3}) at College Green and at Rathmines in Dublin City for January-June 1996.
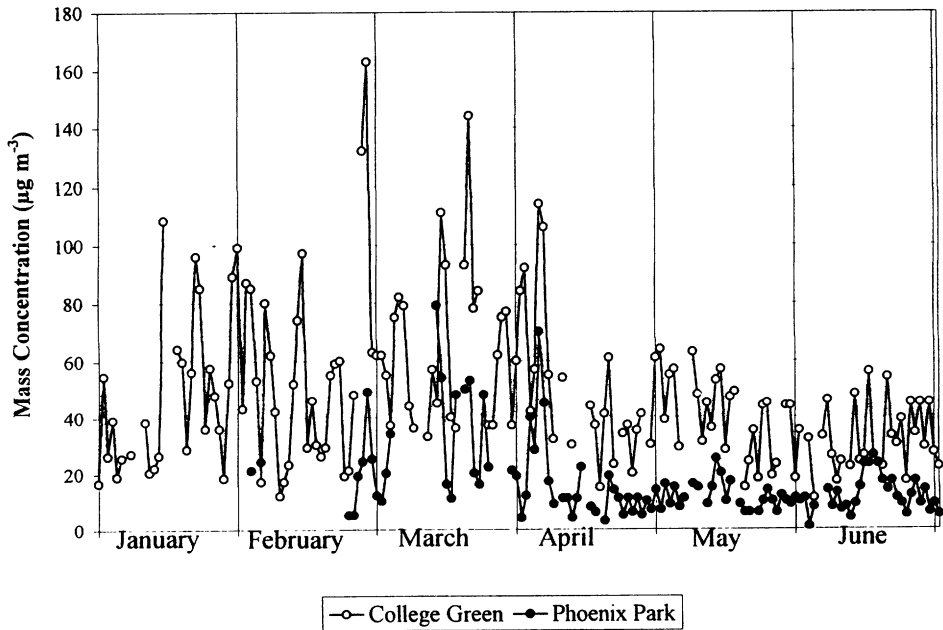
Fig. 3.   Partisol PM$_{10}$ mass concentration (μg m^{-3}) at College Green and at Phoenix Park in Dublin City for January-June 1996.

are generally higher than the Phoenix Park site. The summary statistics from all the sites for the January to June period 1996 are presented in Table II.
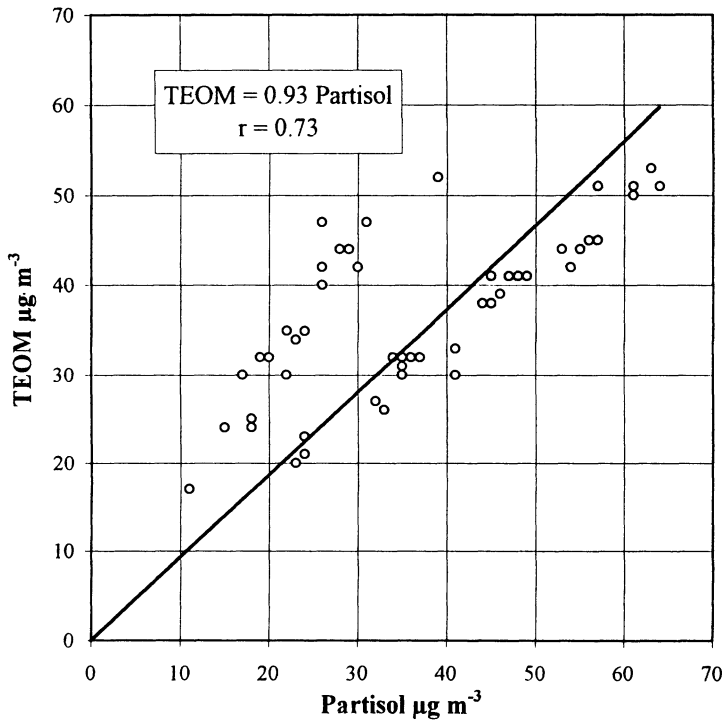
Fig. 4.   TEOM v's Partisol PM$_{10}$ mass concentration (μg m^{-3}) at the College Green site, April-June 1996.

TABLE II
PM$_{10}$ mass concentration (μg m^{-3}) summary statistics for Dublin City sites
for the period January -June 1996

Site	Mean	Maximum	No of Days >50 μg m^{-3}	No of Days >100 μg m^{-3}	Number of measurement days
College Green	49	163	59	7	157
Rathmines	28	90	15	0	134
Ashtown Grove	31	108	16	1	85
Clontarf	14	109	3	1	78
Phoenix Park	17	79	4	0	107

The TEOM and Partisol samplers were collocated at the College Green site from 11 April to 19 June 1996. A comparison was made between the TEOM and Partisol PM$_{10}$ mass concentrations obtained. Good agreement was found to exist between the two methods. A linear relationship of the form *TEOM PM$_{10}$ = 0.93 Partisol PM$_{10}$* was found with a correlation coefficient (r) equal to 0.73 which is deemed to be quite good

agreement. It appears from the graph that the Partisol sampler recorded lower mass concentrations than the TEOM sampler at lower mass concentrations (< 30 μg m$^{-3)}$. Figure 4 shows the scatter plot of the Partisol versus the TEOM PM$_{10}$ mass concentration levels at the College Green site.

Averaged 1/2-hourly PM$_{10}$ mass concentrations are obtained from the TEOM which are very useful is observing short term trends in the PM$_{10}$ levels and also for observing diurnal variations at a particular site. Figure 5(a) shows the averaged 1/2-hourly PM$_{10}$ mass concentrations at the College Green site for the period 11 April -19 June. Each point on the plot is an average of 70 half-hourly values. The general trend of the PM$_{10}$ levels shows a gradual reduction over the period 00:30-05:00, reaching a minimum at around 05:30-06:00. The levels then start to rise reaching a peak between about 08:00 to 09:30. Thereafter, there is a gradual fall off in the levels for the rest of the day with the exception of a slight increase at 18:30. In general the levels tend to decrease as evening time approaches.

A similar analysis was performed at the Rathmines site during the period 09 March -11 April during which the TEOM was operated simultaneously alongside the Partisol. Figure 5(b) shows the diurnal variation in PM$_{10}$. Again the trend shows that the PM$_{10}$ levels show a gradual reduction over the period 01:00 to 05:00. The levels start to rise at 06:30 reaching a maximum at 11:30. There is a decrease in the levels between 11:30 and 14:00. From 14:00 onwards the levels start to increase reaching a maximum at 22:30 in the evening.

3.2.   *RELATIONSHIP BETWEEN PM$_{10}$ AND BLACK SMOKE*

The relationship between daily mean (00:00 to 24:00) PM$_{10}$ and the daily Black Smoke mass concentrations was investigated for three sites, College Green, Rathmines and Ashtown Grove. The relationship between PM$_{10}$ and Black Smoke mass concentrations for the College Green site for the period January-June is shown in Figure 6. The results of the regression analysis for each site are presented in Table III. The best correlation between the two parameters was found at the College Green site, with a correlation coefficient r of 0.75. The other two sites, Rathmines and Ashtown Grove give correlation coefficients of 0.69 and 0.65 respectively. The slopes of the relationship between PM$_{10}$ and Black Smoke vary from site to site with a similar non zero intercept of between about 10-13 μg m^{-3} found at all three sites.

TABLE III
Relationship between PM$_{10}$ and Black Smoke mass concentrations (μg m^{-3})

Site	Regression Line	Correlation coefficient (r)
College Green	PM$_{10}$ = 0.69 Black Smoke + 11.3	0.75
Rathmines	PM$_{10}$ = 1.26 Black Smoke + 9.8	0.69
Ashtown Grove	PM$_{10}$ = 1.58 Black Smoke + 13.3	0.65
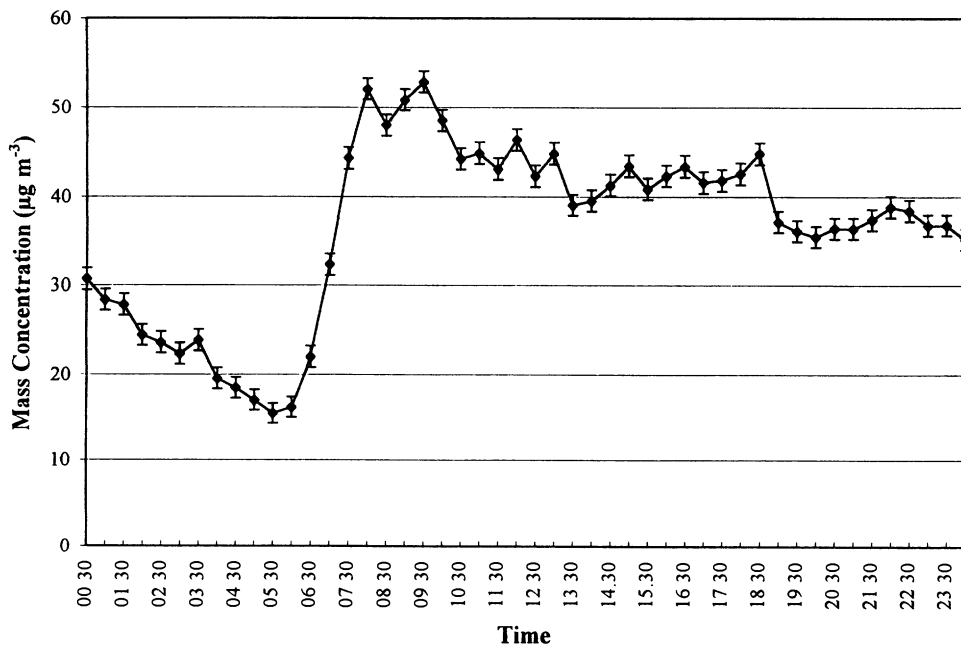
Fig. 5(a). Average 1/2-hourly TEOM PM$_{10}$ mass concentration (μg m^{-3}) at the College Green site,

11 April-19 June 1996.
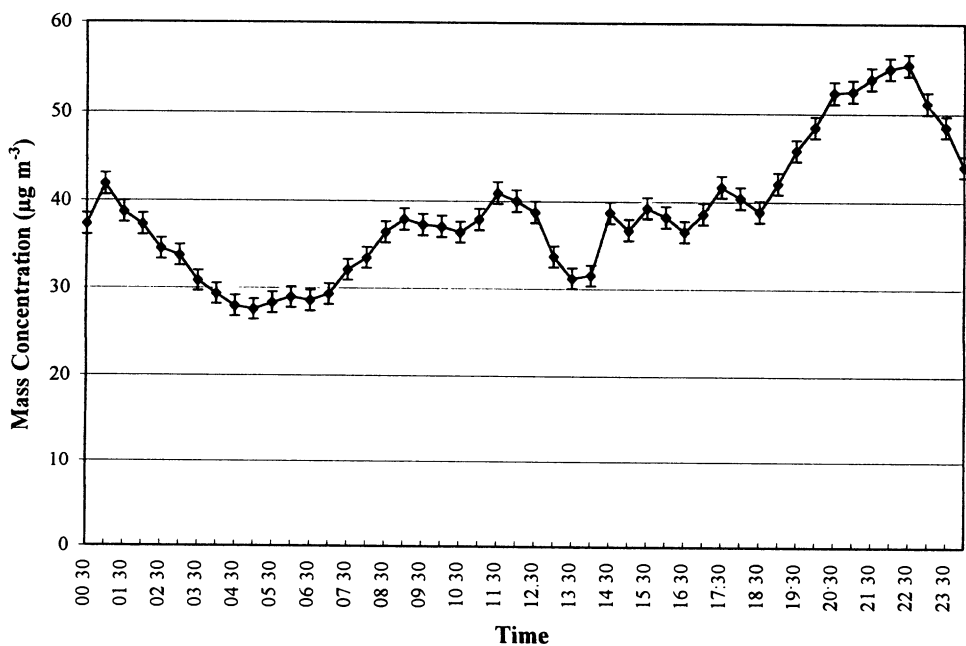
Fig. 5(b). Average 1/2-hourly TEOM PM$_{10}$ mass concentration (μg m^{-3}) at the Rathmines site,

9 March-11 April 1996.

12

3.3. RELATIONSHIP BETWEEN PM_{10} MASS CONCENTRATION AND METEOROLOGICAL PARAMETERS

Correlation analysis between the daily PM_{10} mass concentrations and selected meteorological parameters was performed for five of the sites. The meteorological parameters used in the analysis were wind speed , rainfall rate and air temperature. The correlations for daily PM_{10} mass concentrations versus daily rainfall, wind speed and air temperature at the various sites are shown in Table IV.

The analysis clearly shows that in all cases a negative correlation was found to exist. Figure 7 shows the scatterplot of daily average rainfall rate versus PM_{10} mass concentration at the College Green site for the January to June period. A negative correlation coefficient,
r = -0.21 was found, which suggests that as the rainfall rate increases the PM_{10} values decrease and is probably due to the scavenging effect of the rain.
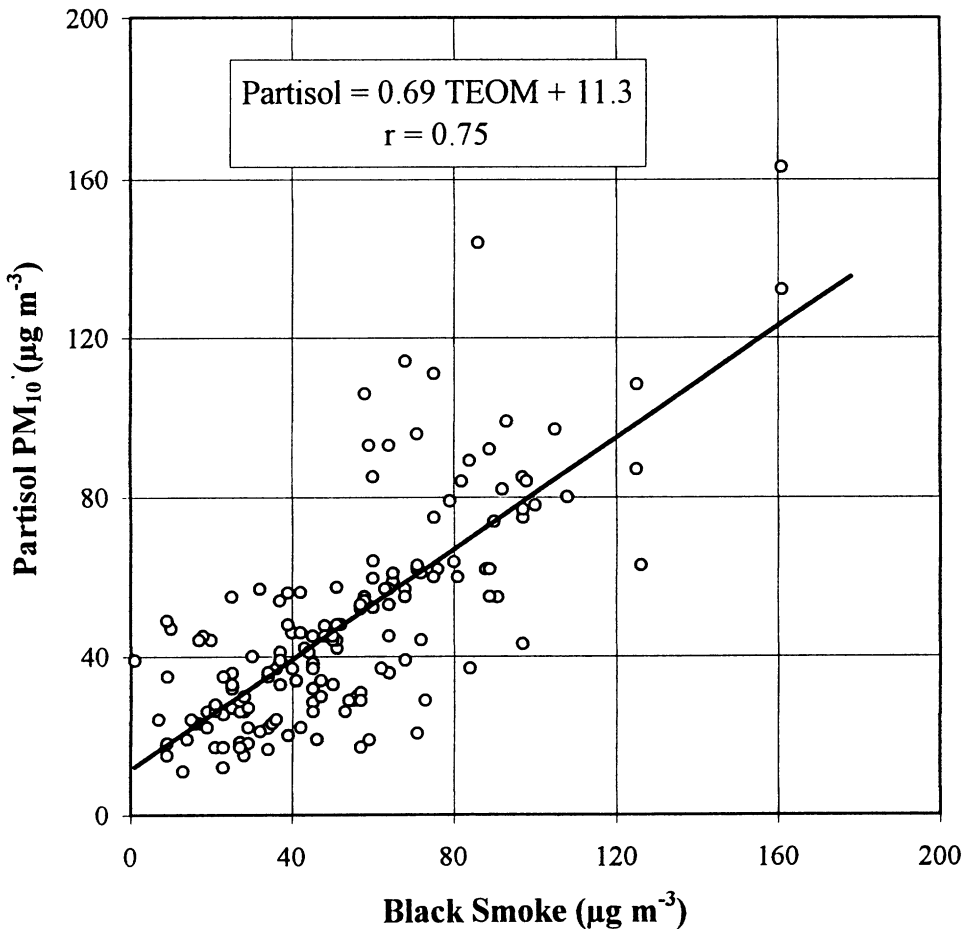
Fig. 6.   Intercomparison of Partisol PM_{10} v's Black Smoke mass concentration ($\mu g\ m^{-3}$) at College Green in

Dublin City for January-June 1996.

TABLE IV
Correlation coefficients (r) between daily PM_{10} mass concentrations and daily rainfall, wind speed and air
temperature values at the Dublin City sites

Site	Rainfall (mm)	Wind Speed (knots)	Temperature (°C)
College Green	-0.21	-0.43	-0.35
Rathmines	-0.09	-0.20	-0.51
Ashtown Grove	-0.14	-0.11	-0.47
Clontarf	-0.13	-0.30	-0.28
Phoenix Park	-0.11	-0.06	-0.42

3.4.   RELATIONSHIP BETWEEN PM_{10} AND TRAFFIC DENSITY

Another objective of this work was to determine if any relationship exists between the PM_{10} mass concentrations and the traffic densities at the various sites. During the operation of the TEOM at the College Green site a traffic survey was carried out (on 27th of May). The numbers of cars, lorries, buses and motorcycles passing the junction every 1/2 hour were manually recorded for a 10.5 hour period (08:00-18:30). A comparison between the PM_{10} mass concentrations and the traffic numbers was performed. Figure 8(a) shows the variation in PM_{10} concentration with car numbers passing per each 1/2 hour period. It can be seen that the PM_{10} levels tend to track the car numbers up to around 14:00, with higher levels occurring in both for the period between 12:00 and 12:30. The variation in PM_{10} mass concentration with lorries and bus numbers is shown in Figure 8(b). With the exception of the period 08:30-11:30 when there is a general reduction in both PM_{10} and bus number density there is no strong evidence of a relationship between the PM_{10} values and the number of lorries and buses passing the site. The influence of diesel operated vehicles (buses and lorries) on the PM_{10} levels is examined in Figure 8(c). Here, the variation of PM_{10} mass concentration ($\mu g\ m^{-3}$) is plotted as a function of the sum of the buses and lorries number density (number passing per 1/2-hour). A weak correlation (r = 0.48) was found between the two parameters, suggesting that there is no strong relationship between the PM_{10} values and the number density of diesel vehicles at the site for that time period.
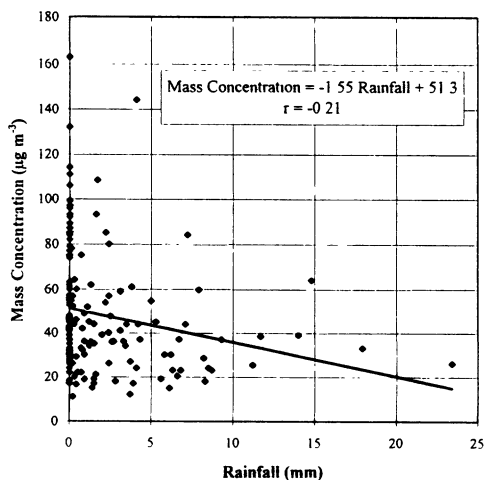
Fig. 7.   Rainfall (mm) v's Partisol PM_{10} mass concentration ($\mu g\ m^{-3}$) at College Green in Dublin City,
January- June 1996.

4. Discussion

PM$_{10}$ measurements carried out at a number of different sites in Dublin City for the first time are reported. The measurements commenced at the beginning of January 1996 and the results reported here cover the period from January to June 1996. The measured mean mass concentrations of PM$_{10}$ were found to vary from site to site. The highest mean mass concentration of 49 µg m^{-3}, was recorded at the College Green site. This site is situated in the city centre at a busy traffic junction so higher levels are expected here due to the influence of higher density road traffic, as determined from the traffic survey data. The high levels recorded at this site are consistent with other recent city centre data on roadside measurements made in both London in 1995 and Birmingham in 1994 (QUARG, 1996) where mean values of 52 µg m^{-3} and 45.5 µg m^{-3} were recorded at these sites. These roadside measurements show a clear elevation over the levels recorded at urban background sites.

The average PM$_{10}$ concentration for the Rathmines site was 31µg m^{-3} and for the Ashtown Grove site was 28 µg m^{-3}. The levels recorded at these sites are similar to the levels observed at the urban background sites in the UK where the average values for 13 sites during 1994 were between 20-34µg m^{-3} (QUARG, 1996). The average values at the Clontarf site were the lowest of all the sites with a value of 14 µg m^{-3}. This monitoring station is located on a main traffic route into the city centre but it is also located very near the coast. The influence of sea breezes is probable causing a reduction in concentrations of PM$_{10}$ at the station. The average value recorded for the Phoenix Park site was 17 µg m^{-3}, which is consistent with it being located away from major sources of traffic. The levels here are similar to the levels recorded at a rural site near Bristol, England (QUARG, 1996) where average concentrations of 14 µg m^{-3} for a 1 month period were measured.

At present no air quality standards exist in Ireland for PM$_{10}$ mass concentrations so that standards of other countries are used to compare the results obtained in this study.
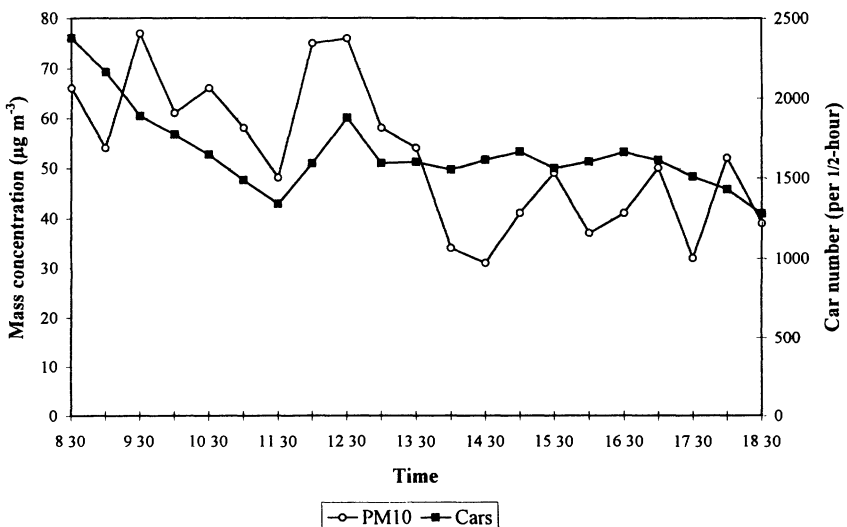
Fig. 8(a). PM$_{10}$ 1/2-hour mass concentration (µg m^{-3}) v's car numbers per 1/2-hour at College Green, 27 May 1996.
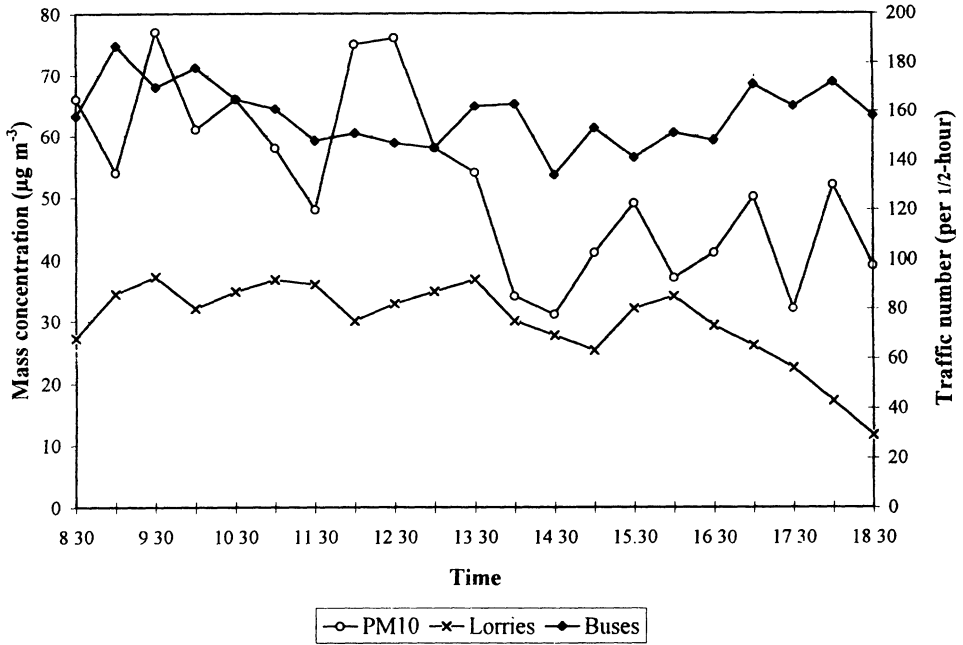
Fig. 8(b). PM$_{10}$ 1/2-hour mass concentration (μg m^{-3}) v's traffic number per 1/2-hour at College Green, 27 May 1996.
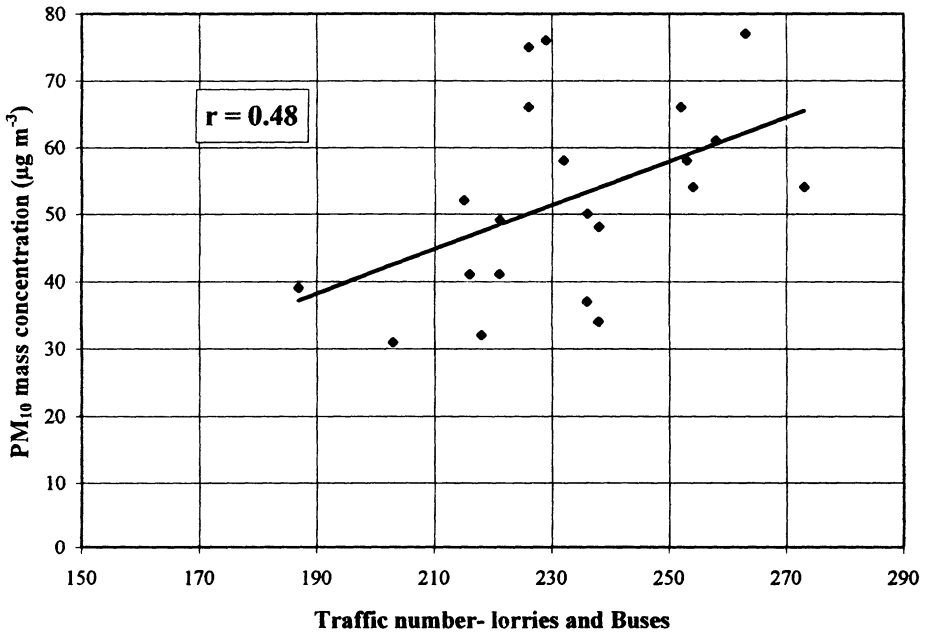
Fig. 8(c). Correlation between PM$_{10}$ 1/2-hour mass concentration (μg m^{-3}) and sum of buses and lorries per 1/2-hour at College Green, 27 May 1996.

In 1987, the US EPA set the following primary standards for ambient PM_{10} concentrations:

A 24 hour mean concentration of 150 µg m^{-3} PM_{10} which is not to be exceeded on more than 1 day in the year and an annual arithmetic PM_{10} mean concentration less than 50 µg m^{-3}.

The 24 hour standard of 150 µg m^{-3} has already been exceeded on one occasion at the College Green site when a 24 hour value of 163 µg m^{-3} was recorded (28th February 1996). The probable reason for this high value was due to winter time inversion conditions existing i.e. slack winds and trapping of the aerosol particulates beneath the inversion. The mean concentrations at the College Green site of 49 µg m^{-3} site for the first six months of 1996 is close to the US EPA annual mean exceedence concentration of 50 µg m^{-3}. The mean PM_{10} values at the other sites are well below the standard exceedence values.

Recently the Expert Panel on Air Quality Standards (EPAQS, 1995) in the United Kingdom has recommended air quality standards for a number of pollutants including PM_{10}. The air quality standard recommended for PM_{10} is 50 µg m^{-3} as a 24-hour rolling average. Table II shows the number of daily exceedences of this recommended standard at each site. It can be seen that on 37% of the days at the College Green site, the PM_{10} mass concentration exceeded 50 µg m^{-3}. The number of exceedences at the other sites is much less, 19% at the Ashtown Grove, 11% at the Rathmines site to a low of 4% at both the Clontarf and Phoenix Park sites.

The TEOM sampler was operated at two sites, College Green and Rathmines for specific time periods during which short term variations and the diurnal variation in PM_{10} levels were measured. An early morning rush hour peak (between about 07:30 and 10:00) was observed at the College Green site. No corresponding evening rush hour peak was obtained. A similar morning peak occurred at the Rathmines site and an increase in the PM_{10} levels was observed during the evening reaching a maximum at 22:30. As the Rathmines site is located in a more populated residential area than the College Green site the influence of domestic heating sources is likely to result in the elevation of levels during the evening.

An investigation of the relationship between the concentration of PM_{10} and Black Smoke was carried out at three of the sites for the period January to May 1996. The regression analysis of the daily means of both parameters indicates that the relationship seems to be site specific. In all three cases the linear regression analysis leads to a significant intercept of between 9.8-13.3 µg m^{-3} PM_{10} as Black Smoke mass concentration goes to zero. This is similar to the results obtained by Muir and Laxen (1995) in their analysis of PM_{10} and Black Smoke measurements in Bristol. Some confusion has arisen over the nature of this non-zero intercept. The Black Smoke method samples the size fraction PM_4, so as Black Smoke goes to zero, PM_{10} need not necessarily go to zero since PM_{10} = Black Smoke + (PM_{10} - PM_4). It is also likely that the non-zero intercept is accounted for by the non-black or non-absorbing component in the PM_{10} fraction of airborne particles which normally resides in the coarse particle size range (diameter $\approx$ 1µm). It is hoped that as this study continues a better understanding of the relationship between both parameters will be obtained using seasonal (winter and summer) PM_{10} and black smoke mass concentration data.

The results of the intercomparison between the PM_{10} levels and three meteorological parameters showed that wind speed, air temperature and rainfall are negatively correlated with the PM_{10} levels. Similar negative correlations between wind speed, air temperature and PM_{10} levels for yearly data have been reported in Switzerland (Monn et al.,1995). The negative correlation between temperature and PM_{10} is mainly due to the inverse seasonal behavior of PM_{10} and temperature. During the winter months in Dublin, higher PM_{10} mass concentrations are expected. This is mainly due to increased usage of domestic heating sources and increases in traffic densities during the winter time. A recent study on the correlation between PM_{10} levels and meteorological parameters (air temperature, wind speed, rainfall and solar radiation) in Edinburgh (QUARG, 1996) found that the relationships are seasonal with a negative correlation in winter and a positive correlation in summer. During the winter months, the greater the wind speed the lower the PM_{10} levels due to the effects of dilution and ventilation but in summer the PM_{10} levels tend to increase with wind speed due to resuspension of surface dust. Further data is required in this study to investigate if this seasonal influence holds for the sites in Dublin City. A negative correlation found between rainfall and the PM_{10} levels is probably due to the scavenging effect of rain. The Edinburgh study (QUARG, 1996) again shows that the relationship is seasonal. In winter there is a negative correlation due to the scavenging effect but in summer the correlation is positive due to the rainfall having the potential to resuspend more material when it falls. Again more data is required to see if this seasonal dependence holds for Dublin City.

The comparison between PM_{10} levels and traffic numbers for the College Green site indicates that there is a positive relationship between the car number density and PM_{10} levels. This is consistant with the QUARG, 1996 report which found that in urban air over 80% of primary PM_{10} emissions can be due to vehicular sources.

5. Conclusions

One can conclude that inner Dublin City sites close to heavy traffic routes will exceed present US EPA PM_{10} limits several times throughout the year, based on this 6 month study of PM_{10} measurements over the period from January 1st 1996 to June 30th 1996. Strong covarience was found between PM_{10} mass concentration and car number density (number passing per each ½ hour) at the central Dublin City site at College Green for the period 08:30 to 13:30 - which provides further evidence of the influence of traffic activity on PM_{10} levels. This is also consistent with the report (QUARG, 1993) that approximately 85% of smoke in London is from traffic - one might expect a similar proportion of smoke in central Dublin City. There is also evidence for close tracking of PM_{10} levels with bus number density during the morning period (08:30 - 11:30) but thereafter there is no strong evidence of a close relationship. More repeated measurements of both PM_{10} and traffic number density are required to establish a more definitive linkage between the two parameters.

Acknowledgments

18

References

Air Quality Guidelines for Europe.: 1995, World Health Organisation. Regional Office for Europe. Copenhagen, WHO Regional Publications, European Series No. 23.

BS 1747. 1969, British Standard Methods for the Measurement of Air Pollution, *Part 2. Determination of concentration of suspended matter.* BS 1747, Part 2 1969, 5-16.

Delfino, R. J., Becklake, M. R., Hanley. J. A.: 1994, *Environ. Res.* **67**, 1-19.

Expert Panal on Air Quality Standards (EPAQS).: 1995, *Particles,* Department of the Environment Expert Panal on Air Quality Standards, HMSO, London.

Federal Register.: 1987, *Revisions to the National Ambient Air Quality Standards for Particulate Matter,*40 CFR Part 50, Federal Register 52:24634.

Glikson, M., Rutherford, S., Simpson, RW., Mitchell, CA. and Yago, A.: 1995, *Atmos. Environ.* **29**, 549-562.

Katsouyanni, K., Zmiro, D., Spix, C., Sunjer, J., Schouten, JP and Ponka, A.: 1995 Short-term effects of air pollution on health: a European approach using epidemiological time-series data: The APHEA project. Eur. Respir. J., **8**, 1030-1038.

Monn, CH., Braendli, O., Schaeppi, G., Schindler, CH., Ackermann-Liebrich, U., Leuenberger, PH. and SAPALDIA TEAM.: 1995, *Atmos. Environ.* **29**, 2565-2573.

Muir, D. and Laxen, D. P. H.: 1995, *Atmos. Environ.* **28**, 959-962.

Mark, D. and Hall, D.: 1993, *Clean Air.* **23**, 193-217.

Patashnick, H. and Rupprecht, E. G.: 1991, *J. Air & Waste Management. Assoc.* **41**, 1079-1083.

Ostro, B.: 1993, Arch. Envir. Hlth. **48**, 326-342.

Pope, C. A., Schwartz, J., Ransom, M. R.: 1992, *Arch. Environ. Health.* **47**, 211-217.

QUARG: (1993) First Report of the Quality of Urban Air Review Group. *Urban Air Quality in the U.K.* Prof. R. M. Harrison, Institute of Public and Environmental Health, University of Birmingham, Edgbaston, Birmingham, England. ISBN 0 9520771 24.

QUARG: (1996) Third Report of the Quality of Urban Air Review Group. *Airborne Particulate Matter in the U.K.* Prof. R. M. Harrison, Institute of Public and Environmental Health, University of Birmingham, Edgbaston, Birmingham, England. ISBN 0 9520771 32.

Schwartz, J. and Dockery, D. W.: 1992a, *Am. Rev. Respir.* Dis. **145**, 600-604.

Schwartz, J. and Dockery, D. W.: 1992b, *Amer. J. Epidemiol.* **135**, 12-19.

Schwartz, J.: 1994, *Environ. Res.* **64**, 36-52.

Spix, C., Heinrich, J., Dockery, D. W., Schwartz, J.: 1993, *Environ. Health Perspect.* **101**, 518-526.

A PASSIVE SAMPLER FOR MONITORING URBAN PARTICULATE: PRELIMINARY RESULTS

R C BROWN, A THORPE and M A HEMINGWAY

Health and Safety Laboratory, Broad Lane, Sheffield S3 7HQ, UK

Abstract. A passive sampling device, developed for personal monitoring of airborne dust levels in industry, has been tested as a site sampler in the urban environment. The device weighs approximately 15g and the essential sampling element is a small disc of electret material (polymer carrying a permanent electric charge). During use it captures particles by electrical attraction, at a rate that depends upon their electrical mobility, but which is independent of the rate at which air flows past the sampler. It collects measurable quantities of particulate, though the sample size tends to be small and correlation with results from conventional samples has not yet been established. Samplers have been exposed to urban particulate for periods of up to seven days, without the electret suffering unacceptable loss of electric charge. It has been shown to be potentially useful for long-term monitoring, a situation in which dispensing with a power source is particularly useful. Being small, the passive sampler is easy to hide or camouflage. It has potential for multiple simultaneous site sampling and for monitoring personal environmental exposure.

1.   Introduction

A passive sampler is a sampler that works without the aid of a pump or external power source. The advantages of such a device have long been known in the field of personal sampling of vapours and personal monitoring of ionising radiation. The devices weigh only a few g, whereas the weight of the pump required for active sampling can often be ~ 1 kg.

A passive sampler for use in monitoring personal exposure to industrial aerosols has been developed (Brown et al 1993, 1994, 1995, 1996), but there are no fundamental problems with its use as a site sampler. For example, site samples have been taken in coal mines, the results of which will be reported in due course. The problem of urban particulate is causing concern, and extensive personal and fixed site monitoring is likely to be necessary (Loth and Ashmore, 1994, Fletcher 1984). If the passive sampler could fulfil these requirements even in part, its value would be considerable. A feasibility study into its use as a site sampler has, therefore, been carried out.

2.   Principles of action of the passive sampler

Any sampling device must have a means of transporting the material to be sampled to the collecting surface. Passive vapour samplers work by molecular diffusion. Although particulate matter does execute random motion, the coefficient of diffusion of a spherical particle of diameter

$0.3\mu m$ more than six orders of magnitude lower than that of an oxygen molecule (Davies,1973) and larger particles diffuse even less. The only external forces that are sufficiently strong to ensure effective capture are gravity and electric forces.

Capture by gravitational forces is highly biased towards large particles, and this is certainly not where the principal hazard of particulate lies. For this reason the passive sampler developed by us relies on the use of electric forces. The device, as used for personal sampling in industry, is shown in Fig 1. The sampling surface is a disc of polymer, 25 mm in diameter, placed centrally within the enclosed region. The surface of the polymer is charged, which makes it adhere to the back plate whilst the sampler is held in its normal, vertical, position. The charging is carried out by a simple corona device and the electret may be charged with either polarity. The initial charge held by the polymer is usually sufficient to give a potential of the order of 1500V, but this decays over a period of approximately 48 hours to about 1000V, after which time the charge is stable for a period of weeks or months. A large number of polymers can be used as electrets but polypropylene appears to be the most suitable simple polymer.
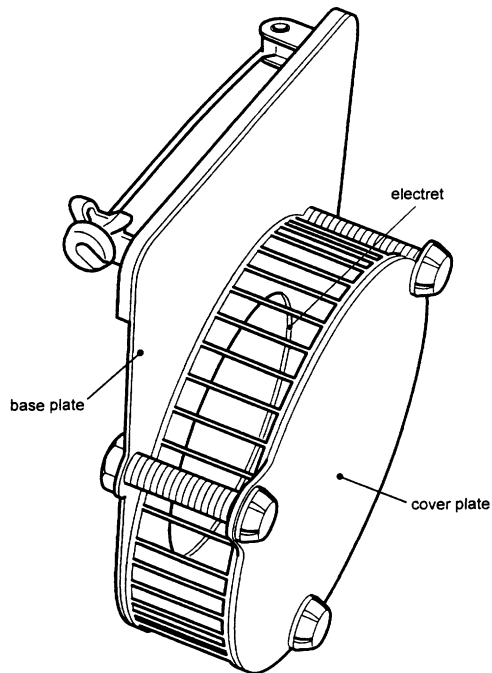
Fig.1. The Electret-based passive dust sampler

All parts of the device except the electret are made from stainless steel, and so their physical contact ensures that they are at a common electric potential. The two parallel conductors in the device are 10 mm apart and so the electric field between them is approximately 10^5 V m^{-1} during use. The grid forming the curved surface of the sampling region allows free ingress of dusty air, but it prevents large objects from making contact with the electret. The electret attracts particles carrying a charge of opposite sign to its surface where they may be monitored. Provided that a low critical air velocity is exceeded the sampling rate of the device does not depend upon the velocity of the air through this region. The reason is simply that if the velocity is doubled, twice as many

dust particles are presented to the electret, but the electric forces have only half the time in which to act. These two effects cancel each other out.

The sample obtained on the electret can be estimated either gravimetrically or by the use of other conventional techniques for analysis of filter samples. The size of the electret has been chosen to match, exactly, the size of conventional sampling filters, so that the electret may be used directly in analytical instruments developed for filters.

In use the passive sampler, which weighs approximately 15 g, has proved very acceptable to wearers. It is also cheap and easy to manufacture. It does, however, have certain drawbacks. The rate at which the device samples particulate is difficult to predict, because it depends on both the size and the electric charge of the dust particles; these usually will not be known in advance. The rate of sampling depends on a particle drift velocity, which follows from the force balance equation of a spherical particle of diameter, d_p, holding n elementary charges of magnitude, e, travelling at its terminal velocity, U, in an electric field of magnitude, E, such that the electric forces and the viscous drag balance

$$neE = 3\pi\eta d_p U \qquad (1)$$

The quotient of the drift velocity, U, and the electric field is termed the electrical mobility of the particle. Most particles are not spherical, and it is difficult to write down an exact equation describing their motion; nevertheless, the electrical mobility can be defined simply as the quotient implicit in equation 1. In order, therefore, to obtain absolute measurements of dust concentration with the device, it is necessary either to measure the electrical mobility of the aerosol by some other means or to obtain a calibration factor from the measurements made with the passive sampler and those made with conventional samplers. This is a difficult problem but attempts to solve it have been made in previous publications (Brown et al 1995,1996).

A second problem is the small sample size. Typically, it is approximately an order of magnitude smaller than the sample obtained with a pumped sampler during the same period of use. If these samples are to be estimated gravimetrically, and this is the simplest method of analysis, a six figure balance is required. With such apparatus, reasonable estimates of masses of 30 µg or more can be obtained.

A third problem is charge stability. If these samplers are held in closed containers charge loss is negligible over a period of months. When, however, they are used in industry, substantial charge loss may occur. For example, in foundries charge losses of 80% may occur over a period of hours. As charge is lost, the sampling rate is reduced, and this will introduce error unless a correction is made. Within the level of accuracy that can be obtained with the device, a reasonable correction based on a linear or exponential loss of charge can be applied to the data, provided that 50% of the charge remains at the end of the sampling period. If significantly more charge than this is lost, one cannot have confidence in the results. The reason for the charge loss is not known for certain, but it is

certainly not caused by the deposition of the aerosol, since there is no correlation between charge loss and aerosol deposit (Brown et al, 1996). It is believed to be caused by the presence of atmospheric ions, since it appears to be more serious in aggressive atmospheres.

3. Modification of passive and pumped samplers for urban particulate monitoring

In order to find out the potential usefulness of the device in the urban environment, it is necessary first to take account of the special problems that sampling here will pose. The concentration of urban particulate is normally lower than that encountered in industry. For this reason effective sampling must be carried out over a particularly long period if a weighable sample is to be obtained. A convincing assessment requires that the passive sampler be used alongside a pumped sampler. A standard battery is capable of running a pumped sampler for a period of only a few hours. In order to run a pumped sampler for a period of 7 days batteries of considerably larger capacity or a mains supply are required.

The second potential problem, that of uncertainty of charge on the aerosol, may be less severe for atmospheric aerosols than for industrials. It is likely that atmospheric aerosol has been aged for a longer period of time than industrial aerosol. As aerosols become aged their charge distribution tends towards that characteristic of thermodynamic equilibrium, in which the mean electrostatic energy of a particle is equal to its mean thermal energy (Bricard and Pradel, 1966). In this situation the mean electric charge, $\bar{n}$, on a particle of diameter d_p (μm) is given by

$$\bar{n} = 2.36 d_p^{\frac{1}{2}} \qquad (3)$$

except in the case of extremely small particles. In this situation it may be possible to give a reasonable estimate of the electrical mobility of a particle, provided that its size is known.

The third potential problem, that of the neutralisation of charge by atmospheric ions, cannot be predicted. It can only be judged from the results of experiments.

4. Experimental method

The exercise was carried out in the winter of 1995/6. A total of five sites were chosen for the comparison tests, all within Sheffield. Two sets of samplers were mounted in a large underground car park in the centre of the city. This had a lot of square ducting situated close to the ceiling, which was inaccessible except by ladder. There was, however, sufficient room between the ducting and the ceiling for both the pumped samplers and the passive samplers, in a vertical orientation.

A second site for the test was in front of a second storey window of a large office block alongside an urban dual carriageway. The sampler was placed at the height of a foot bridge that crosses the road. The third site was on the roof of the same building. The fourth site was on the roof of the HSL Laboratory, and the fifth site was in the underground car park of the same building. In instances where the samplers were used out of doors, it was necessary to protect them from the elements. They were therefore enclosed in meteorological boxes which contain louvred sides to allow free access of air but which prevent rain or snow from entering; it did in fact snow during the exercise.

Electret samplers containing 25 mm diameter electrets, were initially exposed for a period of two or three days so that some indication of the stability on the electrets could be obtained. The charge on the electrets proved so stable that exposures of up to 14 days were carried out.

It became apparent during the exercise that considerable care had to be used in siting the pumped samplers, because they were large and clearly visible. It was important that these devices should not be tampered with or stolen, because they have a value of approximately £500. The passive samplers were easy to hide and have a nominal value of only a few pounds, which is clearly a great practical advantage in their use.

5.   Results and discussion

The electrets were weighed and their mean surface potential was measured both before and after the exercise. These results are shown in Table 1 and Fig 2. The first and most important conclusion to be drawn is that estimable samples of urban particulate were obtained during this exercise but that sample sizes were small. Samples smaller than $30 \mu g$ are subject to a large amount of experimental error, and so should be regarded as semi- quantitative. Nevertheless, it is clearly established that the device may be used to sample urban particulate.

TABLE 1
Data obtained over a seven day period with single-electret passive samplers

Sampler Number	Mass gain (μg)	% voltage loss	Normalised Particulate concentration (mg m^{-3})	Particulate concentration measured with gravimetric sampler (mg m^{-3})
1	12	18.6	0.35	0.028
2	13	36.6	0.22	0.037
3	12	29.4	0.14	0.034
4	5	16.2	0.19	0.039
5	28	9.7	0.30	0.077
6	15	19.4	0.12	0.066
7	10	59.6	0.38	0.037
8	18	31.9	0.23	0.056
9	50	51.5	0.50	0.051
10	21	61.2	0.31	0.043

Secondly, the electrets were sufficiently stable over the period of measurement for quantitative measurements to be made. From the point of view of charge loss urban environmental conditions are not aggressive.

In order to normalise the results obtained with the passive sampler it is necessary to know the value of the mean electrical mobility of the urban aerosol. A value of 4×10^{-9} $m^2V^{-1}s^{-1}$ is assumed, which is a typical mean electrical mobility of a spherical submicrometre particle carrying an equilibrium charge. There is considerable random error, but it is clear that assumption of this level of charge results in a considerable overestimate of the particulate concentration, behaviour similar to that observed previously (Brown et al, 1995).

A second sampling exercise was carried out, with deliberate attempts to increase the sample size. Two electrets were charged to opposite polarity and placed on the opposite faces of the sampler. This doubles the electric field and, since particles of both polarity are captured, it also potentially doubles the sample size, under the reasonable assumption that positively and negatively charged particles are equally numerous. The sample is, therefore, increased by a factor of four. A further improvement can be carried out by reducing the spacing between the plates of the sampler. One style of separating grid contains two wefts and so can easily be cut down to thicknesses of approximately 7.1 mm and approximately 4 mm. In this way two additional models of sampler can be produced, in one of which the electric field is increased by approximately a factor of 1.5 and in the other by a factor of 3. The possible disadvantages are that restricting the space between the plates may also restrict the airflow causing a reduction in sampling, though this effect is least noticeable when the charge on the aerosol is low.

The results obtained in this part of the exercise is shown in Table II and Fig 2. Reducing the spacing of the conductors to 7.1 mm gives increased sample size, but reduction to 4 mm results in poor sampling. In other situations, such as the sampling of a highly charged industrial aerosol, using two electrets and reducing the spacing would result in poorer sampling.

TABLE II
Data obtained over a fourteen day period with double electret passive samplers

Sampler Number	Spacing (mm)	Mass gain (µg)		%Voltage loss		Particulate concentration (mg m^{-3})	
		Top	Bottom	Top	Bottom	Passive Sampler	Pumped Sampler
11	7	48	29	9 3	10.6	0 12	0.093
12	7	46	23	25.9	13.3	0.12	0.103
13	7	86	94	4.9	28.7	0.33	0.107
14	7	67	55	7.6	13.2	0.18	0.093
15	4	-13	5	5.9	14.1	-	-
16	4	-14	12	10.9	19 2	-	-
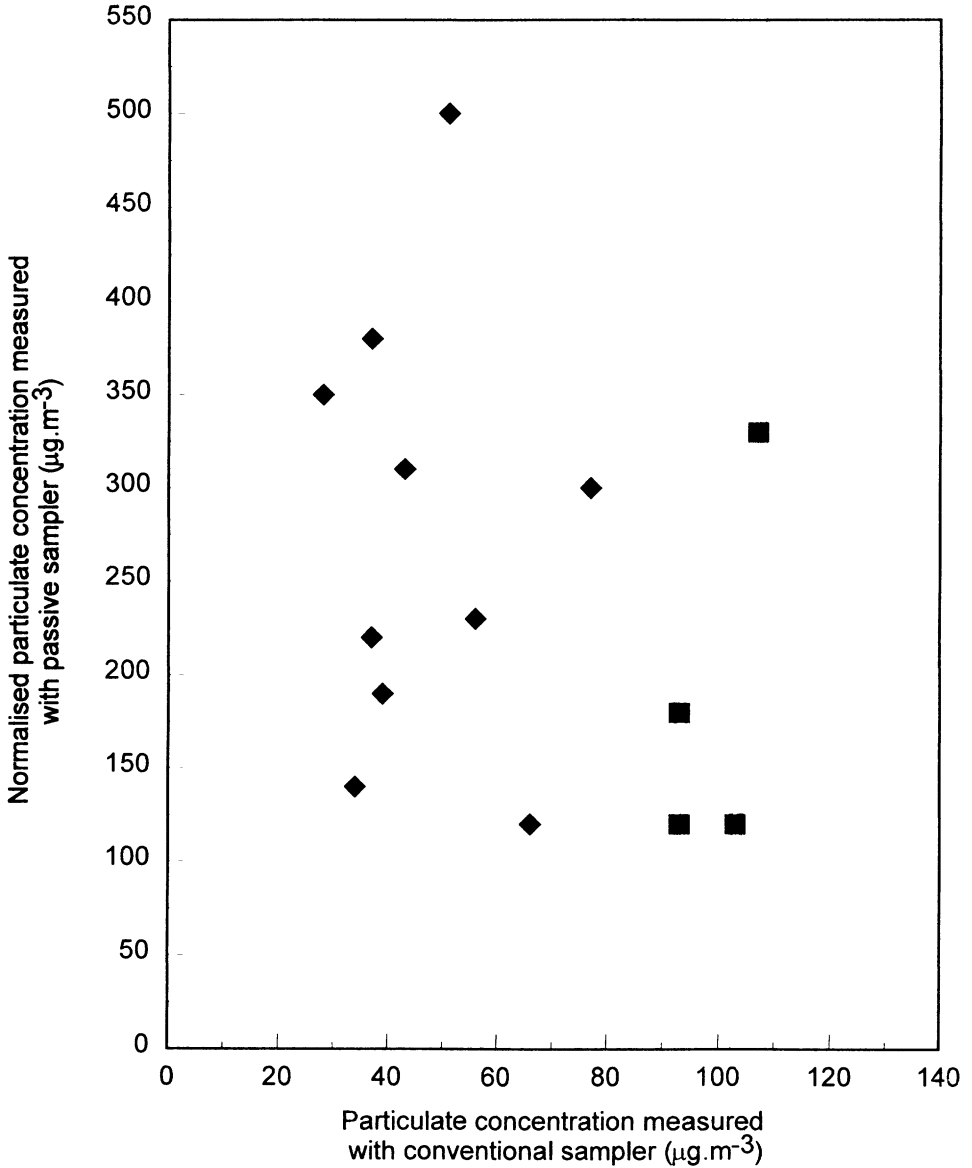
Fig.2 Mass concentrations of urban particulate measured by the passive sampler and by a conventional pumped sampler. ■ - single electret samples, 10 mm spacing; ◆ - double-electret sampler, 7 mm spacing.

26

Negatively charged
electret
(base of sampler)

Positively charged
electret
(base of sampler)

Weight of particulate
collected = 67 µg
Sampling period = 2 weeks

Weight of particulate
collected = 74 µg
Sampling period = 2 weeks

31 mm
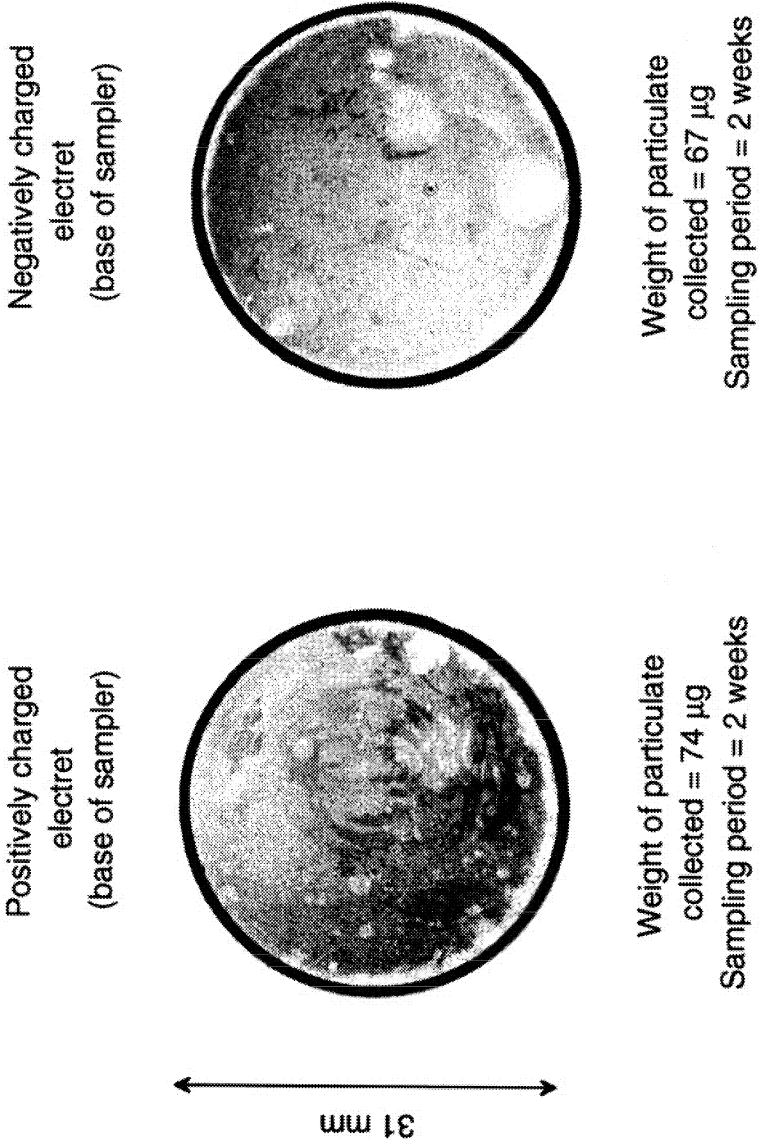
Fig.3. Deposit of urban particulate on the electrets of a passive sampler.

The concentration of aerosol calculated from these results agrees more closely with the gravimetric results, whereas a simple model of aerosol behaviour in electric fields predicts that both should agree equally well. The reason for this is not known. The sample sizes are much larger, but it is not possible to establish correlation on account of the small number of results obtained; further work is necessary.

An example of the deposit, from sampler 14, is shown in Fig 3 where the slightly irregular deposit and the clear circumferential ring indicate the electrostatic nature of the collection mechanism.

The samplers used in the second exercise were exposed for approximately twice as long as those used in the first, but the loss of charge is smaller. This may indicate less efficient capture of ions, and it is certainly an advantage from a practical point of view.

6.   Conclusions

The potential usefulness of a simple electret-based passive sampler in the sampling of urban particulate has been demonstrated. It collects weighable samples and is able to sample over periods of up to about two weeks. It is particularly useful in its two-electret form. Gravimetric analysis is a precision job requiring a six-figure balance, but it is possible that sampling methods involving light scattering, a much easier technique, could be put into effect. The small size of the sampler and its inexpensive manufacture mean that theft or tampering can be avoided, and are not serious if they take place. Moreover, it has potential for multiple simultaneous sampling. Its possible use as a personal sampler in the environments is also, by analogy, demonstrated. The samplers still function when the spacing between the parallel plates is reduced to 7.1 mm, but if the distance is reduced to 4 mm the sampling rate drops drastically, almost certainly as a result of restricted airflow. As stated above, it was assumed that because atmospheric aerosol is aged its charge would have a low and stable level. The results obtained, however, do not support this. There is, at the moment, no clear indication of a simple relationship between samples obtained by the two methods.

Future work will be directed at establishing numerical correlation between passive samples and samples taken by conventional means, and the latter will include estimates of PM_{10} and $PM_{2.5}$. A protocol for the use of the sampler will be developed, and simple analysis techniques will be investigated.

28

References

Bricard, J. and Pradel, J.: 1966, *Aerosol Science*, edited C N Davies, Academic Press, London.

Brown, R. C., Wake, D., Thorpe, A., Hemingway, M. A. and Roff, M. W.: 1993, *J. Aerosol Sci.* **25**, 149-163.

Brown, R. C., Wake, D., Thorpe, A., Hemingway, M. A. and Roff, M. W.: 1994, *Ann. Occup. Hyg.* **38**, 303-318.

Brown, R. C., Hemingway, M. A., Wake, D. and Thompson, J.: 1995, *Ann. Occup. Hyg.* **39**, 603-622.

Brown, R. C., Hemingway, M. A., Wake, D. and Thorpe, A.: 1996, *The Analyst*, **121**, 1241-1246.

Davies, C. N.: 1973, *Air Filtration*, Academic press, London

Loth, K. and Ashmore, M.: 1994, *Clean Air* **24**, 113.

Fletcher, R. A .: 1984, *J. of the Air Pollution Control Assoc.* **34**, 1014-1016.

PM₁₀ PARTICULATES IN RELATION TO OTHER ATMOSPHERIC POLLUTANTS

D. MUIR

*Environmental Quality Section, Directorate of Health & Environmental Services,
Bristol City Council, The Create Centre, B Bond, Smeaton Road, BRISTOL, BS1 6XN.*

Abstract. Concentrations of PM$_{10}$ particulates have been compared to the concentrations of oxides of nitrogen and sulphur dioxide at the fourteen Automatic Urban Monitoring Network (AUN) sites operating during 1993, 1994 and 1995 using fully ratified data.
Factors which are considered include diurnal variations in concentrations of the various substances, ratios between concentrations of PM$_{10}$ and the other substances and differences between relationships in summer and winter and between weekdays and weekends. In addition temporal patterns of concentrations are considered. Variations between different cities is demonstrated. Differences in the seasonal size distribution are identified. It is shown that there is a good degree of consistency in concentrations of PM$_{10}$ across urban areas at background locations and that there is evidence for long range transport of PM$_{10}$.

1. Introduction

Particulate matter with an aerodynamic diameter less than 10 μm (PM$_{10}$) has attracted an increasing amount of interest in recent years. There is a growing body of evidence to link fine particles as contributing to range of health effects including the Six Cities Study carried out in the United States by Harvard University (Dockery et. al 1993, Pope et. al 1996, Ostro 1993). The Six Cities Study showed a near linear relationship between concentrations of PM$_{10}$ and mortality. Far less work has been carried out in the United Kingdom in relation to PM$_{10}$, in part because systematic monitoring of PM$_{10}$ in the UK only commenced in 1992 (QUARG 1996). By 1995 data were available for fourteen sites where PM$_{10}$ is monitored with carbon monoxide, oxides of nitrogen, sulphur dioxide and ozone. The data examined here extend back to January 1993 for nine sites and to January 1994 for the other sites in the UK Automated Urban Network (AUN). This network was originally established as the Enhanced Urban Network (EUN) in 1992 with sites in London Bloomsbury, Birmingham Centre, Cardiff, Belfast, Edinburgh and Newcastle. Sites were added in 1993 in Bristol, Leeds and Liverpool and a local authority site at Birmingham East was affiliated into the network. Further sites were added in 1994 in Hull, Leicester and Southampton and a further local authority site in Swansea was affiliated. At all these sites the pollutants measured are nitrogen oxide (NO), nitrogen dioxide (NO$_2$), total oxides of nitrogen (NO$_x$), sulphur dioxide (SO$_2$), carbon monoxide (CO), sulphur dioxide (SO$_2$), ozone (O$_3$) and particulate matter (PM$_{10}$) (Bower et al 1995, Bower et al 1996). Data from these sites are subjected to a rigorous ratification process at the National Environmental Technology Centre (NETCEN). Until October 1995 the gas analysers were calibrated on a weekly basis using gases which

could be traced to a national standard. From October 1995 the period between calibrations was extended to two weeks. In addition to this each gas analyser is automatically zeroed and span gas run through on a daily basis to enable excessive drift to be detected and rectified. All the instrumentation is audited on a regular basis by NETCEN using travel standards and a reference photometer for ozone to ensure consistency across the network. The Tapered Element Oscillating Microbalance (TEOM) used to measure particulate matter is audited using a set of standard filters.

This study aims to examine variations in the relationship between the concentrations of the various pollutants monitored in the network to attempt to establish common sources. It also aims to examine the spatial variations in PM_{10} concentrations across urban areas and to illustrate seasonal differences between the contribution of the $PM_{2.5}$ fraction to PM_{10} concentrations.

2 Methods

Hourly average diurnal ratios between concentrations of PM_{10} and the other pollutants were calculated for fourteen sites in the network for all data available between January 1993 and December 1995. These averages were calculated for individual days in the week, for weekdays and for weekend days. The analysis of these data also considered the differences between winter and summer with the seasons being arbitrarily defined as 1st October to 31st March and 1st April to 30th September respectively. This analysis provides the baseline for comparison of ratios of concentrations of PM_{10} to other pollutants during episode conditions and provides a means of comparing these ratios between the different cities. The locations of these sites and their commissioning dates are given in Table I.

Table I
Site names and commissioning dates.

Site name	Date	Site name	Date
Belfast Centre	8/3/92	Leeds Centre	4/1/93
Birmingham Centre	18/3/92	Leicester Centre	4/1/94
Birmingham East	1/12/93	Liverpool Centre	25/3/93
Bristol Centre	4/1/93	London Bexley	1/5/94
Cardiff Centre	12/5/92	London Bloomsbury	23/1/92
Edinburgh Centre	4/10/92	Newcastle Centre	8/3/92
Hull Centre	4/1/94	Southampton Centre	4/1/94

Spatial variations in concentrations of PM_{10} were initially examined by making time series plots of daily average data for three sites in Bristol, two operated by National

Power in the Avonmouth area to the North West of the city and the AUN site in the central Broadmead shopping area. This procedure was then repeated using hourly average data from several of the other AUN sites. This was first carried out for the two Birmingham sites and then for the Birmingham sites and the Leicester site, the Bristol and Cardiff sites and for the Hull and Leeds sites. 'data from Birmingham City Council's Hodge Hill site was used to examine the proportion of $PM_{2.5}$ in PM_{10}.

3 Discussion

3.1 RATIOS OF PM_{10} TO OTHER POLLUTANTS

The annual average ratio of concentrations of PM_{10} to nitrogen dioxide are listed in Table II with the site average PM_{10} concentrations.

Table II

Ratios of average PM_{10} concentrations to nitrogen dioxide concentrations

SITE	ANNUAL AVERAGE CONCENTRATION N ($\mu g/m^3$)	ANNUAL AVERAGE PM_{10}:NO_2 RATIO	SUMMER AVERAGE PM_{10}:NO_2 RATIO	WINTER AVERAGE PM_{10}:NO_2 RATIO
BELFAST	28.3	1.59	1.61	1.54
BEXLEY	24.3	1.38	1.50	1.23
BIRMINGHAM CENTRE	23.9	1.21	1.29	1.15
BIRMINGHAM EAST	21.3	1.28	1.43	1.14
BRISTOL	24.8	1.24	1.23	1.29
CARDIFF	29.3	1.64	1.84	1.49
EDINBURGH	20.8	0.89	0.88	0.90
HULL	25.1	1.25	1.37	1.13
LEEDS	26.2	1.01	1.13	0.89
LEICESTER	20.7	1.06	1.21	0.91
LIVERPOOL	25.9	1.32	1.41	1.29
BLOOMSBURY	28.0	0.81	0.86	0.78
NEWCASTLE	25.5	1.30	1.30	1.29
SOUTHAMPTON	22.6	1.14	1.17	1.15
NETWORK AVERAGE	24.8	1.22	1.30	1.16

It is immediately clear that there are marked variations in the absolute numerical values of these ratios. Figure 1 illustrates the diurnal average ratios for two sites where the
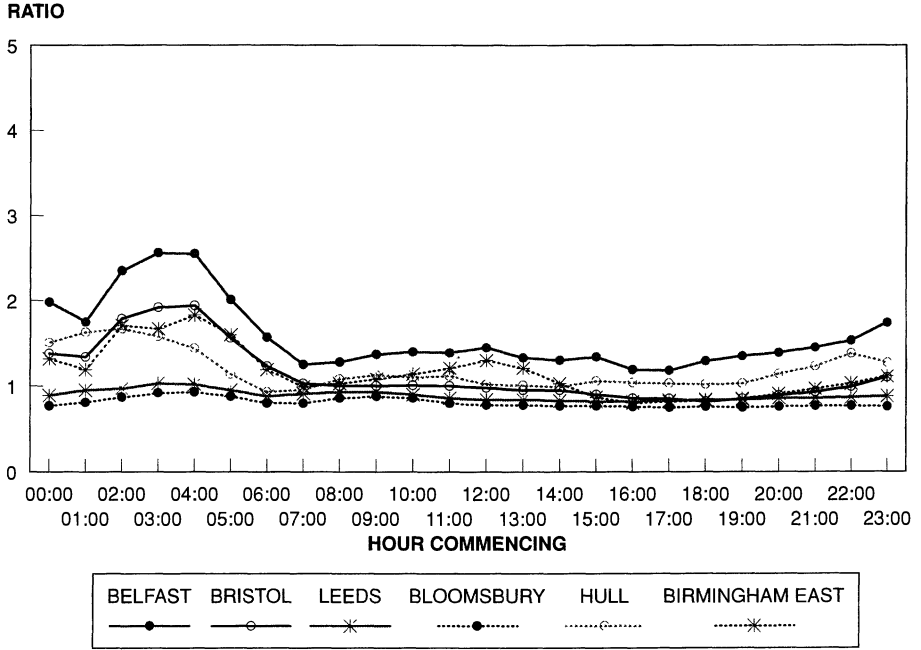
RATIO

Fig. 1 Diurnal average PM$_{10}$: NO$_2$ ratios 1993 - 1995

µg/m³
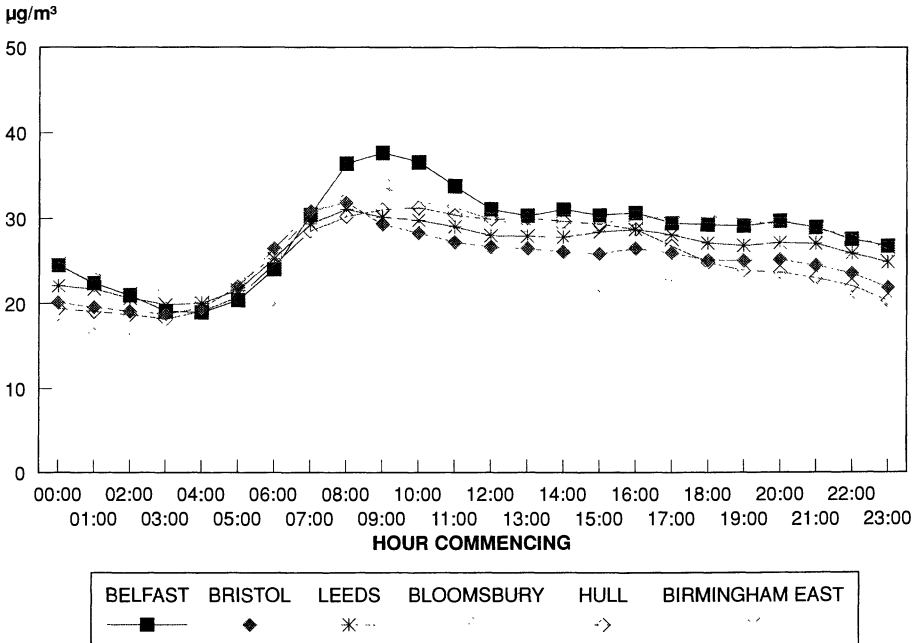
Fig. 2 Diurnal average PM$_{10}$ concentrations 1993 - 1995

average ratio is significantly lower than the network average, two where it is significantly higher and two where the average is almost equal to the network average. From this it is evident that the greatest differences between the three pairings is during the nocturnal hours. Four of the six sites considered here show higher concentrations of PM_{10} relative to NO_2 or conversely lower concentrations of NO_2 relative to PM_{10}. In fact the latter is the case as, in general, diurnal concentrations of PM_{10} are similar at all sites as is illustrated in Figure 2.

The comparable ratios for PM_{10} and sulphur dioxide are given in Table III.

Table III

Ratios of average PM_{10} concentrations to sulphur dioxide concentrations

SITE	ANNUAL AVERAGE PM_{10}:SO_2 RATIO	SUMMER AVERAGE PM_{10}:SO_2 RATIO	WINTER AVERAGE PM_{10}:SO_2 RATIO
BELFAST	2.83	3.50	2.13
BEXLEY	5.53	5.50	5.57
BIRMINGHAM CENTRE	4.75	5.28	4.16
BIRMINGHAM EAST	6.23	6.67	5.81
BRISTOL	5.43	5.27	5.60
CARDIFF	8.61	9.43	7.79
EDINBURGH	4.35	5.19	3.48
HULL	4.77	5.29	4.23
LEEDS	5.06	6.28	3.99
LEICESTER	5.44	6.51	4.35
LIVERPOOL	5.30	6.65	3.89
BLOOMSBURY	4.47	5.04	3.88
NEWCASTLE	6.50	6.83	6.21
SOUTHAMPTON	7.15	8.19	6.31
NETWORK AVERAGE	5.46	6.12	4.81

There are some marked divergences from the averages here, mainly in Belfast and Cardiff. There are well defined reasons for this. In Belfast there is little if any use of gas for heating purposes. Rather coal and smokeless fuel and to a lesser extent oil, both containing sulphur mean that average sulphur dioxide concentration is double that for the remainder of the network (QUARG 1993, Bower et al 1996). In Cardiff the ratio is much higher as a result of higher than average PM_{10} concentrations in 1994 due to construction works (QUARG 1996, Bower et al 1995). This also affected the PM_{10}:NO_2 ratio but not to the same extent. Diurnal ratios are illustrated in Figure 3.

34

3.2 SPATIAL VARIATIONS OF PM_{10}

Examination of daily average concentrations for three sites in the Bristol area for 1994 showed that there was a good degree of agreement between the three sites and, perhaps more significant, the rises and falls in daily average concentrations at the three sites matched well. That this match was not perfect can almost certainly be attributed to local factors such as construction activities. Examples for June and November 1994 are shown in Figure 4. Two of these sites (Avonmouth and Shirehampton) are about 1.5 miles apart and about 7 miles from the Bristol Centre AUN site.
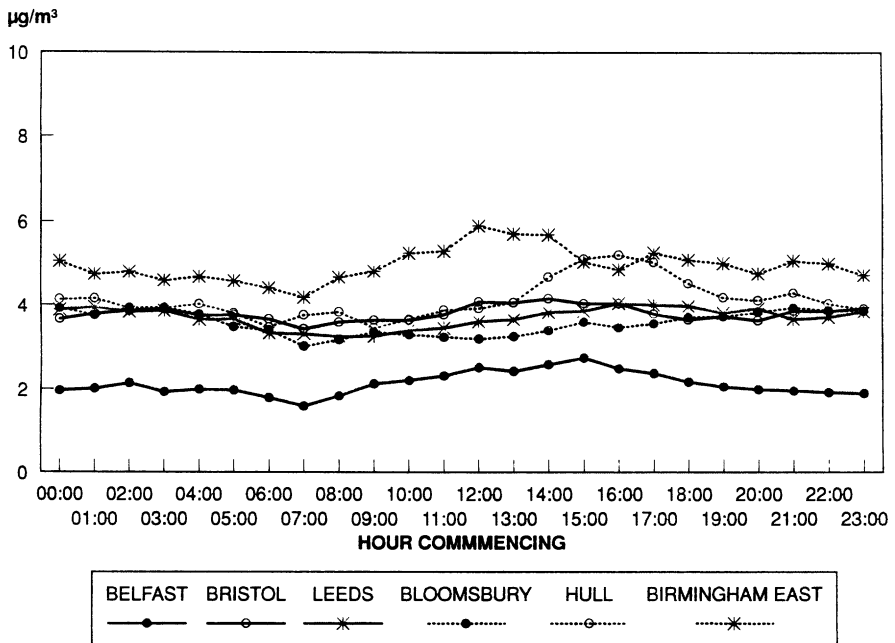
Fig. 3 Diurnal average PM_{10} : SO_2 ratios 1993 - 1995

This analysis has now been repeated for hourly average concentrations at a number of AUN sites. The two Birmingham sites demonstrate a particularly good degree of agreement but there is also good general agreement between the Birmingham sites and the Leicester site and between the Bristol and Cardiff sites. This suggests that even over a distance of 30 to 40 miles conditions for the generation of particulate matter can result in similar concentrations at locations selected under consistent criteria in different cities. When this was repeated for Bristol and Hull, two cities about 200 miles apart, there was still a large number of occasions on which the hourly average concentrations were comparable and when concentrations rose and fell at the same times. This leads to the possibility that a substantial proportion of the PM_{10} being measured in the UK may be the consequence of long range transport, possibly from continental Europe (King & Dorling, 1997). This analysis is illustrated in Figure 5.

3.3 PM_{10} AND BLACK SMOKE

Daily PM_{10} data from the Bristol AUN site has already been compared with Black Smoke data from six urban background sites in Bristol (Muir & Laxen, 1995). This study has now been extended by colocating an automatic 8-port sampler with in the AUN site. The results from this comparison for summer and winter are shown in Figure 6. There is a considerable degree of scatter in these results, some of which may be due to partial exposure of the Black Smoke filters as a consequence of tubes becoming detached or to the relatively small amount of data available, but there is still a difference between the slopes of the estimated best fit lines as is shown in Figure 6.

3.4 PM_{10} AND $PM_{2.5}$

The difference in the slopes of the best fit lines between summer and winter and the fact that there is a positive Y-axis intercept in these plots, features which have been observed in other studies (QUARG 1996), may be attributed to there being a greater proportion of light coloured material present in the particulate matter collected in the summer. The Black Smoke samplers have a nominal cut-off at 4μm so it is reasonable to assume that Black Smoke concentrations will usually be lower than PM_{10} concentrations. The availability of data from colocated PM_{10} and $PM_{2.5}$ monitors at Birmingham City Council's Hodge Hill site makes it possible to compare the contribution of the finer fraction to the total PM_{10} in real time. This comparison again shows a marked difference between summer and winter with a far higher proportion of the PM_{10} being $PM_{2.5}$ in the winter than in the summer. This is illustrated in Figure 7 for a week in each of the months of February and July 1995.

The percentages of PM_{10} which are $PM_{2.5}$ are illustrated for each month in 1995 in Figure 8.

This clear seasonal difference suggests that the particles between 2.5μm and 10μm may be lighter in colour, possibly as a result of their source. It is quite possible that in the summer months there is a greater proportion of particulate arising from entrainment of material by wind and such matter is likely to be less dark than, for example, diesel soot. This may also account in part for differences between summer and winter diurnal patterns for PM_{10} illustrated in Figure 9.

a

PM10 (µg/m³)

b

PM10 (µg/m³)
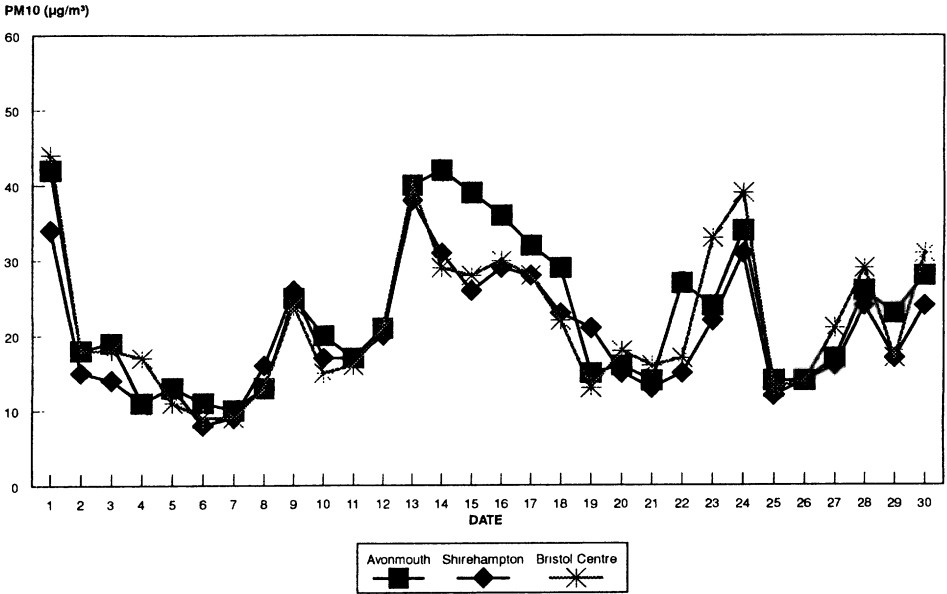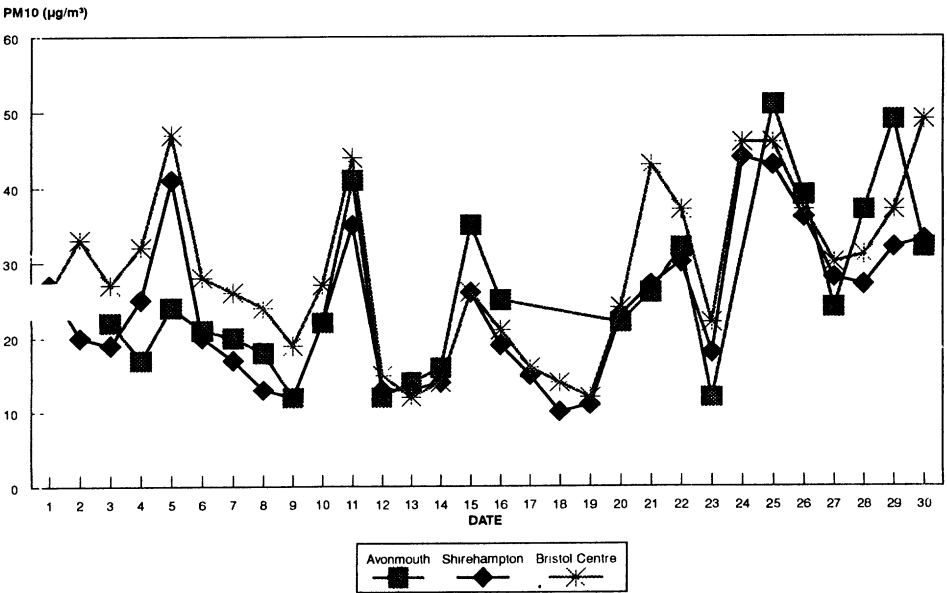
Fig. 4 PM$_{10}$ concentrations at three sites in Bristol 1994 (a = June, b = November)

a

b

c

d
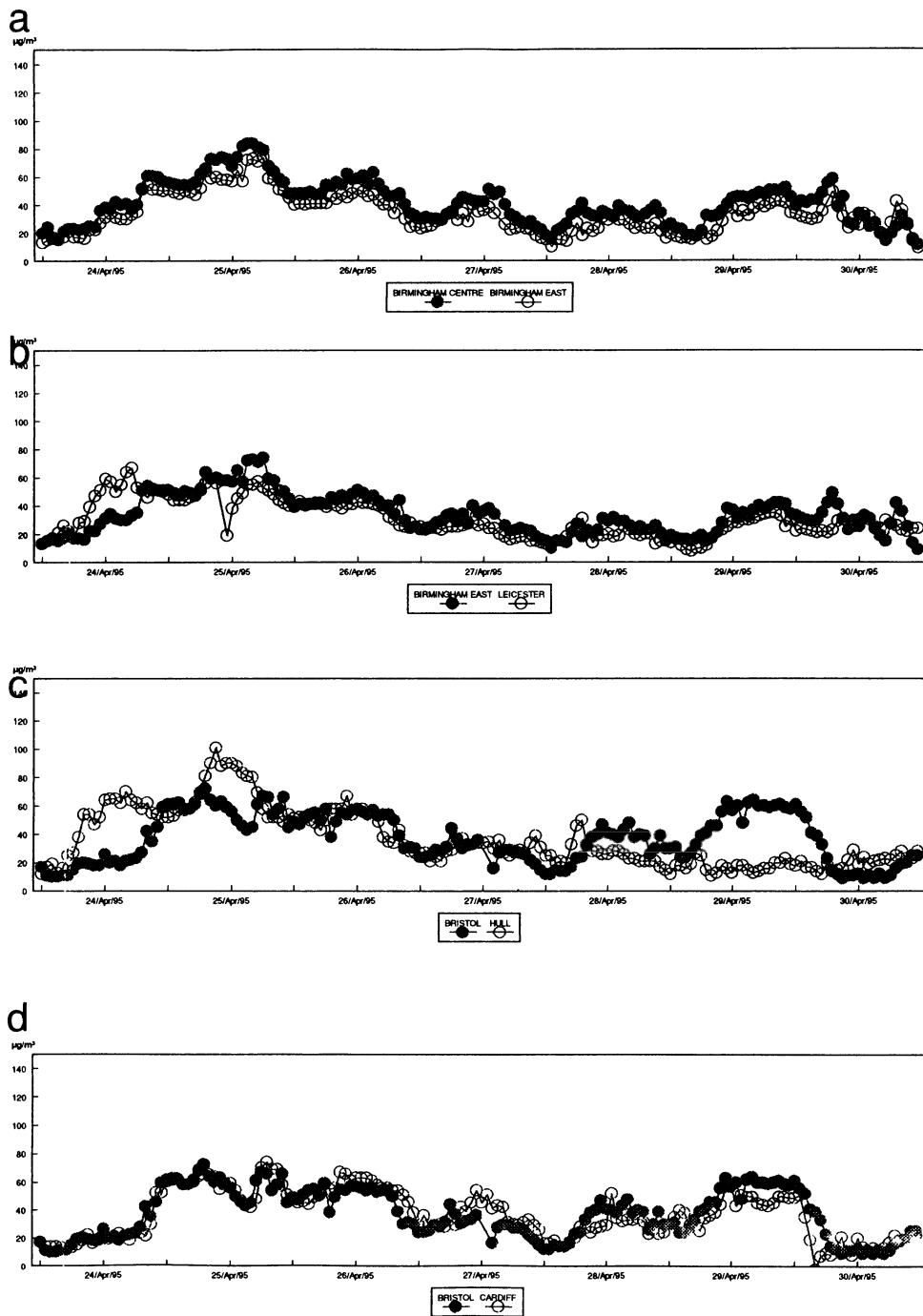
Fig. 5 Spatial variations in PM_{10} concentrations

a
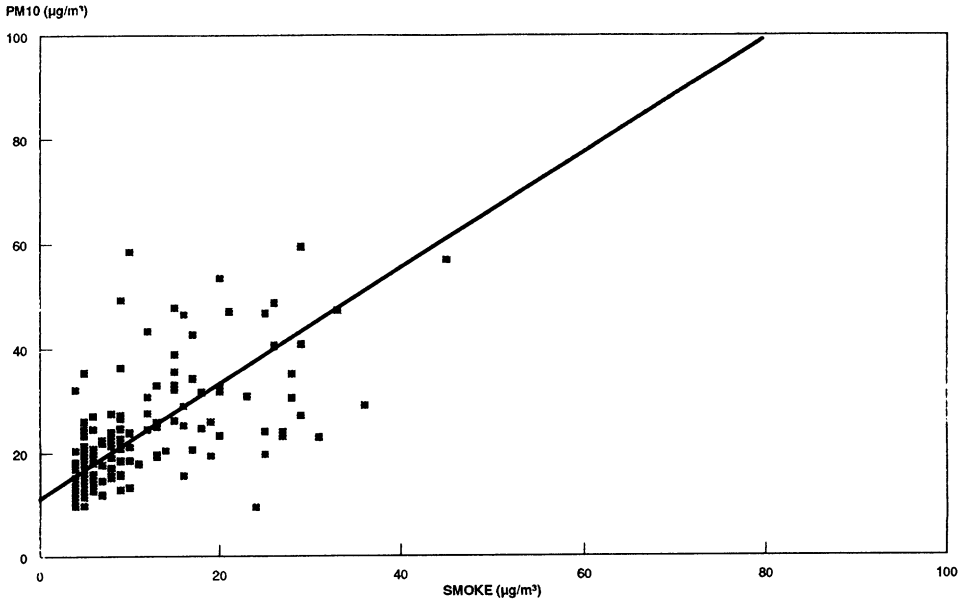
b
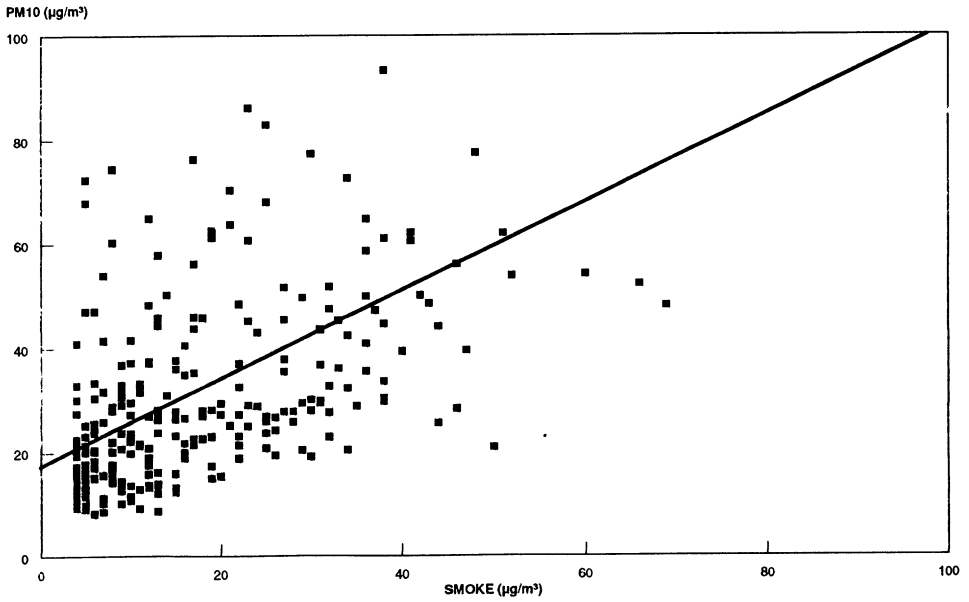
Fig. 6 PM$_{10}$ vs. Black Smoke Bristol AUN (a = Summer, b = Winter)

a

CONCENTRATION (µg/m³)

b
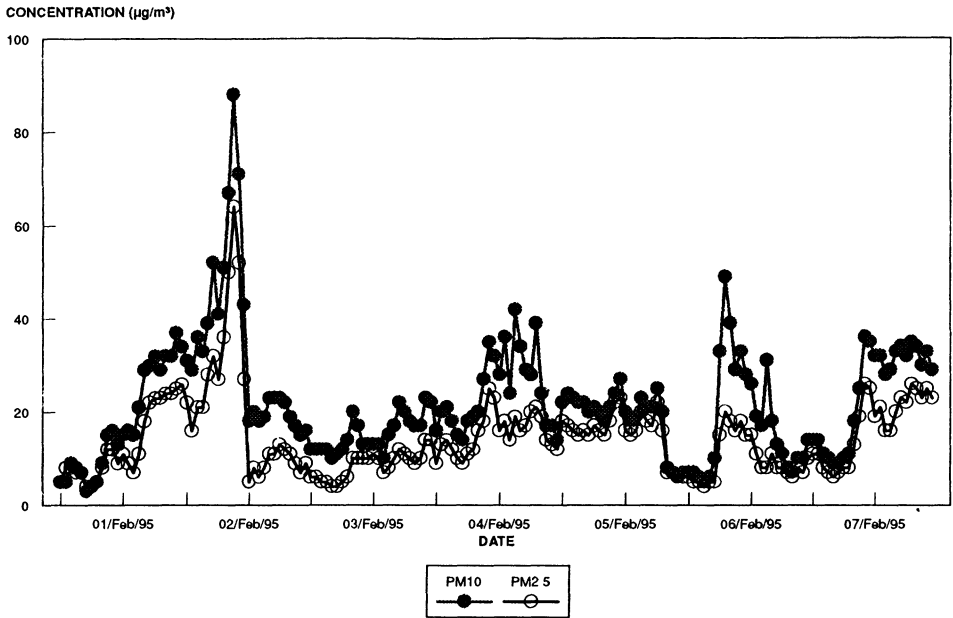
CONCENTRATION (µg/m³)
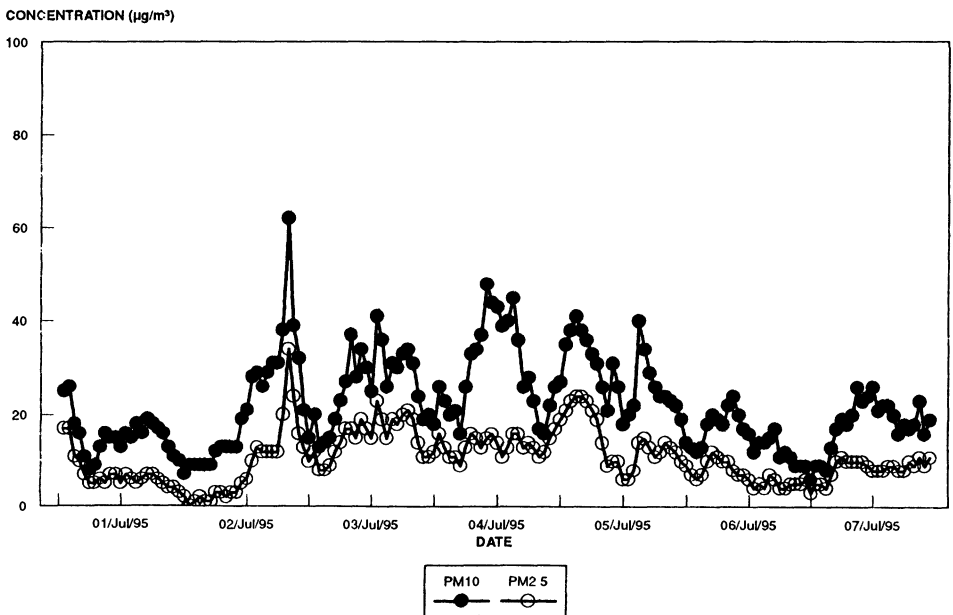
Fig. 7 PM_{10} and $PM_{2.5}$ concentrations Birmingham Hodge Hill (a = February 1995, b = July 1995) ˙
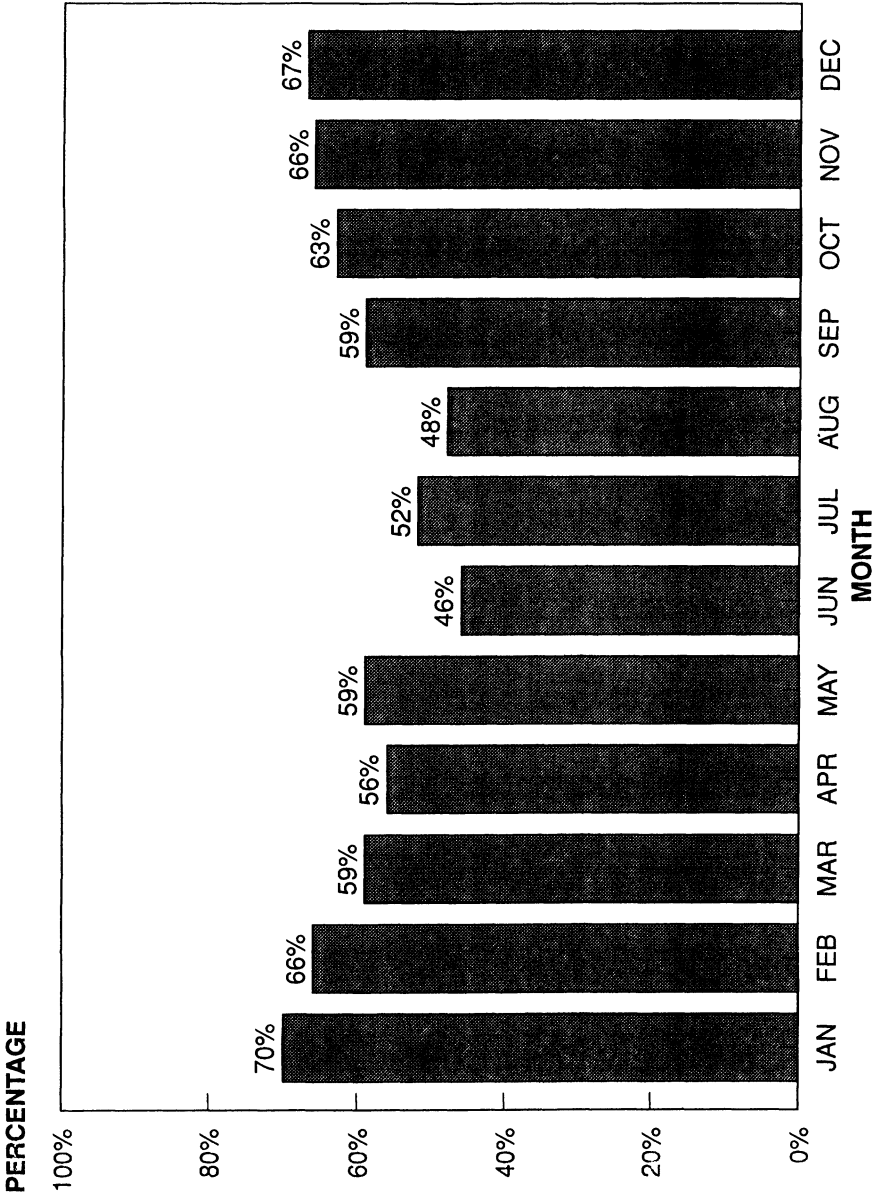
Fig. 8 $PM_{2.5}$ as a percentage of PM_{10} at Birmingham Hodge Hill

a
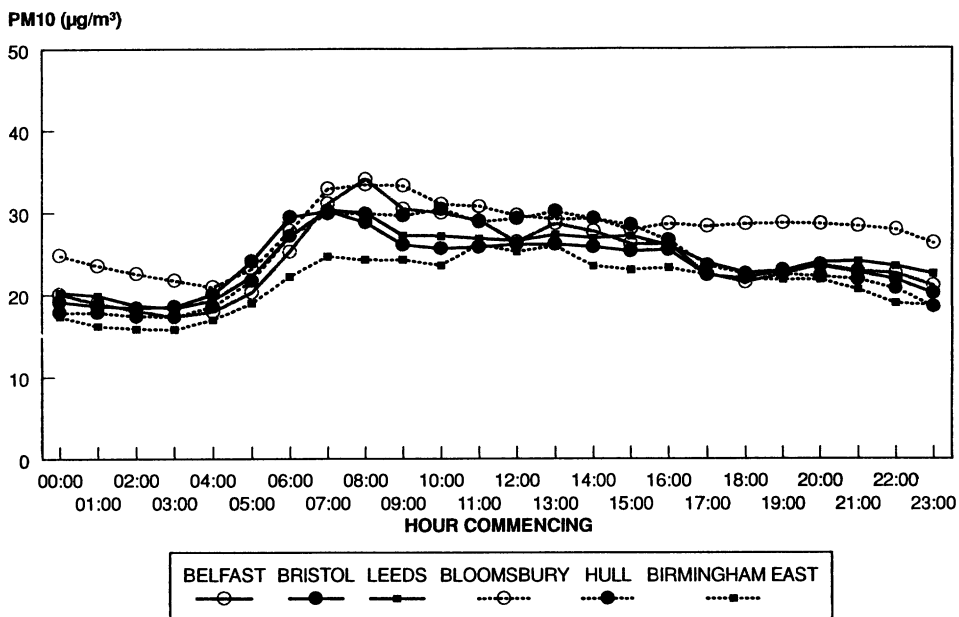
b
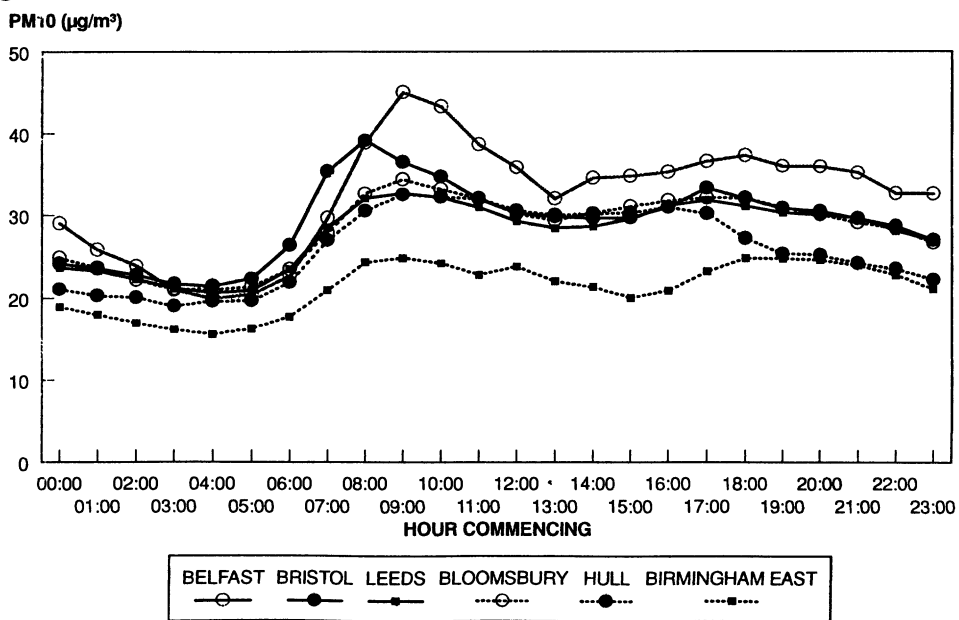
Fig. 9 Diurnal PM$_{10}$ concentrations 1993 - 1995 (a = Summer, b = Winter)

4 Conclusions

There are considerable differences in the ratios of PM_{10} to other pollutants between different cities and the diurnal patterns of these ratios show some variation from city to city. Some of these differences may be explained by readily observed factors such as the higher overall concentrations of sulphur dioxide in Belfast but others require more study. There appears to be a reasonable degree of consistency between PM_{10} concentrations across urban areas at background locations. It has been suggested that some of this similarity may be the consequence of long range transport of PM_{10} but this hypothesis needs to be more fully examined.

There appears to be some relationship between PM_{10} and Black Smoke but this is not strong and a larger data set is needed to make the analysis of any such relationship valid. The proportion of fine particles in PM_{10} changes on a seasonal basis and this may account for the difference in slope in the PM_{10}:Black Smoke scatter plots and, possibly, for the different summer and winter diurnal patterns for PM_{10}.

Acknowledgements

References

Bower J S, Broughton G F J, Willis P G and Clark H, Air Pollution in the UK : 1994, AEA Technology, National Environmental Technology Centre, Culham (1995).

Bower J S, Broughton G F J, Willis P G and Clark H, Air Pollution in the UK : 1995, AEA Technology, National Environmental Technology Centre, Culham (1996).

Dockery D. W., Pope III C. A., Xu X., Spengler J. D., Ware J. H., Fay M. E., Ferris B. G. Jr. and Speizer F. E. (1993) An association between air pollution and mortality in six US cities New Eng. J. Med, **329**, 1753 - 1759.

King A M & Dorling S, PM_{10} particulate matter - the significance of ambient levels, Atmospheric Environment, **31**, 2379 - 2381.

Muir D. and Laxen D. P. H. Black smoke as a surrogate for PM_{10} in health studies Atmospheric Environment, **29**, 959 - 962.

Ostro B., The association of air pollution and mortality, examining the case for interference Arch Envir Hlth, **48**, 326 -342.

Pope III C. A.,Thun M. J., Namboodiri Mohan M., Dockery D. W., Evans J. S., Speizer F. E. and Heath C. W. Jr. (1996) Particulate air pollution as a predictor of mortality in a prospective study of US adults Thorax, **51**, (Suppl 2) 53 - 58.

QUARG (1993), Air Quality in the United Kingdom, First report, Quality of Urban Air Review Group, Dept. Envir, London.

QUARG (1996), Airborne particulate matter in the United Kingdom, Third report, Quality of Urban Air Review Group, Dept. Envir, London.

DIFFUSIVE SAMPLING OF VOLATILE ORGANIC COMPOUNDS IN AMBIENT AIR

V. M. Brown and D. R. Crump

Building Research Establishment, Garston, Watford, Herts. WD2 7JR, UK

Abstract. The Building Research Establishment (BRE) has been using diffusive samplers for the study of VOCs in indoor and outdoor air since 1989. The Perkin Elmer type sampler packed with Tenax TA adsorbent is used for the diffusive sampling of C_6-C_{16} organic compounds. This method was applied in a major study of relationships between the environment and child health carried out during 1990-1993 in the Avon area of the UK. The present paper reports results of an investigation into the repeatability of the sampler in outdoor air and measurements of 6 aromatic hydrocarbons inside and outside a home over a 5 year period and inside and outside an office building over a 12 month period. Both the home and the office were located in Hertfordshire, England. Concentrations of VOCs recorded are similar to those found in the Avon area. Higher concentrations of each of the six compounds were recorded inside the home than outside, whilst greater amounts of benzene and toluene were found inside the office than outside. Seasonal variations in concentrations are observed and measurements recorded outdoors are similar to those recorded by other workers.

1. Introduction

The release of volatile organic compounds (VOCs) to ambient air is of increasing concern because of the role of these compounds in the formation of ozone and the toxicity of some individual compounds such as benzene. VOCs are currently measured at 12 sites by the UK Department of the Environment using continuous monitors. Diffusive samplers offer an opportunity to increase the available data for some VOCs such as the aromatic hydrocarbons for a relatively low cost compared with continuous monitors. They are currently the subject of studies to validate their performance by a number of groups in Europe and work is underway within the International Standards Organisation (ISO TC 146) to prepare a standard procedure for diffusive monitoring of VOCs in air.

The Building Research Establishment (BRE) has applied diffusive samplers to the measurement of VOCs in homes and outdoors since 1989. Results of measurements of VOCs have been reported for 174 homes and at 13 outdoor sites in the Avon area of the UK over a 12 month period as part of a major study of relationships between the indoor environment and child health carried out during 1990-1993 (Berry *et al.*, 1996). The technique has also been applied to provide a relatively low cost means of determining the VOC content of the indoor air where occupants of a building have reported an air quality problem (Brown *et al.*, 1996). The present study involved an investigation into the repeatability of the sampler in outdoor air, together with the measurement of VOCs inside and outside a home in Hertfordshire over a 5 year period and measurements at the workplace of one occupant of the

home over a 12 month period. Results obtained for six VOCs that occur in both outdoor and indoor air are compared with those recorded during the Avon study and with measurements at a range of outdoor locations reported by other workers.

2. Methods

In previous studies of VOCs in air BRE has used the Perkin-Elmer tube type sampler packed with the adsorbent Tenax TA and an exposure period of four weeks. The diffusive sampler has been validated by the UK Health and Safety Executive for the determination of VOCs in workplace air (HSE, 1995). This validation has shown that the performance of the sampler is less influenced by the low air speeds that can occur in indoor environments compared with some other types of samplers such as badges. The diffusive uptake rate of the Perkin Elmer tube type sampler is not affected by air speeds as low as 0.01 m s^{-1}.

Tenax TA is a porous polymeric adsorbent which has a low affinity for water vapour and gives low levels of artifacts on conditioned 'blank' tubes. It is a fairly weak adsorbent and therefore is suitable for the determination of a wide range of VOCs up to a boiling point of about 300°C. This is important for measurements in the indoor environment where compounds such as Texanol (2,2,4-trimethyl -1,3-pentanediol monoisobutyrate) commonly occur. More strongly retaining adsorbents, such as graphitised carbons, are not suitable for thermal desorption of these high boiling compounds, although they do have the advantage of lower back diffusion losses of the more volatile components during sampling.

Diffusive uptake rates for a range of VOCs appropriate to a four week exposure period on Tenax TA have been determined by exposure of the samplers to a standard atmosphere of the compounds of interest in an environmental chamber available at BRE (Brown *et al.*, 1993). Compounds of higher volatility, such as benzene, were found to have a significantly lower net diffusive uptake rate on Tenax TA over this exposure period than less volatile compounds such as 1,2,4-trimethylbenzene. Further work is required to validate the performance of the sampler over the range of pollutant concentrations and environmental conditions encountered during monitoring of ambient air. The European Standards Organisation (CEN) is currently preparing a standard procedure for undertaking such a validation; the work is being carried out by Technical Committee 264 WG11.

Compounds such as benzaldehyde, phenol and acetophenone have been detected on adsorbent tubes packed with Tenax which have been exposed to air containing a high concentration of ozone (Woolfenden, 1997). These compounds appear to be formed from oxidation of the sorbent itself and experiments with and without the presence of ozone showed no artifact formation or analyte degradation resulting from interactions with retained analytes. Further work is required to determine whether any degradation of analytes can occur over an exposure period of 4 weeks in the presence of oxidants such as ozone. Concentrations of ozone in the air were not measured as part of the present study.

The Perkin Elmer tube type samplers were used without diffusive end-caps when placed in indoor locations to be consistent with the study of homes carried out previously where it

was felt that operators unfamiliar with their use may not fit them properly thus resulting in an incorrect length for the diffusive path. When fitted correctly however, diffusive end-caps do offer protection against ingress of dust and insects and the development of turbulence within the diffusive air gap when exposed to high air speeds.

Analysis involves thermal desorption followed by gas chromatography with flame ionisation detection (TD/GC/FID). Peak identities are confirmed using a further TD/GC system equipped with a Finnigan ion trap detector (ITD). Details of the equipment and conditions used are as follows: Perkin Elmer (PE) ATD50 with an 8310 GC and since 1995 a PE ATD400 with an Autosystem GC. Desorption at 250°C for 10 minutes, cold trap low -30°C, cold trap high 300°C, GC column: 25m BP10, 0.25µm film (SGE), temperature programme: 40°C for 1 min, 2°C min^{-1} to 75°C, 5°C min^{-1} to 220°C. A lower split ratio (16:1) is used with the ATD400 than was used with the ATD50 (30:1). This results in a lowering of the detection limit of the sampler. For each instrument the minimum peak area for peak detection selected resulted in detection of five or less peaks during analysis of a clean Tenax tube. This setting is equivalent to a detection limit for toluene of 20 ng on a tube using the ATD50/8310 GC and 2 ng on a tube using the ATD400/Autosystem GC.

3. Results

3.1 REPEATABILITY OF DIFFUSIVE SAMPLER

The repeatability of the sampler for measurement of VOCs in outdoor air was investigated by exposing 6 duplicate samplers at one outdoor location for 5 separate 4 week exposure periods. The site chosen was 12.4m east of the southbound carriageway of the M1 Motorway. In this experiment the samplers were each fitted with a diffusive end-cap and placed in a purpose-built steel open-ended box located close to the ground. The samplers were all positioned less than 0.5m above ground level. Table I shows the results for 6 VOCs and the relative standard deviation which was in the range 1.7 to 10.0%. The lowest mean relative standard deviation over the 5 exposure periods was recorded by benzene (3.8%) and the highest was for ethylbenzene (6.7%). The samplers therefore have a similar repeatability to that found in a parallel experiment in which the same samplers were exposed indoors without diffusive end-caps (Brown *et al.*, 1992). A further repeatability experiment using 3 tubes without end-caps at the same outdoor location for 1 month found a similar relative standard deviation (1.5% - 8.3%) for each of the 6 compounds.

3.2 MEASUREMENTS

Figure 1 shows GC chromatograms given by TD/GC/FID analysis of adsorbent tubes exposed for 4 weeks during March 1995 in the main bedroom and outside a home of a BRE employee in Hertfordshire. The sampler located outdoors was contained in a purpose-built steel open-ended box placed in the back garden, 5m from the house. The chromatograms illustrate the

TABLE I

Repeatability of VOC determination in outdoor air using diffusive sampling

Compound	Mean Concentration (µg m^{-3}) (RSD%)				
	Period 1	Period 2	Period 3	Period 4	Period 5
Benzene	4.8 (1.7)	3.6 (3.0)	3.5 (8.4)	5.8 (3.0)	7.8 (2.7)
Toluene	9.2 (2.8)	4.6 (4.8)	5.7 (7.8)	7.1 (5.6)	14.0 (3.7)
Ethylbenzene	1.4 (4.5)	0.7 (7.0)	0.8 (6.2)	1.1 (7.2)	2.0 (8.7)
M+p-xylene	4.6 (2.9)	2.4 (4.8)	2.9 (1.8)	3.8 (7.4)	6.7 (6.0)
O-xylene	1.8 (3.5)	1.2 (4.8)	1.3 (5.7)	1.7 (10.0)	2.6 (5.9)
1,2,4-TMB	1.3 (4.9)	0.8 (7.9)	0.9 (5.5)	1.2 (7.3)	1.8 (5.8)

differences in the range and amounts of compounds that can be detected indoors and outdoors. Dominant compounds indoors include toluene, xylenes, limonene, C_9-C_{11} aliphatic hydrocarbons and Texanol. In the outdoors, benzene, toluene, ethyl benzene and the xylenes dominate the chromatogram, with lower amounts of less volatile compounds being detected. This range of compounds observed in indoor and outdoor air is consistent with the findings of the study of VOCs in homes and outdoors in the Avon area of the UK (Berry *et al.*, 1996). A total of 256 peaks were detected from the sampler exposed in the bedroom which is greater than the typical number found in the Avon study (generally in the range 50-200). This is in part due to the lower detection limit possible with the present analytical equipment compared with that used in the previous work. A greater number of peaks (121) are also detected outdoors than was found previously (typically 4-24).

Table II shows annual mean concentrations inside and outside the home from 1991 to 1995 for six aromatic compounds with significant outdoor sources. The home is a 1930's built semi-detached building with 4 bedrooms and an integral garage. It is occupied by two adults and three children and there are no smokers resident. It is located in a semi-rural area on the edge of St. Albans but a busy minor road runs in front of the house (20m from the outdoor sampler) and a busy dual-carriageway lies to the rear (100m South East of the house). Significantly higher concentrations of each of the six compounds occur inside the home compared with outside as shown by the indoor-outdoor concentration ratios which range from 2.2 to 4.3.

Samplers were also exposed in the living room of the same home throughout the 5 year period and results (not given in the table) showed annual mean concentrations of each of these six VOCs which were lower in the living room than in the main bedroom but higher than outdoors. This suggests that the concentrations recorded indoors are due to sources inside the building as well as infiltration of outdoor air. Possible sources of VOCs indoors include building materials and consumer products used in the home and it is possible that evaporation
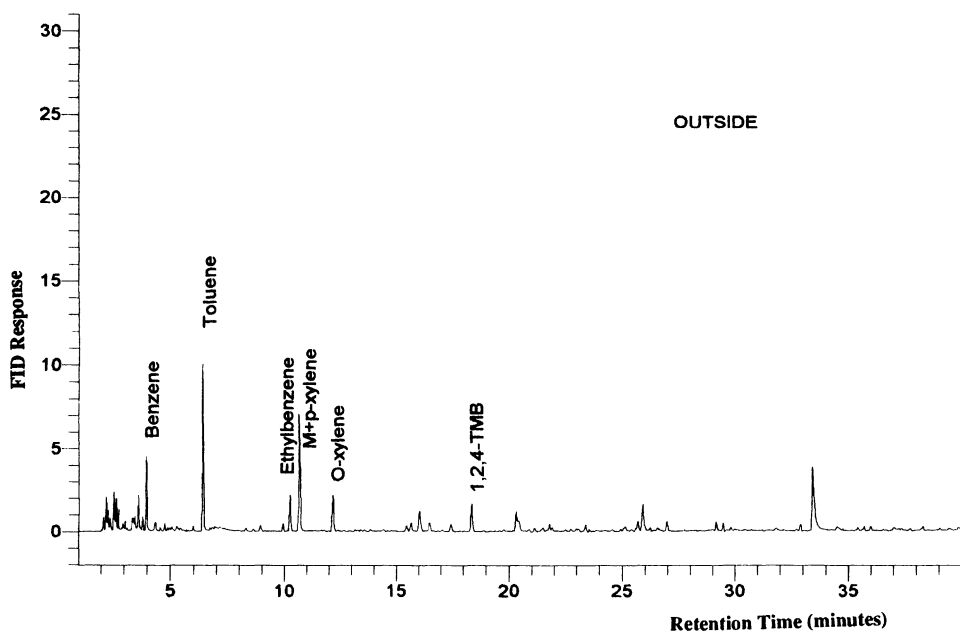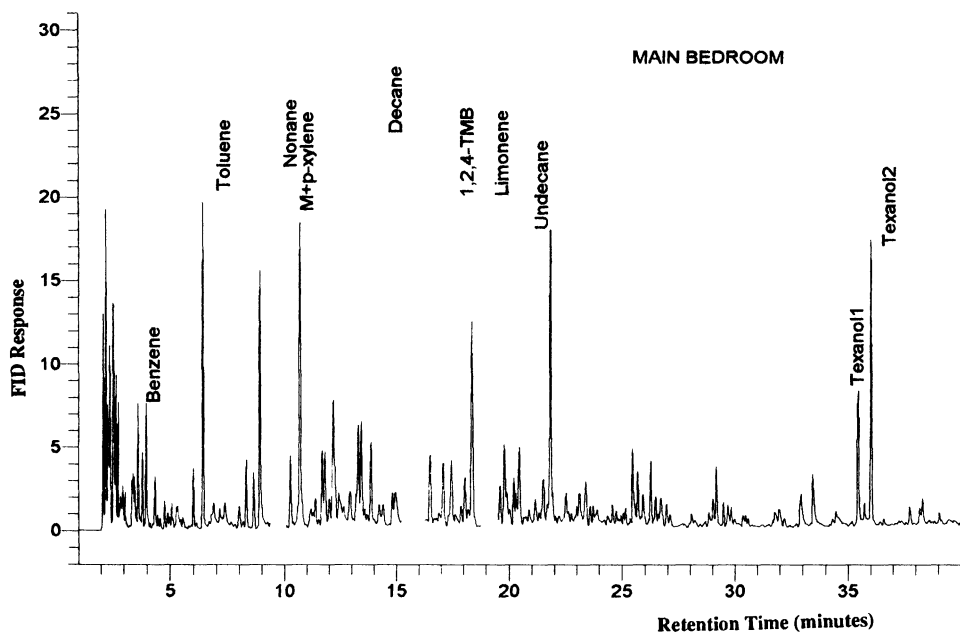
Fig. 1. Chromatograms of air samples from a Hertfordshire home

of fuel and vehicle emissions in the integral garage might contribute to amounts of some VOCs in the home. The results illustrate uncertainties with the monitoring of the outdoor air that is representative of air entering the building. The main bedroom is on the first floor to the front of the house, whilst the living room is on the ground floor to the rear of the building and the outdoor monitor is at ground level to the rear of the house. Further work is required to investigate how representative the back garden location is of air entering the house through ventilation and infiltration.

Table II also shows the ratios of concentrations in the main bedroom and outdoors with respect to benzene. If the ratios inside and outside were the same it might be interpreted that indoor concentrations were due to the outdoor air, but that the outdoor monitoring site was not representative of air entering the building. Some caution is required when making such assumptions however as the indoor source could be similar to that outdoors (eg petrol vapour and motor exhaust in garage) and adsorption of VOCs to internal surfaces could influence concentration ratios. The outdoor ratio shows some differences from the indoors, particularly for xylenes and 1,2,4-TMB, suggesting that there are indoor sources affecting the concentration ratio.

A compound of particular concern due to its classification as a genotoxic carcinogen is benzene (DOE, 1994). Figure 2 shows concentrations of benzene recorded each month in the main bedroom and outside the home over the period from December 1990 to February 1996. All concentrations recorded outdoors were below the recommended air quality standard for benzene in the UK (16 μg m^{-3} as a running annual average). Several individual month's readings in the bedroom exceeded this value, but annual mean concentrations were all below the guideline.

The mean concentrations of benzene recorded over the 6 winter periods (December-February) were significantly higher (20.1 μg m^{-3} in the main bedroom and 8.7 μg m^{-3} outside) than the mean concentrations recorded over the 5 summer periods (6.0 μg m^{-3} in the main bedroom and 3.7 μg m^{-3} outside). The other VOCs investigated also showed a tendency for higher concentrations in winter than in summer both indoors and outdoors. This seasonal variation in concentrations of VOCs in outdoor air is consistent with results of other outdoor measurements of VOCs recorded in the UK (Derwent, 1993). Some observations on longer term trends in VOC concentrations can also be made from this data. Table II shows some decline in concentrations of each of the six compounds recorded between 1991 and 1993 but for the next 2 years levels remained stable.

TABLE II

VOC concentrations inside and outside a home in Hertfordshire

Compound	Location	Annual Mean Concentration (µg m^{-3})						In/Out	Ratio of Concentration to benzene
		1991	1992	1993	1994	1995	Mean		
Benzene	MB	14.9	13.1	10.8	10.3	9.4	11.7	2.2	1
	Out	6.6	7	5.6	4.9	5.4	5.9		1
Toluene	MB	33.5	24.3	17.5	17.7	18.9	22.4	2.4	1.9
	Out	11.9	10.9	6.3	8.5	8.7	9.3		1.6
Ethyl benzene	MB	5.7	3.7	3	3.1	3.3	3.8	2.4	0.3
	Out	2	1.7	1.3	1.4	1.6	1.6		0.3
M+p-xylene	MB	19.5	12.3	8.5	9.6	11.8	12.3	2.4	0.9
	Out	5.8	5.5	3.4	4.2	5.2	4.8		0.8
O-xylene	MB	10.9	6.8	4.8	6.5	10.4	7.9	2.6	0.7
	Out	2.5	2.3	1.3	1.7	2	2		0.3
1,2,4 TMB	MB	10.1	6.1	3.8	5.7	6.4	6.4	4.3	0.5
	Out	2	1.9	1.1	1.3	1.4	1.5		0.2
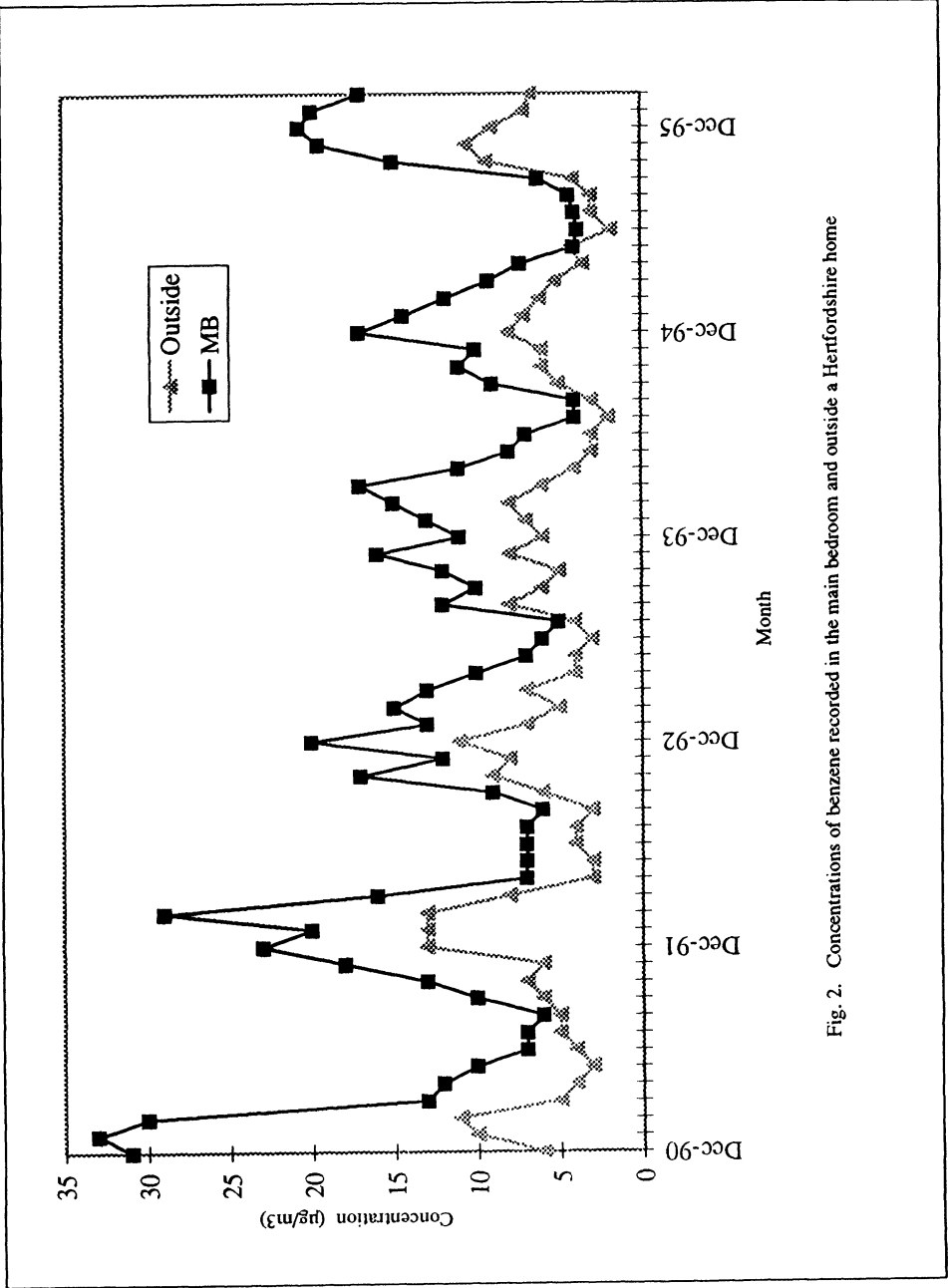
Fig. 2. Concentrations of benzene recorded in the main bedroom and outside a Hertfordshire home

As part of an on-going study of personal exposure, monitoring for VOCs has also been undertaken since March 1995 in an office building at BRE. Samplers were placed in adjacent offices both located on the South side of the third floor of the building and at a site outside the building. One of the offices was a single person office occupied by the employee who's home was also being monitored and the other was a multi-person office. The home monitored in this study was 9.1km from BRE. The sampler placed outside was located on the North side of the building resting on a wall under an overhang of the building (1m from the ground, 2m from the building and 125m from the M1 motorway).

Concentrations of benzene recorded over the 12 month period March 1995-February 1996 inside and outside the building are shown in Figure 3. The results show that in contrast to the home, benzene concentrations outdoors can exceed those indoors. It is possible that the concentration of benzene in the air infiltrating these rooms from outside at third floor level was lower than at ground level. As with the home, further work would be required to determine the position to monitor VOCs outdoors which is appropriate to the infiltration into particular parts of the building. The same seasonal variation is observed in concentrations indoors and outdoors at this location, with a tendency for higher benzene concentrations to be recorded during winter than summer.
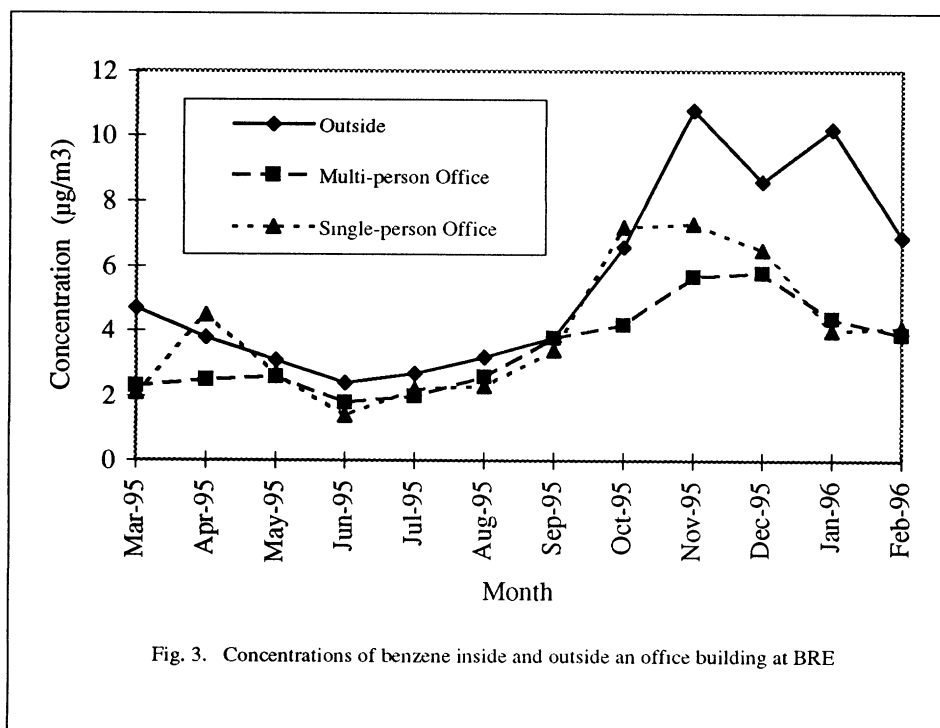
Fig. 3. Concentrations of benzene inside and outside an office building at BRE
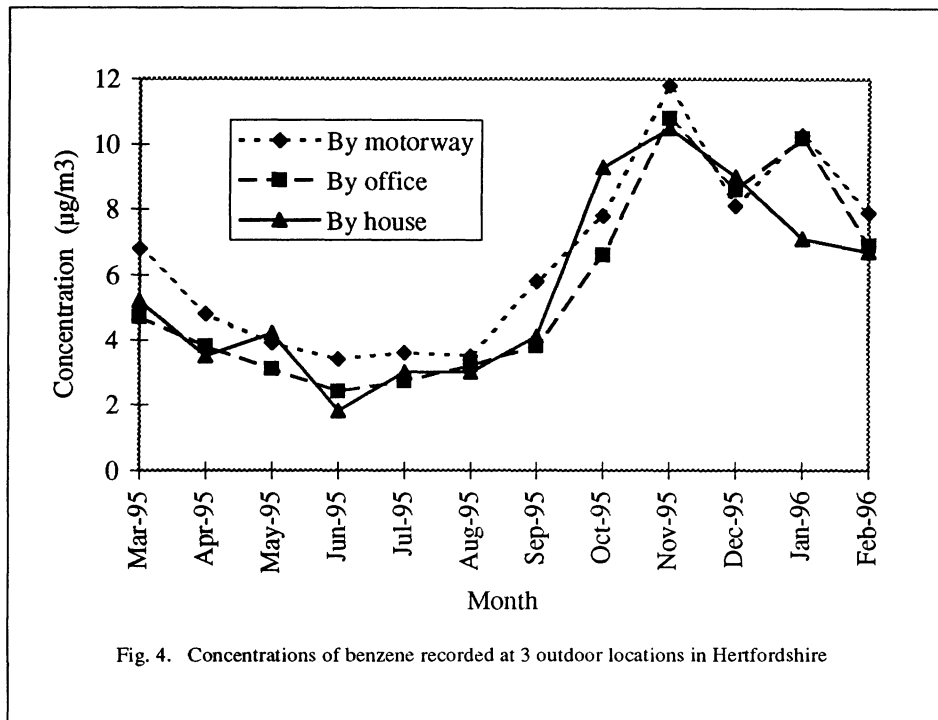
Fig. 4. Concentrations of benzene recorded at 3 outdoor locations in Hertfordshire

A further location monitored was at ground level on the BRE site 12.4m east of the southbound carriageway of the M1 motorway. This sampler was fitted with a diffusive end-cap and placed in an open-ended steel box for protection. Figure 4 shows the concentrations of benzene recorded at this location together with concentrations recorded at the other two outdoor locations. Very similar concentrations were recorded at each of the three locations and each show a similar seasonal variation.

Table III shows the annual mean concentration of the six aromatic hydrocarbons for the period March 1995 to February 1996 for some of the different locations in which the BRE employee spends time. Concentrations given for the home are the mean of individual readings from the living room and main bedroom. Similar annual mean concentrations were recorded for each of the six VOCs outside the home and the office but differences were found in the relative amounts of each compound detected inside the 2 buildings. This suggests the 2 buildings have a different mixture of sources. The annual mean concentrations of benzene and toluene are significantly higher in the home than in the office whilst ethylbenzene, xylene and 1,2,4-TMB concentrations are similar in the 2 buildings. These compounds are all components of white spirit based paints and painting provides a significant source of these

TABLE III

Annual mean VOC concentrations in different micro-environments

Compound	Annual Mean Concentration (μg m^{-3}) (March 1995-February 1996)			
	Home (Mean of Living room and Main Bedroom)	Office	Outside Home	Outside Office
	Mean (SD)	Mean (SD)	Mean (SD)	Mean (SD)
Benzene	8.4 (4.6)	4.0 (2.0)	5.6 (2.9)	5.8 (3.0)
Toluene	17.2 (6.8)	8.6 (3.6)	8.8 (3.9)	10.7 (5.5)
Ethylbenzene	2.7 (1.0)	2.7 (2.8)	1.6 (0.7)	1.8 (0.8)
M+p-xylene	10.9 (4.3)	10.1 (10.9)	5.1 (2.2)	5.9 (2.6)
O-xylene	8.3 (2.6)	4.9 (3.2)	1.9 (0.8)	2.5 (0.8)
1,2,4-TMB	5.8 (1.9)	5.4 (5.7)	1.3 (0.5)	1.8 (0.5)

compounds in indoor atmospheres. High variability recorded in the concentrations of these compounds in the office is due to some high values recorded during painting episodes in January and February 1996. The differences observed between VOC concentrations in the office, home and outdoors illustrates the need to monitor all micro-environments in which an individual spends time to determine their total exposure. Alternatively personal sampling techniques can be applied.

Table IV compares the mean concentrations of VOCs measured in the present study and in the ALSPAC study using diffusive samplers with published results for five sites in England that had continuous monitors (Bertorelli and Derwent, 1995). The five sites are part of the UK Automatic Hydrocarbon Network and employ Chrompack VOCAIR analysers that determine C_2-C_8 hydrocarbons with sampling periods of 30 minutes. Sample heights are 3.5-4.0 m. The Bristol, Birmingham, Middlesborough and Eltham sites are in urban residential areas and the UCL site is at a road kerbside. While direct comparison of the data is not possible because of the different time periods and sampling heights involved, the concentrations of the five VOCs monitored by passive and continuous monitors are similar across sites; benzene 3-6 μg m^{-3}, toluene 6-12 μg m^{-3}, ethylbenzene 1.5-8.5 μg m^{-3}, m+p-xylenes 3-9 μg m^{-3} and o-xylene 2-5 μg m^{-3}. The results suggest that the passive samplers may be giving lower values for ethylbenzene and xylene than the continuous monitors.

TABLE IV

Mean VOC concentrations at outdoor sites in England

Compound	11/90-1/93 Avon[a]	3/95-2/96 BRE, Herts (by office)	3/95-2/96 BRE, Herts (by M1)	3/95-2/96 St. Albans, Herts	1/94-12/94 St. Albans, Herts	1/94-12/94 Eltham, London	1/94-12/94 UCL, London	1/94-12/94 Birmingham	1/94-12/94 Middlesborough	4/94-2/95 Bristol
Benzene	5	5.8	6.5	5.6	4.9	2.7	5.4	4.3	3.7	2.9
Toluene	12	10.7	10.8	8.8	8.5	6.4	10.5	11.2	9.8	7.3
Ethylbenzene	-[b]	1.8	1.7	1.6	1.4	2.0	8.6	6.0	6.3	4
M+p-xylene	4	5.9	5.5	5.1	4.2	2.8	8.6	7.9	6.9	8.2
O-xylene	2	2.5	2.1	1.9	1.7	2.2	4.0	4.5	4.9	3.1
1,2,4-TMB	1	1.8	1.4	1.3	1.3	-[b]	-[b]	-[b]	-[b]	-[b]

[a] 13 sites in Avon, urban, suburban and rural (Berry et al., 1996)

[b] not available

Further work is required to compare the results given by the various methodologies such as continuous monitors based on gas chromatography and the various designs of diffusive samplers that use different adsorbents and analytical methods. Diffusive samplers do provide a low cost method of measuring VOCs in outdoor air and are expected to have an increasing role, in conjunction with the network of continuous monitors, to monitor levels of VOCs in ambient air to ensure compliance with air quality standards and guidelines.

4. Conclusions

Diffusive samplers can provide useful information about the VOC content of indoor and outdoor air which can complement data provided by continuous monitors. They are relatively easy to use and have been found to have good repeatability. Concentrations of benzene, toluene, ethylbenzene, xylenes and 1,2,4-trimethylbenzene can be higher inside a home than outside. Lower benzene and toluene concentrations recorded inside a third-floor office than outside may be due to the outdoor air monitor not being representative of air infiltrating the building. Differences in the amounts of VOCs detected in different micro-environments in which an individual spends time shows the importance of personal sampling to determine an individual's exposure.

References

Berry, R.W., Brown,V.M., Coward, S.K.D. et al., 1996, Indoor Air Quality in Homes-The Building Research Establishment Indoor Environment Study, Building Research Establishment Report, BR 299 and BR 300, BRE, Watford, UK.

Bertorelli V. and Derwent R.: 1995, Air Quality A to Z, Meterological Office, Bracknell, UK.

Brown V.M., Crump D.R. and Gardiner D.: 1992, *Env. Technol.* **13**, 367-375.

Brown V. M.., Crump D.R. and Yu C.: 1993, *Env. Technol.* **14**, 771-777.

Brown V.M., Cockram A.H., Crump D.R and Mann, H.S. : 1996, *Proc. of Indoor Air '96*, Nagoya, **2**, 115-120.

Department of the Environment, Expert Panel on Air Quality Standards, Benzene, HMSO, 1994.

Derwent R.:1993, In: Leslie G. And Perry R (Eds.) Volatile Organic Compounds in the Environment, Lonsdale Press Ltd., London.

Health and Safety Executive, Volatile organic compounds in air - Laboratory method using diffusive solid adsorbent tubes, thermal desorption and gas chromatography. MDHS 80, Health and Safety Executive, 1995.

Woolfenden E., 1997, *J. Air & Waste Manage. Assoc.* 47: 20-36.

DIFFUSIVE SAMPLING OF VOCs AS AN AID TO MONITORING URBAN AIR QUALITY

M.D. WRIGHT, N.T. PLANT and R.H. BROWN

Health and Safety Laboratory, Broad Lane, Sheffield S3 7HQ, England

Abstract. Diffusive sampling of Volatile Organic Compounds (VOCs) onto thermal desorption tubes, followed by gas chromatography, is an established technique for area or personal monitoring of typical workplace concentrations and there has been increasing interest in extending the application to environmental levels, particularly for benzene, toluene and xylene (BTX). Diffusive sampling rates for BTX on Chromosorb 106 and Carbograph-1 (a graphitised carbon) were measured over periods of 1-4 weeks in field validation experiments using ambient air and parallel pumped sampling (the reference method) at the HSL site in central Sheffield. The reference method was also used to investigate the possible bias of an open-path spectrophotometer (OPSIS) used by Sheffield City Council. A bias for BTX was suspected from results of a two-week initial exercise in which several diffusive samplers were placed close to the light path. In the full field validation of the diffusive samplers carried out subsequently, the significant bias of BTX concentrations reported by OPSIS were confirmed when compared with concurrent results from the reference method. OPSIS gave benzene and toluene values up to eight times higher than expected from the GC measurements. Xylene discrepancies were smaller, but in one 3-day peak episode, OPSIS demonstrated a negative correlation with GC.

1. Introduction

It is already mandatory, under existing EC Directives, to assess ambient air quality with respect to SO_2, NO_x, black smoke , PM_{10}, lead and ozone. This list is likely to be extended by the imminent EC Ambient Air Directive to include benzene. Conventionally, benzene and other VOCs have been measured in urban air at fixed monitoring stations using dedicated semi-continuous gas chromatographs. Diffusive samplers offer a low-cost complementary approach and are ideally suited to pollution mapping of small localised areas. They can also be used as a tool for siting fixed stations, for a preliminary assessment of air quality or to test exposure modelling estimates.

However, the valid application of diffusive sampling to environmental monitoring requires an accurate measure of the effective sampling rate of these devices when used over extended periods. In the tube device manufactured by Perkin-Elmer Ltd (Beaconsfield, UK) the geometry of the air gap is reasonably well defined and it is possible to predict from known diffusion coefficients what the theoretical sampling rates will be. The difficulty is that these theoretical rates cannot be sustained without using a very strong sorbent, which is not compatible with good recovery in the thermal desorption step. The choice of sorbent is then a compromise that depends on the application.

Very little has been published to date on the use of the Perkin-Elmer tube for environmental VOC levels. Effective sampling rates for benzene, toluene and undecane over 4 weeks have been measured on Tenax TA (Brown *et al.*, 1993). The choice of Tenax TA is acceptable when one wishes to measure hydrocarbons over a wide volatility range,

however, if just benzene is required then either Chromosorb 106 or a graphitised carbon may be preferred. There have been unpublished studies with Chromosorb 106 (Saunders, 1995) and Carbopack B (Hafkenscheid, 1995), but there has been no published work on these two sorbents involving field validations, where pumped and diffusive samples of ambient air are taken in parallel over several weeks.

For workplace monitoring, typically up to 8 hours, it is feasible to create a mathematical model of the diffusive tube, which allows prediction of effective uptake rates (Van den Hoed and Van Asselen, 1991; Nordstrand and Kristensson, 1994). This indirect method is reasonably accurate if the complete adsorption isotherm is known. Given a 4-week exposure time and the known Freundlich isotherm parameters for benzene on Chromosorb 106, this model predicts significant changes in uptake rate from 1 week to 4 weeks. It is suspected that this large extrapolation of the model may be unrealistic and the actual changes are not very large. Its prediction of the absolute rate may not be greatly in error, considering the magnitude of other errors, but there is a need for direct uptake rate measurements.

The purpose of this paper is to show that at ambient concentrations of up to 50 μg m^{-3}, the Perkin-Elmer tube effective sampling rates for BTX are reasonably stable over periods of 1-4 weeks using either Chromosorb 106 or Carbograph-1 as sorbent; that environmental monitoring is feasible and that diffusive tubes could be used as an independent check on other monitoring systems.

2. Experimental

2.1 VALIDATION OF DIFFUSIVE SAMPLING RATES

Stainless-steel thermal desorption tubes, 89 x 6.35 mm o.d., 5.0 mm i.d. (Perkin-Elmer Ltd, Beaconsfield, UK) were packed with either Chromosorb 106, 60-80 mesh, 300 $\pm$ 30 mg (Chrompack, UK) or Carbograph TD-1, 20-40 mesh, 330 $\pm$ 30 mg (Alltech Associates Inc., USA). Air gaps were measured from the open end of the tube to the fixed sorbent-retaining screen. Any tubes outside the limits 14.0-14.6 mm were rejected for diffusive sampling. The estimated mean effective air gap was 15.9 $\pm$ 0.1 mm, including the diffusion cap. The mean cross-sectional area was 0.193 $\pm$ 0.002 cm^2. Tubes were conditioned for 2-3 hours in a stream of nitrogen prior to first use (Chromosorb 106, 250°C; Carbograph, 300°C). Thereafter, following analysis, tubes were cleaned for 30 minutes at 230°C (Chromosorb 106) or 280°C (Carbograph TD-1).

Sampling tubes were placed just outside the Robens Building at the Health and Safety Laboratory (HSL) Broad Lane site at a height of 15m. Active sampling, with Chromosorb 106 only as the sorbent, was carried out with a personal air sampling pump (SKC model 222-3) calibrated against a water displacement meter traceable to a NIST reference rotameter. The pump was attached to a Perkin-Elmer Sequential Sampler (model STS-25) and set at a nominal flow rate of either 12 mL min^{-1} (12-14 hours per tube) or 55 mL min^{-1} (4-6 hours per tube). The active sampling coverage was >90% of the available time for

periods of 1-4 weeks from October 1995 to February 1996, there being only brief interruptions for tube changeovers and maintenance. Diffusive sampling tubes were placed within 2m of the STS-25. A simple rain shield was made from polythene sheet, but otherwise the diffusive tubes were open to the weather. All diffusion caps were without the optional silicone membrane.

Analysis was carried out using a Perkin-Elmer ATD-400 thermal desorber coupled to a gas chromatograph (Perkin-Elmer Autosystem) equipped with a dual 50m x 0.22mm capillary column configuration (BP-1, d_f = 1.0 μm; BP-10, d_f = 0.5 μm, SGE Ltd., UK) and dual-FID. Primary desorption used 25 mL min^{-1} helium for 10 minutes at 230°C (Chromosorb 106) or 280°C (Carbograph). Secondary desorption from the cold trap (Tenax TA, 25 mg, -30°C) was at 300°C. The GC oven was temperature programmed from 50-130°C at 5°C min^{-1}. The total split ratio was 50:1. Chromatographic signal data was collected with Turbochrom® V4 software (PE Nelson).

Thermal desorption tubes for system calibration were loaded with known amounts of BTX (10-1300 ng) at 4-6 levels by spiking with 5 μL quantities of dilute methanol solutions. Calibration lines were not forced through the origin. The procedure is traceable to primary standards by gravimetry and has been described in detail elsewhere (Wright, 1991).

A diffusive sampling (uptake) rate for each two- and four-week run was determined by comparing about 25 diffusive tube simultaneous measurements with a single integrated active sampling measurement. For some one-week runs the number of diffusive simultaneous measurements was increased to 62.

2.2 FIELD SURVEYS

The beam of an open-path spectrophotometer system (OPSIS AB, Sweden) maintained by Sheffield Environmental Protection Unit (EPU) runs for approximately 300 metres above the Fargate pedestrian street in central Sheffield. The area is away from localised vehicle emissions and measures the general urban background of BTX, NO_x, SO_2, formaldehyde and ozone. During June 1995, weather-proof wooden boxes (loaned by BP Research, Sunbury, UK) were mounted at six points within 25 metres of the path of the beam. Each box was equipped with Chromosorb 106 and Carbograph diffusive tubes in duplicate, together with a pair of blank controls. After two weeks the tubes were removed and analysed for BTX. No pumped sampling was carried out at this initial stage and mean concentrations were estimated from the diffusive uptake measurements of Saunders (1995) and Hafkenscheid (1995).

In a second exercise at the HSL site during November-December 1995, diffusive sampling rates on Chromosorb 106 and Carbograph-TD1 were measured in a field validation, using pumped sampling on Chromosorb 106 as a reference method. It was also anticipated that, since the central Sheffield site of HSL is only 800 metres from the

TABLE I

Diffusive uptake rates on the Perkin-Elmer tube

Sorbent	Sampling time (weeks)	Benzene	Toluene	m/p-Xylene	No. of measurements
			ng ppm^{-1} min^{-1} ± s.d.		
	1	1.46 ± 0.11	1.64 ± 0.07	2.20 ± 0.28	62
Chromosorb 106	2	1.45 ± 0.17	1.89 ± 0.09	2.08 ± 0.07	29
	4	1.47 ± 0.14	2.10 ± 0.09	2.07 ± 0.06	27
	1	1.99 ± 0.19	1.75 ± 0.03	2.16 ± 0.04	23
Carbograph TD-1	2	2.00 ± 0.16	2.11 ± 0.04	2.19 ± 0.09	25
	4	2.00 ± 0.11	2.39 ± 0.05	2.18 ± 0.07	23
Calculated ideal sampling rates *		2.13 ± 0.04	2.29 ± 0.04	2.14 ± 0.04	

* Variance in the ideal sampling rates, expressed as s.d., was estimated from the experimental diffusion coefficient data of Lugg, 1968.

OPSIS beam, another direct comparison could be made with OPSIS data using the continuous pumped sampling results every six hours. The times of the six hour periods were selected on the assumption that levels were strongly related to traffic density. Therefore these were arranged to separate the morning and evening peaks (0700-1300, 1300-1900, 1900-0100, 0100-0700). This was correlated with BTX data derived from OPSIS over the same period, supplied by Sheffield EPU.

3. Results and Discussion

3.1. BACKGROUND BTX LEVELS

During one 54-day period in November-December 1995, about 205 consecutive six hour ambient air samples were taken at the HSL Sheffield site. The concentrations found were (mean of daily average ± s.d., μg m^{-3}); benzene, 2.9 ± 1.7; toluene, 7.5 ± 4.6; m/p-xylene, 5.9 ± 3.6. The peak value for benzene was 15 μg m^{-3} on 9 December 1995, corresponding to an episode of thick fog and still air. The mean ratio of benzene: toluene: m/p-xylene was generally about 2:5:4, with m/p-xylene occasionally diverging to exceed the toluene concentration. The diurnal variation was apparent in the time series data, where the BTX concentration doubled each day from early morning to mid-afternoon.
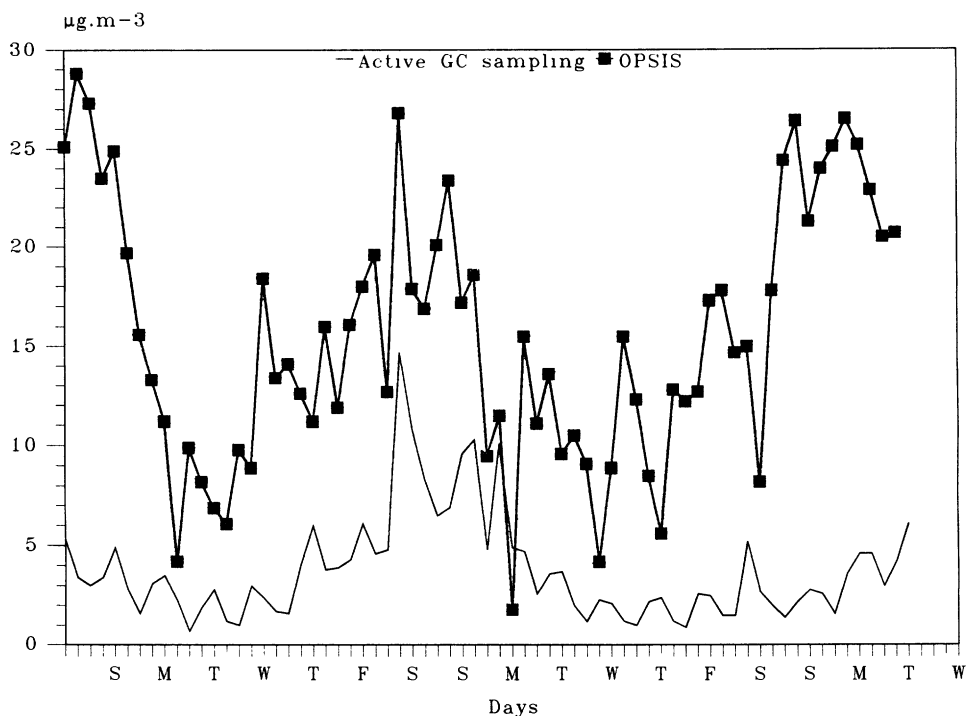
Fig. 1. Benzene concentration in ambient air: comparison of active GC sampling and OPSIS
Central Sheffield 2-19 December 1995.

3.2. VALIDATION OF BTX DIFFUSIVE UPTAKE RATES

The effective diffusive uptake rates were calculated based on the means of all active sampling results over an appropriate matched period and are given in Table 1. Benzene and m/p-xylene results show that these uptake rates are remarkably stable from one to four weeks on both sorbents. The mathematical model of diffusive sampling, originally developed by Van den Hoed and Van Asselen for short-term sampling, predicts a mean uptake rate on Chromosorb 106 that decreases 25% from one week to four weeks (no adsorption isotherm data is available for Carbograph). This indicates that some of the assumptions of the model about the diffusion of VOCs through the porous bed may not be justified for sampling that lasts several weeks.

Toluene, showed an unexpected anomaly, in that the one-week rates were apparently lower than those for four weeks. If there were differences, the opposite would be expected. We believe, based on the ideal sampling rates calculated from diffusion coefficients (Lugg, 1968), that the low one- and two-week results for toluene are artefacts, perhaps due to some GC calibration anomaly involving blank correction. Because the anomaly did not occur for benzene or xylene it was unlikely to be due to breakthrough of toluene or incomplete desorption in the analysis. Sample volumes of 10-20 litres were used, compared with an estimated safe sampling capacity of 80 litres for toluene on 300 mg Chromosorb 106 (Health and Safety Executive, 1993). It was also established that a

μg.m-3
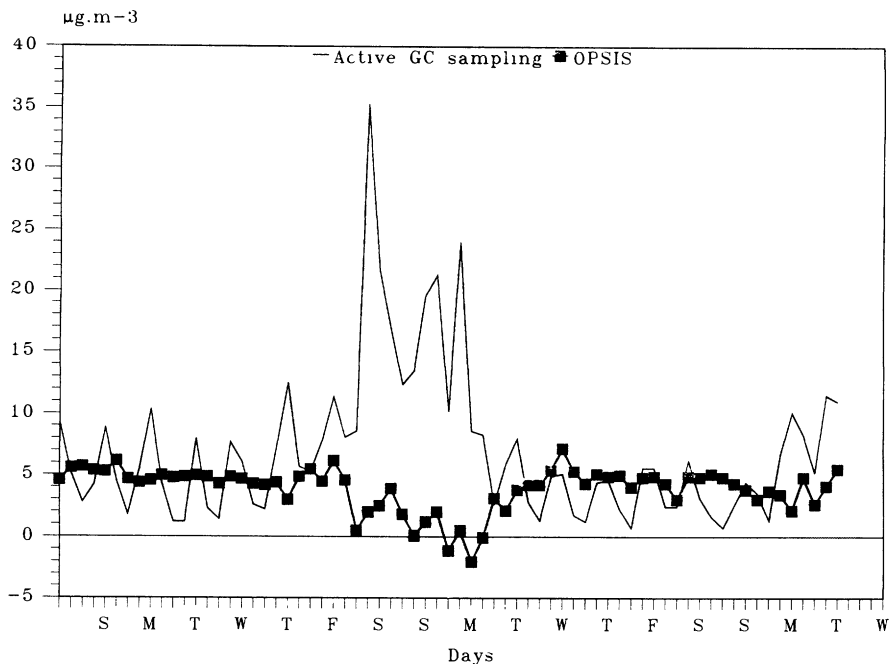
Fig. 2. Xylene concentration in ambient air: comparison of active GC sampling and OPSIS
Central Sheffield 2-19 December 1995.

primary desorption temperature of 230°C was more than sufficient for 100% recovery of
toluene and xylene at 25 mL min^{-1} desorb flow. It is significant that the same anomaly oc-
curred on both sorbents used in the diffusive sampling (Chromosorb 106 + Carbograph).
This points to the ATD-400 flow-path as a possible common source of trace toluene. We
believe this was a transient problem.

The reliability of these results depends on measurements of nanogram amounts of BTX
on thermal desorption tubes, and on the flow rate of the active sampling. Both were trace-
able to primary standards; however, the measurement of BTX mass is subject to more un-
certainty. The greatest contribution to this uncertainty, at least from sampling over one
week, is from the blank. Benzene blank levels on Chromosorb 106 are typically around 5
ng in thermal desorption (equivalent to 1 μg m^{-3} for one week) and cannot be systemati-
cally reduced by repeated conditioning. The benzene blank for Carbograph TD-1 could
not be reduced below about 10 ng, which was unexpectedly high for a grade of graphitised
carbon manufactured specifically for thermal desorption. Toluene blank levels were nor-
mally 1-3 ng for both Chromosorb 106 and Carbograph TD-1.

When choosing diffusive uptake rates it is always desirable to use a single compromise
value, with realistic estimates of uncertainty, even though this figure may represent a range
dependent on time, concentration, humidity, temperature, air velocity and other effects. In
this field validation all these effects are included, though not of course in a systematic way
as they could be in a artificially generated atmosphere. Nevertheless they are not expected
to be significant compared to the uncertainty arising in the analysis.

3.3. COMPARISON WITH OPSIS

In the initial study of June 1995, where diffusive samplers were placed close to the beam, it was found that benzene and toluene values reported by OPSIS were five to ten times greater than the mean result over two weeks from the gas chromatographic analysis of the diffusive tubes, whereas xylene values from the two methods were comparable. Although the bias of each method was uncertain at this stage and the diffusive sampling rates had yet to be confirmed by a reference active sampling method, something clearly was wrong with the BTX ratio given by OPSIS (OPSIS measures the *para*- isomer; the GC system used does not resolve *meta*- from *para*-xylene, but this does not significantly alter the conclusion).

Comparison of OPSIS with sequential six hour active samples from the later validation exercise carried out at the HSL site (800 metres from the beam) gave a more detailed picture. The situation was more confused than expected and showed that comparison over a single day was not sufficient. For benzene (Figure 1) the OPSIS/GC reference ratio averaged about 8 over two weeks but varied between extremes of 0.5 and 10. The diurnal variation seen by OPSIS was not very clear and showed a tendency to negative correlation. A calm foggy period around 9-11 December 1995 was clearly signalled by the GC reference method with peak benzene concentrations of 15 μg m^{-3}. The OPSIS benzene response for this period was smeared out and was not recognisable as an unambiguous peak. The OPSIS xylene response (Figure 2) for the same period was clearly spurious, since there was little or no diurnal variation. The peak episode was represented by a dip in the plot where negative concentrations were reported over several hours.

4. Conclusion

A feasibility study has shown that a simple diffusive tube device originally designed for workplace personal monitoring will give acceptable results at environmental levels. Uptake rates on Chromosorb 106 and Carbograph TD-1, at least for benzene and xylene, were not sensitive to exposure time. The same may be true of Carbopack B which is a graphitised carbon equivalent to Carbograph TD-1. More work is needed to establish whether extending the scope of a mathematical model of diffusive sampling to very long sampling times is justified.

In the course of the validation procedure, large discrepancies between BTX measurements using direct GC analysis (both diffusive and active) and an open-path spectrophotometer were noted. Clearly, diffusive sampling along the line of the beam was unable to give the daily picture, nevertheless it gave a strong indication of an anomaly with the response of the spectrophotometer. Whether this is specific to this instrument or a general problem with such systems requires further investigation.

Although not strictly required by legislation, diffusive tubes could also be used for long-term personal monitoring of workers, such as traffic wardens and enclosed car park attendants, exposed to BTX concentrations higher than the general background.

Acknowledgements

References

Brown, V., Crump D., Gardiner, D. and Yu, C.: 1993, *Environmental Technology*, **14**, 771-777.

Hafkenscheid, T.: 1995, *Personal Communication.*

Health and Safety Executive: 1993, *Methods for the Determination of Hazardous Substances, MDHS 72, Volatile*

    Compounds in Air, ISBN 0-11-885692-8.

Lugg, G. A.: 1968, *Anal. Chem.,* **40**, 1772-1777.

Nordstrand, E. and Kristensson, K.: 1994, *Am. Ind. Hyg. Assoc. J.*, **55**, 935-941.

Saunders, K.: 1995, *Personal Communication.*

Van den Hoed, N. and Van Asselen, O.: 1991, *Ann. Occ. Hyg.*, **35**, 273-285.

Wright, M.D.: 1992, *Health and Safety Executive Internal Report,* IR/L/IA/90/3.

TEMPORAL AND SPATIAL VARIATIONS IN NITROGEN DIOXIDE CONCENTRATIONS ACROSS AN URBAN LANDSCAPE: CAMBRIDGE, UK.

C. KIRBY[1], A. GREIG[1] and T. DRYE[2]

[1]Department of Geography and [2]Applied Computational Sciences Research Unit, Anglia Polytechnic University, East Road, Cambridge CB1 1PT.

Abstract. The acquisition of a comprehensive air quality dataset for a small city environment is described for use in statistical modelling of dispersion processes and micro-scale assessment of polluted zones. The dataset is based on a nitrogen dioxide diffusion tube survey for Cambridge where up to 80 roadside and background sites have been monitored continuously over two years, using a two week exposure period. Site categories are defined by their function within the urban landscape. Spatial and temporal features of the data set are explained in terms of urban location, street geometry, meteorology and traffic behaviour. The highest levels of NO_2 are found in central canyon streets which are narrow with enclosing architecture and slow-moving traffic. In contrast lower levels are found for the wider, more open radial routes where traffic is free-flowing. The influence of street geometry on NO_2 levels for central streets is demonstrated, where canyon sections adjacent to open sections having the same traffic flow record higher concentrations. Whilst all roadside sites are affected by a photochemical pollution 'episode', the greater potential for elevated NO_2 concentrations within the canyon sections is significant. The close proximity of low background levels of NO_2 to roadside 'hot-spots' is important for public exposure assessment. The variation in background levels across the urban landscape is very small and unrelated to location; whether central, suburban or outer city. Seasonal variation, not seen in roadside data, is clearly apparent in background data with a winter maximum and summer minimum.

1. Introduction

Road traffic has been identified as a major contributor to the deterioration of air quality in urban areas, both nationally and globally. Over the decade 1980 to 1990 the UK vehicle population increased by 28%, to just under 25 million vehicles (QUARG, 1993). Despite the introduction of more stringent emission regulations, national inventories show that emissions of traffic-related pollutants increased over the same period (Department of the Environment, 1996). Growth of traffic in Cambridge, however, has exceeded even the national figures with a 50% increase over the decade (Cambridgeshire County Council, 1992). Although a small and compact city with a stable population of just over 100,000 residents, Cambridge is the regional centre for East Anglia which is one of the fastest growing areas in the UK. Since the 1980s Cambridge's transport infrastructure has been under intense pressure as commuting levels have risen dramatically. Traffic congestion has become the norm with little scope within the historic centre for road network improvement.

Reasons for the expansion in traffic growth can be found in the rapid rise in employment levels within the city from 1980 onwards (Cambridge City Council, 1991). Unrestricted central office development, together with the success of high-tech businesses allied to Cambridge University, boosted commuter travel into the city. Altogether 64% of employees in Cambridge now travel to work by private vehicle, the highest percentage in the UK. In addition to the workforce traffic, the city also attracts 4 million visitors each year, many of whom arrive by road. Recent

improvements in motorway and trunk road links to the rest of the UK have made road access even easier.

The traffic problems faced in Cambridge are typical of other towns and cities in the UK and throughout Europe. Indeed Cambridge exemplifies the older European city with its historic centre, pre-dating motorised transport, surrounded by fragmented urban developments where old and new are juxtaposed. Such features impart character to the city but only piecemeal improvements can be made to modernise an urban transport infrastructure designed for an earlier age.

Many current models of atmospheric emission and dispersion processes are based on the American urban grid and block layout and are clearly inappropriate for older European cities. In any case, only a few street-level models exist for application to the wide range of street geometries found in most urban areas, such as the Dutch CAR International model (den Boeft *et al.*, 1996) and the commercially-available ADMS URBAN model. Validation of these models is hindered by a lack of suitable monitoring data; a situation which this study addresses.

This paper describes the acquisition of an extensive air-quality database for a compact urban area where vehicle emissions are the dominant pollution source. The temporal and spatial variations of nitrogen dioxide concentrations, a key urban pollutant, have been measured with particular emphasis on micro-scale effects within pollution 'hot-spots'. A new methodology for selection of sites is presented (see section 2) which takes account of significant features of street geometry and traffic speed and flow to investigate the relationship with measured roadside NO_2 concentrations and dilution to background levels. This systematic 'whole-city' approach has not been taken in previous NO_2 diffusion tube studies. Concurrent traffic data, meteorological variables and descriptors of street geometry have been collated from available sources. In addition, continuous monitoring data from an automated pollution monitoring station is available for a range of traffic-related pollutants. Meteorological measurements are made at a rooftop site, 30 metres above the pollution monitoring station. Statistical analysis of the combined data sets will quantify relationships between contributory factors affecting the spatial and temporal variations in nitrogen dioxide in order to model the dispersion processes. The results of this study will have application to other small city environments, to evaluate public health exposure to nitrogen dioxide and to assess national and local traffic management initiatives aimed at reducing NO_2 levels.

In Cambridge, as elsewhere, the level of public concern over health effects of traffic pollution has never been greater (Cambridge City Council, 1991). However, causal relationships between health and air pollution have been difficult to establish. The need for further research has been recognised (WHO, 1987: UK Department of Health Reports, 1993, 1995) and further work is underway involving both laboratory studies and epidemiological surveys of human exposure to key urban pollutants. The role of geographically-based monitoring data, such as the Cambridge database, to assess the scale of public exposure to urban traffic pollution also needs to be recognised. Detailed micro-scale measurements of urban pollutants are needed to assess the significance of pollution hot-spots in relation to air quality standards and

public exposure. This is essential for effective implementation of national and international air quality standards set to protect public health (Council of the European Communities, 1985; WHO, 1987).

This study contributes to urban air quality assessment in the UK providing detailed information about the size and scale of representative polluted urban zones within a whole city framework. Under UK legislation embodied in the Environment Act 1995, these zones may be designated as local air quality management areas, if air quality standards are likely to be breached. The multi-point monitoring carried out in this survey will help to determine whether confidence can be placed in measurements taken at single site kerbside locations as well as assessing the variation in background levels across broader areas.

Nitrogen dioxide diffusion tubes provide a simple, inexpensive technique allowing measurements to be made with very good spatial resolution and a degree of temporal control (QUARG, 1993). This method has been used to carry out a two year survey of NO_2 levels in Cambridge from Sep.1994 to Sep.1996. An holistic approach has been taken in order to map NO_2 levels across an urban landscape and to determine how urban structure and traffic movement affect distribution of this pollutant. The relationships between nitrogen dioxide, traffic density, urban structure and meteorology is further investigated.

1.1 SAMPLING TECHNIQUE

Passive NO_2 diffusion tubes have found widespread use in the UK for ambient air monitoring as efficient, low cost samplers with few restrictions on siting. Their drawback is that they provide only an average concentration over the period of sampling, usually between one and four weeks depending on the nature of the environment to be monitored. The method was first proposed for occupational hygiene sampling (Palmes *et al.*, 1976) and was subsequently used for indoor air quality surveys (Palmes *et al.*, 1977; Melia *et al.*, 1978). Since then the method has been validated for use in the outdoor environment (Atkins *et al*, 1986). A modification to the preparation of the tubes was introduced by Hargreaves (1989) with additional investigation of temperature, relative humidity and windspeed effects on the uptake of NO_2 by the diffusion tubes.

The sampler consists of an acrylic tube of length 7.1cm and internal diameter 1.1cm, with tight-fitting polythene caps at each end. Triethanolamine-coated meshes are held under one end cap to absorb nitrogen dioxide from the atmosphere following removal of the other end cap. The transport of the gas by molecular diffusion along the tube is described by Fick's Law and by measuring the total amount of NO_2 absorbed on the meshes after exposure, the average NO_2 concentration in the ambient air can be calculated. The unidirectional flow of a gas_1 through a gas_2 is given by Fick's Law:

$$F_1 = -D_{12}\, dc_1\, /dz$$

where F_1 is the flux of gas$_1$ (mol cm^{-2} s^{-1}), D_{12} is the diffusion coefficient for gas$_1$ in gas$_2$ (cm^2 s^{-1}), c_1 is the concentration of gas$_1$ in gas$_2$ (mol cm^{-3}) and z is the length of diffusion (cm). For a cylinder of length z and cross-sectional area πr^2 with a concentration gradient ($c_1 - c_0$) molecule cm^{-3} between its ends, the quantity Q_1 (mol) of gas$_1$ transferred along the tube in t seconds is

$$Q_1 = F_1 \ (\pi r^2) \ t$$

$$Q_1 = -D_{12} \ (c_1 - c_0) \ (\pi r^2) \ t \ / \ z$$

If an efficient absorber is used to remove gas$_1$ then c_0 effectively becomes zero. The negative sign can be ignored as it signifies only that flux is measured in the direction of decreasing concentration of gas$_1$. The diffusion coefficient for NO$_2$ in air has been calculated from gas viscosity data as 0.154 cm^2 s^{-1} (Palmes et $al.$, 1976). Inserting the dimensions for the diffusion tubes (mean length of 7.097cm and mean diameter of 1.106cm) and converting the concentration of NO$_2$ (gas$_1$) from moles cm^{-3} to parts per billion, the concentration of NO$_2$ in air is given by the following equation:

$$\text{NO}_2 \ \text{concentration (ppb)} = Q \ (\mu g) \times 6953 \ / \ t \ \text{(hours)}$$

where Q is the mass of nitrite extracted (μg), and t is the time of exposure of the tubes (hours), assuming 1atm. and 20°C.

Previous studies have investigated the validity of applying Fick's law of diffusion to outdoor conditions. Atkins et al.(1986) reported that changes in temperature were not significant and that sample collection showed no atmospheric pressure dependence. Hargreaves (1989) also found no dependence on temperature and pressure and that the effect of relative humidity was unimportant for outdoor sampling in the UK. Wind turbulence effects were investigated in wind tunnel experiments which showed that at a range of constant windspeeds the tubes did systematically over-estimate NO$_2$ concentrations, however, in field experiments no such over-estimation was found. Comparison to continuous monitors using the chemiluminescent technique was reported originally to give good agreement (Atkins et al., 1986) but later studies have indicated a tendency for the tubes to over-read relative to the continuous monitor (Campbell et al., 1994; Gair et al., 1991). This effect is very variable and appears to depend on site location although the reason for this is not yet known. It has been suggested that atmospheric turbulence at the tube inlet has the effect of reducing the effective diffusion length and therefore enhancing NO$_2$ uptake. Further comparison is being made in the present study and will be reported on in due course. In practice, absolute agreement of a time-integrating method against real-time measurement is probably unrealistic but this does not negate the use of diffusion tubes for investigating relative spatial and temporal patterns of behaviour.

2. Selection of site locations

2.1 BACKGROUND

A crucial part of the Cambridge survey was the systematic selection of both roadside and background sites. This contrasted with earlier surveys where one type of site predominated. For instance the survey of 115 London sites carried out in 1984/85 (Clark and White, 1986) used mainly background sites. Nitrogen dioxide contour maps were compiled showing how background levels varied across a large urban basin, with highest concentrations at the centre falling away towards the outer areas.

Two large-scale national surveys were carried out of urban areas in the UK; the first in 1986 (Bower *et al.*, 1989) and repeated in 1991 (Campbell *et al*, 1994). Here sites were classified by distance from major roads and again were mainly associated with background NO_2 concentrations. No account was taken of the physical location of sites within the urban landscape and only 26 near-road sites were included in the survey out of a total of 243 sites across the UK.

Very few surveys have investigated the proximity of background NO_2 concentrations to the roadside. In London, a short-term survey of two urban 'canyon' streets (Laxen *et al.*, 1987) showed that levels declined rapidly over the first 10-15 metres from the centre of the road and were close to background at a distance of 30 metres. This indicated that NO_2 concentrations decay rapidly away from the road so that at short distances away levels could be indistinguishable from background. Public exposure to traffic pollution at locations above background concentrations is likely to be of short duration.

Roadside variations in NO_2 concentrations were measured by Hewitt (1991) in Lancaster, a small city in north-west England, during a one year survey of four central and two suburban streets. No background sites were included but results indicated that there were significant differences in background concentrations between the city centre and suburban locations. The measurement of background concentrations were shown to be essential, particularly for making comparisons between roadside data from different location types (city centre, suburban, rural).

The Lancaster survey also showed that there was no simple correlation between traffic flow and NO_2 concentration. This was also a conclusion of a previous Cambridge survey of roadside sites carried out by Kirby *et al.* in 1992/93 (Cambridge City Council, 1994). Indeed results for this survey showed that street geometry had a significant influence on NO_2 levels. The sites with maximum concentrations of NO_2 were found to be within the historic city centre where roadways narrowed between high-sided buildings to form street 'canyons'. On other routes of more open topography much lower NO_2 concentrations were found despite higher traffic flows.

70
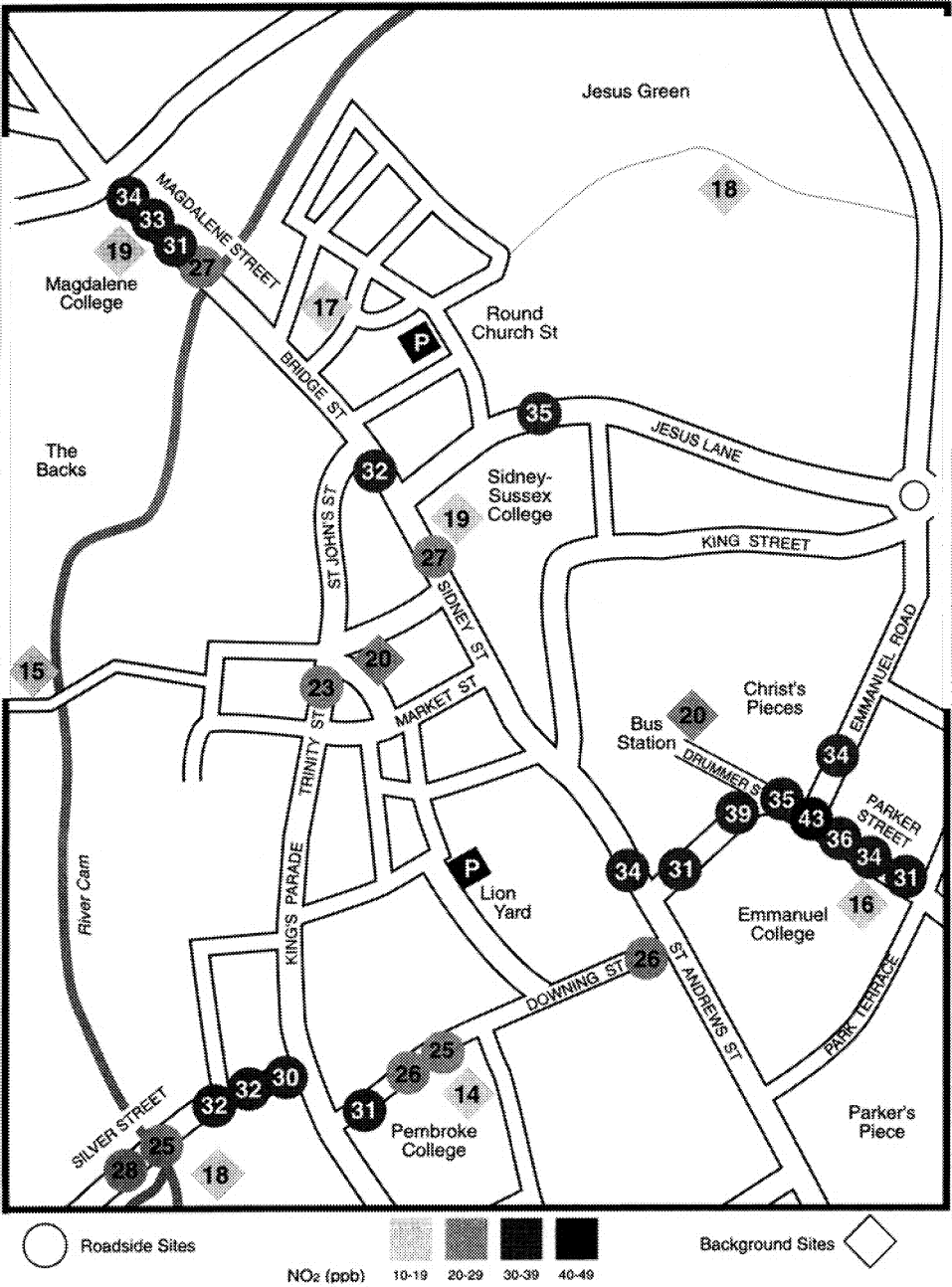
Fig. 1. Inner city site locations showing annual mean NO₂ concentrations in ppb, Sep. 1994 - Sep. 1995.
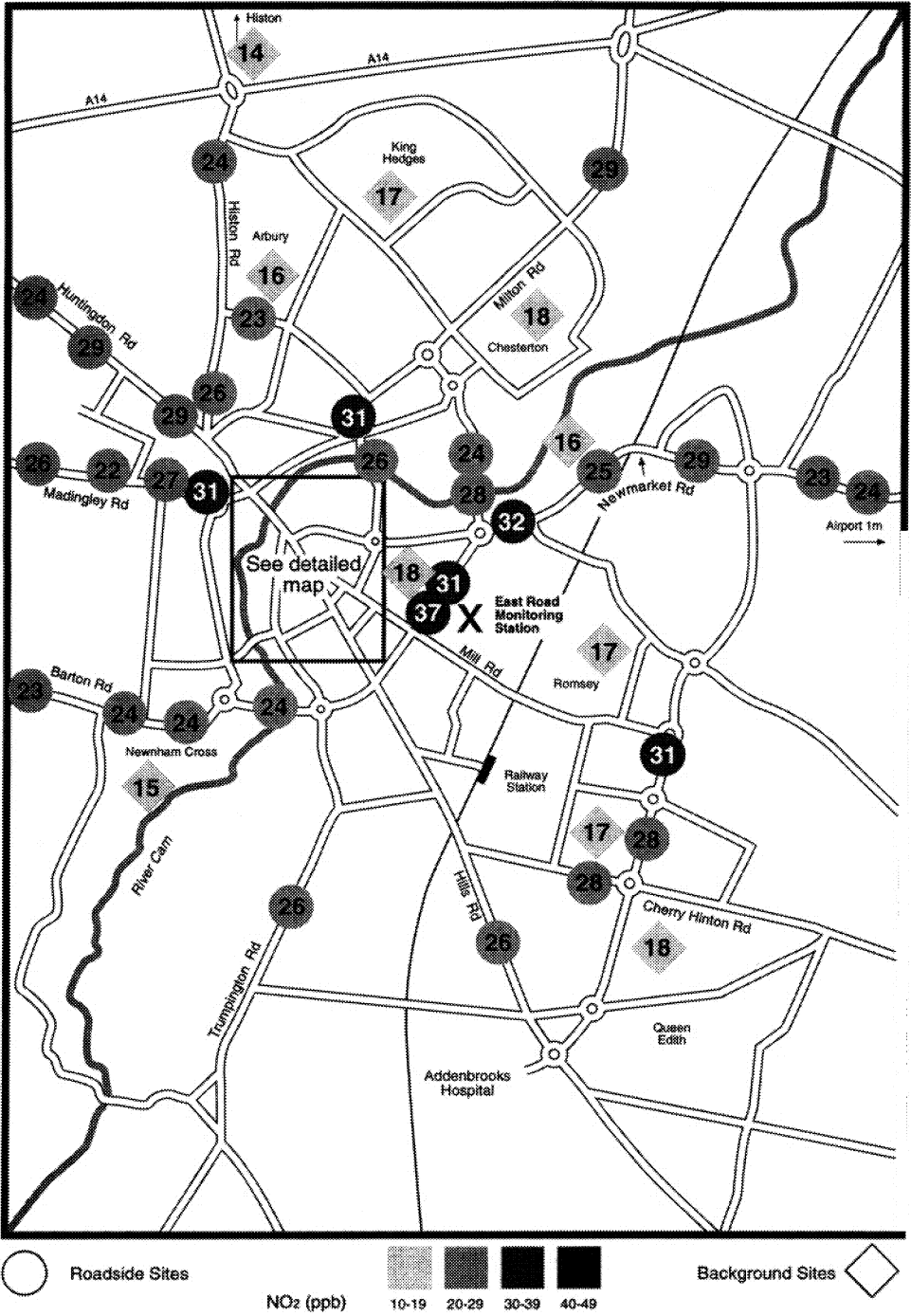
Fig. 2. Outer city site locations showing annual mean NO₂ concentrations in ppb, Sep. 1994 - Sep. 1995.

2.2 SITE LOCATIONS

The compact and symmetrical arrangement of the urban road network in Cambridge has made it an ideal study area for traffic-related pollution. The focus of the survey was to identify and monitor major categories of sites according to their function within the urban structure, ranging from busy roadside to rural background. This was a fundamentally different approach to other NO_2 surveys which have predominantly used background sites well away from traffic sources or, in a few cases, roadside sites defined by distance from a single major road.

The siting criteria described in the 1992/93 survey were adopted for the 1994/96 survey and extended to provide greater spatial resolution of the 'hot-spots' and full coverage of background sites. Sites in both roadside and background categories were defined in terms of their position within the urban landscape. Figs.1 and 2 show the layout of the urban road network, with the inner-city area enlarged to show details of sites. The city centre is encircled on the north and west sides by the River Cam and to the east and south by the inner- and outer-ring roads (Fig.2). The eight main arterial roads radiate out from the inner area, linking directly to the main trunk roads that serve the East Anglian region. For roadside measurement the dominant site categories were identified as the main city centre distributor routes, the outer radials and selected sites on the inner- and outer-ring roads. Sites at junctions were avoided because of ambiguity in defining location and emission sources. For background measurements key areas identified were those near to the city centre distributors, within Cambridge's central parks and pedestrianised areas and also residential areas both within the centre and in the suburbs, lying between the main radials. Other background sites were chosen in rural locations which were not subject to traffic emissions to provide 'clean-air' baseline levels.

Following on from the 1992/93 survey, additional sites were selected within the central canyon streets in order to investigate the effects of street geometry on NO_2 levels, Fig.1. These sites are along Magdalene St., Parker St. and Silver St. Sites along Pembroke St. (Pembroke College) were chosen to study the effects on NO_2 levels of changes in canyon width for the same traffic flow. Of the other city centre roadside sites all were within canyon streets monitored in the 1992/93 survey with the exception of a group of sites close to the bus station where traffic flows were low and dominated by diesel buses and taxis. The radial routes are named in Fig.2 (Histon Rd., Milton Rd., Newmarket Rd., Hills Rd., Trumpington Rd., Barton Rd., Madingley Rd. and Huntingdon Rd.). Sites along certain radials were selected to investigate any differences between inner- and outer-city sections. The list of site categories is given below.

ROADSIDE SITES (all within 1 metre of the kerb):
- Urban traffic 'canyons' with no intersections and distinct topography, including three streets where canyon sections could be compared to adjacent open sections with the same traffic conditions. (Fig.1: 21 sites)

- City centre streets around a bus station with low traffic flows but a high proportion of buses and taxis. (Fig.1: 5 sites)
- Outer radial routes; main arterial roads generally of open aspect. (Fig.2: 21 sites)
- Inner and outer ring roads taking traffic around the city. (Fig.2: 7 sites)
- Suburban link roads between radials. (Fig.2: 3 sites)

BACKGROUND SITES:
- Sites close to traffic canyons; within 7 to 20 metres of roadside. (Fig.1: 7 sites)
- Sites away from major roads; at least 50 to 100 metres distant. (Fig.1: 3 sites; Fig.2: 2 sites)
- Quiet streets in suburban residential areas, located between radials. (Fig.2: 7 sites)
- A semi-rural site located within the city boundary away from roads. (Fig.2: 1 site)
- Rural background sites; located between 10 and 20 km from Cambridge at points lying to the NW, NE, SE and SW. (5 sites, not shown on maps)

In the Cambridge survey 50 sites were continuously monitored over the two years, Sept 1994 to Sept 1996, with simultaneous two-week exposure periods for the NO_2 tubes. For the first year of the survey 80 sites were monitored continuously with up to 30 additional sites providing greater spatial detail and to assess the representation of long-term sites. For the second year of the survey rationalisation of sites reduced the total monitored to 50 sites. Tubes, attached to wooden blocks to ensure free movement of air at the exposed end, were sited on street furniture, either lamp-posts or down pipes. The tubes were placed vertically with the exposed end downwards at heights of approximately 2.3 metres so that they were just above the breathing zone of the public.

3. Experimental

3.1 PREPARATION AND ANALYSIS OF THE DIFFUSION TUBES

The method used in this survey is based on that described by Atkins *et al.* (1986) but with a modification to the tube preparation which was developed by Hargreaves (1989) and is now used by most UK laboratories. Preparation and analysis of tubes was carried out at the laboratory of the Department of Geography, University of Cambridge.

The acrylic tubes were detergent-washed, rinsed with demineralised water and dried in a low- temperature oven. The stainless-steel mesh discs were washed before use in a solution of Decon 90 in an ultrasonic bath, rinsed with demineralised water and dried. The tube preparation involved placing two mesh discs in a coloured end cap and pipetting 30µl of a 10% v/v triethanolamine (TEA)/water solution directly onto the meshes. A tube with a colourless cap on one end was immediately fitted over the coloured cap containing the impregnated meshes, keeping exposure of the

tube to the atmosphere to a minimum. A wetting agent, Brij-35, was added to the absorbent TEA/water solution to aid the coating of the meshes. Once prepared, and also after exposure, the tubes were sealed in polythene bags and stored at 4°C. The tubes were prepared a few days before exposure and analysed within two weeks of collection. A few tubes from each prepared set were retained in storage as 'blanks' for later analysis with the exposed tubes. Each tube was labelled according to its preparation set and location and information was recorded about its start and end date and time of monitoring.

Nitrogen dioxide absorbed as nitrite by TEA was determined spectrophotometrically by a variation of the Saltzman reaction. The colourless caps were removed from the diffusion tubes and 3.15mls of a combined reagent added containing 20 parts of 2% w/v solution of sulphanilamide in 5% v/v orthophosphoric acid to 1 part of 0.14% w/v N-1, naphthylethylenediamine dihydrochloride solution (NEDA). The caps were replaced and the tubes shaken to extract nitrite and mix the reagents. Nitrite present reacted with sulphanilamide to form a diazonium compound that coupled with NEDA to form a purple azo dye. Phosphoric acid was added to the reagent to increase acidity and enhance colour development. The optical absorbance of a range of nitrite standards and the sampler solutions were measured at 540nm on a Cecil spectrophotometer (series CE 2393). The blank reagent solution was used to zero the instrument because of impurities in the reagents. Absorbance readings from the unexposed 'blank' diffusion tubes were averaged for each preparation set and the value subtracted from the readings for exposed tubes. The amount of extracted nitrite found for each tube was used to calculate the ambient NO_2 concentration for its exposure location and time period. Results for all locations and exposure periods were collated on spreadsheets.

4. Results and discussion

The annual mean NO_2 levels for the 80 roadside and background sites from the first year of the survey Sept.1994 to Sept.1995 are shown on the two maps, Figs.1 and 2. All concentration measurements are reported in parts per billion (ppb). Detailed analysis has yet to be carried out but there are significant spatial and temporal features of the data set which can be explained in terms of urban site location, street topography and traffic behaviour.

4.1 SPATIAL COMPARISONS OF ANNUAL MEAN NO_2 CONCENTRATIONS

4.1.1 Roadside
The maps show marked differences in NO_2 levels between outer and inner sites, with the majority of city centre roads having higher concentrations. These differences can be explained by the combined effects of street topography and driving conditions, rather than in terms of traffic flows, Table I. Whilst traffic flows may be two to three times greater on the radial routes than the city centre canyon streets, NO_2

concentrations are lower, 23 to 29 ppb compared to levels above 30 ppb within the canyons. The narrow road widths and enclosing architecture of the canyon streets inhibit dispersion of traffic emissions while the radial routes have a flatter more open topography providing good ventilation. Traffic in the centre is often congested and slow moving while free-flow conditions are more usual on the outer routes.

TABLE I
Comparison of central canyons with outer radial roads

	CANYON SECTIONS	RADIAL ROADS
Traffic flows, daily means	5,000 - 12,000	12,000 - 33,000
Annual mean NO_2	> 30 ppb	23 - 29 ppb

The effects of street geometry are found on a smaller scale along the three multi-sited central streets (Magdalene St., Silver St., Parker St.), where changes in road width and architecture reflect the changes in NO_2 concentrations, Table II. Within the canyon sections, traffic emissions can become trapped and build-up leading to higher concentrations of NO_2. However, where carriageways broaden and buildings are set further back the natural ventilation increases and NO_2 levels are lower. This is evident near the river sites of both Magdalene St. and Silver St., where the added presence of the River Cam also improves dispersion (Fig.1). Air currents over flowing water will cause greater atmospheric turbulence.

TABLE II
Comparison of canyon and open sections within the same street:

STREET	Annual mean NO_2 in ppb		
	CANYON SECTION	OPEN SECTION	BACKGROUND
MAGDALENE ST.	33	27	19
SILVER ST.	32	25	18
PARKER ST.	36	31	16

For the other canyon, Parker St, one end is a congested high-walled junction leading to the bus station. This site records the highest NO_2 levels of any site in the survey, with high levels also found for other sites in streets around the bus station. As vehicle flows are low, the main sources of emissions are diesel-engined buses many of which are old and inefficient. At the other end of Parker St., although still a canyon, the road widens abruptly and there is a drop in NO_2 level. This effect is also

found for the one-way west-to-east route past Pembroke College where the site furthest on the left is within a much narrower canyon than the two sites on the right.

The benefits of a daytime-pedestrianisation scheme in reducing NO$_2$ levels is apparent in Trinity St (23 ppb), but has less impact at another very similar canyon site, Sidney St. (27 ppb) where light- and heavy-goods vehicles queue to leave the pedestrianised area at 10am each weekday.

Differences in road layout and traffic flow also appear to affect NO$_2$ levels along the radial routes (Fig.2) with generally the lowest levels at the outer boundaries of the city, 23-26 ppb, increasing towards the city centre, 26-32 ppb. The outermost sites occur where free-flow traffic conditions prevail, roads are broad and surrounded by open country. Whilst there is some queueing on these routes at peak travel times, as traffic waits to join the motorway and major trunk roads, the emissions are quickly dispersed. Towards the city end of the radial roads the topography changes with roads less wide and bounded by housing close to the road. Traffic also moves more slowly with the approach of major junctions.

A characteristic driving behaviour is found for the ring road sites, with speeds controlled by the frequency of junctions and roundabouts and where traffic levels are maintained throughout the day. NO$_2$ levels are similar to radial roads, 24-32 ppb, with the exception of one site on East Road which recorded a level of 37 ppb (Fig.2). This site faces the site of the automatic monitoring station where the road, although wide, is flanked by very high buildings and shows characteristics of a canyon street (Drye, 1996). The traffic is also heavy and continuous throughout the daytime with queueing and stop-start driving between closely-placed sets of traffic lights.

4.1.2 Background

NO$_2$ levels at background sites which are within a few metres of the canyon streets, are well below levels found at the roadside and are comparable to other more distant background sites (Figs.1 and 2). They appear to be little influenced by their location, showing that traffic-related pollution is contained within the canyon streets falling-off rapidly away from the roadside, Table II. The NO$_2$ concentrations from different background types (city centre, suburban, city rural) show little differences in value, around 1 - 3 ppb, compared to roadside levels differing by up to 20 ppb. Unlike the 1984/85 London survey (Clark and White, 1986) which depicts smoothly rising contours towards the urban centre, there is no evidence of elevated central background concentrations suggesting the presence of an urban pollution 'canopy'. This may be due to the relatively small size of the urban area in Cambridge or to the green 'corridors' which extend from the city's boundaries into the heart of the city. Their effect is to break up the density of the road network and are indeed a much admired part of Cambridge's urban landscape. The measurements of NO$_2$ in rural areas, at 10 to 20 km from Cambridge, are for a later period of the survey and are not yet available for comparison.

4.2. SPATIAL AND TEMPORAL VARIATIONS OF INDIVIDUAL EXPOSURE SETS

In Fig.3 the spatial and temporal variation of nitrogen dioxide levels are depicted for 50 sites for each two-week averaged exposure period across the two year survey. Sites are categorised by type, whether canyon, radial or background and for each exposure period an average NO_2 concentration is found for each category. A clear distinction is apparent for the three categories with central canyon sites having the highest concentrations. The background sites show a marked seasonal variation reaching a minimum in summer and a maximum in winter. This variation, which was noted in a previous survey of rural sites in the UK (Campbell, 1988), is not seen at the roadside being masked by the greater variability between successive exposure sets.

NO_2 in ppb
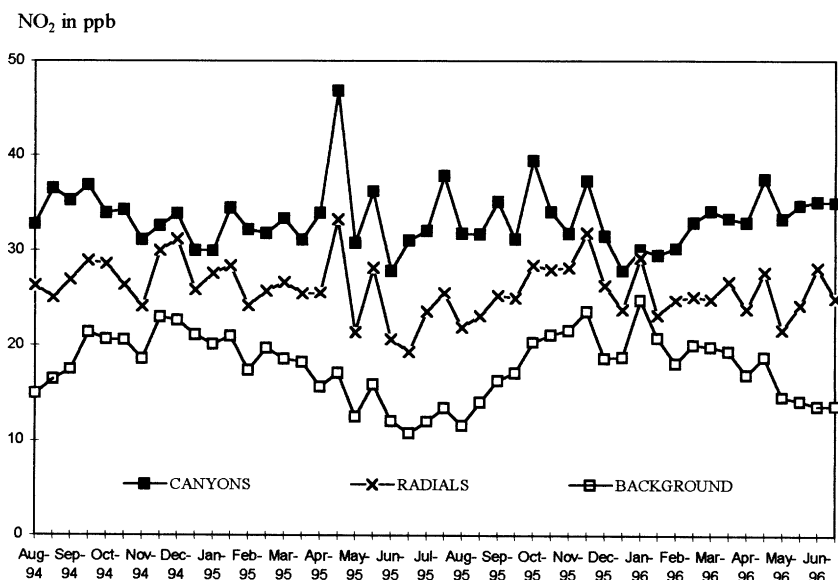
Fig. 3 Average nitrogen dioxide concentrations for three categories of sites (canyon, radial and background) for each exposure period within the survey 1994-1996.

The temporal behaviour across the data-set is extremely variable, particularly for the roadside sites, but there is evidence of a universal pattern for certain exposure periods, showing distinctive peaks or troughs across some or all site categories. One exposure period is particularly significant, 24April-8May1995, with very pronounced peaks for nearly all roadside sites. Meteorological conditions during the latter half of this period caused a photochemical pollution 'episode' which affected NO_2 levels at the roadside but not background levels. This is contrasted to a winter exposure set in mid-January 1996 with a spell of sustained very cold weather when roadside NO_2 levels appear less affected than levels at background and radial sites.

The 'episode' in May 1995 was examined using continuous data from the automated monitoring station and the weather station, both situated on East Road, (Fig.2). For the period 2-7May1995 the weather was very stable, temperatures were consistently high with wind speeds dropping to less than 5 metres sec^{-1} (Fig.4). The dispersion of traffic emissions was at a minimum and conditions were optimum for the photochemical build-up of secondary pollutants such as nitrogen dioxide and also ozone. Maximum 8-hour running averages for both nitrogen dioxide and ozone concentrations were recorded at the inner ring road monitoring station during this time (Fig.5). This was a synoptic-scale photochemical episode reported elsewhere at national monitoring sites (Broughton et al., 1997).

Whilst all roadside sites recorded high levels of NO$_2$, in the range 27-56 ppb compared to annual mean levels of 23-43 ppb, the maximum concentrations of over 50 ppb occurred within the city centre locations. The NO$_2$ concentrations for the three multi-sited canyon streets were compared for this exposure set to the annual mean concentrations, in terms of percentage change from annual mean values (Fig.6). The sites within each street were categorised in terms of street geometry as canyon, open and background. The effects of street geometry on atmospheric dispersion were evident with greater increases in NO$_2$ levels within the high-sided canyon sections, than in the open sections. Background sites appeared unaffected even though close to these roads. The propensity for the canyon streets to become heavily polluted during 'episodes' has been demonstrated and further study will be made to identify critical conditions in terms of meteorology and traffic volume. Although the May 1995 'episode' was widespread amongst the roadside locations, further examination of the data will determine whether more localised events occur affecting different categories of sites.

5. Summary

The results presented in this paper form a small part of the data available from the diffusion tube survey. The selection of both roadside and background sites according to their function within the urban structure has been shown to be justified by interpretation of results. It has been possible to explain spatial and temporal features of the data set in terms of urban site location, street topography and traffic behaviour. Marked differences in annual mean NO$_2$ levels have been found between inner and outer urban sites, with higher levels in central canyon streets, above 30 ppb, compared to outer radial sites, 23 to 29 ppb. The narrow road widths and slow-moving traffic of the canyon streets were contrasted to the wider and more open radial routes with free-flowing traffic. The influence of street geometry on NO$_2$ levels for central streets has been demonstrated, where canyon sections adjacent to open sections having the same traffic flow record higher concentrations.

The temporal behaviour across the data-set is extremely variable, particularly for the roadside sites, but there is evidence of a universal pattern for certain exposure
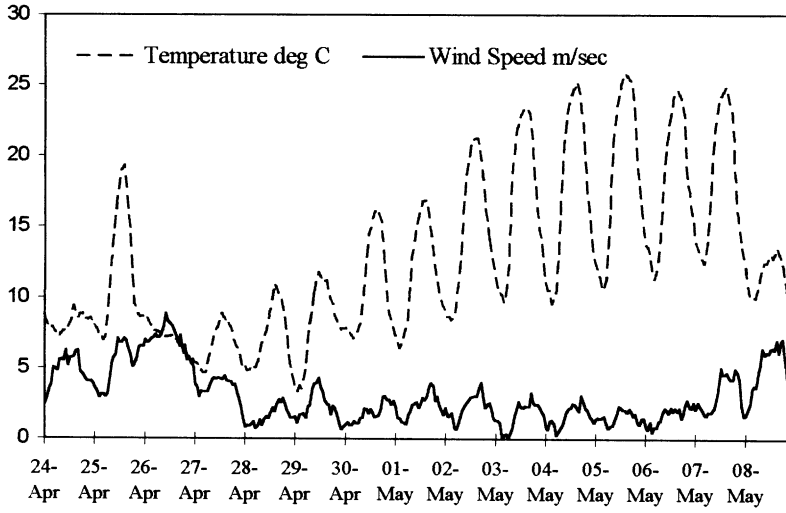
Fig. 4. East Road site: hourly mean temperature and windspeed for 24th April - 8th May 1995
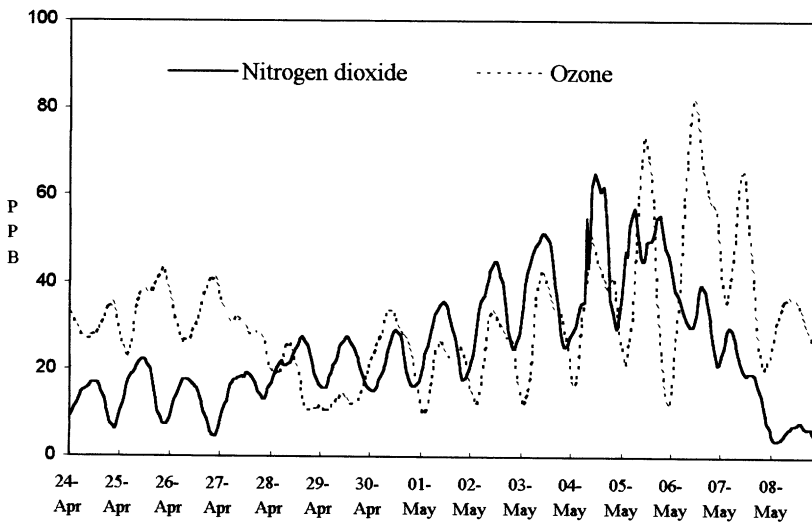
Fig. 5. East Road site: NO₂ and O₃ 8-hour running means for 24th April - 8th May 1995

Y axis = % change in NO$_2$ from annual mean concentration
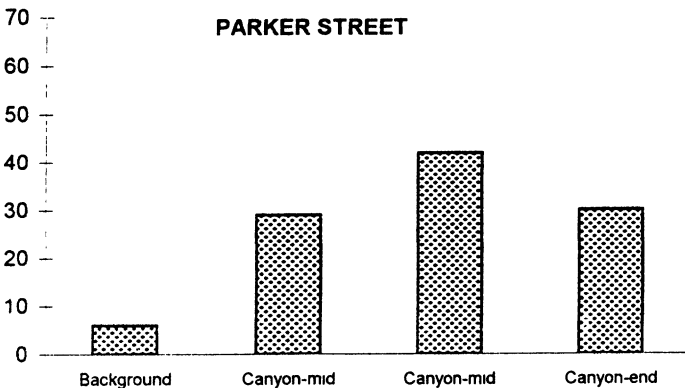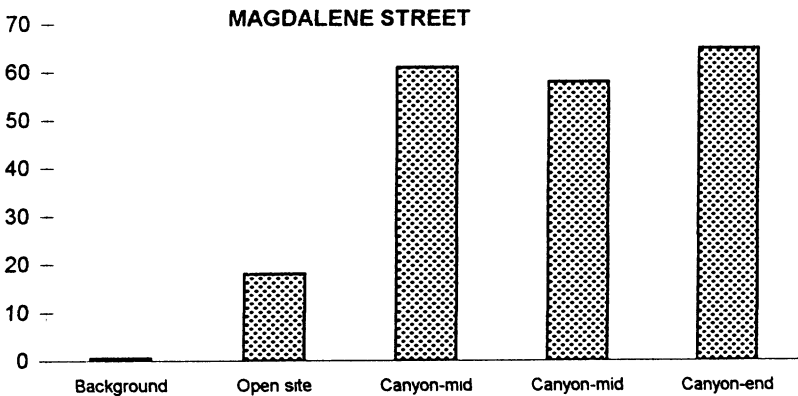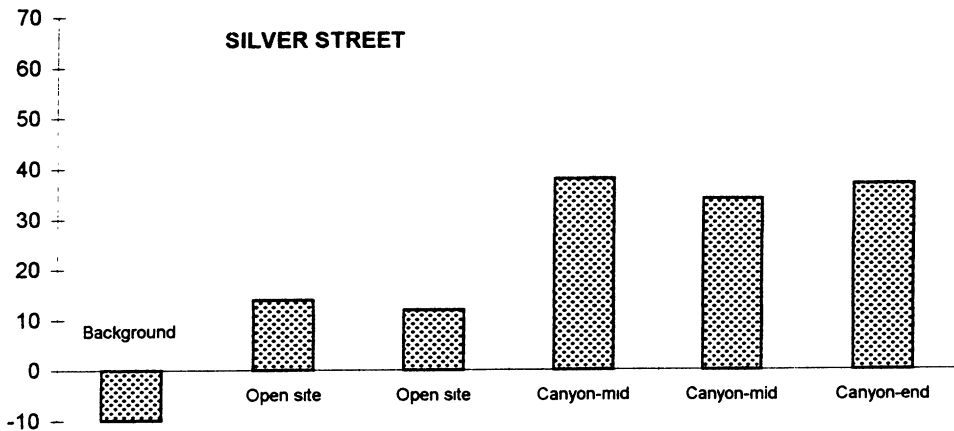
Fig. 6 Site effects on NO$_2$ concentrations within canyon streets: percentage change between 'episode' and annual mean levels.

periods, showing distinctive peaks or troughs across some or all site categories. Whilst all roadside sites were affected by a photochemical pollution 'episode', the greater potential for elevated NO_2 concentrations within the canyon sections was noted. Short-term meteorological events within the data set will be examined further.

The close proximity of low background levels of NO_2 to roadside 'hot-spots' is important for public exposure assessment. The variation in background levels across the urban landscape is very small and appears unrelated to location; whether central, suburban or outer city. Seasonal variations, not seen in roadside data, are clearly apparent in background data where highest concentrations occur in winter and lowest in summer. The summer 'episode' that caused high levels at the roadside did not appear to affect background levels.

The spatial and temporal trends in the data have shown the limited extent of the urban 'hot-spots' and the rapid dilution of nitrogen dioxide concentrations away from the roadside to reach background levels which are consistent across the urban landscape. Where background levels are low, public exposure to high levels of nitrogen dioxide can be expected to be confined to locations at, or very close to, these urban 'hot-spots'. High levels of roadside NO_2 found around the bus station area are a cause of concern for passengers waiting at roadside bus stops who will be exposed to exhaust fumes. Monitoring methods capable of greater time resolution would be needed to investigate significant levels of personal exposure within these locations.

Acknowledgements

References

Atkins, D. H. F., Sandalls, J., Law, D. V., Hough, A.M. and Stevenson, K. J.: 1986, Report AERE R12133, HMSO, London.

Bower, J. S., Lampert, J. E., Stevenson, K. J., Atkins, D. H. F. and Law, D. W.: 1991, *Atmos. Environ.*, **25B**, 255-265.

Broughton, G. F. J., Bower, J.S., Willis, P. G., Clark, H.: 1997, Air Quality in the UK: 1995. AEA Technology, National Environmental Technology Centre, Culham, Oxfordshire.

Cambridge City Council: 1991, *Cambridge Local Plan*, Planning Dept., Guildhall, Cambridge, UK.

Cambridge City Council: 1994, *Cambridge Air Quality Survey 1992/93*, Environmental Health & Protection Service, Cambridge, UK.

Cambridgeshire County Council: 1993, *Traffic Monitoring Report 1992*, Transportation Dept., Shire Hall, Cambridge, UK.

Campbell, G. W: 1988, *Environ. Pollut.*, **55**, 251-270

Campbell, G. W., Stedman, J. R. and Stevenson, K.: 1994, *Atmos. Environ.*, **28**, 477-486.

Clark, R. G. and White, J. R.: 1986, *Environmental Health Aspects of the 1984/85 London Diffusion Tube Survey*, London Environmental Supplement No.14, (former) Greater London Council, UK.

Council of the European Communities: 1985, Directive on air quality standards for nitrogen dioxide. (85/203/EEC). *Off J of European Communities* 1985; L87: 1-7.

Den Boeft, J., Eerens, H.C., den Tonkelaar, W.A.M., Zandveld, P.Y.J.: 1996, *The Science of the Total Environment*, **189/190**, 321-326.

Department of the Environment: 1996, *Digest of Environmental Protection and Water Statistics No 18, 1995*, HMSO, London.

Drye, T.: 1996, Paper presented to "Urban Air Quality - Monitoring and Modelling" Conference, 11-12 July 1996, Univ. of Herts, Hatfield, UK.

Gair, A. J., Penkett, S. A., Oyola, P.: 1991, *Atmos. Environ.*, **25A**, 1927-1939.

Hargreaves, K. J.: 1989, PhD Thesis, University of Nottingham.

Hewitt, C. N.: 1991, *Atmos. Environ.*, **25B**, 429-434.

Laxen, D. P. H. and Noordally, E.: 1987, *Atmos. Environ.*, **21**, 1899-1903.

Melia, R. J. W., Florey, C. du V., Darby, S. C., Palmes, E. D. and Goldstein, B. D.: 1978, *Atmos. Environ.*, **12**, 1369-1381.

Palmes, E. D., Gunnison, A. F., Dimattio, J. and Tomczyk, C.: 1976, *Am. Ind. Hyg. Assoc. J.*, **37**, 570-7.

Palmes, E. D., Tomczyk, C. and Dimattio, J.: 1977, *Atmos. Environ.*, **11**, 869-872.

QUARG: 1993, Urban Air Quality in the United Kingdom, QUARG, London.

UK Department of Health: 1993, *Oxides of nitrogen*, Third Report of the Department of Health's Advisory Group on Medical Aspects of Air Pollution Episodes, HMSO, London.

UK Department of Health: 1995, *Asthma and Outdoor Air Pollution*, Committee on the Medical Effects of Air Pollution, Department of Health, HMSO, London.

World Health Organisation: 1987, *Air Quality Guidelines for Europe*, WHO Regional Publications, European Series 23, Copenhagen.

AIR QUALITY AND MONITORING STRATEGY IN THE HELSINKI METROPOLITAN AREA, FINLAND

K. HÄMEKOSKI and T. KOSKENTALO

Helsinki Metropolitan Area Council (YTV), Environmental Office
P.O. Box 521, 00521 Helsinki, Finland

Abstract. The Helsinki Metropolitan Area Council (YTV) is responsible for air quality monitoring in the Helsinki area. Air quality has been monitored periodically since the late 1950s. An automatic SO_2 monitoring network was constructed in 1975 and TSP measurements were added in 1978. Since then the network has been expanded and currently five automatic multicomponent stations form the basis of the network monitoring SO_2, NO, NO_2, CO, PM_{10} and O_3 concentrations. Manual TSP and PM_{10} measurements are also conducted. Mobile monitoring units are also being used as well as special measurement campaigns. The effects of air pollution on nature are studied in bioindicator monitoring. An air quality index is used in order to inform the public of the current air quality situation. Changes in air quality are reflected in monitoring strategy. SO_2 concentrations have decreased in the past two decades. Annual averages in 1995 were at or below 5 $\mu g/m^3$. Traffic is the major source for pollutants even though catalytic converters have lowered traffic emissions somewhat. The highest annual average NO_2 concentration at an urban site was 49 $\mu g/m^3$ in 1995, and there has been no clear change in NO_2 levels. There has been a decreasing trend in CO concentrations. Maximum annual TSP and PM_{10} averages in 1995 were 92 and 32 $\mu g/m^3$, respectively. The highest average lead concentration was 0.01 $\mu g/m^3$. Elevated concentrations are experienced from time to time. During the spring daily TSP and PM_{10} concentrations can go up to around 300 and 150 $\mu g/m^3$, respectively. This is caused by resuspension mainly due to street sanding. Also a major winter NO_2 episode occurred in December 1995. The highest hourly NO_2 concentrations reached 400 $\mu g/m^3$.

1. Introduction

Helsinki is situated by the Baltic sea at latitude 60°N. The population in the Helsinki Metropolitan Area is 850,000 and the area is 743 km². The mean temperature is -6.2°C in February, 17.2°C in July, and 5.2°C annually. Because of the Gulf stream the climate is warmer than elsewhere at these latitudes. Daylight ranges from 20 h in June to 6 h in December. The area is situated on a flat plain in the boreal vegetation zone.

In general, ambient air quality is reasonably good in the Helsinki area in comparison with several other cities of the same size around Europe (van Zantvoort *et al.*, 1995). There is some evidence (Pönkä, 1990), however, that even these low pollutant levels may cause adverse health effects especially during the cold wintertime. This has also been taken into account in the strict new air quality guidelines in Finland (Sarkkinen *et al.*, 1993, Table I). More research work related to health effects is currently being conducted. PM pollution and occasional high NO_2 concentrations during temperature inversions in winter are exceptions to the relatively good ambient air quality situation in the Helsinki Metropolitan Area.

In this study, we describe the air quality situation and air pollution monitoring strategy in the Helsinki Metropolitan Area.

TABLE I

Air quality guide values in Finland ($\mu g/m^3$, CO mg/m^3)

Pollutant	Averaging time	Guide value	Allowed exceedances
SO_2	hour	250	1 %/month
	day	80	1/month
NO_2	hour	150	1 %/month
	day	70	1/month
TSP	day	120	2 %/year
	year	50	-
PM_{10}	day	70	1/month
CO	hour	20	-
	8 hour	8	-

2. Monitoring

Air quality has been monitored periodically in the Helsinki area since the late 1950s. An automatic SO_2 monitoring network consisting of 5 stations was established in 1976 by the city of Helsinki. High volume manual TSP measurements were started in 1978 at 4 sites. Since 1983, the monitoring has been extended to cover the whole metropolitan area by the Helsinki Metropolitan Area Council (YTV). CO measurement were added in 1985, NO, NO_2 and O_3 in 1986. In 1987, high volume manual PM_{10} measurements were started, and in 1991 continuous PM_{10} measurements were added to the regime. By 1990 thirteen fixed air quality monitoring sites were in use. Since then the number of fixed monitoring sites has been cut down.

Currently five automatic multicomponent stations form the basis of the air quality monitoring network (Figure 1) monitoring SO_2, NO, NO_2, CO, PM_{10} and O_3 concentrations. Manual TSP and PM_{10} concentrations are measured at 6 sites. Pb analyses are performed on TSP and PM_{10} filters at 2 sites. Three mobile stations are also being used monitoring air quality at a given site from 6 months to 1 year. The data are published as monthly and annual reports and as research reports. Air quality indices are also calculated.

Passive samplers are used to assess NO_2 levels at sensitive locations, and levels of different hydrocarbons have been sampled in the centre of Helsinki. YTV has also studied interaction between air quality and corrosion in the area.

Air quality monitoring is also conducted in order to validate dispersion models and there is wide collaboration between YTV and the Finnish Meteorological Institute in refining citywide dispersion models for CO and NO_2 (Kukkonen et al., 1995).
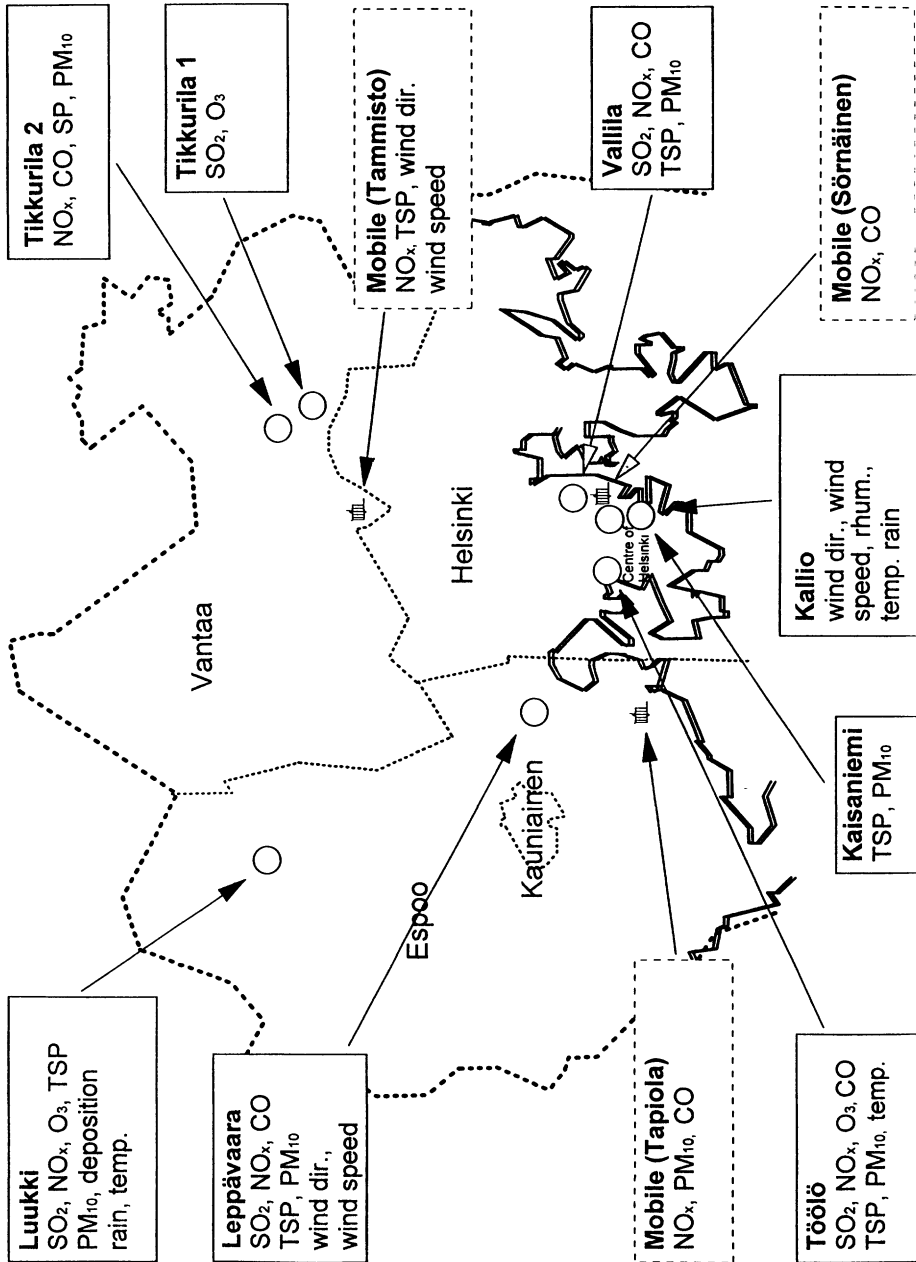
Fig 1. Current air quality monitoring network in the Helsinki Metropolitan Area.

TABLE II

Stationary and mobile source emissions of SO_2, NO_x, PM and CO in the Helsinki Metropolitan Area in 1995

Source		SO_2		NO_x		PM		CO	
		t	%	t	%	t	%	t	%
Energy production	Major power plants	7800	87	9700	37	1200	52	X	X
	Small point sources	430	5	250	1	140	6	X	X
	Area sources	230	3	330	1	50	2	X	X
Road traffic		200	2	13900	53	900	39	41300	99
Aircraft and ships		250	3	2000	8	30	1	400	1
Total		8900	100	26200	100	2300[Y]	100	41700	100

X = unknown, estimated to be small
Y = resuspended particles not included

Gradual changes caused to nature by air pollution are monitored with the use of bioindicators. There are a hundred permanent observation sites in naturally growing spruce and Scots pine forests. At these sites needle losses and tree damages, species diversity of bark-living lichens, and the abundance of certain lichens and algae have been assessed. Pine needles have been analyzed for their sulphur and nutrient levels. Heavy metal and ash deposition have been estimated from moss samples as well as the acidity, nutrient levels, and concentrations of certain heavy metals, including cadmium and lead from humus. The current monitoring programme consist of the determination of needle loss and observations of coniferous trees, epiphytic lichens and needle sulphur concentration every other year.

3. Air Quality

3.1 EMISSIONS

The emissions from energy production have decreased in recent years, most notably those of SO_2 due to increased use of district heating, lower sulphur content in fuels, and effective desulphurization of emissions (Figure 2). About 90 % of households in the Helsinki area have district heating.

Traffic is nowadays a major source of several pollutants (Table II) even though increased use of catalytic converters and reformulated fuels have lowered traffic emissions slightly. Only unleaded gasoline is used. The downward trend in both stationary and mobile source emissions is expected to continue in the future with the exception of CO_2 emissions.
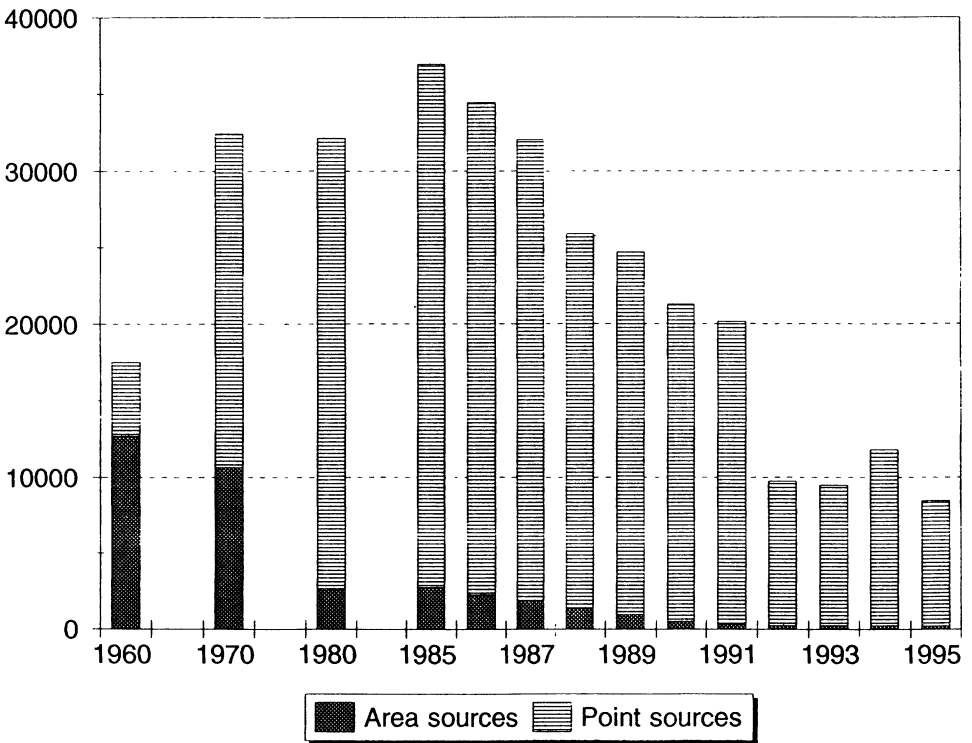
Fig. 2. SO_2 emissions in the Helsinki Metropolitan Area in 1960-1995 (t).

Primary particulate matter (PM) in the Helsinki area originates mainly from large power plants and traffic, because there is no heavy industry in the area (Table II). Particulate matter (PM) emissions from power plants have decreased a lot since the 1980s, which is mainly due to the introduction of effective desulphurization processes also removing PM from the emissions. In addition, the number of area and small point sources and the total emissions from these sources have decreased in recent years. There has also been a slight decrease of direct particle emissions from traffic due to new emission control measures.

As a result of street sanding and salting and the use of studded tires during wintertime resuspension from paved roads is the main source of ambient PM in the Helsinki area. However, there are no proper quantitative estimates available on these indirect particulate emissions. Although photochemical activity can also produce particles from gaseous pollutants in a northern climate, the data suggest that this formation has only a minor impact on ambient PM mass concentrations. PM concentrations are low during photochemically active summer season (Figure 5).

3.2 AVERAGE CONCENTRATIONS

Average ambient air quality is relatively good in the Helsinki Metropolitan Area in comparison with many European cities (van Zantvoort et al., 1995). Traffic is nowadays a major source for concentrations of different pollutants at breathing level because of the low emission height. SO_2 concentrations have noticeably deceased in the past years and are currently low (Figure 3a). While there is a slight decrease in NO concentrations, there is no clear change in NO_2 levels (Figure 3b). Nitrogen oxides occur mainly in the form of NO in emission, and NO is oxidized to NO_2 by O_3. There seem to be no direct correlation between NO_x concentrations and NO_2 concentrations, because NO_2 concentrations are mainly controlled by O_3 concentrations. There has been a decreasing trend in CO concentrations as a result of the increased use of three way catalysts in cars and the use of reformulated fuels (Figure 3a). No local net O_3 formation has been observed as the Helsinki area acts as an O_3 sink (Hämekoski and Lahdes 1990). Average O_3 concentrations are increasing (Figure 3a), most probably due to decreasing NO concentrations. Average lead concentrations are remarkably low due to unleaded petrol. The highest average lead concentration was 0.01 $\mu g/m^3$.

PM pollution is considered as a major air pollution problem even though annual average concentrations of total suspended particulate matter (TSP) have declined in recent years (Figure 3c). The corresponding national guidelines were exceeded in urban traffic environments, and at other sites the concentrations were just below the guidelines. Several measures have been taken in the Helsinki Metropolitan Area in order to solve the air quality problems caused by large indirect PM emissions from the surfaces of paved roads. These measures include:

- faster cleaning of streets after the melting of snow
- improved cleaning methods (e.g. vacuum street sweepers)
- increased use of gravel instead of sand as antiskid material
- use of washed sand and gravel
- reduction in total amount of antiskid material used in winter
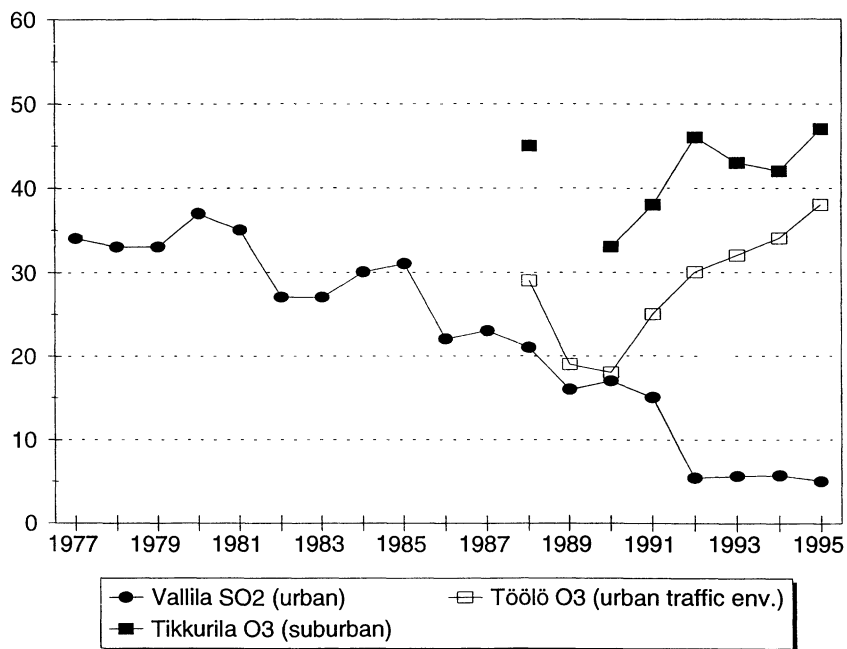
Fig. 3a. Annual averages of SO_2, CO, O_3 concentrations ($\mu g/m^3$, CO: mg/m^3).
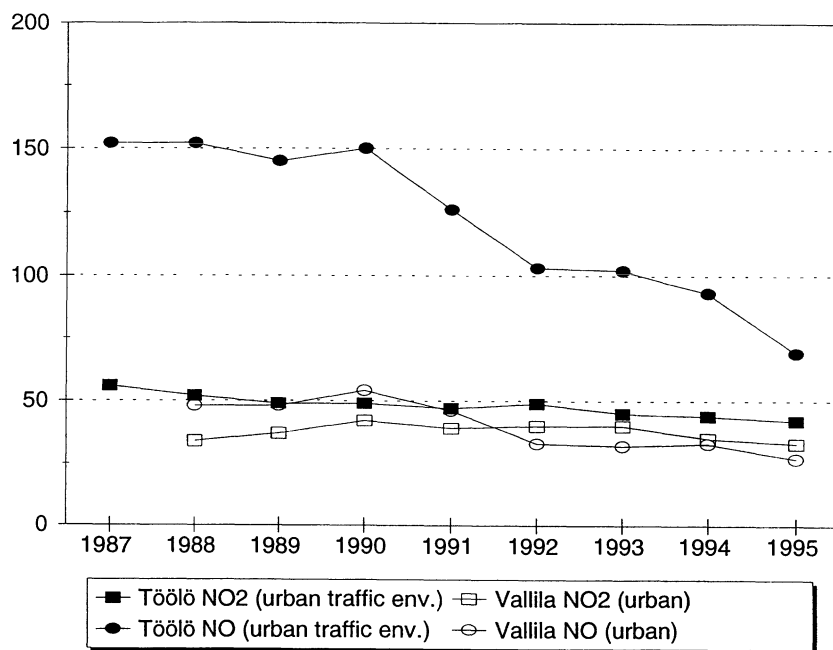
Fig. 3b. Annual averages of NO and NO_2 concentrations ($\mu g/m^3$).
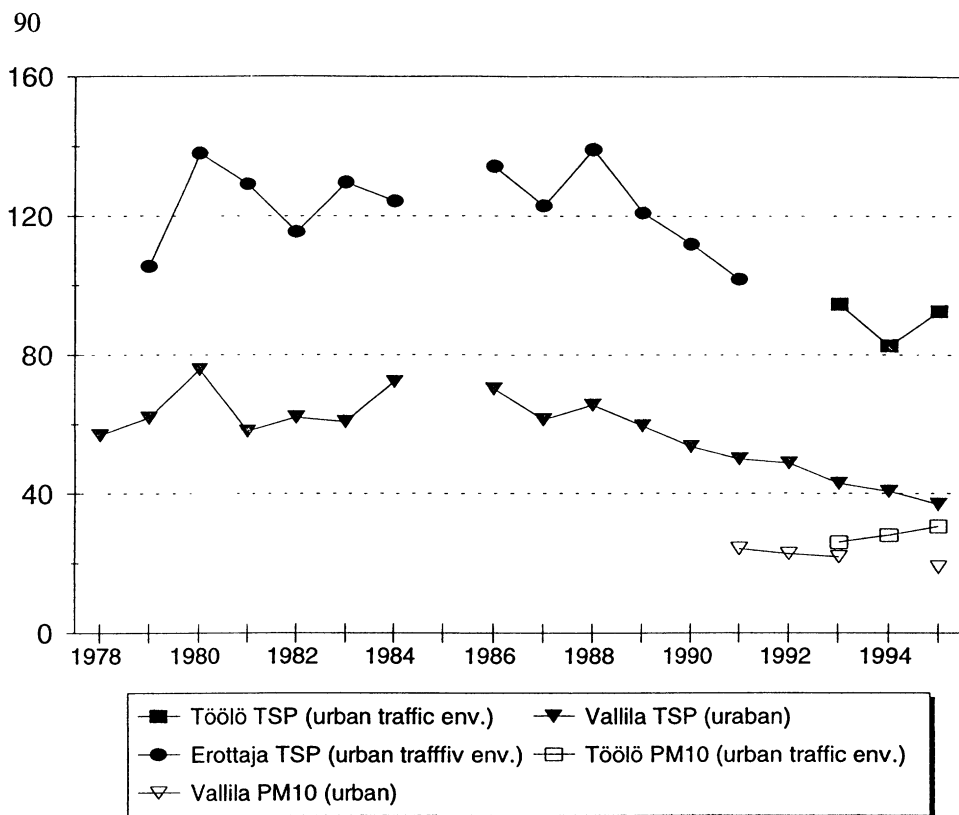
Fig. 3c. Annual averages of TSP and PM_{10} concentrations ($\mu g/m^3$).

In addition, some national measures have probably reduced the indirect PM emissions caused by traffic. The mass of studs in tyres has been reduced and the period for permitted use of studded tyres has become shorter. Campaigns have also been launched to inform maintenance personnel about the necessity of effective street cleaning.

These control measures probably explain the recent downward trend in annual TSP concentrations in the Helsinki Metropolitan Area, but they do not seem to have had a similar effect on annual PM_{10} (PM less than 10 μm aerodynamic diameter) concentrations (Figure 3c) or on episodic high PM_{10} peaks in spring.

Annual average PM_{10} concentrations have been relatively low in recent years and there has not been any clear downward trend as with TSP. However, short-term PM_{10} concentrations have been relatively high. A comprehensive research programme was started in the Helsinki area in spring 1996 by YTV, the Finnish Meteorological Institute and the University of Kuopio in order to study the chemical composition and size distribution of PM_{10}, and to estimate the contribution of different sources to ambient PM_{10} concentrations. The most important question in future epidemiological studies is, whether the episodic high PM_{10} levels caused mainly by resuspended particles are as harmful to human health as currently estimated for PM_{10} pollution in general (World Health Organization, 1995).

Resuspension of road dust dominates ambient TSP concentrations in the Helsinki area and primary emissions from stationary and mobile sources have only small effects. It was estimated in 1987 (Laukkanen, 1990) by calculating PM/SO_2 ratios in emissions and concentrations, that the average contribution of energy production to the TSP concentrations was less than 5 %. Similarly, the contribution of direct traffic emissions was estimated by using PM/Pb ratios and it was less than 10 % (Laukkanen, 1990). Present indirect evidence (Hämekoski *et al.*, 1995) suggests that PM_{10} levels are also caused mainly by resuspension.

3.3 EPISODES

PM pollution and fairly high NO_2 concentrations especially during temperature inversions in winter make exceptions to the relatively good ambient air quality situation in the Helsinki Metropolitan Area. A major winter NO_2 episode occurred in December 1995. The highest hourly NO_2 concentrations reached 400 $\mu g/m^3$ and CO concentrations 17 mg/m^3 (Figure 4). Research work is currently being conducted in order to analyze the causes of high episodic NO_2 concentrations.

Fig. 4. Episode in December 1995 in Töölö (urban traffic environment).

High TSP and PM_{10} concentrations occur especially in spring (Figure 5). The 24-hour average TSP concentration increases to above 300 $\mu g/m^3$ and 24 hour PM_{10} concentrations reach the level of 150 $\mu g/m^3$. When the measured concentrations were compared to the PM_{10} levels used in the newest World Health Organization (1995) health effect assessment, the three-day-average PM_{10} concentration of 50 $\mu g/m^3$ was exceeded on six separate occasions and 100 $\mu g/m^3$ was exceeded once in 1994. The corresponding figures in 1995 were 16 and one exceedances, respectively.

The PM_{10} concentrations of 50 and 100 µg/m^3 are regarded as PM pollution levels, which cause a 5 - 10 % increase in daily mortality, a 10 - 20 % increase in hospital admissions for respiratory conditions, and a 25 - 50 % increase in symptom exacerbations, and a 35 - 70 % increase in bronchodilator use among asthmatic subjects.
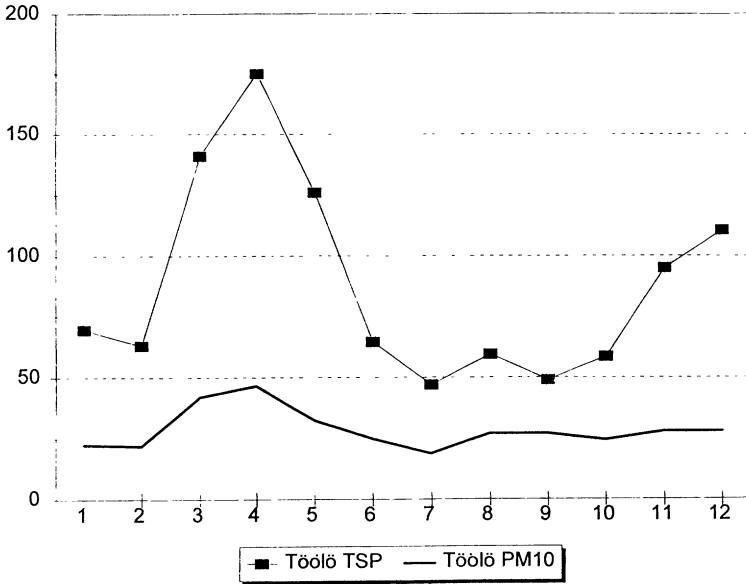
Fig. 5. Monthly averages of TSP and PM_{10} concentrations (µg/m^3) in Töölö (urban traffic environment) in 1993-1995.

However, it is currently unknown how harmful to human health is the relatively high contribution of resuspended particles to these PM pollution episodes. Present indirect evidence (Hämekoski *et al.*, 1995) suggests that episodic high PM_{10} levels are caused mainly by resuspended particles from surfaces of paved roads. The recent results of Timonen *et al.* (1996) suggested that the higher-level PM_{10} pollution in spring may not affect the lung functions of primary school children with chronic respiratory symptoms similarly to the lower-level PM_{10} pollution in winter. It has been hypothesized that this difference may have been due to a lower toxicity of resuspended particles than combustion-related particles, which needs to be tested in future epidemiological studies.

3.4 AIR QUALITY INDEX

Air quality index (AQI) was developed in 1993 in order to inform the public in laymen's terms about the current state of the air pollution situation. It was decided that the AQI should be simple to calculate, clear enough for the public and have a sound scientific basis. Even though the AQI is mainly based on acute health effects, long term effects on nature and man-made structures are also considered.

The pollutants included in the AQI are CO (1 and 8 h), NO_2 (1 and 24 h), SO_2 (1 and 24 h), O_3 (1 h) and PM_{10} (24 h). Sub-indices are calculated hourly for all pollutants and for the given hour the highest sub-index becomes the AQI. Moving averages are used for 24 and 8 hour averages. The AQI incorporates a segmented linear function consisting of 3 breakpoints (Table III) joined by straight line segments. The index level of 100 is based on new guidelines in Finland (Sarkkinen *et al.* 1993, Table I). The guidelines are based on the latest evidence of the health effects of air pollution. The allowed exceedances are not taken into account. The WHO recommendation (1987) is used for ozone. Each AQI index category is associated with characterisation of health and other impacts as well as a colour and descriptive word (Table IV). Combined effects of different air pollutants are not included as there is not enough scientific evidence for this.

TABLE III
Breakpoints of the air quality index in the Helsinki Metropolitan Area
($\mu g/m^3$, CO: mg/m^3)

Index	CO 1 h	CO 8 h	NO_2 1 h	NO_2 24 h	SO_2 1 h	SO_2 24 h	O_3 1 h	PM_{10} 24 h
50	4	4	35	35	40	40	75	35
100	20	8	150	70	250	80	150	70
200	40	16	300	140	500	160	300	140

TABLE IV
Definition of index

Index	Colour	Air quality	Health effects	Other effects (long term)
0 - 50	green	good	no effects	slight effects on ecosystems
51 - 100	yellow	fair	adverse effects improbable	marked effects on vegetation, effects on materials
101 - 150	orange	passable	adverse effects possible on sensitive individuals	marked effects on vegetation, effects on materials
151 -	red	poor	adverse effects possible on sensitive subpopulation	marked effects on vegetation, effects on materials

The AQI has been routinely calculated since 1993 for the urban traffic environment in the centre of Helsinki (Töölö station) and for suburban environments (a combination of the Tikkurila and Leppävaara stations). AQIs are published in a newspaper, on local radio and on colour on-line display in Helsinki. With very few exceptions the highest index values are found in the centre of Helsinki. The highest AQI values in 1995 were caused by 24 hour NO_2 concentrations. The highest recorded index value was 374 in the centre of Helsinki and 292 in suburban areas.

3.5 EFFECTS ON NATURE

According to a bioindicator study (Mäkinen and Pihlstöm, 1995) despite clearly decreased levels of local sulphur and particulate emissions the condition of forests, judged by different indicator methods, has not improved substantially. However, many single bioindicators show positive trends: the concentration of lead in mosses and the sulphur content of needles generally decreased during the period 1988-1993.

The needle loss of conifers increased somewhat during 1988-1993. The magnitude of change is not great, but the trend suggests a persistent slight stress due to air pollution. The distribution of epiphytic lichens reflects long term air pollution zones particularly well. Many species are absent in most parts of the city of Helsinki and in smaller areas elsewhere in the metropolitan area. In the very centre of Helsinki the recolonization of the former lichen desert has occurred, first on broadleaved tree trunks and in the last years also on the more acidic bark of pines. The abundance of epiphytic green algae increased in 1990-1991, probably reflecting mild winter weather and high nitrogen emissions.

Nutrient levels (Ca, K, Mg, Mn) in pine needles have remained rather stable. No leaching, indicating severe acidification, has been detected in the most polluted areas. Due to the role of soil acidification processes in forest decline many soil variables are regularly monitored. No clear large scale decrease in the total amount of available nutrients or slowing down of decomposition has yet been detected. A relative acidification reflected in low values of pH, the base saturation degree and the calcium-aluminium ratio is not concentrated in the central polluted area only.

4. Conclusions

Average air quality has improved in the Helsinki area as far as SO_2, Pb, CO and NO concentrations are concerned. Particulate matter pollution and NO_2 levels especially during temperature inversions in winter make exceptions to the relatively good ambient air quality situation.

The changing air quality situation has also been reflected in air quality monitoring. The number of SO_2 monitoring sites and the number of Pb analyses have been reduced. Current monitoring strategy will concentrate monitoring the air quality in multicomponent fixed sites with additional information collected with mobile units, passive NO_2 samplers, HC measurement campaigns and bioindicator monitoring. The components monitored are directed towards monitoring air pollution caused by traffic. Close collaboration with dispersion modelling work covering the whole metropolitan area has been found useful.

Special attention is currently being paid to particulate matter concentrations and NO_2. Recently started studies on chemical composition and size distribution of ambient PM_{10} in the Helsinki area and associated epidemiological studies are expected to produce new information on the relative harmfulness of particulate matter pollution originating from different sources. This kind of information should help decision-makers in directing PM emission cuts at different sources in a cost-effective way. If resuspended PM_{10} proved to be less harmful than combustion-related PM_{10}, there might be influences on national and international PM_{10} guidelines and standards. Also the behaviour and sources of NO_2 concentrations in inversion situations will be studied in detail.

As the public is increasingly concerned about environmental matters, a simple, understandable air quality index has been developed and found to be a very useful tool for presenting and interpreting air quality data in the Helsinki Metropolitan Area.

Acknowledgements

References

Hämekoski, K. and Lahdes, R.: 1990, *Surface Ozone in the Helsinki Area, Southern Finland*, Tropospheric Ozone and the Environment, Air and Waste Management Association, USA, 664-672.

Hämekoski, K., Aarnio, P., Koskentalo, T., Laukkanen, T.: 1995, *The Behaviour of Particulate Matter in the Northern Climate of the Helsinki Metropolitan Area, Finland,* Particulate Matter: Health and Regulatory Issues, Air & Waste Management Association, USA, 653-663.

Kukkonen, J., Karppinen, A., Härkönen, J., Valkonen, E., Rantakrans, E., Haarala, S., Jalkanen, L., Koskentalo, T., Elolähde, T., Aarnio, P. and Laurikko, J.: 1995. *The influence of traffic on urban air quality - model predictions and their comparison to measurements.* Proc. of the 10th World Clean Air Congress, Espoo, Finland. The Finnish Air Pollution Prevention Society, Helsinki, paper 249

Laukkanen, T.: 1990, *Kokonaisleijuma Helsingissä [TSP in Helsinki]*. Licentiate Thesis. Helsinki University of Technology, Espoo, 129-130

Mäkinen, A., Pihlström. M.: 1995, *Biomonitoring the Effects of Air Pollution on Forest Ecosystem in an Urban Area, Helsinki, Finland,* Proc. of the 10th World Clean Air Congress, Espoo, Finland, The Finnish Air Pollution Prevention Society, Helsinki, paper 414

Pönkä, A.: 1990, *Arch. Environ Health* **46**:262-270.

Timonen, K.L., Pekkanen, J., Salonen, R.O.: 1997, *Eur. Respir. Rev.* (submitted).

Sarkkinen, S., Lumme, E., Salonen, R.O., Säynätkari, T. (eds): 1993, *Ilmanlaadun ohjearvotyöryhmän mietintö [Report of the Working Group on Air Quality Guidelines],* The Ministry of the Environment, Finland, 186 pages.

van Zantvoort, E.D., Sluyter, R.J., Larssen, S. (eds.): 1995, *Air Quality in Major European Cities, Part II: City Report Forms.* National Institute of Public Health and the Environment, the Netherlands, 507 pp.

World Health Organization (WHO): 1995, *Update and Revision of the Air Quality Guidelines for Europe,* 29 pages

ON-SITE COMPARISON OF CANISTER AND SOLID-SORBENT TRAP COLLECTION OF HIGHLY VOLATILE HYDROCARBONS IN AMBIENT ATMOSPHERES

A. CASTELLNOU [1], N. GONZALEZ-FLESCA [2] and J.O.GRIMALT [1]

[1] *Department of Environmental Chemistry (C.I.D.-C.S.I.C.), Jordi Girona,18, 08034-Barcelona. Catalonia. Spain.* [2] *INERIS, Parc Technologique Alata, B.P. 2, 60550 Verneuil-en-Halatte, France.*

Abstract. A field experiment for the comparison of the efficiency of canisters and adsorption multibed tubes for sampling atmospheric highly volatile hydrocarbons at ppbv levels is described. The canister was passivated by the Summa process and the adsorption tubes were filled with Carbotrap C, Carbotrap B and Carbosieve S-III. The sampling with the adsorption tubes was performed at ambient temperature and at -10°C. The highest concentrations were generally obtained with canisters but these results are very similar to those obtained with refrigerated multibed adsorption tubes. Both methods appear to be equivalent for most of the highly volatile hydrocarbons encountered in moderately polluted urban areas. In contrast, sampling with ambient temperature tubes provides lower concentrations. This study has also shown that K_2CO_3 drying efficiently removes humidity from air samples allowing the obtention of reliable concentration data on highly volatile hydrocarbons at ppbv levels. These drying tubes can easily be re-conditioned and tested for blanks and memory effects, which greatly facilitates the control of external contamination and sample cross-contamination.

1. Introduction

It is generally accepted that volatile organic compounds (VOC) are responsible for the increase of tropospheric photochemical pollutants, including ozone, through chemical reactions involving solar radiation and nitrogen oxides. VOC monitoring in urban and semi-urban areas is very relevant for the exposure of human population to these pollutants, including those generated in secondary reactions.

Many VOC monitoring techniques have been used in atmospheric studies. Their reliability depend on the target compounds studied, their range of concentration, molecular weight and the occurrence of other possible interfering pollutants. Both whole-air sampling in canisters and adsorptive sampling by pumping air through sorption cartridges have been widely used for the measurement of light hydrocarbons in the atmosphere. Nevertheless, few studies comparing both sampling techniques have been conducted.

Collection of whole-air samples in electropolished stainless steel containers has been used in the analysis of volatile organic compounds as an alternative to the solid adsorbent-based methods (see recent reviews in Camel and Caude, 1995, and Cao and Hewitt, 1995). The principal advantages of canisters in ambient air VOC monitoring are the flexibility for processing multiple samples from a single canister, the lack of sample

permeation or photo-induced chemical effects and their possible reuse after clean-up. The properties of canisters for VOC sampling have improved after passivation by the Molectric Summa process, which has increased sample integrity and storage stability, providing good recoveries for a wide range of compounds, including those at ppmv (laboratory, industrial, chemical, or other waste products) to pptv concentrations (ambient air).

Stainless steel canisters have been used for measuring VOC concentrations greater than 10 ppmv in gas matrices (Pleil and Stroupe, 1994). Moreover, the usefulness of canisters for VOC measurement at lower concentrations has been evaluated in the analysis of halocarbons -from ppbv (Oliver et al., 1986; Jayanty, 1989) to pptv levels (Harsch, 1980; Müller and Oehme, 1990; Rudolph et al., 1990)-, C_2-C_{10} VOCs -down to the sub-parts-per-billion range (Farmer et al., 1994)-, polar VOCs -at ppbv levels (Kelly et al., 1993)- and non-polar toxics from hazardous waste incineration (Gholson et al., 1989). A comprehensive study on the applicability of canisters to a large number of volatile organic compounds at ppbv levels has recently been reported (Brymer et al., 1996).

On the other hand, the solid adsorbent materials are designed to specifically trap organic vapors from atmospheric samples without enriching water and carbon dioxide (Rudolph et al., 1990; Camel and Caude, 1995; Cao and Hewitt, 1995). Among these, the combination of single adsorbents in multiadsorbent traps has recently received specific attention. This modification allows the integration in one single system of the advantages of the individual adsorbents, widening the number of compounds that can be collected and desorbed in one single tube (Helmig and Greenberg, 1994). One of the major advantages of the adsorbent method concerns the isolation of the compounds of interest from possible interferent species. The main disadvantages involve interferences with artifacts from the adsorbent materials, breakthrough during collection and incomplete desorption. The omnipresence of ozone as well as the high rate constants of the ozonolysis reaction of unsaturated hydrocarbons sometimes leads to the question of the possibility of in situ reactions of analytes during collection (Hoffmann, 1995).

The diverse properties of both sampling methods may give rise to significant biases in the description of airborne VOC (Bayer, 1994). Some authors have used both sampling techniques in studies of human VOC exposure (Michael et al. 1990). However, the differences urge to perform the quantitative comparison of the results obtained with both sampling methods in field studies. In this respect, Berkley et al. (1991) compared the field determination of airborne toxic organic vapors in passivated canisters and in a portable gas chromatograph, concluding that the combination of both methods offers a synergetic approach to source assessment measurements.

The present work is aimed at developing an experiment of field comparison in a low polluted site where VOC are found at ppbv levels. The canister used in this evaluation was passivated by the above mentioned Summa process. The adsorption tubes consisted of a multibed system composed of Carbotrap C, Carbotrap B and Carbosieve S-III. The influence of temperature in adsorptive sampling has also been considered. Thus sampling with solid adsorbents is performed both at ambient and refrigerated (-10°C) temperatures. Canister, ambient and refrigerated temperature adsorption tubes were operated

simultaneously during the comparison experiment.

2. Materials and methods

2.1. ADSORPTIVE SAMPLING

TUBE CONDITIONING

The glass cartridges were filled with a multibed system containing 150 mg each of Carbotrap C, Carbotrap B and Carbosieve S-III, (Supelco; Bellefonte, PA, USA). Four cartridges at a time were conditioned by purging with ultra-high-purity helium at 50 mL/min whilst heating at 350°C for at least 4 hours. After conditioning, the sorbent tubes were capped with stainless steel Swagelock ferrules and nuts and stored in a freezer at -10°C until sampling.

The drying tubes were composed of stainless steel tubes filled with K_2CO_3 (Merck) equipped with a stainless steel frit at each end. These tubes were activated by purging with helium at 50 mL/min whilst heating at 120°C for 4 hours.

SAMPLING

Sampling was performed on a stream of ambient air generated with a stainless steel pipe connected to a high flow rate pump (*ca.* 4 m³/h). This stream was subsampled with either refrigerated or ambient air tubes using low volume pumps (50 mL/min). 3 L samples were collected in each case.

When refrigerated cartridges were used, moisture was avoided by a cooling trap consisting of an empty glass tube refrigerated at -10°C. The sample portion of the air stream was removed from the manifold through Teflon tubes, drawn into the cooling trap and then into the adsorbent cartridge, which was also kept at -10°C in a freezer during sampling.

When ambient temperature cartridges were used, the adsorption tubes were connected directly to the pipe holes. In this case, samples were dried in the laboratory using a K_2CO_3 drying tube which was placed in the thermal desorption unit together with a new multibed adsorption cartridge. The sample was then transferred from the initial adsorption cartridge to one of these drying tubes and then to a new adsorption cartridge. This change prevented the correction of moisture that could freeze in the cryogenic trap.

2.2. SAMPLING WITH CANISTERS

CLEANING

6L-Summa electropolished stainless steel canisters were purchased from Andersen Samplers Inc. (Atlanta, GA, USA). Cleaning was performed by repetitive evacuation and refilling with humidified zero air whilst heating at 100°C. Two canisters at a time were handled by introduction in an isothermal oven and connection to a vacuum pump which

evacuated the canisters to an absolute pressure of 5.10^{-3} mbars. A U-shaped open tubular trap cooled with liquid nitrogen was used to prevent contamination from back diffusion of oil from the vacuum pump. The canisters were refilled with humidified zero air until pressure reached 2 bars. Generally this cycle was repeated three times, until no contaminant peaks could be detected by gas chromatographic (GC) analysis.

SAMPLING

The canisters were evacuated completely before sampling. A pressurized sampling system, Andersen Model 87-200 Volatile Organic Compound Canister Sampler (VOCCS), was used to draw ambient air from the sampling manifold to fill and pressurize the canister. A discharge port on the rear of the instrument cabinet vented the unsampled air. A small portion of this sample air was removed from the manifold by a modified inert diaphragm vacuum pump in conjunction with an electronic mass flow controller. The flow controller device maintained a constant flow (about 30 mL/min) into the canister over the fixed sampling period (about 10 hours) until the target pressure in the canister was achieved (about 20-25 psi). A digital timer was used to preselect sampling periods, start and stop times.

After sample collection, the VOC were measured in the laboratory by transfer of a known volume of air in the canister (*ca.* 1.5 L) to a K_2CO_3 drying tube serially connected to a multibed glass cartridge (mL/min). The drying tubes were replaced every two samples. The air volume was controlled by a flow meter connected after the cartridge.

2.3. INSTRUMENTAL ANALYSIS

Analyses were performed with a Fisons Model 8000 GC (Rodano, Italy) equipped with a thermal desorption unit (TDU) and a conventional flame ionisation detector (FID). The desorption system was a Model 850 Thermal Desorber Envirochem Inc. (Supelco, Bellefonte, PA, USA) coupled to a cryofocussing device Model MFA 815 Cold Trap (Fisons, Rodano, Italy). This cryofocussing unit was a 0.53 mm i.d. fused silica capillary tube cooled with liquid nitrogen to -150°C. VOCs were desorbed at 300°C for 5 minutes at a flow rate of 44 mL/min and transferred into a heated stainless steel tube. Then, they were refocussed on the cryogenic unit and the sample was rapidly desorbed (within 35 s) at 300°C into the gas chromatographic column. Separation was performed on a 30 m x 0.53 mm i.d. porous layer open tubular column coated with aluminum oxide and deactivated with potassium chloride (Chrompack, Middelburg, Netherlands).

Compound identification was performed with a GC coupled to a mass spectrometer Fisons MD-800 (Rodano, Italy). Quantitation was performed using hydrocarbon gas standards from Scott Specialty Gases, Inc. (Durham, NC, USA). Known volumes of these standards were introduced directly into desorption tubes which were analysed as described above.

2.4. Field Study

Samples were taken on the 29th September 1994 at Marignane, a semirural site situated near a coastal pond, the Etang de Berre, which is located in the Fos-Berre region (South of France). The region is well-known for its significant industrial concentrations and large numbers of vehicles. Parallel measurements using canisters (integrated samples) and multibed adsorption tubes (3 L samples every 2 hours, with both refrigerated and ambient temperature collection methods) were performed for comparison. The canister sampler and the stainless-steel pipes were placed at about 15 m from the lake and the distance between them was about 5 m.

3. Results and discussion

Representative chromatograms of ambient air samples collected at Marignane with canisters (Fig. 1) and refrigerated and ambient temperature cartridges (Fig. 2) are shown. The quantitative results corresponding to these determinations are summarized in Table I. The measured concentrations are low, typical of sub-ppbv ambient background levels in areas remote from vehicular traffic or other sources. As described above, the canister provides time-integrated data whereas tube collection, either ambient air or refrigerated, corresponds to two hours periods. A problem of contamination with *n*-octane in the canisters prevented this compound from being included in the comparison. Acetylene was only quantified for canister collection.

The aluminum oxide columns provide high resolution for the separation of light hydrocarbons without the need for using subambient oven temperatures. Thus, baseline separation of linear, cyclo- and *iso*- alkanes, *e.g.* cyclo-, *n*- and *iso*-butane, but-1-ene and pentane, are achieved (Figs. 1 and 2). In this respect, base-line separation of *iso*- and *n*-but-1-ene cannot be achieved with 100% methylsiloxane-coated columns, even when subambient oven temperature programs are used (Farmer *et al.*, 1994).

Unfortunately, the aluminum oxide chromatographic columns are sensitive to humidity, showing retention time changes as a consequence of the adsorption of polar molecules such as water on the active aluminum oxide layers. Humidity excess may even cause column blockage.

Sample humidity may also generate other disturbances which are not specifically related with this type of column. Thus, water vapor may accumulate, freeze and block the cryogenic trap. It may also extinguish the flame on the FID or give rise to problems of overpressurization in the mass spectrometer. Changes in detector response are commonly encountered as consequence of humidity. The significance of these problems obviously depends on the amount of water in the samples. However, when aluminum oxide columns are used water must be eliminated from the samples to ensure retention time reproducibility.

Several solutions have been addressed for drying air samples in the preconcentration and GC analysis of VOCs. The use of permeable membrane dryers allows the selective
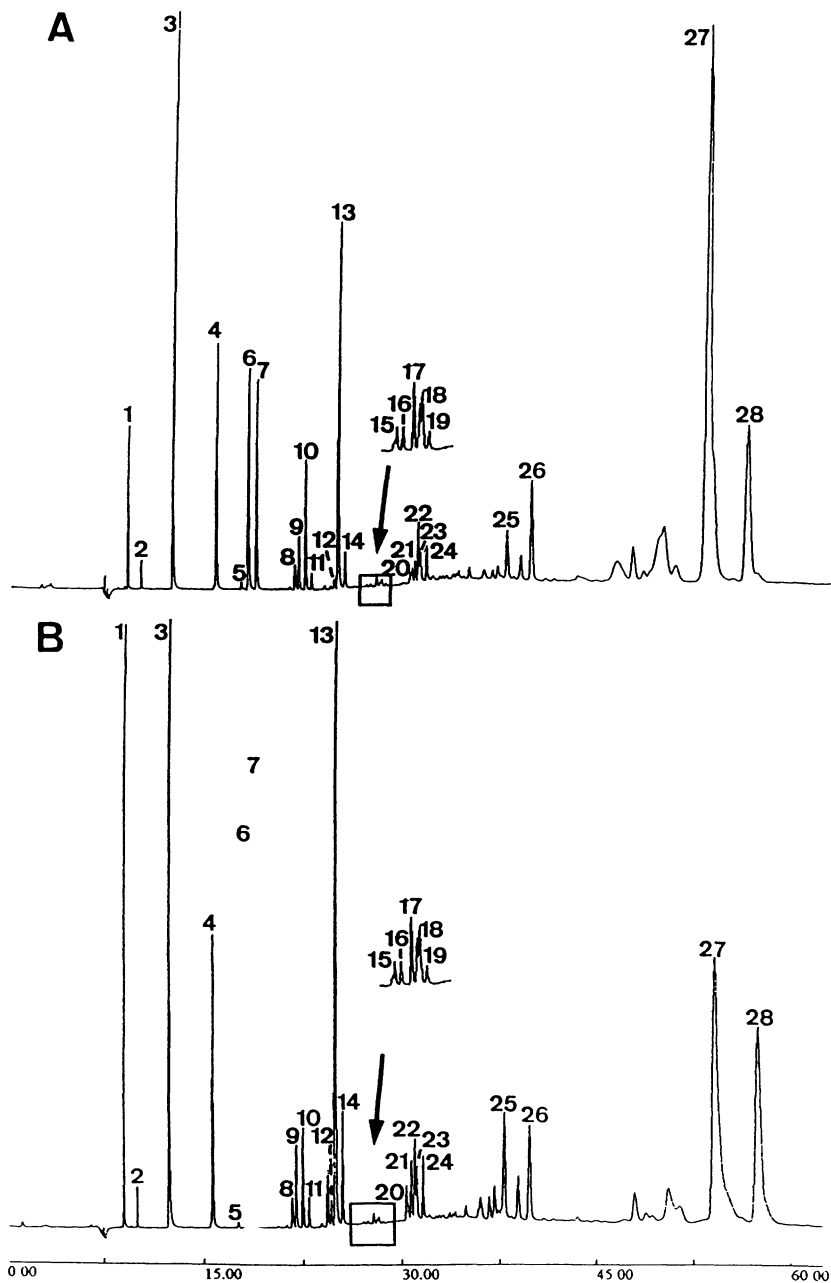
Figure 1. Representative chromatograms of an ambient air sample collected at the Marignane location. A: Ambient temperature adsorption tube. B: Refrigerated adsorption tube. Peak numbers refer to Table I.
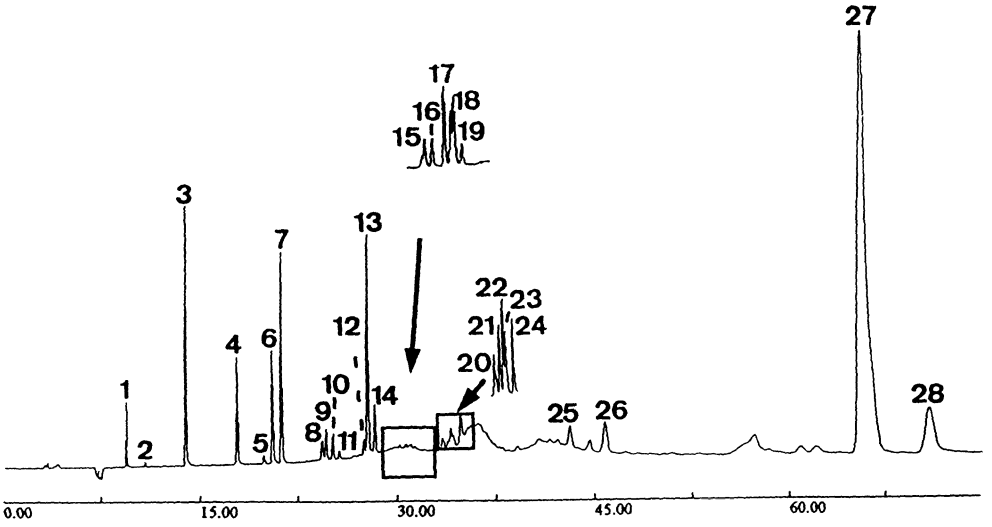
Figure 2. Representative chromatograms of an ambient air sample collected at the Marignane location. Peak numbers refer to Table I.
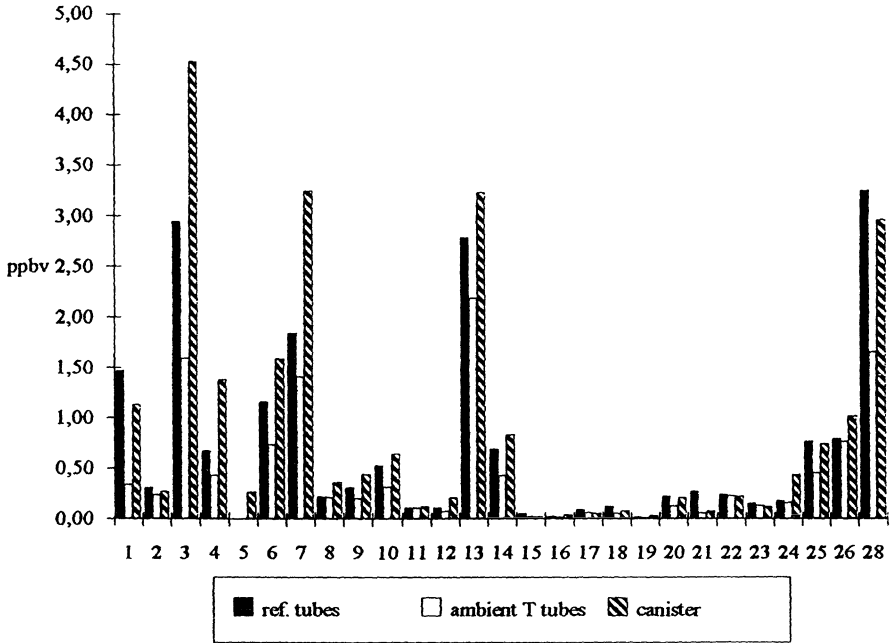

Figure 3. Comparison of the concentrations obtained with canister and solid adsorbent tubes at the Marignane location. Peak numbers refer to Table I.

TABLE I

Volatile organic compounds resulting from the field comparison of sampling with canister and refrigerated and ambient temperature multibed adsorption cartridges. Concentrations in ppbv.

	CANISTER	refrigerated tubes		ambient T tubes	
		mean (n=5)	s.d.	mean (n=10)	s.d.
1 ethane	1.13	1.47	0.73	0.34	0.21
2 ethylene	0.27	0.31	0.27	0.24	0.29
3 propane	4.53	2.95	2.61	1.60	1.14
4 propene	1.38	0.68	0.46	0.43	0.36
5 acetylene	0.26				
6 isobutane	1.59	1.16	0.72	0.74	0.39
7 n-butane	3.25	1.84	0.86	1.41	0.83
8 trans-but-2-ene	0.37	0.22	0.03	0.22	0.11
9 but-1-ene	0.44	0.31	0.16	0.20	0.10
10 iso-but-1-ene	0.65	0.53	0.11	0.31	0.22
11 cis-but-2-ene	0.12	0.11	0.08	0.11	0.08
12 cyclopentane	0.21	0.11	0.03	0.08	0.04
13 iso-pentane	3.22	2.78	1.10	2.18	1.10
14 n-pentane	0.83	0.69	0.23	0.42	0.27
15 trans-pent-2-ene	0.02	0.05	0.04	0.02	0.03
16 2-methylbut-2-ene	0.04	0.03	0.03	0.02	0.02
17 pent-1-ene	0.05	0.09	0.07	0.06	0.05
18 2-methylbut-1-ene	0.08	0.12	0.12	0.05	0.03
19 cis-pent-2-ene	0.03	0.02	0.02	0.01	0.01
20 2,2-dimethylbutane	0.21	0.22	0.19	0.13	0.07
21 cyclohexane	0.07	0.27	0.31	0.06	0.04
22 2-methylpentane	0.22	0.24	0.12	0.23	0.14
23 3-methylpentane	0.12	0.15	0.08	0.13	0.09
24 n-hexane	0.43	0.18	0.08	0.16	0.09
25 2,3-dimethylpentane	0.74	0.77	0.53	0.45	0.36
26 benzene	1.01	0.79	0.11	0.76	0.28
27 n-octane	24.11[a]	4.90	2.83	3.52	2.70
28 toluene	2.95	3.24	2.54	1.65	0.87

[a]Measurement influenced by external contamination.

elimination of water in gas streams (Pankow, 1991; McClenny *et al.*, 1995). However, these membranes may introduce contaminants which interfere with the compounds to be determined in the samples, namely *iso*-but-1-ene, benzene and toluene (Boudrier, 1994). The concentrations of these contaminants are significant for the studies aimed at the determination of trace amounts (ppbv). Another problem related with the use of permeable membrane dryers is the loss of water-soluble VOCs (Oliver *et al.*, 1996). In the cases where this problem may disturb the determination of the target VOC, two-stage trap

methods involving combinations of cartridges filled with different adsorbents have been developed. These methods selectively retain the polar compounds *vs.* water (Kelly *et al.*, 1993; Oliver *et al.*, 1996) although their application to apolar compounds is difficult.

In the case of the highly volatile apolar and low polar compounds of interest in the present study, water adsorption on K_2CO_3 tubes allows an efficient removal of sample humidity without interferences from organic materials (Figs. 1 and 2). These adsorption tubes can be easily re-conditioned and tested for organic contamination and sample memory effects. Comparison of the results summarized in Table I for the canister and trapping with refrigerated tubes show that no major differences between the K_2CO_3 drying system and the serially-connected cryogenic loop are observed. In fact, the concentrations are even higher in the case of K_2CO_3 drying although this may be related with the higher trapping efficiency of the canisters.

The sampling efficiencies of the three collection methods are compared in Figure 3. Higher concentrations are generally found in the case of the canister, except for ethylene, *trans*-pent-2-ene, pent-1-ene, 2-methylbut-1-ene, 2,2-dimethylbutane, 2-methylpentane, 3-methylpentane, 2,3-dimethylpentane and toluene, whose concentrations are similar to those obtained with adsorption with refrigerated tubes. In contrast, adsorption with ambient temperature tubes generally gives rise to lower concentrations than those of the previous sampling systems. The difference is particularly relevant in the case of lightest hydrocarbons C2-C4, like ethane, propane or isobutane. In terms of dispersion, no major differences are observed between the refrigerated and ambient temperature methods, although the latter shows higher dispersion in a major number of cases.

4. Conclusions

The field comparison experiment described in this study shows that sampling with canisters generally provides the highest concentrations. However, these are close to those obtained with refrigerated multibed adsorption tubes. Both methods are in fact equivalent for most of the highly volatile hydrocarbons encountered at ppbv levels. Conversely, sampling with ambient temperature tubes gives rise to lower concentrations, which highlights the need for a close evaluation of this collection method when comparing VOC data from different reports.

This study has also shown that K_2CO_3 drying efficiently removes humidity from air samples allowing the obtention of reliable concentration data on highly volatile hydrocarbons at ppbv levels. These tubes can easily be re-conditioned and tested for blanks and memory effects, which greatly facilitates the control of external contamination and sample cross-contamination.

Acknowledgements

References

Bayer C.W.: 1994, *J. Chromatogr. Sci.* **32**, 312-316.

Berkley R.E., Varns J.L., Pleil J.: 1991, *Environ. Sci. Technol.* **25**, 1439-1444.

Boudrier H.: 1994, Measure et comportement des atmospheres naturelles: Experimentation à la Pointe de Bretagne. Ph.D. Thesis. Université Paris VII. 164 pages.

Brymer D.A., Ogle L.D., Jones C.J., Lewis D.L.: 1996, *Environ. Sci. Technol.* **30**, 1188-1195.

Cao X.-L., Hewitt C.N.: 1995, *J. Chromatogr.* **710**, 39-50.

Camel V., Caude M.: 1995, *J. Chromatogr.* **710**, 3-19.

Farmer C.T., Milne P.J., Riemer D.D., Zika R.G.: 1994, *Environ. Sci. Technol.* **28**, 238-245.

Gholson A.R, Storm J.F., Jayanty R.K.M., Fuerst R.G., Logan T.J., Midgett M.R.: 1989, *JAPCA* **39**, 1210-1217.

Harsch D.E.: 1980, *Atmos. Env.* **14**, 1105-1107.

Helmig D.and Greenberg J.P.: 1994, *J. Chromatogr.* **677**, 123-132.

Hoffmann T.: 1995, *Fresenius J. Anal. Chem.* **351**, 41-47.

Jayanty R.K.M.: 1989, *Atmos.Env.* **23**, 777-783.

Kelly T.J., Callahan P.J., Pleil J., Evans G.F.: 1993, *Environ. Sci. Technol.* **27**, 1146-1153.

McClenny W.A., Oliver K.D., Hunter Daughtrey E. Jr.: 1995, *J. Air and Waste Manag. Assoc.* **45**, 792-800.

Michael L.C., Pellizzari E.D., Perritt R.L., Hartwell T.D., Westerdahl D., Nelson W.C.: 1990, *Environ. Sci. Technol.* **24**, 996-1003.

Müller S. and Oehme M.: 1990, *J. High Resol. Chromatogr.* **13**, 34-39.

Oliver K.D., Pleil J.D., McClenny W.A.: 1986, *Atmos. Env.* **20**, 1403-1411.

Oliver K.D., Adams J.R., Daughtrey Jr.E.H., McClenny W.A., Yoong M.J., Pardee M.A., Almasi E.B., Kirshen N.A.: 1996, *Environ. Sci. Technol.* **30**, 1939-1945.

Pankow, J.F.: 1991, *Environ. Sci. Technol.* **25**, 123-126.

Pleil J.D. and Stroupe M.L.: 1994, *J. Chromatog.* **676**, 399-408.

Rudolph J., Müller K.P., Koppmann R.: 1990, *Anal. Chim. Acta* **236**, 197-211.

MEASUREMENT AND INTERPRETATION OF CONCENTRATIONS OF URBAN ATMOSPHERIC ORGANIC COMPOUNDS

G.JONES[1],N.GONZALEZ-FLESCA[2],R.S.SOKHI[1],T.MCDONALD[1] AND M.MA[1].

[1]*School of Environmental Sciences,University of Greenwich,Creek Road,Deptford,London,SE8 3BW,UK*
[2]*INERIS,Parc Technologique ALATA,BP No 2-60550,Verneuil-en-Halatte,France.* [3] *Atmospheric Science Research Group,Department of Environmental Sciences,University of Hertfordshire,College Lane,Hatfield,Hertfordshire,AL10 9AB,UK*

Abstract. The presence of volatile organic compounds (VOCs) from traffic and other sources in urban areas is a cause for concern about public health. Canister, chemical derivatisation, particulate sampling and adsorption sampling techniques were used to measure VOC concentrations of a wide range of compounds (C_6-C_{40}) during a four day campaign in south London with subsequent laboratory analysis of the samples. Compounds quantified included alkanes, mono- and poly-nuclear aromatic hydrocarbons. Also the first sequential measurements of carbonyl compounds (C_1-C_8) in a UK urban area are presented. Results from canister and adsorption sampling methods are compared. A comparison of the results with other urban data is presented and the temporal variations in VOC concentrations were interpreted with reference to the prevalent wind speeds and directions The CALINE4 line source dispersion model was generally successful in reproducing the daytime 12 hour average concentrations of selected VOCs.

1. Introduction

Many hundreds of volatile organic compounds (VOCs) have been found in urban atmospheres. Some of these compounds, such as benzene, 1,3-butadiene, formaldehyde and polynuclear aromatic hydrocarbons (PAHs), are potential carcinogens and this risk to public health has led to increasing concern about this class of pollutants. In addition, all VOC have a role in the creation of tropospheric ozone (O_3) through their perturbation of the nitric oxide (NO), nitrogen dioxide (NO_2) and O_3 photochemical cycle (Derwent 1995).

The major source of VOCs in urban areas, where industrial uses of organic solvents are absent, is from road transport. Evaporative and exhaust emissions contribute an estimated 30% of total VOC emissions in the UK. The fates of atmospheric organic compounds are their dispersal and eventual surface deposition or oxidation during O_3 creation photochemistry at timescales that vary with the individual reactivity of a VOC.

The ambient concentrations of VOCs in the urban atmosphere are a result of spatial and temporal variability in several parameters. Source characteristics, such as an individual vehicle's fuel type, engine technology and age as well as its operating speed/engine load at any time, all influence individual VOC emission rates. All these factors vary greatly among vehicles so that to characterise the emissions from a whole transport fleet is a complex undertaking. Variations in meteorological parameters of wind speed and direction, atmospheric stability, ambient temperature and solar energy flux influence the dispersion and photochemical oxidation rates of VOCs. These influences are further complicated by the intricate topography of urban areas that can give a local variation to regional meteorology (Field *et al.*,1992).

In view of the concerns outlined above it is necessary to conduct measurement campaigns to characterise spatial and temporal variation in VOC concentrations and to

attempt to develop models for use as tools in predicting the result of future scenarios.

Ambient concentrations of VOC in urban air are usually found in low parts-per-billion by volume (ppbv) mixing ratios. Therefore, they are usually monitored by sampling a volume of air followed by a crucial pre-concentration of the VOCs in the sample volume. The quantitative/qualitative analysis of the sample commonly proceeds by gas chromatography (GC) coupled with flame ionisation detection (FID) or mass spectrometry (MS) respectively (Schaeffer 1989). GC is ideally suited to the separation of the myriad VOCs in a sample. However, the large variability among VOC molecular weights, polarities and stability means that sampling techniques and analytical set-up must be matched to the VOCs one is studying.

Automatic on-line, on-site GC equipment can take a sample and analyse it every hour, producing a large data set with high temporal resolution (Derwent *et al.* 1995). However, the range of VOC it can analyse is limited by time and the GC separation column. The technique is also expensive and needs a constant supply of liquid nitrogen coolant. In these respects the option of taking samples at site and analysing them in a dedicated laboratory offers some advantages. Taking whole-air samples in suitable containers or sampling the VOCs of interest onto an adsorbent bed are two common ways in which this can be achieved.

The US Environmental Protection Agency (EPA) method TO-14 approves the use of passivated stainless steel canisters in sampling 41 specified VOC and this whole air sampling technique has been reviewed (McClenny *et al.* 1991). The method has an excellent advantage in that several analyses from one sample are possible.

Solid adsorbents have been used by many researchers to sample VOCs in the environment (Crisp 1980). Adsorbents such as graphitised carbon blacks and carbon molecular sieves are among the best adsorbents for sampling VOCs in the gas-phase. They can be used either singly or several in combination depending on the application. However, variations in ambient humidity, temperature and VOC concentration affect their adsorption characteristics. Their properties, applications to VOC monitoring and suggested ways of dealing with problems, such as that of humidity, have been extensively reviewed (Matisova and Skrabakova 1995). Polar VOCs, such as aldehydes and other carbonyl compounds, are unstable when adsorbed on carbon adsorbents and so a chemical derivatisation technique is commonly used. They are sampled into a cartridge impregnated with 2,4-dinitrophenylhydrazine (DNPH) and react with this compound to form a more stable derivative that can be analysed by HPLC.

PAHs are found mainly in the condensed phase on particulate matter and so high volume sampling methodology, using filters and back-up adsorbents (to trap material as it desorbs from the particulates) can be employed to monitor their ambient concentrations (Davis *et al* 1987).

A primary aim of this study was to use canister, adsorption, DNPH derivatisation and high volume sampling techniques in an intensive campaign at an urban site to identify and quantify as many VOCs as possible including: 1. monoaromatic hydrocarbons (MAH), aliphatics (C_{7-10}) and carbonyl compounds (C_{1-8}); in the gaseous phase; 2. PAHs adsorbed on to particles (C_{15-40}); and 3. measurements of total non-methanic hydrocarbons (TNMHC). Some VOCs can be identified in samples from more than one sampling technique. This allows results from different methods to be compared which

was another aim of the campaign.

Variations in 12 hour average VOC concentrations during the campaign were interpreted with reference to local meteorological observations and knowledge of source characteristics. Finally, the interpretation was tested using the California Line Source Dispersion Model (CALINE4).

2.Experimental

2.1. SITE DESCRIPTION AND GENERAL SAMPLING EQUIPMENT

Sampling was done from 18th-21st September 1995 at the kerbside of a T-junction on Creek Road in the London Borough of Greenwich. The northern side of the junction (the crosspiece of the "T") had a three storey building as its boundary. The topography was more open for the other three sides. All roads serving the junction were approximately straight for several hundred meters due west, south and east. Weekday traffic flow data for the three roads at were provided by the London Boroughs of Greenwich and Lewisham from their monitoring campaigns during September and April of 1995. Typical am/pm peak flow rates through the junction are of the order of 2000 vehicles/hour with cars comprising approximately 80% of the total traffic. National and regional meteorological data for the sample campaign period was obtained from the London Weather Centre. A monitoring station in the London Borough of Southwark (LBS), some 5km distant from the Creek Road site, provided 1 hour averaged local wind speed, wind direction, standard deviation of wind direction, ambient temperature and nitrogen oxides data.

A main sampling line constructed of cleaned/degreased aluminium tubing was established with its inlet 2.5m above ground-level 3m from the kerbside through which ambient roadside air was drawn by pump at 4L/min. Ports positioned on this tube allowed the main air flow to be sampled to adsorption tubes. Other sample-lines of Teflon tubing fed ambient air to a nitrogen oxides (NOx) analyser (Model 200, Advanced Pollution Instrumentation Inc.), an ozone (O_3) analyser and an Andersen Instruments VOC canister sampler (VOCCS). A filter/polyurethane foam (PUF) sampler (Model PS-1, Graseby GMW) was situated on the ground approximately 15m from the previously described sampling point, 3m from kerbside.

Aromatic and aliphatic VOCs (C_{7-10}) were sampled by stainless steel canisters and single bed adsorbent tubes. The canisters also provided TNMHC measurements. Sep-pak cartridges sampled gaseous aldehydes (C_{1-8}) while the filter/PUF sampler monitored PAHs adsorbed on to particles (C_{15-40}). Blank samples were tested for all the methods and analytical instruments were all calibrated from commercially available standard mixtures.

2.2. ADSORPTION SAMPLING

Adsorption tubes were constructed from silanised glass tubes filled with adsorbent (Carbotrap C) held in place by silanised glass wool (Supelco Inc.) The tubes were heat

conditioned and batch tested for blank signal. All tubes were stored capped with Swagelock fittings which were also used for all sampling line joints. One hour samples were taken at 7am,8am,11am,2pm,5pm and 6pm (to sample during rush hours as well as off-peak times) by drawing air through the adsorption tubes by means of fully charged Gillian battery-operated pumps (calibrated flow rate 75ml/minute). Air was sampled at ambient temperature. Humidity was reduced by passing the air through a drying tube containing conditioned potassium carbonate before entering the Carbotrap C adsorption bed. After sampling, adsorption tubes were re-capped and stored at 5°C approximately until they could be analysed.

Analyses were done in a conventional automated instrument combining a thermal desorption unit (Supelco,Inc.) with heated transfer line into a liquid nitrogen cooled cryofocus that injected the sample into GC-FID/MS apparatus (Fisons). The separation column for the single zone tubes was a CP-Sil 5 CB fused silica column.

2.3. CANISTER SAMPLING

SUMMA® polished stainless steel canisters (Andersen) were prepared by repeatedly heating under vacuum (100°C, 5.10^{-6} bar, 1 hour) then pressurising with humidified zero air (2 bars). Blank samples were then taken from them before finally evacuating the canisters at ambient temperature to the same sub-atmospheric pressure.

Canisters fitted into the VOCCS took 12 hour samples starting at 7am and 7pm to a final pressure of about 1.5 bar ($@20cm^3$/min) and then sealed.

A volume of air from each canister (1.5L) was sampled into single zone adsorption tubes and analysed using the same equipment and methodology as described in section 2.2. In addition, a sample was cryogenically pre-concentrated and analysed by FID with no chromatographic separation to obtain TNMVOC concentrations following the draft ISO standard method ISO/TC146/SC3.

2.4. CARBONYL COMPOUND SAMPLING

Daily 2 hour samples of around 200L were taken at 7am, 11am, 2pm and 5pm using DNPH impregnated Sep-Pak cartridges. An ozone scrubber was used to eliminate interference from this pollutant. Samples were sealed, stored under refrigeration and analysed the following week by HPLC with UV detection.

2.5. PAH SAMPLES

New Whatman 41 filters and PUF conditioned by 24 hour soxhlet extraction with dichloromethane (DCM) were used to sample particulate matter for the PAHs adsorbed on them using high volume sampling techniques. Air was sampled for 4 hours ($@15m^3$/hour) at 7am and 3pm with the two samples taken each day being combined. Samples were kept in cleaned glass vessels under refrigeration and analysed within a month of sampling.

The PAH were recovered from the filter and PUF samples, and prepared for analysis, by 24 hour soxhlet extraction in DCM followed by evaporation of the solvent, and re-solution. The samples were analysed by direct injection to a GC-FID instrument fitted with a PTE-5 column.

3. Results and Discussion

3.1. CAMPAIGN RESULTS

The measured concentrations of VOC found in this study are presented in Tables I-III and in Figures 1, 3 and 4.

Table I presents the 12 hour average concentrations of VOC in the canister samples. Table II presents the 2 hour average carbonyl compound data which are believed to be the first sequential measurements recorded in a UK urban area. Table III shows the one hour mean concentrations of VOC identified in the one zone adsorption tubes. The results of monitoring PAHs are presented later in Figure 4.

Whole missing data entries for the adsorption tubes results are due to a number of samples being used to identify the VOCs by GC-MS analysis. Compounds not detected in any sample are symbolised by ND in the tables.

As can be seen most easily from Table I the general evolution of VOC concentrations throughout the campaign shows decreasing concentrations during the 18th September and fairly constant much lower concentrations for the following two days and into the 21st September until they begin to rise during the evening. In the case of adsorption tube samples a higher resolution of temporal variability is shown. Concentrations were generally higher in the early morning and evening samples as one might expect due to peaks in traffic flow rate and the increased stability of the atmosphere at these times in relation to the rest of the daytime. The general pattern described above is repeated in the results of carbonyl compounds.

TABLE I

Concentration (ppbv) of VOC measured by canister

Compound	18/09/95 day	18/9/95 night	19/09/95 day	19/9/95 night	20/9/95 day	20/9/95 night	21/9/95 day	21/9/95 night
hexane	2.4	1.8	1.7	1.2	1.5	0.7	3.7	2.0
heptane	1.4	1.0	0.9	0.6	0.6	0.6	1.1	1.7
octane	0.8	0.3	0.9	0.7	0.4	0.5	0.7	0.7
nonane	0.2	0.1	0.1	<0.1	0.1	0.1	0.2	0.2
benzene	6.6	4.3	2.2	1.2	2.2	2.1	4.0	5.9
toluene	11.5	7.1	6.0	3.3	2.9	2.9	7.4	10.7
ethylbenzene	1.9	1.1	1.0	0.6	0.6	0.7	1.4	1.7
p-xylene	5.1	2.6	2.4	1.2	1.2	1.4	3.2	4.6
styrene	0.4	0.2	0.2	0.1	0.1	0.1	0.2	0.3
o-xylene	2.5	1.4	1.0	0.6	0.6	0.6	1.6	2.2
cumene	0.2	0.1	0.1	<0.1	<0.1	0.1	0.2	0.2
n - propylbenzene	0.4	0.2	0.2	0.1	0.1	0.1	0.4	0.4
ethyltoluene	1.1	0.5	0.7	0.3	0.3	0.2	0.7	1.1
1,3,5 - trimethylbenzene	0.4	0.3	0.3	0.1	0.1	0.1	0.3	0.5
1,2,4 - trimethylbenzene	1.1	0.5	0.8	0.4	0.3	0.3	0.8	1.4

TABLE II

Concentration (ppbv) of carbonyl VOC sampled by Sep-pak cartridges.

Compounds	18/9/95				19/9/95				20/9/95				21/9/95			
	9am	noon	3pm	6pm	9am	noon	3pm	6pm	9am	noon	3pm	6pm	9am	noon	3pm	6pm
formaldehyde	7.5	8.3	8.9	10.1	4.0	7.0	3.7	2.9	2.2	2.9	2.3	2.2	7.9	3.6	4.7	5.4
acetaldehyde	2.2	2.0	2.2	2.2	1.1	1.7	1.2	0.9	0.9	0.8	0.8	0.5	2.2	1.0	1.9	2.3
acrolein	ND	ND	ND	ND	ND	ND	ND	ND	ND	ND	ND	ND	ND	ND	ND	ND
acetone	0.5	0.7	0.9	0.9	0.4	0.5	0.4	0.3	0.6	0.7	0.4	0.4	0.5	0.4	0.4	0.5
butanal	0.5	0.5	0.2	0.6	0.2	0.4	ND	ND	ND	ND	ND	ND	ND	ND	0.7	0.7
pentanal	0.2	0.2	ND	0.3	ND	ND	ND	0.1	ND	ND	ND	ND	0.2	ND	0.2	0.2
hexanal	0.4	0.4	0.3	0.4	0.3	0.4	0.4	0.4	0.2	0.2	0.2	ND	0.5	0.3	0.3	0.5
heptanal	0.7	0.8	0.5	0.7	0.3	0.4	0.2	0.2	0.3	0.2	0.3	0.2	0.4	0.2	0.2	0.4
octanal	1.4	1.6	1.0	1.4	0.9	1.4	0.8	0.6	1.1	0.8	1.0	0.8	1.2	0.8	0.8	1.4

3.2. TNMVOC, A SIMPLE INDEX OF AIR QUALITY

In view of the exhaustive nature of sampling and analysing VOCs many times by several techniques it would be desirable to have a simpler index of air quality with respect to these compounds. Measurement of TNMVOC from canister samples provides such a tool.

From each canister sample chromatogram, the total area of identified and un-identified peaks were totalled. Taking the FID response factor of a compound representative of the whole sample (in this case hexane was chosen) the VOC concentration of the sample was expressed as the mass equivalent of carbon per unit volume of air ($\mu gC.m^{-3}$) Thus the theoretical TNMVOC concentration from chromatographically analysed samples was determined. TNMVOC concentrations obtained by the draft ISO standard method were calculated similarly. Of course, the lack of chromatographic resolution in this technique meant that only one peak comprising all compounds needed to be treated. This method uses propane as the calibrating compound. However, the similarity of response factor per carbon atom of propane and hexane allows one to compare the two methods of measuring TNMVOC.

Figure 1 shows a scatter plot of these results. It can be seen that the draft ISO method returns greater concentrations than the other method. Some of this difference can be attributed to the compound selectivity of the chromatography column and the peak area threshold level below which no peaks were included in the total peak area addition. Overall however, the draft ISO method adequately reproduces the results of the gas chromatography method. If speciated analysis is not required the former technique can provide a good indication of the general ambient air quality in terms of VOCs.

Table IV presents the correlation coefficients for the daytime 12 hour mean concentrations of several pairs of identified compounds. The general significantly high coefficients indicate that the compounds are all following the same time series trend. This suggests that there is a common source (most likely vehicular) for these compounds and that the concentrations are influenced by common factors of dispersion. In particular the data indicates that formaldehyde is probably a primary pollutant in this study and not a product of photochemical activity.

TABLE III

Concentration (ppbv) of VOC sampled by one zone adsorption tubes

Compounds	18/09/95				19/09/95						20/09/95						21/09/95		
	7am	8am	2pm	5pm	7am	8am	11am	2pm	5pm	6pm	7am	8am	11am	2pm	5pm	6pm	7am	8am	11am
hexane	0.9	2.2	1.0	2.4	0.6	0.7	1.4	0.7	0.5	0.3	0.4	0.3	ND	0.3	0.2	0.4	0.5	ND	0.6
heptane	1.1	1.5	1.1	1.6	0.4	0.6	0.8	0.4	0.3	0.3	0.3	0.5	0.3	0.1	0.1	0.3	0.5	2.0	0.5
octane	0.9	1.2	1.8	1.8	0.7	1.3	1.3	1.0	0.8	0.8	1.2	1.1	0.3	0.8	0.8	0.7	0.3	1.0	1.1
nonane	0.1	0.2	0.2	0.2	0.1	0.1	0.2	0.1	0.1	<0.1	0.1	<0.1	<0.1	<0.1	<0.1	<0.1	0.2	0.3	0.1
benzene	1.8	3.0	1.8	4.1	1.5	1.5	3.0	1.7	0.9	0.8	0.9	0.9	1.0	0.9	0.8	0.9	1.4	1.5	1.4
toluene	2.9	3.9	2.8	4.1	0.9	1.6	2.0	0.7	0.5	0.6	0.5	0.7	0.7	0.3	0.3	0.6	0.9	4.1	1.3
ethylbenzene	2.1	2.5	2.2	3.	0.6	1.2	1.4	0.7	0.4	0.5	0.4	0.3	0.5	0.2	0.2	0.4	0.7	2.8	0.8
p-xylene	6.8	8.1	6.5	9.7	1.8	3.5	4.2	1.5	1.0	1.3	0.9	0.9	1.3	0.6	0.6	1.2	3.0	9.0	2.4
styrene	0.4	0.4	0.4	0.4	0.1	0.2	0.3	0.1	0.1	0.1	0.1	0.2	0.1	ND	ND	0.1	0.1	0.5	0.2
o-xylene	3.2	3.6	2.6	4.0	0.9	1.7	2.0	0.7	0.5	0.6	0.5	0.6	0.6	0.4	0.4	0.6	1.3	3.7	1.2
cumene	0.2	0.2	0.2	0.2	0.1	0.1	0.1	0.1	0.1	<0.1	0.1	0.1	<0.1	<0.1	<0.1	<0.1	0.1	0.4	0.1
n-propylbenzene	0.5	0.6	0.6	0.7	0.2	0.3	0.4	0.2	0.2	0.1	0.1	0.1	0.2	0.1	0.1	0.1	0.3	0.8	0.2
ethyltoluene	2.1	2.4	2.0	2.7	0.5	1.1	1.3	0.4	0.3	0.3	0.3	0.3	0.3	0.1	0.2	0.3	0.9	2.8	0.7
1,3,5-trimethylbenzene	0.8	0.9	0.8	1.0	0.2	0.4	0.5	0.2	0.2	0.2	0.1	0.1	0.1	0.1	0.1	0.2	0.4	1.1	0.3
1,2,4-trimethylbenzene	2.6	2.6	2.5	3.2	0.6	1.2	1.6	0.6	0.4	0.4	0.3	0.3	0.3	0.2	0.2	0.4	1.2	3.2	1.0

$R^2 = 0.7451$

Y-axis: TNMVOC from total area of resolved peaks $\mu g C.m^{-3}$ (0, 50, 100, 150, 200, 250, 300, 350, 400)

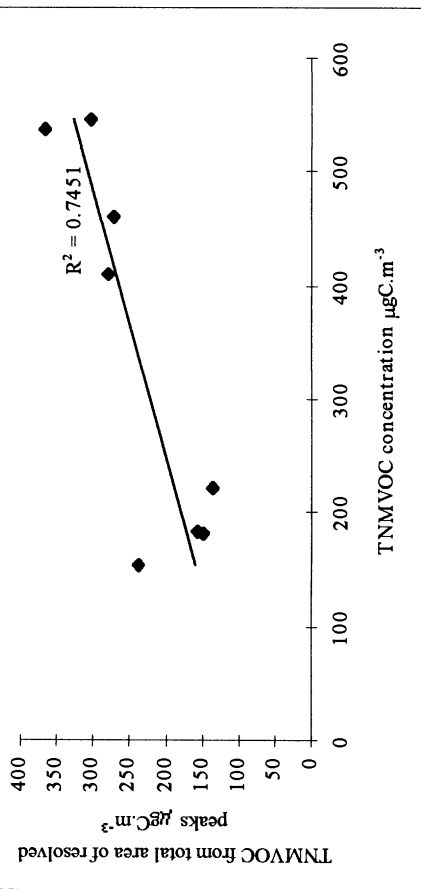X-axis: TNMVOC concentration $\mu g C.m^{-3}$ (0, 100, 200, 300, 400, 500, 600)

Fig.1. Relationship between TNMVOC and theoretical TNMVOC in canister samples.

Table IV
Correlation coefficients of daytime 12 mean concentrations for selected compounds

	toluene from canisters	Formaldehyde	Phenanthrene
formaldehyde	0.977		
phenanthrene	0.995	0.988	
TNMVOC	0.932	0.850	0.923

3.3. SAMPLING METHODS COMPARISON EXERCISE

Certain VOC were identified both in canister and adsorption tube samples. These measurements were used in an exercise to compare the sampling techniques. Daytime 12 hour mean concentrations of the remaining VOCs were arranged in percentile order and are presented as box whisker plots in figure 2 with the sampling technique identified by "c" (for canisters) and "1" (signifying one zone tubes). Large overlap of the two boxplots for any given compound indicates that the fluctuation of concentration with time as well as the range of absolute values were very similar. In such cases the sampling methods are found to be equivalent. VOCs with median concentrations of less than 1ppbv were omitted since, below this concentration, bias in the precision of the analytical method introduces a significant effect to the distribution of results.
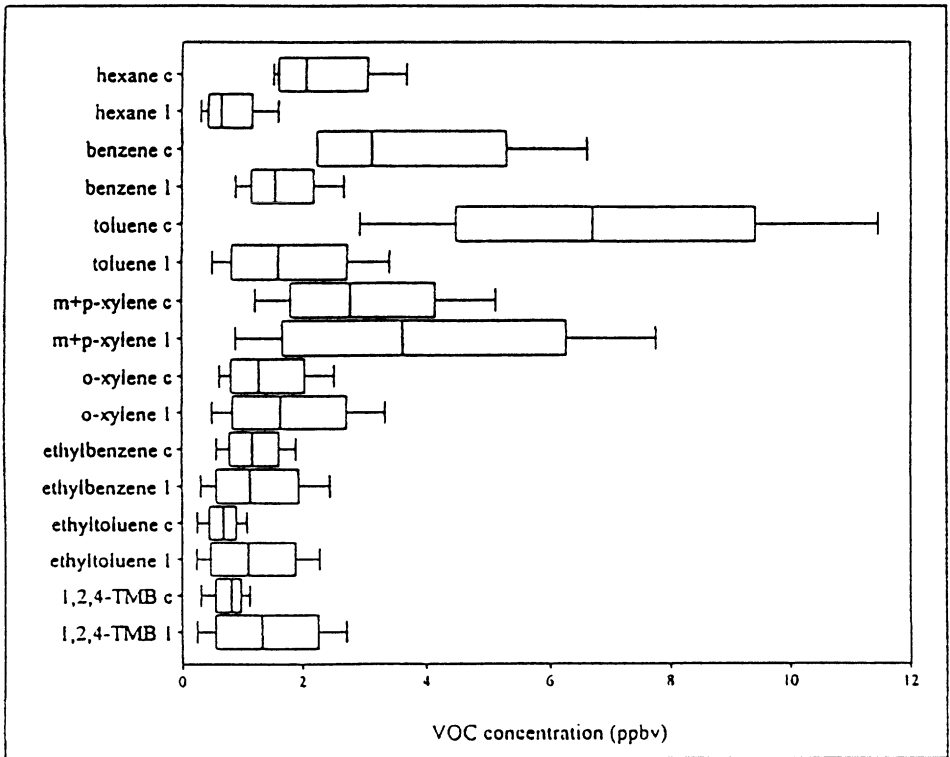

Fig.2. Boxplots of selected VOCs and sampling methods.

It is seen in figure 2 that the canister and adsorption methods are comparable for most of the ring-substituted monoaromatic compounds such as the xylenes. However, for hexane, benzene and toluene there can be variation between the two methods. In particular the adsorption tubes returned much lower concentrations of these compounds than are normally observed in urban atmospheres (section 3.3). This may indicate a compound-selective sample loss mechanism. One possibility is that the hexane, benzene and toluene were irreversibly adsorbed although reviews have noted that graphitised carbon black (GCB) adsorbents such as carbotrap C are almost completely free of the specific adsorption sites that could give rise to the observed losses (Matisova and Skrabakova 1995). Taking only GCB adsorbents, Carbotrap C has the smallest specific adsorption capacity and energies of adsorption. Therefore, breakthrough of the most volatile of the compounds could possibily occur under adverse conditions such as high pollutant concentration. Another factor that could possibly contribute to sample loss is the adsorption of material in the drying tubes during sampling. However, it is difficult to implicate any single factor responsible for the sample loss.

In the light of the discussion above we believe that the canister sampling method may be the more suitable one for the monitoring of hexane, benzene and toluene at normal urban concentrations. Although the canisters are expensive each sample can be analysed cheaply several times if need be. Theoretically canisters can be used to take hourly samples but adsorption tubes still have an advantage in these terms since they are relatively cheap.

3.4. COMPARISON WITH OTHER URBAN CONCENTRATIONS OF VOC

It is worthwhile putting the results of this study in the context of previous studies to look for significant differences or similarities. Since the comparison of methods exercise gave no indication of which one provided the most representative of true VOC concentrations, the daily 12 hour averages for the two methods compared were averaged together and are represented in the following figures as Creek Road 1995. The sources of other average data found in the literature are indicated in the legends of figures 3 and 4 which present this data alongside the data from this study.

From figures 3 and 4 it is seen that this study found concentrations of identified VOCs in London to be similar to other workers' findings; although this campaign was of shorter duration. This data seems to indicate that the MAHs and PAHs measured at Creek Road come from the same general source as that found at other London sites, namely vehicles, and that there is no evidence of local industrial sources contributing to the emissions of these VOCs.

Interestingly, figure 3 shows MAH concentrations and toluene concentrations in particular, to be highest in Paris. Recent work has shown that reductions in the lead content of gasoline in France during the 1980s-90s have been offset by increases in the aromatic content of the fuel from 30% to around 45%. During the same period there was a smaller 5% increase in the aromatic content of UK unleaded fuel (Perry and Gee 1995). The same workers showed that the higher aromatic content in gasoline results in a higher aromatic content in vehicle emissions with toluene emissions being the most enhanced. Although differences in the market share of these fuels between the two countries will also be a determining factor the above the data in figure 3 can be interpreted as corroborating evidence of these differences in urban emission profiles between the UK and France.
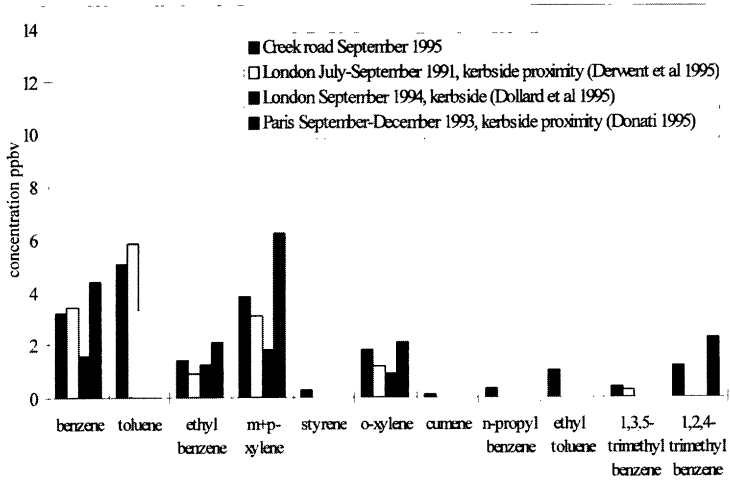
116

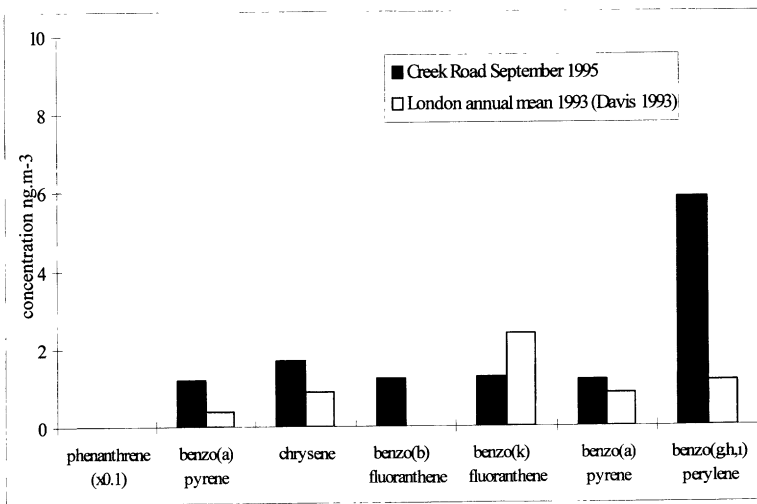Fig.3. Comparison of urban VOC data. Monoaromatic hydrocarbons.

Fig.4 Comparison of urban VOC data. Polynuclear aromatic hydrocarbons.

3.5. INTERPRETATION OF RESULTS

The observed temporal variations in the 12 hour mean concentrations during the sampling campaign were interpreted with reference to the daily weather summaries from the London weather centre and data from the LBS site. The use of data from this site was justified by examining the frequency distribution of the measured 1 hour mean NO_2/NO_x

ratio at Creek Road and the LBS site (fig.5.). In the figure, a similar pattern is seen for the two sites indicating that they were influenced by the same air dispersion factors, pollutant source and transformation reactions of pollutants during the campaign. The meteorological data is summarised in table V.
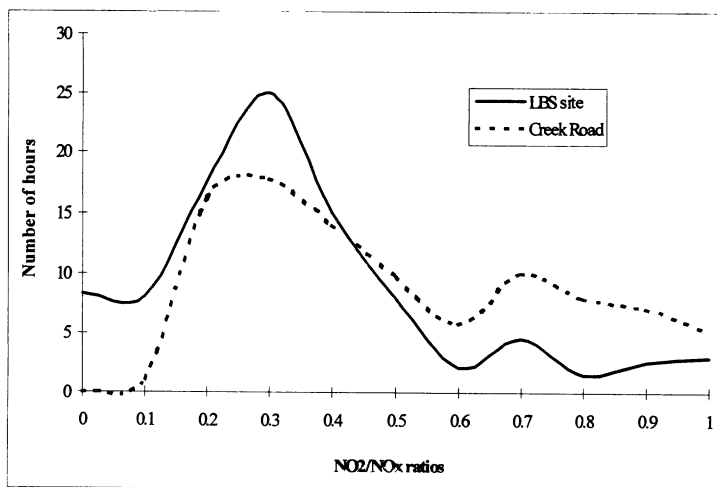
Fig 5 Frequency distribution of 1 hour average NO_2/NOx ratios during this study at the LBS and Creek Road sites

TABLE V
Summarised meteorological data for 18-21/9/95.

Date	Avg. daytime temp. (°C)	Wind direction and average wind speed (m/s)	Observations
18	21	Northerlies and Easterlies (4)	overcast, rain during pm and overnight
19	21	steady Northerlies (7)	overcast but dry, clearing overnight
20	21	steady Northerlies (5)	dry with variable cloud cover
21	21	very variable Southern sector (1)	dry with sunshine, becoming overcast later

The higher wind speeds with a steady northerly direction present during the night of the 18th and throughout the 19th and 20th of September would indicate a period of well ventilated air movement during which VOC emissions from the Creek Road traffic would be dispersed away from the sampling site. Therefore, only the London background source of VOCs would be monitored at these times. The decreasing and then fairly constant VOC concentrations for this period (table I) are in agreement with this interpretation.

The low wind speed from the southerly sector observed on the 21st September would allow Creek Road VOC emissions to be gently dispersed towards the sampling site so resulting in higher measured concentrations. In addition, the easterly winds experienced during September 18th would move air in a direction parallel with Creek Road and, hence, local traffic emissions would contribute to the pollutant concentrations.

The results in table III have not yet been interpreted in terms of possible photochemical transformations. However, the rate constants for the reaction of hydroxyl (OH) radicals with these VOCs under normal atmospheric conditions are the equivalent of

the compounds having 1/e lifetimes of at least several hours (Atkinson 1990). Therefore, the background VOC concentrations may have been influenced by photochemistry in the atmosphere. However, it was assumed that the time scale between the VOCs being emitted from the local source (traffic in Creek Road and junction) and their being sampled was too short for photochemical transformations to have occurred in the prevalent conditions.

3.6. MODELLING EXERCISE

An attempt was made to model the daytime (7am-7pm) 12 hour average concentrations of benzene, toluene, ethylbenzene and the three xylenes with reference to the parameters highlighted in section 3.5. CALINE4 (Benson 1984) was selected for its ability to model pollutant dispersion in the situation of a road junction with changing meteorological conditions, traffic emissions and urban background concentrations of VOCs. The model divides road sections (or links) into elements in which an incremental concentration is derived using Gaussian dispersion theory. Within each link and in regions above and to the side of them the emissions and mixing are assumed to be uniform. The factors assumed to be causing the dispersion are wind speed, turbulence caused by vehicles and thermal convection. CALINE4 cannot model the complex photochemistry of VOCs but, as has been discussed, it was assumed that no transformations were occurring to the road source emissions of these compounds. Another limitation is that the complex urban topography can only be represented by a surface roughness coefficient. The model inputs are contained in table VI with the addition of the temperature and wind speed data from table V.

The model was forced to run in carbon monoxide dispersion mode with results being converted for the different molecular masses of the VOCs. Emission factors from vehicles were assumed to be the same for cars moving at cruise speed or idling at the junction. The emission factors used were the average emissions of a fleet of 25 vehicles driven in UK urban conditions (Bailey et al 1990). 12 hour average background concentrations of VOCs were calculated from data provided by the enhanced urban network London background site at Eltham. These data were taken from AEA Technology pages on the Web (http://www.aeat.co.uk/netcen/aqarchive/auto.html). Roadway, traffic volume and driving mode inputs were the results of observations at the junction and data from the London Boroughs of Lewisham and Greenwich.

The model was run once for each 1hour average wind direction which was sustained for 2 hours or more. Time weighted averages were then calculated for all the results to obtain modelled 12 hour average concentrations.

Figure 6 contains the comparison of measured to modelled VOC concentrations for the campaign. The statistical significance of the reported R^2 values should be tempered by the fact that there were only a very small number of data points from which the values were derived. However, the figure illustrates that the two sets of results are in best agreement (generally to within a factor of three) for the 18th and 20th September. The model underestimates VOC concentrations for the 19th and 20th of the month because the contribution of traffic emissions is eliminated due to the strong wind dispersing pollutants away from the sampling site. In reality the north-sided "bluff" topography of the site could allow air from the roadway to have been re-circulated back towards the site with higher pollutant concentrations being the result. The average wind speed during the

21st of September was 1m/s and, although CALINE4 has 0.5m/s as the minimum speed for which it can function, the model seems to be underestimating the effect of pollutant dispersion on this day. The result is that it predicts higher VOC concentrations than were actually measured. To investigate the relation between measured and modelled values, R^2 values are given for the exercise, although the number of data points is limited. The regression indicates that there is a linear relationship between the two sets of values.

TABLE VI.

All inputs to CALINE4 modelling exercise

Initial inputs

modelling type	aerodynamic roughness coefft. (cm)	pollutant settling velocity (cm/s)	pollutant deposition velocity (cm/s)	altitude above sea level (m)	link mixing zone width (m)
inert gas	108	0	0	10	10

Meteorological inputs

date modelled	wind direction (deg)	standard deviation in wind direction (deg)	Pasquill-Smith stability class	mixing height (m)
18	67,90,112,180,270,315,337	39.6	4	800
19	337	40	4	800
20	337	39.5	5	400
21	90,112,158,202,225,245,292	38.1	5	400

Vehicle emissions and background concentration (ppbv) inputs

compound	benzene	toluene	ethylbenzene	m+p-xylene	o-xylene
emission factor (mg/mile)	313	726	216	684	276
background conc. 18th	0.77	1.67	0.28	0.76	0.29
background conc. 19th	0.48	0.69	0.18	0.49	0.18
background conc. 20th	0.48	1.05	0.21	0.61	0.24
background conc. 21st	2.13	4.55	0.81	2.48	0.98

Road way inputs

link identifier	link type	traffic volume (veh/hr 12hr average) entering link	departing from link	veh. per traffic cycle	veh. delayed per cycle
A	intersection	400	900	8	5
B	intersection	900	400	17	11
C	intersection	500	500	10	7
D	normal highway	500		not applicable	not applicable

Intersection driving mode inputs

deceleration time (s)	idle time at stopline (s)	idle time at end of vehicle queue (s)	acceleration time (s)	cruise speed (miles/hr)
10	45	0	10	14

Although the absolute values of model results sometimes differed from the measured results by up to a factor of five, overall the model satisfactorily reproduced the trends in VOC concentrations that were observed during the campaign.

If the errors in model inputs and assumptions made can be shown to have a linear effect on the model outputs then the model could still be used as a tool for evaluating the proportional impact on VOC concentrations of different scenarios.
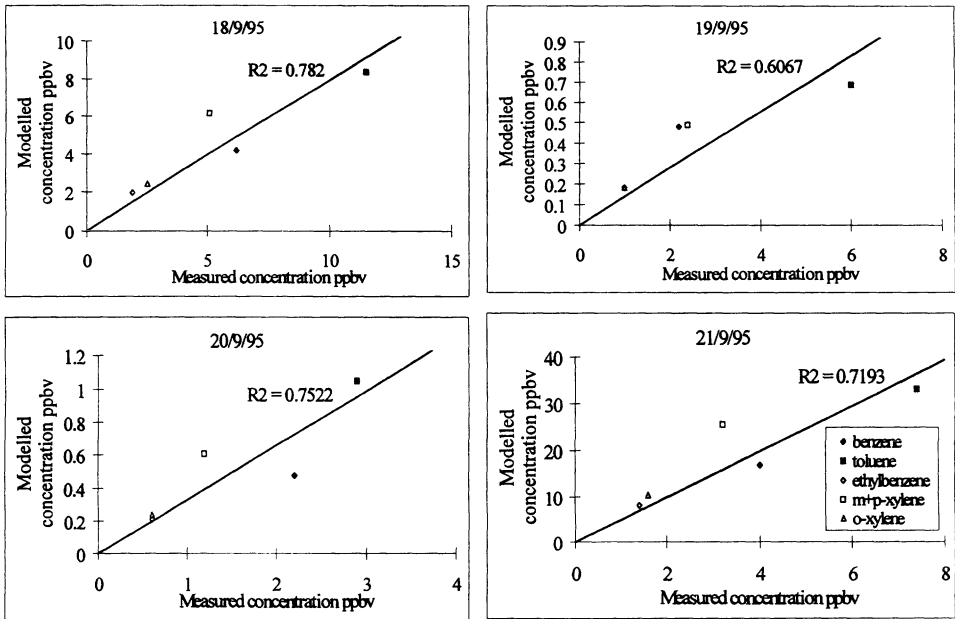
120

Fig 6. Measured vs. modelled VOC concentrations.

4. Conclusions

The campaign successfully measured the sequential concentrations of many VOCs by four different methods. The results indicated that although the canister and adsorption methods were generally equivalent for several compounds the canisters are perhaps more suitable for monitoring hexane, benzene and toluene. TNMVOC measurements not analysed by GC were found to successfully monitor general VOC air quality. The VOC concentrations measured in the sampling campaign were not significantly different from other London studies in most cases and indicated a strong vehicular source of MAHs, PAHs and aldehydes. The variations in the 12 hour average concentrations during the campaign were explained by the changes in wind speed and direction. However, the data indicates that there are significant differences in the proportions of MAH in ambient air between London and Paris. This may be due to differences in fuel compositions between the two countries.

The CALINE4 model can be a suitable tool for modelling VOC concentrations in urban areas for situations where these compounds are assumed to be inert. In this study it reproduced the 12 hour mean concentrations of selected VOCs with some success in spite of limitations in input data, such as the vehicle emission factors for idling engines.

Future work will focus on evaluating other models for their suitability in modelling VOC concentrations in urban areas as well as continuing to work with CALINE4 for the purpose of deriving vehicle emission factors from measured VOC concentrations. In addition, sampling campaigns are to be planned in which the further validation of sampling methods and development of interpretative and modelling tools are envisaged.

Acknowledgements

References

Atkinson R.:1990,*Atmosperic Env.*,**24A(1)**, 1-41.

Bailey J.C.,Schmidl B.,Williams M.L.:1990, *Atmospheric Env.*, **24A(1)**, 43-52.

Benson P.E.:1984, *Report No. FHWA/CA/TL-84/15*, California Department of Transportation, Sacramento, USA.

Crisp S.:1980,*Ann. Occcup. Hyg.*,**23**,47-76.

Davis B.J.:1993,*Toxic organic micropollutants in the atmosphere and in deposition at certain sites in the UK.*,Report LR 997. Warren Spring Laboratory,UK.

Davis C.S.,Fellin P. and Otson R. :1987,*J.A.P.C.A.*,**37**,1397-1408.

Derwent R.G.:1995,"*Volatile Organic Compounds in the Atmosphere*",ed. R.E.Hester and R.M.Harrison,*Issues in Environmental Science and Technology,***4**,Royal Society of Chemistry,Cambridge,UK.

Derwent R.G., Middleton D.R., Field R.A., Goldstone M.E., Lester J.N. and Perry R. :1995,*Atmospheric Env.*,**29**,923-946.

Dollard G.,Broughton G.,Dumitrean P.,Stedman J.,Cambell G.,Davies T.:1995, *Provisional hydrocarbon data summaries AEA Report AEA-CS-18358030/07.* AEA Technology, NETCEN,UK.

Donati J.:1995,*Pollution-Atmospherique*, **Jan-Mars**, 43-51.

Field R.A.,Goldstone M.E.,Lester J.N. and Perry R.:1992,*Atmospheric Env.*,**26A(16)**,2983-2996.

Matisova E. and Skrabakova S.:1995,*J. of Chromatography A*,**707**,145-179.

McClenny W.A.,Pleil J.D., Evans G.F., Oliver K.D., Holdren M.W. and Winberry W.T. :1991,*J.Air Waste Manage. Assoc.*,**41**,1308-1318.

Perry R. and Gee I.L.:1995,*Sci.Tot.Env.*,**169(1-3)**,149-156.

Schaeffer H-J.:1989,*J.of High Resolution Chromatog.*,**12**,69-81.

NITROGEN DIOXIDE IN THE WORKPLACE ENVIRONMENT

I. COLBECK

Institute for Environmental Research, Department of Biological and Chemical Sciences, University of Essex, Colchester, CO4 3SQ, UK

Abstract. Concentrations of nitrogen dioxide were measured in shops and car parks over a 19 week period during the winter. For the shops indoor:outdoor ratios varied from 0.34 to 0.54 with an average value of 0.44. NO_2 levels ranged from 13 to 38 μg m^{-3}. With little or no contribution from indoor sources, ambient concentrations are the primary factor in determining indoor levels. Concentrations of NO_2 in car parks were similar to those measured at the kerb side. Concentrations in the payment booths were higher than those in shops and ranged from 42 to 60 μg m^{-3}. Despite ventilation systems in the payment booths ratios of booth:car park NO_2 varied from 0.65 to 0.86.

1. Introduction

Nitrogen dioxide (NO_2) is an important pollutant and at sufficiently large concentrations, has the capacity to cause damage to humans where the respiratory system is the sensitive target. NO_2 is emitted directly from combustion sources and is also formed in the atmosphere through the oxidation of nitric oxide (NO) by ozone. In urban areas emissions of oxides of nitrogen ($NOx = NO + NO_2$) are dominated by motor vehicle emissions. Establishing any relationship between air pollution and health depends on a good knowledge of the type and distribution of pollutants, both in the outdoor and indoor environments. Since people spend ~90% of their time indoors, it is likely that indoor air pollution is an important source of exposure for some pollutants. To an extent which varies form pollutant to pollutant, outdoor levels influence indoor levels. Some outdoor pollutants, such as fine particles and NO_2, easily penetrate indoors. Others, notably ozone, are so reactive with surfaces that levels are low indoors.

The vast majority of studies on NO_2 in indoor air have concentrated on the domestic environment. Relatively few have been reported in the work place environment. For example measurements have been published on NO_2 in road vehicles (Gatward and Colls, 1990), ice rinks (Yoon *et al.*, 1996) and offices (Ekberg, 1995). High occupational exposure occurred in an incident in which Apollo astronauts were exposed to an average concentration of 470 mg m^{-3} for 4 min prior to splashdown (Hatton *et al.*, 1977). Ice hockey players and spectators have been exposed to 7.5 mg m^{-3} (Hedberg *et al.*, 1989) and levels up to 2.8 mg m^{-3} have been observed in diesel bus garages (Gamble *et al.*, 1987).

Nakai *et al.* (1995) has shown that distance from the roadside is an important factor in determining NO_2 in indoor air. Many shops in the UK front busy roads with

heavy traffic so it is perceivable that workers in these locations will be subjected to enhanced levels of NO_2. Although air pollution levels in car parks are generally adequately controlled few measurements of air quality have been reported. Without suitably controlled accommodation with appropriate ventilation car park attendants may be exposed to high concentrations of certain pollutants

Air quality standards are designed to protect the population for harmful levels of the pollutant. The current guidelines of the World Health Organisation for NO_2 are that the 1 hr average should not exceed 400 μg m^{-3}, and that the 24 hr average should not exceed 150 μg m^{-3}. It is proposed that the 1 hr average should be reduced to 200 μg m^{-3}. The Occupational Exposure Standard for the working environment is 5 mg m^{-3} over an 8 hr time weighted average reference period. In order to understand the levels and the micro-environment conditions of actual human exposure, it is necessary to document both where people spend their times and the pollutant concentrations at those locations. To provide the data necessary for understanding human exposure, we initiated a series of studies to determine NO_2 levels in shops and car parks.

2. Method

Simple passive diffusion tube samplers which collect gas by molecular diffusion were first introduced by Palmes *et al.* (1976) for NO_2 sampling in the field of occupational hygiene. Since then, diffusion tubes have been widely used for both indoor measurements of NO_2, particularly where gas cookers or unflued paraffin space heaters are in use (Ross, 1996; Spengler *et al.*, 1994; Schwab *et al.*, 1994), and in the outdoor environment (Stevenson and Bush, 1995; Bower *et al.*, 1991; Hewitt, 1991). The diffusion tube sampler consists of an acrylic tube approximately 7 cm long and 1 cm in diameter, the ends of which take close-fitting polythene caps. Two stainless steel mesh grids coated with triethanolamine (TEA) were placed on one end of the tube and held in position by a cap. Samplers were mounted vertically, with the cap containing the coated discs uppermost. The diffusion tube samplers were fixed by spring clips to 5 cm wooden blocks. These blocks serve to distance the samplers from surfaces. During the sampling period the lower cap was removed. NO_2 is absorbed by the TEA at a rate determined by the rate of diffusion up the tube. At the end of the exposure period the amount of NO_2 absorbed is determined as nitrite spectrophotometrically by a variation of the Griess-Saltzman method. The analysis involves diazotisation of sulphanilamide by the nitrite, and the formation of a purple azo dye through coupling of the diazonium salt with N-1-naphthylethylenediamine dihydrochloride. The optical density of the solution is measured at 542 nm. The amount of nitrite ion in the sample and hence mass of NO_2 collected, is obtained to a calibration plot derived from the analysis of standard nitrite solutions. The average NO_2 concentration is determined from the mass collected, the sampling time and the calculated sampling rate. The accuracy
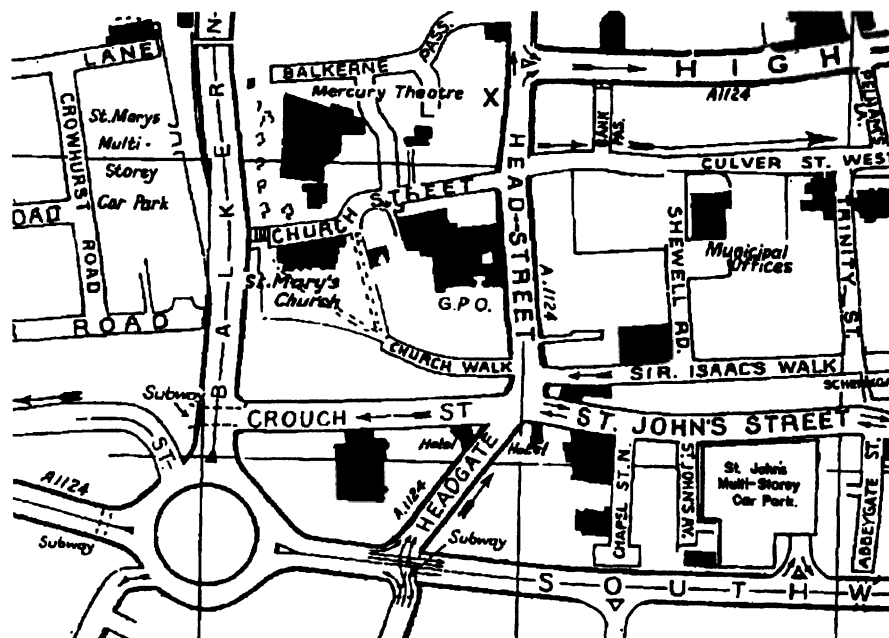
Figure 1. Position of sampling sites. X indicates shops.

of the samplers is reported to be ±10% and precision to be better than 2 ppb for a 1 week sample period (Apling *et al.*, 1979; Boleij *et al.*, 1986). Care must be taken in interpretation of diffusion tube data, and it should not be assumed that the accuracy and precision will match that of the best published data. Quality control is monitored via participation in the annual analytical laboratory intercomparison exercise for the Department of the Environment's UK Nitrogen Dioxide Diffusion Tube Survey. This involves the analysis of field exposed tubes, two sets of artificially doped tubes and a quality control stock solution of sodium nitrite. Full details are given in Stevenson and Bush (1995).

2.1. SAMPLING SITES

Two shops and two car parks within Colchester were selected (Figure 1). Both shops were in Head Street which has a traffic flow of ~9000 vehicles per day. Shop A was adjacent to traffic lights. Entry to the shop, from the road, was via a door approximately 90 cm wide and 2 m high. Shop B was 30 m from the traffic lights with a doors approximately 2 m wide and 2 m high. In each shop two tubes were placed just inside the entrance. Two tubes were also placed on lamp-posts outside each shop at a height of 2.5 m. Shop A was open for 51 hr a week and shop B for 54 hours a week. The tubes were collected and replaced every week from 9 November 1993 to 25 March 1994. There was no indoor source of NO_2 in either shop.
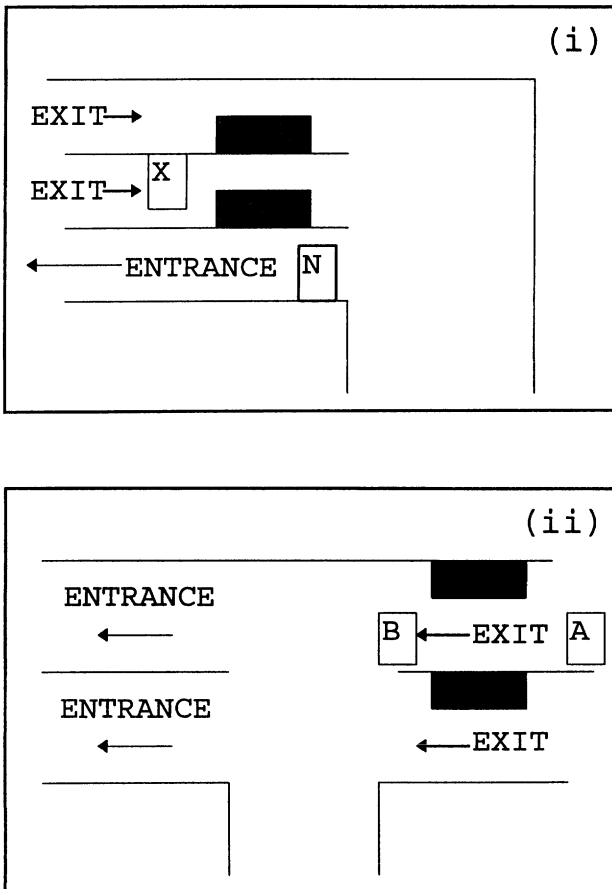
Figure 2. Sampling locations in (i) St John's car park and (ii) St Mary's car park. Payment booths are shaded.

The car parks selected were St John's (11 900 to 12 900 vehicles per week) and St Mary's (9800 to 11 000 vehicles per week). At St John's two tubes were positioned at a height of 1.5 m in the exit (position X, Figure 2) and two in the entrance (position N, Figure 2). A tube was placed in each payment booth, just above the head of the attendant. Due to the different layout of St Mary's two tubes were positioned just before (position A, Figure 2) and just after (position B, Figure 2) the exit barrier. Tubes were also located in the payment booths. Both car parks included an extraction system to remove the exhaust fumes of car queuing to exit. All payment booths were equipped with a ventilation system which operated by drawing air from outside the car park and feeding it into the booths. Again tubes were collected and replaced every week from 9 November 1993 to 25 March 1994.
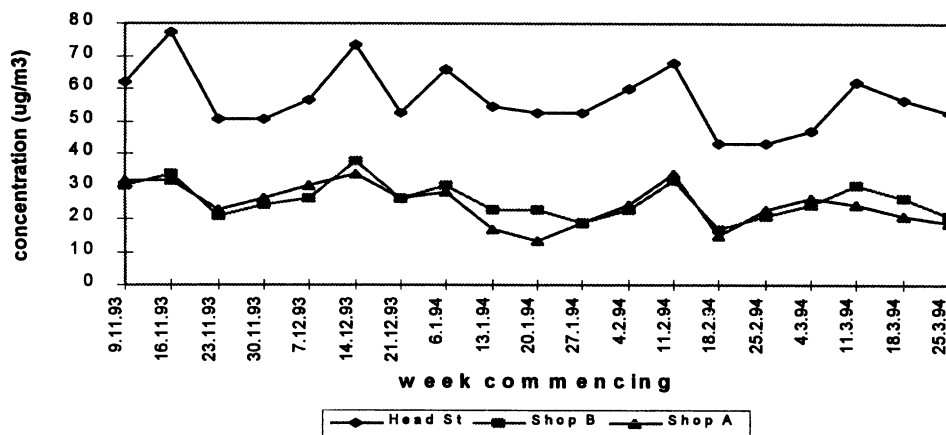
Figure 3. Nitrogen dioxide concentrations in shops and Head Street.

3. Results and Discussion

3.1. SHOPS

Figure 3 shows the variation of NO$_2$ in the two shops and in Head Street. Levels in Head Street are comparable with other roadside sites, with similar traffic densities in the UK (Stevenson and Bush, 1995). The values for Head Street are the average of four tubes (two on each lamp-post). It is known that small differences in the location of the sampler can lead to large differences in average concentrations. In this case concentrations outside shop B were statistically indistinguishable from those outside shop A. The influence of meteorological conditions on dispersion of pollutants can explain much of the week to week variability in ambient NO$_2$ levels. NO$_2$ in both shops follows a similar pattern to that in Head Street with a correlation coefficient of 0.47 and 0.78 for shops A and B respectively. NO$_2$ concentrations in shop A ranged from 13 to 34 μg m^{-3} with an average of 24.5 μg m^{-3}, whilst in shop B NO$_2$ varied from 17 to 38 μg m^{-3} with an average of 25.6 μg m^{-3}. The indoor:outdoor ratio for NO$_2$ ranged from 0.34 to 0.54 with an average of 0.44.

   Little data is available with which to compare these results and like any study relating indoor NO$_2$ to outdoor NO$_2$ generalisation to other situations is difficult. The ratio would be expected to depend not only on indoor sources and infiltration of air but also on the operation and business hours of the shops. Concentrations of NO$_2$ have been reported in shops (Liao *et al.*, 1991) and in offices (Ekberg, 1995). Liao *et al.* (1991) monitored NO$_2$ in offices and shops in Hong Kong. The shops included those with air conditioning as well as those with natural ventilation, whilst all the offices had some form of air conditioning. Sampling, using a passive filter badge, took place during business hours and the average indoor:outdoor ratio was 0.82 and 0.19 for shops and offices respectively. The high ratio in shops is not surprising since the doorways were always left open during business hours

providing easy access not only for customers but also for outdoor air. The offices were all located in medium to high buildings thus reducing the influence of vehicle emissions on indoor air quality. Ekberg (1995) measured NO_2 continuously for a week in four offices in Gothenberg, Sweden. Over a 24 hr period they found an indoor:outdoor ratio of 0.73 for a building with natural ventilation. Many studies of NO_2 in the domestic environment have been reported (IEH, 1996). UK studies where no indoor sources of NO_2 were present report much higher indoor:outdoor ratios than those found in the shops in this study. For instance Meli *et al.* (1990) report indoor:outdoor ratios of 0.99, 0.80 and 0.96 for measurements in the kitchen, living room and bedroom respectively of homes in London during September. In Manchester Raw and Coward (1992) determined an indoor:outdoor ratio of 0.92 for a mixture of urban, suburban and rural homes during the summer. Coward and Raw (1996) monitored NO_2 in a variety of homes in the Avon area over a 12 month period. The indoor:outdoor ratios for the autumn were 0.76, 0.54, 0.63 and 0.70 for rural, suburban, urban and central urban sites respectively.

3.2. CAR PARKS

Figures 4 and 5 shows the variation of NO_2 in the St John's and St Mary's car park respectively. NO_2 in the payment booths follows a similar pattern to that in car parks with correlation coefficients (between booth and car park) of 0.73 and 0.69 for St John's and St Mary's car parks respectively. NO_2 concentrations in St John's car park ranged from 58 to 90 μg m^{-3}, whilst those in the payment booth varied from 43 to 60 μg m^{-3} with an average of 51.3 μg m^{-3}. The respective ranges and values at St Mary's were 54 to 78 μg m^{-3}, 42 to 56 μg m^{-3} and 49.4 μg m^{-3}. At St John's the payment booth:car park ratio for NO_2 ranged from 0.65 to 0.77 with an average of 0.71 whilst at St Mary's it varied from 0.71 to 0.86 with an average of 0.75. The values obtained represent a weekly average. There is little difference in concentrations and trends within the two car parks despite St John's closing between the hours of 00.00 and 07.00 each day and all day Sunday. The absence of any correlation between ambient levels and those in the car parks indicates that week to week variations result from changes in car park usage rather than meteorological conditions. NO_2 concentrations were measured continuously, on three separate occasions, in a payment booth at St John's car park with a Uniresearch LMA-3 Luminox monitor. Figure 6 shows the NO_2 concentration measured on 5 February 1994. Levels were typically around 28 ppb (53 μg m^{-3}) with excursions of a few minutes duration in excess of 40 ppb (75 μg m^{-3}) and one peak reaching 65 ppb (122 μg m^{-3}). These peaks result from the door of the booth being opened and ingress of NO_2 rich air. Concentrations of NOx, carbon dioxide (CO_2), carbon monoxide (CO), volatile organic compounds and particulate material has recently been monitored in 12 underground car parks (Schwar, personal communication), where higher pollutant concentrations would be expected compared to our study. They found the individual users' exposure to
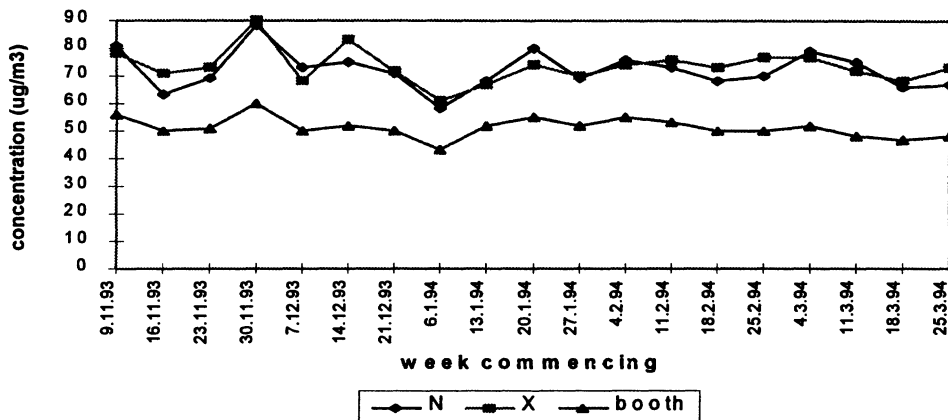
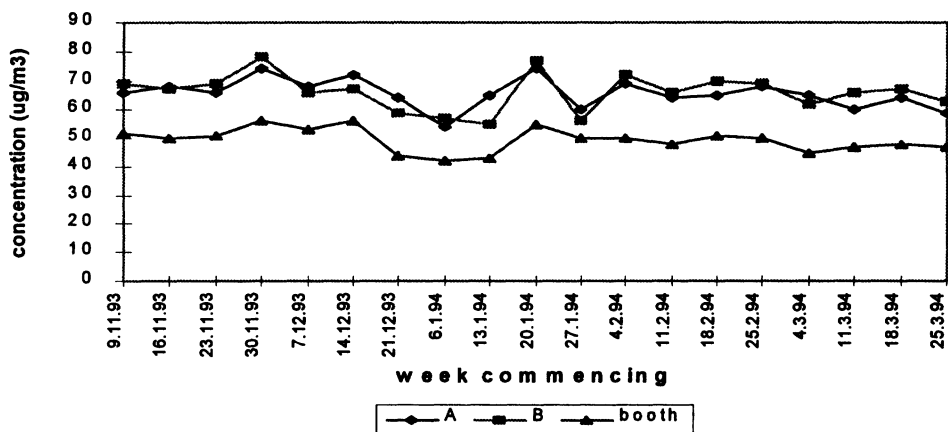*Figure 4.* Nitrogen dioxide concentrations in St John's car park.

Figure 5. Nitrogen dioxide concentrations in St Mary's car park.

NO_2 would only exceed recommended limits if users spent considerable periods in the car park. For car park employees none of the measured pollutants exceed the occupation exposure criteria. Our results support these conclusions.

4. Conclusions

NO_2 was measured in two shops on a weekly basis over 19 weeks. The shops fronted a busy main road. Indoor:outdoor ratios varied from 0.34 to 0.54 with an average value of 0.44. This value is lower than that reported in the domestic environment in the UK. The shops were, however, closed for approximately 68% of the time over a week. The indoor:outdoor ratio should be higher during business hours and also during the summer when shop doors are normally open. With little
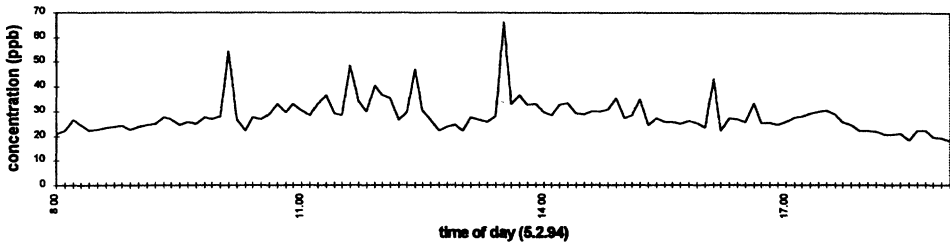
Figure 6. Nitrogen dioxide variation in a payment booth in St John's car park.

or no contribution from indoor sources, ambient concentrations are the primary factor in determining indoor levels.

Concentrations of NO_2 in car parks were similar to those measured at the kerb side. Provided a suitable ventilation system is in operation exposure of staff to NO_2 would only be a problem in the event of plant failure. Exposure of car park users to NO_2 is comparable to that arising in the vicinity of moderately trafficked roads.

References

Apling, A. J., Stevenson, K. J., Goldstein, B. D., Melia, R. J. W. and Atkins, D. H. F.: 1979, *Air pollution in homes 2; validation of diffusion tube measurements*, Warren Spring Laboratory Report LR311(AP).

Boleij, J. S. M., Lebret, E., Hoek, F., Noy, D. and Brunekreef, B.: 1986, *Atmos. Environ.* **20**, 597.

Bower, J. S., Lampert, J. E., Stevenson, K. J., Atkins, D. H. F. and Law, D. V.: 1991, *Atmos. Environ.* **25B**, 4255.

Coward, S. K. D. and Raw, G. J.: 1996, *Indoor Air Quality in Homes: The BRE Indoor Environment Study, Part I NO₂*, Berry, R. W. *et al.* (eds.).

Ekberg, L. E.: 1995, *Build. Environ.* **30**, 293.

Gamble, J., Jones, W. and Minshall, S.: 1987, *Environ. Res.* **42**, 201.

Gatward, J. and Colls, J. J.: 1990, *Environ. Technol.* **11**, 381.

Hatton, D. V., Leach, C. S., Nicogossian, A. E. and di Ferrante, N.: 1977, *Arch. Environ. Health*, **32**, 33.

Hedberg, K., Hedberg, C. W., Iber, C., White, K. E., Osterholm, M. T., Jones, D. B. W., Flink, J. R. and MacDonald, K. L.: 1987, *J.A.M.A.*, **262**, 3014.

Hewitt, C. N.: 1991, *Atmos. Environ.* **25B**, 429.

IEH: 1996, *IEH assessment on indoor air quality in the home, assessment A2*, Institute for Environment and Health.

Nakai, S., Nitta, H. and Maeda, K.: 1995, *J. Expos. Anal. Environ. Epidem.* **5**, 125.

Palmes, E. D., Gunniston, A. F., DiMattio, J. and Tomczyk, C.: 1976, *Am. Ind. Hyg. Assoc.* **7**, 570.

Raw, G. J. and Coward, S. K. D.: 1990, *Proc. of Unhealthy Housing; The Public Heath Response*, Warwick University.

Ross, D.: 1996, *Environ. Technol.* **17**, 147.

Schwab, M., McDermott, A., Spengler, J. D., Samet, J. M. and Lambert, W. E.: 1994, *Indoor Air* **4**, 8.

Spengler, J., Schwab, M., Ryan, P. B., Colome, S., Wilson, A. L., Billick, I. and Becker, E.: 1994, *J. Air Waste Manage. Assoc.* **44**, 39.

Stevenson, K. J. and Bush, T.: 1995, *UK Nitrogen Dioxide Survey, Results for the First Year-1993*, AEA Technology, Report AEA/CS/RAMP/16419032.

Yoon, D. W., Lee, K. Y., Yanagisawa, Y., Spengler, J. D. and Hutchinson, P.: 1996, *Environ. Inter.* **22**, 309.

BIOGENIC EMISSIONS BY OAK TREES COMMON TO MEDITERRANEAN ECOSYSTEMS

V. SIMON, L. DUTAUR, S. BROUARD-DARMAIS, M.L. RIBA and L. TORRES
Laboratoire Chimie Energie- Environnement
Ecole Nationale Supérieure de Chimie de Toulouse
118, route de Narbonne - 31077 Toulouse Cedex 4 - FRANCE

Abstract. The experimental site was a Mediterranean type forest located in Viols-en-Laval near Montpellier (France). The principal species studied were *Quercus ilex* and *Quercus pubescens*. The determination of biogenic emissions was carried out by the enclosure method, which consists in enclosing an intact branch in a Teflon cuvet. The evolution of global terpenic emissions were recorded on June 1995.

For *Quercus ilex* it appears that most terpenic emissions take place during the diurnal period. The evolution of terpenic emission rates versus light (PAR), internal temperature within the cuvet, CO_2 exchange and transpiration (H_2O) were carried out. A close relation between terpene emission and light-triggered physiological activities, was always found. It is obvious that there was no simple correlation between the leaf temperature and the terpenic emission. The temperature of the leaves does not seem to play a significant role in the regulation of the monoterpenic emission. This behaviour allows us to conclude that light with its effect on assimilation and stomatal behaviour is the most important factor for monoterpenic emission by *Quercus ilex* like for *Quercus pubescens* which is an isoprene emitter.

1. Introduction

Important amounts of Volatile Organic Compounds (VOCs) of anthropogenic and/or biogenic origin are regularly released into the atmosphere (Fehsenfeld *et al.*, 1992). With the NO_x, they play an important role as precursors to the photochemical pollution of the air (Brasseur and Chatfield, 1991). Amongst VOCs of biogenic origin, isoprene and monoterpenes are those having the highest impact in tropospheric chemistry due to their predominance in the emissions and their high reactivity. A better knowledge of the atmospheric processes in which these compounds are involved requires a qualitative and quantitative characterization of their principal sources.

The present work was carried out within the frame of the BEMA (Biogenic Emissions in the Mediterranean Area) project. The main objective of our participation was to gain to a better knowledge of the qualitative and quantitative composition of the sources of biogenic compounds emitted by vegetal species being characteristic of the Mediterranean area. We chose to present the results relative to the two principal ones: *Quercus pubescens* and *Quercus ilex*. These results were obtained on 20, 21, 22 June 1995.

2. Materials and methods

2.1. EXPERIMENTAL SITE

The selected experimental site was a Mediterranean type forest located in Viols-en-Laval, 20 km North from Montpellier (France). The site was consisting principally of a clear forest containing *Quercus pubescens* (25 %), *Quercus ilex* (25 %) and also shrubs like *Buxus sempervirens* (5 %), *Juniperus oxycedrus* (3 %). It is located at an altitude of 215 m.

2.2. THE ENCLOSURE METHOD

The determination of biogenic emissions for a given tree was carried out *via* the enclosure method using Teflon cuvets that were kindly supplied by Dr Kesselmeier from the Max Planck Institüt für Chemie, Mainz (Germany) (Kesselmeier *et al.*, 1996a). The emission rates were evaluated by periodical sampling and analysis of both internal and external atmospheres.

The cuvets, having a total volume of 75 l, were made of a 0.05 mm thick Teflon film. A continuous stream of ambient air was circulated through each cuvet at a flow rate of 20-25 l min^{-1}. The cuvets were placed at the top of the canopy. They were equipped with specific sensors allowing a continuous measurement of parameters such as the temperature, the PAR (Photosynthetic Active Radiation), the intensity of H_2O transpiration and CO_2 exchanges.

2.3. SAMPLING DEVICE AND ANALYTICAL METHOD

The air circulating through the cuvets was sampled and analyzed every hour. The trapping device, directly coupled with the injector of the gas chromatograph, was consisting of an unique Pyrex sampling tube (160 x 3 mm ID) packed with 280 mg of TENAX TA (60/80 mesh, Alltech-France). After thermodesorption, the terpenic compounds were thus injected by splitless mode in a HP 5890 II gas chromatograph equipped with Megabore Carbowax 20 M column (Alltech-France, 60 m x 0.53 mm ID, film thickness 1.2 mm). These automatic device for sampling and analysis as well as the calibration procedures have been described in details by Clément *et al.* (1993). The identification of isoprene and monoterpenes was done by using Gas Chromatography/Mass Spectrometry (GC/MS) (HP 5890 II/5971 A).

3. Results and discussion

3.1. *QUERCUS PUBESCENS* EMISSIONS

The only terpene emitted by *Quercus pubescens* is isoprene. Figure 1 displays the diurnal profiles of isoprene emission rates measured between June 20 and June 22. The emissions were found to be high at daytime, between 8 h and 20 h and rapidly decreased to a zero value at night.

Figure 2 shows the diurnal evolution of isoprene emission rates *versus* the evolution of the PAR, the internal cuvet temperature, the assimilation of CO_2 and of H_2O transpiration by the plant.

The emission of isoprene by *Quercus pubescens* is strongly correlated to the light intensity, to the photosynthetic activity and to the transpiration. These results are in agreement with numerous data obtained in laboratories or on sites for a wide number of isoprene emitters (Sanadze, 1991; Loreto and Sharkey, 1993; Guenther *et al.*, 1993).
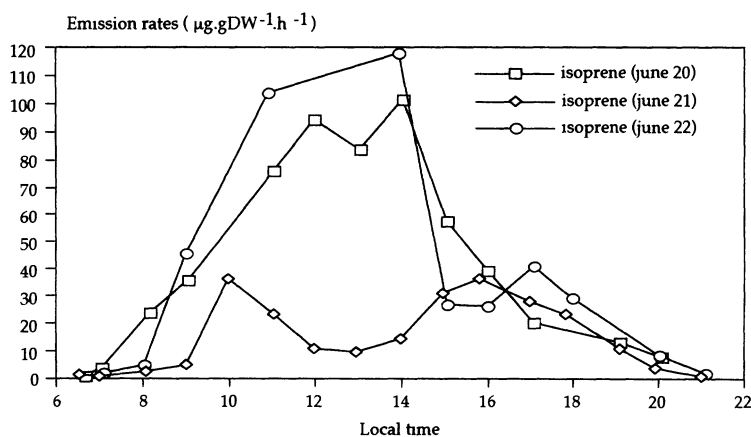
Figure 1: Diurnal profiles of isoprene emission rates for *Quercus pubescens*.

3.2. *QUERCUS ILEX* EMISSIONS

Quercus ilex is a strong monoterpene emitter. The main compounds detected in its emissions are: α-pinene, β-pinene, myrcene, sabinene, limonene, 1,8-cineole and γ-terpinene. Figure 3 shows an example of diurnal cycles of terpenic emission. The profiles indicate maximum emission rates at daytime and minimum ones at night, approaching zero value.

The emission rates vary between maximum values of the order of 10 $\mu g.g^{-1}$ dry weight.h^{-1} for α-pinene and a few tenth of $\mu g.g^{-1}$ dry weight.h^{-1} for the less abundant compounds such as 1,8-cineole and γ-terpinene. The midday depression was observed.
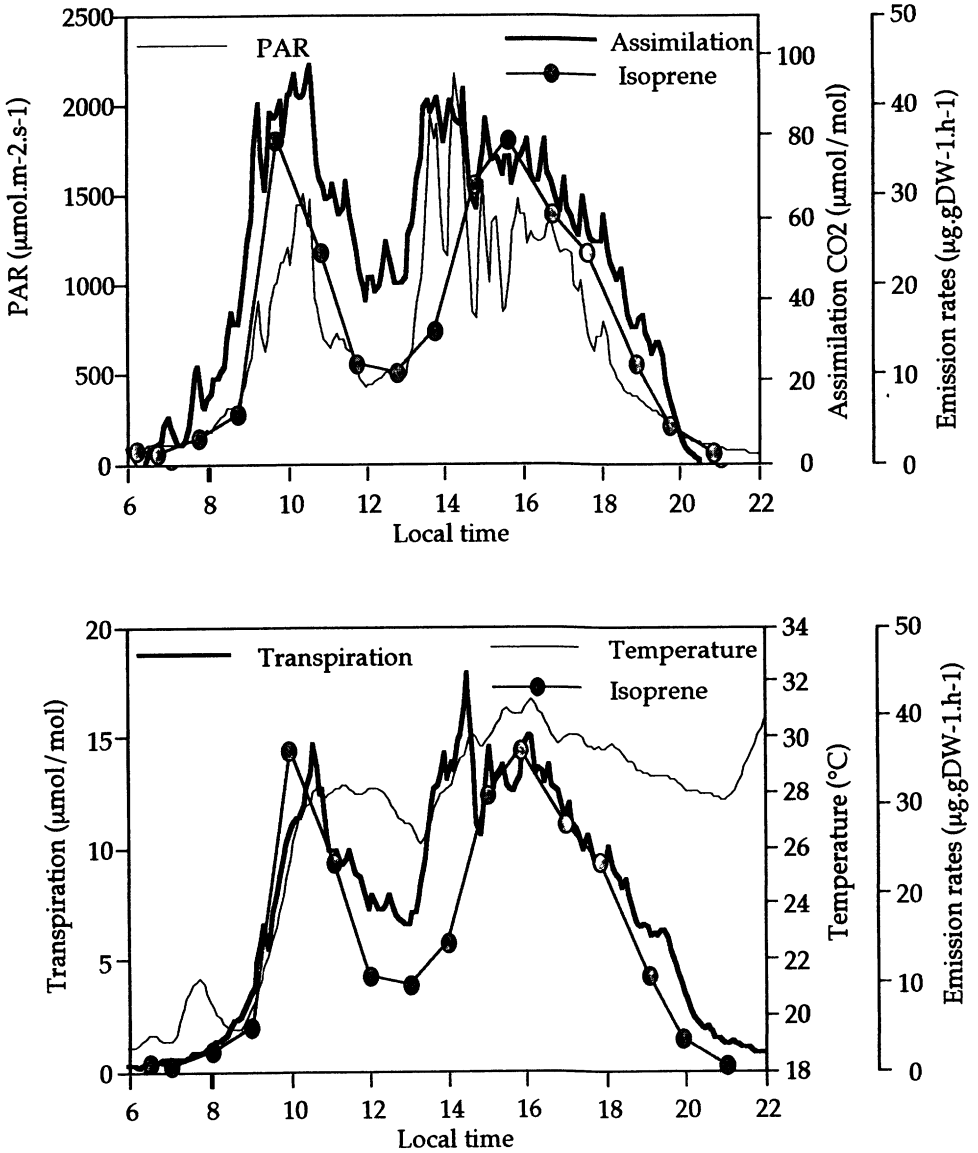
134

Figure 2: Isoprene emission rates, PAR, assimilation, transpiration and temperature profiles for *Quercus pubescens* (June 21).
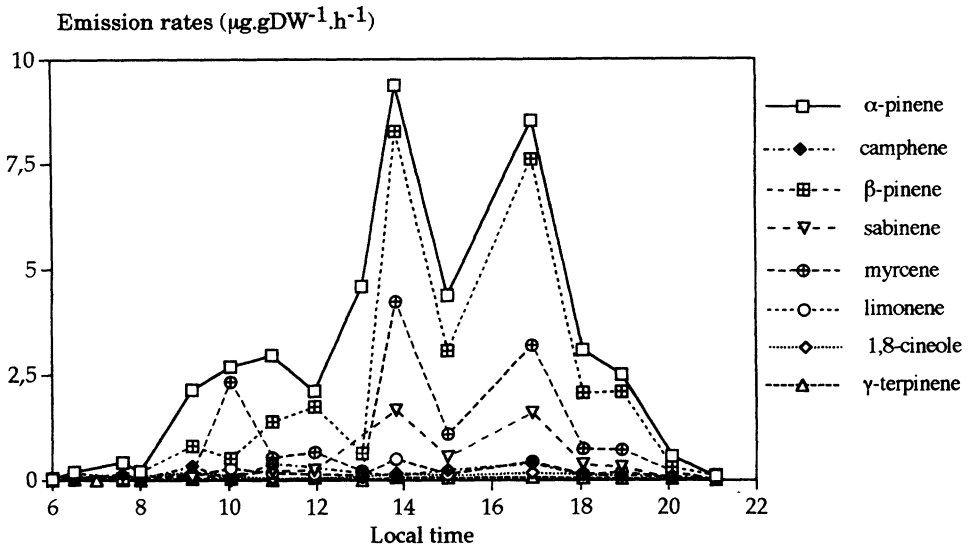
Figure 3: Diurnal profiles of terpenic emission rates for *Quercus ilex* measured on June 21, 1995.

TABLE 1

Relative amounts of principal terpenes emitted by *Quercus ilex* expressed as %.

Compounds	Rome	Montpellier
	May 15, 1994	June 20, 1995
α-pinene	40,5	43,8
β-pinene	26,5	34,1
sabinene	23,4	7,2
myrcene	3,4	11,8
limonene	3,2	2,1
1,8-cineole	1,4	0,4
γ-terpinene	1,6	0,2

The data recorded in the present experiment are listed in table 1 against those recorded on the same vegetal species during a previous experiment carried out in Castelporziano near Roma (Italy) (Kesselmeier *et al.*, 1996b). We note slight changes in the respective amounts of some derivatives, namely sabinene and myrcene in particular. Such a geographical and temporal variability has been already observed (Corchnoy *et al.*, 1992). Our field experiments tend to confirm the light dependency of the emission of monoterpenes by *Quercus ilex*. Figure 4 indicates that the photosynthetic activity and the terpenic emission start almost simultaneously with the lighting of the vegetal plant in the morning. Photosynthesis as well as transpiration and emission are seen to stop in the absence of PAR.

3.3. *QUERCUS PUBESCENS /QUERCUS ILEX*

The terpenic emission rates of *Quercus ilex* and *Quercus pubescens* were found to be correlated with physiological and micrometeorological parameters. Table 2 shows the correlation coefficients. These results tend to confirm the importance of the PAR in the terpenic emission process.

TABLE 2

Correlation coefficients between emission rates and the micrometeorological and physiological parameters of *Quercus ilex* and *Quercus pubescens* (20-21-22 June 1995).

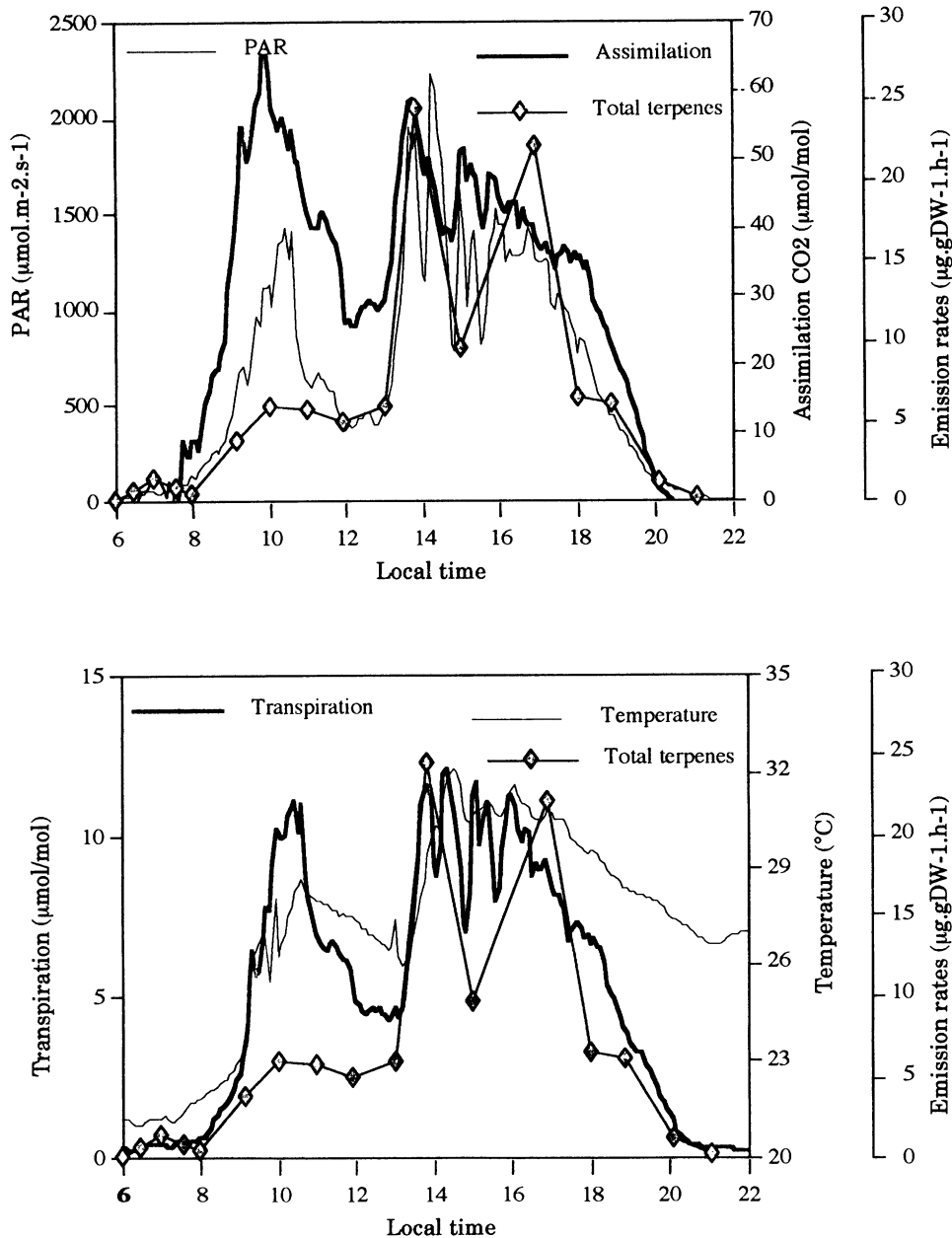|	*QUERCUS ILEX*	*QUERCUS PUBESCENS*
Cuvet temperature	0,62	0,76
PAR	0,76	0,80
Transpiration (H_2O)	0,78	0,88
Assimilation (CO_2)	0,64	0,85

Figure 4: Terpenic emission rates, PAR, assimilation, transpiration and temperature profiles for *Quercus ilex* (June 21).

Figure 5 displays both the isoprene emission rate profiles of *Quercus pubescens* and those corresponding to the total amount of monoterpenes emitted by *Quercus ilex*. For the two oaks, the terpenic emission begins at sunrise and stops completly at sunset. The two identical cuvets installed on both *Quercus* were submitted to the same PAR and internal temperatures. The shape of the two plots is roughly the same, whereas the magnitude of the emissions is seen to vary up to a factor of 4. This tends to indicate that *Quercus ilex*, which synthesizes and emits essentially monoterpenes, exhibits a metabolic behavior being very close to that of *Quercus pubescens* which is almost exclusively an isoprene emitter. These results obtained on the experimental site were recently corroborated by laboratory studies by Loreto *et al*. (1996).
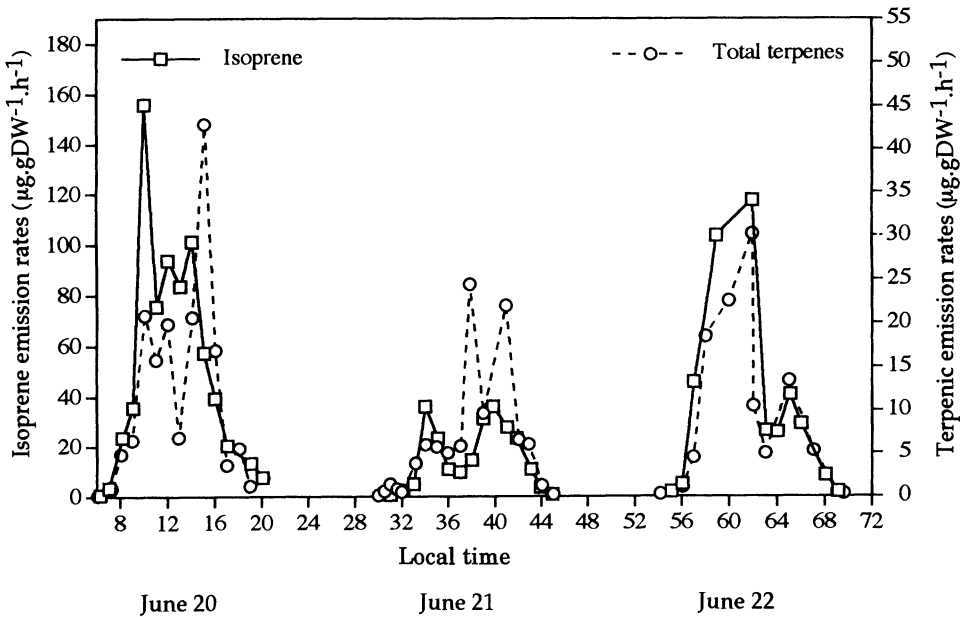

Figure 5: Diurnal profiles of isoprene and total monoterpene emission rates for *Quercus pubescens* and *Quercus ilex*.

4. Conclusion

In contrast to most species belonging to the *Quercus* family, *Quercus ilex* is a very strong emitter of monoterpenes and a very poor emitter of isoprene.

The respective profiles of the monoterpenic emission by *Quercus ilex* and the isoprene emission by *Quercus pubescens* are very similar. They are characterized by a strong emission in the presence of light intensity and an absence of emission during the night.

Our results suggest that *Quercus ilex*, a species producing and releasing monoterpenes, possesses a site of biosynthesis and emission processus which are closely related to that of a species producing and releasing isoprene.

Acknowledgements

R e f e r e n c e s

Brasseur G.P. and Chatfield R.B.: 1991, *Trace Gas Emission By Plants, Sharkey et al., Academic Press, New York, 1-27.*

Clément B., Riba M.L., Simon V. and Torres L.: 1993, *Intern. J. Anal. Chem.*, **50**, 19-27.

Corchnoy S.B., Arey J. and Atkinson R.: 1992, *Atmos. Environ.*, **26B**, 3, 339-348.

Fehsenfeld F., Calvert J., Fall R., Goldan P., Guenther A. B., Hewitt C. N., Lamb B., Liu S., Trainer M., Westberg H. and Zimmerman P.: 1992, *Global Biogeochemical Cycles*, **6**, 4, 389-430.

Guenther A.B., Zimmerman P., Harley P. and Monson R.K.: 1993, *J. Geophys. Res.*, **98**, D7, 12, 609-12, 617.

Loreto F. and Sharkey T.D.: 1993, *Planta*, **189**, 420-424.

Loreto F., Ciccioli P., Cecinato A., Brancaleoni E., Frattoni M., Fabozzi C. and Tricoli D.: 1996, *Plant. Physiol.*, **110**, 4, 1317-22.

Kesselmeier J., Bode K., Hofmann U., Müller H., Schäfer L., Wolf A., Ciccioli P., Brancaleoni E., Cecinato A., Frattoni M., Foster P., Ferrari C., Jacob V., Fugit J.L., Dutaur L., Simon V. and Torres L.: 1996a, *Atmos. Environ.*, (in press).

Kesselmeier J., Schäfer L., Ciccioli P., Brancaleoni E., Cecinato A., Frattoni M., Foster P., Jacob V., Denis J., Fugit J.L., Dutaur L. and Torres L.: 1996b, *Atmos. Environ.*, **30**, 10/11, 1841-1850.

Sanadze G.A.: 1991, *Trace Gas Emission By Plants, Sharkey et al., Academic Press, New York*, 135-152.

NEAR - INFRARED DIODE LASER AIR MONITORING

Robert J.Holdsworth and Philip A.Martin

Department of Chemical and Biological Sciences, University of Huddersfield,
Queensgate, Huddersfield, W.Yorkshire, HD1 3DH
Email: P.A.MARTIN@HUD.AC.UK

Abstract. Inexpensive near-infrared diode lasers are now being used to enable high sensitivity, real time monitoring of gases both in open path measurements of urban air quality and in industrial environments for stack gas emission monitoring. Individual species are detected in a highly selective manner via overtone and combination bands of their vibrational spectra. Operating at room temperature and with simple optical components they can be made into portable instruments, ideal for field measurements. Combined with optical fibres they can be used for accessing remote and possibly dangerous locations. This paper presents current progress on the development of such a system illustrating recent results on ammonia monitoring at 1540 nm and acetylene at 780 nm. Sensitivies of the order of parts per million and below have been attained. Advantages and disadvantages of this approach to air pollution monitoring will be described. Pressure broadening results are also given for the $2v_1$ band of ammonia.

1. Introduction

Much of the recent demand for urban air pollution monitoring is for real time instruments which can measure rapidly varying concentrations of several species. The very low concentrations of most pollutant gases usually means that instruments designed for such measurements are either bulky, thus limiting their portability, or very expensive. Examples, are LIDAR, DIAL and Fourier transform spectroscopy (Sigrist, 1994) techniques. Tunable diode laser absorption spectroscopy also fits into this category and has been used for air pollution monitoring for several years now, offering very high sensitivity (sub-ppb) and high specificity (Fehér and Martin, 1995). The lasers operate at cryogenic temperatures and vibrational transitions of the pollutant gas molecules are detected in the mid-infrared spectral region. An inexpensive extension to this technique is to use a near-infrared diode laser which is very common in optical communications and compact disc technology. Although the technique is not as sensitive in the near-infrared spectral region these lasers operate at room temperature and so are potentially more useful for field measurements.

A portable system based on near-infrared diode lasers has many advantages. It can be used in an open path mode where the laser beam is easily steered in different directions for spatial mapping. With the high time resolution, flux or boundary fence measurements can be made when combined with simultaneous measurement of wind velocities. An example of this application is the determination of methane concentrations over an active landfill site (Hovde *et al*, 1995). In the open path mode the concentrations are integrated over the whole pathlength which can be of the order of 100 m. Alternatively, point source measurements are obtained by using a multipass cell either open or pumping the air through under reduced pressure. High specificity is another major advantage of this technique. Many other methods are plagued by interferences from other species leading to possible inaccuracies in the results. The high spectral

resolution of the laser means that absorption features of the gas of interest are well separated from possible interfering lines.

Each diode laser has a relatively small wavelength tuning range so that different diodes are required for detecting several species. Until recently diodes were only available in specific regions such as 0.67, 0.82, 1.3 and 1.5 μm as a result of their other applications but they are now available at any wavelength between 0.6 and 2 μm. Their use in optical communications means that the laser output is easily coupled to fibre optics which then allows remote locations to be monitored. Sensitivity is usually in the ppm range and below for most gases such as CH_4, NH_3, H_2S (Cooper and Martinelli, 1992). The low operating costs and long term reliability as well as the eye-safe nature of the low-power infrared beams also makes these instruments ideal for industrial environments such as stack gas monitoring.

The aim of this paper is to describe a near-infrared tunable diode laser system for urban air and stack gas monitoring. The first part describes the experimental details and discusses detection limits with specific reference to ammonia with an example of a preliminary field on stack gases. The second part presents some new results on pressure broadening of absorption linewidths in an overtone band of ammonia.

2. Experimental

The measurement principle of the near-infrared diode laser air monitoring system is that of standard infrared absorption spectroscopy. Each pollutant species has a unique spectrum or fingerprint and the intensity of a particular absorption feature is proportional to the concentration of the species within certain limits. *Figure 1* shows a Fourier transform spectrum of ammonia with the various infrared vibrational bands.
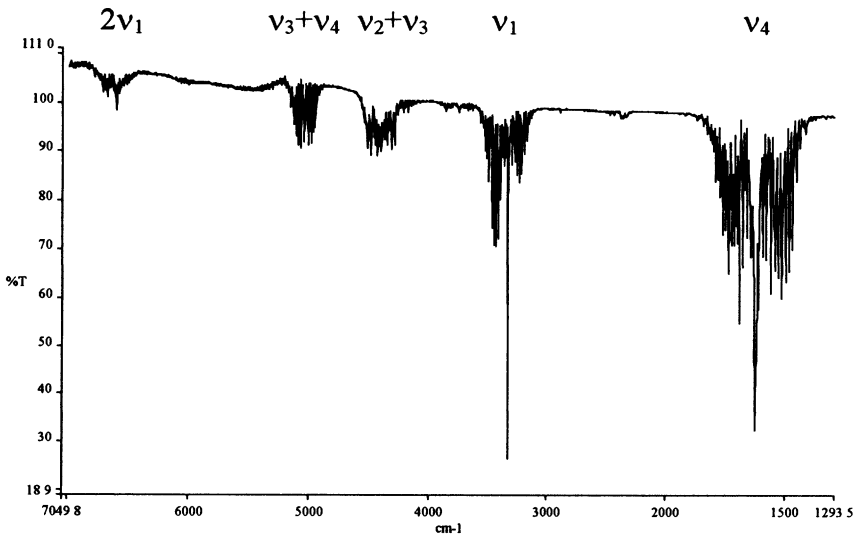

Figure 1. Fourier transform infrared spectrum of ammonia at 50 torr

This is recorded with a resolution of 1 cm^{-1} and thus has many overlapping lines. An individual diode laser can scan over only a small window in this spectrum but at much higher resolution so that many lines can be resolved and contributions from interfering species can be avoided. The laser wavelength is tuned into resonance with a strong absorption peak by varying the temperature and/or the current across the diode (Baumann *et al.*, 1992).

Figure 2 shows the experimental setup for operation of the system in the multipass mode. The laser is mounted on a Peltier cooling element which allows stable temperatures from -10 to +50°C. In the experiments described here the laser is an InP/InGaAsP buried heterostructure type (Hecht, 1992). A White-type multipass gas cell is used to increase the absorption pathlength and thus sensitivity. Polluted air is then pumped through the cell under reduced pressure. Long open path measurements can also be made using a retroreflector to return the beam to a photodiode detector. Two different recording modes are usually employed: amplitude and wavelength modulation. In amplitude modulation the laser beam is chopped at a frequency of around 400 Hz and after amplification the photodiode signal is demodulated with a lock-in amplifier. In wavelength modulation, which is more sensitive, a sawtooth waveform, supplied by a function generator, is applied to the laser current at frequencies of the order 10 kHz which modulates the laser wavelength. Again the signal is demodulated with a lock-in amplifier and usually the 2nd harmonic or 2nd derivative signal (2f) is monitored. The whole system including data acquisition is controlled by computer.
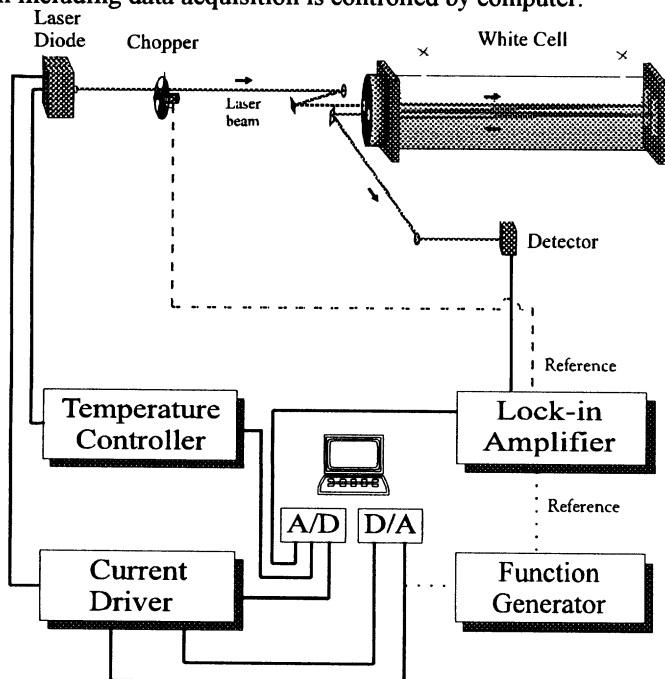

Figure 2. Experimental setup

The instrument can be continuously calibrated by passing 10% of the beam through a reference gas cell containing a known amount of the gas of interest made up with air to the same pressure that the sample is being monitored. Temperature or current instabilities may cause the laser wavelength to drift off the absorption line centre. Longer term stability of the instrument is then achieved by actively locking the laser wavelength to the maximum of the absorption feature of interest by monitoring the first derivative line shape from the reference gas cell. Any drifts away from the line centre are converted into a current adjustment to the laser control via a negative feedback loop (first-derivative line-locking).

3. Detection Limits

The minimum detectable concentrations depend on several factors such as the intrinsic bandstrength or linestrength, gas pressure and pathlength. Monitoring a single vibration-rotation line of the $2v_1$ band of ammonia at 6480 cm^{-1} (see *figure 1*) the minimum detection limit at atmospheric pressure was 66 ppm per metre for a 1s integration time which extrapolates to 1.3 ppm for a 50 m pathlength. The measurements were made under laboratory conditions by introducing a known amount of pure ammonia from a gas cylinder into the multipass cell and diluting to atmospheric pressure with laboratory air. Lower concentrations were then produced by further dilution of the gas mixture with laboratory air. If the total pressure is reduced down to about 80 torr the sensitivity increases to 2 ppm.m or 40 ppb over a 50m pathlength. A signal to noise ratio of 2:1 is taken as the minimum detection limit. The effects of atmospheric pressure on three lines of the $2v_1$ band of ammonia are illustrated in *Figure 3*. The lower figure (b) is the second derivative wavelength modulation spectrum of 5 torr of pure ammonia, whereas in the upper figure (a) air has been added to the same amount of ammonia up to a total pressure of 760 torr. As can be seen the lines become broader. Lower detection limits can be achieved by accessing more intense lines in the $2v_1$ or with a different diode in the $v_3 + v_4$ band around 5000 cm^{-1}. Overtone and combination bands such as these are intrinsically much weaker than fundamental vibrational bands in the mid-infrared spectral region.

Measurements have also been made on acetylene at 780 nm, measured in the same way as described above for ammonia, where the lowest detection limits were 129 ppm.m. This is limited by the low linestrength but diodes in this region are widely available and inexpensive as their main application is for cd players. Approximate calibration of the concentrations have been made in these experiments using a capacitance pressure gauge but for more accurate measurements a permeation tube could be used.
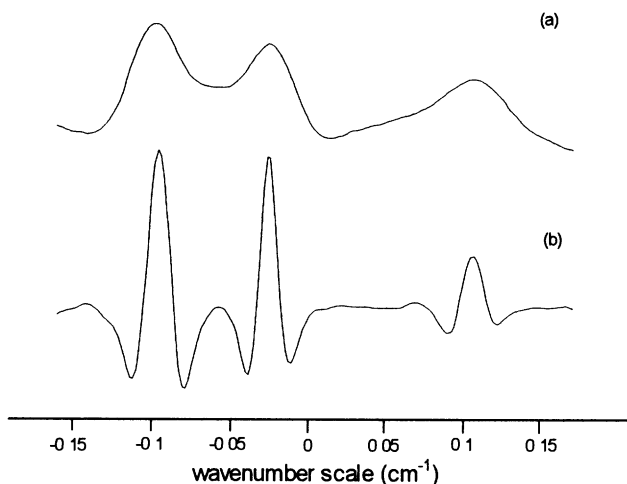
Figure 3. Effects of pressure broadening on 2nd derivative line shapes of ammonia in the region 6480 cm^{-1}. Details are given in the text.

4. Field Trials

Preliminary field trials were made for an ammonia stack gas monitoring application at a large Swiss chemical company. For this trial the air sample was withdrawn from the stack and continuously passed through a 30 cm absorption cell under a reduced pressure of about 100 torr for maximum sensitivity. Laboratory detection limits could be reproduced, although for the short times when ammonia was released into the stack the concentrations were a factor of 100 greater than these limits. Some of the problems encountered were as follows. Transmission losses due to particulates in the stack were minimised by filtering the air sample before analysis. Temperature changes affect the instrument in two ways. Firstly the laser wavelength may drift off the absorption maximum inspite of the laser being mounted on a thermoelectric temperature stabiliser. First derivative line-locking was employed, as described above, to minimise these problems. Secondly, large temperature variations will cause expansion of the optical bench and mounts, thus introducing misalignments. In this application it was not a problem although it could be easily checked by continuously monitoring the laser power. Changes in atmospheric humidity or the concentration of water vapour in the stack gases did not interfere with these particular measurements because the ammonia absorption feature selected was far removed from any water absorptions. Tests were made on a several amines which were also present in the stack to test for possible interferences. These stack gas measurements will be repeated with attention being focussed on the temporal stability of the instrument.

5. Line broadening

Absorption lines at atmospheric pressure are much broader than at low pressure as can be seen in *figure 3*. Accurate measurement of this broadening is extremely useful for simulating atmospheric absorbance at different wavelengths which is often essential for open-path measurements. It also enables the deconvolution of atmospheric lines to give information about the altitude distribution of the molecules. At low pressures (below around 1 torr) the individual vibration-rotation lines are Doppler broadened and have a Gaussian lineshape. At higher pressures collision broadening becomes more important and the linewidth is Lorentzian in shape. At intermediate pressures the lineshape is of Voigt-type (Webster, 1988).
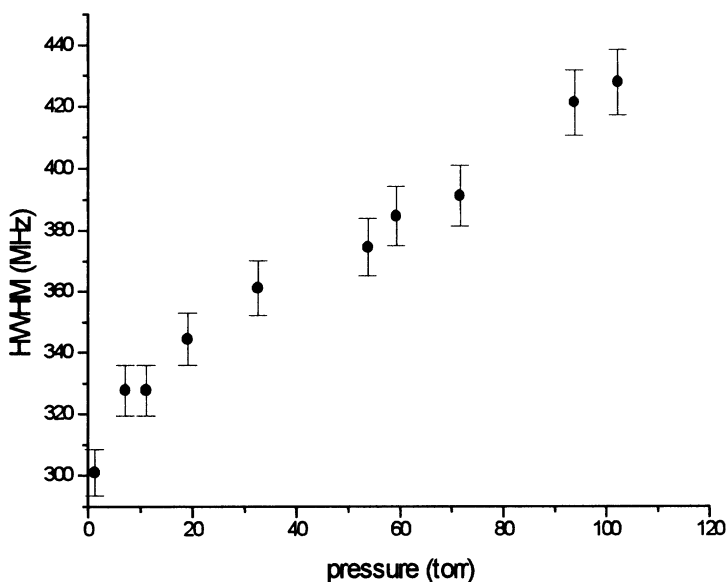

Figure 4. Effect of air broadening on a single vibration-rotation line of ammonia in the $2\nu_1$ band. The initial ammonia pressure was 1.3 torr and the pressure indicated is the total pressure, ammonia plus laboratory air. (HWHM - Half width at half maximum)

Figure 4 shows the increase in the half width at half maximum (HWHM) of an individual vibration-rotation line in the $2\nu_1$ band of ammonia around 6480 cm^{-1} at 1.3 torr when laboratory air is added up to the pressure indicated. From the gradient the air-broadening coefficient was determined to be 1.05 (4) MHz/torr. *Figure 5* shows the linewidth increase as a result of self-broadening with a coefficient of 14.6 (11) MHz/torr

for the same line of ammonia. In this case the broadening is much greater due to the large dipole moment of the NH_3 molecule. This band of ammonia has yet to be analysed so it is not possible to give the assignment.
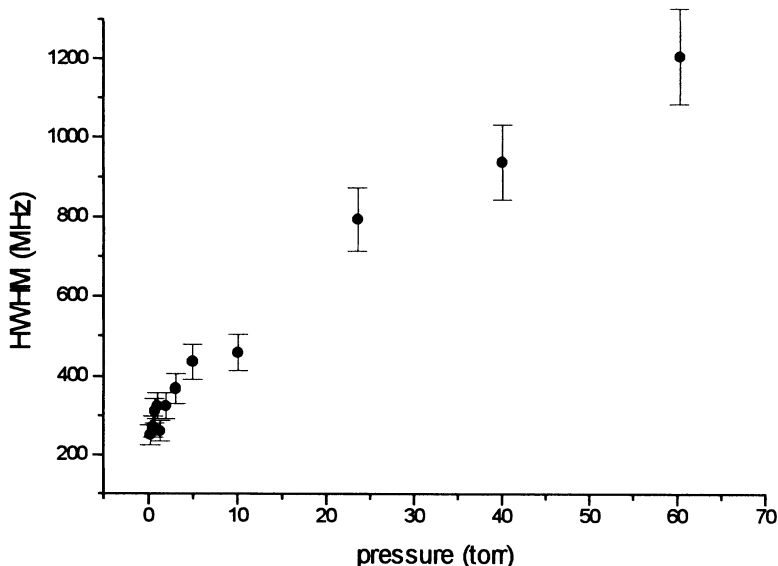

Figure 5. Effect of self-broadening on a single vibration-rotation line of pure ammonia in the $2\nu_1$ band.

6. Discussion and Conclusions

Initial field trials of ammonia stack gas monitoring have shown that the system performs well under field conditions with laboratory detection limits being achieved. Quality control of the results can be obtained by continually monitoring the reference gas concentration which can also be used for wavelength stabilisation. Further checks can be made on the laser power as an indicator of laser malfunction or misalignment problems, including transmission losses due to light scattering off particulate matter. This latter effect would eventually reduce instrument sensitivity.

A near-infrared diode laser based monitoring system has been described which can be used for a wide variety of applications such as spatial measurements of methane on landfill sites, boundary fence monitoring of hydrogen sulphide and as a real-time gas analyser for industrial process monitoring of ammonia. The portable nature of the instrument and the ease of coupling to optical fibres make it ideal for field measurements. Laser technology is continuously improving allowing room temperature operation to be extended beyond the existing range of laser diodes so that different

148

species can be monitored and detection limits can be lowered. Current costs would be about £10000 for an instrument of this type which makes it inexpensive compared to alternative techniques.

Acknowledgements

References

Baumann, M.G.D., Wright, J.C., Ellis, A.B., Kuech, T. and Lisensky, G.C.: 1992, *J. Chem.Educ.* **69**, 89

Cooper, D.E. and Martinelli, R.U.: 1992, *Laser Focus World*, November 133

Féher, M. and Martin, P.A.: 1995, *Spectrochim.Acta A* **51**, 1579

Hecht, J.: 1992, *The Laser Guidebook*, 2nd Ed, McGraw-Hill

Hovde, D.C., Stanton, A.C., Meyer, T.P. and Matt, D.R.: 1995, *J. Atmos. Chem.* **20**, 141

Sigrist, M.W. (Ed.): 1994, *Air Monitoring By Spectroscopic Techniques* (Wiley)

Webster, C.R., Menzies, R.T., and Hinkley, E.D., 1988 *Laser Remote Chemical Analysis* (Wiley) (Ed. Measures, R.M.)

Analysis of Urban Atmospheric Pollution Data in the Bologna Area

G. CLAI, A. KERSCHBAUMER, E. TOSI and S. TIBALDI

University of Bologna- Department of Physics
Atmospheric Dynamics Group (ADGB)

Abstract. Pollutant concentrations relative to the years 1993-1995 measured in the Bologna urban area by a network of automatic stations (S.A.R.A. Sistema Automatico di Rilevamento Ambientale) are analysed to estimate the typical behaviour of the pollutants, especially with regard to periodicities and meteorological dependencies and to attempt prediction for the pollutant daily concentration up to a few days using a statistically based model.

The results obtained show the presence of a very significant weekly periodicity for all the analysed pollutants. A yearly periodicity has been found only for the primary pollutants analysed.

The statistical prediction, using an ARMA model with meteorological variables as transfer functions, shows good predicting capabilities up to one day for carbon monoxide (CO) and sulphur dioxide (SO_2) and up to two days for nitrogen dioxide (NO_2).

1. Introduction

Transport and diffusion of pollutants are strongly influenced by air turbulence (Arya, 1988). The monitoring network does not have adequate spatial and time resolution to allow the initialisation of a numerical prediction model for the air flow in Bologna. Therefore the only possibility is to use a statistically based prediction model.

The construction of a statistical model requires a long enough and reasonably continuous data record, and a careful investigation of the data characteristics (periodicity and autocorrelation) and the investigation on relations with external parameters (meteorological variables in our case). If these relations exist, stochastic methods are a good tool for giving a first answer to the problem (Zanetti,1990).

2. Data sets and data characteristics

This study concentrates on sulphur dioxide (SO_2), carbon monoxide (CO), and nitrogen dioxide (NO_2), that are a subset of pollutants recorded in Bologna by the urban atmospheric network of automatic stations S.A.R.A. (Sistema Automatico di Rilevamento Ambientale). These data are available for the period June 1993-May 1995 an consist of hourly concentrations. The monitoring network S.A.R.A. is composed of nine stations (seven urban, two suburban) placed as shown in Figure 1. The choice of the pollutants to be analysed has been based on data availability (series long enough and with
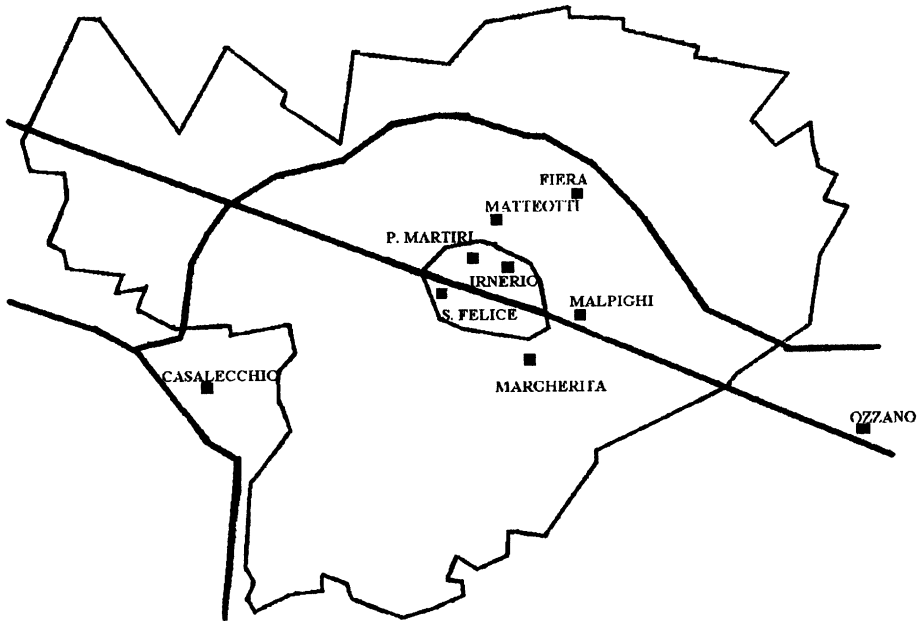
Fig. 1 Map of the monitoring network S.A.R.A.: the inner polygon delimits the historical centre. The outermost

perimeter marks the Municipality limits. Thicker lines represent the main roads and highways.

a limited number of missing observations) and by the fact that the pollutants considered are used to determine traffic restrictions if their concentration exceeds a given threshold.

The meteorological data consist of daily values of relative humidity, wind speed, temperature and ground pressure recorded at the nearby SYNOP station placed at Bologna airport.

Daily means are computed as mean of the hourly measures if these measures are at least 20. For longer gaps the year has been divided in three "seasons": hot, cold and intermediate, assuming that these periods are representative of different traffic regimes (this assumption will be justified later on when the yearly cycles will be presented). The hourly data are used to produce mean daily cycles for each day of the week and for each "season" and these mean values are used to substitute the missing data.

The analysis of variance and spatial correlation used in order to define the spatial representativeness of measuring points of the monitoring network shows that it is possible to identify three different climate types for the pollutant concentration: urban, suburban and neighbouring area. The stations chosen as representative of each climate are: Piazza Martiri, Fiera and Casalecchio for urban, suburban and neighbouring area respectively.

The periodicities in the concentration data are detected by spectral analysis and autocorrelation function (Jenkins,1968). Two main periods are detected: a weekly cycle present in all the three series of pollutant concentrations and an annual cycle present only in SO_2 and CO. The concentration versus time plot of NO_2 (not shown) shows in fact a

different behaviour during the two years of data. The shape of the annual cycle has been determined by repeatedly applying a running mean with a 21 days window and gaussian weights as low-pass filter. Figure 2 shows the annual cycle for SO_2 at Fiera with the unfiltered data superimposed.

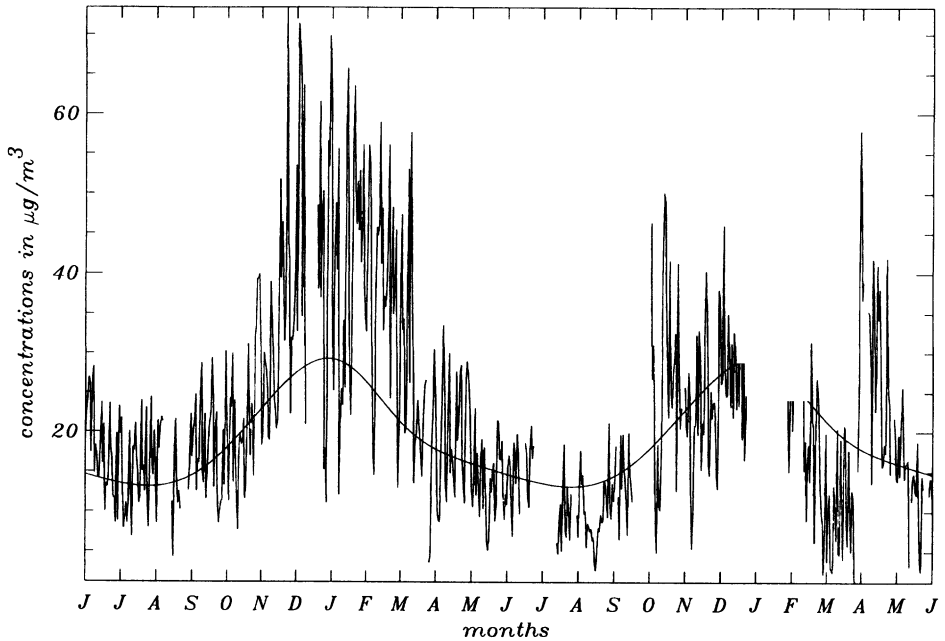Fig. 2. Yearly cycle of SO_2, concentration in $\mu g/m^3$, Fiera station.

The highest concentration values are detected in winter, and decrease approaching summer. The distinction of three regimes in concentration (and then in traffic) is evidently justified. The annual cycle of CO (not shown) has the same behaviour as SO_2.

The weekly cycle is evaluated for each "season" as a simple mean of daily values. Weekly cycles show relevant differences in the three considered "seasons" only for CO and SO_2, these differences are present but less intense for NO_2. Figure 3 shows the three weekly cycles for SO_2 as an example. The shapes of the cycles do not change from one "season" to the other and do not show strong variations from one pollutant to another. An evident decrease is always recorded during weekends and the lowest concentrations are detected on Sundays. These variations are probably due to antropogenic reasons (e. g. car traffic) and are not related to general causes. Unfortunately no traffic data series are available to verify this hypothesis.
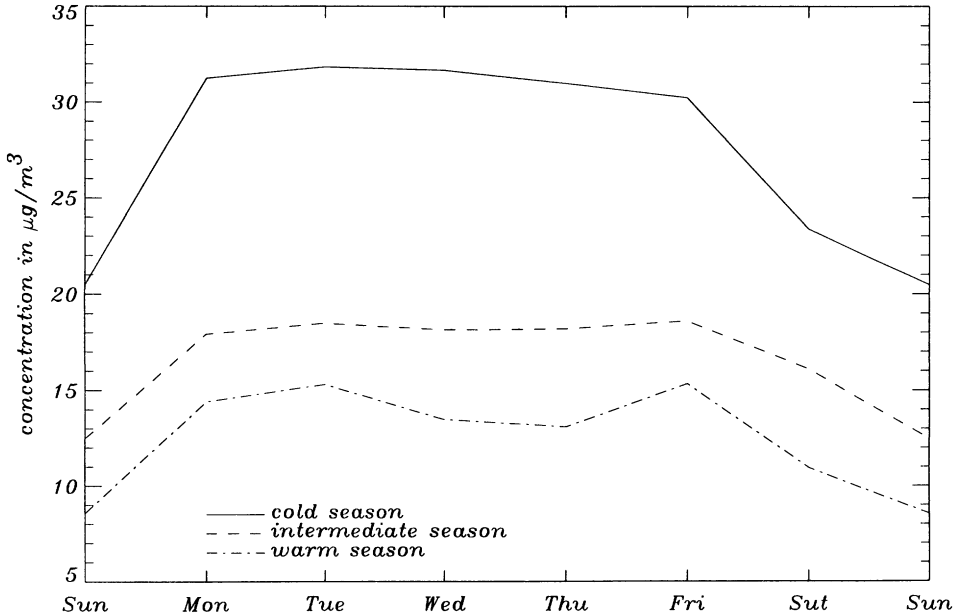
152

Fig. 3 Weekly cycle of SO$_2$, concentration in μg/m^3, Fiera station.

3. ARMA prediction

The autocorrelation function shows a clear autocorrelation up to three days. The correlation coefficients between meteorological variables and pollutant concentrations are not high, ranging from a minimum of 0.11 to a maximum of 0.26. As a first step the weekly and yearly cycles have been subtracted and an ARMA model without transfer functions has been applied. The general ARMA(p,q) model has p autoregressive terms and q moving-average terms that constitute a weighted average of the q values of random series ε, which corresponds to the residual in ordinary regression. We applied an ARMA(1,1) model , using the NAG library.

Then the meteorological variables are introduced as transfer function in order to obtained the maximum improvement of the performances of the autoregressive model, and in fact, the results obtained using the meteorological variables are a little better than those obtained by the autoregressive-moving-average model alone. The fitting coefficients R^2 (Mills, 1990) are shown in Table I and are computed on two years data (June 1993, May 1995). R^2 coefficients are always high, ranging between 0.411 for Fiera CO three days prediction, and 0.993 for Casalecchio NO$_2$ one day prediction. Only one occurrence of a very low coefficient has been found: Fiera NO$_2$ three days prediction (R^2=0.220).

TABLE I

R² Parameter estimates of the ARMA model with transfer functions.

Station	NO_2-1	NO_2-2	NO_2-3	SO_2-1	SO_2-2	SO_2-3	CO-1	CO-2	CO-3
Martiri Square	0 706	0.701	0.587	0.576	0.527	0.499	0.821	0.644	0.514
Commercial Fair	0.479	0.463	0.220	0.599	0.557	0.486	0.561	0.516	0.411
Casalecchio	0.993	0.871	0.753	0.858	0.683	0.580	0.537	0.474	0.415

A simulation experiment of concentration forecasting is made using the concentration data and meteorological observations recorded in the period June- August 1995. For a real forecast the meteorological observations should be substituted by data predicted by a limited area model. The results obtained are not as good as could be supposed from the R^2 coefficients.

As a global measure of the significativity of the forecasts the Theil index defined as:

$$ u = \sqrt{\sum_{1,N} (x_{obs} - x_{pred})^2 \Big/ N} \Big/ \left(\sqrt{\sum_{1,N} x_{obs}^2 \Big/ N} + \sqrt{\sum_{1,N} x_{pred}^2 \Big/ N} \right) $$

where N is the total number of forecasts an x is the forecasted variable, has been used. It is considered significant any prediction with Theil index not higher than 0.35 (Theil, 1971).

The most significant predictions are observed for NO_2 in two stations, Fiera (u=0.183 for one day forecast and u=0.276 for two days forecast (Figure 4) and Casalecchio (u=0.212 for one day forecast and u=0.269 for two days forecast).

Figure 5 shows SO_2 results for one and two days predictions (u=0.284 and u=0.403 respectively) at Fiera station and Figure 6 shows CO results for one and two days predictions (u=0.291 and u=0.415 respectively) at the same station. Two days forecast shows an evident persistence of the signal.

4. Conclusion

The aim of this study is to point out the global characteristics of urban air pollution in the Bologna area, and the methods applied are very general. The qualitative and descriptive results obtained show spatial correlation among the network stations which can be divided in three groups: 1) urban stations; 2) suburban stations; 3) neighbouring areas stations. The most representative station of each group is used in this analysis. Large yearly and weekly periodicities are found in the concentration data. A significant autocorrelation is found up to three days in concentrations data.
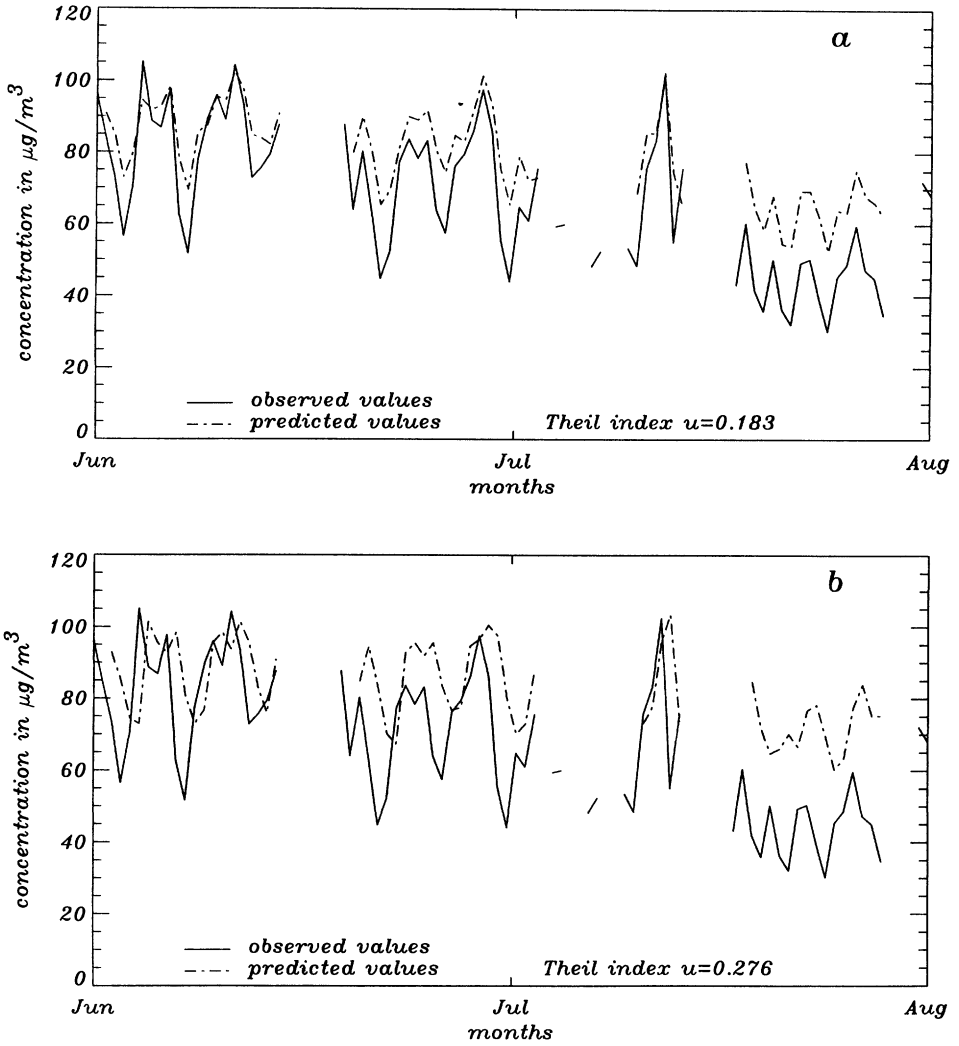
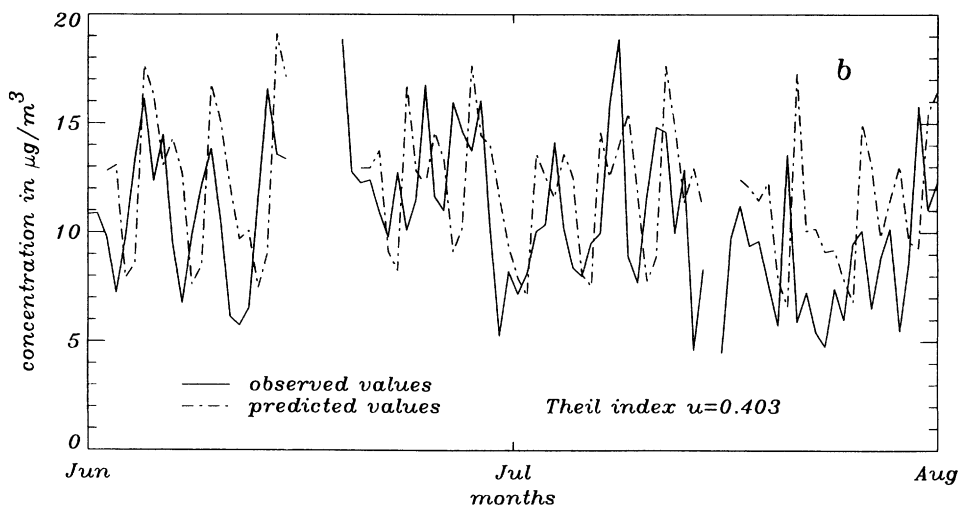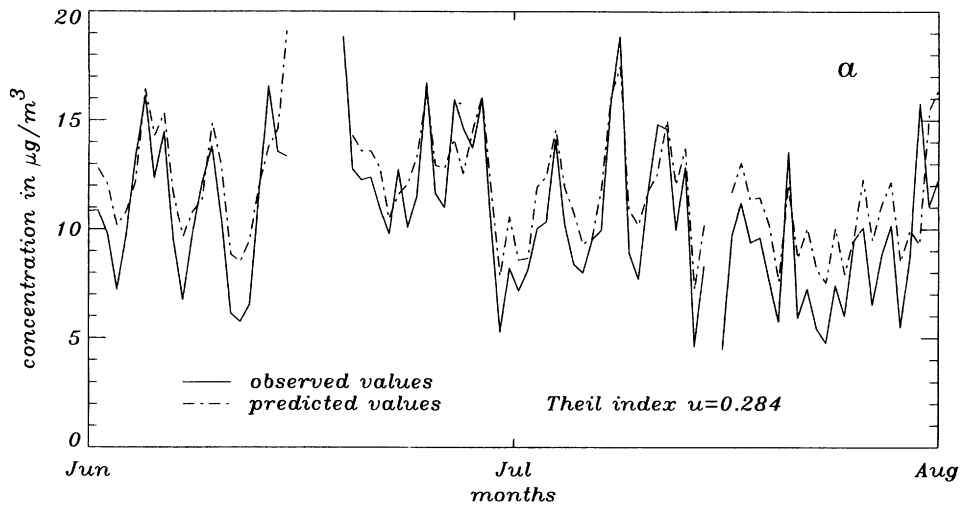Fig. 4.Prediction of concentration for NO_2 at Fiera station. a) One day prediction, b) two days prediction

Fig. 5 Prediction of concentration for SO$_2$ at Fiera station. a) One day prediction, b) two days prediction
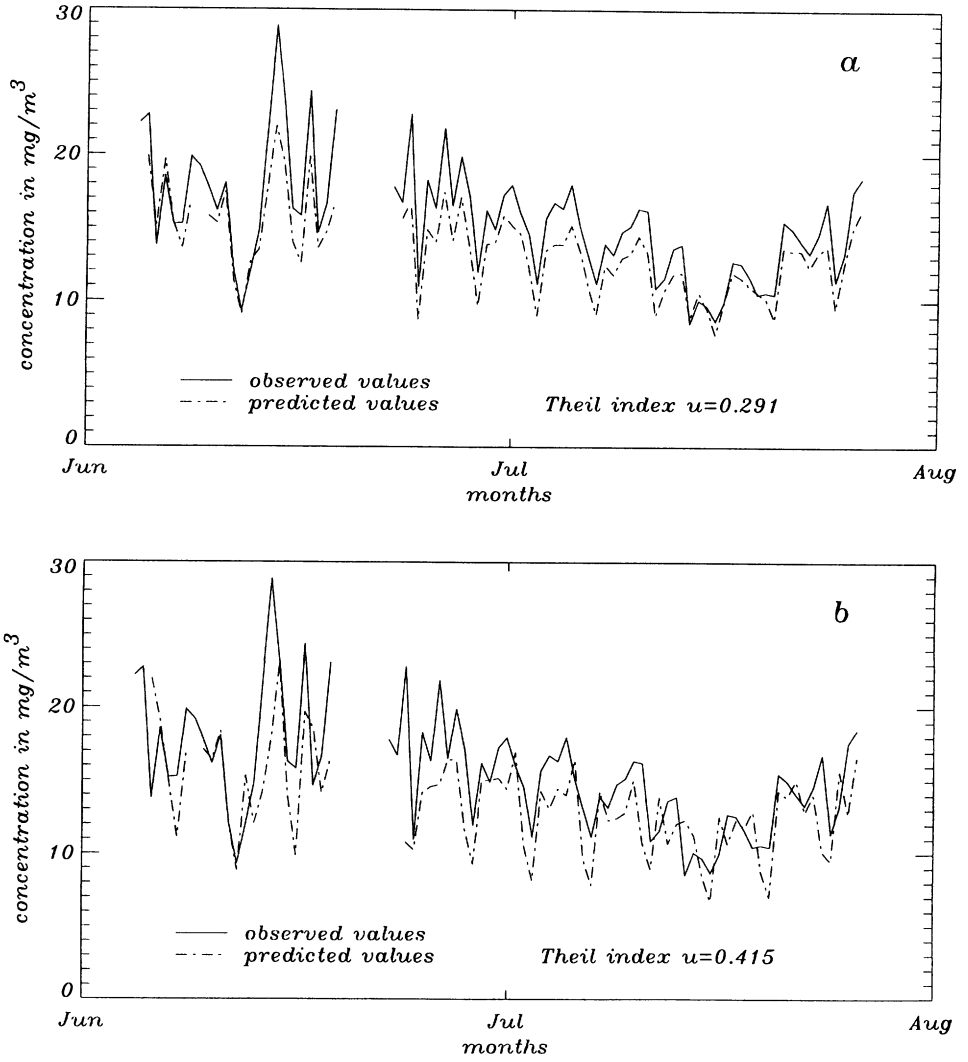
Fig. 6 Prediction of concentration for CO at Fiera station. a) One day prediction, b) two days prediction

The forecasting attempted for one day predictions are the most successful, but two days predictions are also satisfactory in cases.

The introduction of independent meteorological data, with the crude methods used at present, does not result in a satisfactory impact. For this reason it is planned to use information about the vertical structure of the atmosphere, in particular the vertical shear of horizontal wind and vertical stratification, both related to turbulent diffusion and advection.

Acknowledgements

References

Arya S. P.: 1988, Introduction to Micrometeorology, Academy Press, S. Diego

Jenkins G.: 1968, M., Watts D. G Spectral Analysis and its Applications, Holden-Day, S. Francisco

Mills T.: 1990 C. Time Series Techniques for Economists, Cambridge Univrsity Press, New York

Theil H.: 1971, Principles of Econometrics, Wiley, New York

Zanetti P.: 1990, Air Pollution Modelling: theories, computational methods and avaiable software., Computation
        Mechanics Publ, Van Rostrand Reinhold, New York

THE RELATIONSHIP BETWEEN EXTREME NITROGEN OXIDE (NO$_x$) CONCENTRATIONS IN DUBLIN'S ATMOSPHERE AND METEOROLOGICAL CONDITIONS

CONOR DELANEY and PAUL DOWDING

Trinity Air Quality Research Group

Environmental Science Unit, Trinity College Dublin

Republic of Ireland

Abstract: A study was carried out to investigate the effects of meteorological conditions on atmospheric Nitrogen Oxide (NO$_x$ (Nitrogen Oxide and Nitrogen Dioxide)) concentrations at a site in Dublin. Data used in the study (meteorological conditions and hourly NO$_x$ concentrations) were compiled from hourly records for the years 1988-1992. The research identified wind speed, air pressure and wind direction as the most important meteorological parameters for understanding the behaviour of extreme NO$_x$ concentrations in Dublin's air. Daily, weekly and seasonal variation in NO$_x$ concentrations were observed. This work also highlighted the importance of the role played by general synoptic weather conditions over local climatic effects in extreme events.

1. Introduction

In general serious pollution episodes in the urban environment are not directly caused by sudden increases in the emission of pollutants but result from unfavourable meteorological conditions. These unfavourable conditions may reduce the ability of the atmosphere to disperse pollutants, transport pollutants from other areas, or may be a combination of both situations.

Dublin, the capital city of the Republic of Ireland, has a population of approximately one million people. The city is bounded by the sea to the east, mountains to the south, and flat topography to the west and north. The mountains to the south of Dublin effect the wind speed and direction over the city (Irish Meteorological Service, 1983). When the general flow of wind is from the south the mountains deflect the flow to a south westerly or south-easterly direction. Mean annual wind speeds in Dublin are likely to be up to a

third less than over nearby open country. Nitrogen Oxides (NO_x (essentially Nitric Oxide (NO) and Nitrogen Dioxide (NO_2)) concentrations have been monitored hourly at two sites in the city since 1988. In this paper, high concentrations of Nitrogen Dioxide and Nitric Oxide which were recorded during a five year period (1988 to 1992) at a site in Dublin, are studied. This site, in an area called Rathmines, is located on one of the commuter routes to the city centre

The study was carried out to investigate the influence of meteorological conditions on NO_x concentrations in Dublin. This research is the first stage of ongoing work to develop a forecasting model for NO_x concentrations in Dublin.

2. Methodology

The period of this study was 1988 to 1992. It was decided to use this as a development period (1993 to present will be used to validate the eventual forecasting model, see Benarie (1980) p204). Hourly meteorological measurements used in this study were obtained from the Irish Meteorological Service. The measurements were taken at Dublin airport where the Meteorological service maintains a weather station which takes hourly observations of various meteorological parameters. Hourly NO_x concentrations for the Rathmines site were supplied by the Irish Environmental Protection Agency (EPA) which maintains a roadside NO_x monitoring station at Rathmines. The EPA monitor NO_x in order to determine NO_2 concentrations, and are obliged to so by EEC Council Directive 85/203. Rathmines is a main commuter corridor into the city centre and the monitoring site was placed there to reflect the contribution to NO_2 concentrations made by traffic, this is a requirement of the EEC directive. The site is located in a predominantly suburban residential area with commercial premises. Traffic flow data for the time period of was not adequate enough to allow comparisons be made with the air pollution data. However it was reported by Dublin Corporation in 1989 that peak flows of about 3,600 vehicles had been recorded on Rathmines Road Lower between 8.00am and 10.00am and between 4.30pm and 6.30pm (Margo Leddy, 1989). A reduction of 30% was also reported at weekends. The EPA used the chemiluminesence method for the measurement of nitrogen

oxides and they have positioned the sampling inlet 4.9metres above ground level. This technique calculates NO_2 from the difference of measured NO_x and NO concentrations. The NO_x data sets were subdivided into years, seasons, weekends and weekdays. Graphs of the NO_x concentrations were created to investigate the diurnal, weekly, seasonal and yearly trends.

There is no *a* priori reason to expect that air pollutant concentrations should adhere to a specific probability distribution, therefore the frequency distributions of the air pollutants were examined to determine appropriate statistical tests (Seinfield, 1986). The frequency distributions of the NO_x data indicated it to be non normal therefore a non parametric test was chosen when carrying out the correlation of NO_x, NO and NO_2 concentrations against measured meteorological parameters. The test chosen was the Rank Spearman test, this correlation was carried out on one year of data. The results of this correlation indicated which of the meteorological parameters exerted a strong influence on concentrations of NO_x, NO and NO_2.

Case studies of the worst NO_2 pollution episodes for the five years was carried out. It was decided a pollution episode should be any day in which an NO_2 concentration of 105ppb ($200\mu gm^{-3}$) was exceeded at Rathmines. This figure is just below the one hour exposure level of 110pbb ($210\mu gm^{-3}$) that was found to cause slight to mild asthmatics experience bronchonstriction (Orehek *et al.* 1976). The episodic criteria is also 6 times greater than the hourly mean for the study period. Days which met the criteria were then studied in terms of the meteorological parameters considered important by the previous correlation.

Finally synoptic charts were examined to determine the general climatic conditions for episodic days and one of the days was examined in more detail. Synoptic information was gleaned from two sources; *The Monthly Weather Report* by the Irish Meteorological Office and *The Weather Log* by the Royal Meteorological Society.

3. Results

3.1. CONCENTRATIONS OF NO₂ AT RATHMINES

The 50th and 98th percentiles (Figure 1) are the required annual measurement statistics of NO_2 concentration under the Irish implementation of the EEC Council Directive 85/203. This legislation sets an absolute limit value for the 98th percentile of $200\mu gm^{-3}$ (105ppb) and a guideline limit of $135\mu gm^{-3}$ (71ppb).
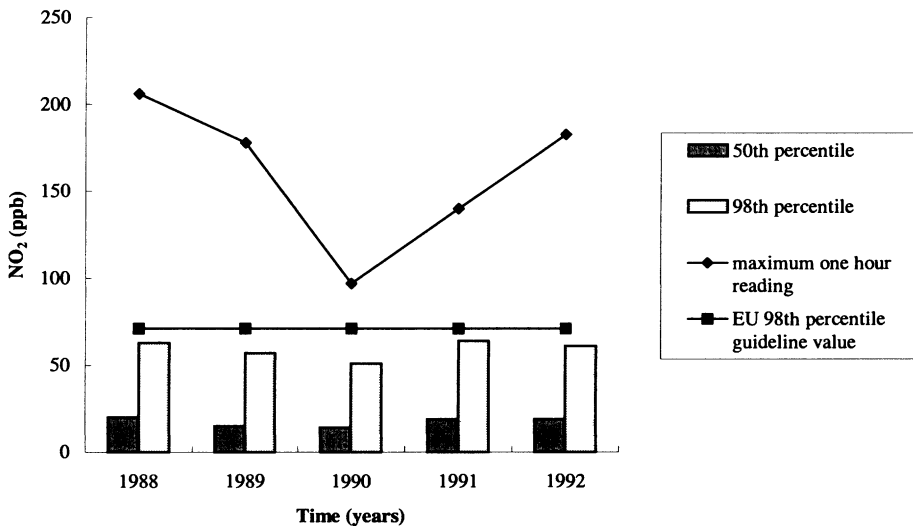

Figure 1. Summary statistics for nitrogen dioxide at Rathmines, Dublin. The E.U. 98th percentile absolute limit value is 105ppb ($200\mu g/m^3$).

At Rathmines, for the five years of this study, neither the absolute or guideline limits for the 98th percentile statistics were exceeded (Figure 1). The yearly maximum one hour reading year ranged from 205ppb to 118ppb, the highest occurring in 1988 and the lowest in 1990.

3.2. PATTERNS IN NO₂ AND NO CONCENTRATIONS

The weekday, weekend and seasonal patterns for NO and NO_2 concentrations were very distinct (Figure 2 & 3). Both of these graphs are derived from weekday hourly averages for five years of readings (1988-92).

There were two peaks for NO concentrations each weekday, one in the morning at approximately 9a.m. and one in the evening around 7p.m. (Figure 2). Peaks for NO_2 weekday concentrations also occur around these times, illustrating how quickly NO gets transformed into NO_2 (Figure 3). In general weekend patterns for NO and NO_2 concentrations did not exhibit these characteristic peaks (Figures 4 & 5). NO_2 weekend concentrations did not follow the weekday hourly trend but did follow the seasonal trend, however during the spring weekend concentrations of NO_2 were as high as weekday concentrations (Figure 3 & 4). The highest mean weekday concentrations of NO occur in the winter and the lowest occur in the summer (Figure 2). NO_2 mean weekday and weekend concentrations are highest in the spring and lowest in the summer (Figure 3 & 4). Mean weekday NO concentrations show greater seasonal variability than the NO_2 concentrations (Figure 2 & 3).
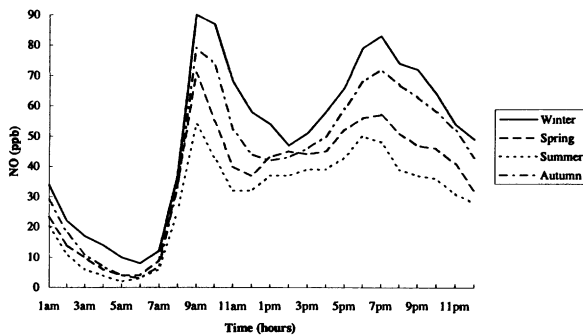
Figure 2. The weekday pattern (based on a five year hourly mean (1988 - 1992)) of NO at Rathmines with seasonal difference.
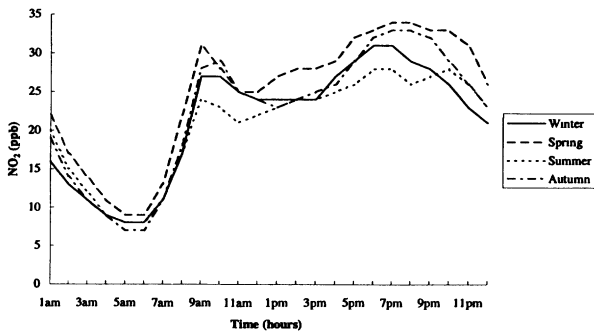
Figure 3. The weekday pattern (based on a five year hourly mean (1988 - 1992)) of NO_2 at Rathmines with seasonal difference.

3.3. CORRELATION OF NO$_X$, NO AND NO$_2$ AGAINST SOME METEOROLOGICAL PARAMETERS

A Spearman Rank correlation was carried out on the 1988 data set. NO$_x$, NO, and NO$_2$ hourly concentrations were correlated against hourly meteorological parameters (Table I). This set was 95% complete thus there were 8389 observations for each variable in the correlation. This correlation was carried out to ascertain which of the meteorological variables were important in describing the fluctuation in the oxides of nitrogen.

	Nitric Oxide	*NO$_x$*	*Nitrogen Dioxide*
Nitric Oxide	1.0		
NO$_x$	0.968	1.0	
Nitrogen Dioxide	0.880	0.957	1.0
Dewpoint	0.012	-0.013	-0.048
Air Pressure	0.183 *	0.213 *	0.243 *
Rainfall	-0.022	-0.033	-0.051
Sunshine Hours	0.052	0.033	0.025
Temperature	0.032	0.0	-0.041
Wind Direction	-0.353 *	-0.359 *	-0.339 *
Wind Speed	-0.385 *	-0.441 *	-0.488 *

Table I Spearman Rank Correlation of some meteorological parameters against the concentrations of NO, NO$_2$ and NO$_x$, for all of 1988 (measurements were taken hourly at Rathmines, Dublin).

The strongest correlations are marked with asterixes and these are; air pressure, wind direction and wind speed. Wind speed correlates strongest with NO$_2$ concentrations as does air pressure.

CASE STUDIES OF EXTREME NITROGEN DIOXIDE CONCENTRATIONS MEASURED AT RATHMINES

There were a total of thirteen days during the five year study period (1988-92) on which NO$_2$ concentrations exceeded 105 ppb (200μgm^{-3}) for at least one hour in the day (Table 2). With one exception, all the extreme days had higher than average air pressure and lower than average wind speed. This exception was Thursday the 25th of August 1988, on

this day the air pressure was lower than the long term mean and the wind speed was higher than the long term mean. Extreme days which occurred in winter or autumn had mean daily temperatures below the long term average (Table II). Summer and spring extreme days (with the exception of the 25th of August 1988) had mean daily temperatures below the long term average (Table II). The average temperature for the exceptional day (25th of August 1988) was below the long term average. The mean daily NO_2 concentrations were much greater than the 5 year seasonal mean. Seasonal means were used for NO_2 to avoid using a possibly weighted monthly average resulting from some gaps in the data set.
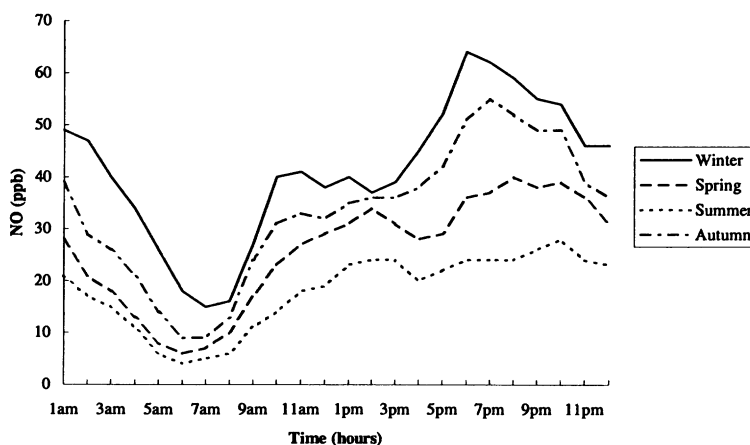
Figure 4. The weekend pattern (based on a five year hourly mean (1988 - 1992)) NO concentration at Rathmines with seasonal difference.
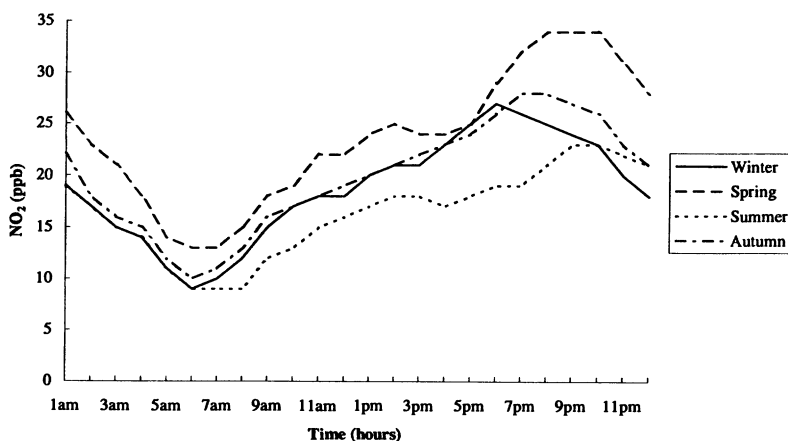
Figure 5. The weekend pattern (based on a five year hourly mean (1988 - 1992)) NO_2 concentration at Rathmines with seasonal difference.

166

	Thurs. 25/8/88	Wed. 23/11/88	Thurs. 24/11/88	Fri. 25/11/88	Thurs. 6/7/89	Mon. 27/11/89	Fri. 4/5/90	Thurs. 29/8/91	Wed. 11/12/91	Mon. 27/1/92	Sun. 20/12/92	Wed. 23/12/92	Thurs. 24/12/92
Air Pressure (hectopascals)	1007	1034	1032	1026	1019	1022	1025	1026	1031	1044	1025	1031	1029
Air Pressure 30 year mean	1014	1012	1012	1012	1014	1012	1015	1014	1011	1011	1011	1011	1011
Wind Speed (ms⁻¹)	7.4	2.5	1.2	0.6	1.2	1.1	0.26	2.2	1.2	1.6	1.7	0.77	1.1
Wind Speed 22 year mean	4	5.7	5.7	5.7	4.1	5.7	4.5	4	6.1	6.3	6.1	6.1	6.1
Temperature (centigrade)	12.6	3.1	1.7	3.5	17.0	5.0	16.79	19.4	1.9	2.3	0.0	3.0	4.9
Temperature 34 year mean	14.6	7.2	7.2	7.2	14.6	7.2	10.4	14.6	5.8	4.9	5.8	5.8	5.8
Nitrogen Dioxide (ppb)	23	55	76	132	52	73	74	73	68	47	61	59	51
Nitrogen Dioxide 5 year mean (seasonal)	19	21	21	21	19	21	24	19	22	22	22	22	22

Table II In the above table are the 13 days of the 5 year study period (1988-1992) on which a recorded nitrogen dioxide level of 105ppb was exceeded for at least one hour. The average meteorological* and nitrogen dioxide values for the appropriate days are included. The long term meteorological means are monthly means and the 5 year NO₂ mean is a seasonal** mean (in bold). The values not in bold are daily means.

* The long term meteorological values come from, *The Climate of Ireland* by P. K. Rohan published in 1986 by the Irish Stationery Office.

** Irish meteorological seasons are: winter (December, January, February); spring (March, April, May); summer (June, July, August); autumn (September, October, November)

3.4. THE SYNOPTIC METEOROLOGICAL SITUATION FOR EACH EPISODIC DAY

General synoptic weather charts for the days included in the case study were examined and were summarised (Table III). The dominant meteorological feature for all days except the 25th of August 1988 were anticyclones to the east of Ireland. On the 25th of August 1988 the dominant meteorological feature was a low pressure system positioned over the North Sea, a warm humid air mass passed over the country from west to east.

Thursday 25th August 1988
Air pressure was below normal and wind speed was above normal. In terms of synoptic conditions the weather in Dublin was dominated by a Low over the North Sea.
Wednesday 23rd to Friday 25th November 1988
Ireland was under the influence of a Polar anticyclone and wind speeds remained very low for three consecutive days.
Thursday 6th July 1989
By the 2nd of July an anticyclone was centred over Britain. This anticyclone had originated on the continent and it brought with it warm weather and low wind speeds it stayed over Britain until the 6th when it then moved back towards the continent.
Monday 27th November 1989
An anticyclone moved down from Polar regions over Ireland on the 25th. It stayed over Ireland until the 28th when it moved eastwards.
Friday 4th May 1990
On the 1st of the month an anticyclone was positioned over the North Sea, this moved onto the continent on the 2nd and was the dominating synoptic feature until the 4th.
Thursday 29th August 1991
An anticyclone which originated in the Bay of Biscay stationed itself generally over Britain and Ireland on the 24th and was the dominating influence until the end of the month. Wind speeds on the 28th and 29th were the lowest, with only these two days going below an average daily wind speed of 2.6 ms^{-1}.
Wednesday 11th December 1991
From the 5th to the 10th of December wind speed was about average and NO$_x$ concentrations were above average. On the 10th the wind speed started dropping reaching its lowest daily mean of 1.2 ms^{-1} on the 11th. The dominant synoptic feature was an anticyclone positioned over Europe.
Monday 27th of January 1992
A continental anticyclone dominated from the 26th to the 31st of the month. Wind speed for the 26th, 27th and 28th was below 2 6 ms^{-1}.
Sunday 20th of December and Wednesday 23rd to Thursday 24th of December 1992
A ridge of high pressure established itself over Britain on the 19th and 20th from a continental anticyclone and it maintained its influence until the end of the month. This weather system brought a period of low wind speeds to Dublin.

Table III. Synoptic information for the episodic days.

One of the episodic days was examined more closely. This was the 6th of the July 1989 and the three days following it. NO_x concentrations where compared with wind speed (Figure 6) and wind speed was compared with wind direction (Figure 7). Differences from mean hourly readings were used for NO_x values rather than absolute NO_x concentrations, this was done to eliminate the weekday/weekend variation. NO_x concentrations can be seen to vary from being above average when the wind direction is easterly/north easterly to being just below average when the wind direction is more westerly (Figure 6). With exception of the 7th wind speeds were below average (Figure 7).

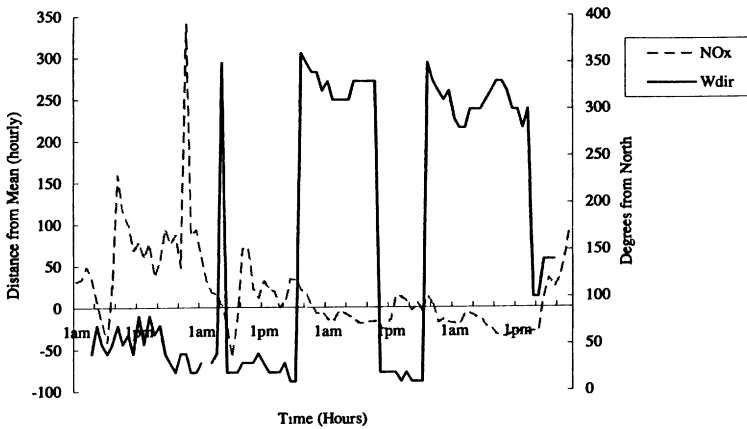**Figure 6.** The 6th to the 9th of July 1989. Observations for NO_x concentrations are the differences from the seasonal hourly means. The observations are from 1am on the 6th to 11pm on the 9th.
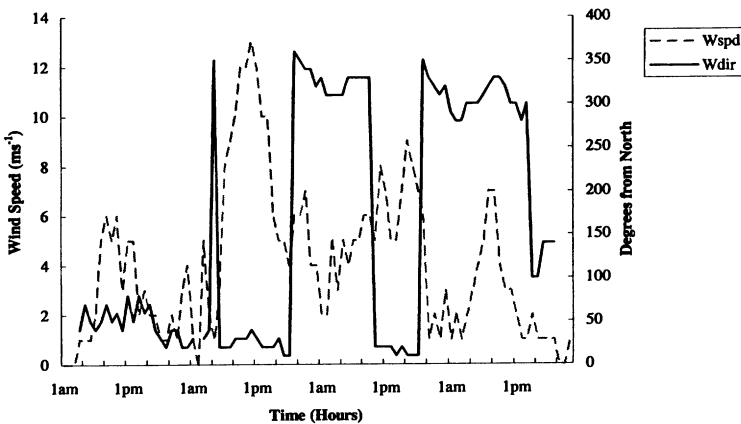

Figure 7. The 6th to the 9th of July 1989. The observations are from 1am on the 6th to 11pm on the 9th. The 22 year mean hourly wind speed for the month of July was 4.1ms^{-1}.

4. Discussion

The NO_2 concentration results at the 50th and 98th percentile (figure 1) for 5 years at Rathmines were very similar and were well within the limit values set out by EC Directive 85/203/EEC of 105ppb ($200\mu gm^{-3}$). Variation existed between the years for the one hour maximum recording of NO_2 concentrations. The most likely explanation for this variation is the influence of meteorological conditions favourable to pollutant dispersal (McGettigan, 1995). Differences between the 98th percentile measure and the maximum one hour reading were indicative of the inability of the 98th percentile measure to account for extreme, short term pollution episodes. However as a measure of overall year-to-year variability the 98th percentile was a robust measure, making it a useful tool for air quality management.

In figures 3 and 4 the diurnal pattern on NO and NO_2 respectively was clear. The morning peak was linked with the morning commuter rush and similarly for the evening peak, a similar diurnal pattern was observed in NO concentrations measured at a roadside site in London (Derwent *et al.*, 1995). Seasonal variations can be seen in both figures, with the variation of NO concentrations more pronounced than those of NO_2. NO concentrations were highest in winter and lowest in summer, with the greatest differences at the 09:00 and 19:00 peaks. Concentrations of NO in spring and autumn were not very different from each other, however the diurnal patterns were different, with spring's pattern more like summer's and autumn's more like winter's. The afternoon concentrations of NO were very similar for each season, this suggests that the morning and evening peak inter-seasonal differences for NO concentrations were linked to seasonal changes in traffic patterns. Seasonal variation for NO_2 was not as pronounced as that for NO; NO_2 attained it highest levels in the spring. Work on NO concentrations in other cities has found seasonal trends which are more distinct than those found in Dublin. For example in Chiba, Japan it was found that winter and autumn were very clearly similar to each other in both the daily pattern and the concentration of NO, spring and summer were also strongly alike (Inoue *et al.*, 1986). The climatic differences between Dublin and Chiba probably account for the differences in the seasonal NO_x trends.

The morning peak of NO_2 which is present in the weekday graph (figure 3) is absent from the weekend graph (figure 5), this can be explained by the absence of commuter

traffic on Saturday and Sunday mornings. The minimum concentrations (9-11ppb NO_2), and the evening maximum for the weekends are the same as those for weekdays NO_2 concentrations. Weekend NO concentrations were much lower than weekday NO concentrations for all seasons.

The parameters with the best correlation with the NO and NO_2 concentrations in the Spearman Rank correlation in table I were wind speed, wind direction and air pressure. Wind speed had a negative value, such that as wind speed increased pollutant concentration was reduced.

Collated in table II are the daily means for NO_2, air pressure, wind speed and temperature. Also included in the table are the relevant long term means and the maximum one hour concentration of NO_2 for each episodic day. All the episodic days, with the exception of the 28th of August 1988, showed similarities. In each case the air pressure was higher, and in most cases very much higher, than the long term average. Wind speeds never exceeded a daily mean of 2.6 ms^{-1}. This high air pressure was caused by anticyclones. Temperature on these episodic days was higher in the summer and spring and lower in the autumn and winter than the seasonal mean. Ireland, positioned as it is in the zone of westerly circulation of middle latitudes, is much subject to the influence of Atlantic weather systems. The strength of the westerlies varies throughout the year allowing other influences, such as airflows from the continent, to dominate. On the episodic days the unusual temperatures suggested that the anticyclonic airflow had originated either from polar or continental regions. Synoptic charts confirmed the influence of continental or polar anticyclone on all the episodic days with one exception. The exception was the 25th of August 1988, on that day wind speed was higher and air pressure was lower than the seasonal average, the dominant synoptic feature was a Low pressure system over the North Sea. This episode occurred as a large peak on the last few hours of the day, which then rapidly dissipated, twelve and twenty-four hours later there were two more peaks but this time they were for NO.

In a study on summer visibility reduction at Dublin airport (Leavey and Sweeney, 1990) it was suggested that summer hazes in Dublin are associated with long-range transport of pollutants from continental and British sources. Continental anticyclones were identified as making a significant contribution to visibility reduction, the clockwise

winds around an anticyclone situated to the east of Ireland bring air from the continent and Britain to Dublin. On the 13th of December 1991 London experienced high concentrations of NO_x. Back-track air mass trajectories for the days leading up to the episode showed that the air mass arriving in London had travelled over the continent (Derwent *et al.* 1995). Dublin also experienced high concentrations of NO_2 and NO during this period.

In figure 6 NO_x concentrations and wind direction for the 6th to the 9th of July 1989 were compared, illustrating the relationship between high NO_x concentrations and wind direction. Figure 7 illustrated that above average easterly wind speeds were also associated with high NO_x concentrations for this period. Synoptically, on the 6th, Ireland was under the weakening influence of an anticyclone which was moving easterly from Britain and a low pressure system moving up from the Bay of Biscay. On the 7th the low pressure had positioned itself over England and on the 8th and 9th the synoptic situation was dominated by anticyclone to the west of Ireland. The synoptic situations on the 6th and the 7th brought with them an air mass which had passed over the continent and Britain, whereas the situation on the 8th and 9th brought an air mass from the Atlantic Ocean.

5. Conclusions

This study has demonstrated diurnal, weekly and seasonal trends in NO and NO_2 concentrations at Rathmines in Dublin. It is expected that while the concentrations of pollutant may vary from site to site in the city seasonal, weekly and diurnal trends should not vary much. The study identified wind speed, wind direction and air pressure as important meteorological parameters in explaining the variation of NO and NO_2 concentrations. It would seem that extreme concentrations of NO_x in Dublin are linked to the general synoptic situation. It is probable that very high concentrations of NO and NO_2 can be expected whenever the synoptic situation affecting Dublin is anticyclonic as this condition can have light winds, low temperatures and strong surface stability which inhibit pollutant dispersal. It is interesting to note the correlation of the anticyclones to the east

of Ireland with extreme concentrations of NO and NO_2 from 1988-1992, this suggests that the air mass arriving to Dublin carries with it NO and NO_2 from Europe.

Acknowledgements

References

Benarie M. M. (1980). *Urban Air Pollution Modelling*. Macmillan, London.

Derwent R. G., Middleton D. R., Field R. A., Goldstone M. E., Lester J. N. and Perry R. (1995). 'Analysis and interpretation of air quality data from an urban roadside location in central London over the period from July 1991 to July 1992' *Atmospheric Environment* **29**, 923-946.

Inoue Takaktsu, Hoshi Mamoru and Taguri Masaaki (1986). 'Regression analysis of nitrogen oxide concentration' *Atmospheric Environment* **20**, 71-85.

Irish Meteorological Service (1983). *The Climate of Dublin*

Leavey M. and Sweeney J. (1990). 'The influence of long - range transport of air pollutants on summer visibility at Dublin' *International Journal of Climatology* **10**, 191 - 201.

Leddy Margo (1989). 'Measurements of Nitrogen Oxides and Suspended Particulates at Two Dissimilar Urban Sites in Dublin' *MSc. Thesis,* Environmental Science Unit, Trinity College Dublin.

McGettigan, M. and O'Donnell, C. (1995) *Air Pollutants in Ireland - Emissions, Depositions and Concentrations 1984 - 1994.* Environmental Protection Agency, Wexford.

Orehek, J., Massari, J.P., Gayrard, P., C., and Charpin, J. (1976). *Journal of Clinical Investigation* **57**, 301.

Seinfield, J. H. (1986). *Atmospheric Chemistry and Physics of Air Pollution.* John Wiley and Sons. New York.

AIR QUALITY EFFECTIVENESS OF TRAFFIC MANAGEMENT SCHEMES: U.K. AND EUROPEAN CASE STUDIES.

H CRABBE and D M ELSOM

Air Quality Management Research Group
Geography Department, Oxford Brookes University, Oxford, United Kingdom, OX3 0BP

Abstract. This paper examines air quality changes that can arise from implementing specific traffic management schemes, based on the findings of current and past impact assessments Air quality changes arising from pedestrianisation, traffic rerouting, traffic calming, and bus priority routes are outlined Case studies are presented where air quality was measured before and after the implementation of a scheme in order to assess how effective traffic management can be in reducing ambient traffic-related pollutant levels Limitations of past and current studies are highlighted. The need for more monitoring studies, and the need for data from those studies to be used to test and validate a range of suitable numerical models, is emphasised

1. Introduction

Many urban areas of the world today are experiencing air pollution problems due to rising traffic levels and congestion. In the UK, the recent expansion in monitoring networks has enabled an assessment to be made of the seriousness of urban air quality problems, by comparing ambient air quality levels to EU standards and UK Expert Panel on Air Quality Standards (EPAQS).   Areas breaching standards are to be designated Air Quality Management Areas (AQMA) and will have to be managed and controlled by local authorities under the new National Air Quality Strategy. Practical measures concerned with reducing transport emissions will have a key role in this process. There is currently little information on how effective traffic management schemes are in reducing pollutant levels. Existing studies of the effect of these measures on pollution have so far relied on either analysing small datasets over relatively short periods, or by using models which have been validated using only small datasets. This paper identifies several studies where air quality changes resulting from recently implemented traffic management schemes have been assessed, or are in the process of being assessed, either by monitoring before and after implementation, or through modelling impact studies.

2. The role of traffic management in air quality management

In meeting air quality standards in congested urban centres, traffic management measures will have an important role to play in improving air quality *locally*, perhaps more so than national or international policy measures such as fuel and engine technology advances. The National Air Quality Strategy recognises this and local authorities will be encouraged to implement traffic management schemes in AQMAs in order to reduce the number of exceedences of standards (Figure 1). Transport authorities will ideally integrate air quality control measures with those related to other traffic objectives such as safety and nuisance alleviation. Each type of scheme will have different spatial and temporal effects on traffic

emission rates and ultimately the air quality in that area. Traffic management options include:

a) Traffic calming. Speed bumps, road narrowings and lower speed limits are introduced to lower average vehicle speeds and, in some cases, to deter some motorists from entering the area e.g. some commuters take short cuts through residential areas.

b) Public transport priority measures. Bus lanes, bus-only streets and giving buses priority at traffic lights (by fitting buses with electronic devices which can delay a red light until the bus has passed through or advance a green light) improve bus service efficiency. This encourages more commuters to switch to public transport systems which emit less pollution per person transported than private cars.

c) Urban Traffic Control (UTC). Telematics systems such as SCOOT (Split Cycle Offset Optimisation Technique) can optimise signal control, improve junction capacity and hence reduce congestion. The proportion of vehicles travelling in the fuel-efficient range of speeds can be increased and the proportion in ranges below or above these speeds can be reduced.

d) Urban road pricing. Using road transport informatics, road pricing can reduce the overall numbers of vehicles entering congested central urban areas as well as spreading out peak travel times so reducing congestion.

e) Re-routing of traffic and pedestrianisation of streets. Restricting, redirecting or even banning vehicles can reduce vehicle emissions in an area and may have the most profound effect on air quality. However, if the number of vehicles in an urban area is not reduced this scheme may shift the pollution hotspot elsewhere.

f) Traffic bans. Traffic bans can be used to reduce the total volume of traffic or specific types of vehicles along specific streets or in a designated area. If this measure encourages a shift to public transport systems then reduced vehicle emissions can improve air quality overall throughout an urban area. Selective bans may include vehicles lacking specified emission-control technology (e.g. catalytic converters, large carbon canisters, diesel particulate traps).

g) Priority (red) routes. Stringent parking controls along major routes can reduce congestion and increase the number of vehicles travelling in the fuel-efficient speed range and reduce the numbers above and below that range.

h) Parking controls. Increased car parking charges, reduction in the number of private workplace and public parking spaces and the shifting of parking spaces from the urban centre to peripheral park-and-ride sites can encourage use of public transport systems, reduce the use of private vehicles and hence total vehicle emissions.

Through the implementation of one or more of these traffic management measures, changes in traffic flow, speed and composition will produce changes in on-road emission rates. Monitoring or modelling the air quality changes achieved by these schemes and comparing the resulting pollutant concentrations with air quality standards will indicate whether additional measures are needed (Figure 1).
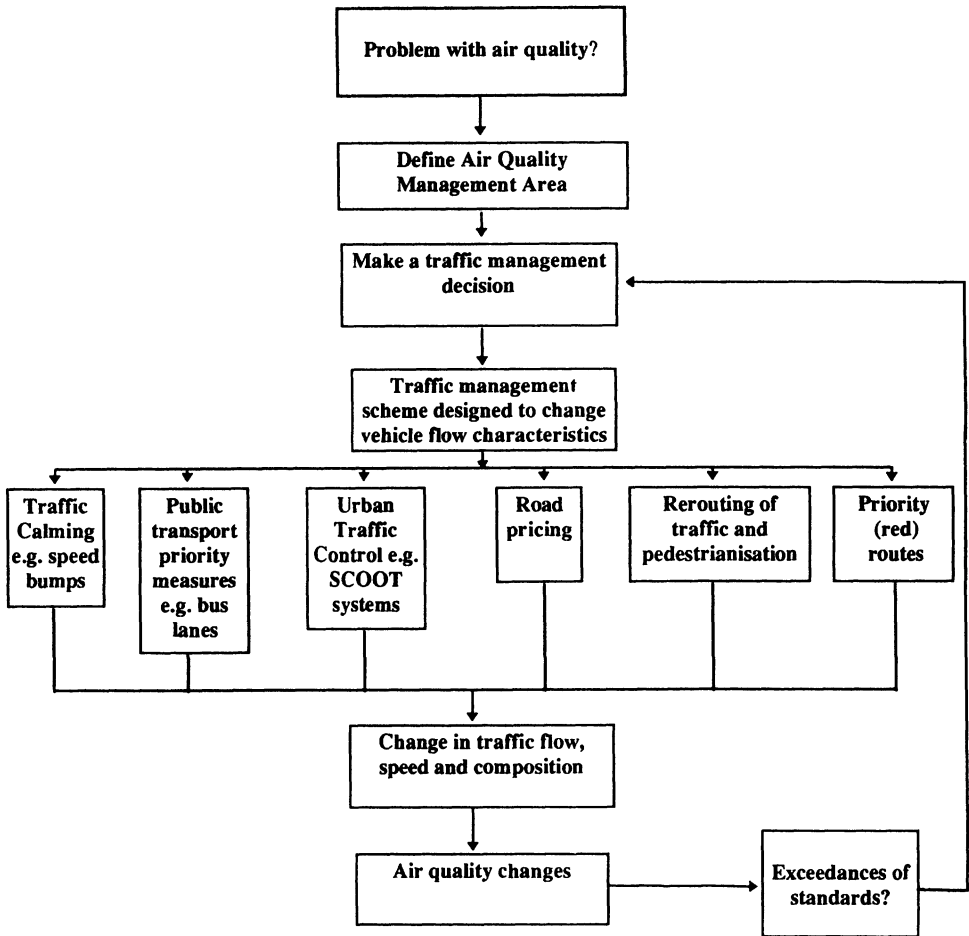
Fig 1 Traffic management scheme options for air quality improvement

3. Current air quality impact assessments

Currently, in the UK, there is a growing realisation that little is known about the detailed effects of transportation strategies, either on the environment or economy of the city, so as a consequence, a few local authorities are now undertaking detailed assessments. Air quality impact assessments of traffic management schemes are being conducted by measuring selected traffic-related pollutants using dedicated equipment both before and after the introduction of a scheme. By detailed comparative time-series analysis, the relative change

in air quality resulting can be determined. Assessment of spatial changes requires a network of monitors to be installed. Alternatively, modelling can provide temporal and spatial assessment of air quality changes providing that the model employed has been validated for the situation to which it is being applied. Selected examples of air quality assessments of traffic management schemes are detailed below to indicate some of the results obtained as well as to highlight the potential problems involved in such studies.

3.1 THE GREATER HULL TRANSPORTATION STRATEGY

Kingston Upon Hull's transport system is being revamped with a package of integrated enhanced highways, new guided bus and railway services, six new park-and-ride sites on the edge of town, various traffic calmed and safety zones, and a series of bus priority routes. Two of the latter (radial) routes are the subject of a monitoring exercise, to assess the effect of the new transportation measures on congestion, bus service efficiency and air quality.

The first (eastern) corridor route, Holderness Road, has been subject to improved public transport and cycling provision. Bus and cycle lanes, revised on-street parking facilities, junction improvements, and traffic calming in adjacent residential areas have recently been added. A mobile trailer laboratory, housing air quality monitoring equipment was positioned along this route some months before these measures were in place. Now that several months data have been collected from this site, the levels before and after can be compared and analysed in detail, by comparing similar time series data with comparable before and after meteorological circumstances and traffic flow levels. For this assessment study, meteorological data and traffic flow data were also parallel inputs (Figure 2).

Bus lanes were implemented as the first stage of the proposals in January 1996 (Figure 3). Initially, daily pollutant averages have been compared for two periods: the first 27 days of data, being the total length of time of monitoring undertaken before implementation, to the 87 days of data after implementation. Comparison of pollutant levels reveals that the average daily concentration of carbon monoxide (CO) decreased, while nitrogen dioxide (NO_2), sulphur dioxide (SO_2), ozone (O_3) and particulates (PM_{10}) increased (Figure 4). The next stage in this study will be to examine air quality changes arising from the bus lanes in more detail and to deal with data limitations. Concerning the latter point, only 27 days of monitoring were undertaken before the bus lanes began operating whereas it would have been desirable to have had say, several months or even a year's duration of monitoring. Problems of availability of the mobile trailer laboratory, resource constraints, budget uncertainties, planning approval delays and difficulties of liaising between the council departments prevented monitoring being in place earlier. Further complications arise because the 27 days of pre-implementation monitoring includes atypical traffic flow conditions associated with the Christmas and New Year public holiday periods (indicated by distinctive pollutant troughs in Figure 3). Limitations may also be present in the post-implementation period used for comparison. For example, a nationwide episode of PM_{10} occurred in March 1996 raising daily means.
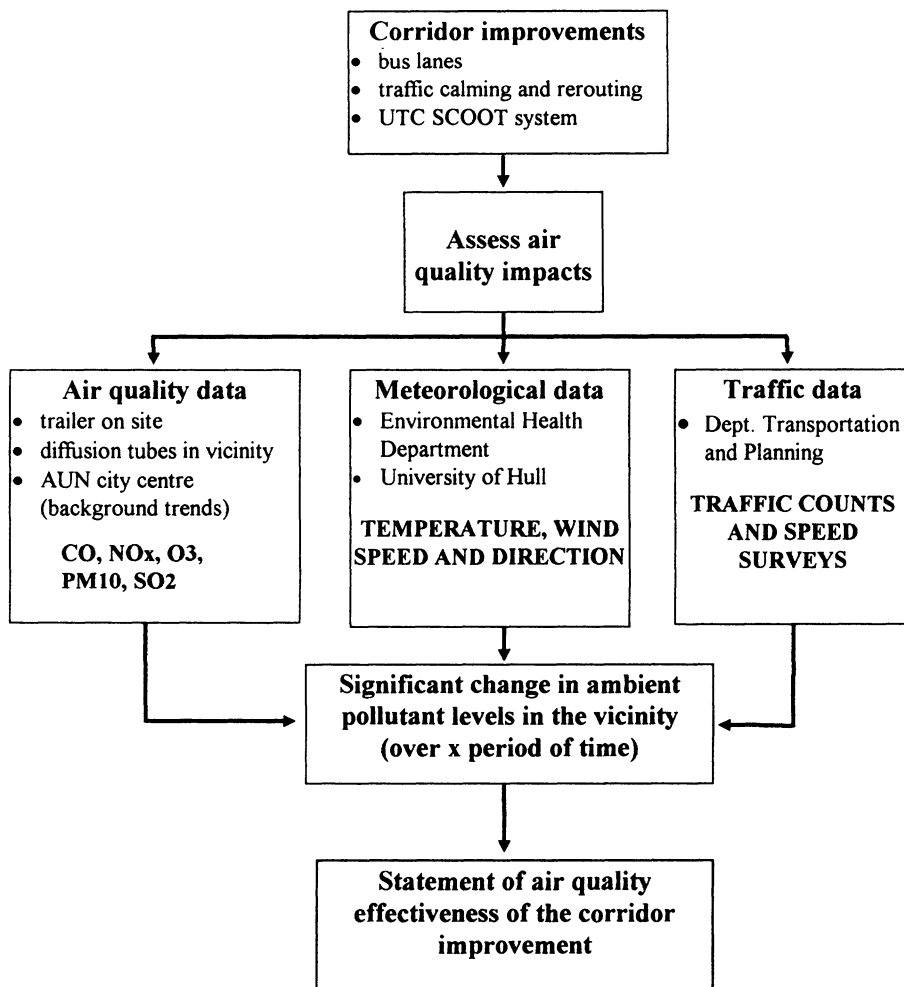
Fig 2 Holderness Road Air Quality impact assessment

The next stage of the analysis will be to eliminate or reduce the effect of some of the complicating factors. Air quality changes during 7.30-9.30am and 4.30-6.30pm, the periods when the bus lanes are in operation, will be examined since average daily pollutant calculations are likely to obscure any changes at these times. Similar periods of traffic flow and meteorological conditions will be chosen, so that any change in pollutant levels can then be identified. The bus lanes and traffic calming measures are only the first of a series of improvements being undertaken along Holderness Road and adjacent residential areas. Time series analyses of pollutant levels are intended to assess the impact of the introduction of the various measures. To assess spatial air quality changes arising from the traffic management measures, a network of diffusion tubes has been located over a wide area. Analysis of diffusion tube data will highlight any changes in air quality arising because of commuters taking short-cuts (`rat-runs') through residential areas. Air quality data from the city centre Automatic Urban
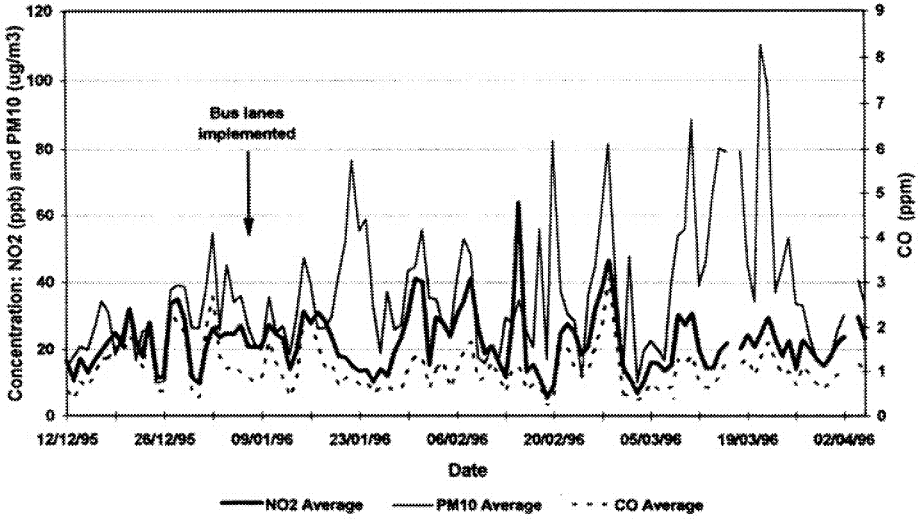
Fig. 3. Daily mean concentration of pollutants measured by the mobile laboratory at Holderness Road, Hull.
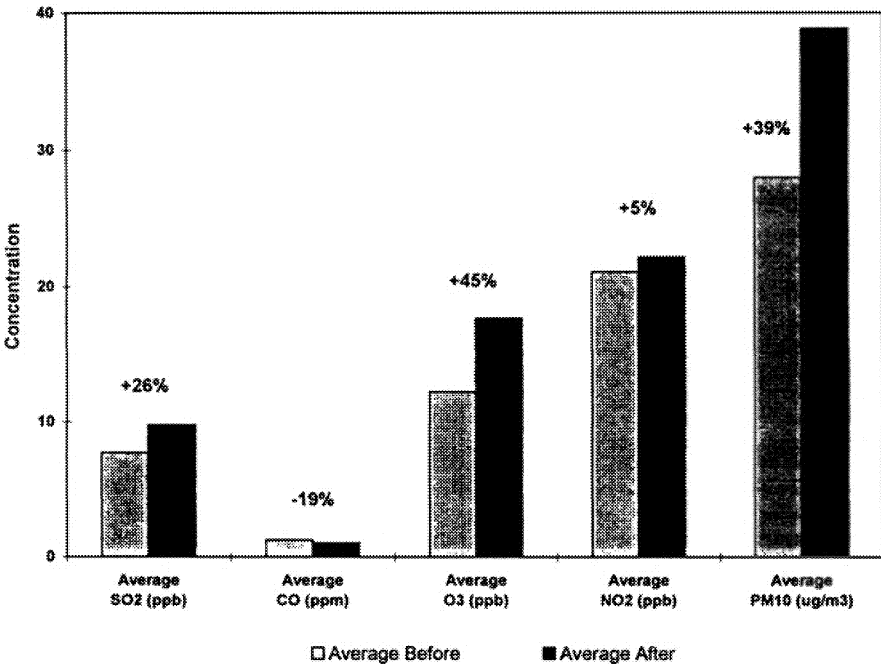
Fig 4. Change in average daily mean concentrations before and after the implementation of bus lanes along Holderness Road, Hull

Network (AUN) monitoring site will be used to detect any change in urban background concentrations as a result of the integrated transportation strategy, especially the impact of the intentional reduction of car traffic as some commuters switch to park-and-ride and other improved public transport facilities.

Given that so few air quality assessments of traffic management schemes have been undertaken in the UK, the Holderness Road study is providing an opportunity to develop a methodology for future air quality assessments not only in Greater Hull (e.g. the western radial route is the next subject for air quality monitoring and impact assessment) but in other urban areas where local authorities have to introduce traffic management schemes to improve air quality in AQMA.

3.2 CITY OF LONDON TRAFFIC MANAGEMENT ZONE

A modelling air quality assessment of the impact of a traffic management zone in the City of London found significant improvements resulting from this scheme. The zone was established as a security measure in July 1993, following terrorist bombing attacks on the City's financial quarter. The security cordon delimited an area of 1.6 km by 1.4 km. Some entry and exit roads were closed and police checkpoints were installed at others to control the entry and exit of vehicles. This measure has decreased traffic flow within the zone by 40%, while redirecting it around the cordon where traffic lights have been adjusted to increase capacity by 20% (TRL, 1995).

From a network of traffic monitoring sites, measuring flow and speeds both inside and outside the cordon, emission estimates of pollutant changes have been calculated at fifteen different receptor points resulting from this traffic management zone. Taking average speeds of vehicles, for hydrocarbons (HC), particulates, NO_x, CO, and carbon dioxide (CO_2) emissions, reductions of 3% overall in the borough's city limit have been calculated. This is a result of emissions within the cordon area decreasing by approximately 15%, and those immediately outside the cordon increasing slightly by 2% due to the re-routing of traffic (Table I).

TABLE I

Calculated percentage change in annual total emissions resulting from the traffic management zone in the City of London (TRL, 1994)

Area	CO	HC	NO_x	CO_2	Particulates
City of London	-2.6	-2.8	-2.9	-2.9	-2.8
Outside cordon	2.2	2.0	1.8	1.8	1.9
Inside cordon	-15 5	-15.2	-14.6	-14.8	-16.2

To complement the model results, air quality changes associated with these emission reductions have been assessed from continuous air quality data within the area. An Opsis path across London Wall, the northern boundary of the cordon, was in operation before the traffic restrictions were implemented. This has measured ambient background (not roadside) levels since September 1992. Preliminary analysis of data from this site shows a decrease of 12% in annual average pollutant levels. This reduction in average pollutant levels is likely to be less than the related emission reduction as pollution infiltrates into the area from nearby traffic and other sources. Further analyses of data from this location together with another site situated alongside a busy route carrying much of the re-routed traffic are to be undertaken. Although security was the reason for establishing the cordon,

the traffic management zone is considered to be so successful in terms of traffic reduction and environmental benefits that it continues to operate and was extended westwards in January 1997. The Corporation of London has foreseen the opportunity to assess the consequences of this, by installing four road-side pollution monitors (measuring traffic and pollution data simultaneously) within this extended area, positioned alongside a variety of effected routes. In time, these sites should be able to detect any air quality changes associated with the new traffic restriction scheme.

3.3 PEDESTRIANISATION AND TRAFFIC RESTRICTIONS IN THE CITY OF CHESTER

Implementation of a pedestrianisation scheme in Chester in 1995 resulted in complaints about poor air quality in Northgate Street, where city centre traffic was concentrated consequently. Complaints from local residents and shopkeepers about poor air quality and a heavy increase in traffic resulted in a monitoring survey, finding that concentrations of NO_2, SO_2 and PM_{10} exceeded some of the relevant air quality guidelines. In March 1996 an experimental one-way system was introduced along Northgate Street, and a further monitoring exercise was undertaken to determine the effects of the new traffic regime on air quality. Pollutant levels consequently were well below the EU and EPAQS standards where available, with the exception of PM_{10}, which breached EPAQS standard of 50 g/m^3 as a 24-hour rolling average on three occasions in 10 days of monitoring (Cheshire County Council, 1996). Comparisons of the two surveys conducted are possible as similar meteorological periods existed. Concentrations of pollutants measured in April 1996, after the one-way system was introduced were significantly lower, by as much as 81%, than those recorded during the comparative study in September 1995 (Table II). The only exception to this was PM_{10}, where no significant reduction was recorded. This was probably due to the location of the monitor, 40 metres from the bus station and adjacent to a lay-by used by tour buses.

TABLE II

Comparison of 1 hour average concentrations from two monitoring surveys of Northgate Street, Chester (ARIC, 1996)

Dates of survey	CO(ppm)	NO(ppb)	NO$_2$(ppb)	NO$_x$(ppb)	SO$_2$(ppb)	Benzene (ppb)	Toluene (ppb)
9-18th Sept 1995	0.81	103.98	32 20	136.18	18.01	0.72	1.48
16-26th April 1996	0.39	19.93	16 85	36.78	6.24	0.58	1.19
Reduction	52%	81%	48%	73%	65%	19%	20%

The idling of diesel-engine vehicles in this area would contribute to the high levels of particulates, even though traffic flows and congestion have been substantially reduced along this route. A network of monitoring stations is being set up across the city to extend the analyses of the effects of current and future traffic management measures.

Chester has also been the subject of an air quality modelling exercise. Chiquetto and Mackett (1995) have modelled the changes in pollutant concentrations resulting from

implementing the pedestrianisation scheme. The model was applied to three separately defined areas (Table III). Large reductions were predicted within the central pedestrianised roads, with corresponding small increases in other central routes. Outside the central area, increases of 2-6% were modelled due to the re-routing of traffic.

TABLE III

Predicted changes in concentrations (expressed as annual average percent) following the implementation of a pedestrianisation scheme in central Chester (Chiquetto and Mackett, 1995).

Location	CO	CO_2	HC	NO_x	PM_{10}
Pedestrianised links	-79	-77	-77	-72	-63
Rest of central area	+22	+16	+17	+2	-1
Non-central area	+6	+5	+5	+2	+2

4. Past assessment studies of transport measures.

Past air quality assessments of traffic management measures have mainly concentrated on assessing emission rate changes rather than undertaking air quality monitoring before and after implementation. By measuring the change in performance of a vehicle before and after a change in the transport infrastructure, emissions can be estimated from the driving cycle. Alternatively, numerical models have been used.

A classic example of a study assessing emission changes following the introduction of extensive traffic calming measures was that undertaken in Buxtehude, Germany, in the 1980s. This study also showed how emission changes varied with driving styles. A network route for pedestrians and cyclist was introduced, having priority over vehicles that were restricted to 30kph speed limits. Reducing speeds and physical traffic restriction measures such as chicanes and narrowed junctions changed driving styles and hence emissions. Table IV shows the results from two driving-cycle tests and the resulting effect on emissions compared to the situation before the traffic calming was introduced, when the speed limit was 50kph.

Traffic calming measures may have negative effects on air quality overall. Road narrowings, road humps, chicanes and raised intersections may, in some cases, lead to increased vehicle emissions if say, drivers decelerate abruptly on approaching a road hump, and accelerate away rapidly before encountering the next hump. Such uneven driving patterns have been modelled by the TRL (1995) considering vehicles originally travelling at a constant 25mph, then subject to traffic calming, with speeds varying from 14-19 mph. Fuel consumption increased by 25%; CO, hydrocarbons and CO_2 emissions rose between 25-50%; while NO_x emissions decreased by 30% (due to the speed/emission relationship curve for NO_x). Therefore, to achieve emission reductions, traffic calming schemes need to encourage steady driving speeds, rather than simply aim to lower average speeds.

TABLE IV

Changes in vehicle emissions from two contrasting driving styles following the introduction of traffic calming measures and 30 kph speed limits in Buxtehude, Germany (Pharoah and Russell, 1989).

Dominant gear and driver behaviour	CO	NO$_x$	HC	Fuel Requirements
Second gear and `aggressive'	-17%	-32%	-10%	+7%
Third gear and `calm'	-13%	-48%	-22%	-7%

Only a very limited number of before and after monitoring studies have been undertaken in the past in the UK. A study in Brighton in 1991 was designed to assess the effect of re-routing traffic from the central area (Bennett et al.. 1992). Peak daytime bans on private vehicles entering the main shopping street together with one-way restrictions and turning bans in adjacent roads were introduced. Monitoring of hourly average pollutant concentrations was undertaken for one month before and one month after the scheme was implemented. Resulting reductions in vehicle flows did not produce corresponding reductions in daily NO$_2$ concentrations, perhaps suggesting pollutant saturation already in the city centre, although a low data capture rate could have affected this conclusion. Increases in CO maximum hourly means were however detected, rising from 8 to 16 ppm. A stronger diurnal pattern was noted in NO$_2$ fluctuations, reflecting the new peak periods in traffic flow and daytime bans. Detailed assessment of the effects of the traffic management scheme proved difficult given the short duration of monitoring (due to resource limitations as well as some technical problems with the equipment). Varying meteorological conditions between the before and after monitoring periods made the assessment even more difficult. The limited results of this Brighton study highlight the need for future studies to include much longer periods of before and after monitoring.

5. Further Work and Conclusions

Very few studies have been undertaken in the UK to measure the changes in air quality resulting from the introduction of traffic management schemes. It is not yet possible to rank or score the relative effectiveness of each type of scheme in reducing pollutants in their vicinity. Moreover, schemes which reduce traffic flow in one area may result in another area being subject to increased traffic flow leading to a deterioration in air quality. Such unwelcome changes, often outside the immediate area in which the traffic management measures are applied, need to be recognised and quantified. Assessing changes to the spatial pattern of air quality requires urban-wide monitoring networks. Data from such networks will highlight whether the original traffic management scheme needs modifying, or additional measures need introducing, in order to ensure that air quality does not worsen in some parts of the urban area.

Monitoring is expensive in terms of the cost of purchase or hire of the equipment and staff time in applying quality assurance and control, processing and analysing the data. Numerical models (e.g. the Dutch CAR model, the Californian CALINE model, the UK

Design Manual for Roads and Bridges model and the UK Meteorological Office AEOLIUS street canyon model) can complement and, when adequately validated, substitute for monitoring in air quality assessments. Models use inputs such as measured or estimated changes in traffic flow, speed and composition as well as location parameters such as distance from the road. The accuracy and applicability of each model in assessing air quality changes arising from traffic management measures have yet to be assessed satisfactorily. This indicates the need for current and future air quality assessments to involve both monitoring and modelling. Only when a sufficient number of combined analyses have been undertaken for a range of traffic management schemes in a variety of urban settings will confidence in using models on their own be gained. Current studies such as those being undertaken in Greater Hull and the City of London provide important contributions towards reaching that goal. Nevertheless, there is a need for many more detailed air quality assessment studies to be undertaken in the UK, particularly in the light of local authorities being required to outline Action Plans to improve air quality in AQMAs (Elsom and Crabbe, 1996).

Acknowledgements

References

ARIC (Atmospheric Research and Information Centre): 1996, *Air Quality Monitoring Survey, Northgate Street, Chester City Centre*. Final report prepared for Cheshire County Council and Chester City Council. Unpublished, ARIC, Manchester Metropolitan University.

Bennett, L. Sandalls, S. and Mackett, R.: 1992, *NO2 and CO in Brighton*, AEA EE 0314, AEA Env. and Energy. Oxfordshire.

Cheshire County Council: 1996, *Environmental Planning and Operations sub-committee*, Decision Paper No. **8**.

Chiquetto, S. and Mackett, R.: 1995, *Sci. Total Environ.* **169**, 265-271.

Elsom, D. M and Crabbe, H.: 1996, Implementing the national air quality strategy in the United Kingdom. In Caussade, B., Power, H. and Brebbia, C.A. (Eds) *Air Pollution IV, Monitoring, Simulation and Control*, Computational Mechanics Publications, Southampton, 823-836.

Pharoah, T. M. and Russell, J. R. E.: 1989. *Traffic Calming: policy and evaluations in three European Countries*. Dept. of Urban Dev. and Policy, South Bank Univ. Occ. Paper, **2/89**, 48.

TRL (Transport Research Laboratory): 1994, *Vehicle emissions in the City of London: Effects of the City's Traffic Management Scheme*. Unpublished TRL Report, Project Ref: **P8716**, TRL, Crowthorne.

TRL (Transport Research Laboratory): 1995, *The Env. Assess. of Traffic Management Schemes: A Literature Review*. TRL Report **174**, TRL, Crowthorne.

AIR-QUALITY PROGNOSIS, FOR THE IMPLEMENTATION OF ABATEMENT STRATEGIES OVER LARGE URBAN AREAS

ANDREAS N. SKOULOUDIS[(1)], ROBERTO BIANCONI[(2)], ROBERTO BELLASIO[(2)]

(1) Environment Institute, Joint Research Centre "Ispra",
TP-250, Ispra (VA), I-21020, Italy
(2) Idea Snc, via Volturno 80, Brugherio (Mi) 20047, Italy

Abstract. State-of-the-art approaches for urban air-quality characterisation have several drawbacks due to a-priori assumptions and/or due to inherent limitations of the concept utilised. For the evaluation of abatement scenarios it is either necessary to embark on extensive monitoring campaigns or to consistently apply numerical models for atmospheric dispersion. The 'ENVISOR' methodology applied here is a mixture of the two approaches. It forecasts pollutant concentrations during real episodes and assesses the impact from the construction of a new highway across a large urban domain of 100x100 km^2. Data from an extensive monitoring network are used to identify real modelling periods and for validating the modelling simulations. The selected periods are aiming to the assessment of 'annual mean' or 'episodic' conditions. These periods are short-listed according to the abatement scenario under consideration. This approach yields accurate forecasts for the concentration of pollutants after extensive validation tests extended over the whole domain. It is foreseen that the impact from the highway construction will be minimal for photochemical pollution whereas, higher impact will result for inert pollutants due to additional emissions from the highway.

1. Introduction

Atmospheric pollution is a major problem in developed world. The principal problem with atmospheric pollution is that it is dynamic, not static. Pollutants emitted from anthropogenic activities are coupled with natural emissions and transported by meteorological fields. Several physical and chemical phenomena can occur during transport and the overall processes can be further enhanced by complex topography. The most common pollutants of interest are carbon monoxide (CO); nitrogen oxides (NO_x); sulphur dioxide (SO_2); ozone (O_3) and particulate matter. The significance of these varies for Northern and Southern cities as well as according to the climatic conditions and the seasonal diversity.

This work concentrates on reviewing current approaches and demonstrating how real-time dispersion simulations for reacting and non-reacting pollutants can be utilised in assessing current urban air-quality. In particular, we focus on the attribution of air-quality conditions into sources and we examine the impact of certain scenarios like the construction of major highway in a domain of 100x100 km^2 containing two metropolitan areas. It is also demonstrated that three-dimensional models can accurately predict the phenomenology of atmospheric dispersion and that these models can be safely used in air-quality forecasts.

2. Techniques and Approaches for Air-Quality Assessment

There are several techniques utilised nowadays for the characterisation of urban air pollution. These are: analysis of time series of monitored concentrations at fixed locations, measurement campaigns conducted for certain short periods, analysis of averaged concentrations from absorption tubes scattered over the domain, and real time dispersion calculations. The ultimate objectives of these are to assess current status over the recording domain. Other objectives are to the forecast the future conditions (short or long term); to evaluate the impact of abatement scenarios, to identify sources of intensive pollution and to evaluate human exposure. Each of these approaches has advantages and limitations.

Time series of concentrations recorded in monitoring stations are sufficient to describe the temporal evolution of pollution at a specific point of measurement. These time series serve primarily to check at fixed locations the compliance with regulatory decisions. However, in an urban area there is a strong dependence of measurements on the exact position and the type of instruments used. Frequently the maximum concentrations for different pollutant are not found at the same position. Thus, a network of expensive monitoring stations can only provide a limited picture of spatial variations. The variety of instruments, the status of their calibration and the occasional non-availability of instruments can further restrict the generalisation process if based on monitoring results only.

Exactly the opposite is achieved by intensive measurement campaigns. Many instruments positioned through the monitoring domain cannot be sustained for long periods. Thus, this approach is usually expensive, and there is always the possibility to miss important episodic conditions. Frequently these campaigns are carried out under inconsistent conditions and the temporal variability is rather limited.

The positioning of absorption tubes over an urban domain is a technique that tackles the problem of spatial distribution. The cost of this technique is primarily on the deployment of these tubes and the measurement of the absorbed concentrations. However, this technique can provide only temporarily averaged concentrations. It is not really suitable for the identifying maximum hourly concentration or for recording rolling averages for the current regulatory monitoring. Besides, absorption tubes are not fully developed for all types of pollutants and the positioning of these tubes can be a subjective process.

For appropriate temporal and spatial characterisation of an urban domain a mixture of the aforementioned approaches could be certainly be applied. However, these approaches can prove to be extremely expensive and time consuming for evaluating abatement scenarios.

Furthermore the previous approaches cannot easily carry out forecasts except with uncertain stochastic methods. These methods have limited only success for certain inert pollutants in cities where photochemical pollution is insignificant. Another crucial limitation is that with the aforementioned methods the attribution of air-quality into emissions sources can not be really achieved. The link between emissions and air-quality through empirical multiplication factors has certain limitations the nature of which is examined below.

During the first European Auto-Oil Programme, (1996), conducted for the European Commission, the European Automobile and Oil Industries a new approach has been developed. This was based on a mixture of the above approaches such as: interpretation of monitoring data for selecting the modelling period; implementation of detailed three-dimensional mathematical models consistently over the domain; validation of the simulations over a base year and future projections under specific emission scenarios. The main elements of this approach form the basis of the "ENVISOR" methodology. The modules of this methodology which are related with forecasts are demonstrated below.

3. Emission Multiplication Factors and their Limitations

Previous abatement strategies are based primarily on emission reductions. Most of these strategies assumed that there is a direct relationship between emissions and air-quality through multiplication factors. Equally, due to the increased number of pollutants which should be elucidated in urban domains, it has been common practice to link one pollutant into another through empirical multipliers. Despite the simplicity of this assumption the establishment of these multipliers has never been a straightforward process. The range of their validity depended only on whether the actual physico-chemical characteristics of these pollutants had similarities or when large tolerance limits are acceptable. The latter is usually the case for long temporal and spatial averages. However, for assessing the effects of abatement strategies it is necessary to identify "hot spots" of high concentrations over the domain and assess the changes of air-quality during severe episodes.

As in any empirical approach, it is always possible to relate two parameters through multiplication factors. However, if we seek to apply these multipliers universally for different physical phenomena in time and space, several implications might occur. These implications originate straight from the nature of the assumptions imposed.

The uncertainties from such an approach are easily demonstrated through the simplified dispersion equation solved in the x-direction for each source category for pollutant-1 (NOx) is as follows:

$$\frac{\partial c_1}{\partial t} - \frac{\partial c_1 u_x}{\partial x} = \frac{\partial}{\partial x}\left(K_{x,1}\frac{\partial c_1}{\partial x}\right) + E_1 \tag{1}$$

where, E_1 is the emission rate, c_1 the air-quality concentrations, K_x is the diffusion coefficient, t is the time and u_x the x-axis velocity. For simplicity, let us consider only one source category; namely the gasoline passenger cars (PC_g). For the concentration of another pollutant c_2 (this could be CO or Hydrocarbons etc) the corresponding equation is:

$$\frac{\partial c_2}{\partial t} - \frac{\partial c_2 u_x}{\partial x} = \frac{\partial}{\partial x}\left(K_{x,2}\frac{\partial c_2}{\partial x}\right) + E_2 \tag{2}$$

We may further assume that: $K_{x,1} \equiv K_{x,2}$ and that from the emission inventories we could establish the following relationship for Gasoline Passenger Cars:

$$E_2 \equiv f_{PC_g} E_1 \tag{3}$$

When eqn-3 is substituted into eqn-2 we have:

$$\frac{1}{f_{PCg}} \frac{\partial c_2}{\partial t} - \frac{1}{f_{PCg}} \frac{\partial c_2 u_x}{\partial x} = \frac{1}{f_{PCg}} \frac{\partial}{\partial x}\left(K_{x,1} \frac{\partial c_2}{\partial x} \right) + E_1 \qquad (4)$$

In order to use only NOx for deriving the concentrations of other pollutants it is necessary to convert eqn-4 into the same form as eqn-1. Thus, it is necessary to assume further that f_{PCg} **is not a time and space dependant** parameter. Only then we shall be able to claim that:

$$c_2 = f_{PCg} c_1 \qquad (5)$$

For the purposes of this work it is sufficient to demonstrate the validity of eqn-5 by examining the spatial variations of f_{PCg} from in the emission inventory and how these are reflected in three dimensional simulations for the concentrations c_1 and c_2.
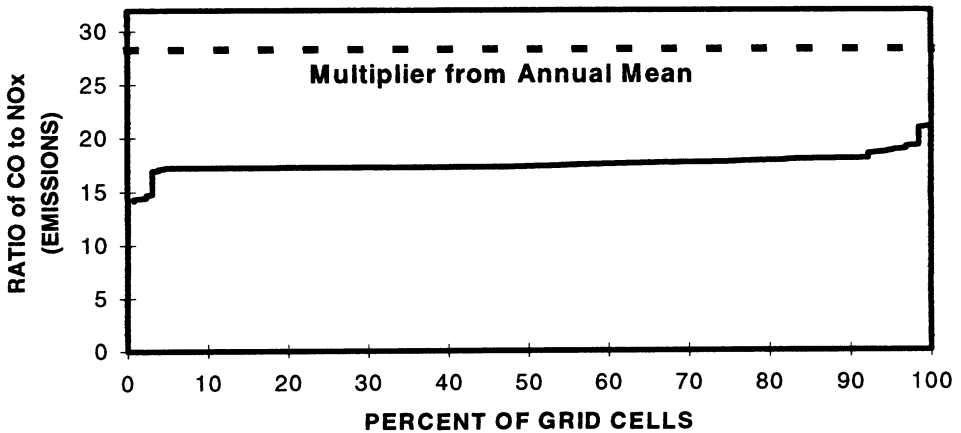

Fig. 1. Percentile distribution of CO/ NOx from the emission inventory of Athens for gasoline passenger cars.

Figure 1 illustrates the grid percentile distributions of E_2/E_1 for gasoline passenger cars in Athens during 1990. With solid line at the same plot is shown the same ratio obtained from annual mean ratios over the whole domain. The latter is overestimating the actual emission ratio of CO/NOx by 30% to 90%. When these emission multipliers are used to calculating the concentrations of CO the ratio of the concentrations $f_{PCg} c_1 / c_2$ is varying up to 260% as shown in Fig.2. Similar conclusions can be drawn for the temporal dependence of the multipliers. Fortunately the availability and reliability of atmospheric dispersion models can safely eliminate the use of multiplication factors whenever accurate assessments are necessary.
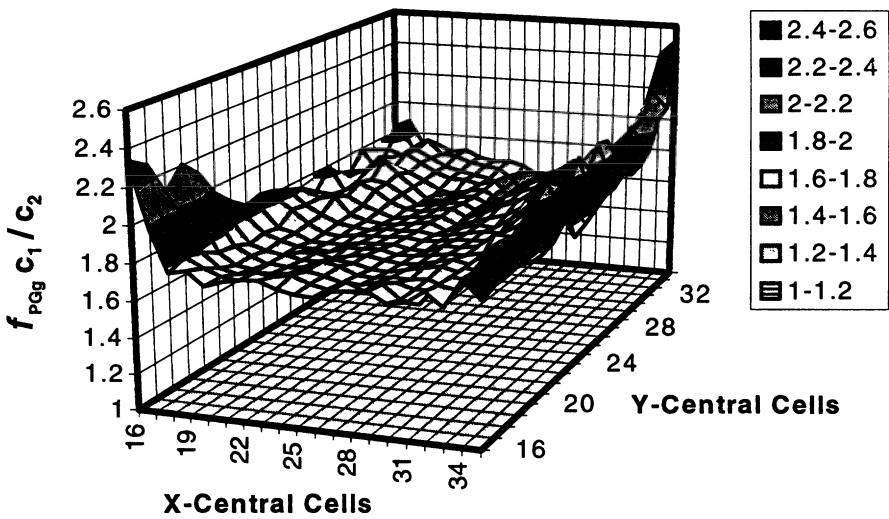
Fig. 2. Comparisons of CO concentrations obtained from emission multipliers to results from 3D dispersion simulation for gasoline passenger cars at the centre of the domain of Athens.

4. The "ENVISOR" Methodology for Urban Air Quality Forecasts

A reliable prognosis of pollutant concentrations for a 'base case', is an essential requirement prior to evaluation of abatement scenarios over urban domains. The forecasting process described here is based on the use of three dimensional, Eulerian dispersion models. The use of these models requires an integrated tackling of several key topics. Such topics are the temporal and spatial characterisation of emissions and the reasonable handling of chemical mechanisms. It further requires the use of high-resolution geographical data and the incorporation of consistent meteorological fields at ground and at higher levels above.

A single numerical tool can not tackle the aforementioned topics. Different mathematical models for the emissions, the atmospheric circulation and the dispersion of contaminants should be applied on urban air sheds. All these components/modules have been consistently incorporated into the "ENVISOR" methodology. The aim of this tool is to furnish a methodological workbench for the establishment and implementation of reliable, objective and comparable regulatory decisions, Skouloudis (1997). Main features of this methodology are:

- Classify urban air-quality over several years and identify episodes according to severity duration and frequency of occurrence.
- Consistently prepare input conditions such as emissions, topography, landuse etc for the dispersion models.
- Standardise input data e.g. harmonisation of source emission categories and provide long term forecasts over a long time horizon.
- Examine the scientific coherence and validate calculated results.

- Demonstrate compliance with agreed standards and limits over large regional and urban domains.
- Demonstrate the spatial representativeness of monitoring stations and optimise the positioning over a metropolitan domain.
- Examine available and planned technological developments from the industry, which will have positive impact on significantly reducing atmospheric pollution.
- Link and optimise emissions, air-quality and cost data according to required similar impact.

For the assessment of key industrial scenarios, several applications of this methodology have been carried out. Most of these have been conducted over North and South European cities for several inert and photochemical pollutants. The length and the severity of episodes have been characteristic of the domain examined. Also, the overall air-quality data were incorporated in a cost-effectiveness optimiser for achieving ideal solutions. Most of these applications are classified for the time being. The following sections demonstrate unclassified simulations with explanations of the main features for this approach.

4.1. CHARACTERISATION OF EPISODES FROM MONITORING DATA

The application of "ENVISOR" in major metropolitan areas requires a grid of 150,000 to 200,000 cells over which meteorological fields and concentrations are calculated on an hourly basis. It is inevitable that the simulation period considered can not be extended to cover a whole year. Besides, neither the emissions nor the initial meteorological conditions are known with such precision so that this calculation will have a significant meaning.

In general, due to the recurring nature of meteorological conditions and the repetitive characteristics of the anthropogenic emissions we could easily identify several classes of real periods that could characterise the whole year. These periods could characterise either episodic or well-ventilated periods similar to annual mean conditions. The advantage of this approach is that there is no need to define artificial diurnal variations and the emission inventories could be tailored to represent the exact anthropogenic activities for the period under consideration.

In order to identify episodes of different severity and duration with the "ENVISOR" methodology, past monitoring data for several years must be analysed. The severity of the episodes can be selected according to the percentile characteristics of each monitoring station. The same approach can be implemented in identifying periods during which the air-quality conditions are similar to the annual mean values. The latter are mainly "surrogate annual mean" episodes and are normally occurring several times per year.

Details can be found in Bellasio and Skouloudis (1997). This characterisation process can be carried out for primary or secondary pollutants from one or many monitoring stations. After the exclusion of non-operational stations, all other stations consistently indicate the similar dates for episodes of equal severity. This is illustrated in Fig 3 for a network of 16 monitoring stations scattered in a domain of 10,000 km^2. The "number of occurrence" indicates how many of the hourly concentrations, corresponding to this date, are within the first 100 places of the ranked file containing annual concentrations.
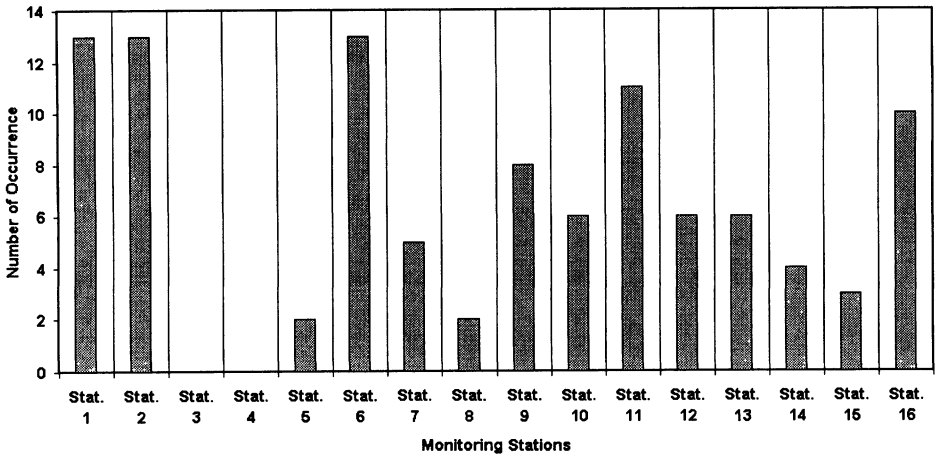
Fig. 3. Number of occurrence of 28 Feb in the 100 highest values recorded during 1992 for 16 different monitoring stations (stations 3 and 4 were not operational).
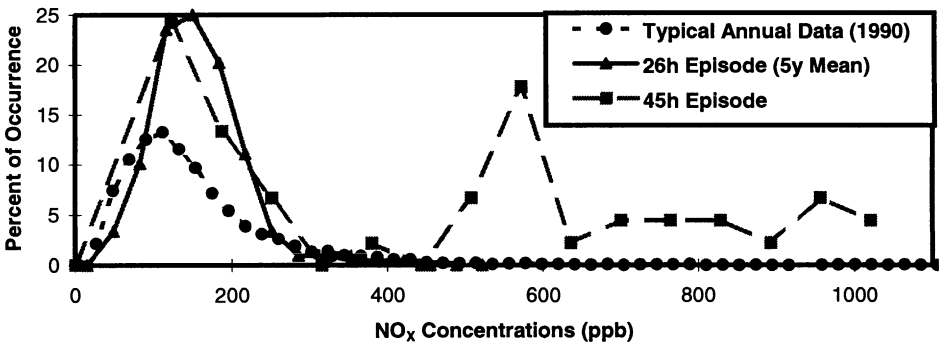

Fig. 4. Typical NO_x distributions for episodes of different duration from London Bridge Place (1988/92).

For demonstrating the significance of episodes of different duration and severity Fig 4 summarises the frequency distributions for episodes of 26 and 45 hours from a single monitoring station used in Auto Oil-1, (1996). The data set for London is the one used for Auto Oil-1 and was obtained from 'AEA Technology', National Environment Technology Centre at Culham, UK. For comparisons, at the same plot is illustrated the frequency distribution for the whole 1990. In this figure is also shown that episodes of short duration are characterised by intermediate concentrations with a higher frequency of occurrence. Whereas, during long episodes, peaks of high concentrations are expected in addition to more frequent intermediate values.
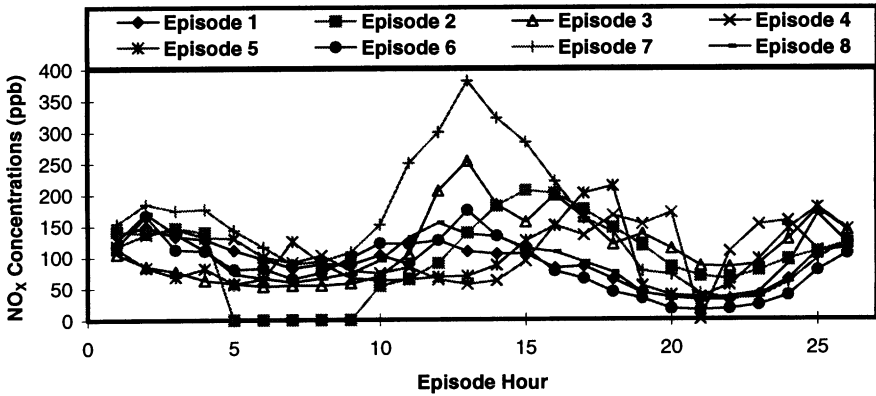
Fig. 5. Time series of hourly concentrations for all episodes lasting 26 hours London Bridge Place (1988/92).

Episodes with inert pollutants lasting 26 hours can frequently occur in an urban domain during winter months. The characteristics of these episodes are demonstrated in Fig 5 for NO_x at the same monitoring station. The time series of all episodes lasting 26 hours show surprising similarities. The mean hourly value of these episodes is used in Fig 4 for comparisons with episodes of different duration.

4.2. EMISSION INVENTORY CONSIDERATIONS

Once the period of episodic conditions or for the surrogate annual mean has been established the emission inventory corresponding to the relevant dates must be constructed. Usually emission data are given on annual basis. In this case temporal and spatial disaggregation of the emission inventory should be carried out. Alternatively the emission inventory needs to be constructed for the exact from a bottom up approach. In the latter case the emissions from each polluting source are aggregated over the whole domain. Before applying either of these solutions it is necessary to know the main source categories which will be used in the abatement strategy.

Within "ENVISOR" both techniques are incorporated. We could start either from general annual inventories and arrive to specific categories disaggregated in time and in space, or start from individual information aggregated into to the desired emission sources for every grid cell and every hour. For example, it is possible to start from fuel consumption and estimate emissions in a particular cell at a particular time. Alternatively, we could process detailed traffic information (number of cars, fleet composition, driven km in a particular site etc) for estimating local emissions in a cell. The same emission inventory can be constructed using a bottom-up approach for certain source categories and a top-down approach for others. This selection of the approach depends strongly on the availability of suitable information.
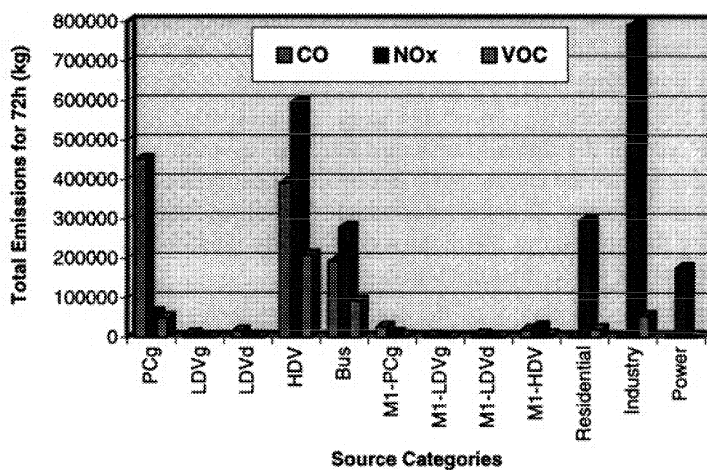
Fig. 6. Source attribution of integrated emissions for CO, NO_x and VOC over the whole domain for 72 hours.
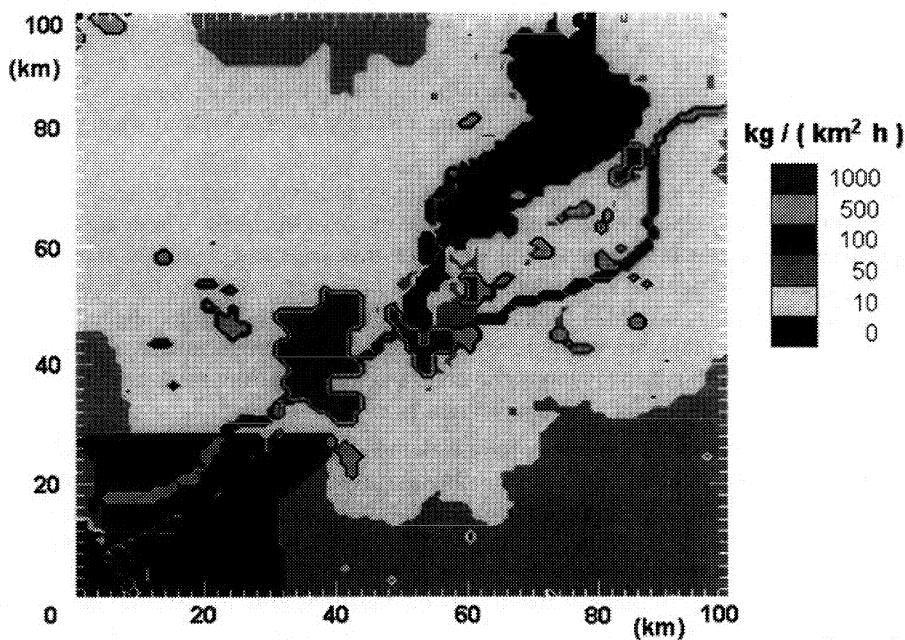

Fig. 7. Spatial disaggregation of CO emissions for 72 hours and all source categories

A typical attribution of sources for an urban domain covering a large metropolitan area is shown in Fig 6 for CO, NO_x and Volatile Organic Compounds (VOC). Emphasis is given to emissions from traffic thus the sources examined are as gasoline passenger cars

(PC$_g$), gasoline light duty vehicles (LDV$_g$), diesel light duty vehicles (LDV$_d$), heavy duty vehicles and buses. Other sources of major emissions on the domain are residential emissions, the emissions from medium industry and from the large power plants.

Because of the forecasting aim of this work, the emissions from the construction of a main highway across the domain are considered as separate sources. These are shown separately in Fig 6 with the letters 'M1'. In Fig 7, is illustrated the spatial variability of CO emissions summed during 72 hours over which modelling simulations are carried out. In the same figure the position of the motorway is clearly identified from north-east towards the south-west corner of the metropolitan domain.

Another important complexity of the emission inventories prepared for photochemical simulations is that VOC emissions must be given into individual components. This speciation process could be carried out in several ways. Within "ENVISOR" different speciation schemes could be utilised for different source categories or sub-categories (i.e. a source category can be traffic and a sub-category can be diesel vehicles).

4.3. DISPERSION CALCULATIONS

Before carrying out any dispersion simulations it is necessary to establish for every hour consistent meteorological fields for each grid-cell of the three-dimensional domain. Naturally, the accurate calculation of wind speed and direction as well as the correct estimation of the planetary boundary layer (PBL) are very important. Wrong winds might move pollutants in wrong directions and wrong PBL depth will result in wrong pollutant concentrations at ground level.

Currently within 'ENVISOR' two meteorological models are incorporated. These are the prognostic model, CSUMM and the diagnostic model, CALMET. These are described respectively by Kessler (1989) and Scire et al., (1995) and can be utilised separately or together. CALMET alone can give satisfactorily results in regions where the topography is not complex. However, CSUMM is necessary for regions with complex terrain with sea-land breezes or with mountain-valley breezes. Generally, the prognostic model is applied over a wide region with relatively large grid cells and the diagnostic meteorological model is applied over a smaller region with smaller cell size.

Following the application of meteorological models the matrices with wind fields, micro-meteorological parameters and emissions are ready for dispersion simulations. In view of the chemistry and the number of the components involved the dispersion calculations can be very expensive. It is inevitable that neither all species nor all chemical reactions occurring in the atmosphere could be taken into consideration. For this reason it is necessary to consider solutions of the dispersion equations only for certain 'explicit' and 'lumped' species. 'Explicit' are the real and most important chemical species usually involved in the formation of ozone (ozone itself, nitrogen oxide, nitrogen dioxide, formaldehyde etc) or very important primary species (as carbon monoxide). 'Lumped' species are obtained from lumping several chemical compounds characterised by similar reactivity. Usually this reactivity is expressed with respect to the hydroxyl radical (OH-).

The photochemical dispersion model used for this work is CALGRID as described by Yamartino et al., (1989) and Scire et al., (1989). The domain is a large metropolitan area

of 10,000 km^2. Over this domain the implications from the construction of a main highway are examined together with its consequence during photochemical episodes.

5. Results and Discussion

An important advantage from the use of 'ENVISOR' is that calculated air-quality concentrations for the 'base case' can be directly validated against real measurements. Extensive validation of 'base case' data sets, lead to realistic and reliable impact assessment of abatement strategies. Several validation criteria for the simulations of urban air-quality have been described by Skouloudis (1996). The main principles behind these criteria are:

- The accuracy of the simulation predictions against measurements is demonstrated
- The reliability of the models is examined through parametric simulations
- The consistency if the important modelling features is demonstrated.

Whenever possible the information extracted from the matrices generated by each simulation should be tested against the ratio of "(predicted - observed)/observed" values. The parameters which could be tested are, the time and area averaged concentrations over the domain as well as the instantaneous values for each pollutant. Similarly, the meteorological fields could be compared at all possible locations. Mass conservation should be checked over the domain for inert pollutants and the area-averaged proportions for each source category should be examined for air quality and emissions.

Regarding the accuracy of a forecasting run, we use the frequency distribution of the hourly concentrations, as indicator as to how close to reality is the simulation. The same is achieved from comparing typical diurnal variations. With the models currently incorporated in 'ENVISOR' an accuracy of 50% is easily achieved for inert (CO, NO) and reactive pollutants (O_3, NO_2) during temporal and spatial comparisons with measurements.

The validation of results and the demonstration of achieved accuracy are usually long processes. It is obvious that for each simulation a large number of validation plots can be created. The presentation of all possible comparisons is a long laborious process. Within 'ENVISOR' most of these processes are carried out automatically. Due to the limited space available, randomly selected comparisons are shown.

First, for spatial trustworthiness, Fig 8 illustrates the concentration of CO 20m above the ground for the whole domain. These concentrations are averaged over 72 hours. Similar plots can be generated for other pollutants. CO has been selected because it corresponds to the x-y plot shown in Fig 7 for emissions. Comparison of the contours of Fig 7 and Fig 8 illustrate how important are dispersion even under episodic conditions without strong winds. The marks in Fig 8 correspond to the position of monitoring stations which are used in demonstrating temporal reliability.

The corresponding time series for three monitoring stations measuring CO are illustrated in Fig 9. These stations are positioned at the centre and the periphery of the domain. The hours indicated at the x-axis are from the beginning of the year and the primary grid lines correspond to 12 hours starting from 0:00 am. For CO the predicted diurnal variations are not as abrupt as the measurements. However, the mean trend during the episode is predicted satisfactorily. The data from station 5 are recorded near a main road. Thus,

higher concentrations are recorded at the point of the measurements than the actual averaged values calculated from the model over an area of 1 km^2. The over-prediction at station 1 is attributed to the proximity of this station to the boundaries of the domain.
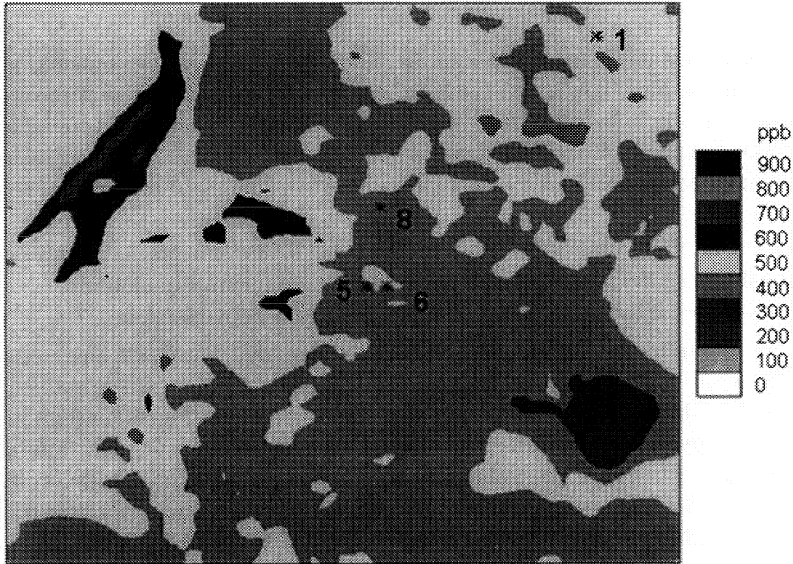

Fig. 8. Time averaged air-quality concentrations for CO over the domain.

Similar comparisons are illustrated in Fig 10 but for ozone. For this pollutant the diurnal variations during the three-day episode are very accurate and the same is true about the predicted maximum values. For station-1, the disagreement of the third peak during the third day of the simulation is also due to close proximity of this station to two boundaries of the domain. Similar accuracy is achieved also for NO and NO$_2$.

Following the validation of the data sets corresponding to 'base case' we are ready to proceed in evaluating the impact of a certain evolution scenario or in assessing the impact of a certain abatement strategy. With the term 'base case' in this work we have considered a severe three-day episode during 1992 and the abatement strategy is the effect from the construction of a highway.

As illustrated in Fig 6, due to the small emissions attributed to the highway, the impact of its construction over the whole domain is rather insignificant. This was actually observed by comparing the frequency distribution of concentrations with and without the highway, during the three days of the episode. Negligible differences are shown at the peak of the frequency distribution only.

On the contrary when the ratio of ground concentrations for 'scenario' to 'base case' is calculated for every grid cell, significant differences are expected at least at the vicinity of the highway. Table 1 shows the 25 highest ratios of the modelling domain for NO and O$_3$.
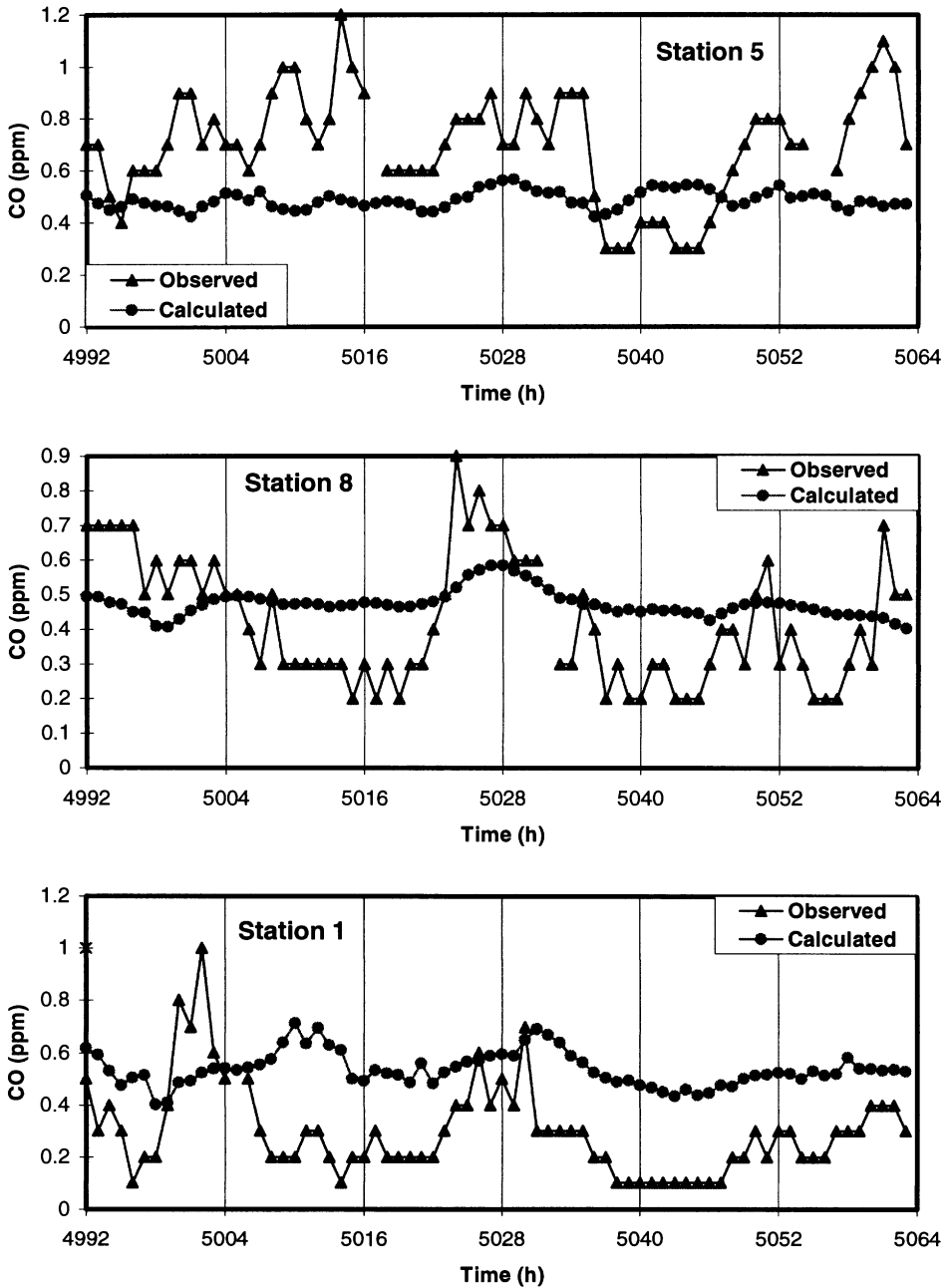
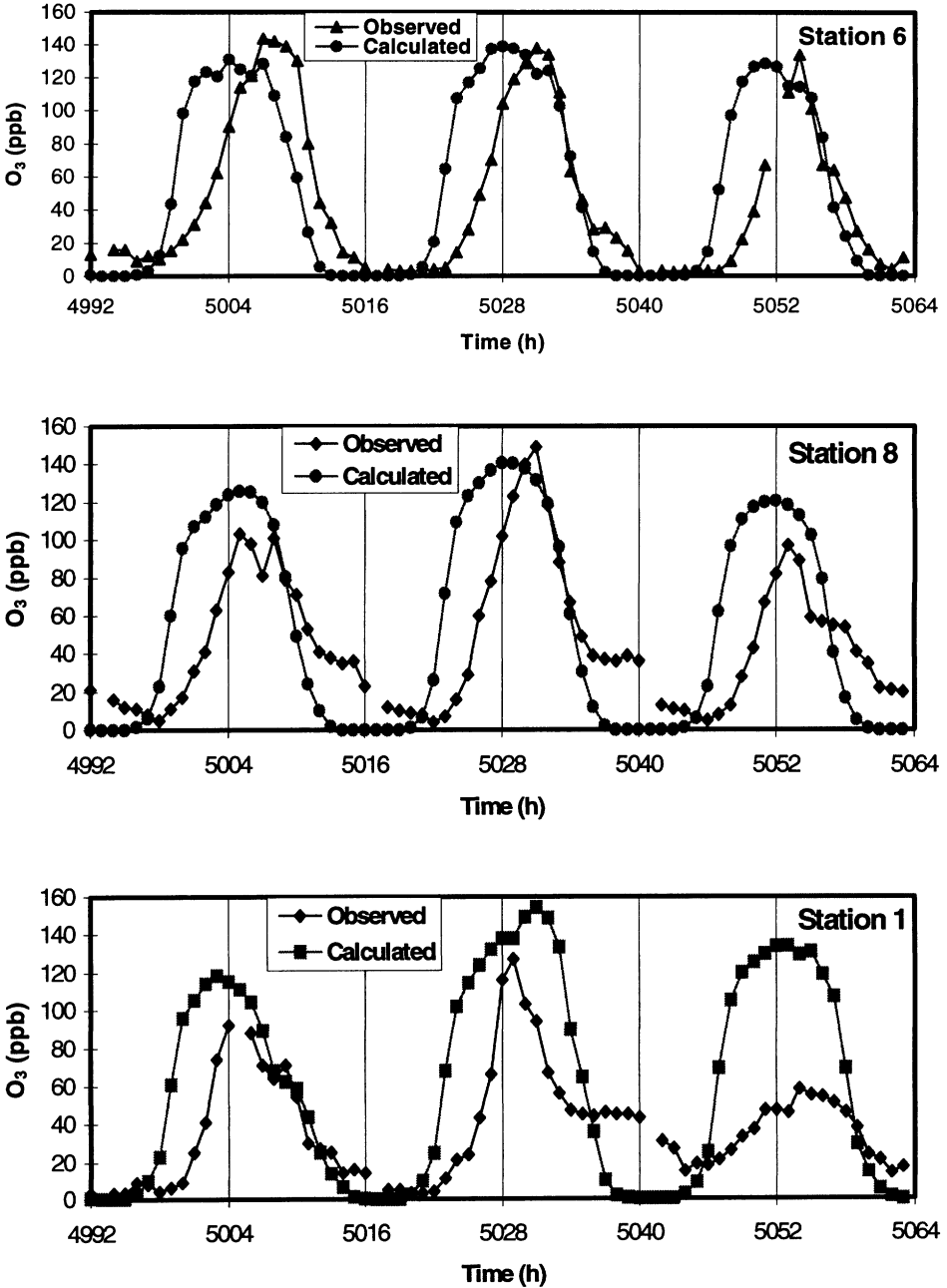Fig. 9. Time series of CO concentrations at selected monitoring stations.

Fig. 10. Time series of O_3 concentrations at specific monitoring stations.

Comparisons can be carried out for two distinct local times during which intense traffic is expected. The x,y is the identification number in km from the south-west point of the domain (as in Fig 7). For NO significant changes are predicted due the construction of the

motorway at the vicinity of the motorway. These changes are more profound during the evening 'rush hour' than in the morning. The cells where the maximum changes occur vary every hour due to the change of meteorological conditions.

Table 1; The 25 largest ratios of NO and O_3 concentrations with and without the Highway.

NO Ratios				O_3 Ratios			
x,y (km)	10:00 am	X,y (km)	8:00 pm	x,y (km)	10:00 am	x,y (km)	8:00 pm
95.81	11.4	89.74	28.1	99.45	1.023	34.25	2.54
96.82	10.0	96.81	26.7	99.41	1.023	43.43	1.69
97.82	9.2	28.31	26.4	97.41	1.022	33.25	1.53
98.82	9.1	95.81	26.2	95.40	1.021	31.28	1.49
95.82	8.6	90.76	24.2	98.43	1.021	42.40	1.38
90.77	8.2	90.77	23.9	89.38	1.021	37.42	1.31
90.78	8.2	29.31	23.5	99.47	1.021	12.17	1.28
78.53	8.1	89.75	20.8	93.39	1.021	41.42	1.27
65.47	7.9	66.48	20.5	95.41	1.021	39.42	1.26
92.80	7.8	95.8	19.3	92.41	1.021	44.44	1.21
94.81	7.5	88.62	19.1	96.42	1.021	6.17	1.21
77.52	7.2	77.52	18.9	96.40	1.021	41.43	1.20
48.44	7.1	87.58	18.0	98.44	1.021	45.43	1.19
66.47	7.1	92.79	18.0	93.41	1.021	14.17	1.17
47.43	7.0	94.8	18.0	98.42	1.021	2.19	1.15
64.47	7.0	89.71	17.9	97.42	1.021	21.30	1.15
70.50	7.0	85.55	17.6	92.40	1.021	2.21	1.14
96.81	7.0	27.31	17.4	97.43	1.021	38.40	1.14
66.48	6.9	91.78	17.4	93.40	1.021	43.42	1.14
72.51	6.8	87.57	17.0	91.40	1.021	2.20	1.14
47.42	6.7	89.73	17.0	94.40	1.021	39.43	1.13
89.76	6.7	86.56	16.8	90.41	1.021	2.18	1.13
63.47	6.6	89.72	16.6	92.38	1.021	2.22	1.12
93.81	6.6	88.58	16.4	90.38	1.021	2.17	1.11
89.75	6.6	98.81	15.5	94.39	1.021	39.39	1.11

In general, during both time periods (10:00am and 8:00pm) the periphery of the highway is more significantly influenced by the presence of this new source of emissions. Different conclusions are made from the observations for O_3. The construction of the highway will introduce insignificant changes for the morning and the evening 'rush hours' in comparison to the NO. During the sampling period at 10:00am the changes, due to photochemical activity, are expected only at cells with appropriate precursor concentrations (i.e. over the rice fields). During the evening period at 8:00pm, photochemical reactions have ceased however, the accumulative ozone produced has dispersed nearly over the domain according the prevailing winds. Hence, cells with

significant changes due to the new source are situated mostly away from the periphery of the highway.

The conclusions drawn from the scenario of a highway is that, despite the load of small emissions, this source might introduce significant changes to the hourly concentration of several pollutants. These need to be accounted for during episodes where excessive instantaneous exposure of the population should be avoided.

6. Conclusions

For the implementation of abatement strategies in large metropolitan areas it is necessary to establish an accurate relationship between air-quality concentration and emissions. In fact, these emissions originate from several anthropogenic sources such as industrial processes, heat and power generation, and traffic. The complexity of the processes associated with emitted pollutants, undergoing chemical reactions, transforming from vapour to particulate and dispersing under complex meteorological conditions makes the distinction of the polluting sources rather prohibitive.

On the other hand, one of the reasons why past emission control strategies have failed to achieve air-quality improvements, is that these strategies were based on simplified representations of atmospheric processes through multiplication factors. These were fundamentally linked to the strength of the emission sources and all atmospheric processes were assumed to be static. The limitations introduced by this approach have been examined and it is recommended to avoid the use of this approach whenever possible. Furthermore, the monitoring of air-quality through networks of measuring stations had limitations in representing reality over large areas. Serious problems might arise when such measurements are extrapolated to locations where data are missing or when interpreting concentration in the proximity of measuring instruments.

The previous limitations have been eliminated in a new approach for the characterisation of urban air-quality. This approach is called "ENVISOR" methodology. It combines state-of-the-art dispersion models coupled with extensive use of monitoring data. It also incorporates emission modelling tools and an automatic validation module of generated data sets. It forecasts pollutant concentrations over real episodes and assesses the impact realistic scenarios for the abatement of urban pollution.

The characteristics and the severity of episodes with different duration have been examined from the hourly concentrations of monitored data for inert and reactive pollutants. It was demonstrated that short and long episodes have distinct frequency distribution of their concentrations. It was also shown that episodes of equal duration are following similar time series.

The prognostic capabilities of "ENVISOR" for a real photochemical episode are also demonstrated in this work. Encouraging results are achieved for the hourly concentrations of ozone and the inert pollutants. Having established good accuracy between several monitored and calculated parameters the data set of the 'base case' is stored and the calculation of different scenarios can be implemented directly at the emission inventory. For a new highway crossing the entire domain the impact of the additional emissions are minimum and there are no significant changes of the ozone concentration. However for NO significant local changes will be introduced at the periphery of the highway.

References

AutoOil-1, Sub Group-2: 1996, 'Air quality report of the Auto Oil programme', Report DG-XI/D3, European Commission , Belgium

Bellasio, R. and Skouloudis, A..N.: 1997, 'An identification methodology for worst pollution episodes in urban atmospheres', Technical Note I.97, Joint Research Centre Ispra, European Commission, Italy.

Kessler, R.C.: 1989, 'Systems applications, Inc. Version of the Colorado State University Mesoscale Model', Prepared for Sigma Corporation Inc., April.

Scire, J.S., Yamartino, R.J., Carmichael, G.R. and Chang, Y.S.: 1989, 'CALGRID: A mesoscale photochemical grid model, Volume 2: User guide', Sigma Research Corporation Inc., Report A049-1, June.

Scire, J.S, Insley, E.M., Yamartino, R.J. and Fernau, M.E: 1995, 'A user's guide for the CALMET meteorological model', Prepared for USDA Forest Service, Sigma Research Corporation Inc., Document 1406, July.

Skouloudis, A..N.: 1996, 'Validation of dispersion simulations in seven European cities for surrogate annual mean and episodic conditions', Technical Note I.97, Joint Research Centre Ispra, European Commission, Italy.

Skouloudis, A..N.: 1998, 'ENVISOR; an integrated methodology for the assessment of current and future air-quality with emphasis to urban traffic', EUR Report on preparation.

Yamartino, R.J., Scire, J.S., Hanna, S.R., Carmichael, G.R. and Chang, Y.S.: 1989, 'CALGRID: A mesoscale photochemical grid model, Volume 1: Model formulation Document', Sigma Research Corporation Inc., Report A049-1, June.

ACCURATE OZONE PROGNOSTIC PATTERNS FOR MADRID AREA BY USING A HIGH SPATIAL AND TEMPORAL EULERIAN PHOTOCHEMICAL MODEL

R. SAN JOSÉ[1], J. CORTÉS[1], J. F. PRIETO[1] and R. M. GONZÁLEZ[2]

[1] Group of Environmental Software and Modelling, Computer Science School, Technical University of Madrid, Campus de Montegancedo, Boadilla del Monte - 28660, Madrid (Spain). [2] Department of Meteorology, Faculty of Physics, Complutense University of Madrid, Ciudad Universitaria, 28040-Madrid (Spain)

Abstract. The ANA Air Quality Model (ANA stands for Atmospheric Mesoscale Numerical Pollution Model for Regional and Urban Areas) has been applied over Madrid during a five day period in June, 1995. The domain is 80 x 100 km^2 and the spatial resolution is 2000 m. The ANA system is driven by a meteorological model REMEST and it includes a detailed emission model for anthropogenic and biogenic sources with 250 m spatial resolution and 60 minutes temporal resolution. Different deposition processes are used such as the Wesely (1989) and Erisman *et al.* (1994) resistance approaches and the simple aerodynamic resistance. The photochemical processes and the general chemistry is based on the CBM-IV mechanism for the organic compounds and solved by the SMVGEAR method (CHEMA module).

The model uses 14 different landuse types which are obtained by using the REMO module which uses the information provided by the LANDSAT-5 satellite image over the domain. The emission module EMIMA takes into account the point, line and area emissions over the domain. Special importance is given to the biogenic emissions which are obtained by using the satellite landuse classification for caducous, perenneal and mixed terrain. The emission module considers the EPA and CORINAIR emission factors. The results show an accurate prediction of the ozone maxima for the five days and also the general pattern of the ozone observed data. The five day simulation is characterized by a local low pressure over the Madrid Area and high pressures over Spain and West of Europe. The ozone surface patterns show the diurnal cycle and the maxima concentrations up to 140-160 ppb for suburban areas during afternoon hours. The general performance of the model is considered quite good. The computer power requirements continue to be very high for standard workstations. Future progress on parallel platforms should improve considerably the computer time requirements.

1. Introduction

Ozone formation in the ambient atmosphere is separated in time and space from emission sources of precursors (volatile organic compounds, VOC, and NO$_x$). Photochemical air pollution is an environmental problem that is both pervasive and difficult to control. The necessity to have a reliable three dimensional mathematical model which allows to predict the ozone three dimensional fields for 24-120 hours is particularly important in the future. Policy makers can find it an essential tool for taking decisions. Public information will be benefited for these mathematical tools. The need to provide public health warnings during ozone episodes is enhanced because these warning will eventually help to reduce or control the ozone episode developments.

An important element of any approach directed at attempting to improve the situation is a reliable means for predicting the air quality impacts of alternative emission control measures. While many different methods have been developed, the most comprehensive and technically defensible approach has been to use mathematical models that describe, in detail, the physical and chemical processes responsible for the chemical

transformation, transport and fate of pollutants in the atmosphere. In the last two decades rapid progress has been made in this direction. Three dimensional mathematical models have been developed that simulate these phenomena to calculate the evolution of ozone and notable among these are: the Urban Airshed Model (Reynolds *et al.*, 1979; Morris and Myers, 1990; System Applications, Inc., 1990; McRae *et al.*, 1982) and the Regional Acid Deposition Model (Chang *et al.*, 1987). The California Air Resources Board Airshed model (CALGRID) (Yamartino *et al.*, 1992) was developed to upgrade and modernize the Urban Airshed Model (UAM) by implementing state-of-the-science improvements in the model. In the European side, the EZM EUMAC Zooming Model (Moussiopoulos, 1994) is the most important representative of the prognostic mesoscale models. This model is the basis of the ANA model which is the model described in this paper. Previously, the E3DUSM (San José *et al.*, 1994) and NUFOMO (San José *et al.*, 1995a) models were used in the ANA model. These models are mesoscale atmospheric prognostic models which are applied over Madrid Area. The former models and applications were made for one day, August, 15, 1991. This contribution shows the results for a longer period and with a much more consolidated system.

ANA stands for Atmospheric mesoscale Numerical pollution model for regional and urban areas. Figure 1 shows a scheme of the different modules of the ANA system. This model is composed on several different codes such as: the CHemical Model for Atmospheric processes (CHEMA), the DEPOsition model (DEPO), the REmote sensing MOdel (REMO), the EMIssion model for MAdrid area (EMIMA) and the REgional MESoscale Transport model (REMEST). All of this modules are in fact independent models which can be applied for specific purposes. The CHEMA model is integrated in the REMEST model under the "on-line" mode which means that the chemistry is solved and updated on the time when the advection and diffusion is simulated by the REMEST model on the actual time step. The EMIMA model is ran under the "off-line" mode which means that the emissions for the simulated days are produced before starting the ANA simulation and stored on a file which is read by ANA during the simulation. In this contribution the set of all this modules which is called ANA is applied for one ozone episode over the Madrid Area during the 5-9, June, 1995 period. June, 5 is Monday and June, 9 is Friday.

The mesoscale meteorological model is based on the MEMO model (Flassak, 1990) which is a non-hydrostatic three dimensional meteorological prognostic mesoscale model characterized by the completeness, consistency, robustness and flexibility. The model has a strict preservation of conservability properties and it uses algorithms which allow estimating the numerical error associated. The Navier-Stokes partial differential equations which describe the prognostic and diagnostic features for the three wind speed components and for the temperature and humidity are solved into the MEMO model. The transport equation is based on the Eulerian approach that solves numerically the advection-diffusion equation on a staggered grid. The form of the equation we adopted is

$$\underbrace{\frac{\partial c_s}{\partial t}}_{I} + \underbrace{\frac{\partial (u_i c_s)}{\partial x_i}}_{A} = \underbrace{\frac{\partial}{\partial x_i}\left[K_{c_{ij}} \frac{\partial c_s}{\partial x_j} \right]}_{D} + \underbrace{S_{c_s}}_{E} + \underbrace{P_{c_s}(c)}_{CH_1} + \underbrace{L_{c_s}(c)}_{CH_2} \tag{1}$$

where c_s denotes the gas phase concentrations of pollutants, u_i are the wind velocity components and K_c is the eddy-diffusivity for scalars (K-theory is used here). The I term is the inertia or storage, A corresponds to the advection, D to diffusion, E to emission (for point and area sources inside the domain), and CH_1 and CH_2 stands for production and loss terms, respectively, regarding gas-phase chemistry.
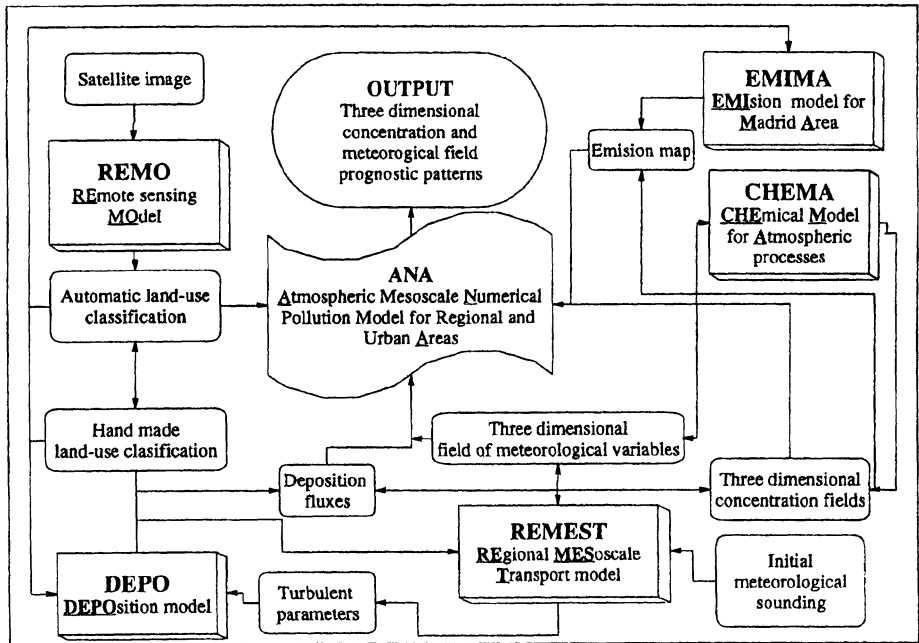

Figure 1.- ANA Model for Air Quality Diagnostic and Prognostic studies.

The 3D eulerian model uses the same computational domain (σ-coordinates, expanding vertical grid, etc.) that the mesoscale meteorological model. The averaged time step is $\Delta t = 30$ s. The temporal discretization adopted makes use of the 2nd order Adams-Bashforth scheme. The vertical diffusion is implemented with the Crank-Nicholson method. For the A term a modification of the original 1D TVD (total variation diminishing) method for the three dimensional case was introduced by Harten (1986). This method achieves a great reduction in the undesirable numerical diffusion but we should point out that this spurious diffusion is not completely removed.

The emission model is a high resolution emission inventory (spatial and temporal) and this information is provided by EMIMA. EMIMA is an emission model of atmospheric pollutants in a domain centered in the Madrid Metropolitan Area following the CORINE methodology. The pollutants which have been taken into account in the current version of the model (2.0) are: SO_2, NO_x and anthropogenic and biogenic VOC's (isoprene and monoterpenes). The model domain comprises an area of 80 km x 100 km with 5,108,144 inhabitants and more than 2,000,000 vehicles. The number of towns is 210.

The city of Madrid (capital of Spain) with more than 3,000,000 people is the main source of anthropogenic emissions and its influence is key for understanding the atmospheric environment of the area. The time resolution is one hour and the sources classification is: line, point and area. The output used in this contribution is 2 km x 2 km for use in the numerical photochemical air quality system (ANA). It is also possible to obtain the emission per grid cell per pollutant and per hour. The area sources include emissions from small industries, tertiary, domestic consumption, biogenic emissions and urban/suburban traffic. The line sources include the emissions from the national roads in the area (six and one important secondary road in the South) and the two ring roads in Madrid City (M-30 and M-40). Six types of vehicles and five types of fuel are considered. Particles are also considered, only 15% of them are assumed to be produced by man-made. Mineral dust, 40% of the total particle emission is considered to be produced by mineral dust in a natural way. The rest of the particle emissions are produced by antropogenic and natural secondary sources. Finally, the point emissions consider the emissions of large industries with more than 100 Tm SO_2/year.

The emission model EMIMA considers 14 types of land use which are also used in the mesoscale meteorological model MEMO and the resistance deposition model DEPO included into the ANA system. The land use types are: caduceus forest, perennial forest, mixed forest, olive, garden, bush, vineyard, fruit, pasture ground, rice, dry land, inland water, urban land and suburban land. We have computed the emissions from the road traffic by the following the expression:

$$E = n.r.c.f \qquad (2)$$

where E is the emitted pollutant in g, n is the number of travelling vehicles of each type, each hour, r is the mean distance travelled by vehicle in km, c is the mean consumption by vehicle in l/km and f is the emission factor for each pollutant given in g/l. The value of n is based on yearly averaged data and then distributed equally on each day and corrected with seasonal variation. This number is corrected with a time dependent factor using information from the Traffic Department of Madrid City. We assume that the traffic during weekends and holidays is 65% on respect of the traffic during working days. The following expression is used for calculating the number of vehicles per cell during working days:

$$n = (people\ in\ the\ cell)\ (0.3)\ (fcnv(hour)\ )\ (NumVehi(type,landuse)) \qquad (3)$$

where $fcnv(hour)$ is the factor associated to the traffic normalized density along the day and $NumVehi(type,landuse)$ is a function of the type of vehicle and the landuse (urban or suburban where the cell is classified). The number of vehicles per person is assumed to be 0.3.

Isoprene emissions depend strongly on the light and on the temperature. The effects of these two parameters are critical on the parameterization of the emission factors for isoprene and monoterpene. Increasing temperature from 25°C to 30°C can cause a 70% increase in isoprene emissions and doubling the available photosynthetically active radiation (PAR) can increase isoprene emissions by 100%. The isoprene emission factor is calculated by the following expression:

$$E(T, PAR) = \frac{E_f E_T(T, PAR)}{E_T(30,400)} \qquad (4)$$

where,

$$log_{10}E_T(T,PAR) = \frac{a}{1+e^{-b(T-c)}+d} \qquad (5)$$

E_f is a specified emission rate factor at 30°C and 400 $\mu Em^{-2}s^{-1}$ and it depends on the corresponding vegetation class, $E_T(T,PAR)$ is the isoprene emission rate obtained from Tingey *et al.* (1980)'s curves at the specified conditions, and $E_T(30,400)$ is the isoprene emission rate at 30°C and 400 $\mu Em^{-2}s^{-1}$. The emission rate of α-pinene and the sum of other monoterpenes does not depend on the light (they are emitted during day and night). It is considered to depend only on the temperature. The land use classification is obtained using the information provided by the LANDSAT-5 satellite. The methodology to obtain this information is based on Ormeo *et al.* (1994). This methodology has been compared with hand-made maps and by sensitivity analysis by using the integrated air quality system ANA for land use sensitivity (San José *et al.*, 1995b) with satisfactory results. The advantage of using remote sensing information is high because of the extraordinary man power involved in hand-made land use classification.

The deposition flux is based on the resistance approach. In this simulation, results are shown by using a simple aerodynamic approach. The chemical processes are represented in this model by the CHEMA code. This code is CBM-IV based mechanism (Gery *et al.* 1989) which is composed by 31 active species, 68 kinetic reactions and 11 photoprocesses. This chemical mechanism is based on the species approach. We have included the isoprene reactions which increase the total number of active species up to 34 and the number of reactions up to 72. The system of chemical reactions is solved by using the SMVGEAR method (Jacobson and Turco, 1994). This is a highly accurate method where the diffusion is strongly reduced. The chemical mechanism is solved every 1800 seconds by using small and variable timesteps. The chemical system is solved for the 80x100 km^2 domain centered in Madrid with 2000 m spatial resolution. The vertical system has 25 different layers. Finest layers are those close to the surface. A total of 50000 cells are solved and advected and diffused by the meteorological module. Ozone appear as a secondary product of the system. The total anthropogenic VOC emissions are splitted (in volume units) following the proposal suggested by the Mechanism Comparison Group (EUROTRAC project) (personal communication, F. Kirchner, Oct'95, Fraunhofer Institut, IFU).

2. Madrid Case Study

The domain is quite rough because of the Guadarrama mountains located in the North and Northwest part of the area. This will create a general mountain and anti-mountain winds which are also combined by the Guadarrama and Jarama rivers which will create

208

the valley and anti-valley winds. Katabatic winds are also presented and well simulated by the non-hydrostatic mode of the simulation. Predicted vertical wind soundings have been compared with those obtained in Madrid airport with good results (San José *et al.*, 1995a). Figure 2 shows the topography of the area. Figure 3 shows the wind patterns for 12h00, 36h00, 60h00 and 84h00 for the five day simulation.
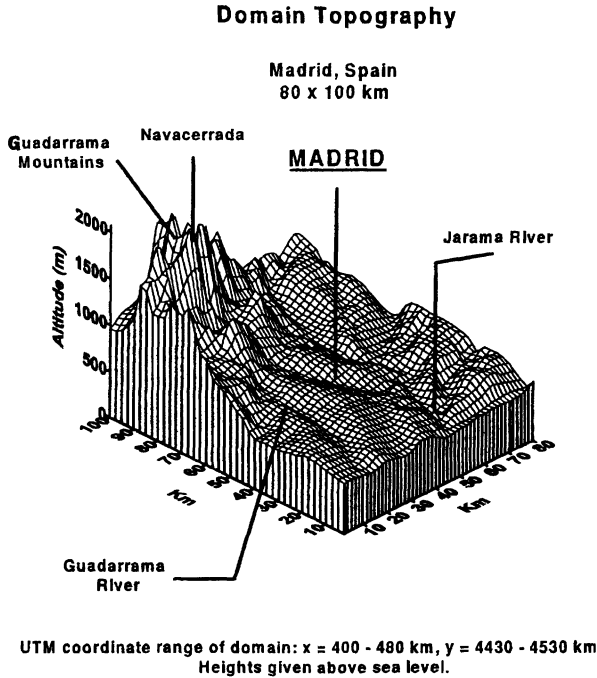
Domain Topography

UTM coordinate range of domain: x = 400 - 480 km, y = 4430 - 4530 km
Heights given above sea level.

Figure 2.- Madrid domain topography.

These patterns show the mountain and valley flows according to the meteorological situation for the June, 5th-9th, 1995. The meteorological conditions are characterized by a local low pressure over the Iberian Peninsula with anticyclonic synoptic conditions for the North and Northwest part of Europe. Pressure values are around 1012 mb for all the week and no significant rain was reported for all the week. Under these conditions, the five days simulation is expected to simulate the meteorological conditions quite well because the wind flows are driven by local topography and diurnal heating cycle.

The meteorological simulation was initialized by using the wind, temperature and humidity vertical soundings at Madrid International Airport located on the Northeast area of the domain. The initial values given for the different species were those obtained by the Madrid Municipality pollution network for the day before (June, 4th, 1995). Two vertical soundings were used (0h00, 12h00, June, 5th, 1995) for running all the 120 hours simulation. The simulation was performed on the Fujitsu vector machine VP-2400 of the Supercomputer Center of Galicia (Spain). The model requires 110 Mb RAM and 4 CPU-hours per simulated day.
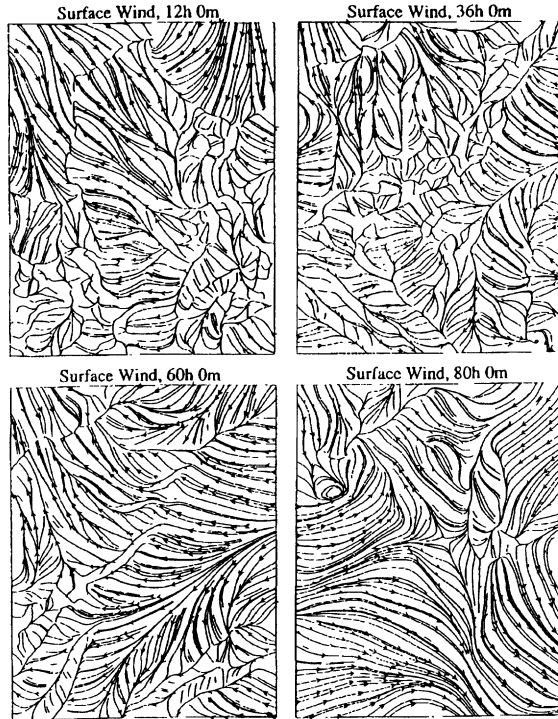
Figure 3.- Simulated wind patterns for the four days case study.

Figure 4 shows the surface ozone patterns for June 6th, 1995 at 0h00, 8h00, 16h00 and 24h00. The 16h00 pattern show the high ozone values outside of the urban area because of the absence of NO_x to consume it. The white spot is located in the Madrid urban metropolitan area. Unfortunately, ozone information in rural areas is not available yet. Some preliminary data taken by mobile stations have confirmed this simulated data. Figure 5 shows the simulated and observed ozone data. The stations are located in the Metropolitan Area. The SREMP station is a station maintained by the authors of this contribution and during June, 8th, 1995 the station was not running because of a failure in the power supply. The Madrid Metropolitan network is calibrated every 20 days and our station was calibrated after the study and the results were into the 3-5 % range.

3. Conclusions

We have presented the comparison between ozone observations in Madrid Metropolitan Area and ozone predictions by using the model ANA which is a complex Air Quality Prognostic and Diagnostic Model. The results are very hopefully however much more observations are required to compare the results and much more simulations are needed. Furthermore, the computer power requirements continue to be a critical demand for these type of studies. The use of new massive parallel computers will become a necessity

in the future. The model has shown the capability to predict the ozone patterns for different locations in a mesoscale area.
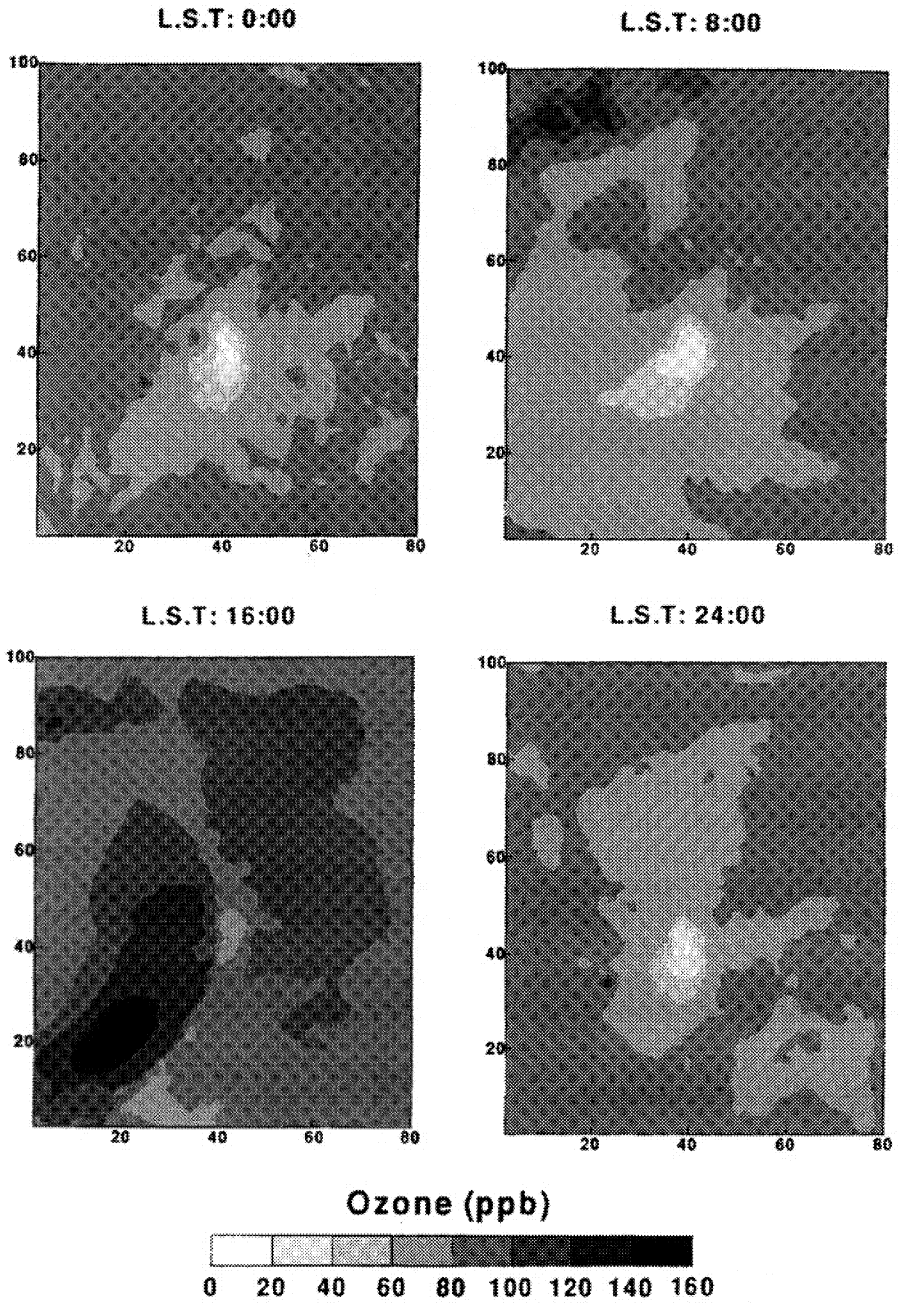

Figure 4.- Simulated surface ozone patterns for June, 6th, 1995

Station 14
Fdez. Ladreda
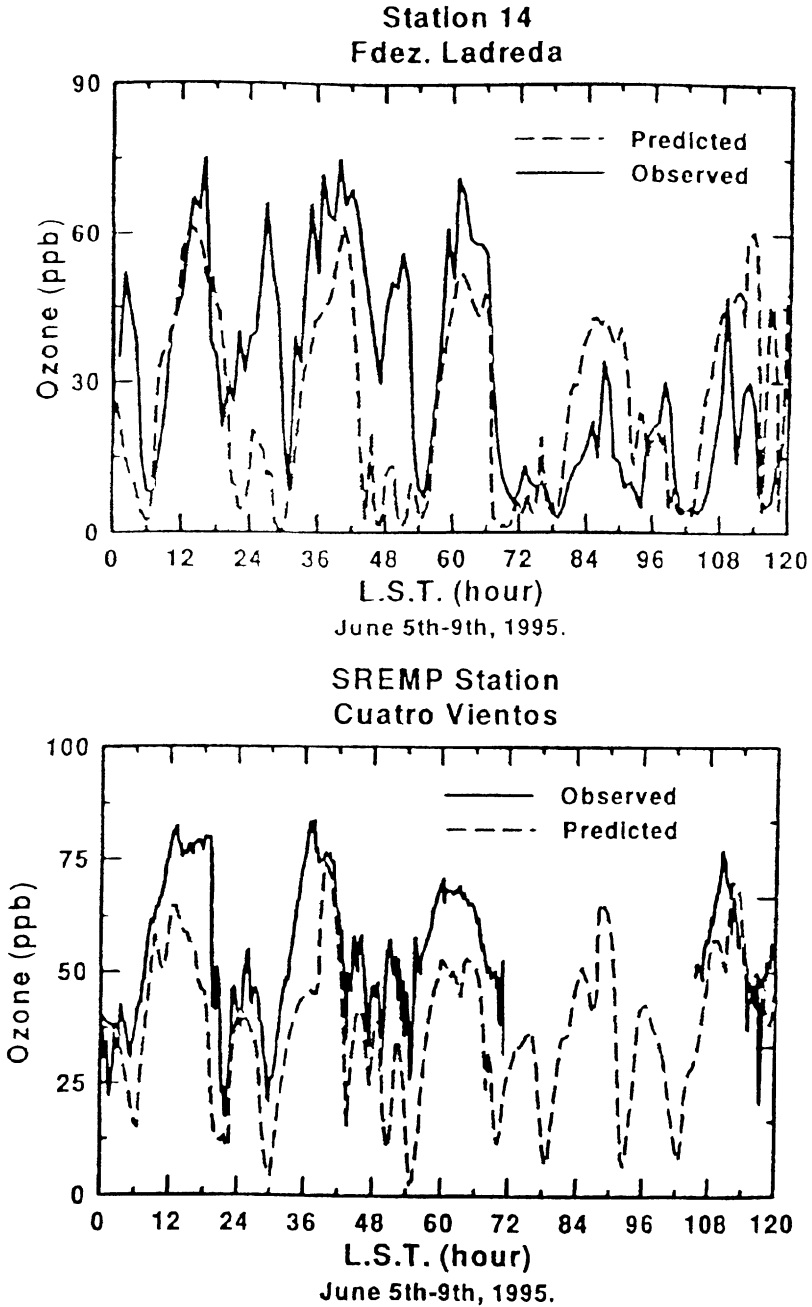

SREMP Station
Cuatro Vientos

Figure 5.- Simulated and observed ozone data for the June, 4-9th, period for two different stations. SREMP station is a station supported by our group.

Acknowledgements

References

Chang J. S., Brost R. A., Isaksen I. S. A., Madronich S., Middleton P., Stockwell W. R. and Walcek C. J. 1987. J. Geophys. Res., **92**, 14681-14700.

Erisman J. W., van Pul A. and Wyers P. 1994. Atmos. Environ., **28**, 2595-2607.

Flassak T. 1990. VDI Verlag, Dusseldorf, pp. 203.

Gery M. W., Whitten G. Z., Killus J. P. and Dodge M. C. 1989. Journal of Geophysical Research, **94**, 12925-12956.

Harten A. 1986. Mathematics of Computation, **46**, 174, 379-399.

Jacobson M. Z. and Turco R. P. 1994. Atmos. Environ., **28**, 273-284.

McRae G. J., Goodin W. R. and Seinfeld J. H. 1982. Atmos. Environ., **16**, 679-696.

Morris R. E. and Myers T. C. 1990. Vol **I**, User's Manual for UAM (CBM-IV), EPA-450/4-90-007 A.

Moussiopoulos N. 1994. in The EUMAC Zooming Model: Model Structure and applications, Ed. N. Moussiopoulos EUROTRAC, International Scientific Secretariat, Garmisch-Partenkirchen, March, 1994, 7-21.

Ormeo S., Madrona H., Castillo M., Hernández J., Delgado M. and San José R. 1994. Computer Techniques in Environmental Studies, Vol II: Environmental Systems, Ed. P. Zannetti, 295-302.

Reynolds S. D., Tesche T. W. and Reid L. E. 1979. SAI Report EF78-53R4-EF79-31.

San José R., Rodríguez L., Moreno J., Sanz M. and Delgado M. 1994. Computer Techniques in Environmental Studies, Vol I: Pollution Modelling. Ed. P. Zannetti, 79-88.

San José R., Sanz M. A., Moreno B., Ramírez-Montesinos A., Hernández J. and Rodríguez L. 1995a. Proceedings EUROPTO Series, Air Pollution and Visibility Measurements, Vol: 2506 Ed. SPIE-The International Society for Optical Engineering, 286-297.

San José R., Marcelo L. M., Moreno B. and Ramírez-Montesinos A. 1995b. 21st NATO/CCMA International Technical Meeting on Air Pollution Modelling and its Applications, Ed. American Meteorological Society, 132-139.

Systems Applications, Inc. 1990, SYSAPP-90/018, San Rafael, CA 94903.

Tingey D. T., Manning M., Grothaus L. C., Burns W. F., 1980. Plant Physiology, **6**, 797-801.

Wesely M.L. 1989. Atmospheric Environment, **23**, 1293-1304.

Yamartino R. J., Scire J. S., Carmichael G. R. and Chang Y. S. 1992. Atmopsheric Environment, **26A(8)**, 1493-1512.

TREATMENT OF URBAN AREAS WITHIN A REGIONAL TRANSPORT MODEL OF SULPHUR AND NITROGEN OXIDES

E. MURPHY-KLIMOVA[1], B. E. A. FISHER[1] and R. SOKHI[2]

[1] *School of Environmental Sciences, University of Greenwich, Deptford Campus, Rachel McMillan Building, Creek Road, London SE8 3BW, UK.* [2] *Department of Environmental Sciences, University of Hertfordshire, Hatfield Campus, College Lane, Hatfield, Hertfordshire AL10 9AB, UK*

Abstract. The air pollution transport model UGEM (The University of Greenwich Evaluation Model) has been developed to evaluate medium-range transport and deposition of sulphur and oxidised nitrogen from all types of sources of emissions in the UK and to estimate their average annual deposition and concentrations across the UK. The model has been tested for its predictions against the available measurements.

This study was focused on a possibility of applying the UGEM model to the assessment of air quality on a local scale. One parameter in the model is crucial, the local deposition fraction. The effect of this parameter on quality of the model predictions has been studied for different scales of UGEM output, such as the whole territory of the UK, a rural region and an urban area.

The results of the study show that the magnitude of the local deposition fraction should be different for each grid square to reach the best agreement of predictions of concentrations with measurements. Applying a local value of the parameter to each grid square will improve the model predictions of the concentrations in urban areas in particular and will not affect the quality of model predictions of the wet deposition.

1. Introduction

Recently passed air quality legislation in the UK (DOE, 1995) requires local authorities to review air quality within their area. The European Union directive on ambient air quality assessment will also require assessment of air quality in urban areas. Both pieces of legislation may require appropriate plans to be produced to improve air quality in a localised area. The assessment will require information to be produced on the amount of pollution imported into quite small areas.

On a European scale much attention has been paid to transboundary pollution between countries. The new legislation will focus attention on crossborder fluxes on a much smaller scale.

Both local emissions and transboundary fluxes coming from other areas contribute to local air quality. So these two factors have to be considered to deal with air pollution problems on a local scale. The first question which a local authority should study is what is the main contributor to air pollution in their area. The management of air quality in an area depends principally on the relative size of the main contributions.

Mathematical modelling is the main method considered for solving this problem. A new model, or a new application of an existing model, is required to evaluate the size of the local contributions and of the transboundary fluxes into small areas. The model should be designed in a way which enables local authorities to understand the contribution of sources outside their area, and to take appropriate action when necessary.

The medium-range air pollution transport model called UGEM has been developed at the University of Greenwich, UK. The possibility of applying the model to assessments of air quality on a local scale are studied. This application will be possible if the model has a good prediction power for each small urban and rural site on a scale of 10 x 10 km^2 or 20 x 20 km^2. This research is focused on one particular parameter of the model, the local deposition fraction. The importance of this parameter for the quality of the model predictions on a local scale is discussed below.

2. Main features of the UGEM model

UGEM is a receptor-orientated, Lagrangian type model, which yields annual average concentrations and depositions of sulphur dioxide (SO$_2$), particulate sulphate (SO$_4$), nitrogen dioxide (NO$_2$), particulate nitrate (NO$_3$) and nitric acid (HNO$_3$) across the UK. UGEM, as a Lagrangian model, provides a method for simulating atmospheric transport and dispersion using air parcels that follow the wind flow. The UGEM model is an approximate solution of the equation (1) for the concentration C^l of pollutant l along air mass trajectories weighted according to wind direction

$$\frac{dC^l}{dt} = -\left(\frac{v_d^l}{h} + k_w^l P + k_c^{m,l} - k_c^{l,m}\right) \times C_0^l \qquad (1)$$

The key parameters of UGEM and their definitions are listed in Table I. All trajectory (Lagrangian) models are version of more less complex solutions of this equation. UGEM employs a constant wind speed and a single wind rose with straight line trajectories. The model time-step is 10 minutes. The boundary layer height is constant at 800 m, but there is a parameter of atmospheric stratification which determines the effective speed of the air parcel in the atmospheric boundary layer. Statistical data of rainfall over the 20 x 20 km^2 grid are used in calculating wet deposition. The model has been described in some detail in Klimova-Murphy and Fisher (1996). The model covers the UK with a 10 x 10 km^2 and/or 20 x 20 km^2 grid for emissions, atmospheric processes and depositions. The time step and grid size may be changed easily in the model. The National Atmospheric Emissions Inventory data of SO$_2$ and nitrogen oxides (NO$_x$) emissions for 1992 for the UK are used as input data of the emissions in UGEM. All sources of emission in each square considered as one effective point source in the centre of that square. Instantaneous mixing through the air parcel is assumed and source height is not taken into consideration since many of the pollutants of interest in urban areas are emitted near ground-level. There is no background element representing sulphur (S) and nitrogen (N) imported into the country from natural or man-made sources. Single dry deposition velocities are assumed, except for SO$_2$ where values are land-use dependent. It is assumed that a fraction α^l of the emission is deposited instantaneously over the grid square from which it is emitted, while the fraction $1-\alpha^l$ is transported along an air mass trajectory, for which the concentration satisfies equation (1). The magnitude of this fraction has been chosen to achieve the best agreement with observations in the UK (see Section 4).

TABLE I

The key parameters of the UGEM model

Symbol	Definition and units	Pollutant	Value
k_w^l	Wet scavenging ratio	SO_2	0.15×10^6
		SO_4	10^6
		NO_2	0
		NO_3	10^6
		HNO_3	1.4×10^6
v_d^l	Dry deposition velocity, mm s^{-1}	SO_2	is given for each 20 x 20 km^2 grid square
		SO_4	1.0
		NO_2	1.0
		NO_3	1.0
		HNO_3	30.0
$k_c^{l,m}$	Chemical conversion rates from pollutant l to pollutant m, s^{-1}	$SO_2 \rightarrow SO_4$	3.2×10^{-6}
		$NO_2 \rightarrow NO_3$	2×10^{-6}
		$NO_2 \rightarrow HNO_3$	1.1×10^{-5}
		$HNO_3 \rightarrow NO_3$	3×10^{-5}
		$NO_3 \rightarrow HNO_3$	1.5×10^{-5}
α^l	Local deposition fraction for each 20 x 20 km^2 grid square	SO_2	0.001
		NO_x	0.01
P	Annual level of precipitation, mm yr.$^{-1}$		is given for each 20 x 20 km^2 grid square
v_0	Average wind speed 10 m above ground, m s^{-1}		7.5
h	Height of the mixing layer, m		800
p_m	Wind - rose in the mixing layer for 12 wind directions (values are given in a clockwise direction starting with the probability of a southerly wind)		0.09, 0.16, 0.15, 0.09, 0.08, 0.08, 0.06, 0.07, 0.07, 0.04, 0.05, 0.06
β^l	Fraction of SO_x emitted directly as SO_4	SO_4	0.05
	Fraction of NO_x emitted as NO_2	NO_2	1.0

Wet removal is represented by a wet scavenging ratio assuming wet removal is equivalent to constant drizzle. For the present application orographic enhancement is not included.

3. Validation of the model

A regression analysis has been used to evaluate the performance of UGEM for predicting spatially distributed concentrations and deposition. It was based on a comparison between measurements and modelling data of the annual average concentrations of SO_2 and NO_2 and wet deposition of S and N in rural areas for 1992. Measurements reported by the Atomic Energy Authority (AEA) National Environmental Technology Centre have been used. Thirty two monitoring sites in rural areas measuring

of S and N in the UK (Review Group on Acid Rain, 1997) have been included in the UGEM validation.

A comparison of UGEM predictions of S and N pollution with measurements has been performed and the results of the regression analysis are grouped together in Table II. Table II shows that the correlation coefficients of calculated and observed data for S concentrations, S wet deposition, N concentrations and N wet deposition all exceed a value of 0.66, which shows that the model has good predictive power for these characteristics with annual averaging. Correlation is perhaps better than expected in a similar model which does not take account of the formation of nitrogen monoxide (NO) to NO_2 in any detail. The model predicts the airborne concentration slightly better than the wet deposition of acid species.

Better correlation of the observed and calculated data for concentrations compared to wet deposition might be due to the following reason. Concentration is the best parameter for evaluating a medium-range transport model of air pollution. The concentrations can show better the pollution over the territory of the UK from indigenous sources of pollution because of the size of the investigated area. Wet deposition usually contains a considerable amount of long-range transported pollutants coming from the outside of the country and hence is less appropriate for modelling on the country-wide or local-range level.

TABLE II

Comparing annual average predictions and measurements using data from 32 monitoring sites in the UK

Characteristic	Units	Regression equation	Regression equation	Correlation coefficient
SO_2 concentrations	$\mu g\ SO_2\ m^{-3}$	$C_2 = 2.1 + 1.2 * C_1$	$C_1 = 0.5 + 0.6 * C_2$	0.87
S wet deposition	$mg\ S\ m^{-2}\ yr.^{-1}$	$C_2 = -140 + 1.5 * C_1$	$C_1 = 469 + 0.3 * C_2$	0.66
NO_2 concentrations	$\mu g\ NO_2\ m^{-3}$	$C_2 = -0.02 + 0.7 * C_1$	$C_2 = 1.8 + 0.97 * C_1$	0.83
N wet deposition	$mg\ N\ m^{-2}\ yr.^{-1}$	$C_2 = 50 + 0.6 * C_1$	$C_2 = 138 + 0.8 * C_1$	0.72

where C_2 = calculated data, and C_1 = observed data.

On the basis of the results and the correlation coefficients, and bearing in mind that these 32 monitoring sites are widely distributed across the country, it may be concluded that UGEM works satisfactorily and can be used to predict S and N concentrations in rural areas of the UK. This analysis shows that the model gives good predictions of the general pattern of S and N pollution over the whole country. To test whether the model is able to give good spatial prediction for quite small regions, a further validation of the model has been considered.

4. Local deposition

A Lagrangian model, of which UGEM is an example, assumes instantaneous mixing of pollutants through the atmosphere. The assumption of instantaneous mixing of emissions

through the air parcel is not realistic and hence leads to the uncertainties in the model predictions. If no correction were made, the model would underestimate near-ground concentrations before complete mixing is achieved, and would underestimate the dry deposition flux. The model would underestimate more significantly in the grid squares with a high emission and this would lead to an underestimate of pollution concentration levels mostly in urban areas.

To compensate, a fraction of the emissions are assumed to dry deposit directly within the emitting grid square in addition to that which is calculated in the normal way, with the remainder available for mixing, transport and further depletion (Norwegian Meteorological Institute, 1995). This fraction is defined by several factors, such as the height of emissions, local topography and local climate, and some urban factors in a particular grid square, such as density and height of buildings. It means that this fraction is expected to be different for each urban grid square.

The fraction of local deposition is an important parameter for Lagrangian type models. On a European scale this parameter had been included for a long time in the EMEP model calculations as constant coefficients for S and N pollutants. The values of 0.15 for S and 0.04 for N are used in EMEP on 150 x 150 km^2 grid (Norwegian Meteorological Institute, 1995). An attempt had been made to calculate this parameter more precisely for SO_2 based on the work of Tuovinen and Kruger (1994). The approach is based on a 'low/high' division of emission sources and an application of different corrections of local depositions for each 150 x 150 km^2 grid square which depend on the height of sources in each particular grid square.

On the UK scale, most of the Lagrangian type models do not include the local deposition correction in their calculation due to the smaller grid size adopted (see for example Metcalfe et al., 1995). In UGEM the fraction of emissions deposited locally in an emission grid square, which also determines local concentrations, has been chosen through experiments with the model to reach the best agreement with observations in the UK for the whole country on a 20 x 20 km^2 grid scale (see Table I). The reason for using smaller values in UGEM in the comparison with EMEP is the much smaller resolution in this model (20 km instead of 150 km).

These values of local deposition fractions gave the best agreement between model predictions and measurements for the whole country. Further research is aimed at looking at this parameter on a local scale.

5. Local sites

Two regions have been chosen for a more detailed analysis of UGEM performance and to look at the importance of the local deposition factor on the model predictions for these regions. One region is situated in Scotland (referred to as the Scottish Region) and the other one is the so-called Thames Gateway Region, east of London. Both of these regions have the same size of 20 x 40 km^2 (see Figure 1).

These regions are very different. The Scottish Region is a rural area with a small amount of diffuse area emissions (source height are below 100 m) and with no point emissions (source height are above 100 m) of NO_x and SO_2. It is also a remote area

away from major sources of N and S emissions. The co-ordinates and the emissions of these regions are presented in Tables III - V.
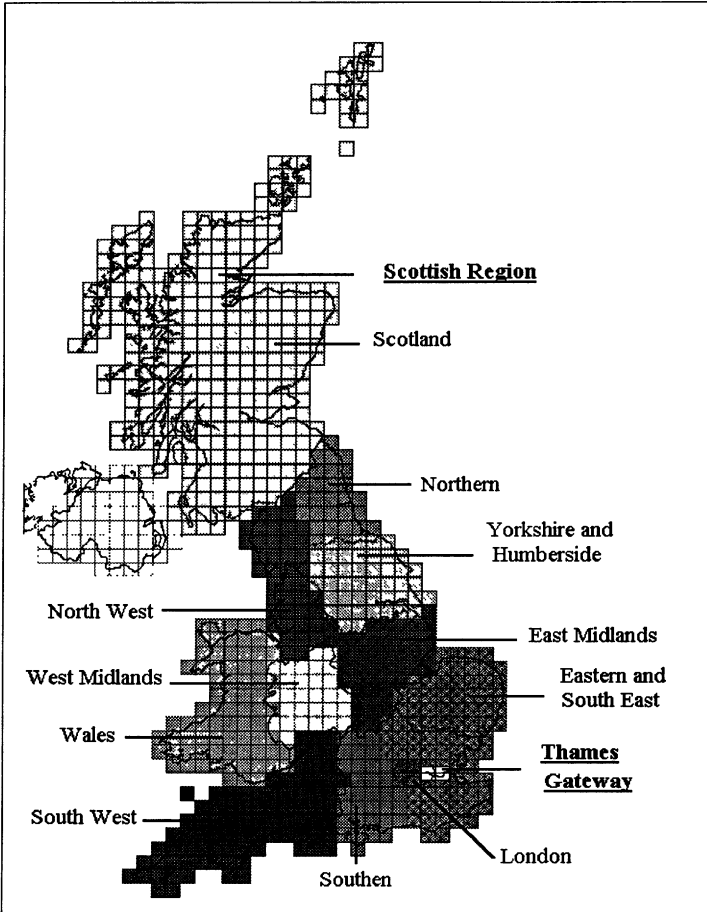

Fig. 1. Regions adopted for the spatial analysis of the UGEM model performance

TABLE III

Area and point sources of the emissions of NO_x in the chosen regions, (emissions as tonnes NO_2 yr^{-1})

Grid square co-ordinate	Scottish Region				Grid square co-ordinate	Thames Gateway			
X =	2200	2300	2400	2500	X =	5400	5500	5600	5700
AREA SOURCES									
Y = 8900	-	2.6	-	105.1	Y = 1800	51541	19501	11370	18965
Y = 8800	4.9	-	-	13.1	Y = 1700	40562	19826	48670	6117
POINT SOURCES									
Y = 8900	-	-	-	-	Y = 1800	-	-	-	22375
Y = 8800	-	-	-	-	Y = 1700	-	56978	61294	-

The Thames Gateway is an urban area, situated to the east of London with significant area and point sources of NO_x and SO_2 both inside (see Tables III - V) and outside of the area. Table V shows that the emissions of SO_2 and NO_x in the Thames Gateway are more than a thousand times higher than the emissions in the Scottish Region.

TABLE IV

Area and point sources of emissions of SO_2 in the chosen regions, (emissions as tonnes SO2 yr.$^{-1}$)

Grid square co-ordinate	Scottish Region				Grid square co-ordinate	Thames Gateway			
X =	2200	2300	2400	2500	X =	5400	5500	5600	5700
AREA SOURCES									
Y = 8900	-	0.6	-	9.2	Y = 1800	10714	2520	10054	8438
Y = 8800	1.2	-	-	3.2	Y = 1700	5874	8730	13376	1120
POINT SOURCES									
Y = 8900	-	-	-	-	Y = 1800	-	-	-	35526
Y = 8800	-	-	-	-	Y = 1700	-	104236	79116	-

TABLE V

Summarised emissions data for the chosen regions

Emissions	NO_2 tonnes NO_2 yr.$^{-1}$	SO_2 tonnes SO_2 yr.$^{-1}$
Emissions from the whole country	2 643 250	3 477 750
Emissions from the Scottish Region	38	7
Emissions from the Thames Gateway	108 730	139 850

6. The model predictions on a local scale

UGEM has been run with different values of the local deposition fraction to investigate the influence of this parameter on the model predictions in both regions. A different grid size for emissions, atmospheric processes and depositions has been used as well. The results are presented in Figures 2 and 3.

Figures 2 and 3 show how the local area mean concentrations, calculated by UGEM, depend on the local deposition fraction. In the model the fraction of emissions deposited locally in the 20 x 20 km^2 grid squares have been chosen through trials with the model to obtain the best agreement with observations in the UK over the whole country (see Table II). The fractions of local deposition were chosen combined to equal 0.01 for NO_2 and 0.001 for SO_2 for all emissions (area and point).

Figures 2 and 3 show that the local deposition fraction has no effect on the Scottish Region for neither NO_2 and SO_2 local concentrations. The predicted NO_2 concentration for the Scottish Region is 1.43 μg NO_2 m^{-3} and the measured concentration is 1.46 μg NO_2 m^{-3} (Review Group on Acid Rain, 1997). The predicted SO_2 concentration for the Scottish Region is 1.6 μg SO_2 m^{-3} and the measured concentration is 0.8 μg SO_2 m^{-3} (Review Group on Acid Rain, 1997).

220

The local deposition fraction has a significant effect on the model predictions in urban areas such as the Thames Gateway (see Figures 2 and 3). If no local deposition fraction is used, the model underprediction of NO_2 concentrations for the Thames Gateway is obvious for both 10 x 10 km^2 and 20 x 20 km^2 grids. For SO_2 concentrations a very low local deposition fraction can be used for a 20 x 20 km^2 grid and is zero for a 10 x 10 km^2 grid (see Figure 3).
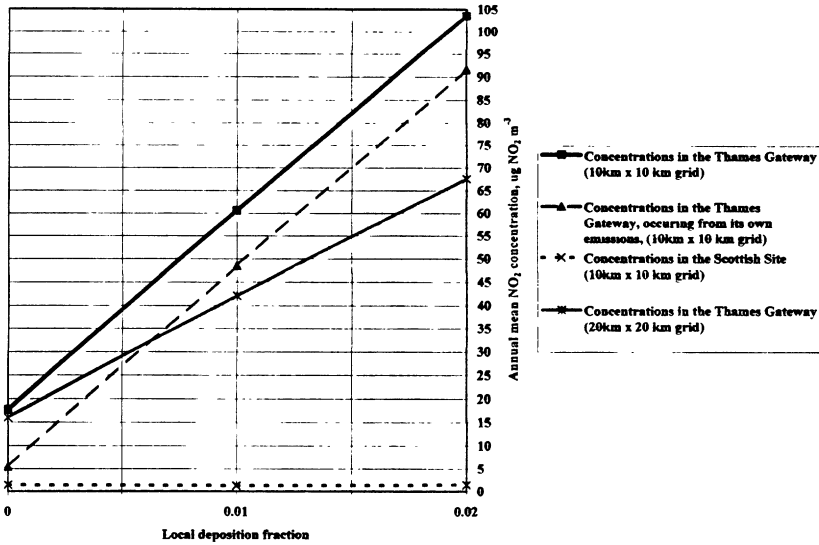

Fig. 2. Local average annual NO_2 concentrations ($\mu g\ NO_2\ m^{-3}$) for different values of the local deposition fraction
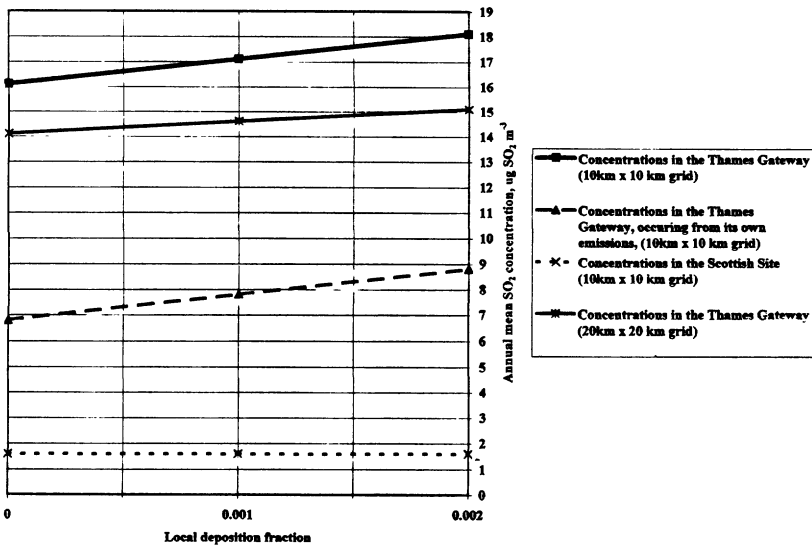
Fig. 3. Local average annual SO_2 concentrations ($\mu g\ SO_2\ m^{-3}$) for different values of the local deposition fraction

Figure 2 shows that using the local deposition fraction equal to 0.01 for NO_2 gives a predictions of 42 µg NO_2 m^{-3} in the Thames Gateway for a 20 x 20 km^2 grid. The Thames Gateway measured NO_2 concentrations in 1993 are about 40-50 µg NO_2 m^{-3} (Bower et al., 1995). To produce the same predictions in UGEM using a 10 x 10 km^2 grid a value of 0.0056 for local deposition fraction should be used. This difference shows the importance of different grid sizes. Emissions outside the region give a contribution of about 12 µg NO_2 m^{-3} to the NO_2 concentrations in the Thames Gateway. This contribution decreases very slowly with an increase in the fraction of local deposition used.

Figure 3 shows that using a local deposition fraction equal to 0.0018 for SO_2 gives a prediction of 15 µg SO_2 m^{-3} in the Thames Gateway for a 20 x 20 km^2 grid. The model predicts concentrations of 16.1 µg SO_2 m^{-3} in the Thames Gateway on a 10 x 10 km^2 grid if a local deposition fraction sets up to zero. Measured SO_2 concentrations in the Thames Gateway in 1993 are about 15 µg SO_2 m^{-3} (Bower et al., 1995). Figure 3 shows that the emissions outside the region give a contribution of about 9.4 µg SO_2 m^{-3} to the SO_2 concentrations in the Thames Gateway. Figures 2 and 3 show the dependence of the local mean values of NO_2 and SO_2 concentrations on the chosen values of the local deposition fraction.

7. Local deposition fractions inside the local area

In the previous Section we looked at the relationships between the local deposition fraction and the model predictions of the local mean concentrations. It is interesting to understand how the model will predict the concentrations inside the local area.

TABLE VI

Ambient annual average NO_2 concentrations in 1991 in the Thames Gateway
(Each grid square has been labelled using the number in brackets)

Grid square co-ordinate	Ambient annual average NO_2 concentrations (µg NO_2 m^{-3}) in the Thames Gateway			
X =	5400	5500	5600	5700
Y = 1800	66.9 (I)	60.8 (II)	46.3 (III)	50.6 (IV)
Y = 1700	62.7 (V)	55.0 (VI)	48.7 (VII)	42.3 (VIII)

Figure 4 shows the Thames Gateway area and average annual NO_2 concentrations on a 5 x 5 km^2 grid (HMIP, 1993). Table VI contains the measured data of NO_2 concentrations in the Thames Gateway (HMIP, 1993), which have been recalculated as average annual concentrations for a 10 x 10 km^2 grid. These data have been used in the comparison with the model predictions. Figure 5 shows a scatter plot of the predicted NO_2 concentrations for each 10 x 10 km^2 grid in the Thames Gateway and the local deposition fraction. The local deposition fractions which give the best agreement with the measurements in each grid are summarised in Table VII.
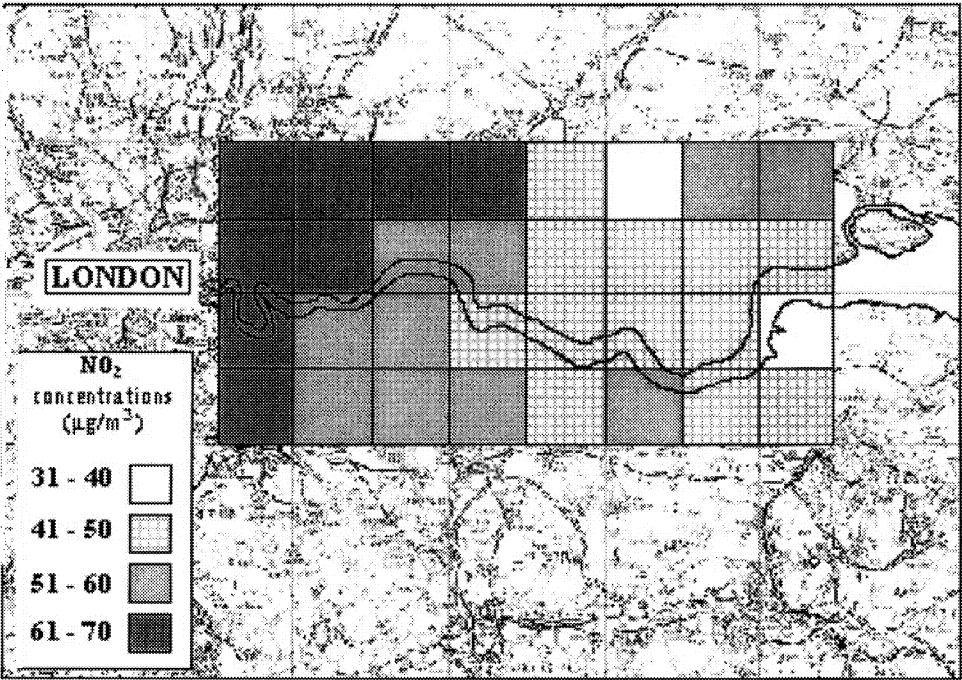
Fig. 4. Ambient average annual NO₂ concentrations (μg NO₂ m⁻³) in the Thames Gateway in 1991 (HMIP, 1993)

Table VII shows that the local deposition fractions differ significantly from grid square to grid square. Some of the grid squares from Table VII include just area sources and some of them include area plus point sources.

TABLE VII

Local deposition fractions which give the best agreement of the model predictions with the measurements

Grid square co-ordinate	Local deposition fractions for each grid square in the Thames Gateway			
X =	5400	5500	5600	5700
Y = 1800	0.009	0.022	0.025	0.008
Y = 1700	0.012	0.005	0.003	0.045

The height of the sources of emission in a grid square has the major influence on the magnitude of the local deposition fraction in the grid square (Norwegian Meteorological Institute, 1995). The contribution from the high sources (point sources) to the concentrations in the grid square will decrease with a decrease of the grid square

size. On the other hand, low-level sources of emissions (area sources) will contribute significantly to the concentrations in a 10 x 10 km² grid square.
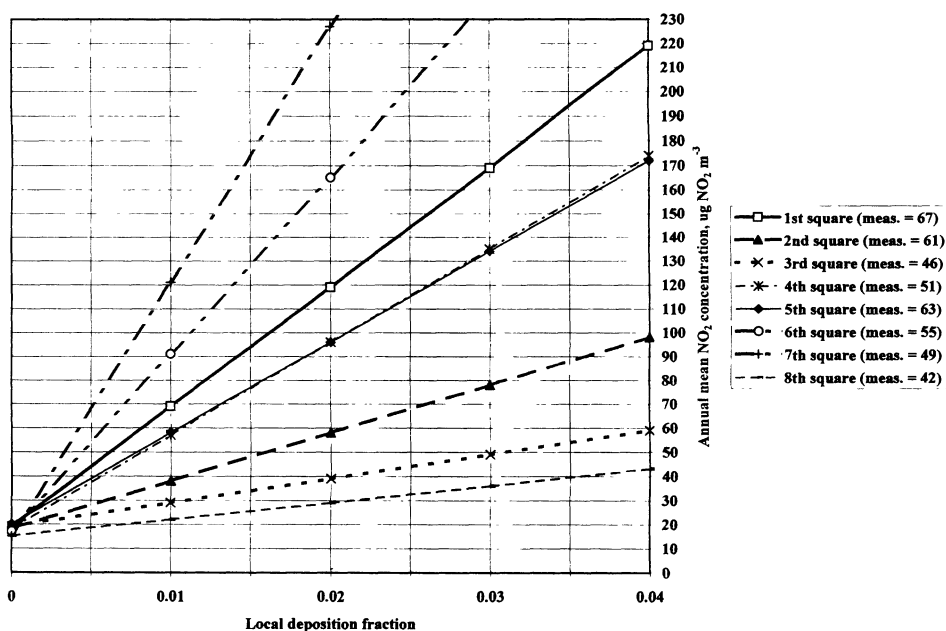

Fig. 5. Average annual NO₂ concentrations (μg NO₂ m⁻³) for each 10 x 10 km² grid square in the Thames Gateway

TABLE VIII

Local deposition fractions for area sources only, which give the best agreement of the model predictions with the measurements

Grid square co-ordinate	Local deposition fractions for each grid square in the Thames Gateway			
X =	5400	5500	5600	5700
Y = 1800	0.009	0.022	0.025	0.017
Y = 1700	0.012	0.019	0.007	0.045

Table VIII shows the local deposition fractions which give the best agreement of the model predictions with the measured ambient annual average NO₂ concentrations in the Thames Gateway if only area sources are taken into account.

224

Table VIII demonstrates that if only the area sources are considered, the local deposition fractions remain different for each grid. This is an important result which shows the local deposition fraction is defined by the emissions distribution, the height of the emission sources in a particular grid square, local topography and local climate, and some urban features of the grid square, such as density and height of buildings. It means that this fraction is unique for each grid square, which contains substantial urban areas.

8. Conclusions

(1) An assumption of instantaneous mixing of emissions through the boundary layer is not realistic feature of regional transport models and leads to uncertainties in the model predictions of airborne concentrations.

(2) The results of this study confirm that the local deposition fraction is an important parameter in the single-layer Lagrangian models. If the local deposition fraction is not included, the model will underestimate concentrations in urban areas.

(3) The local deposition fraction is defined by a variety of factors, such as the emission distribution, the height of the emission sources in the grid square, local topography and local climate, and some urban factors in a grid square, such as density and height of buildings.

(4) The value of the local deposition fraction is different for each grid square.

(5) An application of an optimised value of the local deposition fraction for each grid square in UGEM will improve the model predictions of concentrations in urban areas, but will not affect the model predictions of wet deposition. In principle a local dispersion model should be applied to each grid square but this involves considerable extra complexity. It is hoped that by a careful choice of the local deposition fraction, adequate predictions from regional models can be obtained without the need for excessive complexity.

References

Bower J. S., Broughton G. F. J., Willis P. G. and Clark H.: 1995, *Air Pollution in the UK: 1993/94 AEA Technology, National Environmental Technology Centre.*

Department of the Environment: 1995, *Air Quality Meeting the Challenge.*

The Norwegian Meteorological Institute: 1995, *European Transboundary Acidifying Air Pollution: Ten years calculated fields and budgets to the end of the first Sulphur Protocol,* Research Report no. 17, EMEP MSC-W, Oslo.

HMIP: 1993, *An assessment of the effects of industrial releases of nitrogen oxides in the East Thames Corridor,* HMSO, London.

Klimova-Murphy E. and Fisher B. E. A.: 1996, *Application of a long-range transport model for the assessment of air quality on a local scale,* Proceedings of the 4th Workshop on Harmonisation within Atmospheric Dispersion Modelling for Regulatory Purposes, VITO, May 1996, Belgium.

Metcalfe S. E., Whyatt J. D. and Derwent R. G.: 1995, *Q. J. R. Meteorol. Soc.,* **121**, pp. 1387-1411.

Review Group on Acid Rain: 1997, to be published.

Tuovinen J.-P. and Kruger O.: 1994, *Re-evaluation of the local deposition correction in the Lagrangian EMEP model,* EMEP/ MSC - W, Note 4/ 94, Norwegian Meteorological Institute, Oslo.

MULTI-SCALE ATMOSPHERIC DISPERSION MODELLING BY USE OF ADAPTIVE GRIDDING TECHNIQUES

G. HART*, A. TOMLIN*, J. SMITH✧, M. BERZINS✦

Department of Fuel and Energy, School of Computer Studies* and School of Chemistry✧*
University of Leeds, Leeds LS2 9JT, UK

Abstract

An accurate prediction of the transport-reaction behaviour of atmospheric chemical species is required to fully understand the impact on the environment of pollution emissions. Elevated levels of secondary pollutants such as ozone in the lower atmosphere can be harmful to the health of both plants and animals, and can cause damage to property present in the urban environment. Detailed models of pollution mechanisms must therefore be developed through comparisons with field measurements to aid the selection of effective abatement policies Such models must satisfy accuracy requirements both in terms of the number of species represented, and the spatial resolution of species profiles. Computational expense often compels current models to sacrifice detail in one of these areas. This paper attempts to address the latter point by presenting an atmospheric transport-reaction modelling strategy based upon a finite volume discretisation of the atmospheric dispersion equation. The source terms within this equation are provided by an appropriate reduced chemical scheme modelling the major species in the boundary layer. Reaction and transport discretisations are solved efficiently via a splitting technique applied at the level of the non-linear equations The solution grid is generated using time dependant adaptive techniques, which provide a finer grid around regions of high spatial error in order to adequately resolve species concentration profiles. The techniques discussed are applied in two dimensions employing emissions from both point and area sources. Preliminary results show that the application of adaptive gridding techniques to atmospheric dynamics modelling can provide more accurately resolved species concentration profiles, accompanied by a reduced CPU time invested in solution Such a model will provide the basis for high resolution studies of the multiple scale interactions between spatially inhomogeneous source patterns in urban and regional environments.

1 Introduction

The prediction of primary and secondary pollution generation and transport is required in order to fully understand the impact upon the environment of a range of source types. Elevated levels of ozone in the lower atmosphere can be harmful to animal and plant life and can cause extensive damage to property. Detailed models of pollution mechanisms must therefore be developed to aid effective abatement policies thus ensuring compliance with national and international environmental legislation. The complex interaction of pollutants with atmospheric species, together with the additional effects of meteorological phenomena can cause species production, destruction and dispersion to take place at a long range from the pollutant source. On the other hand the pollution source itself may be of a very small scale, such as a power station plume. This presence of multi-scale behaviour in the atmosphere requires detailed computational grids, in order to resolve concentration profiles over the whole range of dispersion. Comparisons can then be made with field measurements and used in model validation. Such comparisons are useful as they inevitably promote a better understanding of the behaviour of pollutants when released into the atmosphere.

Early Eulerian models of the 1970's only utilised sparse uniform grids over which to solve the atmospheric diffusion equations. Resolution has been improved in second generation (Peters 1995) models due to increases in computer power and memory, and

the application of selectively refined regions of grid points. Regions of high concentration gradient are predicted a-priori and grid points concentrated accordingly, nesting regions of high density grid within the overall domain. These have generally been concentrated in regions of high emissions. However, the complex nature of pollutant species interaction with prevailing meteorological conditions can cause high concentration gradients at a long range from the pollutant source. This makes the use of nested gridding methods more difficult and less effective. There is therefore a need for the application of methods which can refine the grid according to where the solution requires it i.e. time dependent grid adaptive algorithms. There have recently been some applications of adaptive grids for environmental modelling, e.g. Skamarock *et al.* (1989), although as yet these methods have not been implemented in standard air quality models. The present work describes how adaptive gridding techniques, which automatically refine the mesh in regions of potentially high spatial error, can improve on the telescopic or nested approach. The aim of this work is to show that the use of such techniques will lead to a better understanding of the complex multi-scale phenomena that arise from regional scale models.

We have not attempted to develop a comprehensive regional model, but rather to apply a set of numerical modelling tools to a particular test case in order to demonstrate their advantage over traditional techniques. We therefore investigate the solution of the atmospheric transport-reaction problem described by an Eulerian formulation of the atmospheric dispersion equation and a reduced chemical reaction scheme. This problem is solved using a finite volume method over an unstructured grid generated using adaptive techniques. Solution methods presented specifically concentrate upon the release of NO and NO_2 and the subsequent reaction of this effluent with existing atmospheric species to generate secondary pollutants such as ozone.

The paper is structured as follows. In sections 2.1 - 2.3 we briefly introduce the equations which describe the atmospheric transport and reaction problem and the test case over which these equations are solved. Section 2.4 introduces the numerical scheme used to solve these equations. Section 2.5 provides details of the adaptive gridding technique and the criteria for mesh refinement is briefly described. Section 3 presents a comparison of results of the test case using both constant density and adaptive gridding techniques. Finally in sections 4 and 5 we present a discussion and conclusions about the use of adaptive methods in air pollution models.

2 Code Structure

2.1 TRANSPORT-REACTION EQUATION

The 2D transport-reaction behaviour of atmospheric species is modelled by solving the atmospheric diffusion equation for each species ,
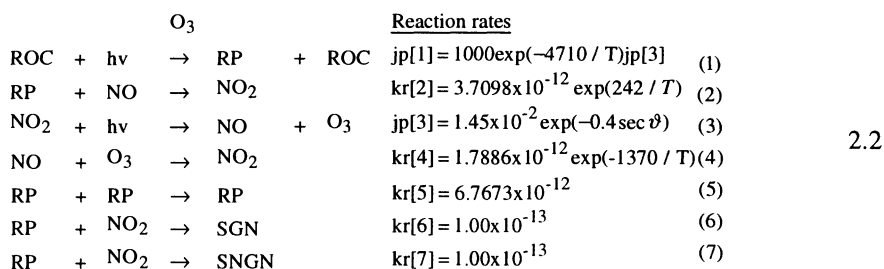
$$\frac{\partial c_s}{\partial t} = -\frac{\partial u c_s}{\partial x} - \frac{\partial w c_s}{\partial y} + \frac{\partial}{\partial x}\left(K_x \frac{\partial c_s}{\partial x}\right) + \frac{\partial}{\partial y}\left(K_y \frac{\partial c_s}{\partial y}\right) + R_s(c_1, c_2, ..., c_n) + E_s - (k_{1s} + k_{2s})c_s \qquad 2.1$$

where:
c_s = the concentration of the s'th compound.
u, w = wind velocities.
K_x, K_y = diffusivity coefficients.
k_{1s}, k_{2s} = dry and wet deposition velocities.
E_s = distribution of emission sources for s'th compound
R_s = source due to chemical reaction .

The above transport-reaction model is solved for n chemical species. This generates an n dimensional set of partial differential equations, each coupled through the non-linear chemical reaction terms.

2.2 CHEMICAL SCHEME

The initial chemical reaction scheme used for code development was introduced by Azzi *et al* (1992). The mechanism, shown in equation 2.2, contains only 7 species and therefore enables fast turn around time in terms of developing the numerical code. Despite its simplicity it represents the main features of a tropospheric mechanism, namely the competition of the fast equilibrating inorganic reactions 3) and 4) with the chemistry of volatile organic compounds, which occur on a much slower time-scale. This separation in time scales generates stiffness in the resulting equations so that sophisticated ordinary differential equation (ode) solvers must be used to solve such schemes. The voc reactions are represented by reactions of a single lumped species, ROC. This is unrealistic in terms of the actual emissions generated in the environment, but the investigation of fully speciated vocs is not the purpose of the present study.

<div>

			O_3			Reaction rates	
ROC	+	hv	→	RP	+ ROC	$jp[1] = 1000\exp(-4710/T)jp[3]$	(1)
RP	+	NO	→	NO_2		$kr[2] = 3.7098 \times 10^{-12}\exp(242/T)$	(2)
NO_2	+	hv	→	NO	+ O_3	$jp[3] = 1.45 \times 10^{-2}\exp(-0.4\sec \vartheta)$	(3)
NO	+	O_3	→	NO_2		$kr[4] = 1.7886 \times 10^{-12}\exp(-1370/T)$	(4)
RP	+	RP	→	RP		$kr[5] = 6.7673 \times 10^{-12}$	(5)
RP	+	NO_2	→	SGN		$kr[6] = 1.00 \times 10^{-13}$	(6)
RP	+	NO_2	→	SNGN		$kr[7] = 1.00 \times 10^{-13}$	(7)

</div>

2.2

where:
ROC = Reactive Organic Compounds.
RP = Radical Pool.
SGN = Stable Gaseous Nitrogen Products.
SNGN = Stable Non-gaseous Nitrogen Products.
$jp[n]$ = Photolosis rates parameterised as a function of solar zenith angle, θ.
$kr[n]$ = Reaction rate.
T = Temperature.

The rate constants have been chosen to be in agreement with those used by Derwent *et al.* (1990). The solar zenith angle θ is calculated as a function of the time of day, the time of year and the latitude. Temperature dependant rate constants are represented by a

standard Arrhenius expression, the temperature calculated as a parameterised function of time of day.

Background atmospheric sources are obtained from the Department of the Environment national atmospheric emissions inventory (Goodwin 1993). This provides NOx and ROC emissions inventories, measured over a 10km x 10km grid, across the UK. These emissions are included as source terms at each computational grid position by interpolating from the 10km x 10km mesh onto the current solution grid. Point sources are represented separately and are averaged over the grid cell in which they are contained. We assume a constant emission ratio of 90% NO and 10% NO_2 for all NOx sources.

An additional sink is included in the form of species dry deposition. Deposition sinks are included at present as a simple parameterised function derived from deposition velocities and the changing height of the boundary layer. Deposition velocities are assumed to be constant across the whole domain.

2.3 DOMAIN AND TEST CASE CONFIGURATION.

A power plant plume or urban plume is a highly concentrated source of NOx emissions which can be carried through the atmosphere for hundreds of kilometres, and so provides a stringent test of whether adaptive gridding methods can lead to more reliable results for complex multi scale models. Since power stations and urban transport provide some of the highest emission sources for NOx it is important to be able to generate an accurate understanding of their impact on not only the total NOx budget, but on the generation of secondary pollutants such as ozone. To achieve this we must consider the interaction of plumes with their surroundings

The model is currently applied over a 2-dimensional domain. This is a necessary simplification while the technique is developed and validated, allowing many of the numerical issues to be resolved before expansion to a more complex, but realistic, 3D case. The domain covers a 500km x 500km region stretching from the English midlands up to the Scottish highlands.

Meteorological data has been kept simple and constant in order to easily identify plumes and to optimise refinement procedures. At present the wind is considered to blow directly from the South at a constant speed of 5m/s. Diffusion only takes place perpendicular to this, the diffusion parameter being set to $50m^2s^{-1}$. Consequently no flow is permitted across the East and West boundaries, Neumann boundary conditions are applied to the North edge of the domain and Dirichlet along the South. At present the concentration at the Southern edge is assumed to be a constant background value, again for simplicity although somewhat unrealistic. In this test case we wish to demonstrate the differences between constant density, telescopic and fully adaptive meshes. We have therefore chosen to refine the initial base mesh around 3 power stations in Northern England to demonstrate the telescopic approach of refining around high emission areas. This can be

seen in Figure 2a. The other point sources are interpolated onto the standard background mesh i.e. constant density for two simple cases and a refined mesh for the adaptive case. For this test case the model is run over a two day period to identify diurnal variations in species concentration and is primarily used to develop an understanding of how NOx and ROC react within the atmosphere to form secondary pollutants such as ozone.

2.4 NUMERICAL DISCRETISATION

The atmospheric diffusion equation described by 2.1 is solved using the flux limited, cell centred finite volume discretisation scheme of Berzins and Ware (1996, 1995). The basis of this finite volume scheme is the space discretisation of the partial differential equation (pde) 2.1 which is reduced from a pde in three independent variables into a system of odes in the single independent variable of time. This is achieved by the integration of 2.1 over each finite volume, use of the divergence theorem and the evaluation of the line integral along the boundary of each volume using the midpoint quadrature rule.

This 'method of lines' approach with the above spatial discretisation scheme results in a system of odes in time which are integrated using the SPRINT2D software tool developed by Berzins and Ware (1996). The SPRINT2D software tool contains a number of solution techniques available for use. For much of the present study the Theta solution method has been utilised, with functional iteration used to solve the resulting system of equations. The Theta option is specifically designed for the moderate accuracy solution of stiff systems with automatic control of the local error in time. The large ode systems which result from the discretisation of flow problems with complex chemistry can result in excessive c.p.u processing times. An approach used here which overcomes this is to use a form of operator splitting based on a decomposition of the pdes into a set of flow terms and a source reactive term (Berzins and Ware, 1996).

2.5 ADAPTIVE GRIDDING

The domain is represented by an unstructured mesh of triangular elements surrounding each grid point, thus forming a small volume over which the solution is averaged. The use of an unstructured triangular mesh more easily enables adequate resolution of the complex solution structures found within multi-scale dispersion modelling. This is especially relevant for cases where we wish to represent point source and urban plumes within a large scale background. The term unstructured represents the fact that each node in the mesh may be surrounded by any number of triangles, whereas in a structured mesh this number would be fixed. The initial unstructured meshes used in SPRINT2D are created from a geometry description using the Geompack (Joe 1991) mesh generator.

The complex nature of the atmospheric dispersion problem makes prespecification of grid density a problem as many complex reactions can take pace at some distance from the pollution source. To this end the dispersion code presented here utilises adaptive gridding techniques to quantitatively evaluate the accuracy of the solution and then automatically refine or derefine the mesh where necessary. This is achieved using a tree-like data structure with a method of refinement based on the regular subdivision of

triangles. Here an original triangle is split into four similar triangles (Figure 1) by connecting the midpoints of the edges. Hanging nodes are removed by joining with nearby vertices to produce the completed refinement. This finer grid may later be coalesced into the parent triangle to coarsen the mesh. This process is called local h-refinement, since the nodes of the original mesh do not move and we are simply subdividing the original elements.

Figure 1: Triangle refinement procedure

original mesh   refine   remove hanging nodes
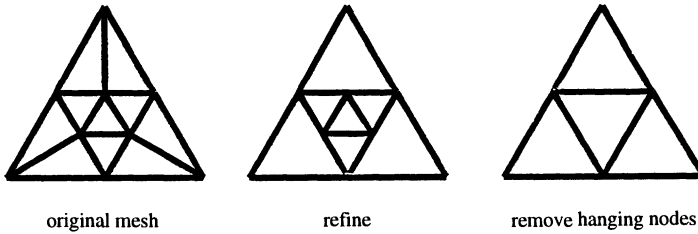
Once a method of refinement and derefinement has been implemented it remains to decide on a suitable criterion for the application of the adaptivity. The ideal solution would be that the decision to refine or derefine would be made on a fully automatic basis. In practice a combination of an automatic technique and some knowledge of the physical properties of the system is used. The technique used in this work is based on the calculation of spatial error estimates. This is achieved by first calculating some measure of error in each species concentration over each triangle. A reliable method for achieving this is to examine the difference between the solution gained using a high accuracy method and that gained using a method of lower accuracy. Clearly over regions of high spatial gradient the difference between high and low order solutions will be greater than over regions of relatively smooth solution and therefore refinement generally occurs in these regions. A refinement indicator for the jth triangle is defined by an average scaled error measured over all *npde* pdes using supplied absolute and relative tolerance:

$$serr_j = \sum_{i=1}^{npde} \frac{e_{i,j}(t)}{\frac{atol_i}{A_j} + rtol_i \times c_{i,j}}$$ 2.3

where: $serr_i$ = average scaled error.
        npde   = number of pdes.
        $e_{i,j}(t)$ = local error estimate of species i over element j.
        $atol_i$ = absolute tolerance applied to species i.
        $rtol_i$ = relative tolerance applied to species i.
        $c_{i,j}$ = concentration of species i over triangle j.
        A_j = area of jth triangle.

This formulation for the scaled error provides a flexible way to weight the refinement towards any species error, and for the user to control the extent of refinement by providing tighter or looser tolerances. An integer refinement level indicator is calculated from this scaled error to give the number of times the triangle should be refined or derefined. Since the error estimate is applied at the end of a time step it is too late to

make refinement decisions. Methods are therefore used for the prediction of the growth of the spatial error using linear quadratic interpolants. The spatial error estimate can also be used to indicate when the solution is being solved too accurately and can indicate which regions can be coarsened.
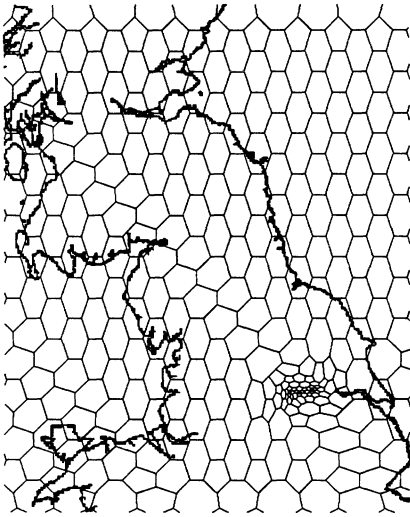

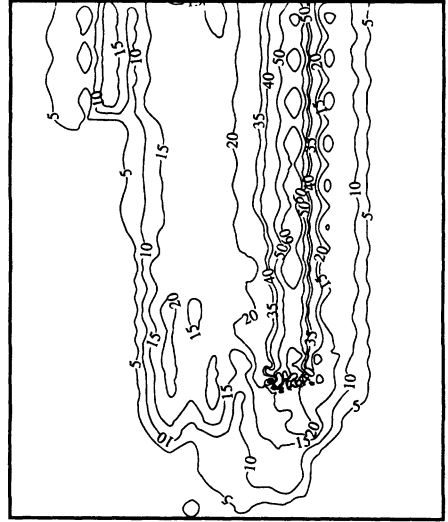Figure 2a: Level 0 constant density dual mesh.　　　　Figure 2b: Level 0 const. density solution.

3.0 Results

To demonstrate the application of adaptive gridding techniques to the reaction-dispersion problem, three different scenarios are presented, and the subsequent effects upon solution accuracy, run time and storage requirements discussed.

The first two solutions presented demonstrate the performance of constant density gridding techniques at low and high grid resolution. The first solution is solved over a coarse constant density grid without refinement, i.e. level 0 except for the telescopically refined area which is refined to level 4 (Figure 2a). The second solution presented is solved over a more refined grid with a density of level 2 over the whole domain (Figure 3a). The third solution presented used adaptive gridding techniques to refined from a constant density level 0 grid, adapting where necessary up to level 2 (Figure 4a). The adaptive gridding technique is configured to adapt around steep spatial NO gradients and thus track and envelop the NOx plumes as they advect Northwards. In Figures 2a, 3a and 4a the vertices of each polygon represent the centre of a triangle on the computational mesh.

3.1 SPATIAL SPECIES DISTRIBUTION

Figure 2b presents the NO solution generated over the level 0, constant density grid. This snapshot of the spatial NO distribution is taken at 12:00 noon on day 2 of the simulation. Contour levels display NO concentrations in parts per billion (ppb). Several plumes can

Figure 3a: Level 2 constant density dual mesh.
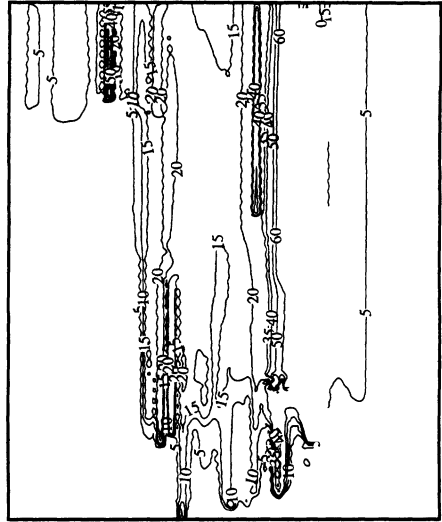
Figure 3b: Level 2 constant density solution.
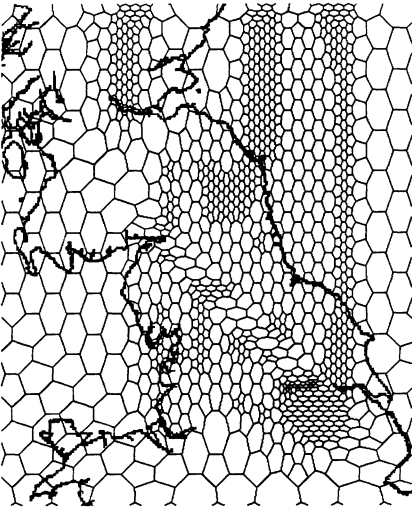
Figure 4a: Adaptive dual mesh.
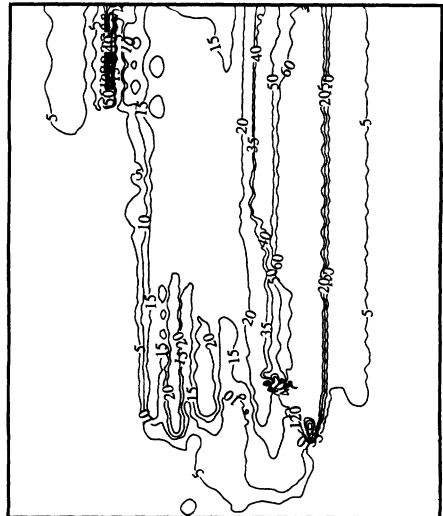
Figure 4b: Adaptive solution.

clearly be identified advecting northwards from high emission sources in urban areas. The most prominent plumes originate from the region around the Yorkshire power stations which was telescopically refined. Figure 3b presents the NO solution at the same instant in time but solved over the much finer level 2 constant density grid. This solution is clearly much less dispersive than the level 0 solution, the plume widths are smaller and much higher NO concentrations are found in the plume cores. The finer grid reduces the artificial spreading of the plumes. This effect is especially marked for plumes originating from sources which were not telescopically refined on the base mesh. The level 2 output is therefore considered to represent a more accurate solution to the scenario described due to the use of a higher resolution grid. However, as the level 2 solution has sixteen times as many more grid points demanding solution, this configuration takes considerably longer to solve. In addition, if the time dependant solution at every grid point is to be saved, much more storage space is required. So, improved performance in terms of solution resolution and accuracy clearly results in greatly increased computational expense.

Figure 4b represents the case where the grid is generated using adaptive techniques. At the start of the simulation the initial mesh is constant density level 0. The code then refines the grid around regions of high spatial error in NO concentration up to a level 2 density. Again, the gross features of the plumes are represented. The effect of using adaptive methods on solution accuracy is perhaps most prominent around the main plume where refinement has occurred around the plume edge (Figure 4a). This has the effect of reducing the artificial dispersion of species via the solution averaging process. The solution achieved using the adaptive gridding process therefore more closely follows that generated by the level 2 constant density grid. If the smaller plumes are examined we see that the level of definition obtained is higher than that achieved by the level 0 grid. The loss of definition obscuring these smaller plumes found in the coarse grid does not arise to such an extent in the adaptive case. Examination of 2D solution profiles alone suggests that a level of accuracy near that of the high resolution constant density grid can be obtained by an adaptive grid using far fewer grid cells. This results in reduced run time and storage requirements.

3.2 CROSS PLUME PROFILES

If a slice is taken through the 2D domain a 1D profile of the solution can be extracted. This profile is useful because it provides a more clear representation of local concentrations. Figures 5 a and b present the cross plume profiles for the three solution strategies obtained by taking a slice across the domain in a West to East direction, 230 km downwind of the 3 main pollution sources. Profiles generated are viewed from a Northerly direction, effectively reversing East and West on the x-axes.

In Figure 5a the level 2 constant density solution is represented by the dashed line and is compared to the level 0 constant density solution. The high resolution solution resolves the high, narrow NO peaks, the main plume represented by the highest peak just East of centre. The level 0 solution can clearly be seen attempting to follow the high resolution

profile but falls short of the main plume peak concentration. In addition the more dispersive level 0 solution smears out the solution profile to the extent that the smaller scale peaks are not represented at all. Figure 5b again presents the solution achieved using level 2 constant density grid but here it is compared to the solution produced using adaptive gridding techniques. The adaptive solution seems to more adequately attain the peak concentration of the high resolution solution. Furthermore the adaptive solution also resolves many of the smaller peaks accompanying the main plume. However, it should be noted that the very small scale plume peaks, such as the peak situated 300km from the Eastern edge, are still not adequately represented. These areas could be resolved using tighter tolerances.

3.3 TOTAL INTEGRATED CONCENTRATION.

As grid density affects the degree of species dispersion the amount of species mixing will be grid dependant which will ultimately alter the total rate of species reaction. The mesh dependency of total species budgets is therefore assessed by examining the total integrated quantity of species over the course of the simulation.

Figure 6 a-d presents the species budgets for all three gridding schemes showing , NO2, NO, O3 and RP. These plots present total integrated species quantities in molecules, within a 1cm layer of the mixing height, against simulation time. Comparison shows that for diurnal variations in NOx-Ozone exchange differences between the gridding regimes are small. Total area under the adaptive and high density NO solutions show only a 0.09% difference. Similar comparison of the adaptive and low density NO solution shows a larger 3% difference, demonstrating that average centreline concentration is a mesh dependant property adequately resolved by the adaptive technique. The most significant differences in total species budget lie in the reactive pool. Large differences in RP quantity exist between solutions gained using the high and low resolution constant density grids. The solution gained using the adaptive gridding regime more closely follows those generated by the low resolution constant density grid. This is because we have chosen to refine around NO concentrations in order to simplify the demonstration of the technique and have consequently not resolved RP structures adequately. This problem is easily solved by applying appropriate tolerance values to RP.

4.0 Discussion

Comparison of the solutions for the two constant gridding scenarios provides a clear demonstration of the effect of grid density on solution. Results demonstrate that as resolution improves clearer identification of small scale structures is possible. In addition, refinement of the grid reduces artificial dispersion of species and therefore the smearing out of detail. Furthermore, examination of cross plume profiles shows that fine
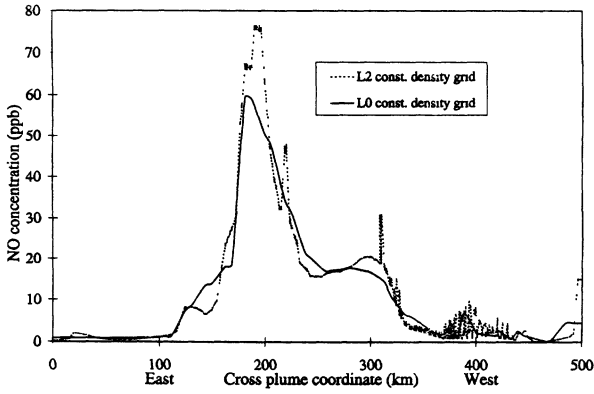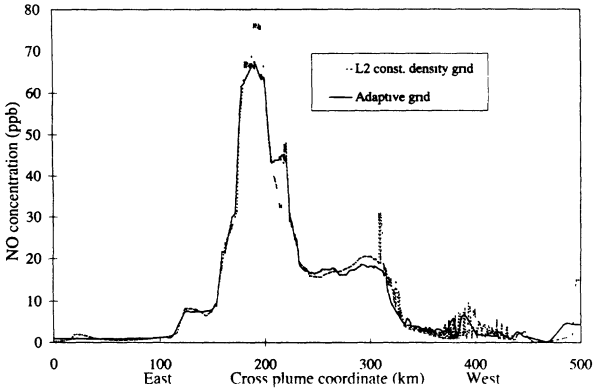
Figure 5a: Level 2/Level 0 cross plume profiles

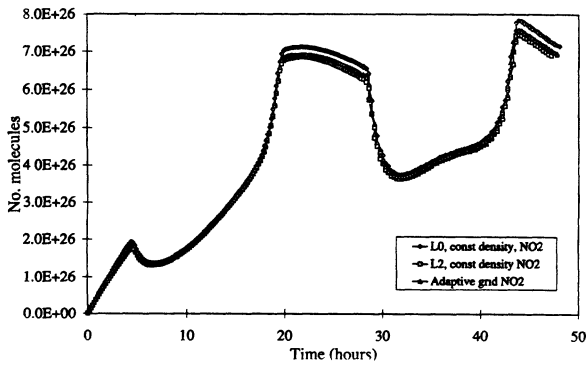
Figure 5b: Level 2/Adaptive cross plume profiles

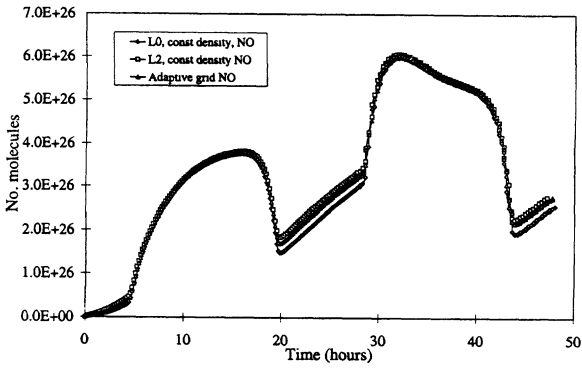Figure 6a: NO$_2$ total species budget
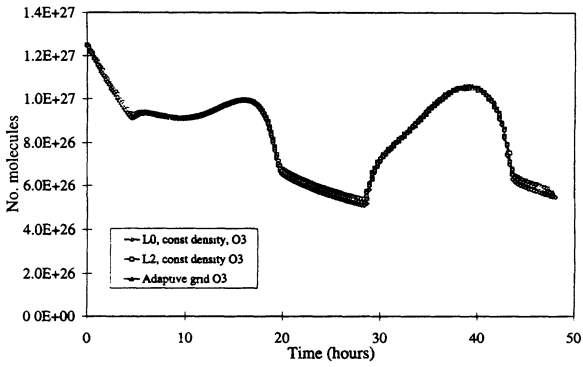
Figure 6b: NO total species budget
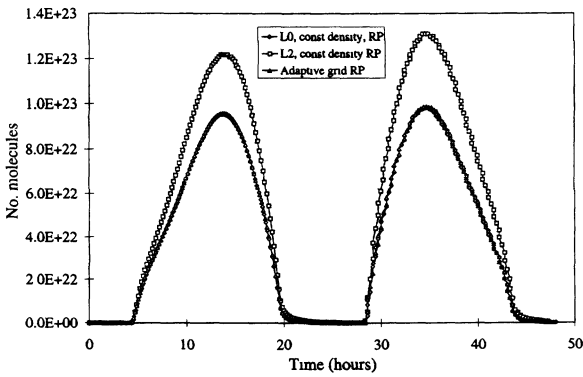

Figure 6c: O_3 total species budget

Figure 6d: RP total species budget

structures within the solution can lead to localised regions of very high species concentration. The resolution of these small scale structures may become very important when comparing numerical results to sparse monitoring data. The large differences between total reactive pool budgets yielded by the different grids are explained in Tomlin (1995) as the result of averaging the non-linear reaction rate over a single finite volume for the coarse grid. The reaction rate averaged over a single volume will only yield an accurate result if the concentration over the surrounding region is smooth, so in regions of steep spatial gradients there are likely to be large errors induced by the non-linear terms. Equation 2.2 shows that RP undergoes several non-linear reactions, accounting for the large discrepancy between high and low resolution results.

Despite improved solution accuracy, code performance is degraded in terms of processing time and storage requirements when using high density grids. This problem has been addressed using time adaptive gridding algorithms. The grid generated using adaptive techniques clearly clusters grid points in regions of potentially high spatial error such as plume edges. Such a grid configuration resolves rapidly changing solution profiles,

identifying structures only represented on a small spatial scale. This degree of accuracy is achieved using far fewer grid points than a constant density grid of similar resolution. In addition, more complex meteorology would make the prespecification of such a grid virtually impossible. The use of adaptive gridding therefore results in a higher accuracy solution solved in less time and requiring much reduced storage. The telescopic approach has shown to be useful in resolving structures close to the high emission areas selected. It is, however, incapable of resolving plume structures as they develop downwind of these sources.

5.0 Conclusion

In this paper we have presented a methodology based upon adaptive gridding techniques which could potentially reduce the computing cost of solving the dispersion problem while maintaining solution accuracy. The code presented successfully detects regions of potentially high spatial error and clusters grid points in these regions. The solutions yielded using such techniques were compared to those achieved using constant density gridding. They were found to be comparable to those gained using higher density grids, and successful in resolving gridding problems which telescopic models only partially address.

Lower resolution grids fail to resolve the small scale structures which may become important when comparing numerical results to monitoring data and in addition disperse species to such an extent that detail is smeared and indistinct. Grid dependency of non-linear reactions has been discussed and the errors possible demonstrated. Total species budgets for NOx and O_3 were not sensitive to grid structure but are highly sensitive for non-linear species such as the radical pool. For our simple scheme these errors did not feed back into major species but this may not be true for other chemical schemes. Local concentrations are far more sensitive to the grid and may require high levels of adaptivity in certain areas in order to be resolved. To achieve adequate solution accuracy using constant grids a high density must clearly be used. However, there is a price to pay in terms of run time and storage requirements when using such grids.

References

Azzi, M., Johnson G. M., Cope M. : 1992, *Proc. 11th Clean Air Conf. 4th Regional IUAPPA Conf., Brisbane*

Berzins, M., Ware, J. M.: 1996 *Appl. Num. Math.* **20**, *83-99*

Berzins, M., Ware, J. M.: 1995 *Appl. Num. Math.* **16**, 417-438

Berzins, M., Gaskell, P. H., Sleigh, A., Spears, W., Tomlin, A., Ware, J. M. : 1995 *Num. Meths for Fluid Dynamics V, pp 311-317, eds Morton, K. W., Baines, M. J., Clarendon Press, Oxford*

Derwent, R. G., Jenkins, M. E. : 1990, *AERE-report-R13736*

Goodwin, J.: 1993, *Personal communication*

Joe B.: 1991, *Adv. Eng. Software* **13**, *No. 5/6, 325-331*

Peters L. K. , Berkowitz C. M. , Carmichael G. R. , Easter R. C. , Fairweather G. , Ghan S. J. , Hales J. M. ,

Leung L. R. , Pennel W. R. , Potra F. A. , Saylor R. D. , Tsang T. T. : 1995, *Atmos. Env.* **29**, *189-222*

Skamarock, W. Oliger, Street, R. L. : 1989 *J. of Comp. Physics* **80**, *27-60*

Tomlin, A., Ware, J., Smith, J., Berzins, M., Pilling, M. J.,: 1995 *On the use of adaptive gridding methods for modelling chemical transport from multi-scale sources - in press*

SIMULATION OF POLLUTION DISPERSION USING SMALL SCALE PHYSICAL MODELS - AN ASSESSMENT OF SCALING OPTIONS

E D OBASAJU[1] and A G ROBINS[2]

[1] BMT Fluid Mechanics Ltd., Teddington, Middlesex TW11 8LZ, UK
[2] A G Robins, EnFlo, University of Surrey, Guildford, Surrey GU2 5QX, UK

Abstract. This paper concerns the role and nature of physical modelling as applied to dispersion studies. The arguments leading to the choice of model scale are discussed. The simulation of atmospheric flows and emissions are described, in particular the similarity conditions linking full scale and model conditions and their implications in terms of facility size and performance. We briefly summarise typical experimental programmes and treat the issues involved in interpreting results. Then we present three examples of laboratory studies. The first illustrates the ability to perform a simple plume rise simulation and the other two demonstrate building affected dispersion simulations. The final discussion centres on applications of physical modelling to urban air quality investigations.

1. Introduction

Local dispersion in an urban environment is a very complex matter, primarily reflecting interactions between the 'external' atmospheric boundary layer and irregular arrays of three-dimensional obstacles, but also affected by differential surface heating, traffic movement, emission conditions and so on. Computer modelling of these processes is generally based on very simplistic concepts which, though often acceptable, will in many cases prove to be inadequate. Examples where this may be so include the dispersion of emissions from point sources, the treatment of special sources (e.g. road tunnels), the prediction of short term concentrations and the interpretation of point measurements. To this list should be added the development and evaluation of improved practical models. The only methods available to resolve questions of this kind are wind tunnel modelling and computational fluid dynamics (CFD). Our paper concerns the former, but we begin with a few words about the latter.

CFD models have been used for some years now to calculate flow and dispersion around buildings, but only recently have the methods reached a suitable stage where this can be undertaken with some confidence of a reasonable outcome (e.g. see Cowan et al, 1996). Even so, the step from one or two buildings to an urban area is a big one and some time will pass before CFD can really tackle such issues. On the other hand, modelling flow and dispersion in complex topography (whether due to terrain or buildings) is readily accomplished in large wind tunnels (e.g. for a detailed discussion see Snyder, 1981). Of course, neither method provides a full and faithful representation of what takes place in the atmosphere, so we must also be aware of these limitations and take proper account of them in planning and executing both experiments and computations and interpreting their results.

We begin by discussing the stages involved in executing a physical modelling study. We discuss the choice of model scale, simulation requirements for the atmospheric flow and the emissions, and the techniques employed to satisfy them. We then summarise the elements of the experiments themselves and some of the issues involved in converting their output to full scale conditions. Finally we present three examples which illustrate the performance of the modelling techniques and discuss their application to dispersion in an urban environment.

We use the term 'physical modelling' as a generic term for laboratory based simulation; this includes water tanks, flumes, rotating tables and so on, as well as wind tunnels. In many places, 'wind tunnel' is used as a generic term for these facilities.

2. The Role and Nature of Physical Modelling

Laboratory based research has been instrumental in developing our understanding of many important fundamental aspects of flow and dispersion in the environment. The following list would probably not be questioned:

1. Plume rise: the entrainment assumption; stratified flow effects; interactions at inversions
2. Buildings: flow and dispersion processes
3. Complex terrain: speed up; stable flows and internal waves
4. Dense gas dispersion
5. Concentration fluctuations; effects of source size and location
6. Convective boundary layer: turbulence structure; dispersion processes

However, we intend to concentrate on the solution of air quality questions, such as dispersion prediction, plant design and stack height determination. Here not only about the experimental methods themselves, but also how the results are to be used must be considered. They will frequently need to be incorporated into some form of environmental impact assessment, implying interpretation in the context of some form of computer-based model which is then used in conjunction with appropriate meteorological data to interpolate or extrapolate to all conditions and output requirements of interest. These concerns are beyond the scope of this paper.

Applications of physical modelling include the study of wind loads on buildings and structures, transport aerodynamics, wind power, manmade hazards (e.g. resulting from the accidental releases of toxic and flammable gases), ventilation systems, and pollutant dispersion. In each case it is the ability to represent in a realistic manner the complex features of the problem that leads to the adoption of a solution based on physical modelling; that, and the established reliability and robustness of the methods themselves. Additionally, and most importantly, experimental conditions are under control, repeatable, and statistically steady.

The main steps in an air quality physical modelling study are basically:

1. the construction of a scale model of the topography, buildings (and so on) of interest,
2. the simulation of an appropriate atmospheric (boundary layer) flow in a wind tunnel,
3. the simulation of the emissions of interest,
4. the experimental programme, and
5. the interpretation and communication of the outcome in relevant (full-scale) terms.

2.1 THE PHYSICAL MODEL

The choice of scale and the extent of the region to be represented are key decisions. They are obviously related as the model size is constrained by the dimensions of the working section. The choice of scale is also a key factor in establishing the flow speed and emission conditions in the wind tunnel (as discussed in Section 2.3).

Figure 1 illustrates how the model and working section sizes are related. Upstream of the emission location a sufficient fetch is needed to establish the required atmospheric flow. The topographical model will generally extend into this region, sufficiently so that important features affecting the flow in the vicinity of the source are included. Then a downstream fetch is required which extends from the source region as far as necessary to answer the air quality questions of issue.
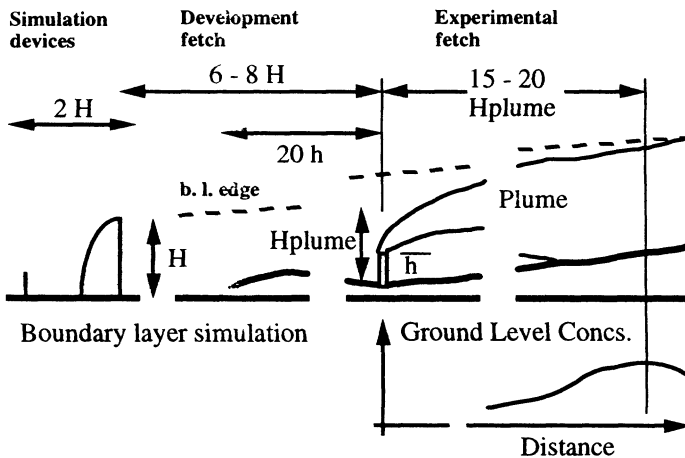
Fig. 1. Factors which determine the length of wind tunnel working section needed to undertake a plume dispersion simulation. H is the depth of the simulated flow, h the stack height and Hplume the plume height.

The figure shows the case of a tall stack where the downstream fetch is extensive. This is by no means always the case; e.g. the other side of the street may be the limit. The

choice of scale also determines the depth of flow to be simulated - this may be the full atmospheric boundary layer or just a fraction of it, as dictated by the working section height. In some special cases the vertical scale may be distorted relative to the horizontal scales in the final model but in most circumstances this is not to be recommended. Decisions have to be made about the degree of detail to be included. As much as possible is a good general rule, but financial and planning considerations may dictate otherwise. A degree of compromise is often necessary, but this must be settled on a case by case basis. Clearly, the model must not be simplified to a level which jeopardises the objectives of the study.

Whatever is decided about scale and detail, we generally require the model's surface to be aerodynamically rough at the lowest operating speed. This can be expressed in terms of the roughness Reynolds number as:

$$u^* . z_o / v > R_{crit}$$

where R_{crit} lies in the range $1 < R_{crit} < 5$, depending on the surface geometry, with u^* the friction velocity, z_o the roughness length and v the kinematic viscosity. In the fully rough regime we have $u^* \propto U_{ref}$ and $z_o \propto d_o$, where U_{ref} is a reference mean wind speed and d_o the height of the surface roughness elements (or model buildings), so this really boils down to a limit on the Reynolds number $U_{ref} . d_o / v$.

Other Reynolds numbers arise which are associated with obstacles, (buildings etc.). The general aim is for these to be high enough to ensure the appropriate flow regime around the obstacle and in its wake. This is a realistic approach for sharp edged buildings but poses problems for smoother shaped obstacles, such as towers and chimneys. A number of solutions have been put forward, such as adding roughness elements or boundary layer trips to force separation from the curved surface at the correct circumferential position. These have limited value.

2.2 THE SIMULATED ATMOSPHERIC FLOW

2.2.1 NEUTRAL CONDITIONS

The aim is to model the non-dimensional profiles of:

> mean flow speed,
> turbulence normal and shear stresses, and
> turbulence length scales

throughout the depth of the simulated flow, H. A number of boundary layer simulation systems have been developed to achieve these properties in as short a fetch of flow as possible: natural development is out of the question, being far too slow. Robins (1979) demonstrates how one such system performs, concluding that a fetch of about 6H is

needed and that thereafter flow development is slow. The latter feature is very important for dispersion modelling, so another prerequisite is that:

$(H/U_{ref}).dU_{ref}/dx \ll 1$

in the absence of topographical modification.

Meeting the fully rough surface condition, together with an equivalent fully turbulent flow condition, is the only factor affecting the choice of reference speed. Other considerations may define a relationship between facility and full-scale wind speeds, but neutral boundary layer simulation itself provides none.

In standard laboratory facilities the flow direction does not change with height above the ground, unlike in the atmosphere where rotational effects generate a change in wind direction of order 10° over the depth of the neutral boundary layer. This is a deficiency which must be borne in mind when assessing the results of any study - it is not normally very significant for short range dispersion studies. Special rotating table facilities have been constructed to investigate this and other effects of the Earth's rotation.

2.2.2 NON-NEUTRAL CONDITIONS

Unlike in the neutral case, there are no generally agreed procedures for modelling stable and unstable atmospheric boundary layers. However, the main requirement is to control the density (or temperature) profile in the flow and the buoyancy (or heat) flux at the surface. This adds an additional length scale to the simulation conditions, the Monin-Obhukov length scale (L_{MO}), and leads to a direct relation between the facility and full-scale wind speed.

A simple case to consider is that of stable flow over terrain. The main flow determining parameter is the obstacle Froude number, F:

$F = U/N.h$

where U is the wind speed, N the buoyancy frequency and h the obstacle height; N is defined as:

$N = \{-(g/\rho).d\rho/dz\}^{1/2}$

where g is the acceleration due to gravity and ρ density. The choice of model scale and simulation conditions are obviously linked and, with a scale ratio and a model density gradient selected, the wind speed is defined by:

$U = F.N.h$

The situation is more complex when we think of boundary layer simulation. In addition to the aims of neutral boundary layer simulation, the profiles of non-dimensional

temperature and turbulent heat flux (or density and buoyancy flux) must also be simulated. An important parameter which emerges from this is the ratio of the boundary layer height and Monin Obukhov scale, H/L_{MO}, and in a heated flow this is given by:

$$L_{MO}/H = -u*^3/\{(k.g.H).(q/T)\}$$

where k is von Karman's constant and q the kinematic heat flux. In this case the choice of model scale, heat flux and wind speed are linked and now the flow speed, here defined by the friction velocity, is:

$$u* = \{(-L_{MO}/H).(k.g.H).(q/T)\}^{1/3}$$

and the choice of model scale, $-L_{MO}/H$, and heat flux can be arranged to provide a workable value for the friction velocity.

2.3 EMISSION SIMULATIONS

The aim is to define model source and wind conditions which will lead to the correct simulation of the non-dimensional plume trajectory (Y_p/H, Z_p/H) and spread (σ_y/H, σ_z/H) as functions of downstream position, x/H. The non-dimensional concentration field, $C.U.H^2/Q$ (with Q the source strength) is then automatically reproduced.

We will illustrate emission simulation by considering a single source (a stack), defining conditions by:

the stack diameter and height: D, h,
the emission velocity and density: W_s, ρ_s, and
the reference ambient wind speed and density: U, ρ.

2.3.1 COMPLETE SCALING

Consideration of the flow equations in non-dimensional form shows that the following parameters need to be conserved:

D/H, D/h, W_s/U, ρ_s/ρ, $g.H/U^2$.

This means that the following are also conserved:

volume flux, Q:	$W_s.D^2/U.H^2 = (D/H)^2.(W_s/U)$
mass flux, Q_M:	$\rho_s.W_s.D^2/\rho.U.H^2 = (\rho_s/\rho).(D/H)^2.(W_s/U)$
momentum flux, F_M:	$\rho_s.W_s^2.D^2/\rho.U^2.H^2 = (\rho_s/\rho).(D/H)^2.(W_s/U)^2$
Richardson number, Ri:	$g.\Delta\rho.H/\rho.U^2 = (1-\rho_s/\rho).(g.H/U^2)$
buoyancy flux, F_B:	$g.\Delta\rho.W_s.D^2/\rho.H.U^3 = (W_s/U).(1-\rho_s/\rho).(g.H/U^2)$,

where $\Delta\rho$ is the density difference, $\rho-\rho_s$. We shall return to these parameters later.

This is termed the complete scaling condition, somewhat euphemistically as a number of source Reynolds number parameters are not conserved. These are, most importantly, the internal Reynolds number, $W_s.D/v$, and the external Reynolds number, $U.D/v$. We have already discussed approaches to the latter problem in Section 2.1. A variety of solutions have been proposed for dealing with the internal flow, the objective being to generate conditions approximating those of a high Reynolds number, turbulent flow at the stack exit. These include internal orifices and nozzles, porous plugs and turbulence generators, though experience leads us to think that in many situations little is lost by ignoring the whole matter providing scaling ratios are not taken to extremes.

The most telling consequence of complete scaling is the relation between model and full-scale wind speeds; i.e. the velocity scaling ratio, V:

$V = Um/U = S^{1/2}$; $S = Hm/H$, the scale ratio.

where 'm' denotes the model state. This demonstrates four things:

1. low wind speeds are necessary at model scale,
2. extreme geometric scale ratios, S, are to be avoided,
3. large facilities are required, and
4. the demands of complete scaling may even then be impossible to meet.

The scale ratio is defined by the arguments set out in Section 2.1. Clearly, scale ratios in the range from S = 1/100 to 1/1000 and beyond follow; e.g. at 1/500 scale a section of wind tunnel 8 m long and 1.5 m high represent 4 km and 750 m at full scale. With this range for S we see that the velocity ratio is in the range from 1/10 to 1/32 and a 5ms^{-1} wind speed is reduced to 0.5 to 0.16 ms^{-1} at model scale. About 0.3 to 0.5 ms^{-1} is the lowest wind speed which can be readily established and controlled in a wind tunnel. Clearly, complete scaling is feasible only for moderate scale ratios and high full scale wind speeds, even in very large wind tunnels.

These arguments demonstrate that the working section of a typical dispersion wind tunnel is likely to be 15 m or more in length and about 1.5 m high, but only needs to operate at low speeds, typically around 0.5 to 2 ms^{-1}.

2.3.2 ENHANCED SCALING

The objective is to relax the strict requirements of complete scaling in some way to obtain a wind speed scaling ratio which is more favourable; i.e. to have:

$Um/U = \beta.S^{1/2}$; $\beta > 1$

The usual approach is to distort the density ratio, $\alpha = \rho_s/\rho$, and to replace the three complete scaling parameters (ρ_s/ρ, W_s/U, $g.H/U^2$) with two physically plausible

substitutes. There are several possibilities, though only combinations of one from W_s/U and F_M together with one from Ri and F_B have generally been used. However, the emission density, ρ_s, has sometimes been used in place of the ambient density, ρ, as a reference property (e.g. see Robins, 1980).

We will now discuss enhanced scaling ESA, based on conservation of F_M and F_B. There is a good reason for choosing these as they arise naturally in plume rise theory and are conserved properties of the emission (at least in a neutrally stable environment). With $\alpha_m = (\rho_s/\rho)_m$ not equal to α, this leads to the result:

$$\beta_A = \{(\alpha/\alpha_m)^{1/2}.(1-\alpha_m)/(1-\alpha)\}^{1/2}$$

and $\beta_A > 1$ if $\alpha_m < \alpha$. By way of illustration, set $\alpha = 0.8$ (typical of a boiler plant emission) and $\alpha_m = 0.2$, to give $\beta_A = 2.8$, a most valuable improvement on complete scaling.

The tests of any proposed method are three in number:

1. do results agree with data from complete scaling (where overlap is feasible),
2. do results agree with full scale observations, and
3. are results insensitive to the degree of density ratio distortion?

Unfortunately, although many enhanced scaling rules have been proposed, few have been examined in this manner. Scaling ESA does conform to these three requirements (Robins, 1980).

Occasions arise with multi-stack studies when the ability to simulate the non-dimensional mass flux, Q_M, is of benefit, so that all sources can be studied simultaneously. Now Q_M and F_B could be selected as the scaling parameters, but this would incorrectly represent the plume trajectory near the source (where the initial momentum is important), which could be a vital error if interaction with a near-by building were an important facet of the problem. However, the three parameters Q_M, F_M and F_B can be conserved if departure from strict geometrical scaling is accepted, allowing the stack diameter ratio, $\delta = Dm/D$, to be treated as an independent parameter. We refer to this as scaling ESB, finding that:

$$\delta_B = S.(\alpha/\alpha_m)^{1/2}$$
$$\beta_B = \{(\alpha/\alpha_m).(1-\alpha_m)/(1-\alpha)\}^{1/2}$$

For the previous example we now find $\delta_B/S = 2$ and $\beta_B = 4$, actually more favourable than Scaling ESA.

We will compare the performance of scaling conditions ESA and ESB in Section 3. Another enhanced scaling, ESC, is included in the comparisons to illustrate the differences which can arises if the scaling parameters are not well chosen. This method

has been used - it is based on conservation of Q_M, F_M and $F_B{}'$, where $F_B{}'$ is an alternative form of the buoyancy flux parameter:

$$F_B{}' = g.\Delta\rho.W_s.D/\rho.U^3$$

which comes about by noting that the length scale H in the denominator of F_B can be replaced by any other length scale, such as D. This is perfectly reasonable providing that H∝D. Used in the context of scaling ESA it would lead to exactly the same result for β. The problem arises when modelling conditions are extended to include the non-dimensional source strength, Q_M. Proceeding as for ESB, but with the modified definition of non-dimensional buoyancy flux, leads to:

$$\delta_c = S.(\alpha/\alpha_m)^{1/2}$$
$$\beta_c = \{(\alpha/\alpha_m)^{1/2}.(1-\alpha_m)/(1-\alpha)\}^{1/2}$$

2.3.3 PASSIVE EMISSIONS

A passive emission is defined as one for which the source momentum and buoyancy parameters, F_M and F_B, are so small that they have no effect on the behaviour of the release. They can effectively be set to zero. There is then no relation between model and full scale wind conditions and a single experiment is sufficient to define concentrations at all wind speeds, since they will collapse when scaled as $C.U.H^2/Q$. The only caveat is that there will generally be a lower limit to the wind speed at which the assumption of passive emission condition fails, since both F_M and F_B are inversely related to the wind speed.

2.4 THE EXPERIMENTAL PROGRAMME

This generally involves a series of experiments in which the parameters of the problem are varied throughout the ranges of interest and resulting concentration levels or dilutions measured. These may be time averaged or 'instantaneous' measurements at a number of points or in a plane, according to the instrumentation used. We do not intend to discuss the techniques involved here, though there is one important point to consider. There are two ways in which physical modelling may be applied, either to predict concentrations or changes in concentration. The first is the obvious, direct application but the second involves determining the changes in concentration levels relative to a 'standard' case. For example, the standard case may be the present state of affairs and the aim to investigate the effects of a new development (say, in an urban area). Experiments are carried for both conditions and used to show how current concentration levels are changed by the development. This proves to be a very robust approach and circumvents many of the questions which surround the interpretation of wind tunnel data.

2.5 DATA INTERPRETATION

For the sake of simplicity we will discus the simulation of a single plume. As pointed out earlier in this Section, the aim of the simulation is to reproduce the non-dimensional concentration field, $C.U.H^2/Q$, and full scale concentrations, C, can be calculated from:

$$C = (Q/U.H^2).(C.U.H^2/Q)m$$

Of course, both C and Q must be measured in consistent units (e.g. mass or volume release rates and concentrations). At model scale C is the concentration of the total emission and Q the total emission rate, whereas at full scale Q will usually be the release rate of the pollutant of interest. When working in volume units we will generally need to reduce the latter to ambient temperature, as Q is defined at the source temperature.

One of the important features of physical modelling is that the experimental conditions are under control, repeatable, and statistically steady. This means that we can measure genuine mean values, unlike in the atmosphere where concentrations are always a function of the time over which they are observed. This leads to the inevitable question: to what averaging time do wind tunnel studies correspond? This is not a simple question and it is made all the more difficult by the rather imprecise way averaging and averaging times are treated in air quality and other atmospheric dispersion studies.

In the laboratory boundary layer turbulence is simulated and this has an integral time scale which is proportional to H/U. The averaging time needed to measure a mean concentration to some acceptable degree of repeatability increases as U decreases; generally it will be of order 100 H/U, typically a few minutes (say U=1 ms^{-1}, H=1 m). If this is translated into atmospheric terms we find we have time scales of order three hours (say U=5 ms^{-1}, H=600 m). However, conditions will not normally be steady on this time scale nor, for that matter, on somewhat shorter ones. The main source of unsteadiness lies in the reference mean wind direction, though the mean wind speed and stability may also vary. In other words, field observations with nominally the same non-dimensional averaging times as a wind tunnel study will tend to show somewhat greater plume spreads (primarily, lateral spread) and, consequently, lower concentrations.

These differences become less significant as the averaging time is reduced and it is generally thought that laboratory simulations can be analysed in terms of 15 to 30 minute averages at full scale. However, there may be considerable ensemble variability at this time scale. To be precise, we should relate the mean concentration obtained from the physical simulation to the ensemble mean atmospheric concentration.

3. Examples

Three examples are presented. The first two demonstrate the efficacy of the scaling arguments, and the third the application of physical modelling to a complex flow and dispersion problem.

3.1 PLUME RISE FROM AN ISOLATED STACK

We start with a simple example to compare the performance of complete scaling and the three enhanced scaling techniques discussed in Section 2.3.2. Figure 2 shows simulated plume rise as a function of distance downstream for all four scaling conditions; full scale conditions are listed in Table 1.

Table 1 Plume rise simulation - full scale conditions	
Stack diameter, D, m	9.3
Stack height wind speed, U_h, ms^{-1}	7.1
Emission speed, W_s, ms^{-1}	21.3
Emission density ratio, $\alpha = \rho_s/\rho$	0.844
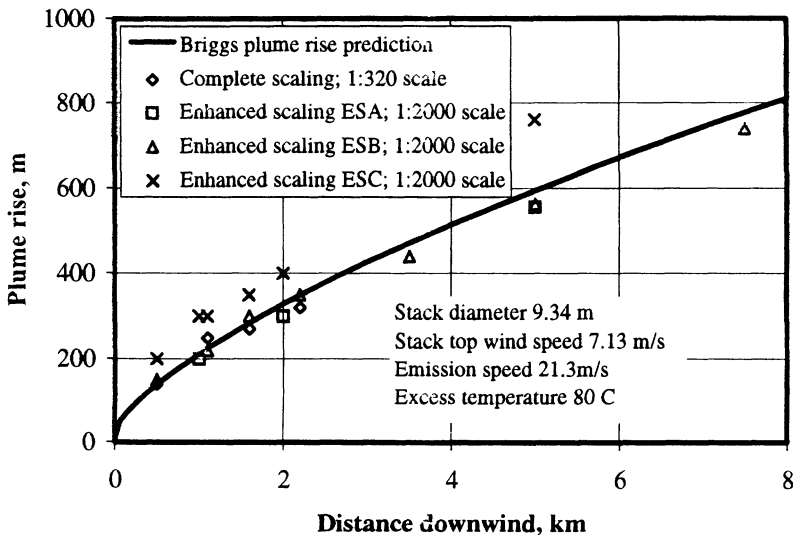
Fig. 2. Simulations of plume rise from an isolated stack; plume height as a function of downwind distance (source conditions and other details in Section 3.1).

These experiments were carried out in the BMT 15 x 4.8 x 2.4 m environmental wind tunnel, in which a deep atmospheric boundary layer was established. Emissions were simulated by mixtures of helium and a hydrocarbon tracer, the concentration of the latter being measured by an array of flame ionisation detectors. Complete scaling was undertaken at a scale ratio, S=1/318, with U_h=0.4 ms^{-1}, the enhanced scaling with

S=1/2000; for ESA we have: α=0.15, U_h=0.57 ms^{-1}; for ESB: 0.15, 0.88 ms^{-1}, with δ=Dm/D=2.35; for ESC: 0.15, 0.57 ms^{-1}, 2.35. The dashed line is a prediction from the Briggs plume rise formula. We see that the results of complete scaling and enhanced scaling ESA and ESB all agree with one another and with the plume rise prediction, whereas enhanced scaling ESC over-predicts the rise. This comes about because, in the context of Brigg's theory, the plume rise contribution from buoyancy is a factor of $\delta^{1/3}$ too large.

3.2 BUILDING AFFECTED DISPERSION, CASE 1

As scaling ESA meets the basic requirements of an adequate procedure (see Section 2.3.2) it was applied to the simulation of a buoyant, roof level emission, to examine sensitivity to changes in the degree of density ratio distortion. Figure 3 shows ground level, centre line concentrations as a function of the reference wind speed at four downstream locations, x/h =5, 10, 20, 30, where h is the building height; in the figure U_{10} represents the equivalent full scale wind speed at a height of 10m. Full scale conditions are listed in Table 2:
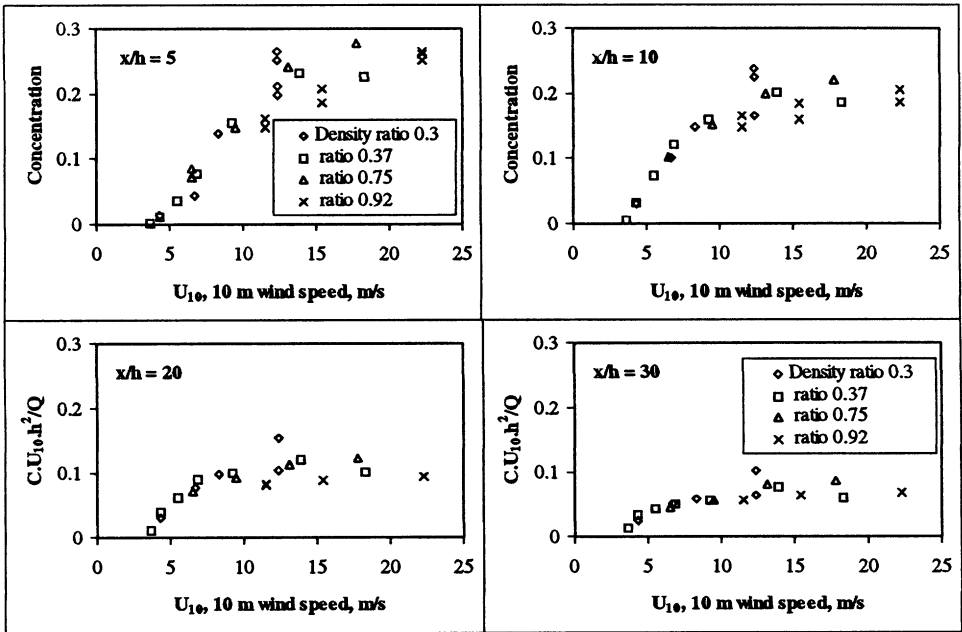
Fig. 3. Simulation of building affected dispersion using enhanced scaling condition ESA; variation in non-dimensional centre line, ground level concentration with 10m wind speed (source conditions and other details in Section 3.2).

Table 2	
Building affected dispersion simulation - full scale conditions	
Building height, h, m	54
Stack diameter, D, m	3.2
Emission speed, W_s, ms^{-1}	12
Emission density ratio, α	0.83
Heat release rate, Q_H, MW	5.8

The experiments were carried out in the Marchwood Engineering Laboratories 20 x 9 x 2.7 m wind tunnel, in which a deep atmospheric boundary layer was established. Emissions were simulated by mixtures of helium, nitrogen and a hydrocarbon tracer, the mean concentration of the latter being measured by a gas sampling and analysis system, using a flame ionisation detector. The simulations were carried out at a scale S=1/400, using a variety of emission density ratios, α, from 0.30 to 0.92. Although there is some scatter, there is no obvious trend with density ratio. In particular, behaviour in the critical wind speed range where the plume begins to be brought to ground in the building wake is unambiguously defined. The plume remains aloft at lower wind speeds and becomes effectively passive (i.e. $C.U_o.h^2/Q$=constant) at high wind speeds.

3.3 BUILDING AFFECTED DISPERSION, CASE 2

Finally, we consider a passive ground level source alongside a large building and illustrate how small scale architectural features can profoundly influence near-field dispersion. In this case there are no constraints imposed on the experimental conditions, other than ensuring passive emission conditions (see Section 2.3.3). The experiments were again carried out in the Marchwood Engineering Laboratories 20 x 9 x 2.7 m wind tunnel, using the techniques described above: in this case the emissions were mixtures of nitrogen and a hydrocarbon tracer. The building lay-out is illustrated in Figure 4; the main building is about 65 m tall and the ground level sources were located at S1, S2 and S3. Sources S2 and S3 were similarly positioned, one on the left and the other on the right hand side of the building, and S1 was near the centre of the building face.

Non-dimensional concentrations observed at receptor A are shown in Figure 5 as a function of wind direction (defined in the figure). Firstly we note the common features for all three sources: the emissions are detectable over a wide range of wind directions when the sources and receptor are in the building's wake, and over a narrower range of directions when both are on the upstream side of the building. The processes responsible are illustrated in the figure. In the first case we have the classical case of dispersion in the recirculation region downstream of a building and in the second the case of dispersion in the recirculation region ahead of a building.

When we look in detail at the three sets of results we see a considerable sensitivity to the actual source location, all of which is due to the presence of the smaller, secondary buildings near to the sources. Sensitivity studies showed that much smaller secondary buildings produced a similar effect. In particular, for wind directions around 0°, the flow close to source S2 is deflected away from receptor A and around the side of the building.

This must also happen to some degree for S3, but clearly to a much lesser degree as much higher concentrations are detected at A.
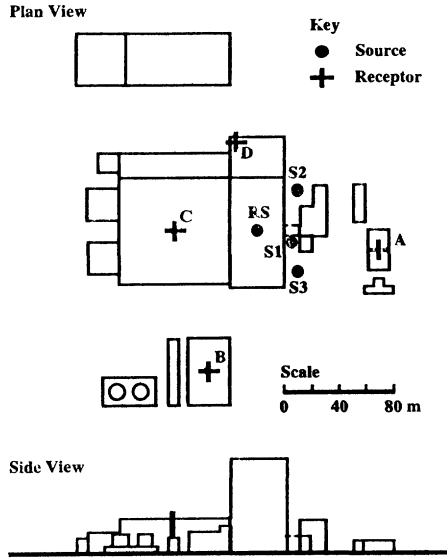

Fig. 4. Simulation of building affected dispersion; building, source and receptor lay-out (source conditions and other details in Section 3.3).
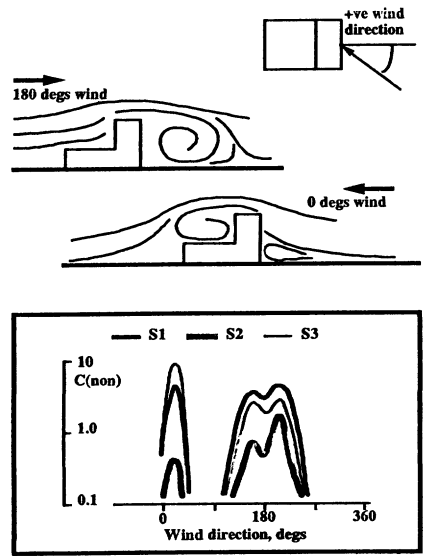

Fig. 5. Simulation of building affected dispersion; variation in concentration at receptor A as a function of wind direction and source position for a passive release (source conditions and other details in Section 3.3).

4. Discussion and Conclusions

We have discussed and illustrated the application of physical modelling to atmospheric dispersion prediction, paying particular attention to the similarity conditions. Of all those proposed (for a list see Snyder, 1981) only a few scaling methods have been subject to detailed examination of any sort. We have presented examples of the performance of the enhanced scaling condition ESA which show that it satisfies the three tests:

1. do results agree with data from complete scaling?
2. do results agree with full scale observations?
3. are results insensitive to the degree of density ratio distortion?

This conclusion is supported by other studies; e.g. Robins, 1980. To a less comprehensive degree we have also shown that scaling condition ESB performs as well as ESA, but ESC is less reliable. Our point is that there are acceptable similarity rules for modelling buoyant emissions (ESA and ESB), but that it is also quite easy to propose rules which are not acceptable (see Robins 1980 for further examples). The examples demonstrate that it is entirely feasible to use wind tunnel methods to study typical urban dispersion problems, such as the interaction between a buoyant emission from a short stack and the buildings in the vicinity of the source.

The second and third examples were chosen because they involved dispersion behaviour which was very sensitive to the complex interactions between emissions and nearby buildings. Both dealt with real sites, as typified by Figure 4. CFD simulations of either of these examples would require some, perhaps considerable, geometrical simplifications, introducing attendant 'scaling' questions in addition to the usual concerns with numerical and modelling error.

A strength of physical simulation methods is the ability to study complex flow and dispersion processes, as our third example illustrates. Again, this is directly applicable to questions of dispersion in built-up areas. Wind tunnels have been widely used to study the behaviour of emissions in street canyons and other idealised environments. Hoydysh and Dabbert (1994) clearly show the importance of three dimensional effects at intersections and how these transport pollutants into side streets. Their study concerned a regular urban network of streets, with uniform buildings. An irregular array is more realistic and this will generate even more complex dispersion patterns. Physical simulation provides a cost-effective tool for studying real environments, defining source-receptor relations, and mapping spatial and temporal variability in the concentration field. The techniques for establishing stratified boundary layers and scaling buoyant emissions can be applied in such simulations to include buoyancy effects, both those associated with surface heating and cooling and those associated with emissions.

5. References

Cowan, I. R., Castro, I. P. and Robins, A. G.: 1996, Numerical considerations for simulations of flow and dispersion around buildings, Proc. Second Int. Symposium on Computational Wind Engineering, Colorado State University, 4-8 August. 1996. To be published in J. Wind Eng. and Industrial Aerodynamics.

Hoydysh, W. G. & Dabbert, W. F.: 1994, Atmos. Environ. 28-11, 1846-1860.

Robins, A. G.: 1980, Studies in Environmental Science 8, 117-124.

Robins, A. G.: 1979, J. Ind. Aero., 4, 71-100.

Snyder, W. H.: 1981, Guideline for fluid modeling of atmospheric diffusion, US EPA Report EPA-600/8-81-009.

VALIDATION OF A STREET CANYON MODEL IN TWO CITIES

A.T. BUCKLAND

Meteorological Office, Bracknell, Berkshire, RG12 2SZ, UK

Abstract. A street canyon model has been formulated based on work published by Hertel and Berkowicz. An outline is given of the theoretical approach used, followed by a modelling of nitrogen oxides and carbon monoxide measurements from sites at Cromwell Road, Central London and Stratford Road, Birmingham. Modelled concentrations were compared with observed mixing ratios for both sites. At Cromwell Road, good agreement was achieved for one month but which was not reproduced as well for the other two months tested. There is uncertainty as to the effect of one of the side streets and whether the general flow is altered during periods of marked solar heating. Also emissions from vehicles may vary from those assumed. The interpretation of the Stratford Road site's results was less straightforward with complications concerning background pollutant levels and changes in emissions from interrupted traffic flow.

1. Introduction

The concentration of pollutants in urban areas due to motor vehicles has become of increasing concern, particularly since the London pollution episode of December 1991. Much work and monitoring have been focused on the background level of airborne substances such as nitrogen oxides (NOx) and carbon monoxide (CO). However, it is at kerbside locations where the general public may suffer exposure to the highest concentrations of pollutants, particularly in a street canyon with large vehicle emissions and reduced dispersion.

Modelling is a useful tool where the collection of data is often relatively difficult in these busy areas. The mathematical techniques are either numerical flow models or simpler parametrizations such as the STREET model (Johnson et al.,1973) or the more developed CPBM or Canyon Plume-Box Model (Yamartino and Wiegand, 1986).

The OSPM or Operational Street Pollution Model (Hertel & Berkowicz, 1989a; 1989b; 1989c; 1991 and Berkowicz et al., 1994) is of the latter kind, calculating short-term (hourly) concentrations. It was developed to be a robust and simple operational model, using concepts developed in the CPBM model. It was tested on data collected from selected sites in Denmark, Norway and the Netherlands. In the present study, the computer code followed their equations given in the literature. The street geometry, traffic flows and vehicle emissions could then be input for a particular site. This version was validated against some of Hertel and Berkowicz's results. It was then tested on field data from two canyon sites in the UK.

2. General Features of OSPM

When the wind blows across a street canyon a vortex is typically generated, with the wind flow at street level opposite to that above roof level. A consequence is lower concentrations of pollutants on the windward side of the street compared with those of

the leeward. The windward side is here defined as the side the roof wind blows to whilst the leeward side is the side the roof wind blows from.

The concentration of pollutant within the street is given by the expression :-

$$C_S = C_d + C_r + C_b. \quad (1)$$

C_d, the direct contribution, is the direct flow of pollutant from vehicles to the monitor; C_r, the recirculation component, results from earlier cycles in the flow around the vortex. C_b is the urban background concentration of pollutant outside the canyon. The quantities, C_d and C_r depend on the angular difference (ϕ) between the wind direction and the street axis and whether the monitor is on the leeward or windward side of the street.

C_d is calculated using a Gaussian plume model. The emission is considered to be distributed uniformly across the street. Q is the emission rate from the whole street width per length along the street ($\mu g\ m^{-1}s^{-1}$). The emissions are modelled as a number of infinitesimal line sources aligned perpendicular to the wind direction at street level. The contribution to the concentration at a distance x from an infinite cross-wind line source of downwind width dx is then given by the expression :-

$$dC_d = \sqrt{\frac{2}{\pi}}\ \frac{dQ}{u_b \sigma_z(x)} \qquad (2)$$

where $dQ = Q\dfrac{dx}{L}$, L is the street width, u_b the wind speed at street level, $\sigma_z(x)$ the standard deviation for plume spread in metres at a distance x. Equation 2 is integrated downwind, i.e. along the wind path at street level. This integration path in Figure 1 depends on wind direction, extension of the recirculation zone and the street width.

If the wind direction at roof level is at an angle ϕ with the street axis, the wind direction at street level outside the recirculation zone is the same. The street level wind within the recirculation zone blows at an angle minus ϕ with the transverse component mirror reflected. The length of the resultant street vortex, L_v , also at angle $\pm\phi$ to the street , is calculated by the expression :-

$$L_v = 2rH_b \quad (3)$$

where H_b is the height of the street buildings and r is a wind speed dependent factor which reflects the strength of the vortex. The component of L_v normal to the street is then $L_v \sin\phi$. The maximum extent of the recirculation zone (i.e. L_r, width of shaded zone in Figure 1) cannot exceed the street width L, or the component $L_v\sin\phi$. So that

$$L_r = Min\ (L, L_v \sin\phi) \quad (4)$$

(Equation 4 is needed because for very tall buildings L_v in equation 3 might be unreasonably large.) r is introduced because at roof level wind speeds below 2 ms^{-1} the vortex often disappears. So r = 1 for u ≥ 2 ms^{-1} or r = u/2 for u < 2 ms^{-1} where u is the wind speed at roof level.

The dispersion of the plume is assumed to depend on two processes: turbulence generated by the wind and mechanical turbulence in vehicle wakes. The effects of thermal stratification in enhancing or suppressing turbulence are neglected: the stability is always neutral in this formulation.

Leeward Side

Roof Level
Wind

Street Level
Wind

ϕ

Street Level
Wind

ϕ

ϕ

Windward Side

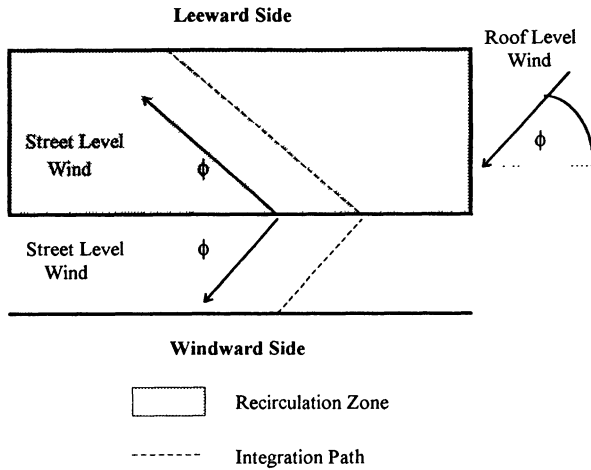☐   Recirculation Zone

--------   Integration Path

Fig 1. Wind flow and formation of recirculation zone in a street canyon.

The traffic created turbulence σ_{w0} depends on traffic intensity and is given by the expression :-

$$\sigma_{w0} = b \sqrt{\frac{V_c N_c S_c^2 + V_h N_h S_h^2}{L}} \quad (5)$$

where N_c and N_h are the traffic intensities of cars and heavy vehicles, respectively, V_c and V_h are the average driving speeds and S_c^2 and S_h^2 are the average horizontal areas. L is the street width and b is an aerodynamic drag coefficient specified as 0.3. σ_w, the combined turbulence, is then given by the equation :-

$$\sigma_w = \sqrt{(0.1 u_b)^2 + \sigma_{w0}^2} \quad (6)$$

u_b, the wind at street level, is calculated using a logarithmic reduction of u with a simplified dependence on ϕ included.

C_r is computed using a simple box model (Figure 2). The principle is that the inflow rate of pollutants into the recirculation zone equals the outflow rate and that the pollutants are well mixed inside the zone. The zone's shape is a trapeze with the length of the upper edge equal to 0.5 L_r and the length of the slant edge is given by :-

$$L_s = \sqrt{(0.5 L_r)^2 + H_b^2} \quad (7)$$

The inflow of pollutant is equivalent to $Q L_r / L$ whilst the pollutants are removed from the recirculation zone by two processes: diffusion through the upper edge and advection through the side edge. The rate of diffusive loss is expressed as $C_r \sigma_{wt} 0.5 L$ and the rate of advective loss is given by $C_r u_d L_s$. σ_{wt} is equivalent to the removal velocity V_d, whilst the advective removal velocity u_d is given by :-

$$u_d = \sqrt{u_b^2 + \sigma_{w0}^2} \quad (8)$$

By equating the inflow and outflow expressions C_r can be calculated.
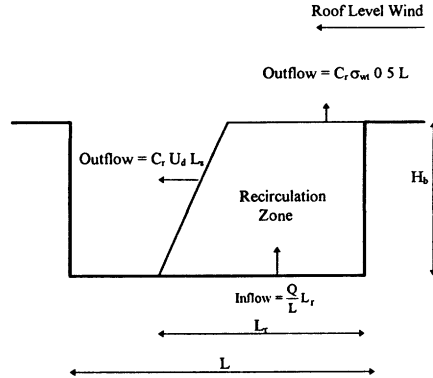
Fig.2. Assumed geometry of the recirculation zone.

There are three situations concerning street canyons, A where the wind blows parallel to the street, B where the wind blows perpendicularly across the street and C with the wind at an oblique direction. In case A **no vortex** occurs so that there is only C_d, with C_r equal to zero. In cases B and C the recirculation zone develops to a greater or lesser extent. By integrating equation 2 the general expression of C_d is given by :-

$$C_d = \sqrt{\frac{2}{\pi}} \frac{1}{\sigma_w} \frac{Q}{L} F \quad (9)$$

where the first part is a Gaussian function and F is a factor that varies according to which of the above cases A, B or C applies. Likewise C_r varies as the dimensions of the trapezoid box change according to the wind direction. Finally the calculated concentration in $\mu g\ m^{-3}$ is converted to a mixing ratio using the molecular weight, temperature and pressure.

4. Verification and Application

4.1 VERIFICATION

To ensure that the model had been coded correctly, model runs were performed for Jagtvej, Copenhagen to attempt to reproduce the work described in Berkowicz and Hertel (1994). The street is oriented 30° to the North. Calculations were performed at 1 m/s intervals from 0 to 8 m/s and for wind directions from 0 to 360° at 5 degree intervals. Figure 3 is Hertel and Berkowicz's run with wind averaging hence the smooth lines. Below, Figure 4, is this study's run for comparison.

The two sets of computed values agree very well with only a few subtle differences. The general shapes of the curves are reproduced with the very low concentrations calculated for wind directions between 265 and 335°. Values of mixing ratios agree to within about 5%.

The verification against measurements is made in Hertel and Berkowicz (1989). In their text Figure 17 shows the scatter plot with good agreement between calculated and measured NO$_x$ for the range 0 to 750 ppb. Figure 18 compares the effect of wind

direction and shows very similar behaviour. In both calculated and measured NO_x plots, minimum values are displayed at similar wind directions.
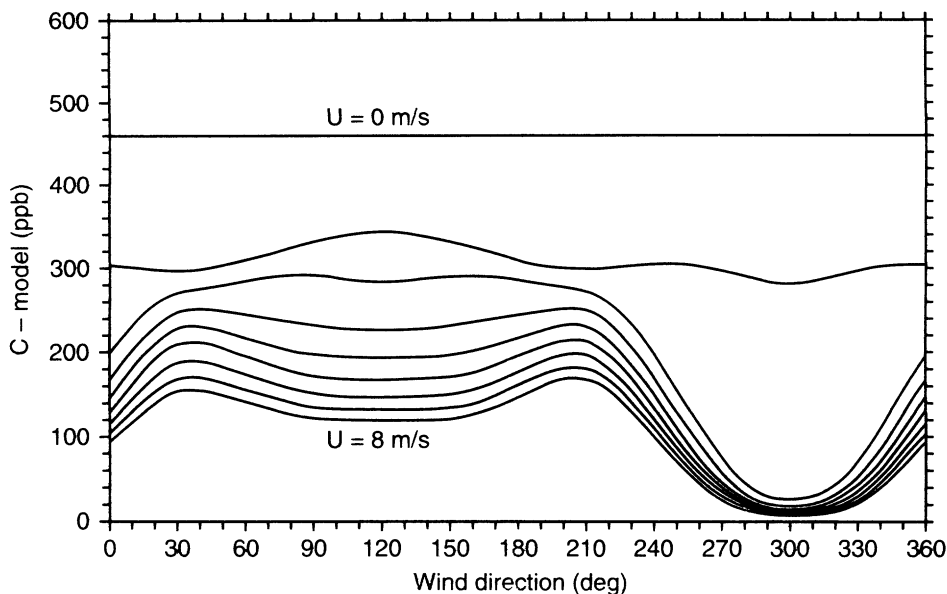
Fig. 3. Hertel and Berkowicz's computed concentrations of NOx for the street of Jagtvej.

4.2 APPLICATION TO CROMWELL ROAD SITE

Figure 5 is a sketch map of the site. Cromwell Road is the A4 route into London, well trafficked and in a well built-up area, with the monitor situated outside the Tudor Court Hotel. Many of the buildings are of similar style, being generally 20 metres high, and the road is 23.5 metres wide. Thus the canyon's height to width ratio is nearly 1. There are also no major road intersections for some distance in either direction.

To calculate Q for NO_x and CO it was necessary to have hourly traffic data and these were available for 23 November 1989, 11 September 1991 and 8 June 1993. All three days were weekdays with counts from 0700-1900 but with some hours missing. These missing hours were filled by assuming linear interpolation or persistence as appropriate. These census days were then used to represent all weekdays for that particular month.

The first two censuses categorised traffic into cars and light goods vehicles, medium goods vehicles, HGVs, buses/coaches and motor cycles. The 1991 count further classified between cars and taxis. It was then a matter of converting traffic flow into Q in units of $\mu g\ m^{-1}s^{-1}$. Using an emission factor q for NO_x or CO in g km^{-1} vehicle^{-1} then with N vehicles hr^{-1} the relationship, $Q= Nq/3.6$ (10), is derived.
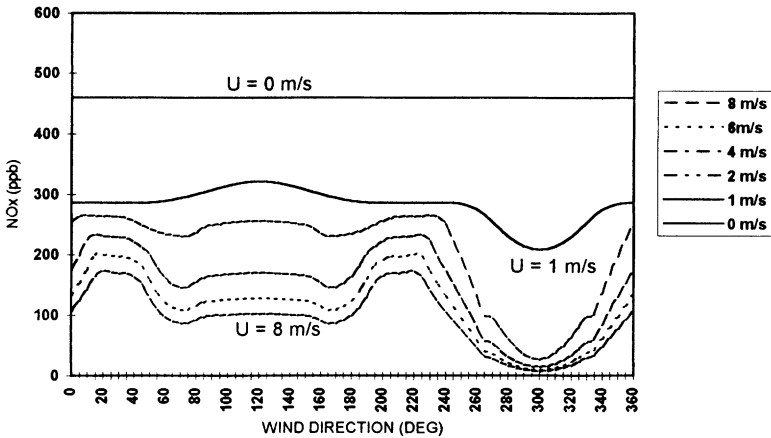
Fig. 4. This study's computed concentrations of NOx for Jagtvej.

Table I shows the road transport emission factors used, Gillham et al (1992). These factors were part of the UK National Emissions Inventory and were broken down into at least eight classes of vehicle. Emission figures from the Design Manual for Roads and Bridges (TRL, 1994) were not used as they are only broken down into two types of vehicle, light duty and heavy duty vehicles.

In the census most categories had readily available emission factors. However a weighted factor was calculated where no distinction was made between cars and light goods vehicles and the types of fuel run on. The London Transport Survey (1991) indicates a ratio of petrol to DERV cars of 9:1 giving an effective factor of 2.11 for NO_x and 19.36 for CO. For light goods vehicles the survey gives a ratio of 1:1 between petrol and diesel, giving a factor of 1.485 and 11.2 for NO_x and CO respectively. These were the factors used in the 1991 census.

The 1989 and 1993 censuses however only had the classification 'light traffic'. The Department of Transport (DoT) count showed that 92% would be cars and taxis with the remaining 8% composed of light goods vehicles. The effective transport factors were calculated to be 2.06 for NO_x and 18.71 for CO. The above counts were also used to derive the traffic intensities of cars and heavy vehicles (N_c and N_h) to calculate traffic induced turbulence (Equation 5). A value of 4.8 m/s was provided by the DoT as a typical speed of busy urban traffic (V_c and V_h).

The nearest meteorological data was from London Weather Centre, which was located at two different sites within the period of study. The older station was operational up to August 1992 at a height of 70 metres above ground level. After August 1992 the station moved a short distance to a new site 48 metres above ground level. Both sites are about 5 km from Cromwell Road so that being in the same geographical area any differences in the pattern of airflow between the locations are expected to have been marginal. The values of the recorded winds were logarithmically reduced to roof and street levels.

The model was run for all weekdays in November 1989, September 1991 and June 1993 to calculate concentrations of NO_x and CO for the hours 0700-1900. It was necessary to add the background concentration, C_b , to produce a final model concentration . Measurements made at Minster House, Vauxhall Bridge were added for November 1989 and measurements at Bridge Place (near Victoria railway station) were added for the other two months. Both sites were considered representative of background levels and any difference between them was considered unsubstantial. They are within 3 km of Cromwell Road. Neither site is near heavily trafficked roads.

Figure 6 is the resulting scatter and time series plots for modelled NO_x against the corresponding observations at Cromwell Road for November 1989. Linear regression analysis was performed using the "least squares method" with the regression line forced through the origin. The full set of equations and correlation coefficients (R) are displayed in Table II.

November 1989's results are clearly the best with the regression lines' gradients approaching 1, and R of nearly 0.8 for both pollutants. For June 1993 there is a disappointing degree of scatter, negative R and gradients significantly above 1. The time series plots confirm the poor agreement as well as the over-calculation of mixing ratios. (Figure 7). September 1991's results were intermediate with gradients close to 1, and R of 0.387 and 0.32 for NO_x and CO.

<div align="center">

TABLE I
Road transport emission factors for urban traffic flow (g km^{-1})

</div>

Vehicle Type	NO_x	CO
Petrol Cars	2.27	21.40
DERV Cars	0.70	1.00
LGV Petrol	2.27	21.40
LGV DERV	0.70	1.00
Medium HGV	12.60	6.00
Large HGV	16.95	7.30
Bus	14.40	6.60
Motorcycle	0.30	20.00

<div align="center">

TABLE II
Sets of equations of best line fit and correlation coefficients for NOx and CO

</div>

MONTH	NOx		CO	
	EQUATION	R	EQUATION	R
NOVEMBER 1989	y=0.8452x	+0.781	y=0.9264x	+0.817
SEPTEMBER 1991	y=0.9476x	+0.387	y=0.8666x	+0.320
JUNE 1993	y=1.2561x	-0.316	y=1.5162x	-0.677

Another way of expressing the model agreement is the error function, E, given by the expression **E = (Calculated Mixing Ratio/Measured Mixing Ratio) (11)**. Table III shows the mean errors for each month. The pattern is similar, November showing an average under-calculation generally $\cong 20\%$ for both pollutants, September having the same bias but with greater variation and June showing an average over-estimate $\cong 28\%$ for NO_x and $\cong 66\%$ for CO.

TABLE III.
Errors in model calculation for Cromwell Road.

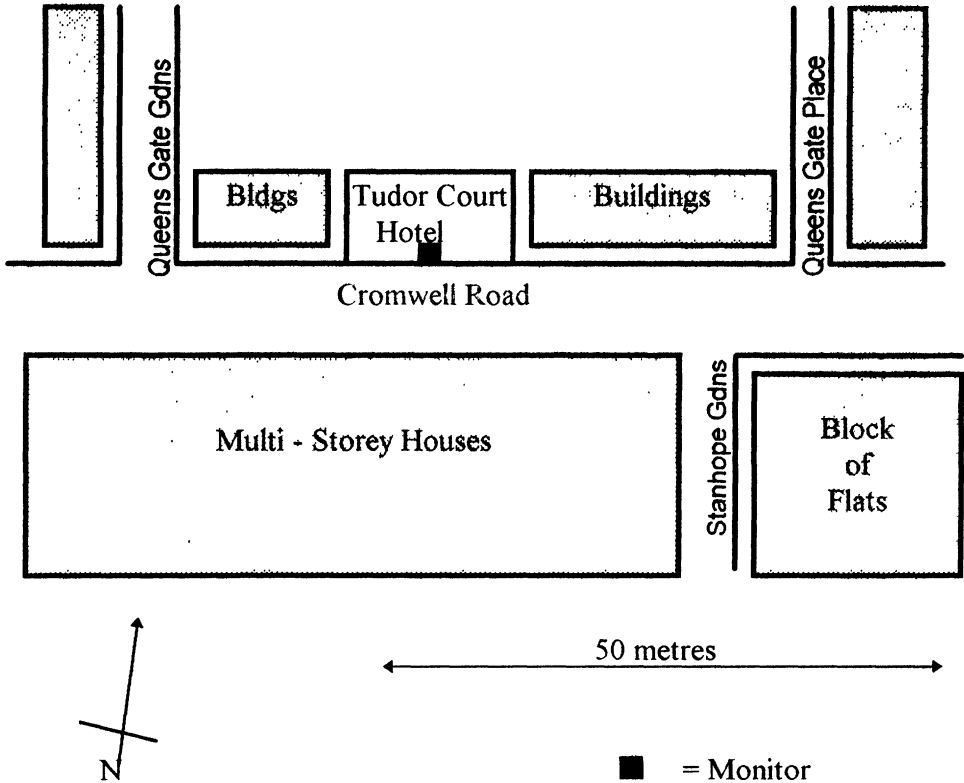| MONTH	$E(NO_x)$	$E(CO)$
NOVEMBER 1989	0.801	0.777
SEPTEMBER 1991	0.648	0.884
JUNE 1993	1.277	1.664

Fig. 5. Sketch map of Cromwell Road.

The cause for the differing performance of the model is uncertain. Changes in the meteorological and background monitoring sites selected were discounted as relatively insignificant. The calculated errors were plotted against temperature, wind speed and direction, sensible heat flux, boundary layer height and Pasquill stability. None gave any notable correlation with the exception of wind direction that showed consistent under-estimation of measured mixing ratios for wind directions between about 150° and 210° for all 3 months. A possible explanation is that at these directions the wind might funnel through Stanhope Gardens and alter the street vortex within Cromwell Road.

There is also the possibility of temporal or seasonal variation of emissions. This study covers a period in which considerable change in the composition of traffic occurred. There has been the advent of the three way catalyst and dramatic increases in diesel sales that would both lead to a reduction in NOx and CO emissions.

Lastly there is the factor of high insolation during the summer. Cromwell Road lies East-West so that on a warm, sunny day the buildings on the north side will be strongly heated. This could lead to a flow venting pollutants out of the canyon or interacting with the street vortex in some way. The model generally calculates excessive concentrations for June 1993, despite the indication from the London Daily Weather Summaries that this month was not especially warm or sunny. Only a suitable field experiment might properly explain this problem.

November 1989
Calculated NOx Vs Measured NOx

$y = 0.8452x$
$R = 0.781$

November 1989
Time Series of Measured and Calculated NOx

Measured NOx ········Calculated NOx
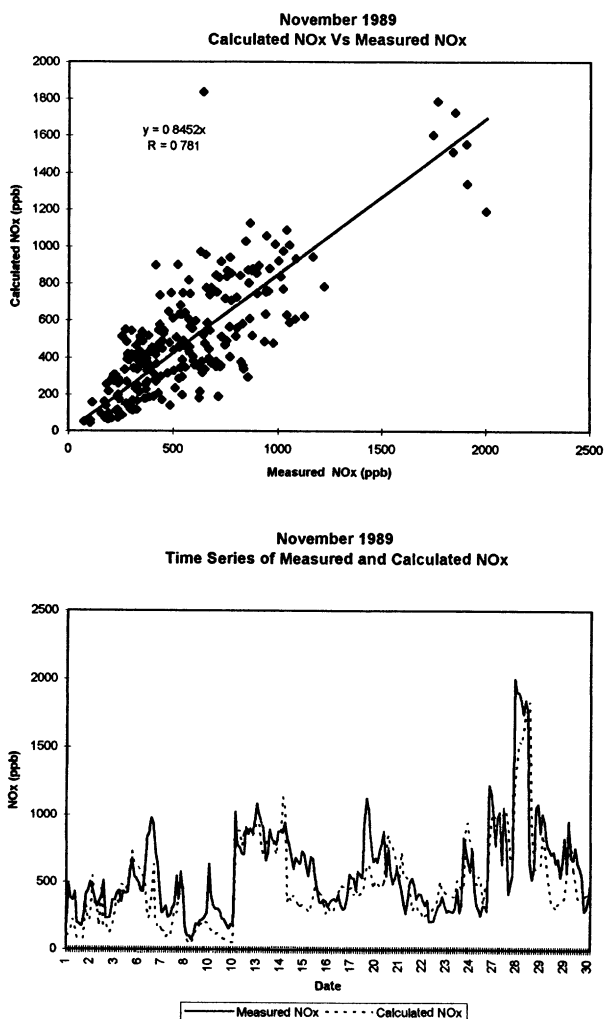
Fig. 6. Scatter and time series plots of NOx for Cromwell Road - November 1989.

4.3. APPLICATION TO STRATFORD ROAD SITE

Figure 8 is the sketch plan of the site. Stratford Road is part of the A34 route into the South of Birmingham, again well trafficked and in a well built-up area. The monitor is situated in front of a row of shops, specifically outside No 828 on the plan. Just to the north there is a pelican crossing. Unlike Cromwell Road the buildings have different heights and the canyon height to width ratio is well below 1. The street axis is close to NNW- SSE and the intersections with Greswolde Road and Grove Road are over 100 metres from the monitor.

Hourly traffic data was available from Saturday 13 May to Friday 19 May 1995. All 24 hours were represented and the traffic categorised into cars and light goods vehicles; medium goods vehicles; HGVs and buses/coaches. The census was assumed to be representative of traffic for a typical week so that extrapolation was performed to cover the month. Q was calculated as before. Average hourly traffic speeds had also been measured so that V_c and V_h were varied instead of being assumed constant as for Cromwell Road (Equation 5).

The nearest meteorological data was from Birmingham Airport (7-8 km distant) and the winds obtained were for a level of 10 metres. The winds were adjusted as before to provide winds at roof and street level. Again any differences in the pattern of airflow between the two locations are expected to have been marginal.

The background concentrations of NO_x and CO were obtained from Centenary Square, a monitoring site in Central Birmingham (5-6 km distant). This site is not located near heavily trafficked roads. Figure 9 shows the resulting scatter plot of modelled against observed concentrations for CO. On the plot a significant number of points deviate from the line of perfect agreement, i.e. y=x, with most of the error through under-calculation. A similar pattern occurs for NOx.

The ratio of measured to calculated concentrations were plotted against parameters such as hour of the day and wind speed and direction. Interestingly for both pollutants the ratio appeared at its greatest for wind directions between 0 and 90° which suggests that there are source or sources of NOx and CO in the NE quadrant. Filtering out those points associated with these wind directions removes many of the points significantly below the y=x line.

The remaining points, well below the line, have no obvious explanation except that only a very few occur at night, virtually all occurring between 0600 and 2200. One explanation put forward is that the pelican crossing interrupts the traffic flow. The result may be a modest increase in NOx emissions through accelerating traffic and a large increase in CO emissions from idling engines. No adjustment of emission factors for vehicle speed could be made as a detailed census of vehicle flow was not available.
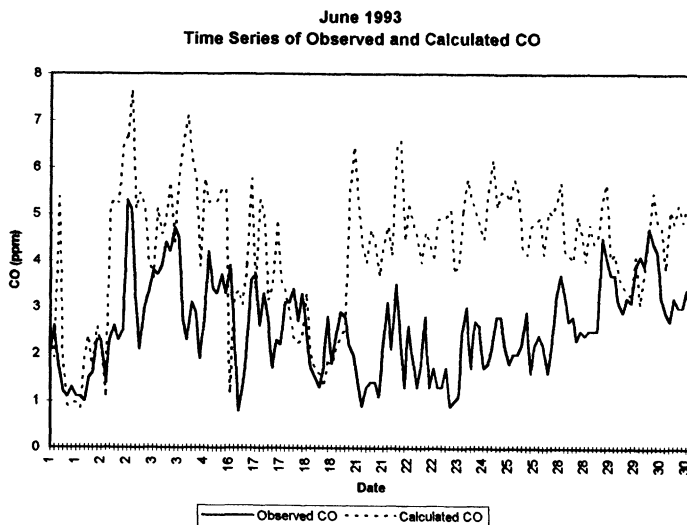
Fig. 7. Time series plot of CO for Cromwell Road - June 1993.

5. Conclusions

This paper describes research to adapt and validate Hertel and Berkowicz's street canyon model to measurements made at heavily trafficked sites in London and Birmingham. This is important because levels of pollution at a kerbside site are often significantly higher than the general urban background concentrations. Also, because of the proximity to areas of general access (e.g. shops, parks, etc.) there is considerable exposure to traffic pollutants for the public.

This work was performed as part of a study to assess the accuracy and validity on the emission factors used to compile national emission inventories. The emission figures from the Department of the Environment (DoE) are derived from measurements taken from samples of vehicle exhausts. These sample sizes vary from 10's to 100's whereas many thousands of vehicles pass these sites each day. The fact that the model produced at least reasonable estimates and at best excellent agreement, vindicates the use of the national vehicle emission factors in the inventories.

Finally the problems such as the emission rates with interrupted traffic flow and the possible change in the street vortex during the summer represent the difficulty in modelling the real world. To the author's knowledge these are at present the two best canyon sites in the UK. However to obtain an ultimately rigorous validation a site should have the following requirements.

1. There should be pollution monitoring on both sides of the street. Measured leeward and windward concentrations would be available thereby enabling the difference between the two to be compared with the difference between their computed counterparts. Hence say **measured** (C_{LEE} - C_{WIND}) would be compared with the **computed** (C_{LEE} - C_{WIND}) with no need for a background quantity.
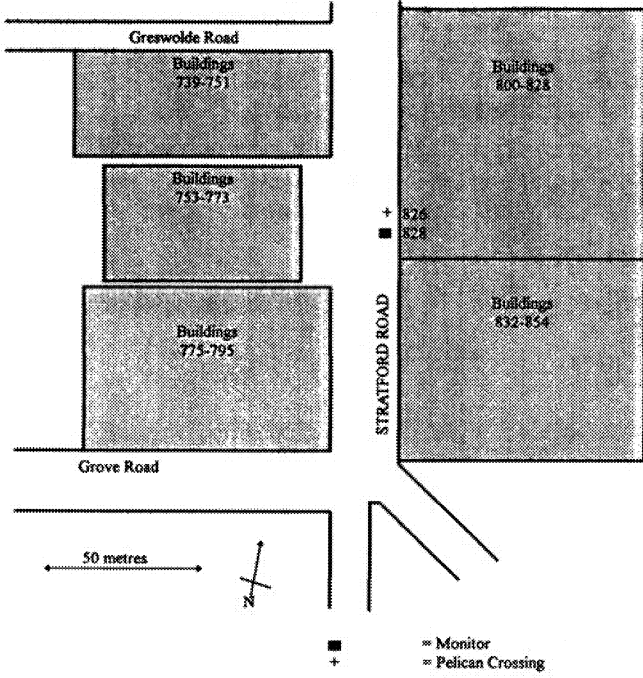
Fig. 8. Sketch map of Stratford Road.
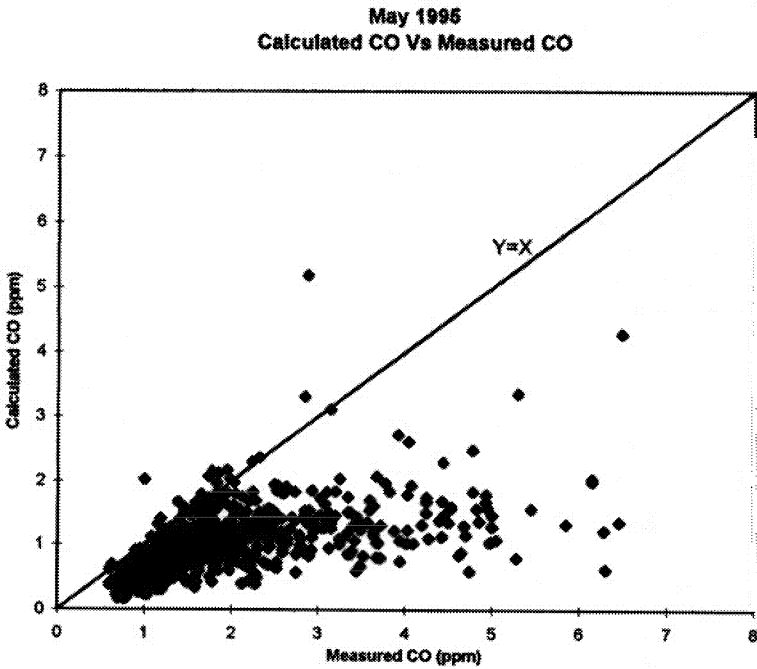
Fig. 9. Scatter plots of CO for Stratford Road - May 1995.

2. It would remain prudent to have background monitoring at four major directions to the canyon site.
3. The canyon should ideally have uniform sides for some distance from the monitor. The street height to width ratio should not vary greatly from 1.
4. There should be no side streets or major intersections for some distance (at least 100 metres) from the monitor. Likewise there should be no zebra or pelican crossings or other features that would interfere with the traffic flow.
5. There should ideally be constant hourly measurements of traffic volume analogous to the hourly measurement of pollutants. There should be a full breakdown of traffic by type of vehicle, fuel and catalytic convertor.
6. An understanding should be acquired as to how the street vortex is modified when the canyon is subjected to strong solar heating and how this relates to wind direction.

Acknowledgments

References

Berkowicz, R.., Hertel, O., Sorensen, N.N., Michelsen, J.A.: 1994 *Modelling Air Pollution From Traffic in Urban Areas: IMA Conference on 'Flow and Dispersion Through Groups of Obstacles'* Cambridge 28-30/3/1994.

Eggleston, H., Gaudioso, D., Goriben, N., Joumard, R., Rijkeboer, R.C., Samaras, Z., Zierock, K.H.: 1991 *CORINAIR Working Group on Emission Factors for Calculating 1990 Emissions From Road Traffic* Volume 1 Commision of the European Communities, Final Report Contract B4-3045 (91) 10PH

Gillham, C.A., Leech, P.K., Eggleston, H.S.: 1992 *UK Emissions of Air Pollutants 1970-1990* DOE Document LR887 (AP)

Hertel, O. and Berkowicz, R.: 1989 *Modelling Pollution From Traffic in a Street Canyon. Evaluation of Data and Model Development.* National Environment Research Institute, Denmark Report DMU Luft A129

Hertel, O. and Berkowicz, R.: 1989 *Modelling NO$_2$ Concentrations in a Street Canyon.* National Environment Research Institute, Denmark Report DMU Luft A131

Hertel, O. and Berkowicz, R.: 1989 *Operational Street Pollution Model (OSPM). Evaluation of the Model Data From St Olavs Street in Oslo.* National Environment Research Institute, Denmark Report DMU Luft A135

Hertel, O. and Berkowicz, R.: 1991 *The Operational Street Pollution Model (OSPM). Air Pollution Modelling and its Application* Ed van Dop, H. and Steyn, D.G., Plenum Press, New York.

Johnson, W.B., Ludwig, F.L, Dabberdt, W.F. and Allen, R.J.: 1973 *J. Air Pollut. Control Ass.* **23**, 490-498

Design Manual for Roads and Bridges - Volume 11 Section 3 Part 1 - Air Quality: 1994 Transport Research Laboratory

Travel in London - London Area Transport Survey 1991: 1994 London: HMSO.

Yamartino, R.J. and Wiegard, G.: 1986 *Atmos Envir* **20**, 2137-2156

A SIMPLE MODEL OF POLLUTANT CONCENTRATIONS IN A STREET CANYON

A. A. HASSAN and J. M. CROWTHER

Department of Physical Sciences, Glasgow Caledonian University,
Glasgow G4 0BA, Scotland, U K

Abstract. A single compartment model has been constructed for predicting hourly concentrationsof pollutant concentrations arising from vehicular emissions within a typical street canyon The model takes account of traffic densities and composition to estimate pollutant emissions within the model compartment Meteorological data on wind speed and direction are used to define the exchanges of pollutants between the compartment and the surrounding air   A parameter is also included to describe the exchange in calm conditions. The pollutant concentrations are then estimated from a steady state mass balance equation for the compartment, assuming conservation of pollutants The model was applied to the prediction of carbon monoxide concentrations in Hope Street, Glasgow   Model parameters were fitted using field measurements, together with concurrent meteorological data and traffic flows estimated from traffic census data for Hope Street The model accounted well for the observed variations in carbon monoxide   It was found that the model parameters varied seasonally, perhaps due to differences in atmospheric stability which have not so far been included in the model formulation

1. Introduction

The term "street canyon" refers to a relatively narrow street between buildings which line up continuously along both sides (Nicholson, 1975).   The prediction of pollutant concentrations in street canyons has great importance because it is those concentrations to which a large part of the population are exposed. The simple empirical model described in this paper was developed for the prediction of hourly concentrations of carbon monoxide (CO) in a particular street canyon (Hope Street, Glasgow: see Fig. 3).   The model is based on the analysis of measured concentrations, meteorological conditions, and emissions estimated from traffic data. The model development has focused on carbon monoxide since it is injurious to human health but relatively inert in the atmosphere, with no significant natural sources or sinks below chimney levels in urban areas. The most important source of CO in the outdoor, urban environment is the motor vehicle and we may investigate the exposure of human beings within a street canyon by modelling the emissions of a conserved tracer (CO) by vehicles into the street canyon, which is ventilated by wind, convection, and vehicle movements.

  The present problem can be simplified by considering a control volume representing the street canyon and applying the principle of mass conservation of pollutants inside the control volume. The model requires only available meteorological data (wind speed and wind direction) and traffic data to give hourly concentrations of carbon monoxide. Several thermal and dynamic urban effects on air flow (such as heat island circulation, buoyant accelerations of exhaust gases, turbulence in the wakes of buildings and vortex circulation produced in street canyons) contribute to dispersion of street-level pollution but are not treated explicitly in the model but in a simple way through empirical model parameters.

2. The Box Model

Air pollution models can range from the simple to the complex. The single box model is the simplest air pollution model and is based on the mass conservation of pollutants inside an Eulerian box, which generally represents a large area such as a city (Lettau, 1970). The atmosphere over the modelling region and within the box is perceived as well-mixed, and the evolution of pollutants in the box is calculated by the conservation of mass principle, including emission, deposition, and chemical reactions. The physical concept underlying the box model approach and the notation are depicted in Fig. 1, where the box covers an area of length L and width W and extends to a height H which is much greater than the building heights.
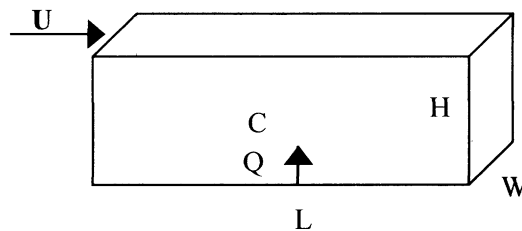
H indicates the time varying mixing height,
L, W are the horizontal dimensions of the box;
C is the average concentration inside the box;
Q is the emission rate per unit area;
U is the constant wind speed entering the box, measured at
a nearby meteorological station.

Fig 1 The single box model

The principle of conservation of mass gives:

$$\frac{\partial(LHWC)}{\partial t} = QLW - CUWH \qquad (1)$$

For a steady state, i.e. $\partial C / \partial t = 0$, Equ. 1 becomes :

$$C = \frac{QL}{UH} \qquad (2)$$

The single box model has frequently been used for predicting both inert and reactive pollutants in cities. Mészáros *et al.* (1978) used the box model for computing the atmospheric sulphur budget over Europe. Jensen and Peterson (1979) used the box model for predicting SO_2 concentrations in a large city, and found good agreement between model results and measurements. Derwent *et al.* (1995) interpreted air quality data from a one year study at an urban roadside location in central London by using simple

statistical techniques, including a box model. It is assumed in the large urban area models that there is no vertical transfer of pollutants through the top of the box, which would either be an inversion layer or the upper limit of the "plume" of pollutants from the urban area within the box. There is an implicit assumption that the pollutants are well-mixed within the volume. With these assumptions the concentration of pollutants in the box is proportional to the emission rate and inversely proportional to the wind speed. The relationships between the wind speed and pollutant concentrations have been widely explored (e.g. Gifford and Hanna, 1973; Simpson, 1992; Benarie, 1980) and confirm that the concentration of pollutants is inversely proportional to the wind speed. In this study also, a negative correlation was found between wind speed and the measured pollutant concentrations in Hope Street (Apling *et al.*, 1981).

Although the Leatu model is intended for application to a whole-city volume of air, it appears to be suitable for application to a control volume of a single street. For example, the street canyon "budget box model" has been developed by Nicholson (1975) to predict average carbon monoxide concentration in street canyons. Input data were wind speed, wind direction and total pollution emission rate. In a street canyon, when the roof-level wind flows perpendicular to the street, a vortex circulation develops with upward transport on the up-wind side and downward transport on the down-wind side, resulting in higher pollution levels at the up-wind side than at the down-wind side. Vortex velocity is predicted by assuming logarithmic wind profiles above the building and street and using the continuity equation. For winds parallel to the street, a bulk wind is predicted by assuming an exponential wind profile in the canyon. Nicholson found that vertical transport was the primary transport when the wind was blowing perpendicular to the street.

A field study of tracer dispersion from an urban street canyon has been analysed by DePaul and Sheih (1985) in order to obtain measurements of pollutant retention times and resulting concentration within the canyon. The retention time is defined as the length of time for a pollutant concentration with its source turned off to reach e^{-1} of its original value. The experiment was conducted in the "South Loop" area of central Chicago. The canyon walls were continuous in the length of one block (80 m), 33.5 m in height on the west side, 40 m on the east side, and the canyon width was 24.5 m. Meteorological data, including the ambient wind speed and wind direction, were measured at a height of 3 m above the upwind roof top. A continuous line source within the canyon was simulated with SF_6, released along the street length at the ground level from tubing with a series of critical orifices uniformly spaced at 2 m intervals. The tracer gas concentrations were measured at various sampling points. The estimates of concentration decay were made by turning off the source after a quasi-steady concentration within the canyon had been reached and then taking measurements.

DePaul *et al.*, (1985) simplified the budget problem by considering a control volume of the street with unit width and applying the conservation of mass to calculate retention time and to predict steady-state concentrations within the canyon. The pollutant retention times were found to range from 0.7 to 3.8 minutes for ambient winds perpendicular to the street between 1.7 and 4.5 m s^{-1}. The corresponding ventilation (vertical) velocity, computed from the retention times, was found to range from 0.15 to 0.8 m s^{-1}.

3. Model formulation

In this study, the box model was applied for an individual street (Hope Street, Glasgow, see Fig. 3) to predict hourly concentrations for inert pollutants (specifically, carbon monoxide) in terms of meteorological data measured at Glasgow Airport and carbon monoxide emission rate in the street. Such simple, empirical, air quality models are not intended to describe explicitly the physical mechanism of air pollutant dispersion, but rather to give an estimate of the mean concentration of the pollutant elements in a simple way. In this study a regression model of the dispersion of CO was developed, based on the mass conservation of pollutants inside a control volume of the street, as illustrated in Fig. 2.
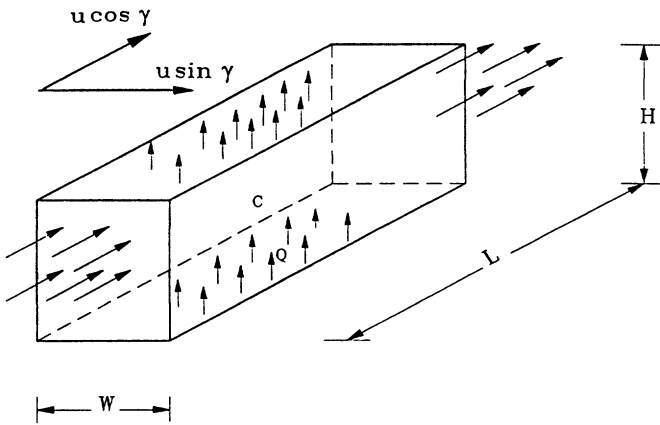
Fig 2 Single Box model application in individual street
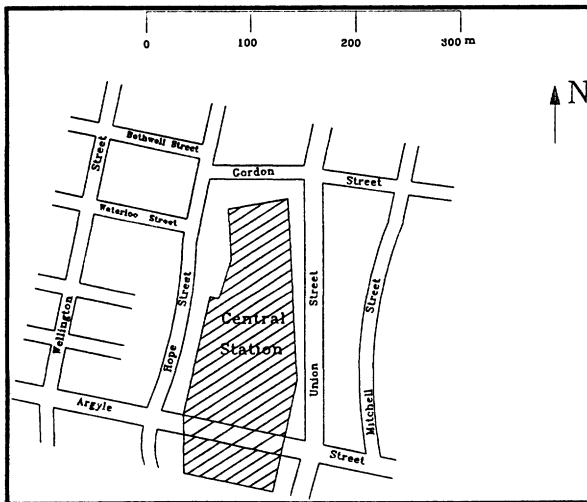
Fig. 3 Sketch map showing the location of Hope Street

The measurement site (Apling *et al.*, 1981) was at the Central Hotel, Glasgow Central Station, on the east side of Hope Street (Fig. 3), approximately 0.5 m in from the road edge and at a height of 2.5 m above the road. It must be emphasised here that the box model is applied with the following assumptions, as shown in Fig. 2 :

1. The box is taken to be rectangular with dimensions: street length L = 160 m, street width W = 17 m between buildings, and building height H = 22 m.
2. The flux of pollutants into or out of the box takes place through the top and ends of the box.
3. There is no deposition within the box.
4. The pollutant source strength is related to vehicular traffic and the pollutants are well-mixed inside the box.
5. The wind speed at roof top, u, is related to the wind speed, U, at a nearby meteorological station (Glasgow Airport, Abbotsinch in this study) by the constant relationship $u = \eta U$.
6. The wind direction does not change between the meteorological site (Abbotsinch) and Hope Street, and makes an angle γ to the street, so that the roof top longitudinal and transverse components of wind speed are $\eta U \cos\gamma$ and $\eta U \sin\gamma$, respectively.
7. Steady state conditions over a time interval and a non-reactive (inert) pollutant.

Equation 1 now takes the form:

$$\frac{\partial(LHWC)}{\partial t} = QLW - (C - C_0)u_E WH - (C - C_0)v_E WL - k_3(C - C_0) \quad (3)$$

where:
C = concentration measured anywhere inside the box (mg m^{-1}),
C_0 = outside concentration (background concentration) (mg m^{-3}), and
Q = source strength (mg m^{-2} s^{-1}),
v_E = ventilation velocity from canyon top = $k_2 \eta U \sin\gamma$
u_E = flushing velocity from canyon ends = $k_1 \eta U \cos\gamma$
k_1 = proportionality constant for the longitudinal component of wind
k_2 = proportionality constant for the transverse component of wind
k_3 = constant for ventilation of the street in calm conditions (m^3 s^{-1}).

Assuming a steady state, $\partial C / \partial t = 0$, the total loss of pollutant across the top and the end of the street is equal to the rate of production, E = QLW, and therefore:

$$C = C_0 + \frac{E}{(k_1 \eta U \cos\gamma)WH + (k_2 \eta U \sin\gamma)WL + k_3} \quad (4)$$

In the next two sections we examine the relationship between the local wind speed and the wind speed at Glasgow airport and the vehicle pollutant emission rate E for carbon monoxide.

4. Relationship between local and airport wind speeds

Since the proposed model predicts concentrations of pollutants in terms of measured data from a meteorological station, it is very important to link the wind speed above the street, u, to the wind speed, U, at the nearest meteorological station. Hourly mean wind speeds are measured at a height of 10 m over a grass covered plain (aerodynamic roughness length = 0.03 m) at Glasgow Airport, Abbotsinch, approximately 12 km away. It is assumed that there is a constant ratio, η = u/U, between local wind speed and measured wind speed at the meteorological station. A significant correlation was found between the locally measured wind speed and measured wind speed at the airport. Table I shows the correlation coefficient, R, and regression line slope, η, between local measured wind speed at Hope Street (u) and measured wind speed at the meteorological station at Abbostinch, Glasgow, (U). The mean value for the year of the ratio, η, was to be found 0.410 with a standard error of 0.016, giving reasonable confirmation of constancy.

Table I
Correlation coefficient, R, and regression line slope, η, between local measured wind speed at Hope Street (u) and measured wind speed at the Glasgow Airport meteorological station, Abbostinch (U)

Month	R	η
Jan.	0.896	0.433±0.002
Feb.	0.923	0.436±0.018
Mar.	0.933	0.366±0.010
Apr.	0.751	0.355±0.021
May	0.702	0.354±0.019
Gun	0.883	0.406±0.016
July	0.901	0.344±0.013
Aug.	0.874	0.421±0.015
Sep.	0.889	0.365±0.014
Oct.	0.827	0.434±0.016
Nov.	0.833	0.485±0.038
Dec.	0.910	0.520±0.041

5. Emission Rates

Emission rates are clearly important because they determine the total quantity of material emitted during the time of interest. A source's emission rate varies with time, over time scales ranging from minutes to hours. In the present study it was assumed that the source of CO is the motor vehicles passing through the street, as there were no industrial establishments close to the study area. The emission rates from motor vehicles depend on various parameters, such as the air-fuel ratio, the physical, and geometrical characteristic of the engine combustion cylinder as well as on the combustion temperature (Seinfeld, 1986). Thus, emission depends fundamentally on the vehicle operation mode: idling, acceleration, cruising or decelerating.

In the present study case there was a lack of detailed information on traffic in Hope Street since it was not equipped with continuous, automatic vehicle-counting equipment. However, for the period of this study, Strathclyde Regional Council Roads Department carried out several manual counts of vehicles entering the Hope Street one-way system at the junction with Argyle Street. These counts correlated well with an inner

city automatic monitoring station at Eglinton Street, Glasgow, which was operated throughout the study period. Based on this correlation in traffic counts, a continuous series of hourly traffic data was constructed for Hope Street, based on the Eglinton Street data.

Emission rates from vehicles depend on the volume of traffic using a street, traffic composition, and the operating mode of the vehicles, which can be expressed as a function of the average speed of the vehicles. In order to simplify the calculation, the following assumptions have been made:

1. All vehicles using a given fuel have similar engine parameters.
2. All streets have a similar traffic profile during the day.
3. In cases where data on traffic composition are missing, vehicles are grouped into two categories according to fuel type used, petrol and diesel, with an assumed percentage of petrol vehicles being 70%.
4. The mean vehicle speed is 20 km h^{-1} (to represent the engine operating mode).

According to the above-mentioned assumptions, the emission factors from motor vehicles must be expressed as a function of the average running speed. The carbon monoxide emission factors for petrol and diesel engines are assumed to be 35 and 3.5 g km^{-1}, respectively, for vehicles running at 20 km h^{-1} average speed. The emission factors have been estimated by Bardeschi *et al.* (1991) from the emission factors determined experimentally by Jounard (1987) for some vehicle samples representative of the 1987 running motor vehicles in France. Thus the following simple expression is used to calculate line source emission:

$$E = \frac{(0.7 \, F_p + 0.3 \, F_d)T \, L}{3600} \tag{5}$$

where:

F_p and F_d are carbon monoxide emission factors for petrol and diesel engines, respectively (mg m^{-1} vehicle^{-1}),
L is the street length (m),
T is the traffic flow, (vehicles h^{-1}).

Hence Equ. 4 becomes:

$$C = C_0 + \frac{(0.7 \, F_p + 0.3 \, F_d) \, T \, L}{3600\big((k_1 \eta U \cos\gamma)WH + (k_2 \eta U \sin\gamma)WL + k_3\big)} \tag{6}$$

6. Results and Discussion

The empirical model equation (Equ. 6) has been applied to the meteorological and air pollution data (CO) for 1979 in the control volume of Hope Street, Glasgow, with dimensions 160, 17 and 22 m, length, width and height, respectively (Fig. 3) and assuming the background concentrations of CO (C_o in Equ. 6) to be equal to zero. This is, of course, an unrealistic assumption but no CO background concentration data were available, and attempts to fit the model with C_o as a constant parameter gave no significant improvement in model accuracy. Variable input data required for the model analysis are: C (hourly concentrations of CO), E (total emission rate of CO within the control volume), $\eta U \cos\gamma$ (longitudinal component of wind speed) and $\eta U \sin\gamma$ (transverse component of wind speed). The model parameters are k_1, k_2, and k_3 which were optimised using a non-linear least squares analysis package: TSP (Time Series Package). Table II and Figs. 4 to 9 show the model parameters, k_1, k_2, k_3 and fitted concentration data for six months.

Table II
The model parameters

Month	k_1	k_2	k_3
Apr.	0.033±0.007	0.005±0.0007	40.3±2.2
Jun.	0.057±0.01	0.016±0.001	64.0±2.3
July	0.089±0.03	0.029±0.003	94.1±4.4
Oct.	0.021±0.009	0.003±0.001	41.2±4.8
Nov.	0.057±0.007	0.005±0.0009	24.3±0.97
Dec.	0.07±0.008	0.007±0.0008	29.8±1.2

The results indicate that the model parameters vary from month to month, presumably representing the varying weather conditions, such as atmospheric stability (Pasquill, 1974; Pasquill and Smith, 1983), which are not included in the model. It was found that k_2 and k_3 were higher in summer than winter. This is consistent with the vertical pollutant flux in summer being greater than in winter because the atmosphere tends to be more unstable. For example, ventilation velocities in July and December are 0.116 m s^{-1} and 0.028 m s^{-1}, respectively, for an ambient wind speed perpendicular to the street equal to 4 m s^{-1}.

     The analysis of the measured CO concentrations shows that the daily concentrations tend to have two peaks, the maximum concentrations occurring in the morning between 0800 and 0900 h and in the evening between 1700 and 1800 h, i.e. the traffic rush hours. The minimum concentrations are between 0300 and 0500 h, when traffic flows are weakest. The concentrations calculated by the box model generally correspond with the above maximum and minimum peaks (Figs. 4 to 9).
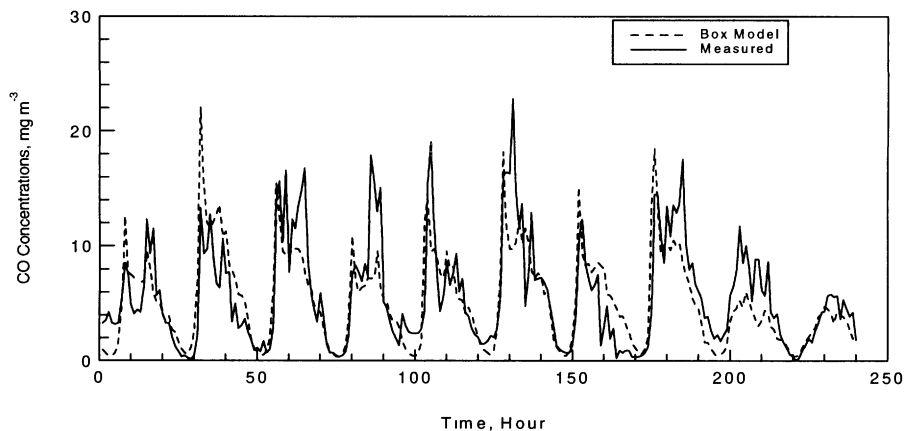
Fig. 4   The hourly simple model calculated and measured concentrations for
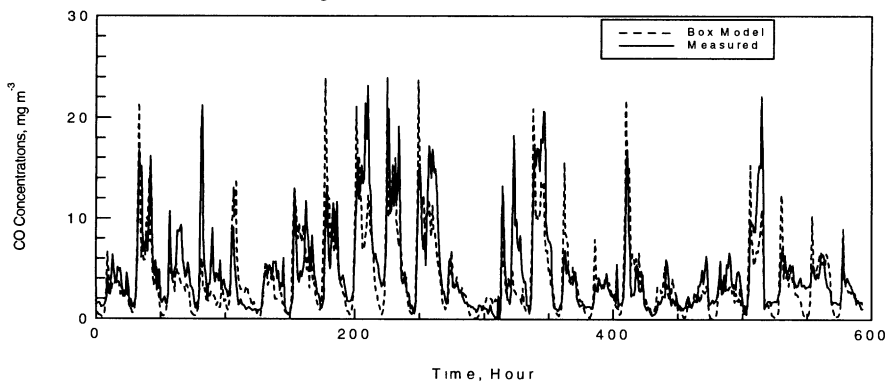CO during October 1979 (240 observations)

Fig. 5   The hourly simple model calculated and measured concentrations
for CO during November 1979 (593observations)
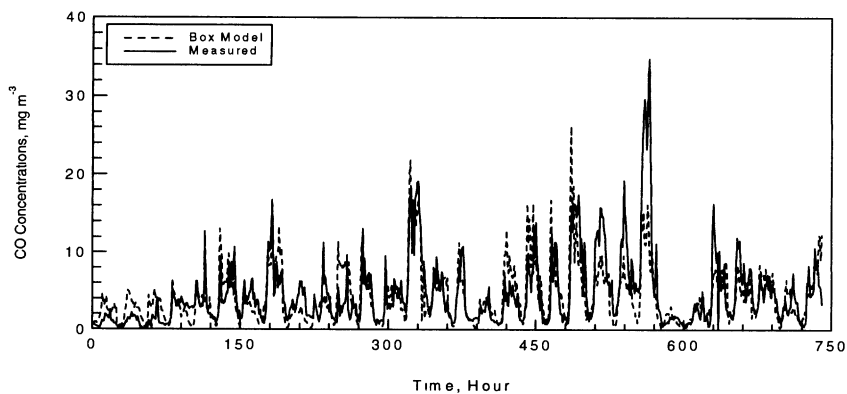

Fig. 6   The hourly simple model calculated and measured concentrations
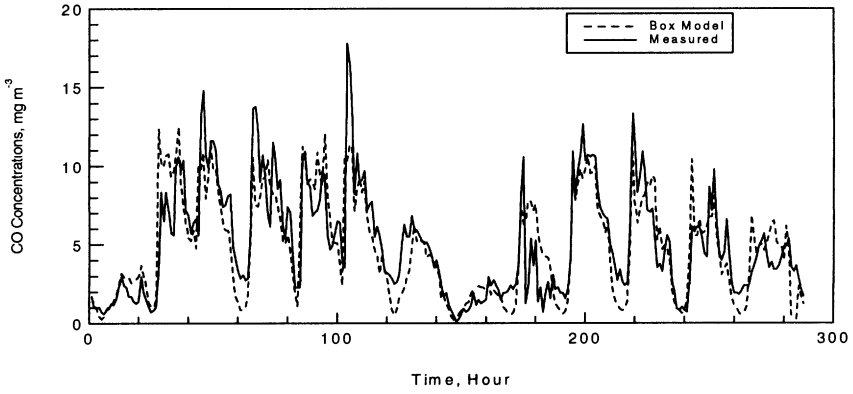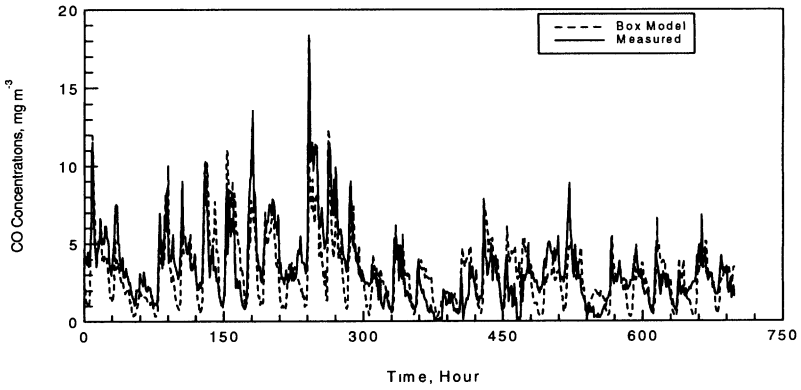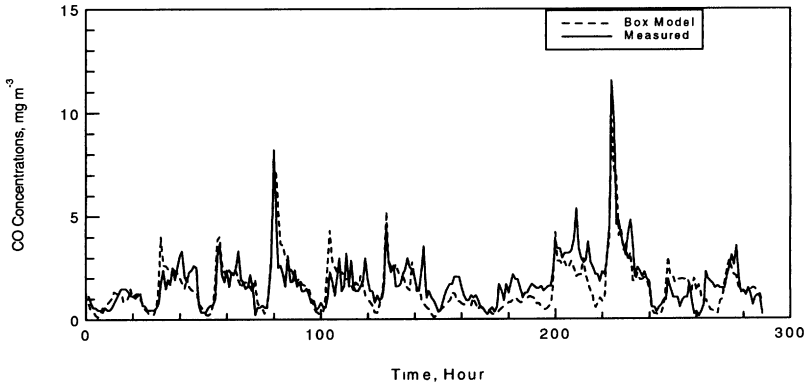for CO during December 1979 (740 observations)

Fig. 7 The hourly simple model calculated and measured concentrations for CO during April 1979 (288 observations)

Fig. 8 The hourly simple model calculated and measured concentrations for CO during June 1979 (698 observations)

Fig. 9 The hourly simple model calculated and measured concentrations for CO during July 1979 (288 observations)

6. Sensitivity of the Model Parameters

The accuracy of the estimated parameters and also the sensitivity of the predicted CO concentration to the calculated model parameters k_1, k_2 and k_3 was examined in order to determine which parameters are significant and which parameters have the greatest effect. These examinations were carried out by calculating the percentage change in concentration when each parameter was increased by 10 % of its fitted value. The results are summarised in Table III. It is clear that the parameter k_3 has a significant effect and so the model would benefit from a more explicit treatment of stability effects, important at low wind speeds.

Table III
Sensitivity of the model parameters

Months	$(C-C_{k1+0.1k1})/C$ %	$(C-C_{k2+0.1k2})/C$ %	$(C-C_{k3+0.1k3})/C$ %
Apr.	1.4	2.4	5.8
Jun	1.0	3.5	5.0
July	1.2	4.3	4.1
Oct.	1.0	1.9	6.7
Nov.	2.8	2	4.7
Dec.	2.7	2.4	4.5

7. Conclusions

The box model presented here predicts a measured concentration at a single sampling point in Hope Street Glasgow in terms of the assumed concentration within the box, which is an average steady state value assumed to apply everywhere within that box. The agreement with the measured data is very good considering the simplicity of the model. The fine details of peaks and troughs are not always reproduced well but this is to be expected when comparing a point measurement with a spatial and temporal average. The model may be expected to perform well in other street canyons but the model parameters will have to be determined afresh to obtain the best fit.

The main difficulty with the model is that the parameters are not constant from month to month, with significant differences between summer and winter. Further work is required to fit several complete years of data to see whether the model parameters follow a discernible seasonal pattern. The model is most sensitive to the parameter k_3 which is required for calm conditions but this could possibly be linked to atmospheric stability class. Stability data are available from the Meteorological Office, and k_3 could be replaced by a formula involving stability class and a different model parameter. This will be investigated in further work and could lead to a better fit with the data and to a lower sensitivity of the predictions to the new parameter.

280

Acknowledgements

References

Apling, A. J., Dorling, T. B., Lilley, K. B., Rogers, F. S. M., Stevenson, K. J. : 1981, *Survey of gaseous air pollutants at selected UK sites. VII. Data digest for Hope Street, Glasgow, 1978-1980.* Report LR 403 (AP), Warren Spring Laboratory,Stevenage.

Bardeschi, A., Colucci A., Gianelle V., Gnagnetti M., Tamponi M., Tebaldi G: 1991, *Atmos. Environ.* **25B**, 415-428.

Benarie, M.: 1980, *Urban air pollution modelling.* Macmillan, London.

DePaul, F. T., Sheih, C. M.: 1985, *Atmos. Environ.* **19**, 555-599.

Derwent, R. G., Middleton, D. R.: 1995, *Atmos. Environ.* **29**, 923-946.

Gifford, F. A., Hanna, S. R.: 1973, *Atmos. Environ.* **7**, 131-136.

Jensen, N. O., Petersen, E. L.:1979, *Atmos. Environ.* **13**, 717-720.

Jounard R.: 1987, *Emissions unitaires des vehicules legers.* Laboratoire Energies Nuisance-Case 24-F 69675, Institut National de Recherche sur les Transports et leurs Securité, Bron Cedex, France.

Lettau, H. H.: 1970, Proceedings of a Symposium of Multiple-Source Urban Diffusion Models, Publication No. AP.86, EPA, USA

Mészáros, G. V., Haszpra, L.: 1978, *Atmos. Environ.* **12**, 2273-2277.

Nicholson, S. E.: 1975, *Atmos. Environ.* **9**, 19-31.

Pasquill, F.: 1974, *Atmospheric diffusion*, 2nd ed., Halsted Press, John Wiley and Sons, New York.

Pasquill, F., Smith, F. B.: 1983: *Atmospheric diffusion*, 3rd ed. Halsted Press, John Wiley and Sons, New York.

Seinfeld, J. H.: 1986, *Atmospheric chemistry and physics of air pollution.* John Wiley and Sons, New York.

Simpson, R. W.: 1992, *Atmos. Environ.* **26B**, 99-105.

MODELLING OF FLUID FLOW AND POLLUTANT DISPERSION IN A STREET CANYON

A.A.Hassan and J.M.Crowther

Department of Physical Sciences, Glasgow Caledonian University
Glasgow G4 0BA, Scotland, UK

Abstract. A two-dimensional steady state numerical simulation has been carried out for a typical street canyon ventilated by a cross-wind. The PHOENICS package from CHAM was used to solve for the air flow above and within the street canyon. The k-epsilon turbulence model was used for turbulence modelling and pollutant sources were added at ground level over the road but not over the pavements. Results for the air flow showed the formation of a longitudinal vortex within the street canyon, as found by other researchers. Pollutant concentrations were predicted with the highest values occurring at the leeward walls of the upwind buildings, and the lowest values on the windward walls of the downwind buildings. The accuracy of these simulations was examined by comparing the predicted results with field observations. Reasonable agreement was obtained, confirming the difference between concentrations on the leeward and windward walls. The results show that the dispersion characteristics can be simulated in terms of structural configurations.

1. Introduction

The term "street canyon" refers to a relatively narrow street between buildings which line up continuously along both sides (Nicholson, 1975). The main source of pollutants in the urban street canyon is the motor vehicle, converting oxygen and fuel to carbon dioxide and water vapour, and emitting various pollutants, such as carbon monoxide, nitric oxide, sulphur dioxide, particulate material, unburnt fuel and several other organic compounds. Some of these pollutants can react with atmospheric oxidants, or with each other to produce secondary products such as nitrogen dioxide, ozone, and sulphuric and nitric acids. The emitted pollutants from motor vehicles thus alter the temperature and composition of the atmosphere through combustion and the introduction of trace gases and particulate material which have potentially injurious effects on human health, vegetation, and materials. The first step in attacking the problem of air pollution is to define the levels at which a pollutant in the atmosphere is considered to be dangerous and have adverse effects. Ambient air quality monitoring is an expensive undertaking and large cities may have only a few monitoring stations. If a location is not being monitored, then how can air pollution control authorities determine the emission rate required from a specific source to meet ambient air quality standards? An answer to this question is to use air quality models both to study the relationship between the source emissions and the resulting atmospheric pollutant concentrations, and also to provide a spatial and temporal interpolation of monitored data.

The prediction of pollutant concentrations within urban street canyons is very important for pedestrians and motorists using the streets and for shop and office staff working in the vicinity. Knowledge of air flow characteristics in and above street canyon is useful, particularly for understanding the mechanisms for transport and dispersion of pollutants from the urban canyon. There have been three main approaches to this problem: full-scale measurements, reduced scale measurements on physical models, and mathematical models.

Full-scale field measurements are the ideal, in the sense that the data are real and unambiguous, but the conditions cannot be controlled and the monitoring points are often few in number and widely positioned. Detailed studies have been conducted to measure the wind characteristics, within real urban canyons by Nunez and Oke (1977), DePaul and Sheih (1986), Nakamura and Oke (1988), and Yamartino and Gotz (1986). These studies generally showed the formation of a vortex within the street canyon but this may not always be the case, especially at low wind speeds. A field study was conducted in three different typical street canyons in Guangzhou city by Qin and Kot (1993) but the wind speed in Guangzhou city is usually low, (the average wind speed during this study being between 0.7 and 0.8 m s^{-1}) and it was rare that a stable vortex was detected in the street canyon. The irregular canyon configurations, low wind speed, and vehicle movement caused air flow in the canyon to be far from ideal and they found that the major factor governing the pollutant dispersion pattern in the street was the canyon configuration, its type and its scale. This same conclusion was reached by Luria *et al.* (1990).

Physical, wind-tunnel model studies are easier to conduct than full-scale studies and can be well-controlled, although inexact boundary conditions and imperfect scaling may introduce errors. Hoydysh and Dabberdt (1988) and Dabberdt and Hoydysh (1991) found that the concentration pattern of pollutants depended on the canyon asymmetry and the aspect ratio of the block, decreasing exponentially in the vertical direction, and being greater on leeward faces than windward faces.

Numerical methods applied to the urban street canyon problem can take several forms: some using a full simulation of the flow field and pollutant transport, and some using empirical models based on field data. Advances in computer hardware technology have provided new opportunities to simulate environmental problems and Johnson *et al.* (1990), Hunter *et al.* (1992), and Shuzo *et al.* (1991) studied the flow field in street canyons, confirming many wind tunnel results, including vortex circulation when the roof-level wind flows are perpendicular to the street canyon. Lee and Park (1993) have developed a two-dimensional, time-dependent flow model in order to assess the effect of various configurations of the street canyon and various flow conditions on the dispersion of pollutants (represented as a time constant). For height-to-width ratios of 2.4:1 or more, these authors found that two contra-rotating vortices may be formed: an upper and a lower. In another study, Moriguchi and Uehara (1993) simulated the concentration distribution of exhaust gases using two- and three-dimensional finite difference models under various configurations. The results of their study showed a significant correlation with experimentally simulated data using a scale model in a wind tunnel.

Johnson *et al.* (1973) developed an empirical model based on full-scale field observation data from San José, California. The model predicted decreasing concentrations away from the line source (vehicular emission) on the leeward side of the canyon and a linear decrease in concentration with height on the windward side. They found that the roof-level wind direction controlled the street-level CO patterns. The CO concentrations at the street level near the leeward sides of buildings were considerably higher than those near the windward sides. However, Qin and Kot (1993) in their work at low wind speeds, as discussed above, used an empirical model based on Johnson *et al.* (1973) for the leeward side only, because they did not detect a difference between windward and leeward sides. Many studies on urban canyons have confirmed that a vortex circulation develops in street canyons when the roof-level wind flows perpendicular

to the street, resulting in upward transport on the leeward side and downward transport on the windward side and hence higher pollution levels on the leeward side than on the windward side (Nicholson, 1975).

Thus the main findings from all three approaches discussed above are that when the wind direction is predominantly perpendicular to the street canyon and the above canyon wind speed is at least 1.5 to 2.0 m s^{-1}, a vortex will form in the street canyon, explaining qualitatively the observed patterns of pollutant concentrations. However, a quantitative explanation depends on the canyon geometry and the magnitude of the above canyon wind speed.

The purpose of the present study is to investigate the use of a fluid flow simulation model for describing the transport and dispersion of pollutants from urban street canyons and to validate the fluid flow model by using field observation data and previous research findings. The PHOENICS package from CHAM was used to solve for the air flow above and within the street canyon, using the k-ε turbulence model, and to solve for pollutant concentrations. The pollutant is assumed to be conserved and this is true in the short term for carbon monoxide used in comparisons with field data.

2. The Model

The model is defined in Equations 1 to 5 and has the objective of predicting mean flows ($\bar{u}, \bar{v}, \bar{w}$) and mean concentrations ($\bar{c}$) as functions of position (x, y, z). In the equations, bars above the symbols denote a time-average of that variable or product of variables. The air is assumed to have a varying pressure p(x,y,z) but a constant density ρ: the usual incompressibility assumption valid at low sub-sonic speeds. The two-equation, k-ε turbulence model (Equ. 3, Equ. 4) is used in this study to represent the effects of turbulence on the mean flows and concentrations. In this scheme, the turbulent kinetic energy per unit mass, k, is created in shear flows at a rate P_k (kinetic energy per unit mass per unit time) and dissipated through molecular viscosity at the dissipation rate ε (kinetic energy per unit mass per unit time). The theory was presented by Launder and Spalding (1972) and by Mohammadi and Pironneau (1994) and the technique has been applied successfully to the air flow characteristics within street canyons by Johnson et al. (1990), Hunter et al. (1992), and Shuzo et al. (1991). The theory predicts the varying eddy viscosity v_t which effectively adds to the kinematic viscosity v_l (applicable to laminar, non-turbulent flows) to produce an effective viscosity. To solve for the mean flow using the k-ε turbulence model, the k and ε transport equations have to be solved together with the usual Reynolds-averaged Navier Stokes equations, involving continuity and momentum conservation (Equ. 1, Equ. 2). To study the transport and dispersion of a pollutant, the conservation equation for species concentration of pollutants (Equ. 5) must be solved together with the above-mentioned equations which describe the flow characteristics.

When the wind direction is assumed to be perpendicular to the street axis (taken parallel to the x-axis), $\bar{u} = 0$ and symmetry precludes any variation in mean wind speeds or concentration along the x-axis. Hence all derivatives with respect to x will be zero and there will be variations only along the vertical (y-axis) or across the street (z-axis).

The set of equations which have to be solved is shown below, following the notation of Mohammadi and Pironneau (1994), with v representing the vertical wind speed and w the horizontal wind speed.

Continuity equation

$$\frac{\partial \bar{v}}{\partial y} + \frac{\partial \bar{w}}{\partial z} = 0 \tag{1}$$

Momentum equations

$$\frac{\partial \rho \overline{vv}}{\partial y} + \frac{\partial \rho \overline{wv}}{\partial z} = -\frac{\partial \bar{p}}{\partial y} + \frac{\partial}{\partial y}\left[\rho(v_l + v_t)\left(\frac{\partial \bar{v}}{\partial y}\right)\right] + \frac{\partial}{\partial z}\left[\rho(v_l + v_t)\left(\frac{\partial \bar{v}}{\partial z}\right)\right] \tag{2}$$

$$\frac{\partial \rho \overline{wv}}{\partial y} + \frac{\partial \rho \overline{ww}}{\partial z} = -\frac{\partial \bar{p}}{\partial z} + \frac{\partial}{\partial y}\left[\rho(v_l + v_t)\left(\frac{\partial \bar{w}}{\partial y}\right)\right] + \frac{\partial}{\partial z}\left[\rho(v_l + v_t)\left(\frac{\partial \bar{w}}{\partial z}\right)\right]$$

k-Transport equation

$$\frac{\partial \bar{v} k}{\partial y} + \frac{\partial \bar{w} k}{\partial z} = \frac{\partial}{\partial y}\left(\frac{v_t}{\sigma_k} \frac{\partial k}{\partial y}\right) + \frac{\partial}{\partial z}\left(\frac{v_t}{\sigma_k} \frac{\partial k}{\partial z}\right) + P_k - \varepsilon \tag{3}$$

ε-Transport equation

$$\frac{\partial \bar{v} \varepsilon}{\partial y} + \frac{\partial \bar{w} \varepsilon}{\partial z} = \frac{\partial}{\partial y}\left(\frac{v_t}{\sigma\varepsilon} \frac{\partial \varepsilon}{\partial y}\right) + \frac{\partial}{\partial z}\left(\frac{v_t}{\sigma\varepsilon} \frac{\partial \varepsilon}{\partial z}\right) + C_{\varepsilon 1} \frac{\varepsilon}{k} P_k - C_{\varepsilon 2} \frac{\varepsilon^2}{k} \tag{4}$$

where:

$$v_t = C_\mu \frac{k^2}{\varepsilon}$$

$$P_k = v_t \left[2\left(\left(\frac{\partial \bar{v}}{\partial y}\right)^2 + \left(\frac{\partial \bar{w}}{\partial z}\right)^2\right) + \left(\frac{\partial \bar{v}}{\partial z} + \frac{\partial \bar{w}}{\partial y}\right)^2 \right]$$

$$C_\mu = 0.09 \quad \sigma_k = 1.0 \quad \sigma_\varepsilon = 1.3 \quad C_{\varepsilon 1} = 1.44 \quad C_{\varepsilon 2} = 1.92$$

Conservation equation for species concentration of pollutants

$$\frac{\overline{v}\partial\,\overline{c}}{\partial\,y}+\frac{\overline{w}\partial\,\overline{c}}{\partial\,z}=\frac{\partial}{\partial\,y}\left(k_y\frac{\partial\,\overline{c}}{\partial\,y}\right)+\frac{\partial}{\partial\,z}\left(k_z\frac{\partial\,\overline{c}}{\partial\,z}\right)+Q \qquad (5)$$

2. Boundary conditions

The above-mentioned equations are solved by using the PHOENICS code for various street configurations and various wind speeds. At the inflow boundaries, the wind field is specified with both the inlet velocity, w_{in} (horizontal velocity) and the mass flow rate (expressed as a pressure boundary condition) assumed to be constant. At the outflow, where the fluid leaves the domain, the pressure is set to zero. For the free stream boundary condition, we assume that the flow is free at a distance 10 m above the canyon according to data analysis by DePaul and Sheih (1984). The inlet values of k and ε are introduced, calculated from the turbulence intensity, I, which is assumed to be 6 percent. Using the definition of turbulence intensity and kinetic energy given by Shaw (1988), we can calculate the value of the inlet turbulent kinetic energy (assumed isotropic) from $k_{in} = 1.5(I\ w_{in})^2$ and the dissipation of kinetic energy from ($\varepsilon_{in}= C_\mu\ k_{in}^2/v_t$) assuming that v_t is 0.015 m^2 s^{-1} at the inlet. The solid wall boundary is described by the wall function, assuming the velocity components parallel to the wall vary logarithmically with the distance from the wall, as found experimentally. The pollutant concentrations $\overline{c}$ are assumed to arise solely from motor vehicles and a complete combustion theory of C_xH_y is used to calculate the total vehicular exhaust emissions. The vehicular exhaust emission source terms Q were then added as fixed-flux boundary conditions at ground level over the road but not over the pavements. The eddy diffusivities K_y and K_z along Y and Z directions are assumed to be identical and equal to the effective viscosity (i.e. $K_y = K_z = v_{eff} = v_t+v_l$).

3. Results and Discussion

3.1. AIR FLOW CHARACTERISTICS

Twenty cases have been studied to examine the flow properties and dispersion of pollutants in a street canyon under different wind speed and canyon aspect ratios. In all cases the wind speed is restricted to be perpendicular to the roadway and the emission rate along the canyon is assumed to be constant, arising from a traffic flow of 1000 vehicles per hour. Concentrations were derived in all cases except one, which served as a comparison of wind speeds only.

The results show that a vortex develops within the street canyon for all cases as shown for example in Figs. 1-a to 1-e. It is clear that the formation of the vortex depends upon the aspect ratio. For height-to-width ratios close to unity, the vortex is approximately circular, but as this ratio is reduced, the vortex becomes elongated in the horizontal. Further reducing this ratio, the vortex forms in the lee of the upwind building and the main air flow penetrates down to the ground level with another vortex forming at the base of the downwind buildings.

The simulation results have confirmed many research findings. For comparison, two previous studies were selected, one a wind tunnel investigation conducted by Hoydysh *et al.* (1988) and the other a field investigation conducted by DePaul and Sheih (1985). Hoydysh *et al.* (1988) have analysed the trajectories of bubbles within the even and step-up notch when the wind direction is perpendicular to the notch. The ratio of the street width to the height of the upwind building was held constant at 0.79 while the ratio of heights of the downwind and upwind buildings was 1 for the even notch and 0.67 for the step-up notch. The analysis indicated that most trajectories were nearly circular or elliptical. In order to validate the present simulation results, a comparison was made between the simulation results and the Hoydysh *et al.* (1988) wind tunnel results. Using the same configurations in the PHOENICS simulation, a reasonable agreement was found as shown in Table I. In the present simulation the ascending and descending velocity were calculated at 0.13, 1.0, 2.6, 4.0, and 5.4 m from the upwind buildings and downwind buildings.

TABLE I.
Comparison of vortex velocities simulated by PHOENICS and those measured by Hoydysh et al. (1988).
$W=19.75$ m, $H_{up}=25$ m (even notch), $H_{up}= 37$ m (step-up notch),
Roof top velocity 2.0 m s^{-1}

Case	Direction	Hoydysh et al. (m s^{-1})	PHOENICS (m s^{-1})
Even Notch	Ascending	0.26±0.07	0.24±0.133
Even Notch	Descending	0.24±0.13	0.27±0.129
Step-up Notch	Ascending	0.34±0.13	0.37±0.21
Step-up Notch	Descending	0.32±0.11	0.44±0.25

Measurements of wind velocities in an urban street canyon have been made by DePaul and Sheih (1986) in central area of Chicago, USA when winds were approximately perpendicular to the street. The mean wind velocities were determined by analysis of the trajectories of tracer balloons that were released in the canyon and photographed in rapid sequence. Field study results by this procedure show that for ambient wind speeds of from 2 to 5 m s^{-1} perpendicular to the street canyon, and with a height-to-width ratio of 1.5, a single vortex cell is contained within the canyon. The vortex seems to disappear for ambient wind speeds less than 1.5-2.0 m s^{-1}. Measurements of vertical and horizontal wind velocity components were taken on one occasion with a constant temperature hot-wire anemometer. Fig. 2 shows a comparison between the field measurements by DePaul and Sheih (1986) within real urban canyon ($W=24.5$, $H_{le}=33.5$ and $H_{up}=40$ m) and numerical results with the same configurations. There is reasonable agreement between the numerical results and the field measurements.
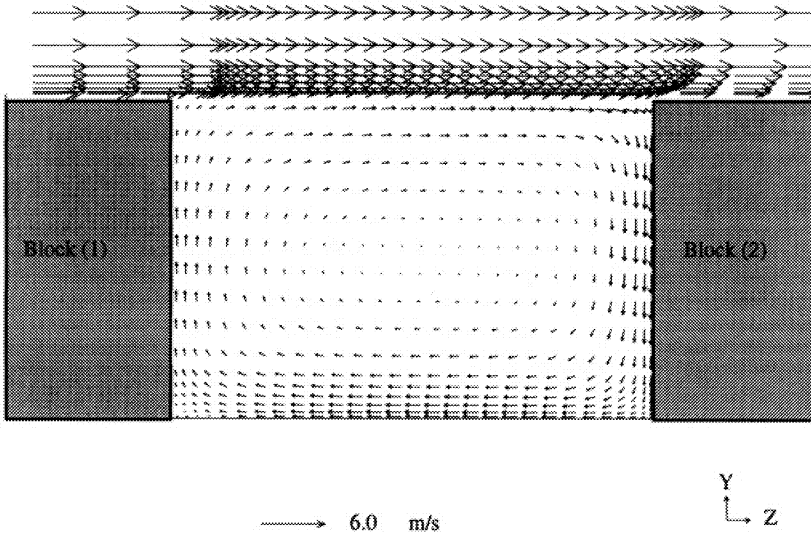
Fig. 1-a Two dimensional simulated wind flow in a street canyon for W=30 m H=20 m

6.0   m/s

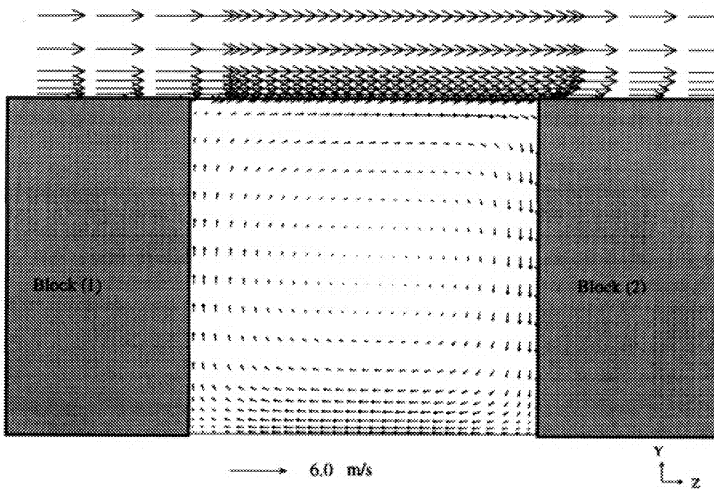Fig. 1-b Two dimensional simulated wind flow in a street canyon for W=20 m, H=20 m

288
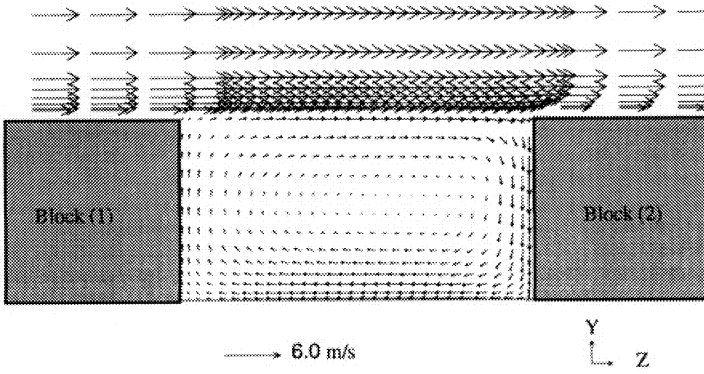

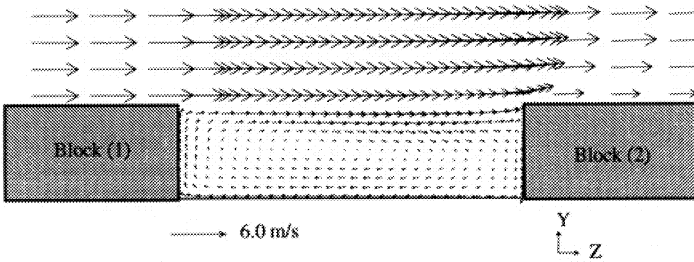Fig. 1-c Two dimensional simulated wind flow in a street canyon for W=20 m, H=10 m

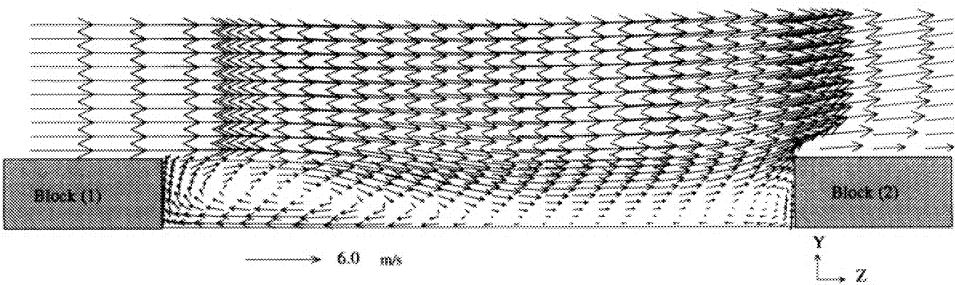Fig. 1-d Two dimensional simulated wind flow in a street canyon for W=20 m, H=5 m

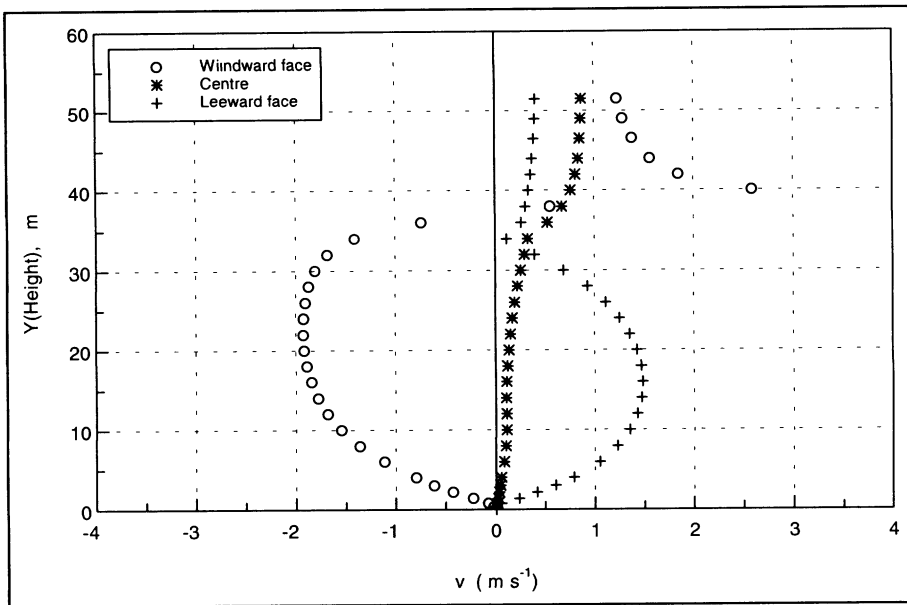Fig. 1-e Two dimensional simulated wind flow in a street canyon for W=40 m, H=5 m

Fig. 2-a Numerical results for vertical wind speed, v, versus height, y
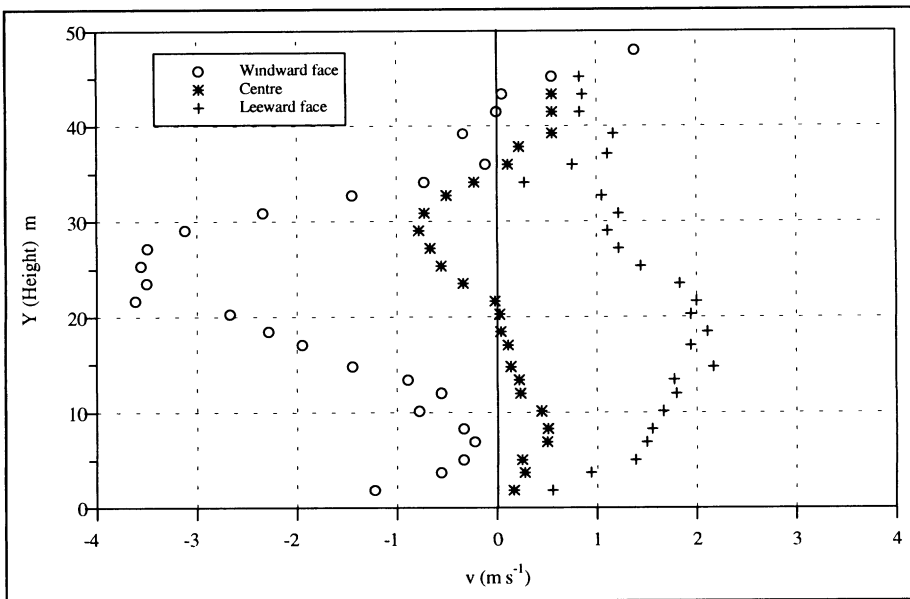
Fig. 2-b Field measurements by DePaul and Sheih (1986) for vertical wind speed, v, versus height, y
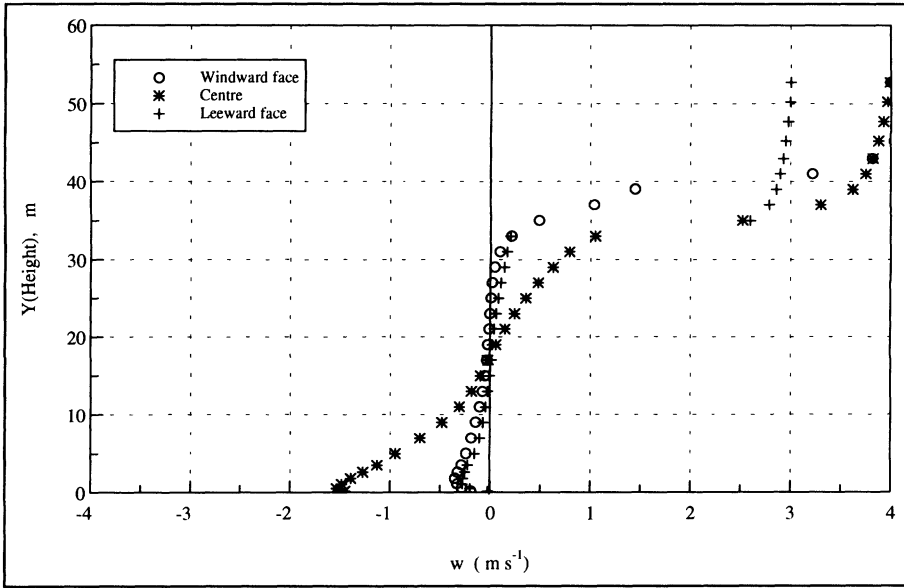
Fig. 2-c Numerical results horizontal wind speed, w, versus height, y
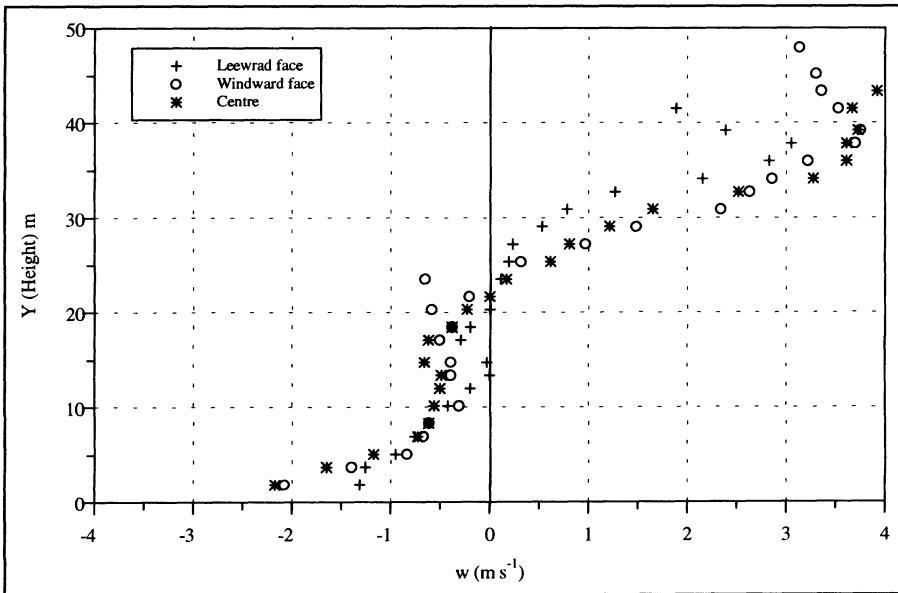
Fig. 2-d Numerical results horizontal wind speed, w, versus height, y

Note that in Figs. 2-a to 2-d, the leeward face refers to Block (1), and the windward face to Block (2) in Fig. 1

3.2. POLLUTANT DISPERSION WITHIN STREET CANYONS

The distribution of pollutants within the street canyon is governed by the air flow characteristics within the street canyon. Contour plots showed pollutants re-circulating within the vortex formed within the canyon as shown in Figs. 3a -3d. The canyon geometry and the ambient wind speed above the canyon are important factors for describing the characteristics of air flow within street canyon and both were investigated. In this study carbon monoxide, CO, dispersion was predicted, since the main source of CO is from motor vehicles and it is a relatively non-reactive gas in the atmosphere. The carbon monoxide emission factors for petrol and diesel engines are assumed to be 35 and 3.5 g km^{-1}, respectively, for vehicles running at 20 km h^{-1} average speed. The emission factors have been estimated by Bardeschi et al. (1991) from the emission factors determined experimentally by Jounard (1987) for representative motor vehicles running in France in 1987. In all cases presented in Figs. 3-a to 3-d, Figs. 4-a to 4-b, and Fig. 5 it is assumed that the traffic is 1000 vehicles per hour.

The results show that CO concentration increases as the aspect ratio increases and the CO concentration decreases exponentially in the vertical direction, the vertical gradient at downward face being less than at the leeward face. The CO concentrations on the leeward face of upwind buildings were considerably higher than the windward face of downwind buildings as shown in Fig. 4. These results confirm many previous results as we mentioned before. The ambient wind speed above the canyon also governs the CO concentration within street canyon as shown in Fig. 5.
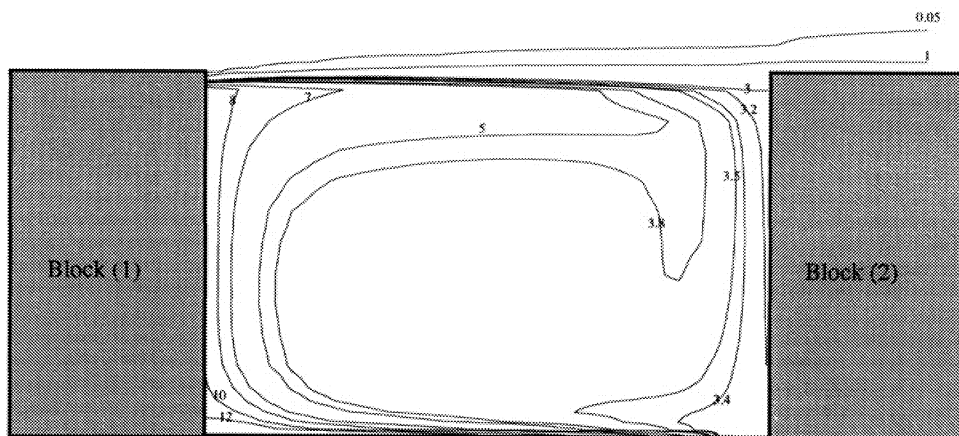

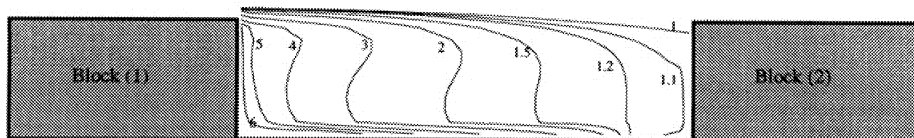Fig 3-a. CO contours (ppm) for a wind speed above building =5 m s^{-1}, W=30 m H=20 m

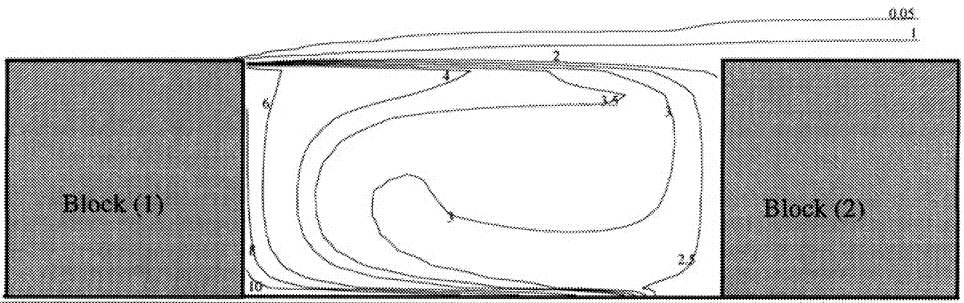Fig. 3-b CO contours (ppm) for a wind speed above building =5 m s^{-1}, W=20 m H=5 m

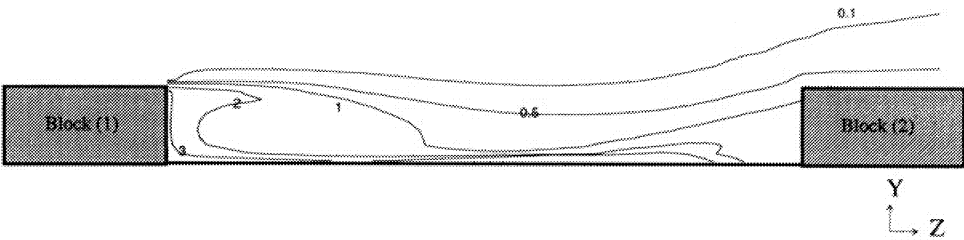Fig. 3-c CO contours (ppm) for a wind speed above building =5 m s⁻¹, W=20 m H=10 m

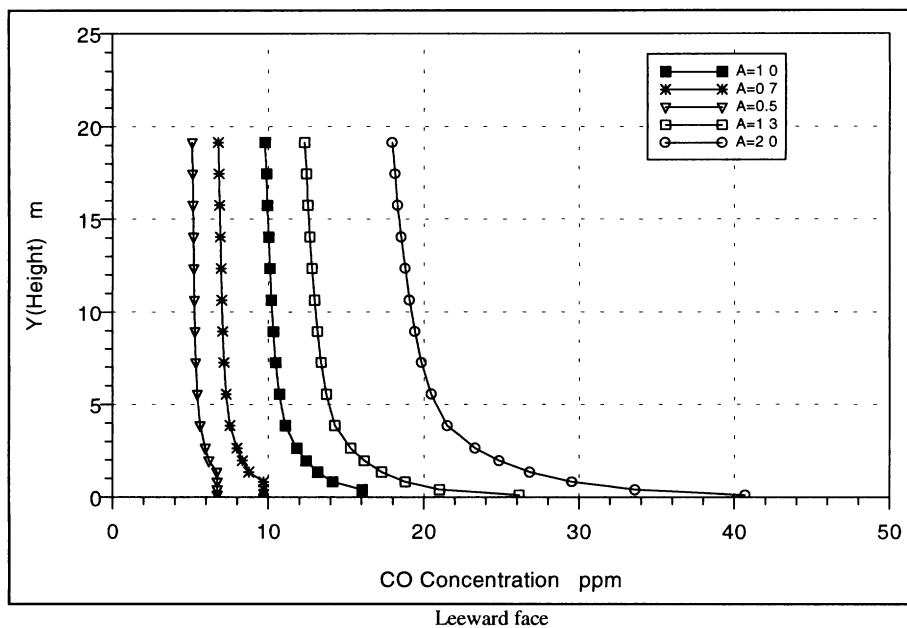Fig. 3-d CO contours (ppm) for a wind speed above building =5 m s⁻¹, W=40 m, H=5 m

Fig. 4a   Calculated vertical CO concentration profiles for different aspect ratios: leeward face of upwind
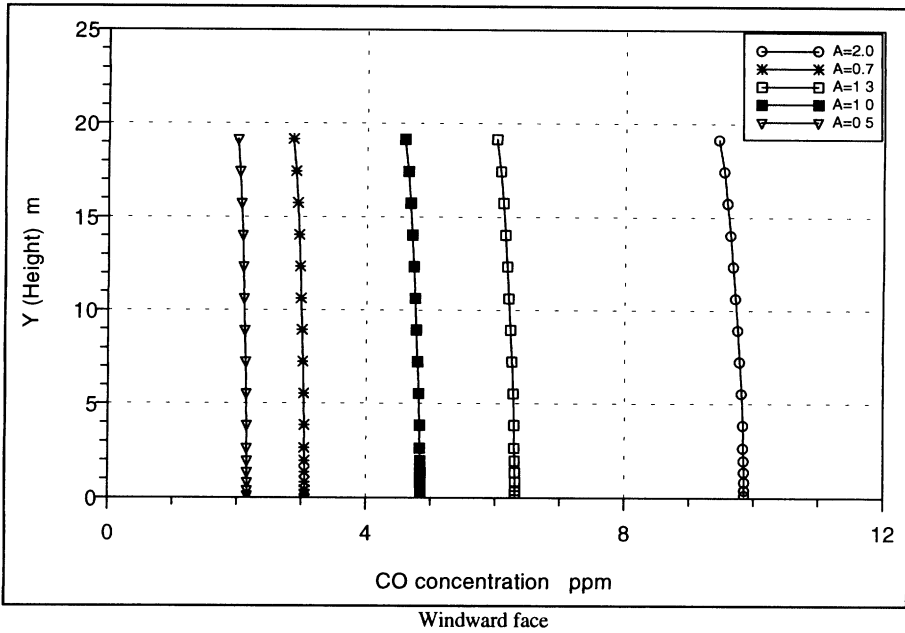building (0.13 m from wall, wind speed = 5 m s⁻¹)

Fig. 4b   Calculated vertical CO concentration profiles for different aspect ratios: windward face of downwind building (0.13 m from the wall, wind speed = 5 m s^{-1})
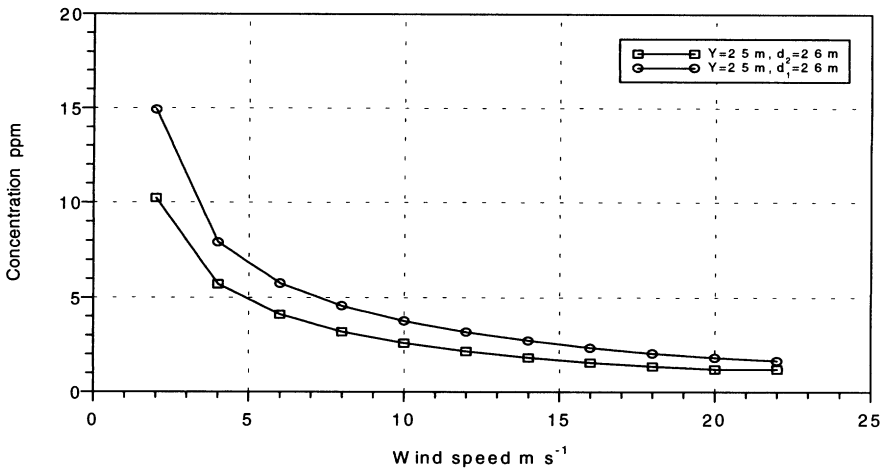

Fig. 5   Calculated CO Concentration vs. wind speed: d_1 = the distance from upwind wall, d_2 = the distance from the downwind wall, Y = the height above the ground.

3.3   APPLICATION TO CARBON MONOXIDE CONCENTRATIONS IN HOPE STREET, GLASGOW

In order to validate the model, a specific application was made for the geometry and typical traffic densities of Hope Street in Glasgow, as counted manually by Strathclyde Regional Council Roads Department.   As in the previous section, the carbon monoxide emission factors for petrol and diesel engines are assumed to be 35 and 3.5 g km^{-1}, respectively, for vehicles running at 20 km h^{-1} average speed. A comparison was made with carbon monoxide concentrations measured within the street during periods when the above street air flow was at approximately 90° and 270° to the street axis.   The measurement station was set up and operated by Warren Spring Laboratory in the Central Hotel, Glasgow Central Station, on the east side of Hope Street. The sample intake was situated 2.5 m above the pavement and 0.5 m in from the kerb. When the wind was from the east (90°) the sampler was on the leeward face, whereas when the wind was from the west (270°) the sampler was on the windward face. Reasonable agreement was obtained, confirming the difference between concentrations on the leeward and the windward faces, as mentioned above. Fig. 6 shows the comparison between the predicted and measured CO concentrations at the leeward and windward faces.
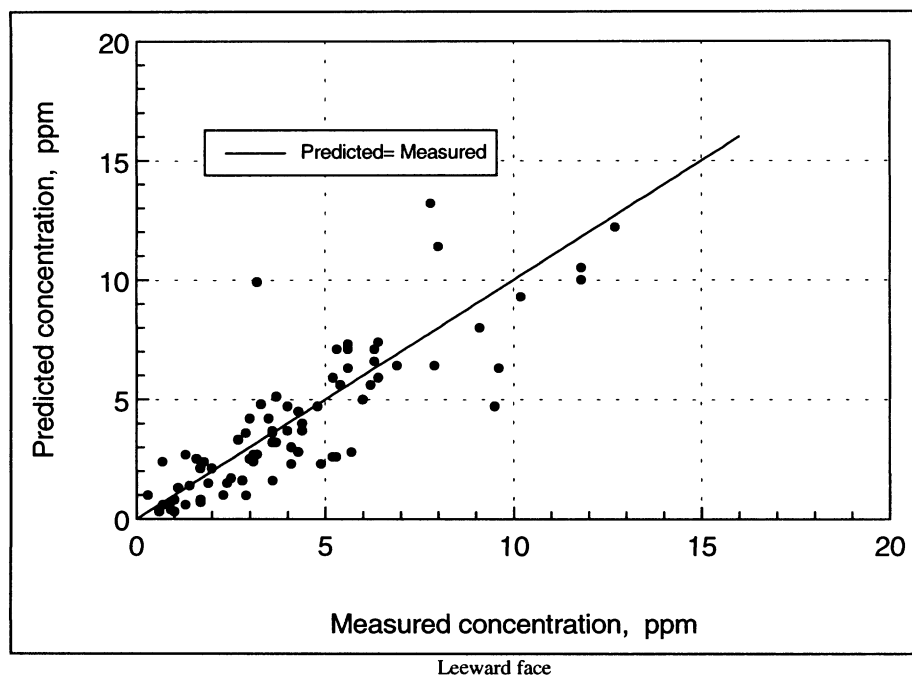

Leeward face

Fig. 6a Comparison between numerical and measured CO for leeward face of upwind building.
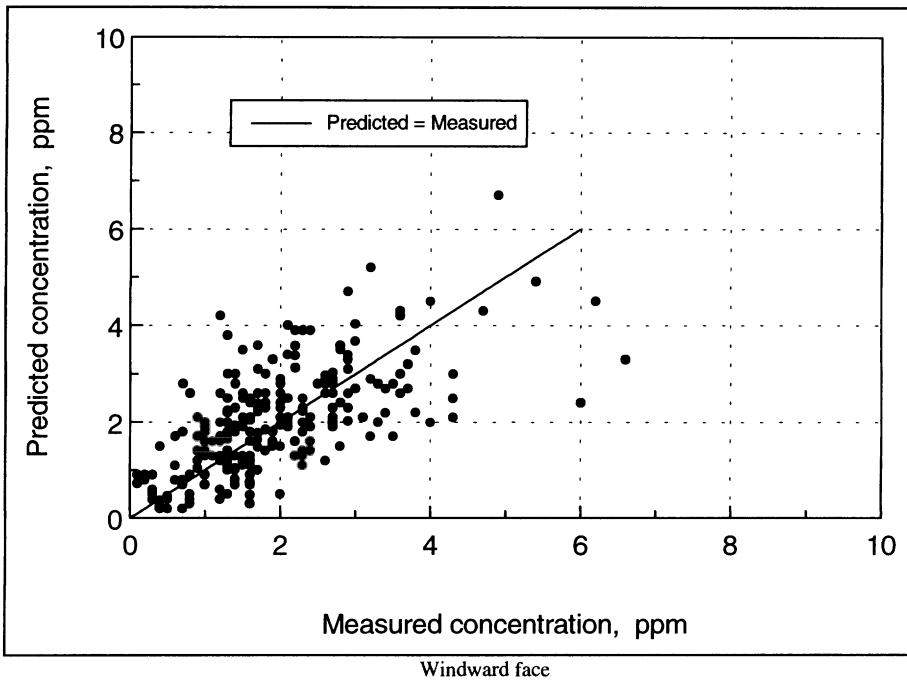
Windward face

Fig. 6a Comparison between numerical and measured CO for windward face of downwind building.

4. Conclusions

In this paper it has been shown that it is feasible to set up the PHOENICS fluid flow simulation package and the k-ε model to solve for the turbulent, two-dimensional flow field in a street canyon. This offers significant improvements over other models using constant eddy viscosity or mixing length theories but adds significantly to the computation. The results confirm the general flow features of wind tunnel studies and field observations, both qualitatively and quantitatively. The representation of the pollutant concentrations is also convincing and gives reasonable agreement with field data for a street canyon.

However, there are insufficient data to provide a comprehensive test of the model simulation, particularly for the within canyon concentration field. What is required is a detailed study of concentration and wind speed, preferably at full-scale, to provide much more observational data.

Work is proceeding on a full three-dimensional PHOENICS simulation involving wind-directions other than perpendicular to the street canyon. The flow structure and concentration fields are more complex than in the two-dimensional cases described here and validation will be more difficult still. However, initial results are encouraging and will be reported in due course.

Acknowledgements

References

Bardeschi A , Colucci A., Gianelle V., Gnagnetti M., Tamponi M., Tebaldi G.: 1991, *Atmos. Environ* **25B**, 415-428.
Dabberdt W.F., Hoydsh W.G.: 1991, *Atmos. Environ.* **25A**, 1143-1153.
DePaul F. T., Sheih C.M.: 1984, Argonne National Laboratory Technical Report ANL/ER-84-1, 84 pp..
DePaul F. T., Sheih C.M.: 1986, *Atmos. Environ.* **20**, 455-459.
Hoydsh W.G., Dabberdt W.F.: 1988, *Atmos. Environ.* **22**, 2677-2689.
Hunter L.J., Johnson G.T., Watson L.D.: 1992, Atmos. Environ. **26B**, 425-432.
Johnson G.T., Hunter L.J., Arnfield A.J. (1990, *Energy and Building,* **15-16**, 325-332.
Johnson W.B., Ludwig F.L., Dabberdt W.F., Allen R.J.: 1973, *J. Air Poll.Control Assoc.* **23**, 490-498.
Jounard R.: 1987, Institut National de Recherche sur les Transports et leurs Securité. Laboratoire Energies Nuisance-Case 24-F 69675, Bron Cedex, France.
Launder B.E , Spalding D.B.: 1972, *Mathematical models of turbulence,* Academic Press, New York.
Lee I.Y., Park H.M.: 1994, *Atmos. Environ.* **28**, 2343-2349.
Luria M., Roni W., Mordechai P.: 1990, *Atmos. Environ.* **24B**, 93-99.
Mohammadi B., Pironneau O.: 1994, *Analysis of the K-Epsilon turbulence model.* John Wiley & Sons, New York.
Moriguchi Y., Uehara K.: 1993, *J. Wind Eng. and Ind. Aerodyn.* **46&47**, 689-695.
Nakamura Y , Oke T.R.: 1988, *Atmos. Environ.* **22**, 2691-2700.
Nicholson S.E.: 1975, *Atmos. Environ.* **9**, 19-31.
Nunez T.R., Oke T.R.: 1977, *J. Appl. Meterol.* **16**, 11-19.
Qin Y, Kot S.C.: 1993, *Atmos. Environ.* **27B**, 283-291.
Shaw C. T.: 1992, *Using computational fluid dynamics,* 1st ed., Prentice Hall International, UK, p. 180.
Shuzo M., Akashi M., Yoshihiko H.: 1990/1991, *Energy and Building,* **15-16**, 345-356.
Yamartino R. J., Gotz W.: 1986, *Atmos. Environ.* **20**, 2137-2156.

FLOW FIELD AND POLLUTION DISPERSION IN A CENTRAL LONDON STREET

C. M. N' RIAIN[1], B. FISHER[2], C. J. MARTIN[3], AND J. LITTLER[1]

[1] Research in Building Group, Department of Architecture and Engineering, University of Westminster, 35
Marylebone Road, LONDON NW1 5LS, [2] Department of Environmental Sciences, University of Greenwich,
Rachel MacMillan Building, Creek Road, Deptford, LONDON SE8 3BW, [3] Energy Monitoring Company Ltd., 3
Chapel Court, Newport Pagnell, Bucks. MK16 0EW.

Abstract. Urban pollution due to roadways is perceived as a major obstacle to implementing low-energy ventilation design strategies in urban non-domestic buildings. As part of a project to evaluate the use of a computational fluid flow model as an environmental design tool for urban buildings, this paper seeks to address the impact of pollution from roadways on buildings in areas of restricted topography and assess dominant influencing factors and other requirements for testing the flow model predictions. Vertical profiles of carbon monoxide (CO) and temperature at the facade of a building in a Central London street, in addition to above-roof wind speed and direction, were measured over a period of three months. The street has a height-to-width (h/W) ratio of 0.6 and is of asymmetric horizontal alignment. The air flows in the area surrounding the building were modelled using a computational fluid flow model for two orthogonal wind directions. CO concentrations were calculated from the steady-state flow field in order to place point measurements in the context of the flow field, identify persistent features in the measured data attributable to the flow structure and, by comparison with measurements, identify further testing requirements.

Some qualitative and quantitative agreement between measured and modelled data was obtained. Measured CO levels at the building facade and vertical variations of CO were small, as predicted by the model. A wake-interference type flow was predicted by the model for wind speeds >2ms^{-1} with formation of a vortex cell occurring for roof-level wind speeds >5ms^{-1} for the cross-wind direction, which was reflected in the measured CO levels and facade gradients. A direction-dependent inverse relationship was noted, both in the model and measurements, between above-roof wind speed and facade CO levels although statistical correlations in the time series were poor. CO concentrations at the facade were found to increase with height frequently, as well as decrease, especially for parallel winds. It is expected that mechanical turbulence due to vehicles was largely responsible. In comparison, thermal stratification appeared to play only a minor role in controlling vertical mixing in the street, under low wind speed conditions.

1. Introduction

The increase of traffic volumes in cities and subsequent rise in vehicle exhaust pollution has caused considerable concern for public health in recent years. However, the restricted geometry of city spaces and the resulting complex flow conditions can give rise to uneven distributions of pollution. Pollution emissions, either from ground-based or elevated emissions sources in the urban core, can be entrained into the wake of buildings where they can create "hot-spots" of pollution. For this reason, concentration distributions of pollutants around buildings in urban streets are of interest to architects and building services engineers when considering where to locate air inlets, particularly for the design of passive low-energy ventilation schemes. In the urban context simple models, developed for homogeneous terrain, which predict air quality from prevailing meteorology and emission rates alone are of limited application.

Previous model studies of microscale dispersion in urban-style geometries have used simple configurations in order to develop generic rules for predicting the amplification of ground-level concentrations due to the presence of buildings. However, experimental studies (Qin and Kot, 1993; Dabberdt and Hoydysh, 1991) have indicated that pollution levels are very sensitive to configuration, and the idealised configurations of model studies are rare in cities. Recent studies (Ní Riain et al, 1996; Murakami et al, 1990) indicate that computational fluid dynamics (CFD) modelling may provide a more practical and versatile alternative to physical modelling for urban design concerns such as design of urban building ventilation strategies, air quality monitoring network design and interpretation of data. However, large uncertainties inherent in the specification of complex boundary conditions and in the numerical techniques employed by model itself currently prohibit its use in the urban environment until reliable input data and modelling guidance exist for this application and confidence has been enhanced by model validation exercises.

This paper presents preliminary investigations into the use of a CFD model for predicting the flow field and pollution distribution around urban buildings for a nearby roadway. This stage looks at spatio-temporal variations in the facade concentrations and temperatures and their relation to above-roof meteorology in order to detect evidence of flow features predicted by a CFD model and to identify the hierarchy of influencing factors to inform model testing requirements.

2. Previous Studies

GEOMETRY, FLOW STRUCTURE AND POLLUTION DISPERSION IN STREET CANYONS

Pollution dispersion in streets depends on the rate at which the street can exchange air vertically with the urban atmosphere above-roof level and laterally with connecting streets. When the incident wind is normal to the canyon axis, Oke (1988) identifies three types of flow regime which occur over 2-dimensional arrays of buildings of increasing height-to-width (h/W) ratios (Fig. 1). The formation of the vortex cell for skimming flow was confirmed in field measurements by de Paul and Sheih (1986) using tracer balloons, for roof-level wind speeds $>2ms^{-1}$. Increased concentrations of vehicle-related pollutants on the leeward side of street canyons have been observed in field studies (Qin and Kot, 1993), while the windward side (facing the oncoming wind) showed decreased levels.

Hunter et al (1990/91) demonstrated in model studies that a sharp transition occurs with increasing block length from a three-dimensional flow structure to two-dimensional for perpendicular wind. Wind tunnel studies (Hall et al, 1995) showed that concentrations of pollutants on the leeward face of a rectangular block, from a ground-based source situated in the lee of the block dramatically increased at the transition point as the
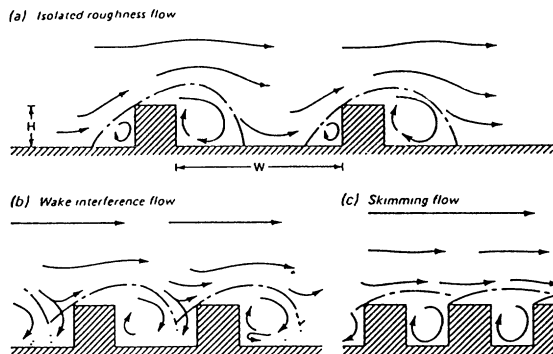
Fig. 1 Flow regimes associated with air flow over building arrays of increasing height/width (h/W) ratios (after Oke, 1988).

length-to-height ratio (L/h) was increased. Wind tunnel studies by Dabberdt and Hoydysh (1991) showed that for shorter block lengths lateral flows can carry pollution emissions from one street to adjoining streets. The contribution from a heavily -trafficked main avenue to an adjoining feeder street could be as much as 20% of the total pollutant budget for that street when the wind perpendicular is to the main avenue, therefore pollution from nearby roadways may also be of concern in building ventilation design.

CONCENTRATIONS AND VERTICAL PROFILES OF POLLUTION IN STREET CANYONS VS. ABOVE-ROOF WIND

Tracer gas measurements by De Paul and Sheih (1985) show clear decrease with height in concentrations over a vertical distance of 24m at the sides of a canyon of h/W=1.5. Model studies by Dabberdt and Hoydysh (1991) found an exponential decrease with height for all angles of the wind, with the slope changing with wind angle. In a later study (Dabberdt and Hoydysh, 1994) they also found that maximum surface concentrations occurred for the wind parallel to the street, while all other wind directions gave rise to roughly equal concentrations. Field measurements by Qin and Kot (1993) also found an exponential vertical decrease at the canyon sides, the slope of which decreased with increasing h/W (0.9→1.2). Concentrations were also found to increase with height on occasion. Carbon monoxide concentrations measured at the canyon centreline (h/W=1.0) were found to decrease to 61% at the sides, while the vertical concentration gradient was found to be on average half that of the horizontal gradient, indicating the significance of initial vertical mixing. Poor correlations were found between roof level wind speed and concentrations in the canyons.

3. Area Description

The area under consideration (Figs. 2a & b) is the area surrounding the University of Westminster Marylebone Campus on Marylebone Road in Central London. The average
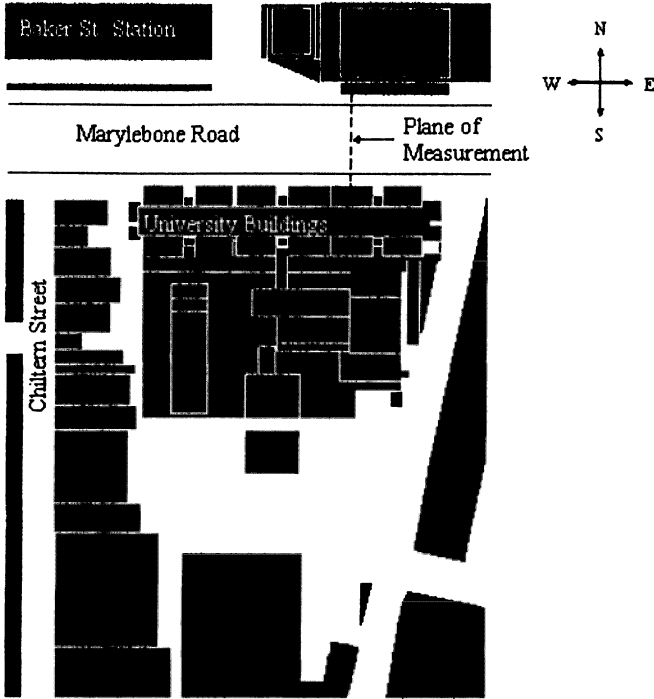
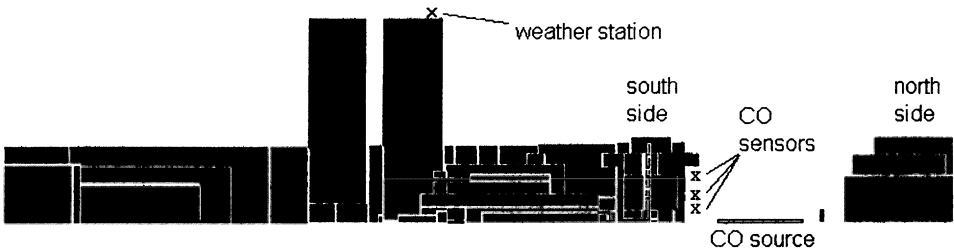Fig. 2a. Marylebone Road area geometry, plan view (X-Y plane)

Fig. 2b. Marylebone Road area geometry, side view (Y-Z plane) with locations of vertically-aligned monitoring stations indicated at heights (z=) 6m, 10m and 17m

building height for the region is 25m. The street network consists of two adjoining orthogonal streets of symmetric height and an asymmetric street surrounding the building complex to the west, north and east. A small park is located immediately to the south of the complex and large park lies to the North of the Marylebone Road. The building complex is constructed around a central courtyard, with a long block facing onto Marylebone Road to the North and bounded at the South by closely-spaced twin towers of 60m height each. The front block is supported on concrete columns, with 50% free area on the ground floor through which air can flow freely into the courtyard from Marylebone Road. The front block also has an overhang of 2.5m at a height of 19m.

Marylebone Road (Fig. 2b) is a six-lane, heavily trafficked road (>60,000 vehicles/day) of east-west orientation. The horizontal asymmetry of the parallel blocks on either side of the road at the point under study means that no individual street segment corresponds to the idealised configurations of Oke (1981) and Hunter et al (1990/91). In the road segment under investigation, the opposing building lengths overlap to form a short, asymmetric canyon-type link of h/W=0.6 and with L/h = 3. On the basis of idealised canyon configurations, the expected flow regime is a transition from skimming to wake interference flow.

The traffic volume increases during the day with a small local peak in the morning rising steadily to a maximum in the evening. Traffic behaviour is difficult to define over shorter timescales due to the presence of two sets of pedestrian-operated traffic lights, one for west-flowing and one for east-flowing lanes. This results in a random stop-start traffic pattern, although congested conditions are frequent during the evening rush-hour.

4. Fluid Flow Model

THEORY

The model used for this investigation is the FloVENT computational fluid dynamics model, developed by the Building Services Resources and Information Association (BSRIA) and Flomerics Ltd. The code adopts a finite-volume approach (as described in Patankar, 1980) to discretize the governing transport equations describing conservation of mass, momentum, thermal energy, turbulence energy and chemical species concentration, which may be represented in the general tensor form:

$$\frac{\partial(\rho\varphi)}{\partial t} + \frac{\partial(\rho u_j \varphi)}{\partial x_j} = \frac{\partial}{\partial x_j}\left[\Gamma_\varphi \frac{\partial \varphi}{\partial x_j}\right] + S_\varphi \qquad (1)$$

where:
$u_j(u_1, u_2, u_3)$ are the time-averaged mean velocity components in the $x_j(x_1, x_2, x_3)$ $x_j(x_1, x_2, x_3)$ coordinate directions; φ are any of the dependent variables: velocity, thermal energy, concentration, turbulence energy; ρ is the fluid density; Γ_φ are the effective diffusion coefficients (laminar + turbulent); S_φ represents the sources and sinks of the variable; t and is the time.

The program uses a staggered grid system to calculate the velocity components (Patankar, 1980). The discretized equations are solved iteratively using a tri-diagonal matrix algorithm (TDMA) and the velocities and pressures are calculated using the SIMPLE (Semi-Implicit Pressure-Linked Equations) algorithm. The standard two-equation k-ε model of turbulence closure (Launder and Spalding, 1974) is employed. A non-uniform Cartesian grid is used. The theory and solution procedures of the code are

the standard techniques as outlined in Patankar (1980), Alamdari et al (1991) and Flomerics Ltd. (1994).

METHODOLOGY

The model was generated in two stages because of the difficulty of estimating the boundary conditions for the urban environment and the hardware requirements of a large computational domain required to set the boundaries at a sufficient distance such that the flow in the area of interest is less affected by the boundaries. A "nested" approach was adopted, whereby the domain size is gradually reduced and the resolution increased by taking boundary information from larger-scale models as improved estimates for the boundary conditions of progressively smaller scale models. Wind and turbulence profiles, for example, vary between cities and it is well-known that the power law profiles and displaced logarithmic wind profiles are crude estimates for this inlet condition.

i. Large-scale Model
A simple (1x1)km 2-dimensional boundary layer model of blocks representative of the average height, height variance and spacing was used to determine the boundaries for the smaller scale Marylebone Area model. Inlet conditions were specified as a displaced logarithmic profile up to a height of 1km with recommended zero plane displacement of 70-80% of the height of the large roughness elements (Panofsky and Dutton, 1984). The profile of turbulence intensity was as recommended from measurements by Kato et al (1992), for terrain category IV:

$$I_u = \begin{cases} 40 * (10/z)^\alpha & \text{for } z > 30\text{m} \\ 0.287 & \text{for } z \le 30\text{m} \end{cases} \tag{2}$$

where α = the power law exponent, taken here as 0.3; and z = height
The profile of turbulence kinetic energy TKE is given by:

$$k_0 = \tfrac{1}{2} I_u^2 U_0^2 \tag{3}$$

and dissipation rate of TKE:

$$\varepsilon_0 = \frac{C_\mu^{3/4} k_0^{3/2}}{\kappa z} \tag{4}$$

The upper boundary (at z=1000m) was modelled as a free stream pressure boundary.
The inlet velocities and surface roughnesses were varied to test for sensitivity.

The profiles at the centre of the last block downwind were taken as input to the larger scale model for the condition of the wind perpendicular to the Marylebone Road canyon (North wind) and one building height downwind of the array of blocks for the parallel wind condition (West wind). Rotach (1995) found that for parallel winds for a canyon of h/W=1 there was little variation between the values of the wind speed and wind variance between the centre of the canyon and the sides of the canyon. This assumption was used when inputting the inlet conditions for the parallel wind case in the Marylebone Road simulations.

ii. Marylebone Area Model

The domain size chosen (180x256x210)m was the maximum permissible by hardware (Sun SparcStation10) for the resolution required in the street. The dimensions in each direction are at least three times the tallest building height (60m) in the model. The inlet, outlet and upper boundary conditions were taken from velocity and pressure fields calculated in the larger-scale model. The assumption was made that the pressure and velocity assigned at the upper boundary would vary little at the height chosen over such a small area of the centre of the city where the height of the roughness elements varied little, compared to the variations over the city as a whole. This assumption is limiting, therefore the resulting flows are considered qualitatively only, and the resulting concentration fields considered only in the light of measurements. Sensitivity tests indicated that the flow features observed for the two velocities modelled varied in magnitude, but were present for the mean measured wind speeds for the area and above.

For this study this source strength is essentially arbitrary as it is the spatial distribution of the gas in the presence of a flow field — the relation between the source and the building facade in this case under different wind conditions — which is the subject of the investigation. A worst-case peak traffic condition was modelled, whereby the roadway is full and the vehicles not moving. The source is represented in the model as an area source of CO (based on an arbitrary emitted CO:Fluid proportion of 5% per tailpipe per second) and composite heat due to vehicles in idle mode (Benson, 1992). No mechanical turbulence was attributed at this stage, although the field data indicate that this needs to be considered in future work. The air flows in area surrounding the building were modelled for two wind speeds (high and low) and directions (parallel and perpendicular to the axis of the main avenue) and the CO concentrations calculated from the steady-state flow field. Both wind profiles gave an above-roof velocity of $>2ms^{-1}$. At best the grid resolution was 0.25m (near the source), but more commonly 1-2m in the street.

5. Experimental Arrangement

EQUIPMENT & METHODOLOGY

Carbon monoxide (CO) and air temperature were measured at the facade of the building, in a vertical line at heights of 6m, 10m and 17m at the canyon segment mid-line (Figs. 2a & b). Electrochemical sensors (City Technology Ltd.) were used to monitor CO. Radiation-shielded thermistors (Campbell Scientific; accurate to $\pm$ 0.5_C) monitor the temperature next to each sensor. The sensor output signals were sampled by Campbell Scientific CR10 dataloggers and stored as five-minute averages. The cells were span-calibrated with a known concentration of carbon monoxide gas. A correction for sensor temperature dependence is applied to the raw data. The estimated total error on each sensor is ±0.5ppm, however the post-correction standard deviations in their relative signals in ambient tests is much less than this (±0.05ppm). The 5-minute averages are

highly correlated (r^2=0.95) in field tests with five-minute averages of a non-dispersive infra-red (NDIR) CO monitor. Wind speed, direction and standard deviation of the wind direction were measured by a cup-and-vane anemometer, located on the tall building (z=60m) immediately south of the University campus and samples averaged over 5-minute intervals.

6. Results & Discussion

Predicted concentration fields (C/C$_{max}$) are presented in plan view approximately in the plane of the 6m sensor (Figs. 3a & b) and vertical section through the street canyon in the plane of the measurements at mid-canyon location (Figs. 4a-l) for both the parallel (west) and perpendicular (north) winds. The predicted concentration levels at the facade at about 0.5h tend to be in the region of between 0.2-0.4 times the road concentration at source height, depending on the wind speed and direction. This was found to be consistent in magnitude with comparisons between measured facade data and kerbside CO measurements made on the same side along the same road (two blocks west of the University site) at the Local Authority monitoring station. Observed CO levels at the facade generally were quite low (average=1.36ppm; max=7.68ppm).

Normalised
Concentration
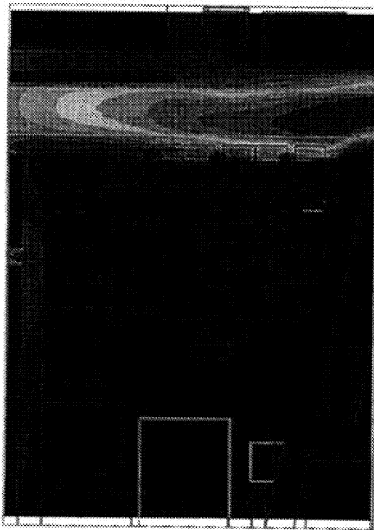
1
0.859
0.712
0.571
0.429
0.288
0.141
0

Fig. 3a. Horizontal plane at z=7m,
parallel wind, U$_{roof}$=3ms^{-1}
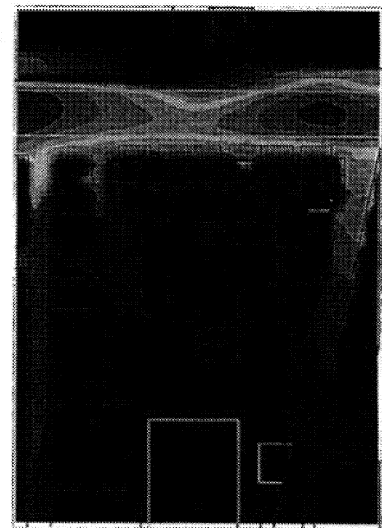
Fig. 3b. Horizontal plane at z=7m,
perpendicular wind, U$_{roof}$=2.7ms^{-1}
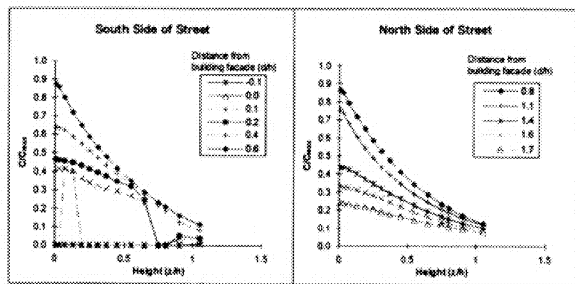
(a) West wind, $U_{roof}=3ms^{-1}$ (b) (c)
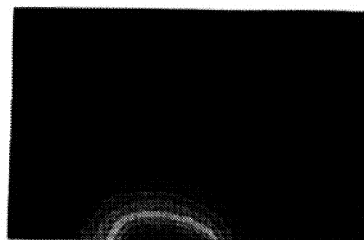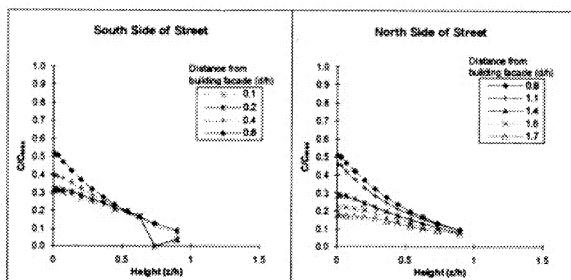
(d) West wind, $U_{roof}=6.5ms^{-1}$ (e) (f)

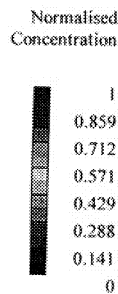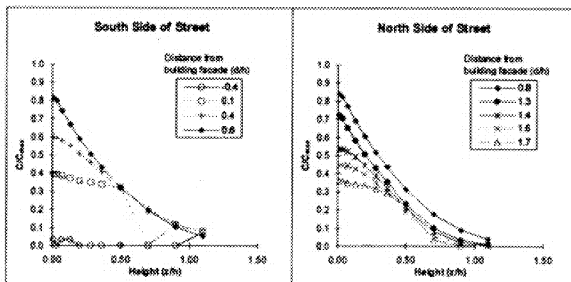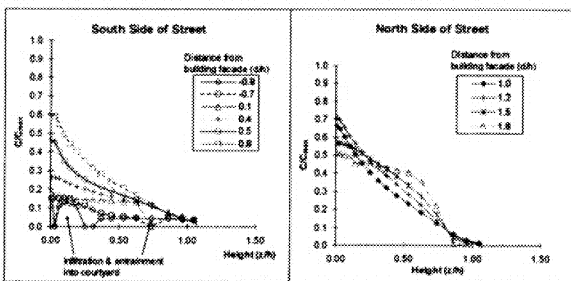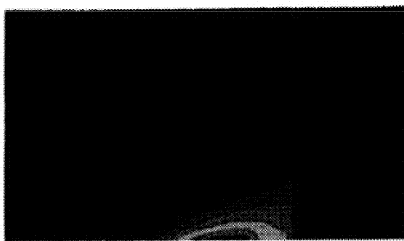(g) North wind, $U_{roof}=2.7ms^{-1}$ (h) (i)

(j) North wind, $U_{roof}=7\ ms^{-1}$ (k) (l)

Fig. 4 Vertical dispersion profiles and concentration distributions at mid-canyon cross-section

CO LEVELS AND ABOVE-ROOF METEOROLOGY

No significant statistical correlations existed in the raw measured data between CO levels and above-roof wind behaviour, although time series (eg. Fig. 5) clearly show low concentrations during periods of very high wind speed. This is as expected, due mostly to variations in the source behaviour, and the phase-lag which exists between the summer diurnal wind speed pattern and apparent diurnal source patterns. The facade position of the sensors should, in theory, also increase the sensitivity of the measured CO levels to factors such as wind speed and direction. A rough estimate of the daily traffic trend, generated from low wind speed hourly-averaged data, showed promising improvements in the statistical correlations, although the spread of data is still very large. As expected, wind speed emerges as the most significant influencing factor (r=-0.5). Closer source-monitoring (traffic factors and kerbside CO at the site) is planned for the next experimental phase.
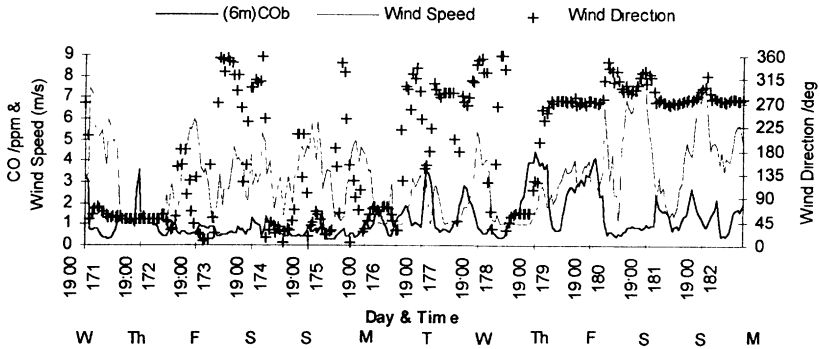
Fig. 5. Typical time series of CO at z=6m on the facade of the building, with above-roof wind speed and direction data for an eleven-day period

A direction-dependent inverse relationship between facade CO levels and wind speed is apparent the measured data, although the spread of data is large. A vertical vortex is predicted by the model for the higher perpendicular wind speed condition (Fig 6b), while the lower wind speed (Fig. 6a) shows the structure of wake interference-type flow, although the roof-level speed is $>2ms^{-1}$. This explains why measured concentrations for north wind (which passes over a large park) were consistently lower in the field than for other directions for above-roof wind speeds $>1ms^{-1}$; below $1ms^{-1}$ the spread of data is larger (Fig 7).

In the model, the facade concentrations on the leeward side increase with wind speed for perpendicular wind, while the windward side concentrations decrease (Figs. 4g-l), which is consistent with the field observations of Qin and Kot (1993). Measured facade concentrations were seen to increase for winds from the south, when the facade is in the lee of the wind, with maxima at SE and SW directions where the "effective" block

(a)   Reference Vector 3 5ms⁻¹ ————▶

(b)   Reference Vector 8 5ms⁻¹ ————▶
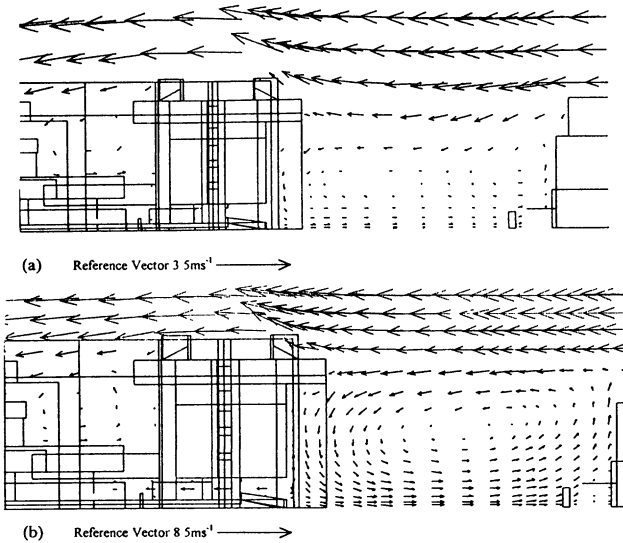
Fig. 6 Air flows in the Y-Z plane at mid-canyon position showing wind vectors for north wind for (a) U_{roof}=2.7ms⁻¹ and (b) U_{roof}=7ms⁻¹.

length, as seen by the incident wind, is greatest. South-westerly winds are cited as the dominant condition for the London area. However, these directions were poorly represented during the monitoring period and require further investigation.

The spread of measured data for parallel winds is large for all wind speeds, as found by Dabberdt and Hoydysh (1994) in wind tunnel studies (Fig. 7). This is due to variations in contributions to the source from the upwind road segments. As a result, measured concentrations for parallel winds are generally higher at the facade than other wind directions.

North Wind (Perpendicular)   **West Wind (Parallel)**
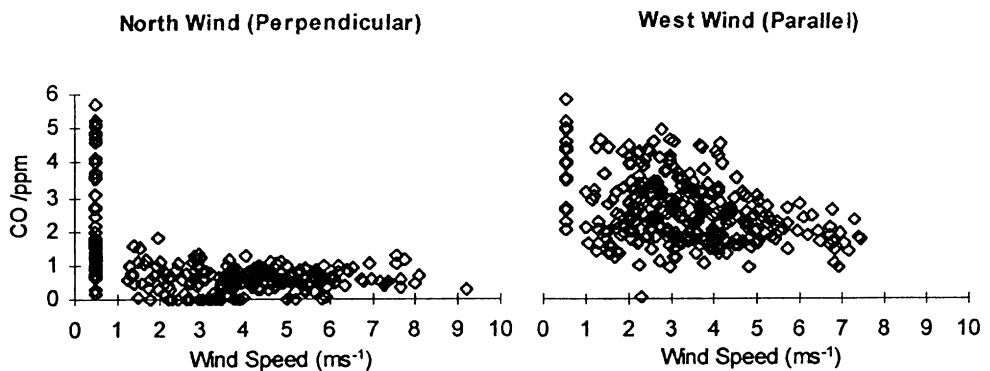
Fig. 7. CO levels at z=6m at the building facade for north and west winds, evening peak data: slow traffic conditions and negative thermal gradients

VERTICAL CO VARIATIONS

The vertical variations of CO detected at the facade of the building were small, mostly falling in the region of about ±1ppm differences between 6m and 17m. While this lies close to the estimated error on each sensors (±0.5ppm), it lies well outside the measured standard error in their relative signals when tested together in ambient conditions (±0.05ppm). The variations are also small in the flow model. CO was often found to increase with height as well as decrease, which was also found by Qin and Kot (1993). The reasons for this appear to be varied, but it is suspected that initial vertical dispersion in the vicinity of the roadway due to vehicle-induced turbulence (not measured or modelled at this stage) is the dominant factor. As this is very variable, no clear patterns emerge in the aggregated data although however the following observations have to date been made:

(i) Facade CO Variations and Wind Direction

Positive (increasing with height) and negative (decreasing with height) gradients were experienced for all wind directions. The incidence of positive gradients is much higher for parallel winds, due to dispersion from upwind roadway sections, and for above-roof wind speeds <1ms^{-1} (Fig. 8). Gradients for north wind tended to be either very small or negative for wind speeds >1ms^{-1}, which is consistent with the flow patterns predicted by the flow model. A positive gradient was observed for the south wind on the few occasions which it occurred which accords well with preliminary model calculations. No positive gradients were observed in the model for north and west winds, but the model calculations were for near-neutral thermal stratification and vehicle-induced turbulence was not modelled at this stage. As with the experimental study of Qin and Kot (1993), the horizontal gradient of CO between the centreline and the side is about twice that with height at the sides, at mid-canyon (Fig. 9). At a height of 2m the CO value deteriorates horizontally to about 60% its centreline value. This suggests that the vertical dispersion parameter is twice that of the horizontal, depending on wind speed of course, without the inclusion of vehicle-induced turbulence.
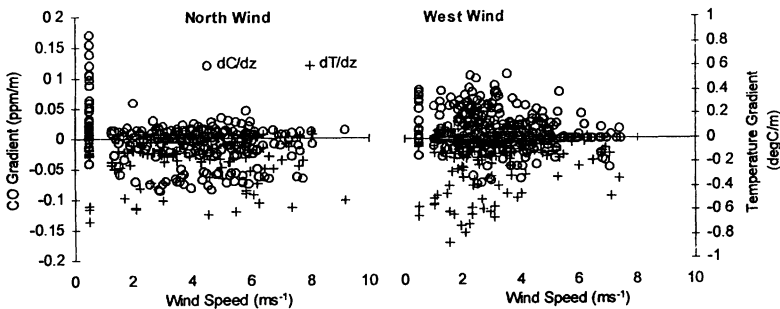

Fig. 8. CO and temperature "gradients" on the building facade for north and west winds, evening peak data (negative=decreasing with height; positive=increasing)
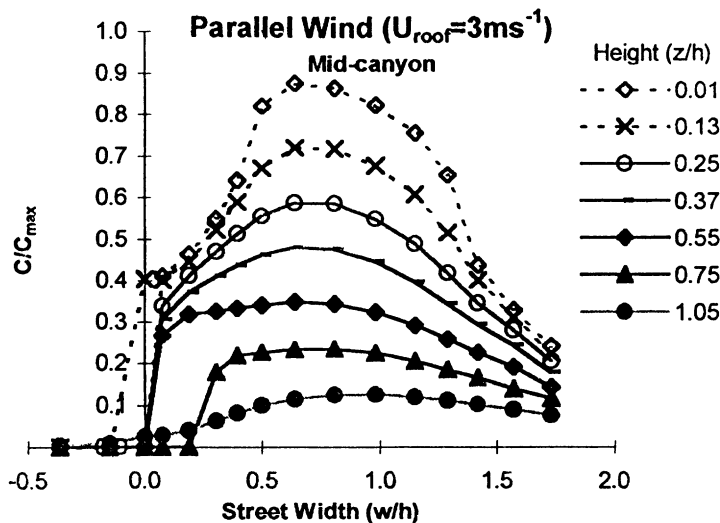
Fig. 9. Horizontal variation of CO concentration (vertical section) across the street at different heights (z/h) at mid-canyon section level.

(ii) CO and Temperature Gradients at the Facade

The air temperature difference near the facade between 6m and 17m varied with a diurnal pattern between $\pm 3°C$, the slope ($\Delta T/\Delta z$) being negative (temperature decreasing with height) from noon-8pm — "maximum" negative slope occurring between 5-6pm, when the suns rays are parallel to the street and solar access is at peak — and turning positive around midnight (max. at around 3am) as the air is no longer being heated from above and the canyon fabric is slowly releasing absorbed heat. In this climate thermal gradients in the street appeared to play only a supporting role in the vertical variances of CO on the building facade, compared with the influence of wind speed and vehicle-induced turbulence. This was in evidence when the wind speed aloft was less than $1ms^{-1}$. Under near-neutral or unstable thermal stratification the incidence of positive CO gradients increases. However, when the temperature profile is weakly stable negative CO gradients are dominant.

(iii) CO Gradients and Street Geometry

The effect of the building geometry on the facade concentrations is also apparent from the model. For the parallel wind condition only, the horizontal distribution at mid-canyon has the appearance of a distorted Gaussian distribution, distorted by both the horizontal and vertical asymmetries of the street. The parameters of the distribution varies along the length of the canyon (Figs. 3a & b). The difference in building facade design is reflected in the vertical profile differences between the north and south sides. Lateral air and contaminant infiltration are observed into the courtyard of the south side building (just below the 6m measurement point) for all but high parallel wind (Fig. 4d). As the perpendicular wind increases, entrainment of pollutants into the wake of the block (upper) as well as through the apertures into the courtyard is evident (Fig 4j). Lateral

flows at lower levels into adjoining streets (Fig. 3a) should reduce concentrations at the facade especially for the north wind condition, as observed in the field.

SIGNIFICANCE OF FACADE VARIATIONS: MODEL PREDICTIONS VS. MEASUREMENT

Comparing the model with negative CO gradients in the measured data only for evening peak times when the temperature gradient is negative: when the wind speed is $3ms^{-1}$ both the model and measurements agree on a 40% decrease in concentration between 6m and 17m for the parallel wind condition and 11% (model)/15% (measurement) decrease for the north wind condition. The mean above-roof wind speed was $2.5ms^{-1}$ over entire the monitoring period. However, when the wind speed is doubled the model predicts only a small change (to 35% decrease) compared with measurement (0.5% decrease) for the parallel wind condition, which is attributable to underestimation of upwind concentrations and dispersion characteristics in the model. The facade concentration variation in the north wind model increases to 19% while measurements record a much larger mean increase with wind speed of 40%.

The implications for ventilation design are as yet inconclusive. The low facade concentrations are probably as a result of the canyon being relatively shallow and the building set some 10m from the kerbside. Closer to the road, the model predicts an exponential decreases in concentration with height, which has been observed in field and wind tunnel studies in streets of higher h/W ratios (Dabberdt and Hoydysh, 1991). It is therefore expected that the implications will be greater for buildings set closer to the roadway in streets of higher h/W ratios, in particular for pollutants which exist in concentrations which regularly exceed health guidelines. In this respect the validation of the flow model in this instance serves as a prerequisite for the investigation of potentially more sensitive scenarios.

7. Summary and Conclusions

For a shallow canyon no single dominant factor was found to affect *dispersion* in the street, although source factors are clearly directly responsible for contaminant *levels*. The resulting distribution is a function of several variables: wind speed and direction, geometry, mechanical turbulence due to vehicles with thermal gradients in a supporting role. Facade concentrations were found to increase as well as decrease with height which appeared to be attributable to vehicle-induced turbulence. The gradients at the facade were small, both in practice and in the model. The predicted flow fields did contain many flow features which agreed well qualitatively with the field observations and previous field and model studies and there was some quantitative agreement between measured and modelled facade concentration variations which was encouraging, but further work is required. Discrepancies between the model and field studies indicated the potential

importance of factors such as mechanical turbulence which had not hitherto been included in the study for practical reasons. The relative benefits of a fluid flow model for quantitative use in building environmental design in the urban environment are, as yet, uncertain due to the complexity of environment although much further work is necessary in both experimental validation and investigation of the boundary conditions to establish the limits of its use.

Acknowledgements

References

Alamdari, F, Edwards, SC and Hammond, GP (1991) "Microclimate performance of an open office building: a case study in thermo-fluid modelling", In CFD - tool or toy? *Proc. IMechE Conference*, London, 1991.

Benson, P E (1992), A review of the development and application of the CALINE3 and CALINE4 Models, *Atmospheric Environment*, **Vol. 26B, No. 3**, 379-390.

Dabberdt, WF and Hoydysh, WD (1991) Street canyon dispersion: sensitivity to block shape and entrainment, *Atmospheric Environment*, **25A**, 1143-1153.

Dabberdt, WF and Hoydysh, WD (1994) A fluid modelling study of concentration distributions at urban intersections, *The Science of the Total Environment*, **146/147**, 425-432.

de Paul, FT and Sheih, CM (1985) A tracer study of dispersion in an urban street canyon, *Atmospheric Environment*, **19**, 555-559.

de Paul, FT and Sheih, CM (1986) Measurements of wind velocities in a street canyon, *Atmospheric Environment*, **20**, 455-459.

FloVENT User Manual, Flomerics Ltd. 1994.

Hall, DJ, Kukadia, V, Walker, S and Marsland, G (1995) Plume Dispersion from Chemical Warehouse Fires, BRE Client Report No. CR 56/95.

Hunter, LJ, Watson, ID and Johnson, GT (1990/91) Modelling air flow regimes in urban canyons, *Energy and Buildings*, **14-15**, 315-324.

314

Kato, N, Okhuma, T, Kim, JR, Murakawa, H and Nahori, Y (1992) Full scale measurements of wind velocity in two urban areas using an ultrasonic anemometer, *J. Wind Eng. Ind. Aerodyn.*, **41-44**, 67-78.

Launder, BE and Spalding, DB (1974) The numerical computation of turbulent flows, *Computer Methods in Appl. Mech. and Eng.*, **3**, 269-289.

Murakami, S, Mochida, A, Hayashi, Y and Hibi, K (1990/1991) Numerical simulation of velocity field and diffusion field and diffusion field in an urban area, *Energy and Buildings*, **15-16**, 345-356.

Ní Riain, C, Croxford, B, Littler, J and Penn A, "City Space and Pollution Dispersion: a monitoring and modelling exercise", In Jenks, M, Burton, E and Williams, K (eds.) The *Compact City: a sustainable urban form?*, E & FN Spon, London, 1996.

Oke, TR (1988) Street design and the urban canopy layer, *Energy and Buildings*, **11**, 103-113.

Panofsky, HA and Dutton, JA, Atmospheric Turbulence, John Wiley & Sons, New York, 1984.

Patankar, SV, Numerical Heat Transfer and Fluid Flow, Hemisphere, Washington, 1980.

Qin, Y and Kot, SC (1993) Dispersion of vehicular emissions in street canyon, Guangzhou City, South China (P.R.C.), *Atmospheric Environment*, **27B**, 283-291.

Rotach, M W (1995) Profiles of turbulence statistics in and above an urban street canyon, *Atmospheric Environment*, **29**, 1473-1486.

Sini, J-F, Anquetin, S and Mestayer, PG (1996) Pollutant dispersion and thermal effects in urban street canyons, *Atmospheric Environment*, **30B**, 2659-2677.

A NEW BOX MODEL TO FORECAST URBAN AIR QUALITY: BOXURB

D.R. MIDDLETON

Meteorological Office, Bracknell, Berks RG12 2SZ

Abstract. This paper presents a model to forecast concentrations of nitrogen dioxide NO_2 in urban areas. A box model provides a simple and robust description of air quality in urban areas, especially where emissions data are only available on a fairly coarse grid. BOXURB is a box model with some novel features. It can use synoptic observations of the meteorology, or numerical forecasts of wind and cloud. Traffic emissions are adjusted by time and day of week, and space heating emissions by degree hours. The urban heat flux combines an urban heat store adjustment, a space heating term, and the rural heat flux. Pollutants accumulate with the onset of light winds. NO_2 is forecast by subdividing the NO_x into its constituents, NO (nitric oxide) and NO_2. The subdivision is empirical for most of the year, but in ozone episodes the photostationary state is invoked. The forecasts are sent by the Met Office to NETCEN AEA Technology for use in the Department of Environment's Air Quality Bulletin System.

1 Introduction

A simple box model is described in Derwent et al. (1995), and the use of emissions from a typical grid square in the national emissions inventory is discussed in Derwent and Middleton (1996). Let Q be the emissions of NO_x, tonnes of NO_2 per year per 10 km × 10 km grid square, and q the flux (rate of emission per unit area), microgrammes per square metre per second:

$$q = 3.171 \times 10^{-4} Q \qquad (1)$$

For a downwind strip of city length x, wind speed u and depth of polluted layer h, the concentration for pollutant emission flux q is:

$$C = \frac{qx\chi}{hu} \qquad (2)$$

where χ converts units to ppb; it depends on the molecular weight W of the compound and the absolute temperature T_0 and pressure p; at temperature T_0=273.15 K, and pressure p=1013.25 mbar, $\chi = 0.487$ for NO_2. In the new model h, u, and

q depend on the numerical weather forecast (Middleton, 1995a, b) as this paper now describes. The inputs required by BOXURB from the forecast are wind speed, temperature, pressure, total cloud, and low, medium and high cloud covers. Wind direction is not required for a box model. Strictly, the box model formula requires u to be the mean wind speed through the polluted layer; in practice it is sufficient to use a wind speed at height 10 m.

2 Sensible Heat Flux H

Pasquill (1961) classified atmospheric stability by time of day, wind speed, and cloud cover. The new model adjusts the stability for urban energy flows. To do this, it estimates the rural sensible heat flux H Wm^{-2}, then adds the urban adjustments. The combined heat flux is then used to diagnose stability.

Following Smith (1979), net solar radiation R is $c_A Z$ Wm^{-2}, where c_A allows for total cloud, and solar energy Z Wm^{-2} varies with time of day and season. The rural heat flux was given by

$$H = 0.4(R - 100.0) \tag{3}$$

which is described by Smith (1979) as 'modestly reliable with standard error about 55 W m^{-2}'. Values of c_A range from 1.07 (clear sky) to 0.23 (8 oktas). H recognises the transition period within one hour of sunrise or sunset which was recommended by Pasquill (1961). However, in this work, we used

$$H = 0.4c_A(Z - 100.0) \tag{4}$$

This formulation does not alter the period for which $H \geq 0.0$. This is important because any adjustments to the timing of the evening transition (from unstable to stable conditions) will be described below under urban heat store.

By night, Farmer (1984) models the sensible heat flux by

$$H = (0.1748N_m - 2.36)\exp(0.375u) \tag{5}$$

for wind speed at 10 metres, u m s^{-1}, and cloud expressed as a modified cloud cover, N_m oktas, which is defined below.

3 Modified cloud amount, N_m.

The cloud amount is modified to take account of the relative effects of the various cloud types on the long wave radiation. Nielsen et al. (1981) derived N_m from the low, medium and high cloud cover:

1. If total cloud $N_t = 9$, the sky was obscured or fog or darkness, $N_m = 9$.
2. If total cloud $N_t = 0$, clear sky, $N_m = 0$.

3. If $max(N_1, N_2) \geq N_3$, low cloud N_1 or medium cloud N_2 predominate, $N_m = N_t$, the total cloud.

4. If $max(N_1, N_2) < N_3$, high cloud N_3 is dominant so
$N_m = N_t$ if $N_t < 3$, or $N_m = 2$ if $N_t = 3$, or $N_m = N_t - 2$ if $N_t > 3$.
This scheme reduces effective cloud cover slightly when high cloud is the main type of cover. The model uses cloud at three levels from observations or forecasts.

4   Friction Velocity u_*

Friction velocity to calculate boundary layer depth is obtained by solving the surface layer equations after Bull and Derbyshire (1990). Their subroutine SUBMOHFBC for u_* uses wind speed difference Δu, surface roughness length for momentum z_0, the height difference Δz, and the upward surface temperature flux T_f

$$T_f = \frac{H}{\rho C_p} \tag{6}$$

Assuming that the wind speed is negligible at the roughness height $z_0 = 0.1$ m, $\Delta u = u$ m s^{-1}, and $\Delta z = 9.9$ m. Then u_* is a rural value. Here u may be an observed wind speed at 10 m, or a forecast wind speed. For temperature 283.15 K and pressure 1000 mbar, we have $\rho C_p = 1235.05$ J m^{-3} K^{-1}. To economise on computation H is the urban heat flux Q_{Hu} from Section 9.

5   Boundary Layer Depth z_i

The boundary layer develops over a considerable distance upwind of the city, with the heat flux and surface roughness as for the rural case. A shallow layer limits the vertical mixing. After Smith and Blackall (1979), the neutral depth is

$$z_n = 0.25 \frac{u_*}{f} \tag{7}$$

for Coriolis parameter f at latitude θ. For rural flux of sensible heat $H < 0.0$ the stable depth is

$$z_s = 21500 \frac{u_*^2}{(|H|)^{\frac{1}{2}}} \tag{8}$$

and to join with the neutral depth

$$z_i = \left(\frac{1}{z_n^3} + \frac{1}{z_s^3}\right)^{\frac{1}{3}} \tag{9}$$

If the rural flux of sensible heat $H > 0.0$ the unstable depth is

$$z_i = \sqrt{z_n^2 + 1400 S_i} \tag{10}$$

where $S_i = \Sigma H_i$ is the summation of hourly rural heat fluxes H_i since dawn. As the program runs, the summation is initialised to zero at each sunrise, then increases at each daytime hour.

6 Stability Index P

Pasquill (1974) describes Smith's curves for stability index P. Curves to represent Pasquill's (1961) stability table are in Figure 6.10 of Pasquill and Smith (1983) third edition. In the box model, Smith's curves are treated according to stability using equations in Farmer (1984), viz:

Unstable conditions (positive heat flux) $P < 3.6$: P depends on wind speed and sensible heat flux.

$$P = 7 - [2.26 + 0.019(U_8 - 5.6)^2][0.1H_p + 2 + 0.4U_8^{3/2}]^{[0.28 - 0.004(U_8 - 2)^2]} \qquad (11)$$

with $U_8 = min(u, 8)$ for wind speed u m s^{-1}, and $H_p = max(H, 0)$ for surface sensible heat flux H W m^{-2}. When $H_p = 0.0$ W m^{-2}, P is given between 3.4 and 3.7, depending on u. This is close to Smith's definition that $P = 3.6$ for neutral stability, Class D, at zero sensible heat flux.

Stable Conditions (negative heat flux) $P > 3.6$: P depends on wind speed and cloud cover.

$$P = 3.6 + 10^{(0.08 - 0.025U_8^2)}(|0.1H|)^{1.54 - 0.011U_8^2} \qquad (12)$$

where the nighttime sensible heat flux was $H = 3.333(N_m - 8)$. Cloud cover N_m from 0 to 8 oktas gives H in the range -26.7 to 0.0 W m^{-2}. For u from 1 to 8 m s^{-1}, P was returned in the range 8.7 down to 3.6. Fog may be associated with poor air quality, but its stability is not defined by this scheme. Cloud cover coded as 9 (sky obscured) in synoptic observations requires special consideration e.g. restricted mixing.

7 Vertical Dispersion Parameter: $\sigma_z(x, P, z_0)$

Vertical spread depends upon distance travelled x, stability P, and surface roughness length z_0. Smith (personal communication, 1993) provided an empirical function for σ_z. Define:

$$K = 0.165 - 0.017P \qquad (13)$$

$$L = 1.0 - 0.032P \qquad (14)$$

$$M = 0.77 - 0.022P \qquad (15)$$

$$N = 0.386 \times 10^{-3}P \qquad (16)$$

For surface roughness length z_0,

$$S_0 = log_{10}z_0 \tag{17}$$

For downwind distance x in metres (i.e. city size) ,

$$X = log_{10}x - 3.0 \tag{18}$$

Then A,B,C,D depend on X:

$$A = 1.365 - 0.192X + 0.022X^2 + 0.05X^3 \tag{19}$$

$$B = 0.45 - 0.2738X + 0.0352X^2 + 0.0086X^3 \tag{20}$$

$$C = 0.075 - 0.074X + 0.019X^2 - 0.0005X^3 \tag{21}$$

$$D = 0.005 - 0.0045X + 0.0026X^2 - 0.0031X^3 \tag{22}$$

The empirical formula for σ_z is:

$$\sigma_z(x, P, z_0) = \frac{Kx^L}{(1 + Nx^M)}(A + BS_0 + CS_0^2 + DS_0^3) \tag{23}$$

8   Box Model Cloud Height: h

Stability P is obtained via synoptic observations or forecast products. Then σ_z is estimated at distance x over the surface roughness where the pollutant is released: $z_0 = 0.3$ m for suburb, or $z_0 = 1.0$ m for city. A constant factor α allows for the distribution of concentration in the vertical being represented by a well mixed layer in the box model. In BOXURB, α is set to 1.25. Here h is usually less than the boundary layer depth, but is constrained: $h \leq z_i$. This constraint seldom arises. Thus

$$h = \alpha\sigma_z(x, P, z_0) \tag{24}$$

9   Urban Heat Store and Stability

Changes to the rural energy balance are caused by urbanisation through differences in albedo, thermal capacity, thermal conductivity, and evaporation. They combine with anthropogenic heat release to alter the sensible heat flux and the stability. This affects dispersion. Pasquill and Smith (1983) page 292 discuss urban heat release. Oke(1990) p 283ff presents measurements for Vancouver showing the larger heat flux in the suburb compared to the country. The onset of stable conditions is delayed in the town. We therefore expect that summer evening pollution peaks will be delayed or suppressed. We now describe a physical model of Oke's data. The sensible heat
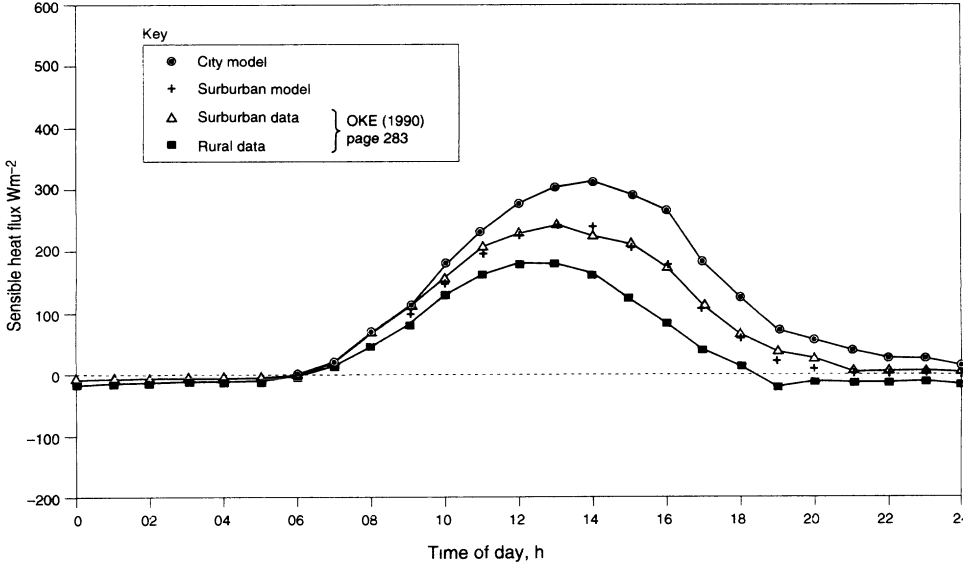
Figure 1: Plot of sensible heat flux W m^{-2} versus time of day read from Oke's (1990) measured curves in the rural and suburban sites. The plot also shows the curve fit for Oke's suburban data ($f = 0.023$, $\tau = 2.6875$ hours), and extrapolated to an imaginary city centre ($f = 0.046$, $\tau = 4.0$ hours). The model city achieves a larger daytime flux which remains convective until later into the summer evening.

flux in the rural case is Q_{Hr} and in the urban case Q_{Hu}. Then ΔQ_H is a difference between urban and rural heat fluxes due to stored solar energy warming the city. We call ΔQ_H the urban heat store correction. Let ΔQ_A be a sensible heat flux addition due to anthropogenic sources (industrial and space heating), e.g 3 W m^{-2} which is a conservative estimate; much larger values appear in Chell and Hutchinson, 1993. Neglecting seasonal changes in ΔQ_A, the urban heat flux is

$$Q_{Hu} = Q_{Hr} + \Delta Q_H + \Delta Q_A \tag{25}$$

Warming: Let Q_i^* be the net all-wave radiation flux density received in hour t_i during the day. We find R (Section 2) for Q_i^* at each hour. With sunrise at t_r and sunset at t_s, the mid-afternoon maximum in the urban heat flux is at time

$$t_m = t_r + 1.0 + 3(t_s - t_r)/4 \tag{26}$$

Assume the additional sensible heat depends on the energy stored in the city, so is some fraction f_s of the accumulated solar input:

$$\Delta Q_H = f_s \Sigma Q_i^* \tag{27}$$

Summation ocurs at each hour t_i whilst $t_r < t_i \leq t_m$; at mid-afternoon t_m summation halts and the maximum ΔQ_H is denoted $(f_s \Sigma Q_i^*)_m$.

Cooling: After t_m, $(f_s \Sigma Q_i^*)_m$ is constant. We assume stored energy is lost to cooler air entering the city from nearby countryside. For $t_i > t_m$, by analogy with Newton's law of cooling,

$$\Delta Q_H = (f_s \Sigma Q_i^*)_m \exp(-\frac{(t_i - t_m)}{\tau})$$ (28)

In these equations, ΔQ_H increases from sunrise, then decays from mid-afternoon into the evening. This method automatically adjusts for cloudy or clear conditions as well as time of year through Q_i^*. In winter or when overcast, the net radiation Q_i^* is small and ΔQ_H will have minimal impact on the stability. This automatic adjustment ΔQ_H is preferred to the method used by Roberts et al. (1992); they used a constant shift in heat flux and no temporal changes to the duration of unstable conditions.

Our parametrisation of the urban heat flux fits Oke's(1990) data with f_s=0.023, τ=2.6875 h, ΔQ_A=0 W m^{-2}. It easily reverts to rural conditions if we set f_s=0.0. It is simple and robust (Middleton, 1995a). Figure 1 shows the curves for rural (no heat store), suburb (fitted to Oke's data) or city (extrapolated) values. The method can be used on heat fluxes estimated from synoptic data or from model products for any day of the year at any location.

Heat store values used in the model BOXURB:

rural	f_s=0.0	τ= not used	ΔQ_A=0 W m^{-2}
suburb	f_s=0.023	τ=2.6875 hours	ΔQ_A=3 W m^{-2}
city	f_s=0.046	τ= 4.0 hours	ΔQ_A=6 W m^{-2}

The urban heat store adds to the sensible heat flux and leads towards more unstable conditions i.e. reduces P. It will have greatest effect on clear summer evenings. Neutral conditions are much more likely in the city: the early evening P is moved towards 3.6. Figure 2 shows the effect on concentrations of NO_2. This work suggests that stable conditions will occur less often in suburb or city than in the rural case. Air quality forecasts and environmental impact assessments are thus made sensitive to the urban stability classes. Further measurements are needed to test these ideas.

10 Episodes: Accumulation in Light Winds.

Let x_{max} be distance across the city, and Δt a time interval, usually 1 hour, between timesteps. Let $i = 0$ be the current timestep, $i = 1$ the previous timestep, and so on to the oldest timestep $i = n$.
In strong wind, when $u.\Delta t \geq x_{max}$,

$$C = \frac{q_0 x_{max} \chi}{h(x_{max}, P, z_0) u}$$ (29)
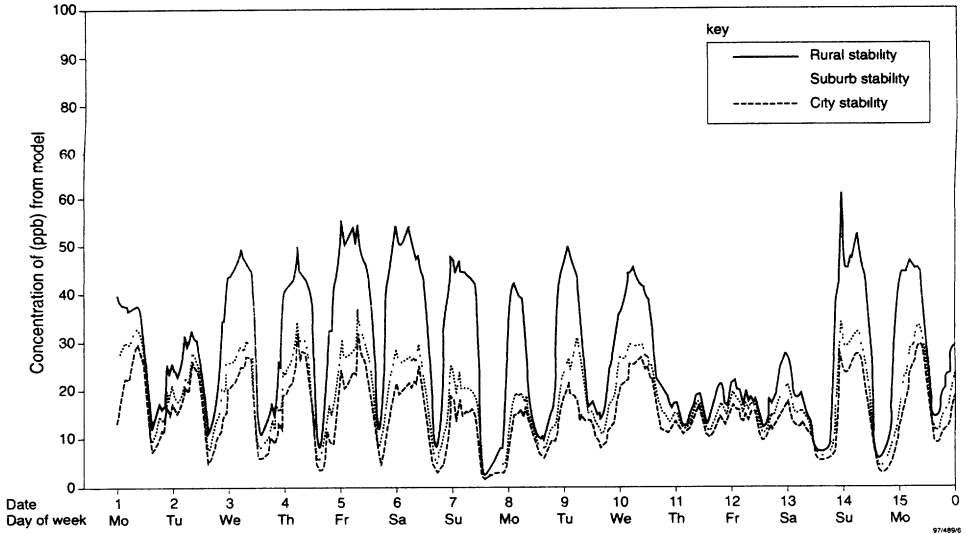
Figure 2: Sensitivity of the calculated concentration of NO_2 to the changes in stability index P caused by the urban heatstore and space heating additions to the sensible heat flux.

as in the original box model: clean air is entering the box.

In light wind, when $u.\Delta t < x_{max}$, pollutants accumulate, Figure 3. The very first parcel is calculated with distance $x_0 = u_0\Delta t$:

$$C_0 = \frac{q_0\Delta t\chi}{h(u_0\Delta t, P, z_0)} \tag{30}$$

During timestep i the parcel is displaced a distance $u_i\Delta t$; after i steps,

$$x_i = \Sigma_0^i u_j\Delta t \tag{31}$$

Subscript j denotes the sequence of steps through which the ith parcel has passed. Retaining the original stability P and roughness length z_0:

$$h(x_i, P, z_0) = 1.25\sigma_z(x_i, P, z_0) \tag{32}$$

Since $x_i > x_{i-1}$, we have $h(x_i, P, z_0) > h(x_{i-1}, P, z_0)$ i.e. the contribution C_i decreases as the parcel ages and its depth h increases:

$$C_i = \frac{q_0\Delta t\chi}{h(x_i, P, z_0)} \tag{33}$$

where q_0, u, P are for the time the parcel was created (with $i = 0$). In terms of the previous concentration:

$$C_i = C_{i-1}\frac{h(x_{i-1}, P, z_0)}{h(x_i, P, z_0)} \tag{34}$$
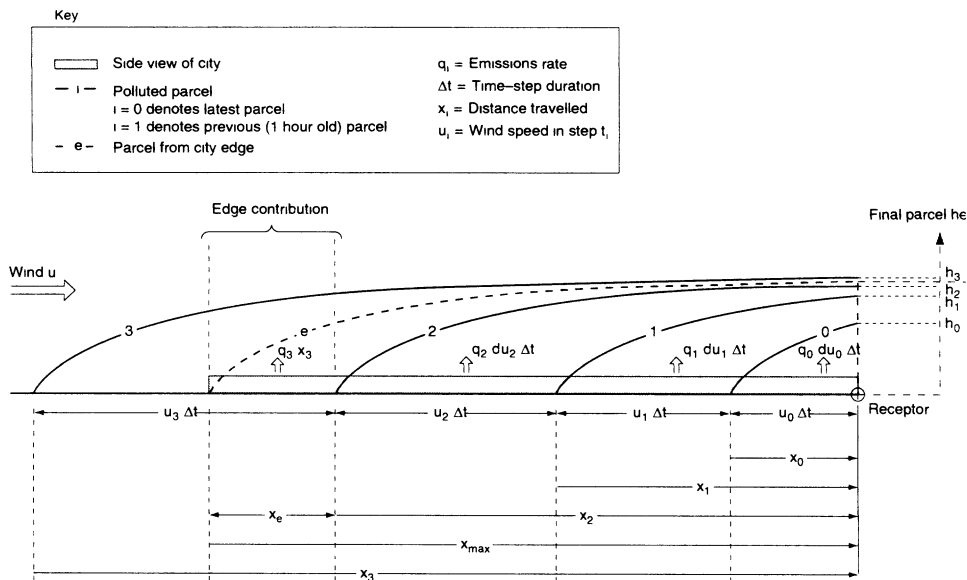
Figure 3: Diagram of the air parcels used in the low wind speed accumulation model.

and this is the form that is coded in the program. During accumulation the current term C_i and earlier terms must be summed:

1. For $x_i \leq x_{max}$, the whole term C_i is used.
2. For $x_{i-1} < x_{max} < x_i$, only a part of the term C_i is used, i.e. the edge contribution C_e.
3. For $x_{i-1} > x_{max}$, the term C_i lies beyond the city and does not contribute.

The edge contribution C_e is caused by pollutant emissions from an area of width d and length $(x_{max} - x_{i-1})$:

$$C_e = \frac{q_0(x_{max} - x_i)\chi}{h(x_{max}, P, z_0)u} \tag{35}$$

At the upwind edge of the city C_e replaces C_i; subsequent terms are ignored:

$$C = \Sigma_0^l C_i + C_e \tag{36}$$

where the upper limit $l \leq n$ and n is the number of terms stored in the array, which was coded with 20 rows of data, one per timestep. The summation starts at subscript $i = 0$, which uses the current and most recent timesteps first. It halts when condition 2 is true and then $l = i - 1$. In principle, contributions from 20 earlier hours could be used, but this is unlikely as the city edge is usually reached first.

At the upwind edge of the city:

$$C_e = C_{l+1} f_h f_x \tag{37}$$

where the dilution reset

$$f_h = \frac{h(x_{l+1}, P, z_0)}{h(x_{max}, P_{l+1}, z_0)} \tag{38}$$

recognises that the parcel height for row $l + 1$ was calculated for a larger distance than x_{max} and the dilution must be adjusted to that from just x_{max}. Similarly, the emissions reset allows for the last part of the city's emissions area:

$$f_x = \frac{(x_{max} - x_l)}{(x_{l+1} - x_l)} \tag{39}$$

Advantages of the low wind speed algorithm:
1. Accumulates pollution from sources near the ground.
2. Reverts to a simple box model once winds are strong and $u\Delta t > x_{max}$.
3. Delays the timing of the peak concentration during pollution episodes when winds become light over many hours.
4. Retains the relative simplicity and robustness of a box model with small computational costs.

11   Emissions from Traffic and Heating

The model BOXURB is used to forecast the total oxides of nitrogen, NO_x comprising nitric oxide NO and nitrogen dioxide NO_2. Only after NO_x has been forecast is it possible to apportion it into NO and NO_2 (cf Section 12). Emissions inventories are important in the management of air quality and in forecasting air quality. Emissions depend upon the nature of the pollutant and its source e.g. heating or transport. They vary with the season and time of day. They may depend upon special meteorological factors, such as fog when traffic speeds decrease, or cold weather when space heating increases. Emission rate Q has three components:
1. Q_P large point sources are ignored; their tall stacks are designed for negligible contribution in the immediate area.
2. Q_S stationary sources is multiplied by a seasonal factor S_λ as emissions reach a maximum in winter.
3. Q_M mobile sources i.e. transport is multiplied by a diurnal factor T_λ as traffic flow varies each hour of the day.
The combined emission rate of oxides of nitrogen (cf Q in equation 1):

$$Q_\lambda = Q_S S_\lambda + Q_M T_\lambda \tag{40}$$

Emissions were calculated by NETCEN AEA Technology for circles of radius 5.64 km (the same area as for emission squares). The dispersion distance across the city is not altered by the use of these circular emission estimates. Values of these annual fluxes ranged from $Q_M = 17551$ and $Q_S = 4073$ centred on London Bloomsbury, through 10062 and 2544 respectively at Birmingham Centre, down to 1878 and 927 respectively for Belfast Centre.

Mobile Sources: T_λ The emissions adjustment factor T_λ is given below:

hour	0 to 6	7 to 9	10 to 15	16 to 18	19 to 23
T_λ	0.275	1.667	1.227	1.684	0.931

On Saturdays the mobile emissions are multiplied by an extra factor of 0.5, or 0.3333 on Sundays. Over all 7 days this leads to an average factor of 0.833. For a proper summary of traffic flows, representative data are needed from each town, for each hour of the week. These were not available in this work.

Stationary Sources: S_λ The seasonal adjustment factor S_λ in pollutant emissions from stationary sources is dominated by space heating. Mean temperature indicates heating requirement (Ahrens, 1991). Heating engineers use degree-day, defined as the amount by which mean daily temperature $\overline{T}$ has fallen to below a fixed temperature such as 18C. When temperatures rise above 18C, the demand for heating is negligible, and degree-day DD is set to zero. For $\overline{T} \geq 18.0$, $DD = 0.0$. When $\overline{T} < 18.0$,

$$DD = 18.0 - \overline{T} \tag{41}$$

Lehman and Warren (1994) support a linear dependence of natural gas consumption in the domestic sector upon degree-days. There is a non-heating consumption which occurs even when degree-days are zero. Secondary factors included the influence of the cost of the fuel. Similarly, van den Berg (1994) has modelled the sales of natural gas in the Netherlands, with temperature, time of day and day of week, the wind speed, and solar radiation, as controlling factors. His function reduces to temperature dependence in winter episodes when it is very cold, winds are light, and fog attenuates the weak incoming solar radiation.

In the box model, when temperatures rise above 18C (negligible demand for heating), degree-hour DH_i is set to zero. For temperature T_i forecast below 18 C at hour i,

$$DH_i = 18.0 - T_i \tag{42}$$

The stationary source emission rate is $S_\lambda Q_S$, since

$$S_\lambda = \frac{DH_i}{\overline{DH}} \tag{43}$$

where S_λ is the normalised degree hour. The denominator is the average degree-hours:

$$\overline{DH} = \frac{\Sigma DH_i}{N} \tag{44}$$

N is the total number of valid temperature observations T_i averaged over a long period, preferably 10 years. Values of $\overline{DH}$ were found to be between 6.9 C and 9.5 C at 17 UK sites.

Some processes, such as in factories, may use fuel irrespective of the daily temperature. Following Lehman and Warren (1994) a fraction f_λ of the fuel may be

used independently of degree-hour: we chose $f_\lambda = 0.1$. Then the stationary source emission rate would become $(1.0 - f_\lambda)S_\lambda Q_S + f_\lambda Q_S$. Combining the emissions from stationary and mobile sources,

$$Q_\lambda = ((1.0 - f_\lambda)S_\lambda + f_\lambda)Q_S + Q_M T_\lambda \tag{45}$$

We illustrate the method by example. The temperature at Heathrow airport fell to 1.1 C at 06 Z on the 22 December 1994. The heating degree hour is then 16.9 C, so dividing by mean heating degree hour 7.5188 C, $S_\lambda = 2.248$. Since $Q_S = 4239.60$, $S_\lambda Q_S = 9529.35$. The new scheme for forecasting emissions would thus give, at this time and date, an emissions rate from space heating that is increased by 2.248 times relative to the annual average for stationary sources which is held in the national emissions inventory. Although central heating for example is often set by a time clock with morning and evening settings, the temperature based model does not apply according to time of day, but only to the degree hour at each hourly time step.

12 NO_2 Forecasts

The box model calculates the concentration (denoted $[NO_x]$) of NO_x. To estimate the amount of NO_2 in the mixture, Derwent and Middleton (1996) show data in the range 0 to 1300 ppb NO_x, and give an empirical function (concentrations in ppb):

$$[NO_2] = 2.166 - [NO_x](1.236 - 3.348A_{10} + 1.933A_{10}^2 - 0.326A_{10}^3) \tag{46}$$

where
$$A_{10} = \log_{10}([NO_x]) \tag{47}$$

By definition
$$[NO_x] = [NO] + [NO_2] \tag{48}$$

and the empirical ratio R_e uses $[NO_2]$ (Equation 46) and $[NO_x]$:

$$R_e = \frac{[NO_2]}{[NO_x]} \tag{49}$$

Below 9.0 ppb NO_x, $R_e = 0.7226$ avoids spurious negative values. It represents most of the NO having been oxidised to NO_2 after large dilution and significant reaction have occurred. Above 1141.5 ppb NO_x, $R_e = 0.25$. This region spans three orders of magnitude up to high concentrations found in vehicle exhaust. R_e in this region is uncertain, as episodes are unusual and data few. Forecast NO_x concentrations often lie in the range 10 to 1500 ppb. The smallest value is $R_e = 0.1327$ at $[NO_x]$ between 470 ppb and 486 ppb.

The function must be modified in a photochemical episode when ozone levels are high. The photostationary state assumes equal rates of formation and removal of
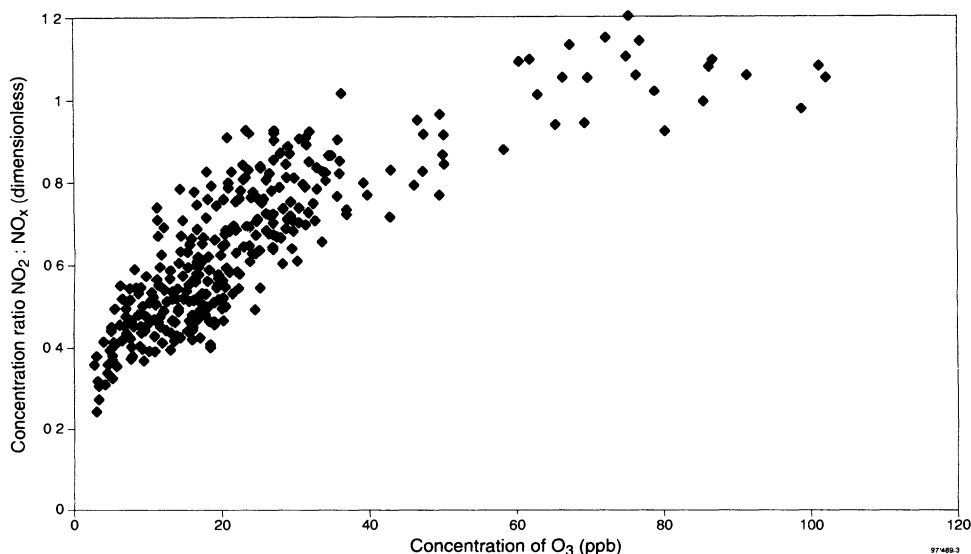
Figure 4: The ratio $[NO_2]{:}[NO_x]$ versus $[O_3]$ at the DoE site in Bloomsbury, London showing all daytime observations (diamonds) for the period 1/4/1995 to 10/5/1995 at hours 09:00 to 18:00 inclusive.

NO_2 by two dominant processes:

1. Reaction between NO and O_3 to form NO_2: its rate is $k[NO][O_3]$, where k is a rate constant. Other reactions such as oxidation of NO to NO_2 by O_2 are neglected.
2. Photolysis of NO_2: the rate is $J[NO_2]$, where J combines the light intensity (number of photons absorbed) and the quantum efficiency (the number of molecules destroyed per photon absorbed). J varies with position of the sun in the sky and with cloud cover.

Writing $A = J/k$ (a dimensionless quantity), it can be shown (Middleton 1995b) that the photostationary state ratio

$$R_p = \frac{[NO_2]}{[NO_x]} = \frac{[O_3]}{A + [O_3]} \tag{50}$$

R_p passes through 0 as $[O_3]$ tends to 0, and is asymptotic to 1 as $[O_3]$ tends to infinity.

Figure 4 shows $[NO_2]{:}[NO_x]$ versus $[O_3]$ using measurements at the DoE site (London Bloomsbury) from the period 1/4/95 to 10/5/95. Most points lie between 0 and 1. There are values above unity which implies $[NO_2]>[NO_x]$, but this is contrary to the definition of $[NO_x]$. This may be due to calibration errors in the monitors, or other artifacts. Given these practical limitations, we conclude that R_p has the correct form. In summer with reasonable light intensity, once $[O_3]$ is above say 30 ppb, the value of R_p is quite insensitive to the exact value of A that might be chosen ($4 \leq A \leq 16$), Figure 5. There is then little dependence of $[NO_2]_p$ on $[O_3]_f$, giving
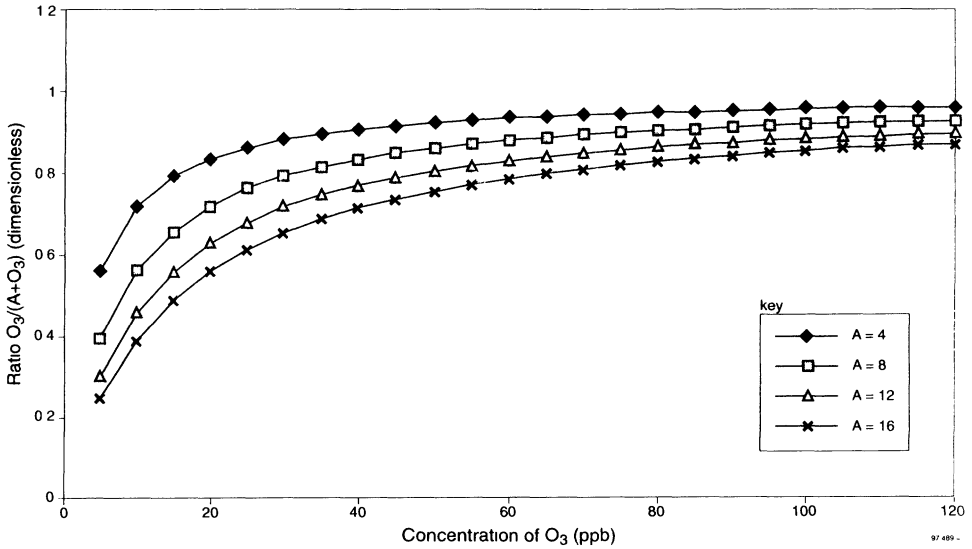
Figure 5: The ratio R_p calculated (smooth curves for $A = 4$, 8, 12, 16) by the photostationary state relation $[O_3]/(A+[O_3])$ showing asymptotic behaviour with lack of sensitivity to A or $[O_3]$ for $[O_3] > 30$ ppb (cf Figure 4).

us a robust forecasting aid.

Currently there are 20 sites with a single midday forecast of $[O_3]$. The box model uses the nearest 4 of these daily values for an averaged ozone forecast $[O_3]_f$. Let the forecast for NO_x at time t be denoted $[NO_x]_f$. For April to September and $8 \leq t \leq 19$, the forecast via the photostationary state approximation will be:

$$[NO_2]_p = R_p[NO_x]_f \qquad (51)$$

where R_p uses $A = 8.7591$ in Equation 50. At all other times, $[NO_2]_p = 0$. On the numerous occasions at night or out of summer when this method is not relevant, the BOXURB model reverts to $[NO_x]_f$ in equation 46 to find $[NO_2]_f$. The output $[NO_2]$ is the larger of $[NO_2]_p$ and $[NO_2]_f$. Figure 6 plots the original forecasts $[NO_2]_f$, and the larger $[NO_2]_p$ as a time series for 1st to 22nd June 1995. The photostationary results (Equation 51: broken line) on some days reach double the values from the empirical function (Equation 46: solid line). On other days the photostationary results show little change, indicative of little photochemical activity.

The Met Office runs a trajectory following box model to forecast the midday ozone concentration. The chemical reaction scheme is represented by a production term and a removal term, Stedman and Williams (1992). Ozone accumulates along the whole trajectory, and this might take up to 96 hours. Elevated ozone episodes form relatively slowly. Local emissions of urban NO_x might then be added to the air. The insensitivity of NO_2 to O_3 indicates that the two processes of long range ozone
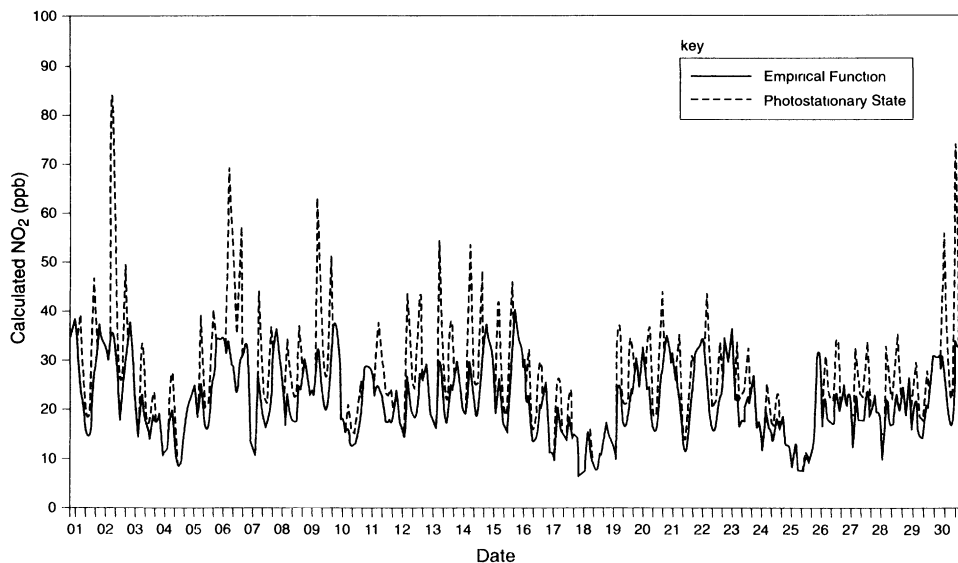
Figure 6: Time series plot for June 1995 showing $[NO_2]$ from the empirical function (solid) and the increased $[NO_2]$ (dashed) from the photostationary state ($A = 8.7591$), using the midday forecast $[O_3]$ and the hourly forecast $[NO_x]$. Concentrations are ppb.

formation and of local NO_2 formation may be treated as if dynamically uncoupled. BOXURB assumes that the NO and NO_2 behave as if entering ambient air containing O_3 at its forecast level. Strictly speaking, both the chemical kinetics and the rates of dispersion should be modelled together, but will not be considered here.

13   Conclusions

This paper describes the urban box model BOXURB which is run by the Met Office every day in order to forecast the likely concentration of NO_2. A validation plot (Figure 7) shows the time series for measured (point monitor) and forecast (city wide average) values, along with the error term, ln(bias). The latter type of plot is a useful means of assessing forecast performance.

The new model allows for the effect of urbanisation on stability diagnosis by lengthening the unstable daytime period to beyond sunset. The model has accumulation of pollutants when the wind decreases, the role of temperature in influencing heating emissions, a function to estimate NO_2 from NO_x, and a simple forecasting rule (using the photostationary state) to estimate elevated NO_2 when O_3 is forecast to

London NO$_2$ May 1996

London NO$_2$ May 1996 – New Box Model

London NO$_2$ May 1996 – New Box Model
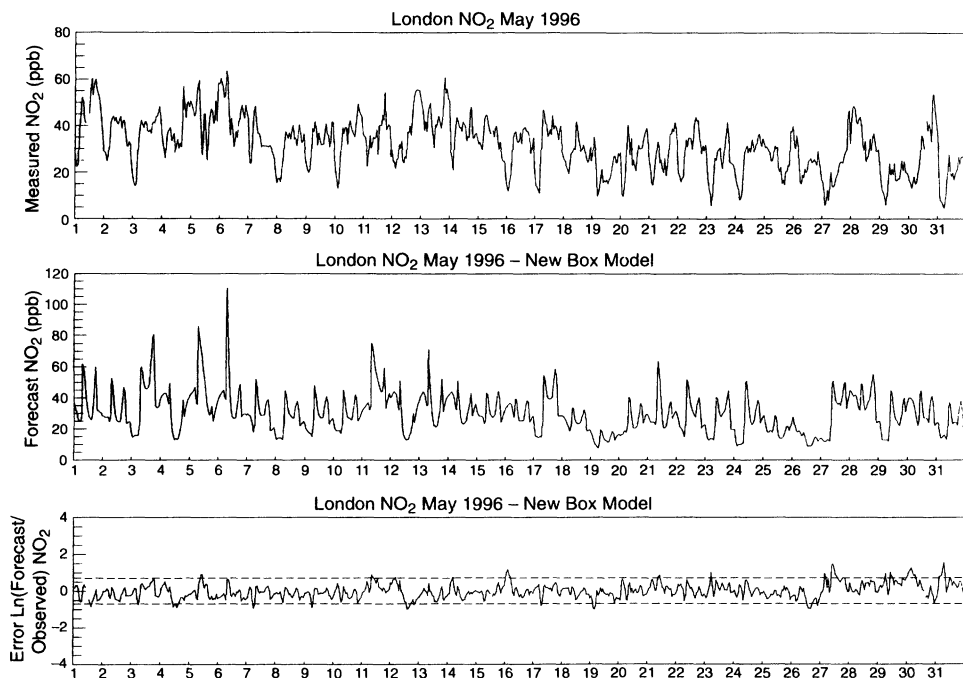
Figure 7: Validation plot for the new box model BOXURB, May 1996, London Bloomsbury, showing time series of NO$_2$ concentrations (ppb). Top: measured. Middle: NO$_2$ forecast 1 day ahead; broken line denotes poor air quality banding 100 ppb. Bottom: Error term ($ln(forecast/observed)$); broken lines denote factor of 2 error limits ($ln(2) = 0.693$).

be high. Forecasts obtained to date with the new model show that underforecasting is a problem in small towns. Research is in hand to identify the relative errors arising from uncertainties in the numerical weather forecasts, description of pollutant dispersion in towns, and the modelling of emission rates. It is possible to use the model with other pollutants such as carbon monoxide or fine particles, provided that they are emitted predominantly from sources near the ground. This would be the case for carbon monoxide, but will not always be true for particles where vehicles and domestic solid fuel may be dominant in winter episodes, but atmospheric chemistry may more important in summer. Finally, the urban heat flux scheme described above could be used to adapt Monin Obukhov stability to urban areas.

Acknowledgements

Nomenclature

A	Coefficient, Section 2.8
A_{10}	Variable used in NO_2:NO_x function, dimensionless
B	Coefficient, Section 2.8
c_A	Cloud cover attenuation of incoming radiation, dimensionless
C	Concentration of pollutant, dimensionless ratio ppb by volume
C	Coefficient, Section 2.8
C_i	Concentration associated with timestep t_i, μg m^{-3}
C_e	Concentration from edge of city, μg m^{-3}
C_p	Specific heat at constant pressure, Joule K^{-1} kg^{-1}
C_0	Concentration of pollutant, μg m^{-3}
d	Crosswind width of urban pollution plume, m
D	Coefficient, Section 2.8
DD	Heating degree day (see Ahrens, 1991), C
DH	Heating degree hour, C
$\overline{DH}$	Average heating degree hour, preferably over 10 years, C
f	Coriolis parameter, s^{-1}
f_s	Fraction of incoming radiation integral for urban flux, dimensionless
f_h	Ratio of previous to current parcel depths, dimensionless
f_x	Ratio of current to previous emission distances, dimensionless
f_λ	Fraction of fuel consumption for stationary sources used for non heating purposes, dimensionless
g	Acceleration due to gravity, m s^{-2}
h	Depth of polluted layer in box model, m
H	Turbulent sensible heat flux, W m^{-2}
H_p	Turbulent sensible heat flux (≥ 0), W m^{-2}
i	Denotes the current time step (dimensionless)
$i - n$	Denotes the nth previous timestep (dimensionless)
j	Summation subscript for each timestep, h
k	von Karman's constant, dimensionless
l	Number of steps to reach city edge (dimensionless)
K	Coefficient, Section 2.8

L	Coefficient, Section 2.8
L	Monin Obukhov length, m
M	Coefficient, Section 2.8
n	Maximum number of terms in low wind summation (dimensionless)
N	Coefficient, Section 2.8
N	Number of valid observations, dimensionless
N_m	Nielsen et al. (1991) modified cloud amount, oktas
N_t	Total cloud cover, oktas
N_1	Low cloud cover, oktas
N_2	Medium cloud cover, oktas
N_3	High cloud cover, oktas
p	Pressure, mbar
P	F B Smith stability index value (dimensionless)
q	Emissions flux, μg m^{-2} s^{-1}
q_0	Emissions flux in current step, μg m^{-2} s^{-1}
Q	Rate of pollutant emissions per annum from emission square, tonnes per 10 kilometre square per annum
Q_λ	Emissions rate Q after seasonal and diurnal adjustment tonnes per 10 kilometre square per annum
Q_M	Emissions per annum from mobile sources in emission square tonnes per 10 kilometre square per annum
Q_P	Emissions per annum from point sources in emission square tonnes per 10 kilometre square per annum
Q_S	Emissions per annum from stationary sources in emission square tonnes per 10 kilometre square per annum
Q^*	Net all wave radiation flux, Oke (1990), W m^{-2}
Q_i^*	Value of Q^* for time t_i, W m^{-2}
Q_H	Turbulent sensible heat flux, Oke (1990), W m^{-2}
Q_{Hs}	Suburban turbulent sensible heat flux, Oke (1990), W m^{-2}
Q_{Hr}	Rural turbulent sensible heat flux, Oke (1990), W m^{-2}
Q_{Hs-r}	Suburb heat flux minus rural flux, Oke (1990), W m^{-2}
Q_{Hu}	Urban turbulent sensible heat flux, Oke (1990), W m^{-2}
ΔQ_H	Difference in Oke's (1990) curves, suburb-rural, W m^{-2}
ΔQ_A	Space heating flux of sensible heat from man's activities, W m^{-2}
R	Net incoming solar radiation, W m^{-2}
R_e	Empirical ratio [NO$_2$]:[NO$_x$] (ppb v/v), dimensionless
R_p	Photostationary ratio [NO$_2$]:[NO$_x$] (ppb v/v), dimensionless
S_0	Coefficient, Section 2.8
S_λ	Seasonal adjustment factor for stationary sources Q_S, dimensionless (obtained by normalised degree hour)
t_i	Hour i in the day, h
t_r	Hour of sunrise, h
t_s	Hour of sunset, h
t_m	Hour of mid afternoon maximum heat flux, h
T	Temperature, C
T_f	Flux of surface temperature, K m s^{-1}

T_0	Absolute Temperature, K
$\overline{T}$	Average daily temperature, C
T_λ	Diurnal adjustment factor for mobile sources Q_M, dimensionless
U_8	Wind speed (not exceeding 8), m s^{-1}
u	Wind speed, m s^{-1}
u_i	Wind speed at time t_i, m s^{-1}
Δu	Vertical difference in wind speed, m s^{-1}
u_*	Friction velocity, m s^{-1}
W	Molecular weight, kg kmole^{-1}
x	Distance travelled by polluted parcel since emission, m
x_{max}	Distance to upwind edge of city, m
X	Coefficient, Section 2.8
z	Height, m
Δz	Height difference, m
z_0	Roughness length, m
Z	Incoming solar radiation (before attenuation in cloud), W m^{-2}
z_i	Boundary layer depth, m
z_n	Neutral boundary layer depth, m
z_s	Stable boundary layer depth, m
α	Factor to derive polluted layer depth from vertical plume spread, m
δ_i	Difference according to day number (see Section 6.3)
Δt	Timestep between box model forecasts (1 hour), s
χ	Conversion factor from μg m^{-3} to ppb
$\chi(\mu_*)$	Polynomial in μ_*
$\chi_2(\mu_*)$	Polynomial in μ_*
$\chi_3(\mu_*)$	Polynomial in μ_*
θ	Latitude, degrees
λ	Seasonal and diurnal adjustment to the retrieved emissions rate Q
μ	Kazanski-Monin stability (see Smith, 1979)
μ_*	Parameter related to μ as in Equation 25
ρ	Ratio of vertical dispersion parameters of different roughness lengths, dimensionless
ρ	Density of air, kg m^{-3}
σ_z	Vertical dispersion parameter, m
τ	Time constant for decay of stored urban heat flux, h
τ_u	Shear stress component, N m^{-2}
τ_v	Shear stress component, N m^{-2}

References

Ahrens C.D.(1991)
Meteorology today. An introduction to weather, climate and the environment.
4th Edition, pp 100-101.
West Publishing Co., St Paul, Minnesota.

334

Bull J.M. and Derbyshire S.H. (1990)
Numerical Solution of the Surface Layer Equations.
Met.O.(P) Turbulence and Diffusion Note No. 197. Unpublished.
The Meteorological Office.

Chell M. and Hutchinson D. (1993)
London Energy Study. Energy Use and the Environment.
London Research Centre.

Derwent R.G., Middleton D.R., Field R.A., Goldstone M.E., Lester J.N., Perry
R. (1995)
Analysis and interpretation of air quality data from an urban roadside location in
Central London over the period from July 1991 to July 1992.
Atmospheric Environment 29(8) 923-946.

Derwent R G and Middleton D R (1996)
An empirical function for the ratio NO_2:NO_x.
Clean Air Vol 26 (3) Autumn 1996 National Society for Clean Air.

Farmer S.F.G. (1984)
A comparison of methods of estimating stability category and boundary layer depth
using routine surface observations.
Special Investigations Technical Note No 37. Unpublished.
The Meteorological Office.

Lehman R.L. and Warren H.E. (1994)
Projecting monthly natural gas sales for space heating using a monthly updated
model and degree-days from monthly outlooks.
Journal of Applied Meteorology, 33, pp 96-106.

Middleton D.R. (1995a)
A new box model to forecast urban air quality: BOXURB
Turbulence and Diffusion Note No 221. Unpublished.
The Meteorological Office.

Middleton D.R. (1995b)
Operation of new box model to forecast urban air quality: BOXURB
Turbulence and Diffusion Note No 225. Unpublished.
The Meteorological Office.

Nielsen L.B. et al. (1981)
Net incoming radiation estimated from hourly cloud observations.
Journal of Climatology Vol 1, 255-272
(see pages 257, 261 for N_m)

Oke T R (1990)

Boundary Layer Climates
Routledge

Pasquill F. (1961)
The estimation of the dispersion of windborne material.
The Meteorological Magazine, 90 No 1063, pp33-49.

Pasquill F. (1974)
Atmospheric Diffusion The Dispersion of Windborne Material from Industrial and
other Sources
2nd Edition, pages 366 to 379
Ellis Horwood Ltd, Chichester

Pasquill F. and Smith F.B. (1983)
Atmospheric Diffusion The Dispersion of Windborne Material from Industrial and
other Sources
3nd Edition, page 337 to 338
Ellis Horwood Ltd, Chichester

Roberts C.S., Timmis R.J., Hackman M.P., Williams M.L. (1992)
Assessment and application of an advanced gaussian plume model.
In Air Pollution Modeling and its Application
Ed Van Dop H., Kallos G. (1992)
Plenum Press, New York

Smith F.B. (1979)
The relation between Pasquill stability P and Kazanski-Monin stability μ (in neutral
and unstable conditions).
Atmospheric Environment 13, pp 879-881

Smith F.B. and Blackall R.M. (1979)
The application of field experiment data to the parametrisation of the dispersion of
plumes from ground level and elevated sources.
In Proc. Mathematical Modelling of Turbulent Diffusion in the Environment. page
201ff.
Edited by Harris C.J.
Academic Press.

Stedman J R and Williams (1992)
A trajectory model of the relationship between ozone and precursor emissions.
Atmospheric Environment Vol 26A (7) pp 1271-1281

van den Berg W. D. (1994)
The role of various weather parameters and the use of worst-case forecasts in pre-
diction of gas sales
Meteorological Applications 1, pp 33-37

THE ADEQUACY OF THE EXECUTION AND PRESENTATION OF A SELECTION OF RECENT AIR QUALITY MODELLING ASSESSMENTS WITHIN THE UK

T. STEBBINGS[1], K. SIMMS[2], S. GRIMES[1]

[1] Centre for Environmental Research, Brunel University, Uxbridge, Middlesex, UK
[2] WS Atkins Science and Technology, Epsom, Surrey, UK.

Abstract.

The Environmental Protection Act 1990 has resulted in a large number of air quality modelling assessments being carried out to predict the effects on ambient air quality of various individual industrial sources as a part of the application process for authorization to operate. Currently there is no standard approach to carrying out air quality modelling assessments in the UK and, consequently, the content and quality of studies can vary enormously. To examine this variation, twenty five assessments which included dispersion modelling were selected and assessed against criteria derived from consideration of the requirements of these studies. The criteria derived also took account of two sets of guidelines. One set has been produced by the Institute of Environmental Assessment and the other by the Royal Meteorological Society. It should be noted, however, that this paper does not set out to produce a "user's manual" for air quality modelling studies, but rather to examine various studies against set criteria.

Aspects of each assessment which have been examined include: the site description; the objectives of the study; the representativeness and reliability of the input data; the assumptions made; and the communication of the results. Each category considered has been evaluated and marked against a common scoring scheme.

In general the resulting scores were poor with 56% of the assessment scoring less than 50% and only 8% of the assessments scoring more than 70%. Many of the assessments examined would not be capable of being fully audited or reproduced because they contained insufficient details of the input data used or the assumptions made.

In the context of ever increasing concern regarding the effects of air quality there needs to be a clear understanding of the efficiency and effectiveness of the tools which are being used to measure or predict air quality. Also in light of the UK Department of the Environment's air quality management initiative it is necessary for there to be a clear understanding of the most appropriate ways in which such tools should be applied.

1. Introduction

Air quality assessments, which include predictive modelling of anticipated ground level concentrations of pollutants, can be used for a number of purposes, including:-

1   Identifying the main sources contributing to unsatisfactory air quality within an area;
2   To assess compliance with air quality criteria;
3   As a tool in the design of monitoring networks;
4   To determine the impact of development in an area;
5   To predict the consequences of changes in transportation and planning policy;
6   To determine the effects of legislative development and future technological changes.

Air quality modelling assessments are carried out for a variety of reasons and many such studies have recently been undertaken for submission to Her Majesty's Inspectorate of Pollution (HMIP), now the Environment Agency, as part of applications for authorization to operate industrial facilities under the Environmental Protection Act, 1990. This act introduced

a system of authorizations for controlling the pollution arising from a range of industrial processes, including that from mobile sources. The prescribed processes were divided into the more potentially polluting processes, termed Part A processes, which were subject to control by HMIP for emissions to air, land and water in line with the concept of Integrated Pollution Control and, the less polluting, Part B, processes which were subject to control by local authorities for emissions to air only.

Operators of prescribed processes are obliged to apply for an authorization, which the enforcing authority may issue, possibly with various conditions attached. Enforcing authorities are required to maintain a public register containing copies of applications, authorizations, any variation, enforcement, prohibition or revocation notices, documentation relating to appeals and monitoring data.

The application form for an authorization for certain of the processes asks the applicant to state "What are the consequences of the release of prescribed substances, taking into account local circumstances." This question is often addressed with a predictive study, the specific objectives of which may include:

1   Identification and prioritisation of abatement and/or control technology;
2   Assessment of harm;
3   Identification of the Best Practical Environmental Option (BPEO);
4   Determination of monitoring requirements.

It appears to be fairly rare for an air quality modelling assessment to be carried out for the smaller Part B processes which are regulated by local authorities, however a number of air quality modelling assessments, carried out by a range of organisations, have been submitted to HMIP under the Environmental Protection Act 1990 for Part A processes.

Little guidance exists in the UK for Air Quality Assessments, and their application. The Institute of Environmental Assessment has produced the documents "Practical Experience of Environmental Assessment in the UK" (1993) and "Guidelines for Environmental Assessment of Road Traffic Guidance Note No.1" which considered some of the broader aspects of air quality modelling but did not relate specifically to industrial emissions from point sources. The Royal Meteorological Society has produced a "Policy Statement on Atmospheric Dispersion Modelling: Guidelines for the Justification of Choice and Use of Models, and the Communication and Reporting of Results" (1995) which discusses aspects of air quality modelling relating to meteorological dispersion. The Department of the Environment has produced "Released Substances and their Dispersion in the Environment" which provides guidance for applicants for process authorisation under integrated pollution control (March 1996) . One chapter specifically deals with the dispersion and fate of releases to the Environment, including to the air. The document touches upon results presentation.

The objective of the study was to examine a range of modelling assessments for different types of processes, produced by different organisations, in order to identify any deficiencies. To this end, this paper sets out the findings of a review of 25 modelling assessments obtained from HMIP Part A public registers, with reference to a common scoring scheme. The results presented then reflect the degree to which the study could be reproduced rather than the technical accuracy of the predictions.

The common scoring scheme used was derived frojm the documents produced by the Institute

of Environmental Assessment and the Royal Meteorological Society. The 25 selected assessments, and a study carried out for HMIP into the impacts of pollution from Part A processes situated alongside the Thames to the east of London, were considered against the scoring scheme, which covered factors such as consistency, adequacy, appropriateness and reliability of individual assessments. The East Thames Corridor Study was included for reference purposes. While the scale and objectives of this study are different to those for a single process trying to obtain an authorization, the document represents the only form of guidance, albeit indirectly, from HMIP on how such assessments should be conducted.

2. Methodology

The twenty five assessments were selected randomly from those held on the public register of Part A processes at the HMIP offices in Fleet (Hampshire) and Bedford (Bedfordshire). The objective of the scoring scheme was to make the evaluation of each assessment as objective and as consistent as possible. Various related elements were grouped under sub-headings which sought to examine different aspects of the study such as the input data or communication of results. The scoring scheme was broken down into a series of sub-headings and a total score out of 100 points awarded under each of these sub-headings. Within each of the individual sub-headings different aspects were given different weighting. For example, under the first sub-heading "Title and Outline" the site description was considered to be more important than naming the author, and this was reflected in the maximum score which could be achieved. The review criteria used included the following sub-headings:

TITLE AND OUTLINE (INCLUDING SITE DESCRIPTION)

The title, person or organisation undertaking the assessment and date of the study, which should be clearly stated as a means of identification. There should also have been some mention of the purpose of the study and a site description including a description of the locality, details about the site layout and the heights of nearby buildings where appropriate.

DEFINITION OF THE PROBLEM

This covered the need for the study and the background to it. The objectives and approach to the study were considered including the scope of the study and the scenarios examined. The study domain, both spatial and temporal, should be clear and the scope of the assessment and scenarios identified as well as the study's objectives. All the relevant air quality impacts should be identified and there should be justification for the exclusion of any impacts.

FITNESS OF THE MODEL

The tools used to carry out the assessment were considered under a separate sub-heading. The model used should be stated and some detail regarding the type of model and its suitability for the purpose given. Any quality assurance evaluation of the model should be highlighted and there should be an explanation for the choice of method in relation to the objectives. The uncertainty and variability associated with the model should be identified and an indication of the confidence to be placed in the results should also be outlined.

DATA

The input data used by the model is one of the most important aspects effecting the results

produced. Emissions and engineering data, baseline conditions and meteorological data were considered. The emissions included in the modelling procedure should be identified. The sources of emissions data (direct or derived) should be made explicit, and the quality and representativeness of the data should be discussed. The limitations imposed by the availability of suitable data should be explained and the uncertainty and variability of the assessment due to emissions data should be explored. Again an indication of the confidence to be placed on the results should be outlined.

It was usually not clear from the assessments examined whether there were any cost limitations attached to the assessments, or indication of the impact such constraints would have on the comprehensiveness of the data used. However, such a financial constraint would not preclude the author from indicating the representativeness of the data used and the impact on the uncertainty of the final result.

The representation of baseline conditions should be explained and an outline of data used, details of the monitoring sites and length of monitoring periods should be included. It should be established how the data requirements of the model have been met and the implications of any deficiencies. The representativeness of data should be considered and the limitations imposed by availability of suitable data should be explained. Again the uncertainty and variability associated with the ambient data should be commented on. An indication of the confidence to be placed on the results should be outlined.

An outline of the meteorological data used should be included, the sources of data should be made explicit and the quality and representativeness of data should also be considered. Finally the limitations imposed by non-availability of suitable data should be explained and an indication of the confidence to be placed on the results should be outlined.

RESULTS

Any sensitivity analysis carried out should be explained and the quantitative prediction of the impact should be identified. This prediction should take account of all other relevant emissions and combine the ground level concentrations associated with emissions from the plant with existing baseline conditions before comparing with air quality standards. Negative impacts should be recognised and given equal prominence to positive impacts and possible mitigation of any adverse effects should be discussed. Again an indication of the confidence to be placed on the results should be outlined.

APPROACH AND METHOD

All the assumptions, including correction factors and conversions must be made explicit. Any qualitative descriptions should be fully explained or defined. Overall the study should contain sufficient information to allow it to be reproduced or audited. In addition the meaning of individual results and an understanding of the total impact should be conveyed. The overall uncertainty and variability associated with the results should be identified and an indication of the confidence to be placed in the results should be outlined.

COMMUNICATION OF RESULTS

The final sub-heading related to the actual communication of the results and conclusions. The report should be logically laid out and technical terms should be used appropriately and

explained where relevant to the reader. Information should be comprehensible to the those who need to understand the implications of the findings but who may not be specialists in the area of modelling. The report should be clearly presented and include, as appropriate, an index, a glossary, full references, a non-technical summary and graphical summaries to enhance the clarity of the results. All numerical quantities must be clearly labelled with appropriate units and all conclusions should be explicit and expressed in a manner that bears a close relationship to the stated objectives and to the results obtained from the modelling procedure.

The Standard Scoring Scheme

Category		High	Medium	Low	Points
Title and Outline	Title	Clearly stated, for identification purposes.	Ambiguous	None	0-20
	Author and Date	Clearly stated	One or the other stated	Neither stated	
	Purpose	Purpose of the modelling study clearly stated e.g. as part of an IPC application.	Purpose could be inferred from other parts of the report, or the title.	Unclear	
	Site description	Description of locality, details about the site lay-out and heights of nearby buildings. Includes a site map and/or plan depicting the lay-out of the site.	Some text describing the site.	No site description.	0-80
Sub Total				100	
Definition of the problem	Objectives	Clearly defined.	Could be inferred form the report	No apparent objectives	0-20
	Study Domain	A clear statement of the distance over which predictions were made, and the averaging period in which the predictions were quoted, which must be appropriate.	Distance over which the predictions were made could be inferred from graph axes and time period either stated or inferred from which type of model was used.	Spatial and/or temporal boundaries unclear.	
	Impacts	Justification or discussion relating to choice of impacts.	Impacts considered identified.	Impacts not identified or inconsistencies later	0-40

				in report regarding impacts examined.	
	Standards	Relevant air quality standards fully referenced or reproduced.	Relevant air quality standards referred to.	Air quality standards not referred to at all or inappropriate standards presented.	0-40
Sub-Total				100	
Tools	Model	Name of model stated and some detail regarding type of model and suitability for purpose.	Name of model stated.	Name of model not given.	0-20
	Quality Assurance (QA)	Detailed discussion regarding the reliability of the model used and the quality assurance procedures it has been subjected to.	Limited discussion regarding the quality assurance procedures the model had been subjected to.	No discussion regarding the reliability of the model.	0-50
	Uncertainty and variability	The uncertainty associated with the modelling results actually quantified.	Some mention of the uncertainty associated with the modelling results.	No mention of the accuracy of the modelling results.	0-30
Sub-Total				100	
Data	Emission sources and data	Sources of emission data used clearly stated and/or explained. Where the data was derived from monitoring data, details about the monitoring, including the monitoring period, should also be stated. Where data were calculated, all calculations should be clearly explained. All relevant emissions data, particularly emission rates, stated or referenced.	Emissions data sources stated but not fully explained. e.g. missing calculations or monitoring period etc. Some emission data, including the emission rates and not other details such as stack heights stated.	Source of data not stated. Emission rates not stated.	0-40
	Emission uncertainty	Discussion regarding the	Limited reference regarding the	No discussion regarding the	

and variability	reliability of the emission data used and some appreciation of their importance with regard to the final result.	reliability of the emission rates used.	reliability of the emission data used.	
Baseline conditions	Full data sets for the site specific ambient air quality survey used as part of the assessment either contained in the reports or referenced. Details of monitoring methodology, monitoring period or source of the data should be included.	Summary of ambient air quality data for the locality, collected from other sources, considered as part of the assessment and referred to.	Ambient conditions not considered and the plant considered in isolation.	
Ambient uncertainty and variability	Quality and sufficiency of ambient data used, considered. Also the representativeness of the data used would have to be considered.	Some discussion regarding the representativeness of the data used.	No discussion as to the representativeness of data, or no data used.	
Meterological data	The data used must be justified as being representative. For example, the use of theoretical meteorological conditions may be suitable for worst-case analysis (For example a range of stability class/wind speed combinations used with have first been "tested" to determine those producing the worst-case conditions). For more detailed analysis, three years meteorological data from a nearby weather station may be appropriate. A	Some effort has been made to select representative weather data but it has not been fully referenced or reproduced.	The conditions used to represent meteorological conditions have not been justified as being representative. Certain stability class/wind speed combinations have simply been selected without any apparent justification, or the source of meteorological input is unclear.	0-30

		summary of the data should be contained in the report or fully referenced.			
	Metrologic al uncertainty and variability	Discussion regarding the representativeness of the data used, which should include consideration of the proximity of the metrological station used.		No discussion regarding the representativeness of the metrological data used.	
Sub-Total				100	
Results	Sensitivity analysis	Included, and the approach used added something to the quality or reliability of the overall results.	Included where required.	Nt included but would have been appropriate.	0-5
	Prediction of impact magnitude	Clear quantitative impacts predicted, presented in a summary table alongside the relevant criteria. The results took account of all relevant factors, and combined the emissions from the plant with existing ambient concentrations before comparison to relevant air quality standards.	The results presented in the text alone and took account of all relevant factors, and combined the emissions from the plant with existing ambient concentrations before comparison to relevant air quality standards.	No clear quantitative prediction or predictions that considered emissions from the plant in isolation.	0-75
	Negative impacts	Negative aspects recognised and discussed.	Limited reference to negative aspects.	Obvious negative impacts which were ignored.	0-10
	Mitigation	Discussion regarding reducing emissions.		No discussion of mitigation where warranted and obvious.	0-5
	Uncertaint y and variability	Discussion regarding the uncertainty associated with the	Limited discussion regarding uncertainty associated with the	No discussion regarding the uncertainty associated with the	0-5

		quantified impacts.	results.	results.	
Sub-Total				100	
Approach and Method	Assumptions	All assumptions clearly identified.	Most of the assumptions identified, or could be inferred.	Assumptions unclear.	0-30
	Qualitative descriptions	All qualitative descriptions explained fully.		Significant qualitative descriptions not fully explained.	0-5
	Factually incorrect	No factually incorrect statements.		Factually incorrect statement(s)	0-5
	Auditability	The assessment contained sufficient information including all input data (or references) and all assumptions were clear, making it possible to fully reproduce the results.		The assessment contained insufficient detail to allow the results to be reproduced.	0-30
	Overall uncertainty and variability	Discussion regarding the overall uncertainty associated with the results.	Limited discussion regarding the overall uncertainty associated with the results.	No discussion regarding the overall uncertainty associated with the results.	0-30
Sub-Total				100	
Communication of Results	Presentation	Report logically laid out with appropriate headings. Clear, legible text, well set out tables, good English and punctuation.			0-15
	Technical terms	Appropriate use of technical terms.		Inappropriate use of technical terms.	0-3
	Comprehensible	Fully comprehensible.		Confusing.	0-10
	Index	Included.		Not included.	0-3
	Glossary	Included.		Not included.	0-3
	References	Included.		Not included.	0-4

Non-technical summary	Included.		Not included.	0-10
Graphical summaries	Where a graphical summary is appropriate, clear contour plots for each pollutant, overlaid onto a map, showing areas of significance such as residential areas and SSIs	Where a graphical summary is appropriate, a graph depicting downwind ground level concentration with increasing distance from the source.	No graphical summary where one would have been appropriate.	0-25
Findings communicated	Yes.	Some ambiguity.	No.	0-5
Units	Clearly stated appropriate units.		None stated.	0-2
Explicit numerical conclusions	Explicit and numerical conclusions summarising the results and their relevance.	Conclusions either not explicit or numerical.	No explicit numerical conclusions.	0-25

Sub-Total		100
Total		100

3. Study Results

OVERALL RESULTS

All of the twenty five assessments, plus the East Thames Corridor Study, were considered against the criteria, and summary results of all the assessments are presented. In addition, examples of both good or poor assessments are reported. The results of the examination of the East Thames Corridor will be related to the other assessments, and is included because this is the only indication from HMIP of how modelling should be performed.

Title	Total Score	Title and Outline	Definition of the Problem	Tools	Data	Results	Approach and Method	Communication of Results
Power	24%	10	37	35	17	40	10	19

Station								
Power Station	29%	15	39	40	27	30	20	35
Willesden London	30%	17	48	40	23	35	15	35
District Heating Scheme	30%	20	40	40	20	20	20	40
Cement Works	34%	15	47	25	27	35	45	45
Cement Works	36 %	15	47	40	27	40	45	37
Sugar refinery	36%	20	40	40	40	40	20	20
Combined heat & power plant	40%	30	65	25	30	51	25	51
Hospital Boiler Plant	43%	20	60	40	80	40	20	40
Hospital Incinerator	46%	30	65	30	50	40	50	55
Brick Works.	49 %	25	76	40	57	68	35	44.
Boiler Plant	49%	80	40	40	40	40	40	60
Power Station	49%	30	60	35	40	60	45	74
Combined Heat and Power Plant	49%	35	55	30	45	75	50	55
Incinerator	50%	20	70	30	65	55	50	61

| Steel works	52%	20	70	40	70	40	53	68
Co-generation plant	55%	80	55	45	50	75	25	58
Clinical Waste Plant.	55%	20	71	40	66	75	30	82*
Coffee factory	56%	20	80	40	70	40	60	80
Masons Works, Ipswich	62%	70	77	40	75	78	45	50
Poultry Litter Power Station	64%	40	83	35	57	84	65	84
Brewery, Mortlake	67%	60	90	55	70	60	65	69

Eighty eight per cent (88%) of the assessments had been submitted as part of an IPC application, while the other twelve per cent (12%) did not state why they had been commissioned. The site description was considered an important feature of the report as local topography and terrain may affect the approach taken for an assessment. Forty four per cent (44%) of the studies contained no site description and a further thirty two per cent (32%) contained only limited information. Twenty four per cent (24%) of the assessments contained an adequate site description, that is it included a description of the locality, details about the site lay-out and heights of nearby buildings and perhaps even included a site map or plan.

The pollutants examined would relate to the type of process. Most of the assessments (92%) considered emissions of oxides of nitrogen (NO_x) and/or nitrogen dioxide (NO_2). The following graph illustrates the other pollutants considered.
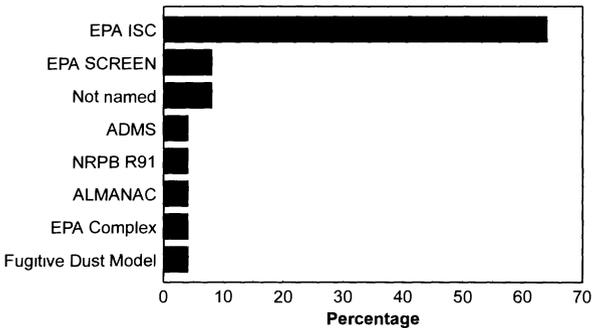
Pollutants Considered as Part of Modelling Assessment
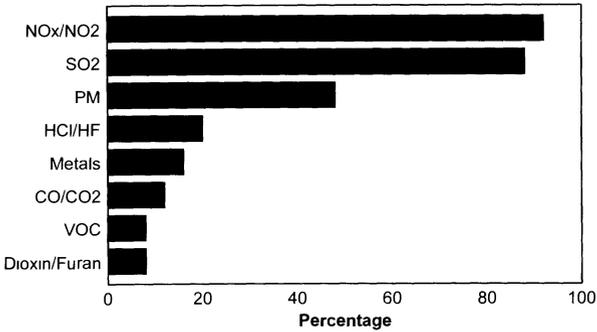
Air Quality Standards Considered as Part of the Modelling Assessment
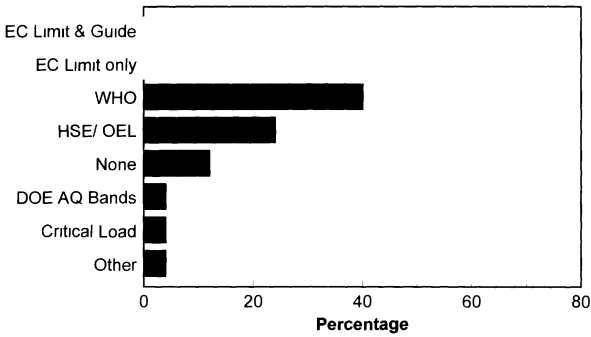
Model Used

When considering predicted ambient pollutant levels, most studies (68%) considered these against EC Limit and Guide Values, however twelve per cent (12%) did not consider any air quality standards.

The most commonly used models were the United States Environmental Protection Agency Industrial Source Complex models (both long term and short term).

Various approaches were taken in the studies for ascertaining emission rates to be used as input data to the model. The majority (44%) based emission rates on results of stack emission monitoring at the site. Thirty six per cent (36%) did not state the source of the emission rates used. The remainder used calculated emissions rates.

Baseline conditions were estimated in a number of ways, the most popular method (60%) being to base conditions on historical data collected from a number of sources, including local authorities and the Department of the Environment. In twenty per cent (20%) no consideration was given to baseline conditions. Specific monitoring for the purpose of the assessment was carried out in twelve per cent (12%) of the studies and the remainder estimated baseline

conditions.

Meteorological conditions were simulated in the model by the use of data from a weather station in forty four per cent (44%) of the assessments and in a further twenty per cent (20%) conditions thought to represent worst case conditions were selected. In twelve per cent (12%) of the assessments worst case conditions were again represented by a combination of unfavourable wind speed and stability category, but after screening to find the combination that produced the highest ground level concentrations. A further twelve per cent (12%) selected conditions thought to represent common weather conditions and in eight per cent (8%) of the assessments it was not clear how meteorological conditions had been simulated. Finally, in the remainder of the assessments, other input data were used.

Scores awarded to the East Thames corridor study have been included to allow comparison, although this study was much more detailed than would be expected for a single process.

4. Discussion and Conclusions

Generally the higher scoring assessments were good in most areas and the low scoring assessments poor in most areas.

As previously mentioned the final score is not a measurement of the accuracy the results of an air quality modelling assessment but represents the ability of the assessment to be reproduced and to be used for its intended purpose, for example, to demonstrate the effect of a process on ambient levels. Where a low score was achieved this is not meant to imply that the process should not have been authorised, instead a low score reflecs a lack of detail particularly regarding input data or assumptions which would allow judgement to be made regarding the effectiveness of the assessment and the results.

Some assessments did appear to be incomplete and were probably submitted as part of a larger document which may have addressed some of the more general issues, such as the site description. However, this should have been made clear in the assesmet.

In general, when the assessments were compared against the criteria, which were not particularly onerous, even the better assessments did not perform very well and some performed very poorly. Consequently, it would seem appropriate to question the usefulness within the authorization process of many of these studies.

This paper demonstrates that there is a need for comprehensive guidelines for performing air quality assessment. These would need to specify how studies should be undertaken, the competence required of individual undertaking studies, which models are appropriate for which uses, and their limitations and merits in relation to specific situations. In addition, practical advice on how to select appropreate input data for modelling is clearly required. Currently, there is a great deal of research being undertaken into predictive air quality modelling, however, from this study, it would appear that effeort is also required into how modelling should be applied.

References

Department of the Environment (1995) HMIP The East Thames Corridor Study

Department of the Environment (1996) *Released Substances and their Dispersion in the Environment* HMSO

Institute of Environmental Assessment 1993 *Practical Experience of Environmental Assessment in the UK*

Institute of Environmental Assessment *Guidelines for Environmental Assessment of Road Traffic Guidance Note No.1*

Royal Meteorological Society 1995 *Policy Statement Atmospheric Dispersion Modelling: Guidelines for the Justification of Choice and Use of Models, and the Communication and Reporting of Results* Published in collaboration with the Department of the Environment